Heterologous Expression of Thiostrepton A and Biosynthetic Engineering of Thiostrepton Analogs

A Dissertation
Presented to
The Academic Faculty

By

Feifei Zhang

In Partial Fulfillment
of the Requirements for the Degree
Doctor of Philosophy in the
School of Chemistry and Biochemistry

Georgia Institute of Technology
December, 2014

Heterologous Expression of Thiostrepton A and Biosynthetic Engineering of Thiostrepton Analogs

Approved by:

Dr. Wendy L. Kelly, Advisor
School of Chemistry and Biochemistry
Georgia Institute of Technology

Dr. Julia M. Kubanek
School of Chemistry and Biochemistry
School of Biology
Georgia Institute of Technology

Dr. Raquel L. Lieberman
School of Chemistry and Biochemistry
Georgia Institute of Technology

Dr. Alfred H. Merrill
School of Biology
Georgia Institute of Technology

Dr. Adegboyega K. Oyelere
School of Chemistry and Biochemistry
Georgia Institute of Technology

Date Approved: August 28, 2014

Happiness can be found even in the darkest of times, if one remembers to turn on the light.
---Albus Dumbledore

ACKNOWLEDGEMENTS

I am deeply grateful to my supervisor, Dr. Wendy L. Kelly, who is an extraordinary scientist. I would like to thank her for supporting me and guiding me to the right direction throughout my doctoral studies. Not only did she show me her dedications to science, her constant encouragement and motivation helped make the completion of my graduate work possible. I also appreciate her for training me and challenging me to be a good scientist.

I would like to offer my sincerest gratitude to my thesis committee members, Dr. Julia M. Kubanek, Dr. Raquel L. Lieberman, Dr. Alfred H. Merrill and Dr. Adegboyega K. Oyelere. Many thanks go to their precious time, extreme patience, valuable advice and intellectual contributions which helped to advance my thesis projects.

Warmest acknowledgements go to all current and previous Kelly laboratory members, especially Dr. Chaoxuan Li, Dr. Katy R. Rommel, Lisa T. Bain, Karen M. Goeders, Po-Yu Fang, Rayaj A. Ahamad, Hiroyuki Ichikawa, Daniel S. Sircar, Dr. Atahualpa Pinto, Dr. Wangsa T. Ismaya, Dr. Sridhar R. Kaulagari, and Juan Pablo Argon, who provided an outstanding environment of collaboration, an excellent network of knowledge, and great support. I would like to thank Dr. Chaoxuan Li and Lisa T. Bain for training me on molecular biology related techniques. Additional thanks go to Dr. Chaoxuan Li, who is a wonderful collaborator and excellent scientist. I am also grateful to Dr. Katy R. Rommel for her expertise in HPLC and NMR and for proof-reading many of my reports.

My sincere appreciations extend to Scott H. Nguyen, Leigh M. Matano, Cori C. Parker, Erik A. Oldfather and Emily Yasi. I would like to thank them for challenging me

to be a qualified and good mentor. I would like to specially thank Scott H. Nguyen, a brilliant undergraduate researcher, for assisting me with my projects, teaching me, and many more.

Special thanks go to Dr. Chiaolong Hsiao (currently at National Taiwan University) for his guidance on modeling studies. I would also like to thank David Bostwick at the Georgia Institute of Technology Bioanalytical Mass Spectrometry Facility and Dr. Fred Strobel at the Emory Mass Spectrometry Center for their excellent technical assistance and suggestions with mass spectrometry analyses. Special thanks go to Dr. Leslie T. Gelbaum at the Georgia Institute of Technology NMR Center for NMR training and valuable suggestions. My gratitude extends to Dr. John Glushka at the University of Georgia Complex Carbohydrate Research Center NMR spectroscopy facility. I would like to thank Dr. Glushka for his expertise, intelligence, and helping me with experiments on the 800 and 900 MHz NMR instruments.

I am deeply grateful to Dr. Cameron J. Tyson. Thank you for all your support, advice, and suggestions. I would also like to thank Mrs. Leslie Dionne White for coordinating things to make my projects running smoothly.

One of the most treasurable and priceless things I have received during my doctoral studies is the friendship, especially from Po-Yu Fang, Yanrong Shi, Chun Huang, Zhijun Zhao, Yang Li, Hongfeng Ren, Hui Lin, Xuejia Yan, Jun Jia, Karen M. Goeders, Lisa T. Bain, Katy R. Rommel, and Scott H. Nguyen. I am grateful for all your support. Thank you Yanrong and Chun, for picking me up at the airport when I first landed at Atlanta and many many more. I still remember all the good days when we were together. Thank you Karen, for all your help, for exercising with me, and for being a

wonderful friend. I cannot express enough of my gratitude and appreciation for their friendship. Thank you for being that I have ever needed.

I wish to thank my biking friends, Po-Yu Fang, Rayaj A. Ahamed, and Po-Kuei (Bob) Huang. I enjoyed all the ridings we did together. Especially to Po-Yu and Bob, thank you for encouraging me to bike to Alabama from Georgia. The non-stop, over 70 miles biking is one of the greatest things that I have achieved during the past many years.

最后，我想要感谢我的家庭，感谢他们一直以来对我的支持和无条件的爱。在我漫长的求学路程中，有过很多的困难，沮丧，和失败。感谢他们的鼓励，让我可以在跌倒后继续爬起来，一直前行。也正是有了他们的信任和支持，才塑造了今天的我，让获得博士学位成为一件可能的事情。我想要感谢我最伟大的妈妈，含辛茹苦抚养我长大，教育我为人处事的方式，教会我明辨是非黑白，引导我成为一个正直的人。我感谢我们所经历的困难，正是这些困难，才让我们更坚强地成长。我会继续努力，成为一个更优秀的人，成为您的骄傲。我想要感谢我的父亲，是您教会了我要正视困难，要乐观地生活，鼓励我成为一个更好的自己。谢谢您对我信任和教诲。我要感谢我的外公，谢谢您给我树立了一个生活的榜样。我还需要感谢我勤劳的外婆，在您的身上，我看到了劳动人民的伟大与智慧。苍白的语言无法表述我数不清的感谢，我想要告诉每一位家庭成员：谢谢你们，谢谢你们为我付出的一切，我爱你们！

TABLE OF CONTENTS

LIST OF TABLES

LIST OF FIGURES

LIST OF SYMBOLS AND ABBREVIATIONS

º	degree
×	times
α	alpha
β	beta
Δ	deletion
δ	chemical shift
ε	molar extinction coefficient
λ	lambda
µg	microgram
µL	microliter
µM	micromolar
µm	micrometer
aa	amino acid
Abs	absorbance
ADP	adenosine-5'-diphosphate
AMP	adenosine-5'-monophosphate
amp	ampicillin
amp^R	ampicillin resistance gene
apra	apramycin
$apra^R$	apramycin resistance gene
AMT	aminotransferase
Arg	arginine
Asn	asparagine
Asp	aspartic acid
ATP	adenosine-5'-triphosphate
AU	absorption units
bp	base pairs
br	broad

ºC	degree Celsius
C	cysteine
c	concentration
$CDCl_3$	deuterated chloroform
CD_3OD	deuterated methanol
CH	methine
CH_2	methylene
CH_3	methyl
$CHCl_3$	chloroform
chl	chloramphenicol
chl^R	chloramphenicol resistance gene
CH_3OH	methanol
cm	centimeter
CTD	C-terminal domain
COSY	correlation spectroscopy
C q	quaternary carbon
Cys	cysteine
dIH_2O	distilled water
d	doublet
D	aspartic acid
Da	dalton
DCM	dichloromethane
dd	doublet of doublets
DEPT-135	distortionless enhancement by polarization transfer with a 135º proton pulse
Dha	dehydroalanine
Dhb	dehydrobutyrine
DMF	dimethylformamide
DMSO	dimethyl sulfoxide
DNA	2'-deoxyribonucleic acid

dNTP	2’-deoxynucleotide-5’-triphosphate
dATP	2’-deoxyadenosine-5’-triphosphate
dCTP	2’-deoxycytidine-5’-triphosphate
dGTP	2’-deoxyguanosine-5’-triphosphate
dTTP	2’-deoxythymidine-5’-triphosphate
E	glutamic acid
EF-G	elongation factor G
ESI	electrospray ionization
F	phenylalanine
F	foward
FMN	flavin mononucleotide
$FMNH_2$	reduced FMN
FOXM1	forkhead box M1
G	glycine
g	gram
g	gravity
gDNA	genomic DNA
Gln	glutamine
Glu	glutamic acid
Gly	glycine
GTP	guanosine triphosphate
GTPase	guanosine triphosphate hydrolase
H	histidine
h	hour
^{1}H	proton
H bond	hydrogen bond
His	histidine
HMBC	heteronuclear multiple-bond correlation spectroscopy
HPLC	high performance liquid chromatography

HR	high resolution
Hz	hertz
I	isoleucine
Ile	isoleucine
IC_{50}	half maximal inhibitory concentration
J	coupling constant
K	lysine
k	kilo
kan	kanamycin
kan^R	kanamycin resistance gene
kb	kilobase pairs
kDa	kilodaltons
L	leucine
L	liter
LB	Luria-Bertani
Leu	leucine
Lys	lysine
M	methionine
m	multiplet
MALDI	matrix-assisted laser desorption/ionization
Me	methyl
Met	methionine
mg	miligram
Mg^{2+}	magnesium (II)
MHz	megahertz
MIC	minimum inhibitory concentration
min	minute
mL	mililiter
mM	milimolar

mmol	milimole
mol	mole
MRSA	methicillin-resistant *Staphylococcus aureus*
MS	mass spectrometry
MT	methyltransferase
mult	multiplicity
MW	molecular weight
m/*z*	mass to charge ratio
N	asparagine
NaCl	sodium chloride
$NADP^+$	nicotinamide adenine dinucleotide phosphate
NADPH	reduced $NADP^+$
nm	nanometer
nM	nanomolar
nmol	nanomole
NMR	nuclear magnetic resonance
NOESY	nuclear overhauser effect spectroscopy
nt	nucleotide
NTD	N-terminal domain
OD_{600}	optical density at 600 nm
orf	open reading frame
P	proline
p	plasmid
PCR	polymerase chain reaction
PDB	protein database
pfu	*Pyrococcus furiosus*
Phe	phenylalanine
P_i	inorganic phosphate
ppm	parts per million

Pro	proline
Q	glutamine
q	quartet
QA	quinaldic acid
R	arginine
R	reverse
RNA	ribonucleic acid
ROESY	rotating frame nuclear overhauser effect spectroscopy
RP-HPLC	reversed phase-high performance liquid chromatography
rpm	revolutions per minute
S	serine
s	second
S. actuosus	*Streptomyces actuosus* ATCC25421
SAM	*S*-adenosyl-L-methionine
S. coelicolor	*Streptomyces coelicolor* CH999
Ser	serine
S. laurentii	*Streptomyces laurentii* ATCC 31255
S. lividans	*Streptomyces lividans* TK24
sp.	species
T	threonine
t	triplet
Taq	*Thermus aquaticus*
Thr	threonine
TOMM	thiazole/oxazole-modified microcin
Trp	tryptophan
TSB	tryptic soy broth
Tyr	tyrosine
UV-Vis	ultraviolet-visible
V	valine

Val	valine
VRE	vancomycin-resistant *Enterococcus*
VREF	vancomycin-resistant *Enterococcus faecium*
W	tryptophan
X	one-letter abbreviation for any amino acid
Xxx	three-letter abbreviation for any amino acid
Y	tyrosine

SUMMARY

Thiopeptides are posttranslationally-processed macrocyclic peptide metabolites, characterized by extensive backbone and side chain modifications that include a six-membered nitrogenous ring, thioazol(in)e/oxazol(in)e rings, and dehydrated amino acid residues. Thiostrepton A, produced by *Streptomyces laurentii* ATCC 31255, is one of the more structurally complex thiopeptides, containing a second macrocycle bearing a quinaldic acid. Thiostrepton A and other thiopeptides are of great interest due to their potent activities against emerging antibiotic-resistant Gram-positive pathogens, in addition to their antimalarial and anticancer properties.

The ribosomal origins for thiopeptides have been established, however, few details are known concerning the posttranslational modification steps. Alteration to the primary amino acid sequence of the precursor peptide provides an avenue to probe the substrate specificity of the thiostrepton posttranslational machinery. Due to the difficulties in the genetic manipulation of *S. laurentii*, the heterologous production of thiostrepton A from alternate streptomycete hosts (*Streptomyces actuosus* ATCC 25421, *Streptomyces coelicolor* CH999, and *Streptomyces lividans* TK24) was sought to facilitate the biosynthetic investigations of the peptide metabolite. The production of thiostrepton A from the non-cognate hosts did not lend itself to be as robust as *S. laurentii*-based production, therefore an alternate strategy was pursued for the production of thiostrepton variants. The introduction of a fosmid used in the heterologous production of thiostrepton A, harboring the entire thiostrepton biosynthetic gene cluster, into the *tsrA* deletion mutant permitted restoration of thiostrepton A production to that of the wild-type level. The fosmid was then engineered to enable the

replacement of wild-type *tsrA*. Introduction of expression fosmids encoding alternate TsrA sequences into the *S. laurentii tsrA* deletion mutant led to the production of thiostrepton variants retaining antibacterial activity, demonstrating the utility of this expression platform toward thiopeptide engineering. This work was published in *Mol. BioSyst.* in 2011.

The seventh residue of thiostrepton A is predicted to be critical for the metabolite's antibacterial activity. Using the previously developed mutagenesis platform, the Thr7 position was targeted, and variants of TsrA at the biologically critical Thr7 residue were successfully generated. Substitution of Thr7 in the thiostrepton A precursor peptide disrupts both biological activity and successful biosynthesis of the analogs. A shunt metabolite, SL105-1, was produced by *S. laurentii* TsrA Thr7Ala variant. The identification of this analog grants insight into the late stages of thiostrepton biosynthesis, suggesting that epoxidation of quinaldic acid and subsequent closure of this loop occur late during thiostrepton maturation. This work was published in *Chem. Commun.* in 2012.

A mutation of the TsrA core peptide, Ala4Gly, supported the successful production of the corresponding thiostrepton variant. To more thoroughly probe the thiostrepton biosynthetic machinery's tolerance toward structural variation at the fourth position of the TsrA core peptide, we reported the saturation mutagenesis of this residue using a fosmid-dependent biosynthetic engineering method and the isolation of 16 thiostrepton analogs. Several types of side chain substitutions at the fourth position, including those that introduce polar or branched, hydrophobic residues, are accepted, albeit with varied preferences. In contrast, proline and amino acid residues inherently

charged at physiological pH are not well-tolerated at the fourth position by the thiostrepton biosynthetic system. These newly generated thiostrepton analogs were assessed for their water solubilities, antibacterial activities, and abilities to inhibit the proteolytic functions of the 20S proteasome. We demonstrate that the identity of the amino acid residue at the fourth position in the thiostrepton scaffold is not critical to effectively inhibit either the ribosome or the proteasome *in vitro*. This work is currently being prepared for publication.

Prior efforts in engineering the thiostrepton precursor peptide, TsrA, led to production of thiostrepton Ala2Gly, which demonstrated strong antibacterial activity. This observation prompted a systematic study of the proteinogenic amino acid residues at the second position of TsrA core peptide that will support the production of a mature thiostrepton A analog. Only eight thiostrepton Ala2 variants were isolated, suggesting that the thiostrepton biosynthetic system is somewhat restrictive towards structural modifications at this position, and. Two thiostrepton analogs truncated at the N-terminus by one amino acid, bearing a shortened quinaldic acid-containing macrocycle, resulted from the Ala2Ile and Ala2Val substitutions in the precursor peptide. This is the first report revealing that the size of the quinaldic acid loop is amenable to alteration. Although the identity of the residue at the second position of the core peptide does influence thiostrepton analog biosynthesis, it may not be crucial for the antibacterial and proteasome inhibitory activities of the full-length variants. The quinaldic acid loop size does affect thiostrepton's antibacterial potency as revealed by the greatly diminished abilities of Ala2Ile-ΔIle1 and Ala2Val-ΔIle1 analogs to inhibit bacterial growth and *in vitro* protein synthesis. In contrast, these two ΔIle1 analogs retained their inhibitory

activities against the proteasome, albeit slightly reduced. This work is currently being prepared for publication.

CHAPTER 1: INTRODUCTION

Adapted from the publication:

Zhang, F.; Kelly, W. L. *In vivo* generation of thiopeptide variants. *Methods Enzymol.* **2012,** *516,* 3-24.

1.1 Thiopeptides

Anti-infective agents have been successfully used to treat bacterial and malarial infections. However, emerging microorganism resistance to common drugs has complicated their clinical treatment. Currently, there is a pressing need for the development of new compounds, especially molecules displaying new modes of action, which could be incorporated into human medicine to fight against ever-adapting pathogens.[1] Great interest has been placed on a class of ribosomally synthesized and posttranslationally modified peptide metabolites (RiPP), thiopeptides (Figure 1.1), since their discovery in 1948.[2] More than 100 thiopeptides have been identified from several genera of marine and terrestrial Gram-positive bacteria.[3-7] Thiopeptides, also referred to as polythiazolyl peptides, are distinguished from other peptide metabolites by their six-membered central nitrogen-containing ring substituted by up to three thiazolyl groups to form a rigid central molecular framework.[8-9] In addition to multiple azol(in)e rings, dehydroalanine (Dha) and dehydrobutyrine (Dhb) residues are often present within the thiopeptide scaffold.

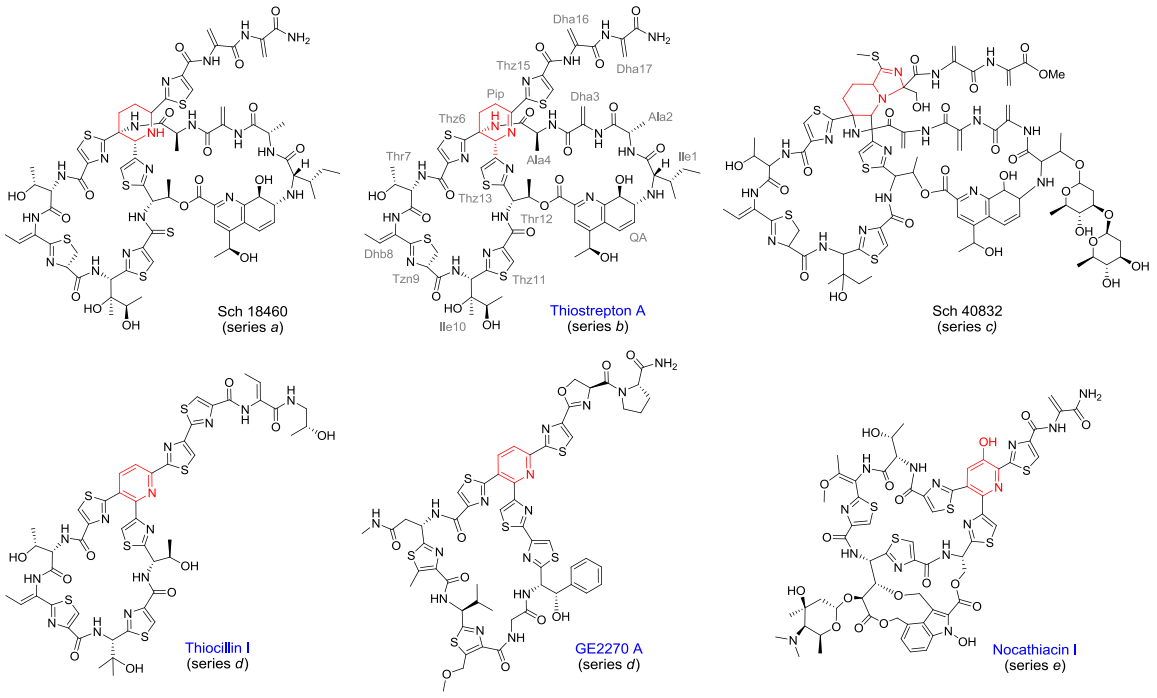

Figure 1.1. Examples of thiopeptides. The central six-membered nitrogenous ring is highlighted in red. The names of the thiopeptides with known biosynthetic gene clusters are shown in blue. The thiostrepton A residues are abbreviated using a three-letter code and labeled in grey. Dha, Dhb, Tzn, and QA refer to dehydroalanine, dehydrobutyrine, thiazoline, and quinaldic acid, respectively.

1.2 Structural classification of thiopeptides

Thiopeptides are divided into five classes based on the oxidation state and substitution pattern of the central nitrogen-containing ring (Figure 1.1).[8, 10] A tetrasubstituted piperidine ring characterizes series *a* thiopeptides, while in series *b*, the piperidine is replaced by a dehydropiperidine, as observed in thiostrepton A (Figure 1.1). Series *c* contains a single member, Sch 40832, with an unusual dihydroimidazopiperidine ring system.[11] Series *d*, the largest subfamily, includes a trisubstituted pyridine. Series *e* metabolites display a hydroxypyridine or alkoxypyridine moiety. Only one macrocycle is found in series *d* thiopeptides (e.g. thiocillin I, Figure 1.1) but the other series incorporate

both the core thiopeptide macrocycle and a second macrocycle harboring an L-tryptophan-derived quinaldic or indolic acid residue (Figure 1.1).

1.3 Biological activities of thiopeptides

The thiopeptides are best recognized for their antibacterial activities, owing to their potent inhibition of drug-resistant Gram-positive bacterial pathogens such as methicillin-resistant *Staphylococcus aureus*, vancomycin-resistant *Enterococci*, and penicillin-resistant *Streptococcus pneumonia*.[8, 12] They typically disrupt bacterial protein synthesis by one of two mechanisms. One group, including thiostrepton A, nosiheptide, and thiocillin I, binds to the 50S ribosomal subunit adjacent to the GTPase-associated center (Figure 1.2).[13-18] This region of the ribosome interacts with a number of translation factors, including elongation factor G (EF-G) that utilizes GTP hydrolysis to drive the movement of the A and P site tRNA-mRNA complex to the P and E sites of the ribosome. Thiopeptides interfere with the conformational changes required for this translocation.[14, 16, 19-20] A second mode of action is exemplified by GE2270 A, which binds to elongation factor Tu (EF-Tu) and prevents the formation of a stable EF-Tu·GTP·aminoacyl-tRNA complex, thus impeding the delivery of aminoacyl tRNAs to the ribosomal A site following translocation.[21-22]

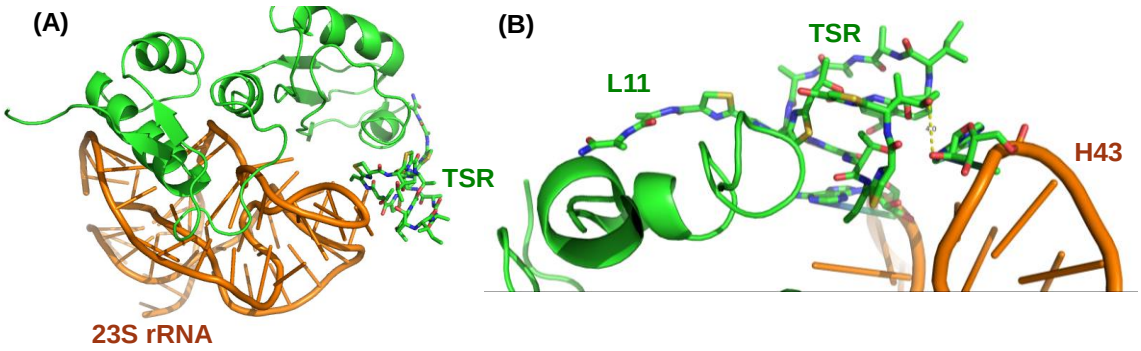

Figure 1.2. Thiostrepton A bound to the 50S ribosome. (**A**) Local view of the binding site of thiostrepton A on the 50S ribosome.[14] (**B**) Enlarged view of thiostrepton A in the complex. Thiostrepton A is abbreviated as TSR and labeled in green. The 23S rRNA and ribosomal proteins are shown in orange and green, respectively.

In addition to their antibacterial activities, thiopeptides have antimalarial and anticancer properties. Thiostrepton A exerts its antimalarial activity by targeting two aspects of protein homeostasis in *Plasmodium falciparum* (*P. falciparum*). Thiostrepton A and other thiopeptides prevent the prokaryotic-like translational machinery within the apicoplast, a plastid-like organelle essential for the survival of *P. falciparum*.[23-26] In addition, thiostrepton A inhibits the *P. falciparum* 20S proteasome within the cytosol, interfering with protein degradation and recycling.[27-28] The anticancer activity recently reported for thiostrepton A also likely results from the engagement of two cellular targets. Here, thiostrepton A induces apoptosis both by proteasome inhibition and by direct interference with the binding of forkhead box M1 (FOXM1) transcription factor to its affiliated promoter regions.[29-31]

1.4 Thiopeptide biosynthesis

For more than 60 years, it was unclear whether the thiopeptides were the products of a nonribosomal peptide synthetase assembly-line or the extensive posttranslational

modification of a ribosomally-synthesized precursor peptide. In 2009, five thiopeptide biosynthetic gene clusters were identified, revealing that these metabolites are derived from genetically-encoded precursor peptides (Figure 1.3).[32-36] Since these initial reports, several other thiopeptide biosynthetic gene clusters have been uncovered (Figure 1.3).[37-42]

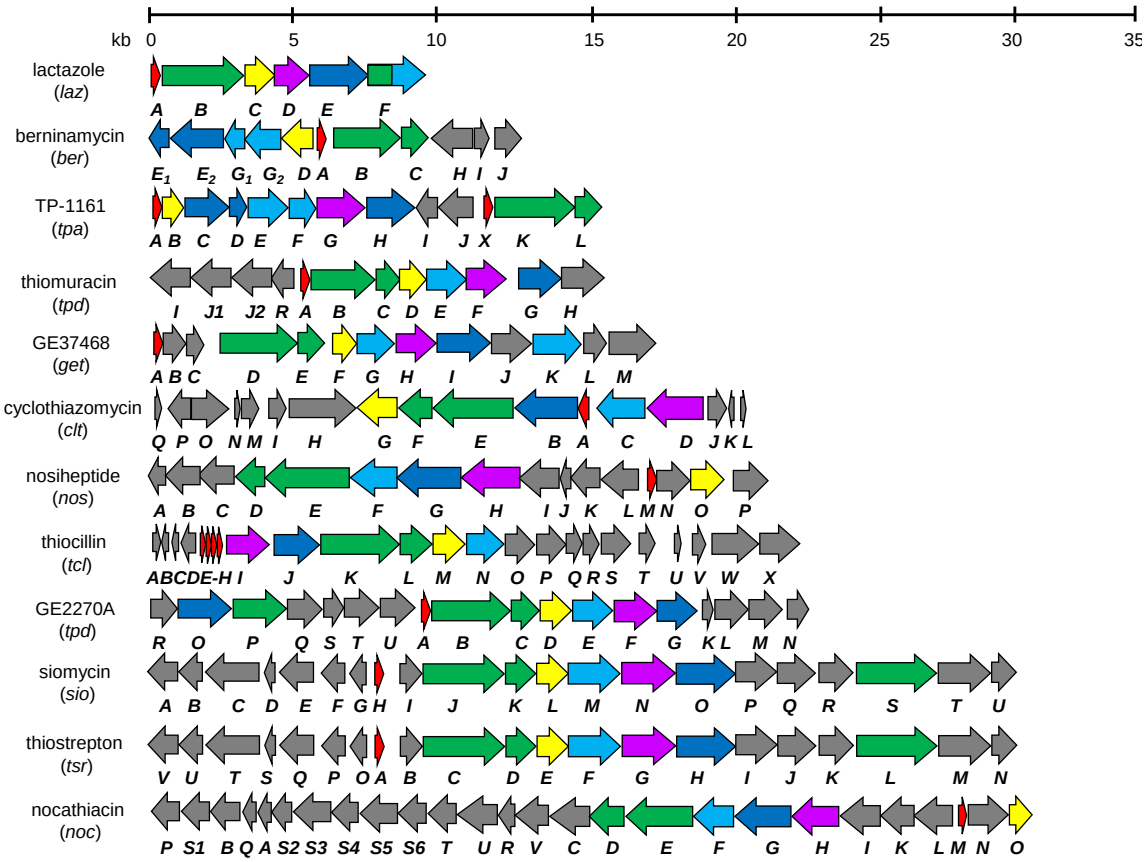

Figure 1.3. Genetic organization of the reported thiopeptide gene clusters. The precursor peptide encoding genes are highlighted in red. LanB-type dehydratase homologs are shown in green. Putative cyclodehydratases and dehydrogenases are presented in dark blue and light blue, respectively. Two gene products that are likely involved in the central core ring formation are displayed in yellow and purple. Lactazole (*laz*)[42], berninamycin (*ber*)[41], TP-1161 (*tpa*)[37], thiomuracin (*tpd*)[35], GE37468 (*get*)[38], cyclothiazomycin (*clt*)[40], nosiheptide (*nos*)[36], thiocillin (*tcl*)[33-34], siomycin (*sio*)[34], thiostrepton (*tsr*)[32, 34], and nocathiacin (*noc*)[39].

Each thiopeptide biosynthetic gene cluster contains a small precursor peptide-encoding gene and six genes conserved among all thiopeptide biosynthetic gene clusters. The nomenclature proposed by our group for the thiostrepton A biosynthetic gene (*tsr*)

cluster will be used here in an overview of thiopeptide biosynthesis.[32] The precursor peptides (TsrA) are composed of two regions: an N-terminal leader peptide that is cleaved during the course of precursor peptide processing and a C-terminal core peptide that supplies the backbone for the mature thiopeptide. TsrCDEFGH appear to be the minimal set of proteins needed to construct the thiopeptide scaffold. TsrC and TsrD resemble LanB-type lanthipeptide dehydratases, and one or both of them likely effects the dehydration of Ser and Thr residues to provide Dha and Dhb residues, respectively (Figure 1.4).[43] In contrast to the well-known phosphorylation mechanism involved in the dehydrations catalyzed by other families of lanthipeptide dehydratases, LanB-type NisB dehydrates the Ser and Thr residues in the precursor peptide, NisA, via a glutamylated intermediate, and it is expected that the thiopeptide LanB-like dehydratases would also employ this catalytic strategy.[44-47]

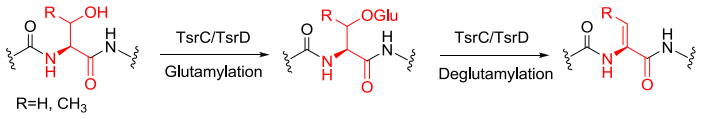

Figure 1.4. Proposed generation of a Dha or Dhb residue by the thiopeptide dehydratase(s). Dha and Dhb stand for dehydroalanine and dehydrobutyrine, respectively.

Bioinformatic analyses revealed a putative cyclodehydratase (TsrH) and a dehydrogenase (TsrF), both resembling enzymes that introduce the azoline and azole rings in the *E. coli* peptide microcin B17 (Figure 1.5).[48] Two independent mechanistic studies have been performed with other RIPP cyclodehydratases: TruD from the cyanobactin biosynthetic pathway and BalhD from a thiazole/oxazole-modified microcin (TOMM) biosynthetic pathway.[49-50] The Naismith group suggested that TruD generates an azoline group using an adenylation-type mechanism (Figure 1.5A).[49] In contrast, Mitchell *et al.* demonstrated that, in the heterocyclization catalyzed by BahlD, ATP

directly phosphorylates the substrate (Figure 1.5B).[50] The thiopeptide cyclodehydratase, TsrH, more closely aligned to TruD, likely adapts a similar adenylation strategy to effectuate an azoline formation.

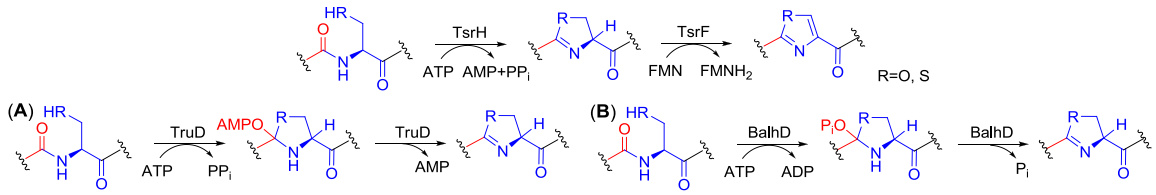

Figure 1.5. Proposed generation of a thiazole or oxazole moiety by thiopeptide cyclodehydratase(s) and dehydrogenase(s). Two mechanisms involved in the formation of an azoline moiety (**A**) using ATP as a molecular machine. (**B**) using ATP to phosphorylate the substrate.

The central piperidine/dehydropiperidine/pyridine ring and core macrocycle of the thiopeptides are suggested to arise from a [4+2] cycloaddition of two dehydroalanine residues in a linear precursor peptide, but this mechanism is cryptic (Figure 1.6). One hypothesis is that the central ring could be closed by a concerted hetero-Diels-Alder cyclization (Figure 1.6, pathway A).[51] Alternatively, Kelly *et al*. proposed that the nitrogenous ring could be formed via a stepwise fashion by adapting the neighboring thiazole group as an electron sink as seen in the reactions catalyzed by thiamine pyrophosphate-dependent enzymes (Figure 1.6, pathway B).[32, 52] Inactivation of *tclM*, a *tsrE* homolog, in a thiocillin-producing *Bacillus cereus* strain led to the accumulation of a linear peptide bearing multiple posttranslational modifications, including the two anticipated dehydroalanine residues.[53] This metabolite implicates a role for TclM/TsrE in forming the central nitrogen-containing ring, suggesting that installation of thiazoles, dehydroamino acid residues, and other core peptide modifications may very likely precede intramolecular cyclization.[53] The sixth conserved protein, TsrG, has no strong similarity to proteins of known function.

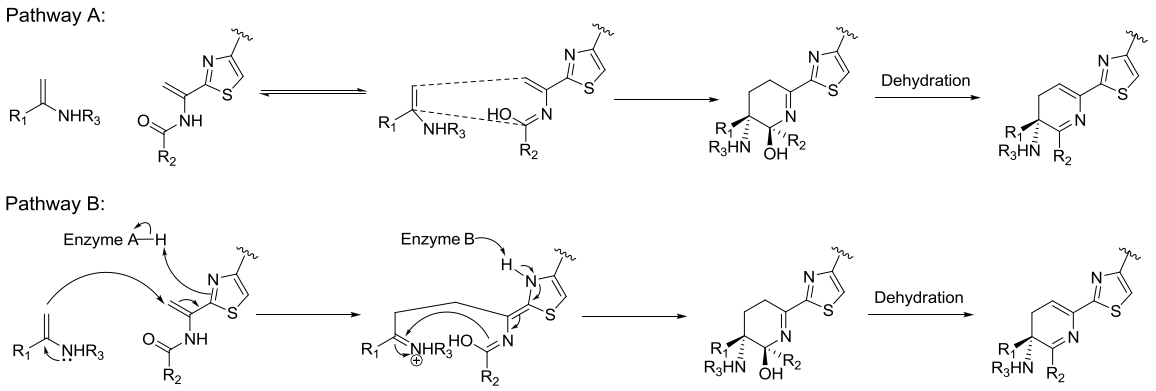

Figure 1.6. Two proposed biosynthetic pathways to the central six-membered nitrogen-containing ring.

Other modifications in individual metabolites include hydroxylations, methylations, and modifications to the C-terminus. Although there is general knowledge of the steps involved in thiopeptide maturation, detailed biochemical studies are still needed to decipher the relative timing of the various posttranslational modification steps.

1.4.1 Biosynthesis of thiostrepton A

Thiostrepton A (Figure 1.1) is produced by at least two species: *Streptomyces azureus* ATCC 14291 and *Streptomyces laurentii* ATCC 31255 (*S. laurentii*), and is one of the best studied thiopeptides.[7, 54] A prototypical example for series *b* thiopeptides, thiostrepton A bears a dehydropiperidine ring and a second highly modified macrocycle wherein a quinaldic acid moiety links a Thr side chain from the core thiopeptide macrocycle to the N-terminus.[10, 55-56] The *S. laurentii* thiostrepton A biosynthetic gene (*tsr*) cluster consists of 21 open reading frames, spanning nearly 30 kb.[32, 34] TsrA, a 58-amino acid precursor peptide, is composed of a 41-amino acid leader peptide followed by a 17-amino acid core peptide.[32] The apparent minimal set of biosynthetic proteins encoded by *tsrCDEFGH* presumably installs the core thiopeptide framework and the remaining proteins likely mediate additional modifications, including the generation and

attachment of the quinaldic acid residue (Figure 1.7) and amidation of the peptide's C-terminus (Table 1.1).[32]

Table 1.1. Deduced functions of the open reading frames in the *tsr* locus

Core Peptide Tailoring	Quinaldic Acid	Unknown Function, Export, Regulation
TsrA: Precursor Peptide	TsrJ: Adenylation Enzyme	TsrB: Putative Hydrolase
TsrC: Dehydratase	TsrM: Radical-SAM-Methylcobalmine-Dependent-Methyltransferase	TsrI: Cytochrome P450
TsrD: Truncated Dehydratase	TsrV: Aminotransferase	TsrK: Cytochrome P450
TsrE: Putative Hetero-Diels-Alderase	TsrN: NAD(P)H-Dependent Reductase	TsrO: Hypothetical Protein
TsrF: Thiazoline Dehydrogenase	TsrQ: Flavin-Dependent Dehydrogenase	
TsrG: Hypothetical Protein	TsrS: Cyclase	
TsrH: Cyclodehydratase/ Docking protein		
TsrL: Dehydratase		
TsrP: Carboxyl Methyltransferase		
TsrT: Amidotransferase		
TsrU: Carboxylesterase		

Earlier feeding studies demonstrated that the quinaldic acid moiety in thiostrepton A is derived from L-tryptophan.[57] It was originally proposed that the biosynthesis of the quinaldic acid begins with forming L-2-methyltryptophan from L-tryptophan catalyzed by an *S*-adenosyl-L-methionine (SAM)-dependent methyltransferase, TsrM (Figure 1.7).[32, 58] Feeding studies completed by Floss *et al.* revealed that the methyl group retained its stereochemistry upon transfer, suggesting the participation of a radical SAM enzyme.[59] This hypothesis was recently confirmed by the Berteau group. TsrM was biochemically characterized as a novel radical SAM enzyme using methyl-cobalmine as the direct methyl group donor.[60] Next, TsrV, a pyridoxal 5'-phosphate (PLP)-dependent aminotransferase, converts 2-methyltryptophan to 3-(2-methylindolyl)pyruvic acid (Figure 1.7).[32] This intermediate is oxidized by TsrQ followed by a ring rearrangement (Figure 1.7).[61] An oxidoreductase TsrN further reduces the ketone to an alcohol in a stereospecific manner, forming 4-(1-hydroxyethyl)quinoline-2-carboxylate, which is

thought to be activated by a putative adenylation enzyme TsrJ prior to its attachment to the Thr12 side chain hydroxyl group.[32, 61-62]

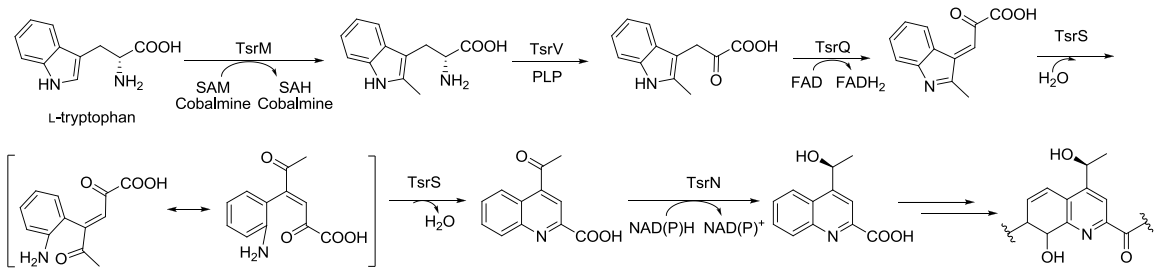

Figure 1.7. Proposed biosynthetic pathway for the thiostrepton quinaldic acid moiety.

1.5. Semi-synthesis of thiopeptides

Despite thiopeptides' promising biological activities, development of these metabolites into clinically useful agents is hindered, at least in part, by their poor water solubility. Structural modifications of the thiopeptide scaffold may generate biologically active analogs that overcome solubility limitations. Total syntheses of several thiopeptides have been achieved, but often involve complicated procedures with low net yields.[63-65] Thus, semi-synthetic modification of naturally-occurring thiopeptides may be a more viable solution. The Arndt and the Balasubramanian groups have successfully generated a series of thiostrepton analogs by semi-synthetic derivatization.[27-28, 31, 66-69] It was reported that selective removal or modification of the thiostrepton C-terminal Dha residues resulted in the analogs generally with retained antibacterial and proteasome inhibitory activities.[27-28, 66, 68] In contrast, at least one of the two C-terminal Dha residues was suggested to be important for thiostrepton's binding to the FOXM1 target.[31] Converting the Ile10 dihydroxyl groups of thiostrepton A to a ketal form resulted in the formation of an analog with retained anticancer activity, whereas reacting the endocyclic

quinaldic acid double bond with Danishefsky's diene led to cycloaddition products lacking any inhibitory activity against MCF-7 human breast cancer cells (Figure 1.1).[31] Oxidizing the 9th thiazoline to an aromatic thiazole gave rise to active thiostrepton derivatives against proteasome inhibition, while a thiostrepton analog in which the ester bond connecting Thr12 to the quinaldic acid moiety was opened resulted in a less effective proteasome inhibitor (Figure 1.1).[68] The D-configured thiazoline at position 9 is likely to be important for the inhibitory activity of thiostrepton A against protein synthesis, as suggested by the greatly reduced binding affinity of the L-epimer to the ribosome.[28] Interestingly, a thiostrepton analog obtained by reducing the central dehydropiperidine to a piperidine demonstrated an increased affinity for the L11/rRNA complex (Figure 1.1).[28] Among the efforts placed on developing thiopeptides as antibiotics, the C-terminal tail has been a popular region by introducing polar functional groups.[70-74] Indeed, semi-synthetic nocathiacin derivatives have been prepared that retain potent antibacterial activity with improved aqueous solubility and a GE2270 A derivative is currently being investigated for the treatment of gastrointestinal *Clostridium difficile* infections.[73-74] However, the semi-synthetic derivatization usually operates within the restrictions of the naturally occurring scaffold of a thiopeptide and no analog has been made with alternations to the peptide backbone.

1.6 Biosynthetic engineering of thiopeptides

Biosynthetic engineering offers a feasible strategy to augment semi-synthetic efforts toward generation of thiopeptide derivatives. One advantage of producing variants *in vivo* by site-directed mutagenesis of a precursor peptide is that the engineered

thiopeptide can be obtained from bacterial fermentation, potentially in high yield. Moreover, it reveals the collective posttranslational machinery's tolerance toward alternate substrates and may provide insights into the thiopeptide maturation process. There are several platforms to access thiopeptide analogs by precursor peptide engineering.[38, 41-42, 53, 75-79] Biosynthetic engineering of thiostrepton A is the focus of my thesis project and my results will be described in detail in the following chapters. Here, only the efforts toward generating thiocillin analogs via mutating precursor peptide, and providing thiostrepton and nosiheptide variants by gene inactivation are briefly discussed.

1.6.1 Thiocillin analogs obtained by precursor peptide mutagenesis

The thiocillins, series *d* thiopeptides, provide an exquisite illustration of broad thiopeptide production across bacterial genera and ecological niches. The thiocillins closely resembling micrococcin P_1 and P_2 were first reported in 1976 from a variety of terrestrial *Bacillus* strains, and metabolites YM-266183 and YM-266184 were later isolated from a marine-derived *Bacillus* species.[5-6] A micrococcin was the very first thiopeptide identified, obtained from an Oxford sewage *Micrococcus* isolate in 1948 and closely related analogs have also been reported from *Bacillus pumilis* and *Staphylococcus equorum* WS 2733.[80-82] A close inspection of the thiocillins, micrococcins P_1 and P_2, YM-266183 and YM-266184 reveals that they could all stem from an identical core peptide sequence. Using a genome-mining approach, two groups identified a thiocillin biosynthetic gene cluster in *Bacillus cereus* ATCC 14579 (Figure 1.3).[33-34] Walsh and coworkers established that this strain produces eight thiocillin derivatives, including thiocillin I (Figure 1.1), the previously identified micrococcins, YM-26618, and YM-266184.[33] The conserved set of thiopeptide biosynthetic proteins is encoded by

tclIJKLMN. The thiocillin precursor peptide is encoded in four identical gene copies (*tclE-H*) and is composed of a 38-amino acid leader peptide and a 14-amino acid core peptide.[33-34] To access thiocillin analogs by precursor peptide engineering, Walsh *et al*. constructed a *B. cereus tclE-H* deletion mutant, permitting introduction of a single variant copy of *tclE* on a plasmid *via* Campbell integration. Each residue of the TclE core peptide was replaced by site-directed mutagenesis and several thiocillin analogs were generated.[53, 75]

1.6.2 Gene inactivation to produce nosiheptide analogs

Nosiheptide, produced by *Streptomyces actuosus* ATCC 25421 (*S. actuosus*), is a representative member of the series *e* thiopeptides and is sold as a feed additive in animal husbandry (Figure 1.1).[83-85] Nosiheptide features a hydroxypyridine within the core scaffold and a second macrocycle in which an indolic acid residue is linked to two side chains from the core macrocycle. The indolic acid appendage is tethered by thioester and ester bonds to a cysteinyl thiol and the γ-carboxyl of a hydroxylated glutamyl residue, respectively. The region encompassing the nosiheptide biosynthetic gene (*nos*) cluster spans nearly 35 kb and contains 26 genes (Figure 1.3).[36] The minimal set of proteins needed to install the thiopeptide scaffold is proposed to be encoded by *nosDEFGHO*. The nosiheptide precursor peptide, NosM, is composed of a 50-amino acid leader peptide and a 13-amino acid core peptide.[36] Only the first 12 amino acids of the NosM core peptide are found in nosiheptide and the 13th residue is cleaved during maturation.[36, 86]

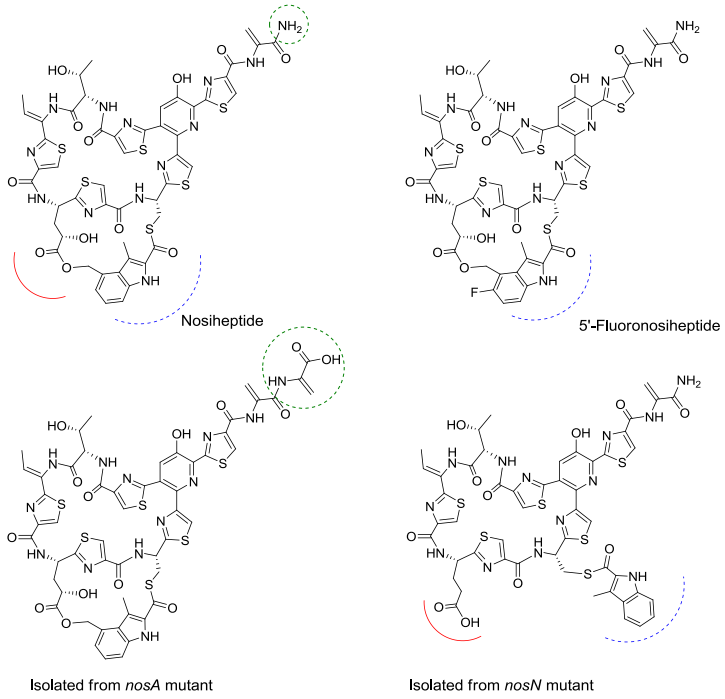

Figure 1.8. Nosiheptide and analogs generated by gene inactivation. The modified C-terminus is circled and the alterations to the indolic acid residue and glutamyl side chain are indicated with a hashed arc and solid arc, respectively.

Nosiheptide analogs have been generated either by supplementing fermentation medium with an analog of L-tryptophan, the precursor to the indolic acid residue, or by inactivating tailoring genes.[36, 86-87] NosL was recently demonstrated to be a radical *S*-adenosyl-L-methionine (SAM)-dependent enzyme that rearranges the L-tryptophan carbon skeleton to provide 3-methyl-2-indolic acid and it accepts 5- and 6-fluoro-DL-tryptophan as substrates.[87] This promiscuity was exploited in *S. actuosus* to generate the first halogenated thiopeptide (Figure 1.8).[87] Inactivation of genes encoding nosiheptide tailoring enzymes also yielded nosiheptide analogs in two separate studies. NosN, proposed to be a radical SAM-dependent methyltransferase, is proposed to install the 4-methyl group on the indolic acid residue.[36] Deletion of *nosN* leads to the accumulation of a nosiheptide analog with an indolic appendage lacking the anticipated 4-methyl group and, as a consequence, an incomplete second macrocycle (Figure 1.8).[36] NosA catalyzes

formation of the C-terminal amide by an eneamide dealkylation.[86] Deletion of *nosA* permits interception of a nosiheptide biosynthetic intermediate bearing the cryptic 13th residue at the C-terminus (Figure 1.8).[86]

1.6.3 Gene inactivation to produce thiostrepton analogs

Thiostrepton derivatives have also been obtained by inactivation of genes encoding enzymes that elaborate the thiopeptide scaffold late during the maturation process. Our group and Liu *et al.* have deployed this strategy to obtain what appear to be intermediates in thiostrepton A biosynthesis.[32, 88] TsrU resembles members of the α/β hydrolase superfamily, and disruption of the corresponding gene leads to accumulation of a thiostrepton derivative bearing a methyl ester at the peptide's C-terminus (Figure 1.9).[32, 88] *In vitro* biochemical analysis of TsrU verified this enzyme is an esterase that hydrolyzes the C-terminal methyl ester to liberate methanol and the carboxylate-containing thiostrepton C (Figure 1.9).[88] Inactivation of *tsrT*, which encodes a protein homologous to amidotransferases, abrogates thiostrepton A production and permits accumulation of thiostrepton C.[32] The metabolites isolated following inactivation of *tsrU* and *tsrT* suggest that formation of the C-terminal amide may be a late, if not the final, step of thiostrepton A biosynthesis.[32, 88] Thiostrepton C is ca. 50% more water soluble than thiostrepton A, but is nearly 10-fold less effective against *Bacillus subtilis*.[88]

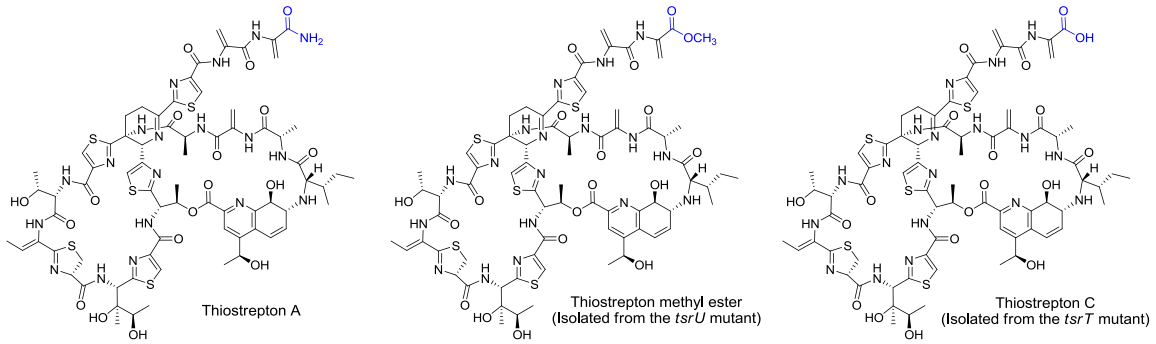

Figure 1.9. Thiostrepton A and analogs generated by gene inactivation. The modified C-terminus in each variant is highlighted in blue.

1.7 Scope of this work

Despite the potent biological activities described for thiostrepton A, its clinical application is currently limited due, at least in part, to poor water solubility and bioavailability. In contrast to the general structural knowledge of how thiopeptides affect protein translation, rather limited information is available concerning how a thiopeptide is also able to engage the recently recognized 20S proteasome and FOXM1 targets. It is therefore unknown whether the same or differing structural regions of thiostrepton A are critical for each of the three major biological activities. However, the limitations posed by naturally available chemical handles for modification of thiostrepton A have prevented its structure-activity relationships from being fully explored. Here, a fosmid-dependent biosynthetic engineering platform for thiostrepton A was developed and a series of thiostrepton analogs were successfully produced adapting this method. The newly generated thiostrepton variants were then interrogated for their water solubilities, antibacterial and proteasome inhibition properties. The information gathered from current studies will be used to refine thiostrepton's structure-activity relationship, providing

insight into the key features of its scaffold that impart specificity toward each biological target.

1.8 References

1. Gammon, K., Drug discovery: Leaving no stone unturned. *Nature* **2014,** *509*, S10-S12.

2. Arnison, P. G.; Bibb, M. J.; Bierbaum, G.; Bowers, A. A.; Bugni, T. S.; Bulaj, G.; Camarero, J. A.; Campopiano, D. J.; Challis, G. L.; Clardy, J.; Cotter, P. D.; Craik, D. J.; Dawson, M.; Dittmann, E.; Donadio, S.; Dorrestein, P. C.; Entian, K. D.; Fischbach, M. A.; Garavelli, J. S.; Goransson, U.; Gruber, C. W.; Haft, D. H.; Hemscheidt, T. K.; Hertweck, C.; Hill, C.; Horswill, A. R.; Jaspars, M.; Kelly, W. L.; Klinman, J. P.; Kuipers, O. P.; Link, A. J.; Liu, W.; Marahiel, M. A.; Mitchell, D. A.; Moll, G. N.; Moore, B. S.; Muller, R.; Nair, S. K.; Nes, I. F.; Norris, G. E.; Olivera, B. M.; Onaka, H.; Patchett, M. L.; Piel, J.; Reaney, M. J.; Rebuffat, S.; Ross, R. P.; Sahl, H. G.; Schmidt, E. W.; Selsted, M. E.; Severinov, K.; Shen, B.; Sivonen, K.; Smith, L.; Stein, T.; Sussmuth, R. D.; Tagg, J. R.; Tang, G. L.; Truman, A. W.; Vederas, J. C.; Walsh, C. T.; Walton, J. D.; Wenzel, S. C.; Willey, J. M.; van der Donk, W. A., Ribosomally synthesized and post-translationally modified peptide natural products: overview and recommendations for a universal nomenclature. *Nat. Prod. Rep.* **2013,** *30*, 108-160.

3. Biskupiak, J. E.; Meyers, E.; Gillum, A. M.; Dean, L.; Trejo, W. H.; Kirsch, D. R., Neoberninamycin, a new antibiotic produced by *Micrococcus luteus*. *J. Antibiot.* **1988,** *41*, 684-687.

4. Mukai, A.; Fukai, T.; Hoshino, Y.; Yazawa, K.; Harada, K.; Mikami, Y., Nocardithiocin, a novel thiopeptide antibiotic, produced by pathogenic *Nocardia pseudobrasiliensis* IFM 0757. *J. Antibiot.* **2009,** *62*, 613-619.

5. Nagai, K.; Kamigiri, K.; Arao, N.; Suzumura, K.; Kawano, Y.; Yamaoka, M.; Zhang, H.; Watanabe, M.; Suzuki, K., YM-266183 and YM-266184, novel thiopeptide antibiotics produced by *Bacillus cereus* isolated from a marine sponge. I. Taxonomy, fermentation, isolation, physico-chemical properties and biological properties. *J. Antibiot.* **2003,** *56*, 123-128.

6. Shoji, J.; Hinoo, H.; Wakisaka, Y.; Koizumi, K.; Mayama, M., Isolation of three new antibiotics, thiocillins I, II and III, related to micrococcin P. Studies on antibiotics from the genus *Bacillus*. VIII. *J. Antibiot.* **1976,** *29*, 366-374.

7. Trejo, W. H.; Dean, L. D.; Pluscec, J.; Meyers, E.; Brown, W. E., *Streptomyces laurentii*, a new species producing thiostrepton. *J. Antibiot.* **1977,** *30*, 639-643.

8. Bagley, M. C.; Dale, J. W.; Merritt, E. A.; Xiong, X., Thiopeptide antibiotics. *Chem. Rev.* **2005,** *105*, 685-714.

9. Zhang, Q.; Liu, W., Biosynthesis of thiopeptide antibiotics and their pathway engineering. *Nat. Prod. Rep.* **2013,** *30*, 218-226.

10. Hensens, O. D.; Albers-Schönberg, G., Total structure of the peptide antibiotic components of thiopeptin by ^{1}H and ^{13}C NMR spectroscopy. *Tetrahedron Lett.* **1978,** *19*, 3649-3652.

11. Puar, M. S.; Chan, T. M.; Hegde, V.; Patel, M.; Bartner, P.; Ng, K. J.; Pramanik, B. N.; MacFarlane, R. D., Sch 40832: a novel thiostrepton from *Micromonospora carbonacea*. *J. Antibiot.* **1998,** *51*, 221-224.

12. Newman, D. J.; Cragg, G. M., Natural products as sources of new drugs over the last 25 years. *J. Nat. Prod.* **2007,** *70*, 461-477.

13. Bausch, S. L.; Poliakova, E.; Draper, D. E., Interactions of the N-terminal domain of ribosomal protein L11 with thiostrepton and rRNA. *J. Biol. Chem.* **2005,** *280*, 29956-29963.

14. Harms, J. M.; Wilson, D. N.; Schluenzen, F.; Connell, S. R.; Stachelhaus, T.; Zaborowska, Z.; Spahn, C. M.; Fucini, P., Translational regulation via L11: Molecular switches on the ribosome turned on and off by thiostrepton and micrococcin. *Mol. Cell.* **2008,** *30*, 26-38.

15. Lentzen, G.; Klinck, R.; Matassova, N.; Aboul-ela, F.; Murchie, A. I. H., Structural basis for contrasting activities of ribosome binding thiazole antibiotics. *Chem. Biol.* **2003,** *10*, 769-778.

16. Porse, B. T.; Leviev, I.; Mankin, A. S.; Garrett, R. A., The antibiotic thiostrepton inhibits a functional transition within protein L11 at the ribosomal GTPase centre. *J. Mol. Biol.* **1998,** *276*, 391-404.

17. Egebjerg, J.; Douthwaite, S.; Garrett, R. A., Antibiotic interactions at the GTPase-associated centre within *Escherichia coli* 23S rRNA. *EMBO J.* **1989,** *8*, 607-611.

18. Thompson, J.; Cundliffe, E.; Stark, M., Binding of thiostrepton to a complex of 23-S rRNA with ribosomal protein L11. *Eur. J. Biochem.* **1979,** *98*, 261-265.

19. Cameron, D. M.; Thompson, J.; March, P. E.; Dahlberg, A. E., Initiation factor IF2, thiostrepton and micrococcin prevent the binding of elongation factor G to the *Escherichia coli* ribosome. *J. Mol. Biol.* **2002,** *319*, 27-35.

20. Modolell, J.; Cabrer, B.; Parmeggiani, A.; Vazquez, D., Inhibition by siomycin and thiostrepton of both aminoacyl-tRNA and factor G binding to ribosomes. *Proc. Natl. Acad. Sci. U.S.A.* **1971,** *68*, 1796-1800.

21. Heffron, S. E.; Jurnak, F., Structure of an EF-Tu complex with a thiazolyl peptide antibiotic determined at 2.35 Å resolution: atomic basis for GE2270A inhibition of EF-Tu. *Biochemistry* **2000,** *39*, 37-45.

22. Parmeggiani, A.; Krab, I. M.; Okamura, S.; Nielsen, R. C.; Nyborg, J.; Nissen, P., Structural basis of the action of pulvomycin and GE2270 A on elongation factor Tu. *Biochemistry* **2006,** *45*, 6846-6857.

23. Clough, B.; Strath, M.; Preiser, P.; Denny, P.; Wilson, I. R., Thiostrepton binds to malarial plastid rRNA. *FEBS Lett.* **1997,** *406*, 123-125.

24. McConkey, G. A.; Rogers, M. J.; McCutchan, T. F., Inhibition of *Plasmodium falciparum* protein synthesis. Targeting the plastid-like organelle with thiostrepton. *J. Biol. Chem.* **1997,** *272*, 2046-2049.

25. Rogers, M. J.; Cundliffe, E.; McCutchan, T. F., The antibiotic micrococcin is a potent inhibitor of growth and protein synthesis in the malaria parasite. *Antimicrob. Agents Chemother.* **1998,** *42*, 715-716.

26. Clough, B.; Rangachari, K.; Strath, M.; Preiser, P. R.; Wilson, R. J. M., Antibiotic inhibitors of organellar protein synthesis in *Plasmodium falciparum*. *Protist* **1999,** *150*, 189-195.

27. Aminake, M. N.; Schoof, S.; Sologub, L.; Leubner, M.; Kirschner, M.; Arndt, H.-D.; Pradel, G., Thiostrepton and derivatives exhibit antimalarial and gametocytocidal activity by dually targeting parasite proteasome and apicoplast. *Antimicrob. Agents Chemother.* **2011,** *55*, 1338-1348.

28. Jonker, H. R. A.; Baumann, S.; Wolf, A.; Schoof, S.; Hiller, F.; Schulte, K. W.; Kirschner, K. N.; Schwalbe, H.; Arndt, H.-D., NMR structures of thiostrepton derivatives for characterization of the ribosomal binding site. *Angew. Chem. Int. Ed. Engl.* **2011,** *50*, 3308-3312.

29. Bhat, U. G.; Halasi, M.; Gartel, A. L., Thiazole antibiotics target FoxM1 and induce apoptosis in human cancer cells. *PLoS One* **2009,** *4*, e5592.

30. Pandit, B.; Bhat, U. G.; Gartel, A. L., Proteasome inhibitory activity of thiazole antibiotics. *Cancer Biol. Ther.* **2011,** *11*, 43-47.

31. Hegde, N. S.; Sanders, D. A.; Rodriguez, R.; Balasubramanian, S., The transcription factor FOXM1 is a cellular target of the natural product thiostrepton. *Nat. Chem.* **2011,** *3*, 725-731.

32. Kelly, W. L.; Pan, L.; Li, C., Thiostrepton biosynthesis: Prototype for a new family of bacteriocins. *J. Am. Chem. Soc.* **2009,** *131*, 4327-4334.

33. Wieland Brown, L. C.; Acker, M. G.; Clardy, J.; Walsh, C. T.; Fischbach, M. A., Thirteen posttranslational modifications convert a 14-residue peptide into the antibiotic thiocillin. *Proc. Natl. Acad. Sci. U. S. A.* **2009,** *106*, 2549-2553.

34. Liao, R.; Duan, L.; Lei, C.; Pan, H.; Ding, Y.; Zhang, Q.; Chen, D.; Shen, B.; Yu, Y.; Liu, W., Thiopeptide biosynthesis featuring ribosomally synthesized precursor peptides and conserved posttranslational modifications. *Chem. Biol.* **2009,** *16*, 141-147.

35. Morris, R. P.; Leeds, J. A.; Naegeli, H. U.; Oberer, L.; Memmert, K.; Weber, E.; LaMarche, M. J.; Parker, C. N.; Burrer, N.; Esterow, S.; Hein, A. E.; Schmitt, E. K.; Krastel, P., Ribosomally synthesized thiopeptide antibiotics targeting elongation factor Tu. *J. Am. Chem. Soc.* **2009,** *131*, 5946-5955.

36. Yu, Y.; Duan, L.; Zhang, Q.; Liao, R.; Ding, Y.; Pan, H.; Wendt-Pienkowski, E.; Tang, G.; Shen, B.; Liu, W., Nosiheptide biosynthesis featuring a unique indole side ring formation on the characteristic thiopeptide framework. *ACS Chem. Biol.* **2009,** *4*, 855-864.

37. Engelhardt, K.; Degnes, K. F.; Zotchev, S. B., Isolation and characterization of the gene cluster for biosynthesis of the thiopeptide antibiotic TP-1161. *Appl. Environ. Microbiol.* **2010,** *76*, 7093-7101.

38. Young, T. S.; Walsh, C. T., Identification of the thiazolyl peptide GE37468 gene cluster from *Streptomyces* ATCC 55365 and heterologous expression in *Streptomyces lividans*. *Proc. Natl. Acad. Sci. U. S. A.* **2011,** *108*, 13053-13058.

39. Ding, Y.; Yu, Y.; Pan, H.; Guo, H.; Li, Y.; Liu, W., Moving posttranslational modifications forward to biosynthesize the glycosylated thiopeptide nocathiacin I in *Nocardia sp.* ATCC202099. *Mol. Biosyst.* **2010,** *6*, 1180-1185.

40. Wang, J.; Yu, Y.; Tang, K.; Liu, W.; He, X.; Huang, X.; Deng, Z., Identification and analysis of the biosynthetic gene cluster encoding the thiopeptide antibiotic

cyclothiazomycin in *Streptomyces hygroscopicus* 10-22. *Appl. Environ. Microbiol.* **2010,** *76*, 2335-2344.

41. Malcolmson, S. J.; Young, T. S.; Ruby, J. G.; Skewes-Cox, P.; Walsh, C. T., The posttranslational modification cascade to the thiopeptide berninamycin generates linear forms and altered macrocyclic scaffolds. *Proc. Natl. Acad. Sci. U.S.A.* **2013,** *110*, 8483-8488.

42. Hayashi, S.; Ozaki, T.; Asamizu, S.; Ikeda, H.; Omura, S.; Oku, N.; Igarashi, Y.; Tomoda, H.; Onaka, H., Genome mining reveals a minimum gene set for the biosynthesis of 32-membered macrocyclic thiopeptides lactazoles. *Chem. Biol.* **2014,** *21*, 679-688.

43. Chatterjee, C.; Paul, M.; Xie, L.; van der Donk, W. A., Biosynthesis and mode of action of lantibiotics. *Chem. Rev.* **2005,** *105*, 633-683.

44. Chatterjee, C.; Miller, L. M.; Leung, Y. L.; Xie, L.; Yi, M.; Kelleher, N. L.; van der Donk, W. A., Lacticin 481 synthetase phosphorylates its substrate during lantibiotic production. *J. Am. Chem. Soc.* **2005,** *127*, 15332-15333.

45. Müller, W. M.; Schmiederer, T.; Ensle, P.; Süssmuth, R. D., In Vitro bosynthesis of the prepeptide of type-III lantibiotic labyrinthopeptin A2 including formation of a C-C Bond as a post-translational modification. *Angew. Chem. Int. Ed. Engl.* **2010,** *49*, 2436-2440.

46. Goto, Y.; Okesli, A.; van der Donk, W. A., Mechanistic studies of Ser/Thr dehydration catalyzed by a member of the LanL lanthionine synthetase family. *Biochemistry* **2011,** *50*, 891-898.

47. Garg, N.; Salazar-Ocampo, L. M.; van der Donk, W. A., In vitro activity of the nisin dehydratase NisB. *Proc. Natl. Acad. Sci. U.S.A.* **2013,** *110*, 7258-7263.

48. Li, Y.-M.; Milne, J. C.; Madison, L. L.; Kolter, R.; Walsh, C. T., From peptide precursors to oxazole and thiazole-containing peptide antibiotics: Microcin B17 synthase. *Science* **1996,** *274*, 1188-1193.

49. Koehnke, J.; Bent, A. F.; Zollman, D.; Smith, K.; Houssen, W. E.; Zhu, X.; Mann, G.; Lebl, T.; Scharff, R.; Shirran, S.; Botting, C. H.; Jaspars, M.; Schwarz-Linek, U.; Naismith, J. H., The cyanobactin heterocyclase enzyme: A processive adenylase that operates with a defined order of reaction. *Angew. Chem. Int. Ed. Engl.* **2013,** *52*, 13991-13996.

50. Dunbar, K. L.; Melby, J. O.; Mitchell, D. A., YcaO domains use ATP to activate amide backbones during peptide cyclodehydrations. *Nat. Chem. Biol.* **2012,** *8*, 569-575.

51. Bycroft, B. W.; Gowland, M. S., The structures of the highly modified peptide antibiotics micrococcin P1 and P2. *J. Chem. Soc., Chem. Commun.* **1978**, 256-258.

52. Frank, R. A. W.; Leeper, F. J.; Luisi, B. F., Structure, mechanism and catalytic duality of thiamine-dependent enzymes. *Cell. Mol. Life Sci.* **2007,** *64*, 892-905.

53. Bowers, A. A.; Acker, M. G.; Koglin, A.; Walsh, C. T., Manipulation of thiocillin variants by prepeptide gene replacement: Structure, conformation, and activity of heterocycle substitution mutants. *J. Am. Chem. Soc.* **2010,** *132*, 7519-7527.

54. Dutcher, J. D.; Vandeputte, J., Thiostrepton, a new antibiotic. II. Isolation and chemical characterization. *Antibiot. Annu.* **1955,** *3*, 560-561.

55. Anderson, B.; Hodgkin, D. C.; Viswamitra, M. A., The structure of thiostrepton. *Nature* **1970,** *225*, 233-235.

56. Mocek, U.; Beale, J. M.; Floss, H. G., Reexamination of the ^{1}H and ^{13}C NMR spectral assignments of thiostrepton. *J. Antibiot.* **1989,** *42*, 1649-1652.

57. Mocek, U.; Zeng, Z.; O'Hagan, D.; Zhou, P.; Fan, L. D. G.; Beale, J. M.; Floss, H. G., Biosynthesis of the modified peptide antibiotic thiostrepton in *Streptomyces azureus* and *Streptomyces laurentii*. *J. Am. Chem. Soc.* **1993,** *115*, 7992-8001.

58. Frenzel, T.; Zhou, P.; Floss, H. G., Formation of 2-methyltryptophan in the biosynthesis of thiostrepton: isolation of *S*-adenosylmethionine:tryptophan 2-methyltransferase. *Arch. Biochem. Biophys.* **1990,** *278*, 35-40.

59. Zhou, P.; O'Hagan, D.; Mocek, U.; Zeng, Z.; Yuen, L. D.; Frenzel, T.; Unkefer, C. J.; Beale, J. M.; Floss, H. G., Biosynthesis of the antibiotic thiostrepton. Methylation of tryptophan in the formation of the quinaldic acid moiety by transfer of the methionine methyl group with net retention of configuration. *J. Am. Chem. Soc.* **1989,** *111*, 7274-7276.

60. Pierre, S.; Guillot, A.; Benjdia, A.; Sandström, C.; Langella, P.; Berteau, O., Thiostrepton tryptophan methyltransferase expands the chemistry of radical SAM enzymes. *Nat. Chem. Biol.* **2012,** *8*, 957-959.

61. Duan, L.; Wang, S.; Liao, R.; Liu, W., Insights into quinaldic acid moiety formation in thiostrepton biosynthesis facilitating fluorinated thiopeptide generation. *Chem. Biol.* **2012,** *19*, 443-448.

62. Smith, T. M.; Priestley, N. D.; Knaggs, A. R.; Nguyen, T.; Floss, H. G., 3,4-Dimethylindole-2-carboxylate and 4-(1-hydroxyethyl)quinoline-2-carboxylate activating

enzymes from the nosiheptide and thiostrepton producers, *Streptomyces actuosus* and *Streptomyces laurentii*. *J. Chem. Soc., Chem. Comm.* **1993**, 1612-1614.

63. Hughes, R. A.; Thompson, S. P.; Alcaraz, L.; Moody, C. J., Total synthesis of the thiopeptide antibiotic amythiamicin D. *J. Am. Chem. Soc.* **2005,** *127*, 15644-15651.

64. Nicolaou, K. C.; Dethe, D. H.; Leung, G. Y.; Zou, B.; Chen, D. Y., Total synthesis of thiopeptide antibiotics GE2270A, GE2270T, and GE2270C1. *Chem. Asian. J.* **2008,** *3*, 413-429.

65. Nicolaou, K. C.; Safina, B. S.; Zak, M.; Lee, S. H.; Nevalainen, M.; Bella, M.; Estrada, A. A.; Funke, C.; Zecri, F. J.; Bulat, S., Total synthesis of thiostrepton. Retrosynthetic analysis and construction of key building blocks. *J. Am. Chem. Soc.* **2005,** *127*, 11159-11175.

66. Schoof, S.; Baumann, S.; Ellinger, B.; Arndt, H.-D., A fluorescent probe for the 70S-ribosomal GTPase-associated center. *ChemBioChem* **2009,** *10*, 242-245.

67. Schoof, S.; Arndt, H. D., D-cysteine occurrence in thiostrepton may not necessitate an epimerase. *Chem. Commun.* **2009**, 7113-7115.

68. Schoof, S.; Pradel, G.; Aminake, M. N.; Ellinger, B.; Baumann, S.; Potowski, M.; Najajreh, Y.; Kirschner, M.; Arndt, H.-D., Antiplasmodial thiostrepton derivatives: Proteasome inhibitors with a dual mode of action. *Angew. Chem. Int. Ed. Engl.* **2010,** *49*, 3317-3321.

69. Baumann, S.; Schoof, S.; Bolten, M.; Haering, C.; Takagi, M.; Shin-ya, K.; Arndt, H.-D., Molecular determinants of microbial resistance to thiopeptide antibiotics. *J. Am. Chem. Soc.* **2010,** *132*, 6973-6981.

70. Naidu, B. N.; Sorenson, M. E.; Zhang, Y.; Kim, O. K.; Matiskella, J. D.; Wichtowski, J. A.; Connolly, T. P.; Li, W.; Lam, K. S.; Bronson, J. J.; Pucci, M. J.; Clark, J. M.; Ueda, Y., Nocathiacin I analogues: synthesis, in vitro and in vivo biological activity of novel semi-synthetic thiazolyl peptide antibiotics. *Bioorg. Med. Chem. Lett.* **2004,** *14*, 5573-5577.

71. Naidu, B. N.; Sorenson, M. E.; Matiskella, J. D.; Li, W.; Sausker, J. B.; Zhang, Y.; Connolly, T. P.; Lam, K. S.; Bronson, J. J.; Pucci, M. J.; Yang, H.; Ueda, Y., Synthesis and antibacterial activity of nocathiacin I analogues. *Bioorg. Med. Chem. Lett.* **2006,** *16*, 3545-3549.

72. Xu, L.; Farthing, A. K.; Dropinski, J. F.; Meinke, P. T.; McCallum, C.; Leavitt, P. S.; Hickey, E. J.; Colwell, L.; Barrett, J.; Liu, K., Nocathiacin analogs: Synthesis and

antibacterial activity of novel water-soluble amides. *Bioorg. Med. Chem. Lett.* **2009,** *19*, 3531-3535.

73. LaMarche, M. J.; Leeds, J. A.; Amaral, A.; Brewer, J. T.; Bushell, S. M.; Deng, G.; Dewhurst, J. M.; Ding, J.; Dzink-Fox, J.; Gamber, G.; Jain, A.; Lee, K.; Lee, L.; Lister, T.; McKenney, D.; Mullin, S.; Osborne, C.; Palestrant, D.; Patane, M. A.; Rann, E. M.; Sachdeva, M.; Shao, J.; Tiamfook, S.; Trzasko, A.; Whitehead, L.; Yifru, A.; Yu, D.; Yan, W.; Zhu, Q., Discovery of LFF571: an investigational agent for *Clostridium difficile* infection. *J. Med. Chem.* **2012,** *55*, 2376-2387.

74. Xu, L.; Farthing, A. K.; Dropinski, J. F.; Meinke, P. T.; McCallum, C.; Hickey, E.; Liu, K., Synthesis and antibacterial activity of novel water-soluble nocathiacin analogs. *Bioorg. Med. Chem. Lett.* **2013,** *23*, 366-369.

75. Acker, M. G.; Bowers, A. A.; Walsh, C. T., Generation of thiocillin variants by prepeptide gene replacement and *in vivo* processing by *Bacillus cereus*. *J. Am. Chem. Soc.* **2009,** *131*, 17563-17565.

76. Li, C.; Zhang, F.; Kelly, W. L., Mutagenesis of the thiostrepton precursor peptide at Thr7 impacts both biosynthesis and function. *Chem. Commun.* **2012,** *48*, 558-560.

77. Li, C.; Zhang, F.; Kelly, W. L., Heterologous production of thiostrepton A and biosynthetic engineering of thiostrepton analogs. *Mol. BioSyst.* **2011,** *7*, 82-90.

78. Bowers, A. A.; Acker, M. G.; Young, T. S.; Walsh, C. T., Generation of thiocillin ring size variants by prepeptide gene replacement and in vivo processing by *Bacillus cereus*. *J. Am. Chem. Soc.* **2012,** *134*, 10313-10316.

79. Young, T. S.; Dorrestein, P. C.; Walsh, C. T., Codon randomization for rapid exploration of chemical space in thiopeptide antibiotic variants. *Chem. Biol.* **2012,** *19*, 1600-1610.

80. Su, T. L., Micrococcin, an antibacterial substance formed by a strain of *Micrococcus*. *Br. J. Exp. Pathol.* **1948,** *29*, 473-481.

81. Fuller, A. T., A new antibiotic of bacterial origin. *Nature* **1955,** *175*, 722.

82. Carnio, M. C.; Holtzel, A.; Rudolf, M.; Henle, T.; Jung, G.; Scherer, S., The macrocyclic peptide antibiotic micrococcin P_1 is secreted by the food-borne bacterium *Staphylococcus equorum* WS 2733 and inhibits *Listeria monocytogenes* on soft cheese. *Appl. Environ. Microbiol.* **2000,** *66*, 2378-2384.

83. Benazet, F.; Cartier, J. R., Effect of nosiheptide as a feed additive in chicks on the quantity, duration, prevalence of excretion, and resistance to antibacterial agents of Salmonella typhimurium; on the proportion of *Escherichia coli* and other coliforms resistant to antibacterial agents; and on their degree and spectrum of resistance. *Poult Sci* **1980,** *59*, 1405-1415.

84. Casteels, M.; Bekaert, H.; Buysse, F. X., Zootechnical evaluation of a new antibiotic, nosiheptide, using swine. *Rev. Agric. (Brussels)* **1980,** *33*, 1069-1078.

85. Prange, T.; Ducruix, A.; Pascard, C.; Lunel, J., Structure of nosiheptide, a polythiazole-containing antibiotic. *Nature* **1977,** *265*, 189-190.

86. Yu, Y.; Guo, H.; Zhang, Q.; Duan, L.; Ding, Y.; Liao, R.; Lei, C.; Shen, B.; Liu, W., NosA catalyzing carboxyl-terminal amide formation in nosiheptide maturation via an enamine dealkylation on the serine-extended precursor peptide. *J. Am. Chem. Soc.* **2010,** *132*, 16324-16326.

87. Zhang, Q.; Li, Y.; Chen, D.; Yu, Y.; Duan, L.; Shen, B.; Liu, W., Radical-mediated enzymatic carbon chain fragmentation-recombination. *Nat. Chem. Biol.* **2011,** *7*, 154-160.

88. Liao, R.; Liu, W., Thiostrepton maturation involving a deesterification-amidation way to process the C-terminally methylated peptide backbone. *J. Am. Chem. Soc.* **2011,** *133*, 2852-2855.

CHAPTER 2: HETEROLOGOUS EXPRESSION OF THIOSTREPTON A

From the publication:

Li, C.*; Zhang, F.*; Kelly, W. L. Heterologous production of thiostrepton A and biosynthetic engineering of thiostrepton analogs. *Mol. BioSyst.* **2011,** *7,* 82-90. (*Authors contributed equally to this work)

2.1 Introduction

Thiostrepton A is one of the more extensively studied members of the thiopeptide antibiotics.[1] The proposed thiostrepton biosynthetic gene (*tsr*) cluster is nearly 30 kb in length, containing 21 open reading frames.[2-3] TsrA encodes the precursor peptide which is composed of a leader peptide and a core peptide.[2] Considerably more genetic and biochemical studies are required to uncover the details concerning the transformation of the precursor peptide into thiostrepton A, a process requiring over one dozen chemical modifications. Although gene inactivation can be performed in the thiostrepton producer *Streptomyces laurentii* ATCC 31255 (*S. laurentii*), this strain has been recalcitrant to further manipulation of the thiostrepton biosynthetic locus, including attempts to replace the gene encoding the precursor peptide with one encoding an alternate amino acid sequence.[2, 4] One strategy to circumvent this limitation of *S. laurentii* is to heterologously express the entire *tsr* cluster in a more genetically tractable host bacterium. Such an approach may permit the multiple genetic manipulations that would be necessary to engineer the production of thiostrepton analogs. In this chapter, the heterologous production of thiostrepton A by two *Streptomyces* host strains is discussed.

2.2 Materials and Methods

2.2.1 General

Unless specified, common chemicals, solvents, enzymes and other materials were purchased from standard commercial sources and used as provided. The QIAprep Spin Miniprep Kit (Qiagen, Valencia, CA) was used for the isolation of plasmids and fosmids from *E. coli* strains. *Streptomyces* genomic DNA was isolated using the Wizard® Genomic DNA Purification Kit (Promega, Madison, WI) according to the manufacturer's recommendations. High performance liquid chromatography (HPLC) analysis was performed on a Beckman Coulter System Gold instrument. HPLC-MS was performed at the Georgia Institute of Technology Bioanalytical Mass Spectrometry Facility with a Phenomenex Syngeri RP column (250 mm × 2 mm, 4 μm) (Torrance, CA) and developed with 20% solvent B in solvent A for 8 min followed by a gradient from 20-100% solvent B over 35 min (solvent A: 5% acetonitrile and 0.1% formic acid; solvent B: 95% acetonitrile and 0.1% formic acid) at 0.25 mL/min.

2.2.2 Bacterial strains, plasmids and growth medium

Streptomyces laurentii ATCC 31255 (*S. laurentii*) and *Streptomyces actuosus* ATCC 25421 (*S. actuosus*) were obtained from American Type Culture Collection (ATCC). All strains and plasmids are listed in Table A.1, and primers are listed in Table A.2. All *Escherichia coli* (*E. coli*) strains were grown in Luria-Bertani liquid or solid medium with the appropriate antibiotic(s). For the selective growth of *E. coli* or *Streptomyces*, the following antibiotics and concentrations were used: kanamycin (50 μg/mL), apramycin (50 μg/mL), ampicillin (100 μg/mL), nalidixic acid (25 μg/mL), and chloramphenicol (30 μg/mL). R2YE solid medium was used for the growth and

sporulation of *S. lividans* and *S. actuosus*, and for the protoplast transformation of *S. lividans*.[5] MS agar was used for the intergeneric conjugation of all *Streptomyces* strains.[6]

2.2.3 Fosmid engineering

Fosmids pCC1FOS and JA3A10 were retrofitted for integration into the chromosome of various *Streptomyces* hosts by employing λ Red-mediated recombination.[6-7] First, a 4.4 kb fragment containing *aac(3)IV, int, attP* and *oriT* was amplified from pSET152 by polymerase chain reaction (PCR) using the primers CTSR1-F and CTSR1-R. Next, the resulting PCR product was used to replace the chloramphenicol resistance gene (chl^R) located on the fosmid backbone, generating the fosmids int-3A10 and int-pCC1FOS. The allelic replacements in the resulting fosmids were confirmed by PCR and by sequence analysis of the amplified products.

2.2.4 Heterologous production of thiostrepton

As an initial step for *S. lividans* only, pSE34 was introduced by protoplast transformation following established protocol.[5] Each fosmid (int-3A10 or int-pCC1FOS) was introduced by intergeneric conjugation into *S. lividans* and *S. actuosus*, providing the strains *S. lividans* FZ1, *S. lividans* FZ2, *S. actuosus* FZ1 and *S. actuosus* FZ2. The presence of int-3A10 in *S. lividans* FZ1 and *S. actuosus* FZ1 was confirmed by PCR amplification of *tsrK*, *tsrN*, and *tsrV*, and by sequence analysis of the amplified products.

2.4.5 Evaluation of thiostrepton A production in *Streptomyces*

The fermentation of *S. actuosus* was carried out in a three-step process. Briefly, 50 mL of tryptic soy broth (TSB) was inoculated with 50 µL of *S. actuosus* mycelium glycerolic stock and grown at 28 °C and 220 rpm for 7 days in a 250-mL Erlenmeyer

flask. Next, 500 µL of the *S. actuosus* preculture was inoculated to 50 mL seed medium (30.0 g/L glucose, 0.234 g/L $MgSO_4$, 20.0 g/L soytone, 20.0 g/L corn steep liquor, 3.0 g/L $(NH_4)_2SO_4$, and 5.0 g/L $CaCO_3$, pH 6.8)[8] in a 250-mL Erlenmeyer flask. After 96 h of incubation at 28 °C and 220 rpm, 1 mL of the seed culture was inoculated to 100 mL fermentation medium (5.0 g/L L-glutamate, 1.0 g/L L-arginine, 1.0 g/L L-aspartate, 0.29 g/L K_2HPO_4, 0.469 g/L $MgSO_4$, 2.0 g/L Na_2SO_4, 0.01 g/L $ZnSO_4 \cdot 7\ H_2O$, 0.02 g/L $FeSO_4 \cdot 7H_2O$, 3.0 g/L $CaCO_3$, and 40.0 g/L glucose, pH 7.25)[8] in a 500-mL Erlenmeyer flask. The fermentation culture was incubated at 28 °C and 220 rpm for 7 days.

The fermentation of *S. lividans* was carried out in a three-step process. First, 50 mL of tryptic soy broth in a 250-mL Erlenmeyer flask was inoculated with 50 µL of *S. lividans* mycelium glycerolic stock and grown at 28 °C and 220 rpm for 48 h. Next, 0.5 mL of the *S. lividans* preculture was used to inoculate 50 mL of seed medium (50 g/L glucose, 15 g/L soybean flour, 15 g/L soluble starch, pH 7.2)[9] in a 250-mL Erlenmeyer flask. After 7 days at 28 °C and 220 rpm, 1 mL of this seed culture was then used to inoculate 100 mL of fermentation medium (5.0 g/L L-glutamate, 1.0 g/L L-arginine, 1.0 g/L L-aspartate, 0.29 g/L K_2HPO_4, 0.469 g/L $MgSO_4$, 2.0 g/L Na_2SO_4, 0.01 g/L $ZnSO_4 \cdot 7\ H_2O$, 0.02 g/L $FeSO_4 \cdot 7H_2O$, 3.0 g/L $CaCO_3$, and 40.0 g/L glucose, pH 7.25) in a 500-mL Erlenmeyer flask.[8] The resulting culture was incubated at 28 °C and 220 rpm for 7 days. *S. coelicolor* strains were cultivated following the same conditions used for *S. lividans* and *S. actuosus*. To harvest thiostrepton A, the whole culture was extracted twice with an equal volume of chloroform. The chloroform layers were pooled together and solvent removed *in vacuo*. The solid residue was dissolved in 2 mL of chloroform. Samples were analyzed by HPLC with a Phenomenex Luna C18(2) column (250 × 4.6 mm, 5 µm). The

column was developed using a gradient of 0-100% acetonitrile in water over 30 min at a flow rate of 1 mL/min. Absorbance was monitored at 254 nm. Under these conditions, thiostrepton elutes with a t_R of about 22 min. Under the conditions used for HPLC-MS, thiostrepton A elutes at a t_R of about 28 min providing ions at *m*/*z* 1664.4 $[M+H]^+$ and 832.9 $[M+2H]^{2+}$. The predominant ion for thiostrepton A was $[M+2H]^{2+}$, whereas $[M+H]^+$ was only a minor species.

2.3 Results and Discussion

An *S. laurentii* genomic fosmid library was previously constructed using the vector pCC1FOS, and it was determined that fosmid JA3A10 possessed the entire proposed *tsr* cluster.[2] Using λ Red-mediated recombination, the fosmid was retrofitted with the elements necessary to support the intergeneric transfer from *E. coli* into a *Streptomyces* species and the integration into a *Streptomyces* chromosome.[6-7, 10-11] The chloramphenicol resistance-imparting gene of the fosmid backbone was replaced with a cassette from pSET152 containing an integrase (*int*), an *attP* sequence, an origin of transfer (*oriT*), and an apramycin-resistance gene (*aac(3)IV*) to yield int-3A10 (Figure 2.1).[12] A control fosmid was also prepared in this fashion from pCC1FOS to provide int-pCC1FOS.

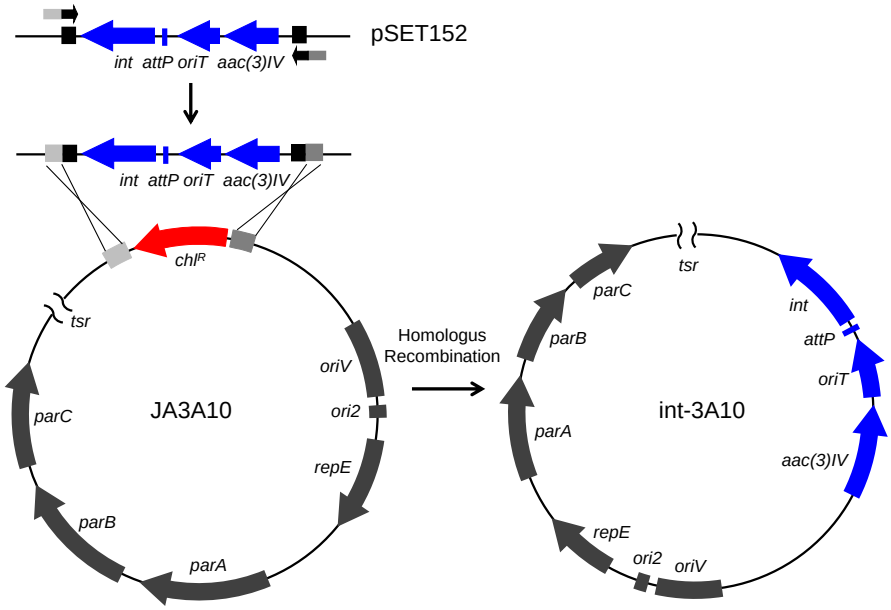

Figure 2.1. Construction of int-3A10. A fragment containing *aac(3)IV*, *int*, *attP*, and *oriT* was amplified from pSET152 and used to exchange the chloramphenicol resistance gene (*chl*^{R}) on JA3A10, yielding int-3A10. Location of the *tsr* cluster within the fosmid is indicated by "*tsr*."

The heterologous hosts chosen for this study were *Streptomyces lividans* TK24 (*S. lividans*) and *Streptomyces actuosus* ATCC 25421 (*S. actuosus*). Since the established resistance-imparting gene for thiostrepton A is not co-localized with the *tsr* cluster, it was necessary to take additional measures in *S. lividans* to avoid any toxicity that would result from thiostrepton A production.[2, 13] The vector pSE34, which harbors the rRNA methyltransferase imparting thiostrepton A resistance, was introduced into *S. lividans* to yield *S. lividans*/pSE34. *S. actuosus*, on the other hand, produces another thiopeptide, nosiheptide.[14] This strain is inherently cross-resistant to thiostrepton A, negating the need to introduce a gene specifically conferring thiostrepton A resistance.[15-16] The retrofitted fosmids were then introduced into *S. lividans*/pSE34 and *S. actuosus* by intergeneric conjugation to provide *S. lividans* FZ1 and *S. actuosus* FZ1 (strains containing int-3A10) and *S. lividans* FZ2 and *S. actuosus* FZ2 (strains containing int-pCC1FOS). The presence

of int-3A10 in *S. lividans* FZ1 and *S. actuosus* FZ1 was confirmed by PCR amplification of *tsrK*, *tsrN*, and *tsrV* (Figure 2.2),

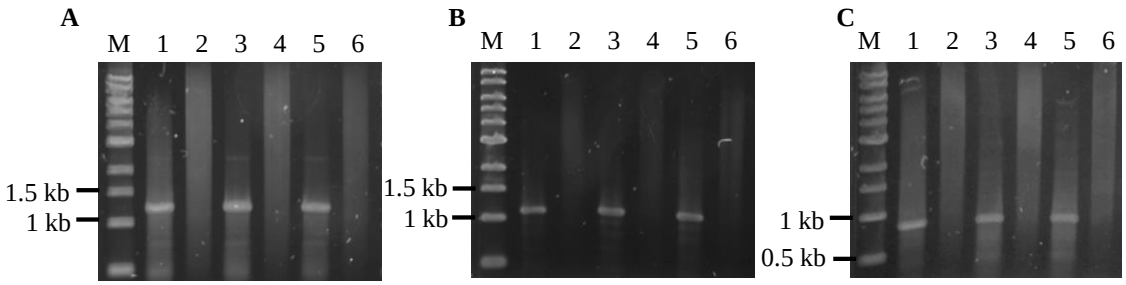

Figure 2.2. PCR analysis of *S. actuosus* FZ1 and *S. lividans* FZ1. (**A**) Amplification of *tsrK* using primers TSRK-F and TSRK-R. (**B**) Amplification of *tsrV* using primers TSRV-F and TSRV-R. (**C**) Amplification of *tsrN* using primers TSRN-F and TSRN-R. Lanes: (*M*) 1 kb ladder; (*1*) JA3A10; (*2*) pCC1FOS; (*3*) *S. actuosus* FZ1; (*4*) *S. actuosus* FZ2; (*5*) *S. lividans* FZ1; (*6*) *S. lividans* FZ2.

Analysis of the culture extracts by HPLC (Figure 2.3) and HPLC-MS (Figures B.1 and B.2) revealed that thiostrepton A was indeed produced in *S. actuosus* FZ1 and *S. lividans* FZ1. In contrast, none of the strains possessing int-pCC1FOS, which lacks the *tsr* cluster, produced thiostrepton A (Figure 2.3). Parallel with these studies, int-3A10 and int-pCC1FOS were introduced into *Streptomyces coelicolor* CH999 (*S. coelicolor*), but no thiostrepton A was detected in the culture extract from the *S. coelicolor* host strain (data not shown). The ability of int-3A10 to impart thiostrepton-production capabilities upon its heterologous host demonstrates that all essential genes for the biosynthesis of thiostrepton A are contained within the fosmid int-3A10. Unfortunately, the production of thiostrepton A in *S. lividans* FZ1 (0.2 mg/L) and *S. actuosus* 3A10 (1.0 mg/L) was significantly lower than the level of thiostrepton A production in *S. laurentii* (44 mg/L). A potential complication to the heterologous production of thiostrepton A and other thiopeptides is the presence of the thiostrepton-inducible proteins in various streptomycetes, including strains of *S. lividans* and *S. coelicolor*.[16-18]

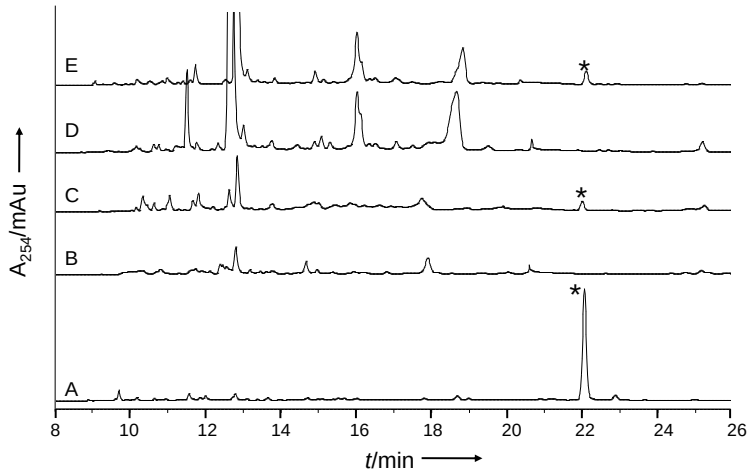

Figure 2.3. HPLC analysis of culture extracts from (**A**) wild-type *S. laurentii*, (**B**) *S. lividans* FZ2, (**C**) *S. lividans* FZ1, (**D**) *S. actuosus* FZ2, (**E**) *S. actuosus* FZ1. The asterisks indicate thiostrepton A. Absorbance was monitored at 254 nm.

The TipAS and TipAL proteins from *S. lividans* 66 have been characterized to some detail. In response to complexation with thiostrepton A, TipAL activates its own promoter, *ptipA,* and induces the expression of two alternate translation products from the *tipA* gene: TipAL (itself) and TipAS.[19] TipAS, the dominant thiostrepton-induced protein in *S. lividans* 66, forms an irreversible lanthionine adduct upon binding thiostrepton A, using a TipAS cysteine residue to attack a thiostrepton A dehydrolanine residue and sequester the thiopeptide.[20] Although this may explain one limitation to achieving high-yield production of thiostrepton A from non-cognate streptomycetes, it is unlikely to be the sole contributing factor. In addition to its interactions with TipAL and TipAS, thiostrepton A has been implicated in modulating the expression of other genes in actinomycetes.[17-19] Furthermore, it is not unusual to observe lower titers of a metabolite from a heterologous host versus that of the native producer, and optimization of the fermentation conditions may overcome low production of the metabolite.[21-22] For example, the production of epothilone D in *Myxococcus xanthus* was increased from less than 0.2 mg/L to 23 mg/L through a series of modifications to the culture conditions.[23] In

any event, the low titre of thiostrepton A production in *S. lividans* FZ1 and *S. actuosus* FZ1 restricts the utility of this integrative fosmid-based heterologous production platform to query the roles of the thiostrepton biosynthetic genes or to engineer thiostrepton derivatives. Genetic manipulations of the *tsr* cluster are apt to generate biosynthetic intermediates or analogs produced at lower levels relative to the wild-type biosynthetic system, and such metabolites may easily escape the limits of detection if using the heterologous hosts developed here.

2.4 Conclusions

Due to the difficulties in the genetic manipulation of *S. laurentii*, the heterologous production of thiostrepton A from an alternate streptomycete host was sought to facilitate the biosynthetic investigations of the peptide metabolite. We have been able to develop a methodology for the heterologous production of thiostrepton A in a *Streptomyces* host and the successful production of thiostrepton in the heterologous hosts demonstrates that all essential genes for the biosynthesis of the antibiotic are contained within the fosmid int-3A10. Unfortunately, the production of thiostrepton A in *S. lividans* FZ1 and *S. actuosus* 3A10 was low, which hinders further application of this platform to generate thiostrepton analogs. Therefore, rather than undergoing a complex and likely extensive effort in an attempt to improve thiostrepton production in either heterologous host, the same methodology toward the engineering of thiostrepton variants in the native thiostrepton-producing bacterium, *S. laurentii*, will be discussed in the next chapter.

2.5 References

1. Trejo, W. H.; Dean, L. D.; Pluscec, J.; Meyers, E.; Brown, W. E., *Streptomyces laurentii*, a new species producing thiostrepton. *J. Antibiot.* **1977,** *30*, 639-643.

2. Kelly, W. L.; Pan, L.; Li, C., Thiostrepton biosynthesis: Prototype for a new family of bacteriocins. *J. Am. Chem. Soc.* **2009,** *131*, 4327-4334.

3. Liao, R.; Duan, L.; Lei, C.; Pan, H.; Ding, Y.; Zhang, Q.; Chen, D.; Shen, B.; Yu, Y.; Liu, W., Thiopeptide biosynthesis featuring ribosomally synthesized precursor peptides and conserved posttranslational modifications. *Chem. Biol.* **2009,** *16*, 141-147.

4. Li, C.; Kelly, W. L., *Unpublished*.

5. Kieser, T.; Bibb, M. J.; Buttner, M. J.; Chater, K. F.; Hopwood, D. A., *Practical Streptomyces Genetics* The John Innes Foundation: Norwich, England, 2000.

6. Gust, B.; Challis, G. L.; Fowler, K.; Kieser, T.; Chater, K. F., PCR-targeted *Streptomyces* gene replacement identifies a protein domain needed for biosynthesis of the sesquiterpene soil odor geosmin. *Proc. Natl. Acad. Sci. U.S.A.* **2003,** *100*, 1541-1546.

7. Datsenko, K. A.; Wanner, B. L., One-step inactivation of chromosomal genes in *Escherichia coli* K-12 using PCR products. *Proc. Natl. Acad. Sci. U.S.A.* **2000,** *97*, 6640-6645.

8. Houck, D. R.; Chen, L.-C.; Keller, P. J.; Beale, J. M.; Floss, H. G., Biosynthesis of the modified peptide antibiotic nosiheptide in *Streptomyces actuosus*. *J. Am. Chem. Soc.* **1988,** *110*, 5800-5806.

9. Priestley, N. D.; Smith, T. M.; Shipley, P. R.; Floss, H. G., Studies on the biosynthesis of thiostrepton: 4-(1-hydroxyethyl)quinoline-2-carboxylate as a free intermediate on the pathway to the quinaldic acid moiety. *Bioorg. Med. Chem.* **1996,** *4*, 1135-1147.

10. Zhang, Y.; Buchholz, F.; Muyrers, J. P. P.; Stewart, A. F., A new logic for DNA engineering using recombination in *Escherichia coli*. *Nat. Genet.* **1998,** *20*, 123-128.

11. Zhang, Y.; Muyrers, J. P. P.; Testa, G.; Stewart, A. F., DNA cloning by homologous recombination in *Escherichia coli*. *Nat. Biotechnol.* **2000,** *18*, 1314-1317.

12. Bierman, M.; Logan, R.; O'Brien, K.; Seno, E. T.; Rao, R. N.; Schoner, B. E., Plasmid cloning vectors for the conjugal transfer of DNA from *Escherichia coli* to *Streptomyces spp*. *Gene* **1992,** *116*, 43-49.

13. Smith, T. M.; Jiang, Y. F.; Shipley, P.; Floss, H. G., The thiostrepton-resistance-encoding gene in *Streptomyces laurentii* is located within a cluster of ribosomal protein operons. *Gene* **1995,** *164*, 137-142.

14. Benazet, F.; Cartier, M.; Florent, J.; Godard, C.; Jung, G.; Lunel, J.; Mancy, D.; Pascal, C.; Renaut, J.; Tarridec, P.; Theilleux, J.; Tissier, R.; Dubost, M.; Ninet, L., Nosiheptide, a sulfur-containing peptide antibiotic isolated from *Streptomyces actuosus* 40037. *Experientia* **1980,** *36*, 414-416.

15. Cundliffe, E.; Thompson, J., The mode of action of nosiheptide (multhiomycin) and the mechanism of resistance in the producing organism. *J. Gen. Microbiol.* **1981,** *126*, 185-192.

16. Yun, B. S.; Hidaka, T.; Kuzuyama, T.; Seto, H., Thiopeptide non-producing *Streptomyces* species carry the *tipA* gene: a clue to its function. *J. Antibiot.* **2001,** *54*, 375-378.

17. Kumar, C. V.; Martin, J. F., Thiostrepton induced proteins in *Streptomyces*, *Amycolatopsis*, and *Nocardia* species. *FEMS Microbiol. Lett.* **1994,** *118*, 107-112.

18. Murakami, T.; Holt, T. G.; Thompson, C. J., Thiostrepton-induced gene expression in *Streptomyces lividans*. *J. Bacteriol.* **1989,** *171*, 1459-1466.

19. Holmes, D. J.; Caso, J. L.; Thompson, C. J., Autogenous transcriptional activation of a thiostrepton-induced gene in *Streptomyces lividans*. *EMBO J.* **1993,** *12*, 3183-3191.

20. Chiu, M. L.; Folcher, M.; Griffin, P.; Holt, T.; Klatt, T.; Thompson, C. J., Characterization of the covalent binding of thiostrepton to a thiostrepton-induced protein from *Streptomyces lividans*. *Biochemistry* **1996,** *35*, 2332-2341.

21. Julien, B.; Shah, S., Heterologous expression of epothilone biosynthetic genes in *Myxococcus xanthus*. *Antimicrob. Agents. Chemother.* **2002,** *46*, 2772-2778.

22. Xu, Z.; Jakobi, K.; Welzel, K.; Hertweck, C., Biosynthesis of the antitumor agent chartreusin involves the oxidative rearrangement of an anthracyclic polyketide. *Chem. Biol.* **2005,** *12*, 579-588.

23. Lau, J.; Frykman, S.; Regentin, R.; Ou, S.; Tsuruta, H.; Licari, P., Optimizing the heterologous production of epothilone D in *Myxococcus xanthus*. *Biotechnol. Bioeng.* **2002,** *78*, 280-288.

CHAPTER 3: SITE-DIRECTED MUTAGENESIS OF THE THIOSTREPTON PRECURSOR PEPTIDE AT ALA2, ALA4 AND THR7

From the publications:

Li, C.*; Zhang, F.*; Kelly, W. L. Heterologous production of thiostrepton A and biosynthetic engineering of thiostrepton analogs. *Mol. BioSyst.* **2011,** *7*, 82-90. (*Authors contributed equally to this work)

Li, C.; Zhang, F.; Kelly, W. L. Mutagenesis of the thiostrepton precursor peptide at Thr7 impacts both biosynthesis and function. *Chem. Commun.* **2012,** *48*, 558-560 .

3.1 Introduction

The heterologous production of thiostrepton A was described previously, however, with low yields. Here, we adapted the platform developed for heterologous production toward a pliable system for the generation of thiostrepton analogs from *S. laurentii* itself. The thiostrepton A precursor peptide, TsrA, contains a 17 amino acid core peptide region that is incorporated into the final thiostrepton scaffold.[1] Of the seventeen amino acids remaining in thiostrepton A, only three residues are unaltered by the posttranslational modification machinery: Ala2, Ala4, and Thr7. These three residues were chosen for the initial round of mutagenesis, since none are expected to be directly involved in a potentially critical transformation in precursor peptide processing, such as dehydration or cyclization. Conservative alterations at these positions may therefore elicit a minimal disturbance upon the maturation of a thiopeptide variant.

Thiostrepton A exerts its antibacterial effect by binding the prokaryotic 50S ribosomal subunit near the GTPase-associated center and disrupting the action coordinated between the ribosome and its initiation and elongation factors.[2-3] The binding

pocket for thiostrepton A includes both the 23S rRNA and the ribosomal protein L11.[4] The Ala2 and Ala4 residues of thiostrepton A appear to be solvent-exposed while the Thr7 residue makes critical contacts with the 23S rRNA.[4] Despite the implication that the thiostrepton Thr7 plays an important role in the antibacterial function of thiostrepton A, no analogs with alterations to this residue have yet been generated. To probe the importance of the Thr7 residue, this position was targeted for additional modifications. The newly isolated thiostrepton analogs were further assayed for their antibacterial activities.

3.2 Materials and Methods

3.2.1 General

Unless specified, common chemicals, solvents, enzymes and other materials were purchased from standard commercial sources and used as provided. The QIAprep Spin Miniprep Kit (Qiagen, Valencia, CA) was used for the isolation of plasmids and fosmids from *E. coli* strains. *Streptomyces* genomic DNA was isolated using the Wizard® Genomic DNA Purification Kit (Promega, Madison, WI) according to the manufacturer's recommendations. High performance liquid chromatography (HPLC) analysis was performed on a Beckman Coulter System Gold instrument. HPLC-MS was performed at the Georgia Institute of Technology Bioanalytical Mass Spectrometry Facility with a Phenomenex Syngeri RP column (250 mm × 2 mm, 4 μm) (Torrance, CA) and developed with 20% solvent B in solvent A for 8 min followed by a gradient from 20-100% solvent B over 35 min at 0.25 mL/min (solvent A: 5% acetonitrile and 0.1% formic acid; solvent

B: 95% acetonitrile and 0.1% formic acid). High-resolution matrix-assisted laser desorption/ionization mass spectrometry (HR-MALDI-MS), and MALDI-MS/MS were also performed at the Georgia Institute of Technology Bioanalytical Mass Spectrometry Facility. High-resolution electrospray ionization mass spectrometry (HR-ESI-MS) was performed at the Emory University Mass Spectrometry Center. Proton and carbon NMR spectra were recorded on a Bruker 500 MHz spectrometer. All NMR experiments were performed according to standard pulse sequences supplied with the instrument.

3.2.2 Bacterial strains, plasmids and growth medium

Streptomyces laurentii ATCC 31255 (*S. laurentii*) was obtained from American Type Culture Collection (ATCC). *S. laurentii* NDS1 (Δ*tsrA*), *S. laurentii* NDS1/int-3A10 (encoding wild-type TsrA), int-3A101 (encoding TsrA Ala2Gly), int-3A102 (encoding TsrA Ala4Gly), int-3A103 (encoding TsrA Thr7Gly), int-3A104 (encoding TsrA Thr7Ser), int-3A105 (encoding TsrA Thr7Ala) and int-3A106 (encoding TsrA Thr7Val) were all generated by Dr. Chaoxuan Li. All strains and plasmids are listed in Table A.1, and primers are listed in Table A.2, All *Escherichia coli* (*E. coli*) strains were grown in Luria-Bertani liquid or solid medium with the appropriate antibiotic(s). For the selective growth of *E. coli* or *Streptomyces*, the following antibiotics and concentrations were used: kanamycin (50 μg/mL), apramycin (50 μg/mL), ampicillin (100 μg/mL), nalidixic acid (25 μg/mL), and chloramphenicol (30 μg/mL). MS agar was used for the intergeneric conjugation of *S. laurentii* NDS1.[5]

3.2.3 Fermentation of *S. laurentii*

The fermentations of *S. laurentii* mutant strains were carried out in a three-step process as described previously.[1] First, 50 mL tryptic soy broth (TSB) with apramycin

was inoculated with 50 µL of glycerolic mycelium stock of a *S. laurentii* mutant strain and grown at 28 °C and 220 rpm for 24 h in a 250-mL Erlenmeyer flask. Next, 500 µL of the *S. laurentii* variant preculture was inoculated to 50 mL seed medium (15 g/L soybean flour, 50 g/L glucose, 15 g/L soluble starch, pH 7.2) in a 250-mL Erlenmeyer flask. After 48 h incubation at 28 °C and 220 rpm, 10 mL of the seed culture was inoculated to 100 mL fermentation medium (11 g/L yeast extract, 50 g/L glucose, 15 g/L TSB, 1 g/L trace elements solution (5 g/L $CoCl_2 \cdot 6H_2O$, 0.5 g/L Na_2MoO_4, 0.5 g/L H_3BO_3, 1.0 g/L $CuSO_4 \cdot 2H_2O$, 1.0 g/L $ZnSO_4 \cdot 7H_2O$)) in a 500-mL Erlenmeyer flask. The fermentation culture was incubated at 28 °C and 220 rpm for 4 days and extracted twice with an equal volume of chloroform. The chloroform layers were pooled and removed *in vacuo*. The solid residue was dissolved in 4 mL chloroform for HPLC and HPLC-MS analyses. Crude culture extracts were analyzed by HPLC with a Phenomenex Luna C18(2) column (250 × 4.6 mm, 5 µm). The column was developed with a gradient of 0-100% acetonitrile in water over 30 min at 1 mL/min and absorbance was monitored at 254 nm.

3.2.4 Purification and structural determination of thiostrepton analogs

Crude extracts from *S. laurentii* NDS1/int-3A101 (encoding TsrA Ala2Gly) (5 L) and *S. laurentii* NDS1/int-3A102 (encoding TsrA Ala4Gly) (4 L) fermentation culture were purified by HPLC with a semi-preparative Phenomenex Luna C18(2) column (250 x 10 mm, 5 µm) while monitoring absorbance at 254 nm. For the purification of thiostrepton Ala2Gly, column was developed using solvents A (water) and B (acetonitrile) at a flow rate of 4.7 mL/min as follows: the mobile phase was increased from 10% to 40% solvent B over 5 min, then held constant at 40% solvent B for 5 min, then increased from 40% to 50% solvent B over 5 min, then held constant at 50% solvent

B for 5 min, then increased from 50% to 100% solvent B over 5 min, and finally held constant at 100% solvent B for 5 min. For the purification of thiostrepton Ala4Gly, the column was equilibrated with 10% solvent B and developed as follows: the mobile phase was increased to 40% solvent B over 5 min, then held constant at 40% solvent B for 5 min, then increased to 45% solvent B over 5 min, then held constant at 45% solvent B for 5 min, then increased to 100% solvent B over 2 min, and finally held at 100% solvent B for 5 min. Thiostrepton Thr7Ala and SL105-1 from the culture extract of *S. laurentii* NDS1/int-3A105, and thiostrepton Thr7Val and SL106-1 from the culture extract of *S. laurentii* NDS1/int-3A106 were all purified by Dr. Chaoxuan Li.[6] All samples were stored under argon at -80 °C. Thiostreptons Ala2Gly and Ala4Gly were analyzed by HPLC-MS, HR-ESI-MS and NMR. Thiostreptons Thr7Ala, Thr7Val, SL105-1 and SL106-1 were analyzed by HPLC-MS, HR-ESI-MS or HR-MALDI-MS, and MALDI-MS/MS. NMR experiments were also performed with thiostrepton Thr7Ala and SL105-1. The spectral data are included in Appendix C and HR-MS data are included in Table F.1.

3.2.5 Antibacterial activity of thiostrepton analogs

Antimicrobial activity of *S. laurentii* culture extracts was qualitatively assessed by solid agar disc-diffusion assays. 3 mL of Luria-Bertani (LB) liquid medium was inoculated with 3 µL of a cell stock of either *Bacillus* sp. ATCC 27859 (*Bacillus* sp.), or *E. coli* ATCC 27856 (*E. coli* 27856). Brain heart infusion broth (3 mL) was inoculated with 3 µL of a cell stock of vancomycin-resistant *Enterococcus faecium* ATCC 12952 (VRE) or methicillin-resistant *Staphylococcus aureus* ATCC 10537 (MRSA). All strains were incubated at 37 ºC and 220 rpm for 18 h. Infused solid medium was prepared by adding 200 µL of overnight bacterial culture to 20 mL of respective molten medium agar

cooled to 42 °C. Eight 7 mm filter paper disks were spaced evenly on the surface of the solid medium. To each disk, 10 μL of *S. laurentii* strain extract in DMSO was deposited and the plates were incubated at 37 °C for 18 h. The positive antibiotic control used for *Bacillus* sp., *E. coli* 27856, and VRE was 10 μL of chloramphenicol (1 mg/mL) and the positive antibiotic control used for MRSA was 10 μL of vancomycin (0.5 mg/mL). The negative control used for all bacterial strains was 10 μL of DMSO. Antibacterial activity was qualitatively determined by the presence or absence of a growth inhibition zone.

Minimum inhibitory concentrations (MICs) of thiostrepton analogs against MRSA, VRE and *Bacillus* sp. were further determined using liquid microdilution method. Briefly, MRSA, VRE, and *Bacillus* sp. were grown overnight at 37 °C in nutrient broth, brain heart infusion and LB broth, respectively. Overnight cultures of the individual strains were each diluted 1000-fold with the respective medium and transferred to a 96-well plate. Thiostrepton A and its analogs were prepared in DMSO and quantified by UV spectroscopy using the extinction coefficient ε_{280} = 0.027 /(cm μM).[7] Serial dilutions of test samples and controls were performed to assess growth inhibition. The positive antibiotic control used for *Bacillus* sp. and VRE was chloramphenicol, whereas the positive control for MRSA was vancomycin. DMSO was used as the negative control in all assays. Cell growth was monitored by comparing the optical density at 600 nm at the time of treatment and after 18 h incubation at 37 °C. A difference in OD_{600} was considered grown and lowest concentration causing complete suppression of visible bacterial growth defined MIC.

3.3 Results and Discussion

3.3.1 Deletion of *tsrA* in *S. laurentii*

Given the concentration-dependent limitations of thiostrepton production encountered in the heterologous hosts (see Chapter 2), the approach used for the genetic inactivation of *tsrA* was reevaluated. Previously, an apramycin resistance cassette was inserted into the *tsrA* sequence, leading to the loss of thiostrepton production.[1] *In trans* complementation of *tsrA* in this mutant strain, however, never met with success, raising the possibility of a secondary effect within the insertional mutant.[8] In an effort to overcome this limitation of complementation and, ultimately, to spur the production of thiostrepton variants, Dr. Chaoxuan Li constructed a markerless, in-frame deletion mutant of *tsrA* to provide *S. laurentii* NDS1. As observed in the *tsrA* insertional mutant, deletion of *tsrA* in *S. laurentii* also abolished thiostrepton production (Figure 3.1). Unfortunately, the re-introduction of *tsrA* alone into *S. laurentii* NDS1 was still insufficient to revive thiostrepton production (experiment performed by Dr. Chaoxuan Li and data not shown). Introduction of the integrative fosmid int-3A10 into *S. laurentii* NDS1 to yield *S. laurentii* NDS1/int-3A10 by Dr. Chaoxuan Li, however, did permit the robust production of thiostrepton A at 113 ± 35 mg/L (Figure 3.1).

3.3.2 Production of thiostrepton analogs in *S. laurentii*

With a functional platform in hand for complementation of *S. laurentii* NDS1, it is now feasible to interrogate the tolerance of the thiostrepton biosynthetic machinery toward alternate precursor peptide substrates. To facilitate the substitution of the precursor peptide-encoding gene, wild-type *tsrA* in int-3A10 was replaced with a dual-selection cassette imparting resistance to chloramphenicol (chl^R) and a widely-used

counterselection marker, the *Bacillus subtilis sacB* gene by Dr. Chaoxuan Li, to provide int-3A100.[9] When *E. coli* and other Gram-negative bacteria are grown in media containing sucrose, the presence of *sacB* inflicts a lethal effect upon its host.[9-10] Thus, the loss of *sacB* permits growth of *E. coli* on sucrose-containing medium and provides a useful screen for its allelic replacement. An advantage to this fosmid-based system for *tsrA* replacement is that all genetic manipulations involving *tsrA* can now be conducted in *E. coli* in a comparatively facile manner by PCR-targeted gene replacement.[11] Following the successful replacement of wild-type *tsrA* with a variant *tsrA*, Dr. Chaoxuan Li introduced the engineered fosmid into *S. laurentii* NDS1 to assess analog production.

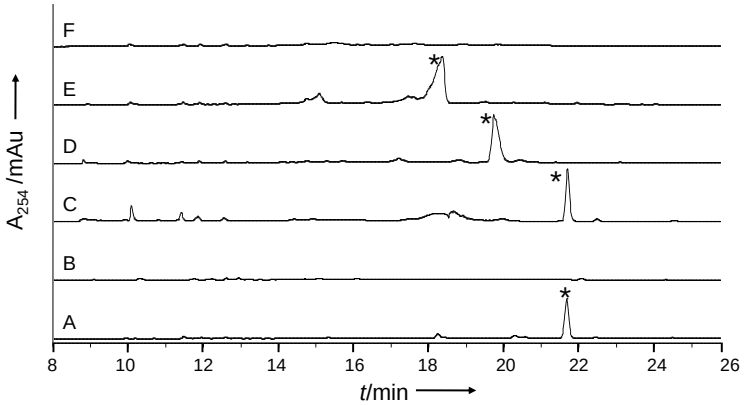

Figure 3.1. HPLC analysis of culture extracts from (**A**) wild-type *S. laurentii*, (**B**) *S. laurentii* NDS1 (Δ*tsrA*), (**C**) *S. laurentii* NDS1/int-3A10 (endoding wild-type TsrA), (**D**) *S. laurentii* NDS1/int-3A101 (endoding TsrA Ala2Gly), (**E**) *S. laurentii* NDS1/int-3A102 (endoding TsrA Ala4Gly), (**F**) *S. laurentii* NDS1/int-3A103 (endoding TsrA Thr7Gly). The asterisks indicate either thiostrepton A or a thiostrepton analog. Absorbance was monitored at 254 nm.

Three integrative fosmids, each encoding a separate mutant of TsrA, were constructed by Dr. Chaoxuan Li and designated as follows: int-3A101 (encoding TsrA Ala2Gly), int-3A102 (encoding TsrA Ala4Gly), and int-3A103 (encoding TsrA Thr7Gly) (Figure 3.2). Dr. Chaoxuan Li individually introduced the fosmids int-3A101 to int-3A103 into *S. laurentii* NDS1 by intergeneric conjugation to provide *S. laurentii*

NDS1/int-3A101 to *S. laurentii* NDS1/int-3A103, respectively. Two new metabolites with similar UV-visible absorption spectra to thiostrepton A were observed in the HPLC analysis of the culture extracts of *S. laurentii* NDS1/int-3A101 and *S. laurentii* NDS1/int-3A102 by Dr. Chaoxuan Li (Figure 3.1). Further analysis of the extracts by HPLC-MS confirmed that the masses of the two metabolites were consistent with those expected for the engineered thiostreptons Ala2Gly and Ala4Gly.[12] In contrast, Dr. Chaoxuan Li did not detect thiostrepton Thr7Gly in the culture extract of *S. laurentii* NDS1/int-3A103 either by HPLC or HPLC-MS.

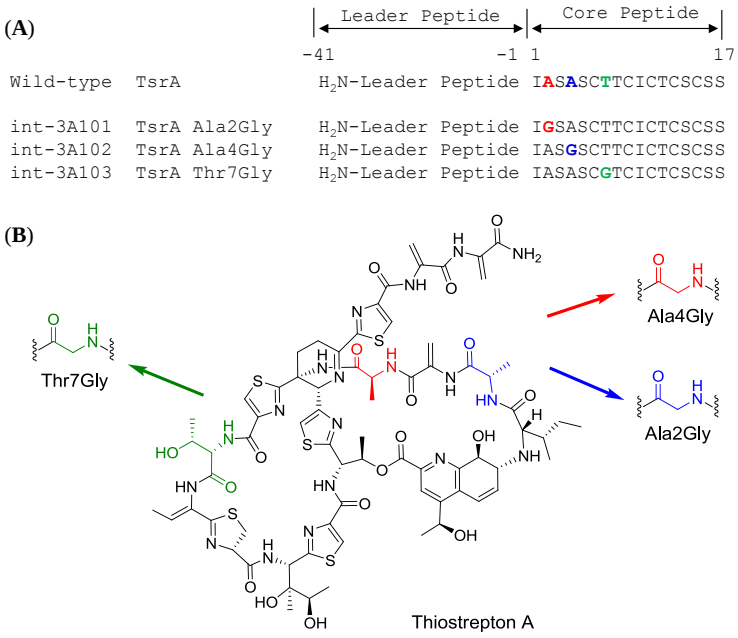

Figure 3.2. Thiostrepton A and the expected analogs to be generated by site-directed mutagenesis of TsrA. (**A**) Comparison of wild-type TsrA with the TsrA mutants encoded in the three fosmids (int-3A101 to int-3A103). The mutated amino acid residues are indicated in red, blue and green. (**B**) Structures of the expected thiostrepton analogs.

3.3.3 Antibacterial activities of thiostreptons Ala2Gly and Ala4Gly

An initial assessment of the antibacterial activity of the new thiostrepton variants by disc-diffusion of the *S. laurentii* culture extracts against bacteria-infused solid media revealed that thiostreptons Ala2Gly and Ala4Gly both retained antibacterial properties

(Figure 3.3). Thiostreptons Ala2Gly and Ala4Gly were purified and their structures were verified by one-dimensional and two-dimensional NMR analyses (Appendix C). The minimum inhibitory concentrations (MICs) of the thiostrepton analogs were determined against methicillin-resistant *Staphylococcus aureus* ATCC 10537, vancomycin-resistant *Enterococcus faecium* ATCC 12952, *Bacillus* sp. ATCC 27859, and *Escherichia coli* ATCC 27856 (*E. coli* 27856) (Table 3.1). None of the thiostreptons demonstrated antibacterial activity against *E. coli* 27856 (Data not shown). Both engineered thiopeptides retained antibacterial activity against the tested Gram-positive strains, although thiostrepton Ala4Gly did reveal a reduction in efficacy (Table 3.1).

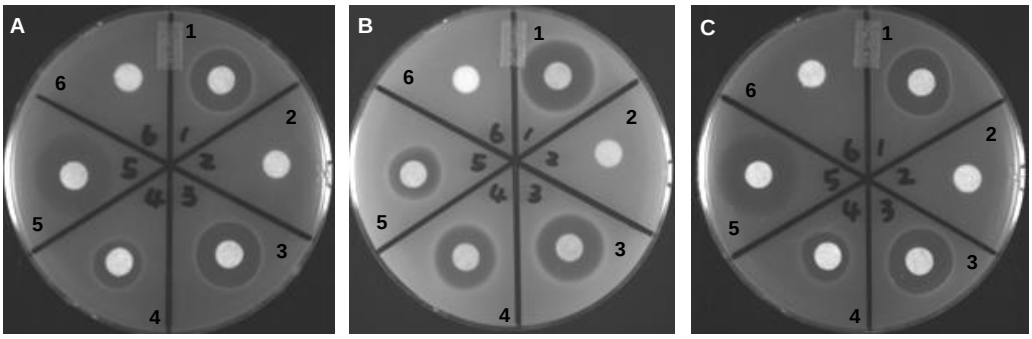

Figure 3.3. Disc diffusion antimicrobial assays of culture extracts from S. laurentii strains producing thiostrepton variants. (**A**) *Enterococcus faecium* ATCC 12952, (**B**) *Staphylococcus aureus* ATCC 10537 and (**C**) *Bacillus sp.* ATCC 27859. For region 1 through region 4, culture extracts of the following strains were added, respectively: wild-type *S. laurentii*, *S. laurentii* NDS1, *S. laurentii* NDS1/int-3A101, and *S. laurentii* NDS1/int-3A102; region 5, chloramphenicol (in **A** and **C**), vancomycin (in **B**); region 6, dimethyl sulfoxide.

Table 3.1. Summary of the antibacterial activity of thiostrepton analogs

Compound	MIC[a] (μg/mL)		
	MRSA[b]	VRE[c]	*Bacillus*[d]
Thiostrepton A	0.012	0.012	0.025
Thiostrepton Ala2Gly	0.023	0.019	0.19
Thiostrepton Ala4Gly	0.12	0.12	0.46
Vancomycin	0.39	ND[e]	ND
Chloramphenicol	ND	3.9	0.98

[a] Minimum inhibitory concentration.
[b] *Staphylococcus aureus* ATCC 10537.
[c] *Enterococcus faecium* ATCC 12952.
[d] *Bacillus* sp. ATCC 27859.
[e] Not determined.

Both Ala2 and Ala4 reside within thiostrepton's second macrocycle, the quinaldic acid loop. Much of this region, excepting quinaldic acid, is likely exposed to solvent upon binding to the ribosome and is not likely to participate in any direct interactions with either the ribosomal protein L11 or the 23S rRNA.[4] Retention of antibacterial activity in the Ala4Gly and Ala2Gly variants is consistent with this expectation. The position of the core thiopeptide macrocycle corresponding to Thr7 of thiostrepton A does appear to be critical for antibacterial activity. This unmodified amino acid residue of the ribosome-binding thiopeptides is highly conserved and substitutions at the corresponding position of thiocillin I resulted in a loss of antibacterial activity.[13-14] The precise orientation of the thiopeptide macrocycle, when bound to the ribosome, appears to dictate the specific contacts assigned to this conserved threonine residue. For micrococcin P_1 and thiocillin I, it is presumed that the threonine-containing edge of the macrocyclic loop forms several contacts with ribosomal protein L11.[4, 14] In contrast, this conserved edge in thiostrepton A macrocycle forms several contacts with the 23S rRNA.[4, 15] Furthermore, the Thr7 side chain comes within 4-5 Å of A1067 and A1095, two RNA nucleotides known to be critical to the antibacterial activity of thiostrepton A.[4, 15]

3.3.4 Generation of additional thiostrepton Thr7 analogs

Earlier efforts toward generating thiostrepton Thr7Gly was unsuccessful.[12] It was therefore uncertain whether or not variants of Thr7 could be generated and used to probe the importance of this residue for thiostrepton's antibacterial activity. Here, Thr7 residue was targeted with additional modifications. Three mutant strains, *S. laurentii* NDS1/int-3A104 (encoding TsrA Thr7Ser), *S. laurentii* NDS1/int-3A105 (encoding TsrA Thr7Ala) and *S. laurentii* NDS1/int-3A106 (encoding TsrA Thr7Val) were constructed by Dr. Chaoxuan Li as previously described. Dr. Chaoxuan Li also evaluated the culture extracts of the three strains for the presence of thiostrepton-related metabolites by both HPLC and HPLC-MS (Figures 3.4 and C.17). Thiostrepton Thr7Ser (Figure 3.5) was only faintly detected by HPLC-MS and was not observable by HPLC analysis, precluding isolation of this analog in a quantity sufficient to support biological or structural evaluation.

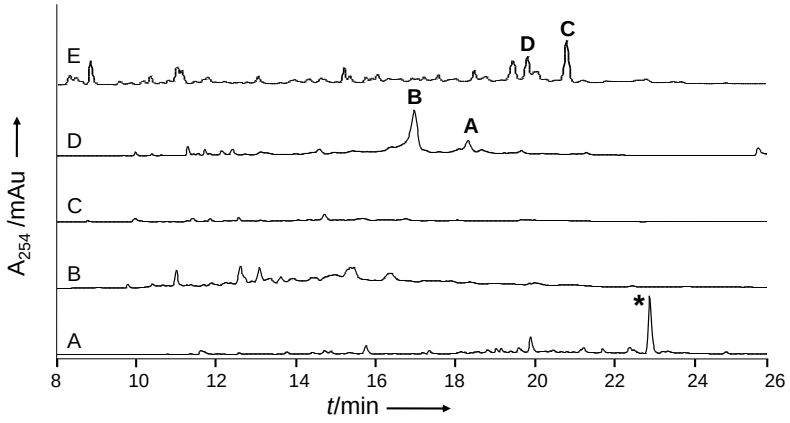

Figure 3.4. HPLC analysis of cultures extracts from (**A**) wild-type *S. laurentii*, (**B**) *S. laurentii* NDS1, (**C**) *S. laurentii* NDS1/int-3A104 (encoding TsrA Thr7Ser), (**D**) *S. laurentii* NDS1/int-3A105 (encoding TsrA Thr7Ala), and (**E**) *S. laurentii* NDS1/int-3A106 (encoding TsrA Thr7Val). The asterisk indicates thiostrepton A. Absorbance was monitored at 254 nm.

In the case of the extract from *S. laurentii* NDS1/int-3A105, two new metabolites, **A** and **B** were observed by HPLC eluting with a t_R of 16.9 min and 18.5 min, respectively

(Figure 3.4). Metabolite **A**, a minor component of this culture extract, possesses an UV-visible absorption spectrum similar to that of thiostrepton A and further analysis by HPLC-MS confirmed that the mass of **A** was consistent with that expected for thiostrepton Thr7Ala, with an *m/z* 817.9 $[M+2H]^{2+}$. On this basis, **A** was purified by Dr. Chaoxuan Li and analyzed by mass spectrometry (Appendix C).

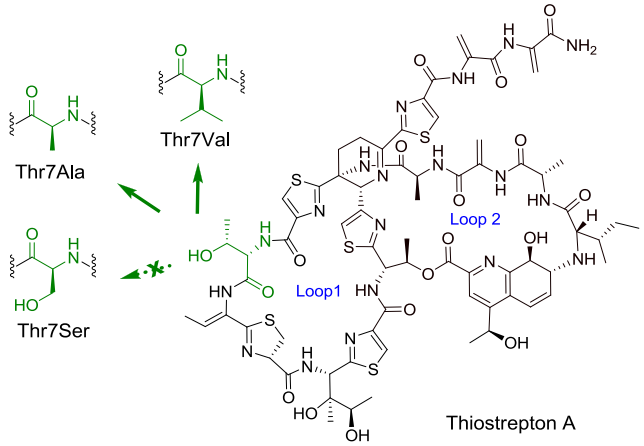

Figure 3.5. Thiostrepton A and analogs to be generated by mutagenesis of TsrA. Thr7 is indicated in green.

3.3.5 Structural characterization of SL105-1

The UV-visible absorption spectrum of **B**, on the other hand, revealed a strong absorbance at 242 nm that is absent from mature thiostrepton analogs (Figure C.17). Compound **B** was isolated by Dr. Chaoxuan Li, designated as SL105-1, and deduced to have a molecular formula of $C_{62}H_{67}N_{16}O_{15}S_5$ by HR-MALDI-MS (*m/z* 1435.3575 $[M+H]^+$, calculated *m/z* 1435.3618). One- and two-dimensional NMR experiments for compounds **A** and **B** were carried out by Feifei Zhang. Dr. Wendy L. Kelly analyzed the NMR data for compound **B** and examination of the NMR spectra for compound **A** was performed by Feifei Zhang. Initial comparison of the ^{1}H and ^{13}C NMR spectra of thiostrepton Thr7Ala and SL105-1 suggested some structural similarities.[6] However,

several distinctions were noted, including differences in the resonances correlating to the thiostrepton quinaldic acid residue and an absence of the first three residues (Ile1, Ala2, and Dha3) in SL105-1.[16-17] Further analysis of SL105-1 by DEPT-135, COSY, HMBC, HSQC and MALDI MS/MS suggested the presence of 4-(1-hydroxyethyl)quinolone-2-carboxylic acid (HEQ) moiety that, unlike thiostrepton A and Thr7Ala analog, is not connected to the N-terminal amine of the peptide backbone.

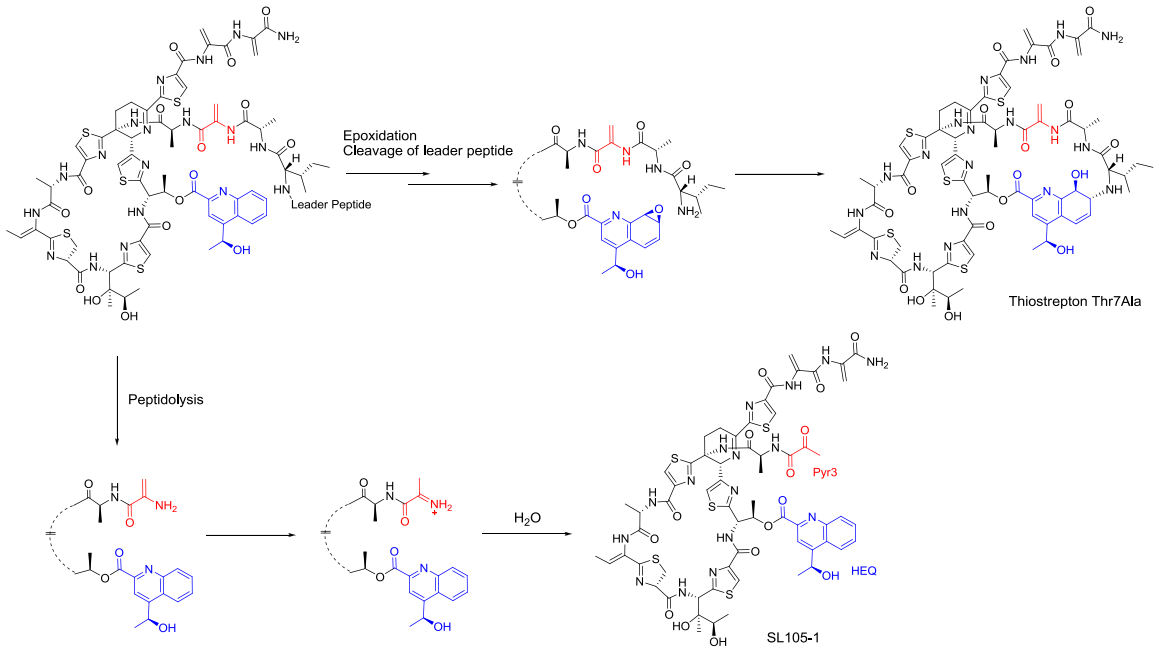

Figure 3.6. Proposed biosynthesis of thiostrepton Thr7Ala and SL105-1. The positions corresponding to the pyruvyl residue (Pyr3) and HEQ are shown in red and blue, respectively.

Notably, a MALDI MS/MS spectrum of SL105-1 indicated elimination of the HEQ moiety by the appearance of a fragment ion at *m/z* 1218.1, a loss of 217 Da from the parent ion at *m/z* 1435.4 $[M+H]^+$.[6] A carbon at δ_C 196.3 and a singlet integrating to three protons at δ_H 2.14 indicate the presence of a methyl group adjacent to a ketone. HMBC correlations from the methyl group at δ_H 2.14 to δ_C 196.3 and δ_C 159.6 support this conclusion and suggest the presence of a pyruvyl moiety at the N-terminus of the peptide.

Together with additional NMR and MS analyses, these data support the molecular formula suggested by HR-MALDI-MS (Table F.1) and the structure proposed for SL105-1 by Dr. Wendy L. Kelly (Figure 3.6).

To evaluate the effect of a Thr side chain isostere, *S. laurentii* NDS1/int-3A106, encoding TsrA Thr7Val, was prepared by Dr. Chaoxuan Li. HPLC (Figure 3.4) and HPLC-MS analysis of the culture extract from this strain revealed the presence of thiostrepton Thr7Val and SL106-1, a Val-containing analog of SL105-1. Metabolites **C** (thiostrepton Thr7Val) and **D** (SL106-1) were isolated by Dr. Chaoxuan Li and subjected to HR-MS and MALDI-MS/MS analysis.[6]

3.3.6 Antibacterial activities of thiostrepton Thr7 analogs

Thiostrepton Thr7Ala, Thr7Val, SL105-1, and SL106-1 were evaluated for their antibacterial properties. As expected, all thiostrepton analogs were devoid of activity toward *E. coli*. The MIC of each analog was at least 300-fold greater than that of thiostrepton A (Table 3.2). The diminished antibacterial activities for thiostreptons Thr7Ala and Thr7Val are consistent with the critical role proposed for the Thr7 residue. An unmodified threonine residue in the corresponding position within Loop 1 (Figure 3.5) is highly conserved among ribosome-binding thiopeptides, and this side chain likely participates in critical contacts in the thiopeptide binding pocket.[4] The exact nature of that contact, however, differs according to the individual thiopeptide.[4] Thiocillin I, another ribosome-binding thiopeptide, contains an unmodified threonine residue analogous in location to Thr7 of thiostrepton A.[4] While Thr7 of thiostrepton A appears to interface with the 23S rRNA, the corresponding thiocillin I threonine (Thr3) instead approaches the ribosomal protein L11, reflecting the differences in how individual thiopeptides can

bind to the prokaryotic ribosome.[4] Mutagenesis of Thr3 in the thiocillin precursor peptide to Ala, Asp, and Lys led to generation of thiocillin analogs that, like thiostreptons Thr7Ala and Thr7Val, were all impaired in their antibacterial activities, whereas the serine variant retained activity.[13-14] Irrespective of the exact binding mode adopted by a thiopeptide core macrocycle to the 50S ribosome, the conserved threonine residue is indeed essential for the thiopeptide's antibacterial function.

Table 3.2. Summary of the antibacterial activity of thiostrepton analogs

Compound	MIC[a] (μg/mL)		
	MRSA[b]	VRE[c]	*Bacillus*[d]
Thiostrepton A	0.012	0.012	0.025
Thiostrepton Thr7Ala	>3.4	>3.4	>3.4
SL105-1	>3.4	>3.4	>3.4
Thiostrepton Thr7Val	>3.4	>3.4	>3.4
SL106-1	>3.4	>3.4	>3.4
Vancomycin	0.39	ND[e]	ND
Chloramphenicol	ND	3.9	0.98

[a] Minimum inhibitory concentration.
[b] *Staphylococcus aureus* ATCC 10537.
[c] *Enterococcus faecium* ATCC 12952.
[d] *Bacillus* sp. ATCC 27859.
[e] Not determined.

Although the Thr7Ala substitution may contribute to the diminished antibacterial efficacy for SL105-1, this analog also lacks an intact quinaldic acid-containing loop. Indeed, Arndt *et al*. revealed that linearization of Loop 2 (Figure 3.5) by cleavage of the ester bond between Thr12 and the quinaldic acid moiety of thiostrepton A yields an thiostrepton variant devoid of antibacterial activity.[18-19] The crystal structure of thiostrepton A indicates that the hydroxyl group in the quinaldic acid forms an intramolecular hydrogen bond with the Thr7 hydroxyl side chain, and this interaction likely contributes to thiostrepton A's overall conformation.[20] Furthermore, the X-ray crystal structure of thiostrepton A bound to the ribosome reveals that the quinaldic acid of is within 3.5 Å of A1067 of the 23S rRNA.[4] The exact parameters leading to the diminished activity remain to be determined, however, it is possible that the absence of

an intact Loop 2 leads to in improper orientation of the quinaldic acid moiety, preventing the analog from effectually binding to the ribosome.

HEQ is a discrete intermediate in the biosynthesis of thiostrepton A. Floss and coworkers reported the presence of an enzyme in *S. laurentii* cell-free extracts that activates HEQ in an ATP-dependent manner, presumably, immediately prior to the tethering of HEQ to the Thr12 side chain.[21-22] The proposed epoxidation of HEQ followed by a nucleophilic attack from the Ile1 N-terminal amine, released following cleavage of the TsrA leader peptide, could then forge the quinaldic acid-containing macrocycle (Figure 3.6).[17, 22] In the case of the TsrA Thr7Ala variant, this process appears to largely derail at an advanced stage of thiostrepton maturation, likely preceding the proposed epoxidation of HEQ (Figure 3.6). Following peptidolysis of the leader peptide and the two N-terminal proteinogenic amino acids, a dehydroalanine is transiently exposed at the N-terminus prior to tautomerization and hydrolysis to provide the shunt product SL105-1 (Figure 3.6).

The alterations to TsrA Thr7 explored thus far do not permit the robust production of alternative thiostreptons. Furthermore, this residue appears to be critical not only for the biological activity of thiostrepton, but also for efficient maturation of the thiostrepton precursor peptide. The Thr7Gly substitution completely abrogates production of a mature thiostrepton, whereas the Thr7Ser variant permits only trace quantities of the final metabolite.[6, 12] The reason(s) these TsrA Thr7 variants failed to be processed to a thiostrepton analog is(are) not yet clear, and inefficient processing of alternate precursor peptides can occur at any transformation steps during thiostrepton biosynthesis. The intramolecular hydrogen bond between Thr7 and the quinaldic acid may play a key role

during thiostrepton maturation by stabilizing an intermediate's conformation for enzymatic processing. The production level of thiostrepton A is typically 115 ± 35 mg/L. The mature thiostrepton analogs Thr7Ala and Thr7Val were produced at 6 ± 2 and 12 ± 3 mg/L, respectively. During posttranslational processing, a notable portion of the TsrA Thr7Ala and Thr7Val precursor peptides are diverted toward shunt products SL105-1 and SL106-1 (9 ± 3 and 3 ± 1 mg/L, respectively).

3.4 Conclusions

A fosmid-dependent method to rapidly generate variants of thiostrepton A was developed and alteration to the primary amino acid sequence of the precursor peptide provides an avenue to probe the substrate specificity of the thiostrepton posttranslational machinery. The introduction of a fosmid used in the heterologous production of thiostrepton A, harboring the entire thiostrepton biosynthetic gene cluster, into the *tsrA* deletion mutant, *S. laurentii* NDS1, permitted restoration of thiostrepton A production to that of the wild-type level. The fosmid was then engineered to enable the rapid replacement of wild-type *tsrA*. Introduction of fosmids encoding alternate TsrA sequences into the *S. laurentii* NDS1 led to the production of thiostreptons Ala2Gly and Ala4Gly with retained antibacterial activities. These results demonstrated the utility of this expression platform toward thiopeptide engineering. Furthermore, we successfully generated thiostrepton analogs at the biologically critical Thr7 residue. Although low levels of mature thiostreptons resulted from these mutations, thiostreptons Thr7Ala and Thr7Val did accumulate to levels sufficient to permit both structural characterization and assessment of their biological activities. As predicted by the crystal structure of

thiostrepton A bound to the ribosome, the Thr7Ala and Thr7Val substitutions indeed result in greatly impaired antibacterial activities. The presences of SL105-1 and SL106-1 grant insights into thiostrepton biosynthesis, and suggest that epoxidation of HEQ and quinaldic acid loop closure occurs late during thiostrepton maturation.

3.5 References

1. Kelly, W. L.; Pan, L.; Li, C., Thiostrepton biosynthesis: Prototype for a new family of bacteriocins. *J. Am. Chem. Soc.* **2009,** *131*, 4327-4334.

2. Brandi, L.; Marzi, S.; Fabbretti, A.; Fleischer, C.; Hill, W. E.; Gualerzi, C. O.; Stephen Lodmell, J., The translation initiation functions of IF2: Targets for thiostrepton inhibition. *J. Mol. Biol.* **2004,** *335*, 881-894.

3. Modolell, J.; Cabrer, B.; Parmeggiani, A.; Vazquez, D., Inhibition by siomycin and thiostrepton of both aminoacyl-tRNA and factor G binding to ribosomes. *Proc. Natl. Acad. Sci. U.S.A.* **1971,** *68*, 1796-1800.

4. Harms, J. M.; Wilson, D. N.; Schluenzen, F.; Connell, S. R.; Stachelhaus, T.; Zaborowska, Z.; Spahn, C. M.; Fucini, P., Translational regulation via L11: Molecular switches on the ribosome turned on and off by thiostrepton and micrococcin. *Mol. Cell.* **2008,** *30*, 26-38.

5. Gust, B.; Challis, G. L.; Fowler, K.; Kieser, T.; Chater, K. F., PCR-targeted *Streptomyces* gene replacement identifies a protein domain needed for biosynthesis of the sesquiterpene soil odor geosmin. *Proc. Natl. Acad. Sci. U.S.A.* **2003,** *100*, 1541-1546.

6. Li, C.; Zhang, F.; Kelly, W. L., Mutagenesis of the thiostrepton precursor peptide at Thr7 impacts both biosynthesis and function. *Chem. Commun.* **2012,** *48*, 558-560.

7. Draper, D. E.; Xing, Y.; Laing, L. G., Thermodynamics of RNA unfolding: Stabilization of a ribosomal RNA tertiary structure by thiostrepton and ammonium ion. *J. Mol. Biol.* **1995,** *249*, 231-238.

8. Li, C.; Kelly, W. L., *Unpublished.*

9. Schweizer, H. P.; Hoang, T. T., An improved system for gene replacement and *xylE* fusion analysis in *Pseudomonas aeruginosa*. *Gene* **1995,** *158*, 15-22.

10. Gay, P.; Le Coq, D.; Steinmetz, M.; Berkelman, T.; Kado, C. I., Positive selection procedure for entrapment of insertion sequence elements in Gram-negative bacteria. *J. Bacteriol.* **1985,** *164*, 918-921.

11. Datsenko, K. A.; Wanner, B. L., One-step inactivation of chromosomal genes in *Escherichia coli* K-12 using PCR products. *Proc. Natl. Acad. Sci. U.S.A.* **2000,** *97*, 6640-6645.

12. Li, C.; Zhang, F.; Kelly, W. L., Heterologous production of thiostrepton A and biosynthetic engineering of thiostrepton analogs. *Mol. BioSyst.* **2011,** *7*, 82-90.

13. Acker, M. G.; Bowers, A. A.; Walsh, C. T., Generation of thiocillin variants by prepeptide gene replacement and *in vivo* processing by *Bacillus cereus*. *J. Am. Chem. Soc.* **2009,** *131*, 17563-17565.

14. Bowers, A. A.; Acker, M. G.; Koglin, A.; Walsh, C. T., Manipulation of thiocillin variants by prepeptide gene replacement: Structure, conformation, and activity of heterocycle substitution mutants. *J. Am. Chem. Soc.* **2010,** *132*, 7519-7527.

15. Lentzen, G.; Klinck, R.; Matassova, N.; Aboul-ela, F.; Murchie, A. I. H., Structural basis for contrasting activities of ribosome binding thiazole antibiotics. *Chem. Biol.* **2003,** *10*, 769-778.

16. Mocek, U.; Beale, J. M.; Floss, H. G., Reexamination of the ^{1}H and ^{13}C NMR spectral assignments of thiostrepton. *J. Antibiot.* **1989,** *42*, 1649-1652.

17. Mocek, U.; Zeng, Z.; O'Hagan, D.; Zhou, P.; Fan, L. D. G.; Beale, J. M.; Floss, H. G., Biosynthesis of the modified peptide antibiotic thiostrepton in *Streptomyces azureus* and *Streptomyces laurentii*. *J. Am. Chem. Soc.* **1993,** *115*, 7992-8001.

18. Schoof, S.; Arndt, H. D., D-cysteine occurrence in thiostrepton may not necessitate an epimerase. *Chem. Commun.* **2009**, 7113-7115.

19. Jonker, H. R. A.; Baumann, S.; Wolf, A.; Schoof, S.; Hiller, F.; Schulte, K. W.; Kirschner, K. N.; Schwalbe, H.; Arndt, H.-D., NMR structures of thiostrepton derivatives for characterization of the ribosomal binding site. *Angew. Chem. Int. Ed. Engl.* **2011,** *50*, 3308-3312.

20. Bond, C. S.; Shaw, M. P.; Alphey, M. S.; Hunter, W. N., Structure of the macrocycle thiostrepton solved using the anomalous dispersion contribution of sulfur. *Acta Crystallogr. D Biol. Crystallogr.* **2001,** *57,* 755-758.

21. Smith, T. M.; Priestley, N. D.; Knaggs, A. R.; Nguyen, T.; Floss, H. G., 3,4-Dimethylindole-2-carboxylate and 4-(1-hydroxyethyl)quinoline-2-carboxylate activating enzymes from the nosiheptide and thiostrepton producers, *Streptomyces actuosus* and *Streptomyces laurentii*. *J. Chem. Soc., Chem. Comm.* **1993**, 1612-1614.

22. Priestley, N. D.; Smith, T. M.; Shipley, P. R.; Floss, H. G., Studies on the biosynthesis of thiostrepton: 4-(1-hydroxyethyl)quinoline-2-carboxylate as a free intermediate on the pathway to the quinaldic acid moiety. *Bioorg. Med. Chem.* **1996,** *4*, 1135-1147.

CHAPTER 4: SATURATION MUTAGENESIS OF TSRA ALA4 UNVEILS A HIGHLY MUTABLE RESIDUE OF THIOSTREPTON A

From the work:

Zhang, F.; Kelly, W. L. Saturation mutagenesis of TsrA Ala4 unveils a highly mutable residue of thiostrepton A. **2014,** *In preparation*.

4.1 Introduction

Thiostrepton A (Figure 4.1) is one of the more extensively studied metabolites of thiopeptides and has exhibited antibacterial, antimalarial, and anticancer properties.[1-4] It contains a dehydropiperidine ring and a quinaldic acid loop, in addition to the core macrocycle that is observed in all thiopeptides.[5] In contrast to the general structural knowledge of how thiostrepton A affects protein translation, rather limited information is available concerning how it is also able to engage the recently recognized 20S proteasome and the forkhead box M1 (FOXM1) transcription factor. It is therefore unknown whether the same or differing structural regions of thiostrepton A are critical for each of the three major biological activities. Recently, we developed a biosynthetic engineering platform to produce thiostrepton analogs in *Streptomyces laurentii* ATCC 31255 (*S. laurentii*) by the site-directed mutagenesis of TsrA.[6-7] In this initial study, mutation of the fourth residue of the TsrA core peptide from alanine to glycine supported the production of thiostrepton Ala4Gly that retained antibacterial activity, suggesting that this residue is amenable to substitution.[6] Herein, we more thoroughly probe the range of amino acid residues tolerated at the fourth position of the TsrA core peptide by saturation mutagenesis. The newly generated thiostrepton variants are then interrogated for their

antibacterial and proteasome inhibition properties to determine whether or not the identity of the fourth residue is critical for either activity.

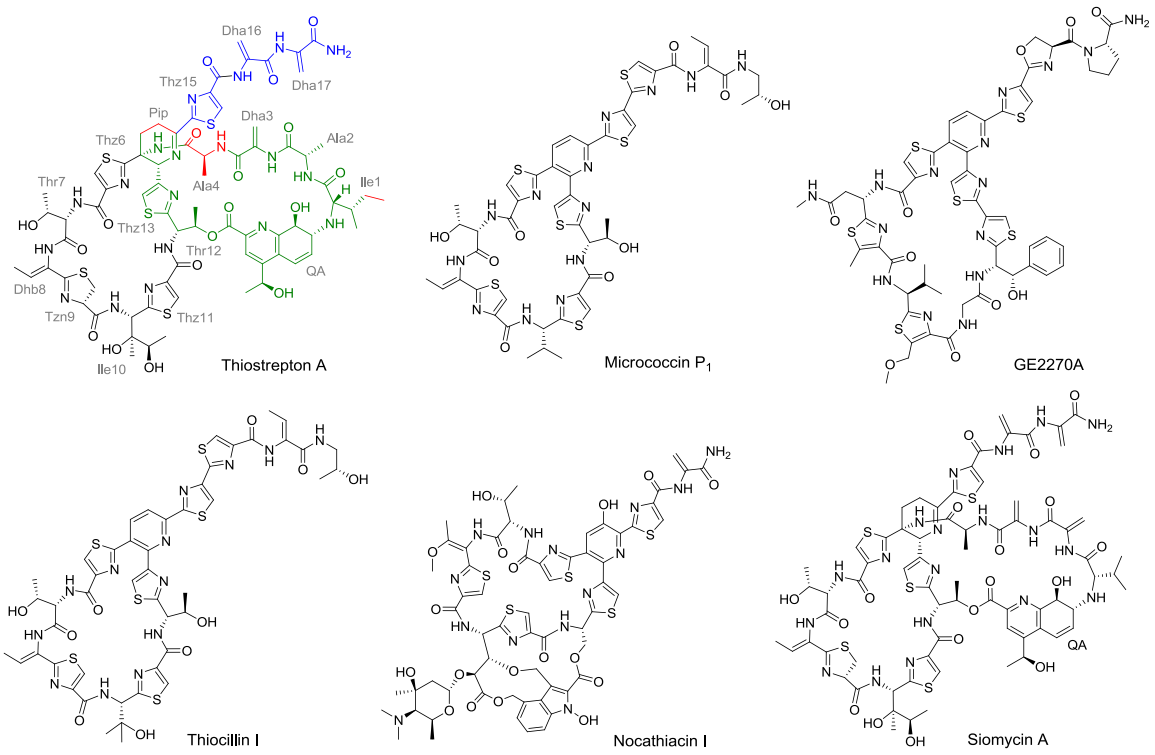

Figure 4.1. Examples of thiopeptides. The thiostrepton A residues are abbreviated using a three-letter code and labeled in grey. The quinaldic acid (QA)-containing loop and the C-terminal dehydroalanine residues are highlighted in green and blue, respectively. The Ala4 residue of thiostrepton A is shown in red.

4.2 Materials and Methods

4.2.1 General

Unless otherwise indicated, all chemicals and solvents were reagent grade, purchased from common vendors, and used as received. Enzymes and buffers were purchased from New England Biolabs (Beverly, MA). The QIAprep Spin Miniprep Kit and DirectPrep 96 MiniPrep Kit from Qiagen (Valencia, CA) were used to prepare

plasmids and fosmids from *E. coli* strains. *Streptomyces* genomic DNA isolation was performed using the Wizard® Genomic DNA Purification Kit (Promega, Madison, WI). The StrataClone Blunt PCR Cloning Kit (Agilent Technologies, La Jolla, CA) was adapted for PCR product cloning purposes. 96-well tissue culture plates and 96-well black with clear flat bottom plates were obtained from Becton Dickson (Franklin Lakes, NJ) and Corning (Tewksbury, MA), respectively. 384-well black plates were purchased from PerkinElmer (Waltham, MA). A BioTek H4 Multi-Mode Microplate Reader (Winooski, VT) was used for optical density, fluorescence, and luminescence measurements.

High performance liquid chromatography (HPLC) analysis was performed on a Beckman Coulter System Gold instrument. HPLC-mass spectrometry (HPLC-MS) was completed on Micromass Quattro LC at the Georgia Institute of Technology Bioanalytical Mass Spectrometry Facility with a Phenomenex Synergi RP column (250 mm x 2 mm, 4 μm; Torrance, CA). The column was developed with 20% solvent B in solvent A for 8 min followed by a gradient from 20-100% solvent B over 35 min at 0.25 mL/min (solvent A: 5% acetonitrile and 0.1% formic acid in water; solvent B: 5% water and 0.1% formic acid in acetonitrile). Unless indicated otherwise, high-resolution matrix-assisted laser desorption/ionization mass spectrometry (HR-MALDI-MS), and MALDI-MS/MS were conducted on Applied Biosystems 4700 Proteomics Analyzer at the Georgia Institute of Technology Bioanalytical Mass Spectrometry Facility. High-resolution electrospray ionization mass spectrometry (HR-ESI-MS) was performed on Thermo LTQ-FTMS at the Emory University Mass Spectrometry Center. Proton and carbon NMR experiments were conducted on a Bruker 500 MHz spectrometer (School of

Chemistry and Biochemistry, Georgia Institute of Technology) according to standard pulse sequences supplied with the instrument.

All oligonucleotides were synthesized by Integrated DNA Technologies (Coralville, IA) and DNA sequencing was completed by Eurofins MWG Operon (Huntsville, AL). Sequence analysis was performed using the VectorNTI® software package from Invitrogen (Carlsbad, CA).

4.2.2 Bacterial strains, plasmids, and growth media

Streptomyces laurentii ATCC 31255 (*S. laurentii*), methicillin-resistant *Staphylococcus aureus* ATCC 10357 (MRSA), vancomycin-resistant *Enterococcus faecium* ATCC 12952 (VRE), *Bacillus* sp. ATCC 27859 (*Bacillus*) and *Escherichia coli* (*E. coli*) ATCC 27856 were obtained from American Type Culture Collection (ATCC). *E. coli* EPI300 was purchased from Epicentre® (Madison, WI). All strains, plasmids, and fosmids are itemized in Table A.1, and primers are listed in Table A.2. All *E. coli* strains were grown in Luria-Bertani liquid or solid medium with the appropriate antibiotic(s). For the selective growth of *E. coli* or *Streptomyces*, the following antibiotics and concentrations were used: apramycin (50 μg/mL), kanamycin (50 μg/mL), ampicillin (100 μg/mL), nalidixic acid (25 μg/mL), and chloramphenicol (12.5 μg/mL). ISP3 agar was used for the sporulation of *S. laurentii* strains and MS agar was used for the intergeneric conjugation of *S. laurentii* NDS1.

4.2.3 Engineering TsrA Ala4 variants in *S. laurentii*

A synthetic ultramer, containing a degenerate codon (NNS) at the fourth position of the *tsrA* core peptide-encoding region and regions homologous to fosmid int-3A100, was used as the template for the initial amplification of mutant *tsrA* genes by polymerase

chain reaction (PCR), using the primers Amp-TsrA-SP-F and -R. The amplicons were cloned into pSC-B-amp/kan and the resulting plasmids were analyzed by DNA sequencing. Inserts containing the highest percentage of synonymous codon usage for *Streptomyces* were selected for further studies.[8] The mutant plasmids served as the templates for amplification for each mutant *tsrA* gene, using the primers Amp-TsrA-SP-F and -R. The resulting amplicons were used to replace the dual-marker disruption cassette in fosmid int-3A100 by PCR-targeted gene replacement.[9-10] Fosmids from the chloramphenicol-sensitive and sucrose-tolerant colonies were transformed into chemically competent *E. coli* EPI300 cells to induce high copy number before isolation and further analysis by restriction digestion with *Eco*RI. Samples that displayed the same restriction digestion pattern as fosmid int-3A10 were selected for DNA sequence analysis to confirm the allelic replacement of wild-type *tsrA* by each mutant *tsrA* gene. Mutant int-A4X fosmids were transformed into *E. coli* ET12567/pUZ8002, and then introduced into *S. laurentii* NDS1 through intergeneric conjugation.[10-11] Colonies resistant to apramycin were confirmed by PCR using the primers SD3-F and -R, and the strains were annotated as *S. laurentii* NDS1/int-A4X, according to the introduced mutation.

4.2.4 Evaluation of thiostrepton Ala4 analog production in *S. laurentii*

Growth of *S. laurentii* was carried out in a three-step process as described previously.[12] First, 50 mL tryptic soy broth (TSB) containing apramycin in a 250-mL Erlenmeyer flask was inoculated with 50 μL of glycerolic mycelium stock of the *S. laurentii* strain of interest and grown at 28 °C and 220 rpm for 24 h. Next, 0.5 mL of this preculture was used to inoculate 50 mL seed medium (15 g/L soybean flour, 50 g/L glucose, 15 g/L soluble starch, pH 7.2) in a 250 mL-Erlenmeyer flask. After 48 h

incubation at 28 °C and 220 rpm, 10 mL of this seed culture was used to inoculate 100 mL fermentation medium (11 g/L yeast extract, 50 g/L glucose, 15 g/L TSB, 1 g/L trace elements solution (5 g/L $CoCl_2 \cdot 6H_2O$, 0.5 g/L Na_2MoO_4, 0.5 g/L H_3BO_3, 1 g/L $CuSO_4 \cdot 2H_2O$, 1 g/L $ZnSO_4 \cdot 7H_2O$)) in a 500-mL Erlenmeyer flask. The resulting culture was incubated at 28 °C and 220 rpm for 4 days. The whole culture was extracted twice with an equal volume of chloroform. The chloroform layers were pooled together and the solvent was removed *in vacuo*. The solid residue was dissolved in 4 mL chloroform for HPLC analysis. Samples were analyzed by HPLC with a Phenomenex Luna C18(2) column (250 x 4.6 mm, 5 μm) which was developed at 1 mL/min using a gradient of 0-100% acetonitrile in water over 30 min. Absorbance was monitored at 254 nm.

4.2.5 Purification and mass spectrometric analyses of thiostrepton Ala4 analogs

Crude culture extracts from *S. laurentii* variant fermentations were first crystallized as described previously.[13] Briefly, each crude culture extract was dissolved in a minimum volume of chloroform and 10 volumes of *n*-hexane was added to the sample before centrifugation at 4000 rpm (2559 x *g*) for 5 min at 25 °C. Next, the precipitate was resuspended with a minimum volume of dichloromethane:ethanol at a ratio of 4:1. Diethyl ether (5 volumes) was then added to the sample and the resulting mixture centrifuged at 4000 rpm (2559 x *g*) for 5 min at 25 °C. Finally, the precipitated sample was dissolved in chloroform:methanol (4:1) and was further purified by semi-preparative HPLC with a Phenomenex Luna C18(2) column (250 x 10 mm, 5 μm) while monitoring absorbance at 254 nm and using gradients of acetonitrile (solvent B) in water (solvent A) as described below.

For the purification of thiostreptons Ala4Asn Ala4Dha, Ala4Ile, Ala4Leu, Ala4Ser, and Ala4Val, the column was developed using a gradient of solvent B in solvent A at 4.5 mL/min as follows: 0% to 50% solvent B over 10 min, then 50% to 60% solvent B over 5 min, then held at 60% solvent B for 5 min, then 60% to 100% solvent B over 5 min, and the mobile phase was finally held constant at 100% solvent B for 3 min. For the purification of thiostreptons Ala4Cys F1, Ala4Cys F2, Ala4Gln, Ala4His, Ala4Met, Ala4Phe, Ala4Trp, and Ala4Tyr, the column was developed at 4.3 mL/min using a gradient of 0-100% solvent B in solvent A over 30 min. For the purification of thiostrepton Ala4Dhb, the column was developed at 4.5 mL/min using a gradient of solvent B in solvent A as follows: 0% to 40% solvent B over 5 min, then 40% to 50% solvent B over 10 min, then 50% to 100% solvent B over 2 min, and the mobile phase was finally held constant at 100% solvent B for 3 min. Purified samples were stored under argon at -80 °C and analyzed by HPLC-MS, MALDI-MS/MS, and either HR-MALDI-MS or HR-ESI-MS (Table F.1 and Appendix D).

4.2.6 Truncation of thiostrepton A and thiostrepton analogs

The C-terminal truncations of thiostrepton A and its analogs (Ala4Asn, Ala4Cys F1, and Ala4Cys F2) were performed following published procedures with slight modifications.[14-15] Briefly, 0.48 mmol of thiostrepton analog was dissolved in 160 μL chloroform. Following the addition of 16 μL diethylamine, the resulting solution was gently mixed before incubation at 0 °C for 24 h. The reaction mixture was dried under argon. The residue was dissolved in 200 μL chloroform and analyzed by HPLC-MS.

4.2.7 Kinetic solubility of thiostrepton analogs

The kinetic aqueous solubilites of thiostrepton A and its analogs were measured following a previously described protocol.[16] First, the thiostrepton A analog was dissolved in DMSO and quantified by absorption at 280 nm using an extinction coefficient of 0.027/ (cm μM) to make a 1 mM stock solution.[17] The thiostrepton sample was diluted in the assay buffer (10 mM MOPS, 5 mM $MgCl_2$, and 200 mM KCl, pH 7.0) to a nominal concentration of 20 μM, containing 5% DMSO. The resulting sample was incubated at 25 °C for 2 h followed by centrifugation at 25 °C and 14,000 rpm (18,000 x *g*) for 10 min to remove any precipitate. The UV absorbance of the supernatant at 280 nm was used to calculate the solubility of the thiostrepton analog and each analysis was performed in triplicate. The aqueous solution of the shunt metabolites SL105-1 and SL106-1 were similarly prepared, but with the concentrations quantified by HPLC against a standard calibration curve of SL105-1 and assuming comparable spectral properties for the two metabolites.[7]

4.2.8 Antibacterial activity assay

Minimum inhibitory concentrations (MICs) of thiostrepton analogs against indicator strains (MRSA, VRE, *Bacillus*, and *E. coli* ATCC 27854) were determined following the liquid microdilution method described previously.[6] Thiostrepton A and its analogs were prepared in DMSO and quantified by absorbance at 280 nm as described above. Chloramphenicol was used as a positive control for *Bacillus* and VRE, whereas vancomycin served as a positive control for MRSA. DMSO was used as the negative control in all assays. Cell growth was evaluated by comparing the optical density at 600 nm (OD_{600}) at the time of inoculation and after 18 h incubation at 37 °C. A difference in

OD_{600} was considered growth, and the lowest concentration that completely inhibited bacterial growth defined the MIC.

4.2.9 *In vitro* trancsription-translation coupled assay

In vitro transcription-translation coupled assays were completed using the *E. coli* S30 Extract System for Circular DNA and Luciferase Assay System from Promega (Madison, WI). The inhibition assays were conducted according to manufacturer's protocol, except that the experiment was performed using a 10 μL reaction volume containing 1 μL amino acid mixture, 4 μL S30 premix, 3 μL S30 *E. coli* extract, 1.25 μL nuclease-free water, 0.25 μL thiostrepton analog, and 0.5 μL pBESTLuc^{TM} template. The luciferase substrate was reconstituted as recommended by the manufacturer. Thiostrepton A and its analogs were prepared in a range of concentrations in DMSO and quantified by absorbance at 280 nm or HPLC as described above. The reaction was incubated at 37 °C for 1 h, at which time 5 μL of the reaction mixture was transferred to a well in a 96-well plate. Luciferase substrate (50 μL) was added to each well immediately before luminescence was measured. Relative activity, obtained by normalizing luminescence to that of a DMSO control, was plotted against compound concentration. Each assay was performed in triplicate and the half maximal inhibitory concentration (IC_{50}) was calculated for each compound by fitting the data to the Hill equation using GraphPad Prism 5 (La Jolla, CA).

4.2.10. Structural modeling

The crystal structure of thiostrepton A complexed with the ribosome from *Deinococcus radiodurans* (*D. radiodurans*) (PDB entry: 3CF5) was used as the source to build the *in silico* model of the thiostrepton Ala4Cys analogs bound to the ribosome.[3]

Thiostrepton A interacts with helices 43 and 44 (H43/44) of *D. radiodurans* 23S rRNA and ribosomal protein L11. By visual inspection, the local complex structure, including thiostrepton A, H43/44, and L11, were extracted from the crystal structure and exported to ChemDraw 3D Ultra 12.0 (CambridgeSoft, Cambridge, U.K.) The thiostrepton analogs, Ala4Cys F1 and F2, were manually built in ChemDraw 3D using the crystal structure of thiostrepton A complexed to the ribosome (PDB entry: 3CF5) as the template.[18] The analog structures were energy minimized using the MM2 force field in ChemDraw 3D, where H43/44 and L11 were immobilized during minimization.[19] The energy minimized structures of the thiostrepton Ala4Cys analogs were modeled into the ribosome, and the interactions of the complex, were visualized using PyMOL.[20]

4.2.11 20S Proteasome inhibition assay

Components used to assay inhibition of the 20S proteasome were acquired from Enzo Life Sciences (Farmingdale, NY), including the purified human 20S proteasome and the fluorogenic substrates Boc-Leu-Arg-Arg-AMC (AMC: 7-amino-4-methylcoumarin), Suc-Leu-Leu-Val-Tyr-AMC, and Ac-Nle-Pro-Nle-Asp-AMC, which were used to measure the trypsin-like, chymotrypsin-like, and caspase-like activities of the 20S proteasome, respectively. Thiostrepton A and its analogs were prepared in DMSO and quantified by absorption at 280 nm or HPLC as described above. DMSO and bortezomib were included as controls. The assay was executed in a final volume of 50 μL in a 384-well plate consisting of: 5 μL test compound, 10 μL 1 μg/mL 20S proteasome, 10 μL 50 uM fluorogenic substrate and 25 μL assay buffer (20 mM Tris-HCl, 1 mM EDTA, pH 7.5) and each assay was performed in triplicate. The 20S proteasome was incubated with the test compound for 15 min at 37 °C, followed by the addition of the

appropriate fluorogenic substrate. Fluorescence was measured using an excitation wavelength of 360 nm and an emission wavelength of 460 nm. Emissions were documented every 50 s for 1 h and the arbitrary fluorescence units (AFU) were plotted against time for each compound to acquire the slope of the linear fit. Relative activity, obtained by normalizing the compound slope to the DMSO control slope, was plotted against compound concentration and fit to the Hill equation using GraphPad Prism 5 to calculate IC_{50}.

4.3 Results and Discussion

4.3.1 Engineering *tsrA* variants in *S. laurentii*

The thiostrepton biosynthetic engineering platform utilizes a *tsrA* deletion mutant of *S. laurentii* (*S. laurentii* NDS1) and an *E. coli*-*Streptomyces* shuttle fosmid, int-3A100, allowing for *tsrA* mutagenesis to be carried out in *E. coli*.[6] Fosmid int-3A100 harbors the entire *tsr* biosynthetic gene cluster, except that the TsrA core peptide-encoding region is replaced by a dual-marker selection cassette consisting of chl^R (a chloramphenicol resistance gene) and a levansucrase-encoding *sacB* gene.[6] The *tsrA* genes varying at the position encoding the core peptide's fourth residue were introduced into the fosmid by PCR-targeted gene replacement and the resulting fosmids were transferred into *S. laurentii* NDS1 by intergeneric conjugation.[9-10] By this method, 18 different *S. laurentii* NDS1/int-A4X (where "X" is the one-letter amino acid code for the introduced mutation) variants were successfully generated, in addition to the previously constructed *S. laurentii* NDS1/int-A4G.[6]

(A)

		Leader Peptide	Core peptide
		-41 -1	1 17
int-3A10	Wild-type TsrA	H_2N-Leader Peptide	IAS**A**SCTTCICTCSCSS
int-A4R	TsrA Ala4Arg	H_2N-Leader Peptide	IAS**R**SCTTCICTCSCSS
int-A4N	TsrA Ala4Asn	H_2N-Leader Peptide	IAS**N**SCTTCICTCSCSS
int-A4D	TsrA Ala4Asp	H_2N-Leader Peptide	IAS**D**SCTTCICTCSCSS
int-A4C	TsrA Ala4Cys	H_2N-Leader Peptide	IAS**C**SCTTCICTCSCSS
int-A4Q	TsrA Ala4Gln	H_2N-Leader Peptide	IAS**Q**SCTTCICTCSCSS
int-A4E	TsrA Ala4Glu	H_2N-Leader Peptide	IAS**E**SCTTCICTCSCSS
int-A4G	TsrA Ala4Gly	H_2N-Leader Peptide	IAS**G**SCTTCICTCSCSS
int-A4H	TsrA Ala4His	H_2N-Leader Peptide	IAS**H**SCTTCICTCSCSS
int-A4I	TsrA Ala4Ile	H_2N-Leader Peptide	IAS**I**SCTTCICTCSCSS
int-A4L	TsrA Ala4Leu	H_2N-Leader Peptide	IAS**L**SCTTCICTCSCSS
int-A4K	TsrA Ala4Lys	H_2N-Leader Peptide	IAS**K**SCTTCICTCSCSS
int-A4M	TsrA Ala4Met	H_2N-Leader Peptide	IAS**M**SCTTCICTCSCSS
int-A4F	TsrA Ala4Phe	H_2N-Leader Peptide	IAS**F**SCTTCICTCSCSS
int-A4P	TsrA Ala4Pro	H_2N-Leader Peptide	IAS**P**SCTTCICTCSCSS
int-A4S	TsrA Ala4Ser	H_2N-Leader Peptide	IAS**S**SCTTCICTCSCSS
int-A4T	TsrA Ala4Thr	H_2N-Leader Peptide	IAS**T**SCTTCICTCSCSS
int-A4W	TsrA Ala4Trp	H_2N-Leader Peptide	IAS**W**SCTTCICTCSCSS
int-A4Y	TsrA Ala4Tyr	H_2N-Leader Peptide	IAS**Y**SCTTCICTCSCSS
int-A4V	TsrA Ala4Val	H_2N-Leader Peptide	IAS**V**SCTTCICTCSCSS

(B)

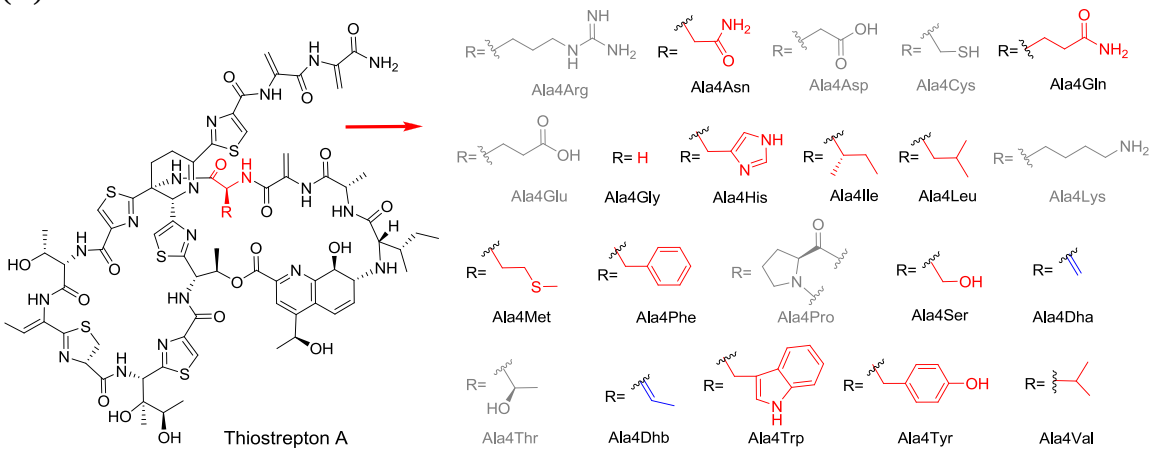

Figure 4.2. Thiostrepton A and the analogs to be generated by site-directed mutagenesis of TsrA. (**A**) Comparison of wild-type TsrA with the TsrA Ala4 variants encoded in the mutant fosmids. (**B**) Structures of thiostrepton Ala4 analogs. The amino acid residue is abbreviated using a three-letter code. The analogs in grey are not produced. The observed analogs possessing no modification of the variant residue are highlighted in red, while the ones resulting from a modification of the variant residue are highlighted in blue. Dha and Dhb refer to dehydroalanine and dehydrobutyrine, respectively.

4.3.2 Production and structural characterization of thiostrepton analogs

Culture extracts of the *S. laurentii* strains encoding TsrA Ala4 variants were evaluated for thiopeptide production by HPLC and HPLC-MS. Structures of the anticipated thiostrepton analogs are shown in Figure 4.2. Mature thiostrepton analogs were not detected in the extracts of *S. laurentii* NDS1/int-A4D, A4E, A4K, and A4R,

either by HPLC or HPLC-MS, suggesting that the amino acid residues inherently charged at physiological pH are not well-tolerated by the thiostrepton biosynthetic system at the fourth position. The Ala4Pro substitution, which introduces conformational constraints on the precursor peptide backbone, is also not processed into a mature thiostrepton derivative, as thiostrepton Ala4Pro was not present in the *S. laurentii* NDS1/int-A4P extract. A majority of the Ala4 substitutions in TsrA, however, did yield the expected mature thiostrepton analogs, including Ala4Asn, Ala4Gln, Ala4Gly, Ala4His, Ala4Ile, Ala4Leu, Ala4Met, Ala4Phe, Ala4Trp, Ala4Tyr, and Ala4Val (Figure 4.2). These analogs were purified by semi-preparative HPLC and their identities confirmed by HR-MS and MALDI-MS/MS (Appendix D and Table F.1).

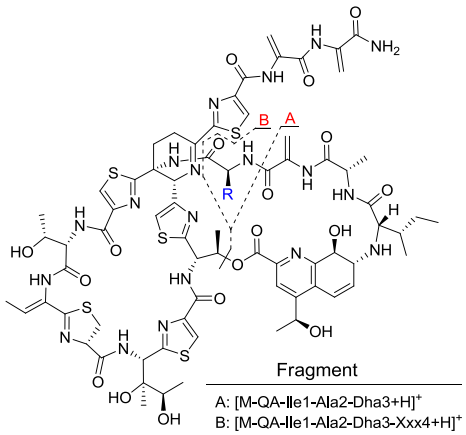

Figure 4.3. Two characteristic fragments from MALDI-MS/MS used to confirm the identity of the fourth residue of a thiostrepton analog. Fragment **A** corresponds to the loss of the quinaldic acid (QA) moiety and the three N-terminal residues Ile1, Ala2, and Dha3 (Dha: dehydroalanine) from the parent ion and fragment **B** additionally lacks the fourth residue (Xxx4).

Loss of the quinaldic acid (QA) moiety and sequential fragmentation of the newly exposed N-terminal residues are consistently observed in most thiostrepton analogs during MALDI-MS/MS, often allowing for unambiguous identification of the residues in the QA-containing loop.[7] The mass difference between two key fragments is particularly

diagnostic for the identity of the fourth residue: fragment **A** corresponds to the loss of the QA moiety and the three N-terminal residues (Ile1, Ala2, and Dha3 (Dha: dehydroalanine)) from the parent ion and fragment **B** additionally lacks the fourth residue (Xxx4) (Figure 4.3 and Appendix D).

The variant peptides TsrA Ala4Thr and Ala4Ser both led to thiostrepton analogs bearing a modification at the newly introduced residue. For *S. laurentii* NDS1/int-A4T, a major metabolite displaying a similar UV-visible absorption spectrum to that of thiostrepton A was detected by HPLC analysis of the culture extract. Further investigation by HPLC-MS revealed a species 18 Da less than that expected for thiostrepton Ala4Thr, suggesting thiostrepton Ala4Dhb (Dhb: dehydrobutyrine) as the product of a dehydration of the newly introduced threonine residue (Figure 4.2). Meanwhile, two thiostrepton analogs were readily observed by HPLC analysis of the *S. laurentii* NDS1/int-A4S culture extract. Initial HPLC-MS analyses of the extract revealed masses consistent with the anticipated thiostrepton Ala4Ser in addition to thiostrepton Ala4Dha, resulting from dehydration of the introduced Ser residue (Figure 4.2). These three analogs were purified and then analyzed by MALDI-MS/MS and HR-MALDI-MS (Appendix D and Table F.1). The proposed structures of thiostreptons Ala4Dha and Ala4Dhb were further verified by one- and two-dimensional NMR analyses (Figures D.21-D.26 and D.29-D.34). Relative to thiostrepton A, the Ala4Dha analog revealed an additional quaternary carbon (δ_C: 138.2) and an unsaturated CH_2 (δ_C: 102.9 and δ_H: 5.82, 5.25), each characteristic of a Dha residue (Table D.3). Additional resonances corresponding to a quaternary carbon (δ_C: 131.8) and an unsaturated CH (δ_C: 121.8 and

δ_H: 5.87), suggestive of a Dhb residue, were observed in thiostrepton Ala4Dhb (Table D.4).

Dehydration of a Ser or Thr residue at the fourth position of thiostrepton could be catalyzed by the dehydratase(s) encoded within the thiostrepton biosynthetic gene (*tsr*) cluster: TsrC, TsrD, and TsrL.[12] TsrC and TsrD, homologous to NisB and the LanB family of lanthipeptide dehydratases, have homologs in all reported thiopeptide biosynthetic systems, and are proposed to dehydrate Ser and Thr residues of the core peptide during thiopeptide maturation.[21-22] The additional LanB-type dehydratase, TsrL, is not conserved among all thiopeptide biosynthetic gene clusters, and its role is currently unclear.[12] In contrast to other families of lanthipeptide dehydratases, which employ phosphorylation to activate the β-hydroxyl as a leaving group, NisB dehydrates the serine and threonine residues of the nisin precursor peptide NisA via a glutamylated intermediate, and the LanB-like dehydratases involved in thiopeptide maturation likely adopt a similar catalytic strategy.[22-24] The LanB family of dehydratases appear to be flexible in their abilities to dehydrate Ser and Thr residues introduced by precursor peptide engineering, demonstrating a broad tolerance toward non-native peptide substrates.[25-27] Lys12Ser and Lys12Thr mutants of the nisin A precursor peptide both led to the production of a mixture of nisin analogs either unprocessed or dehydrated at the twelfth position, with dehydration of the threonine residue predominating.[28] An *in silico* analysis of 37 lanthipeptides has suggested that Ser residues may be more likely than the Thr side chain to be incompletely processed.[29] Consistent with these lanthipeptide observations, *S. laurentii* expressing TsrA Ala4Thr only yielded the Ala4Dhb derivative, but the strain expressing TsrA Ala4Ser supported the production of both thiostreptons

Ala4Ser and Ala4Dha at about a 1:14 ratio. All thiopeptides isolated thus far from the structural series *a* and *b* contain an unmodified Ala4 residue, but the lone member reported for series *c*, Sch 40832 possesses a Dha4.[5] The naturally-occurring and engineered thiopeptides from series *a*-*c* suggest that the dehydratases for the QA loop-containing thiopeptides may be biased toward dehydration if a suitable residue presents at the fourth position of the core peptide.[30] Insertion of Ser residues in the precursor peptide for thiocillin, a series *d* thiopeptide, also led to dehydration of the newly introduced residue.[31] It therefore appears that, like their lanthipeptide dehydratase counterparts, thiopeptide dehydratases are not highly restrictive in their substrate specificities and this flexibility can be further explored for directing the introduction of dehydrated amino acids into engineered thiopeptides.

Several metabolites with UV-visible absorption spectra comparable to that of thiostrepton A were observed during the HPLC analyses of the *S. laurentii* NDS1/int-A4C culture extract. We focused on two of the more abundant metabolites whose masses were consistent with that expected for thiostrepton Ala4Cys and those two compounds were assigned as thiostreptons Ala4Cys F1 and F2. The identical masses could result from two scenarios: either Cys4 retains the umodified thiol group or, via a Michael addition, the Cys4 thiol attacked one of the thiostrepton dehydro residues to form a lanthionine or methyllanthioine (Lan or MeLan, respectively) bridge, as observed in lanthipeptides.[32] To distinguish between these two possibilities, both Ala4Cys analogs were analyzed by MALDI-MS/MS. If the newly introduced Cys4 residue remains unmodified, the two distinguishing **A** and **B** fragments would be observed (Figure 4.3). However, MS/MS fragments of thiostreptons Ala4Cys F1 and F2 both revealed only the

presence of fragment **A** (Figures D.3 and D.11). This observation suggested that the Cys4 residue was probably now contained within either a Lan or MeLan residue. A lanthionine ring likely does not involve Dha3, which would otherwise result only in the formation of fragment **B**. There are three additional dehydrated amino acid residues in the thiostrepton scaffold: Dhb8, Dha16, and Dha17. Cys4 is not expected to form a thioether linkage with Dhb8 due to the relative positioning of the core macrocycle and the QA loop, which places the two residues on opposing faces of the molecule.[33] One- and two-dimensional NMR studies were further performed with purified thiostreptons Ala4Cys F1 and F2 (Appendix D). The expected ^{1}H and ^{13}C resonances for Dha3 and Dhb8 in both F1 and F2 analogs were indeed present, confirming that these two residues remain intact.[34] In contrast, the resonances corresponding to one of the C-terminal Dha residues of thiostrepton A changed dramatically. The β proton resonances of a Dha residue typically appear between 6.7 and 5.2 ppm, whereas the resonances of a Lan residue's β protons should occur upfield, around 3 ppm.[6-7, 34-36] The NMR analyses revealed only two unsaturated CH_2's in both thiostreptons Ala4Cys F1 and F2, as opposed to three in thiostrepton A (Dha3, Dha16, and Dha17). The absence of proton signals corresponding to one of the C-terminal Dha residues and the appearance of new resonances near 3 ppm in the ^{1}H spectra of thiostreptons Ala4Cys F1 and F2 suggested that a Lan ring could be formed between Cys4 and either Dha16 or Dha17.

To help delineate whether the dehydroalanine of the 16th or 17th residue of thiostreptons Ala4Cys F1 and F2 are incorporated into the Cys4-initiated Lan rings, the analaogs were subjected to a diethylamine-mediated truncation of their C-termini and the reactions monitored by HPLC-MS.[14-15] Using this method, the two C-terminal Dha

residues can be sequentially removed from the thiostrepton to provide two truncated products lacking Dha17 or both Dha17 and Dha16.[14-15] If the Lan ring was formed from Dha17, no truncated product would be observed; however, if Dha16 was attacked by Cys4 instead, a product shortened by the loss of Dha17 would be generated. The expected Dha17 and Dha17 plus Dha16 truncation products were identified by HPLC-MS in the positive control reactions of thiostrepton A and thiostrepton Ala4Asn (Figure D.2). Following exposure of thiostreptons Ala4Cys F1 and F2 to the truncation conditions,[14-15] ions suggestive of the corresponding diethylamine adducts of the intact metabolites were observed, but no products consistent with a C-terminal cleavage event were detected (Figure D.2). Based on the MS, NMR, and chemical modification studies, we propose that thiostreptons Ala4Cys F1 and F2 are stereoisomers and, in each analog, the Lan residue is formed by the adventitious Michael addition of the Cys4 β-thiolate to the terminal alkene of Dha17.

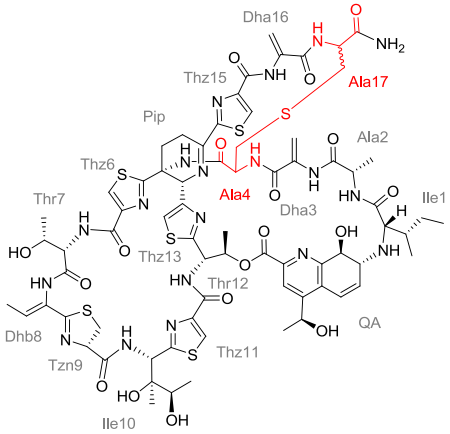

Figure 4.4. Structures of thiostreptons Ala4Cys F1 and F2. Thiostreptons Ala4Cys F1 and F2 are proposed to be diastereomers differing in configuration at the α carbon of the 17th residue. The residues comprising the lanthionine are each annotated in the structure as "Ala" and are highlighted in red.

The thiazoline residue (Tzn9) of thiostrepton A occurs in a D-configuration, however, nonenzymatic epimerization at this site has been reported.[34, 37] For a D-

configured Tzn9, the chemical shift of the α proton appears at approximately 4.8 ppm and the resonances of the β protons appear at about 3.5 ppm and 3.0 ppm. In contrast, the corresponding resonances for an L-configured Tzn9 appear at about 4.6, 3.4, and 3.1 ppm, respectively.[37] Examination of the ^{1}H resonances of Tzn9 in the two Ala4Cys analogs revealed chemical shifts closely aligned to those of thiostrepton A and our previously reported thiostrepton analogs, which presumably all adopt the D-configuration (Tables D.1 and D.2).[6-7, 34] Collectively, the data suggest that thiostreptons Ala4Cys F1 and F2 are diastereomers differing in the configuration at the α-carbon of the 17th residue, however, their absolute configurations were not determined (Figure 4.4).

In class I lanthipeptide biosynthesis a Ser or Thr residue is first dehydrated by a LanB-dehydratase and then a LanC-cyclase mediates Lan or MeLan ring closure between the dehydrated amino acid and Cys residues.[38] Although no lanthionine cyclase homolog is encoded in the *tsr* cluster, a LanC homolog encoded elsewhere in the *S. laurentii* chromosome that could affect Lan formation for the thiostrepton Ala4Cys analogs cannot be definitively ruled out. Lanthipeptide synthesis has revealed that Lan ring formation from a free cysteine thiol and a dehydrated residue can be readily achieved near physiological pH.[39-40] A nonenzymatic 1,4-addition of the Cys4 thiol to the α,β-unsaturated alkene of Dha17 seems to be the most reasonable explanation for the Lan ring observed in thiostreptons Ala4Cys F1 and F2.

In total, sixteen thiostrepton analogs have been successfully produced from the saturation mutagenesis of TsrA Ala4, however, the titers of these analogs varied significantly (Table F.2). TsrA Ala4 variant peptides with hydrophobic alkyl or linear thioether chains (Ile, Leu, Met, and Val) are well-tolerated by the thiostrepton

biosynthetic system, as suggested by their robust production titers (> 40 mg/L) compared to that of wild-type thiostrepton A (115 ± 35 mg/L). Exchanging Ala4 of TsrA with a β-heteroatom-containing residue also enables maturation of the precursor peptide to a thiostrepton at a reasonable overall quantity. TsrA Ala4Ser and Ala4Thr were efficiently channeled to thiopeptide derivatives dehydrated at the engineered site whereas the Ala4Cys metabolites detected suggest that this residue largely escaped posttranslational processing by the thiopeptide cyclodehydratase. When the polar residues Asn, Gln, and His are used to replace Ala4, the anticipated thiostrepton analogs are generated, but these species were produced at levels ranging from abundant (near 40 mg/L for Asn) to relatively impaired (< 5 mg/L for Gln and His). Likewise, substitution of Ala4 with the aromatic residues Phe, Trp, and Tyr only supported analog production reduced nearly 40-fold from wild-type thiostrepton A, suggesting that, while permitted, aromatic residues at the fourth residue are not favored by the collective thiostrepton biosynthetic machinery. In contrast, TsrA core peptides bearing a positively or negatively charged residue (Arg, Lys, Asp, and Glu) or Pro at the fourth position were not transformed into a mature thiopeptide. At this time, it is not known which step(s) contribute(s) to low or failed thiostrepton analog production, and it is certainly possible that multiple enzymes are not able to efficiently accommodate the alternate substrates.

4.3.3 Aqueous solubility of the thiostrepton Ala4 analogs

One of the goals behind the biosynthetic engineering of thiostrepton variants is to enable development of analogs with improved aqueous solubility while retaining the desired bioactivity. The thiostrepton analogs prepared here were therefore assessed for their kinetic solubilities, a method widely used in the prescreening process during drug

development, to inform on any trends within this family of derivatives.[41] As expected, the polar side chains introduced into thiostreptons Ala4Asn, Ala4Gln, and Ala4Ser contributed to slightly improved aqueous solubilities compared to thiostrepton A, and the loss of the methyl side chain in thiostrepton Ala4Gly also led to a moderate improvement (Table 4.1). Not surprisingly, analogs bearing aromatic or hydrophobic alkyl chains at the fourth residue exhibited reduced water solubility compared to the parent compound, consistent with the decreased polarity of the introduced side chains relative to the Ala methyl group. These data suggested that the identity of the fourth residue can indeed influence the solubility of a corresponding thiostrepton derivative.

Table 4.1. Water solubility of thiostrepton analogs

Compound	Water solubility (μM)
Thiostrepton A	8.10 ± 0.24
Ala4Asn	12.28 ± 0.46
Ala4Cys F1	8.16 ± 0.87
Ala4Cys F2	11.02 ± 0.21
Ala4Dha	7.38 ± 0.53
Ala4Dhb	6.61 ± 0.21
Ala4Gln	10.70 ± 0.26
Ala4Gly	11.78 ± 0.87
Ala4His	7.06 ± 0.16
Ala4Ile	2.22 ± 0.29
Ala4Leu	1.51 ± 0.15
Ala4Met	0.59 ± 0.11
Ala4Phe	1.37 ± 0.06
Ala4Ser	10.36 ± 0.27
Ala4Trp	0.19 ± 0.04
Ala4Tyr	0.84 ± 0.08
Ala4Val	1.84 ± 0.22
Thr7Ala	19.29 ± 0.80
SL105-1	6.17 ± 1.70
Thr7Val	17.61 ± 1.82
SL106-1	11.01 ± 0.87

4.3.4 Antibacterial activities of the thiostrepton analogs

The antibacterial activities of the purified thiostrepton Ala4 variants were evaluated using a previously described liquid microdilution method.[6-7] When Ala4 is

substituted by nonpolar aliphatic or aromatic amino acids, the resulting thiostrepton analogs showed minimum inhibitory concentrations (MICs) comparable to the values for thiostrepton A against three indicator strains of *Staphylococcus aureus*, *Bacillus* sp. and *Enterococcus faecium* (Table 4.2). The antibacterial activities of thiostreptons Ala4His, Ala4Ser, Ala4Dha, and Ala4Dhb decreased moderately by approximately 10 to 50-fold, whereas the amide side-chain containing Ala4Asn and Ala4Gln variants were reduced in activity between 100 to 300-fold. Among all the Ala4 analogs tested, thiostreptons Ala4Cys F1 and F2 suffered the greatest impairments in their MIC values, by as much as 300-fold. Neither thiostrepton A nor its Ala4 variants displayed any antibacterial activity against the *E. coli* indicator strain ATCC 27856 (Data not shown).

Table 4.2. Antibacterial activities of thiostrepton analogs

Compound	MIC[a] (μg/mL)		
	MRSA[b]	VRE[c]	*Bacillus*[d]
Thiostrepton A	0.012	0.012	0.025
Ala4Asn	1.6	3.3	3.3
Ala4Cys F1	>3.4	>3.4	>3.4
Ala4Cys F2	>3.4	>3.4	>3.4
Ala4Dha	0.10	0.20	0.40
Ala4Dhb	0.25	0.25	0.50
Ala4Gln	1.3	2.7	2.7
Ala4Gly	0.12	0.12	0.46
Ala4His	0.16	0.43	1.30
Ala4Ile	0.026	0.026	0.013
Ala4Leu	0.015	0.015	0.029
Ala4Met	0.014	0.014	0.029
Ala4Phe	0.013	0.013	0.013
Ala4Ser	0.42	0.21	1.04
Ala4Trp	0.014	0.007	0.014
Ala4Tyr	0.028	0.007	0.055
Ala4Val	0.015	0.015	0.015
Thr7Ala	>3.4	>3.4	>3.4
SL105-1	>3.4	>3.4	>3.4
Thr7Val	>3.4	>3.4	>3.4
SL106-1	>3.4	>3.4	>3.4
Vancomycin	0.39	ND[e]	ND
Chloramphenicol	ND	3.9	0.98

[a] Minimum inhibitory concentration.
[b] *Staphylococcus aureus* ATCC 10537.
[c] *Enterococcus faecium* ATCC 12952.
[d] *Bacillus* sp. ATCC 27859.
[e] Not determined.

The observed loss of antibacterial activity could be due to either a diminished capacity of the newly generated analogs to bind the target ribosomal site, or instead be caused by off-target effects, such as cell permeability or metabolite stability. To distinguish between these possibilities and to more directly assess the inhibition of protein synthesis by the thiopeptide derivatives, a coupled *in vitro* transcription-translation assay was employed using a luciferase reporter system and the translation inhibition curves are shown in Figure G.2. Surprisingly, all thiostrepton Ala4 derivatives revealed half-maximal inhibitory concentrations (IC_{50}'s) against *in vitro* protein synthesis comparable to that of the parent compound, thiostrepton A (Table 4.3). The IC_{50} for the Ala4Trp variant could not be measured due to solubility limitation; however, its MIC values against the indicator strains suggest that binding of this analog to the ribosome is not dramatically affected (Tables 4.2 and 4.3).

Table 4.3. *In vitro* translation inhibition by thiostrepton analogs

Compound	IC_{50} (μM)
Thiostrepton A	0.63 ± 0.01
Ala4Asn	0.64 ± 0.01
Ala4Cys F1	0.66 ± 0.03
Ala4Cys F2	0.64 ± 0.01
Ala4Dha	0.44 ± 0.02
Ala4Dhb	0.69 ± 0.02
Ala4Gln	0.41 ± 0.01
Ala4Gly	0.44 ± 0.02
Ala4His	0.35 ± 0.02
Ala4Ile	0.49 ± 0.02
Ala4Leu	0.50 ± 0.04
Ala4Met	0.33 ± 0.01
Ala4Phe	0.67 ± 0.01
Ala4Ser	0.71 ± 0.05
Ala4Trp	> 0.19[a]
Ala4Tyr	0.56 ± 0.02
Ala4Val	0.32 ± 0.01
Thr7Ala	> 19[a]
SL105-1	> 6[a]
Thr7Val	> 17[a]
SL106-1	> 11[a]

[a] IC_{50} not determined due to solubility limitation.

To rule out any non-specific inhibition of the *in vitro* transcription-translation system by the thiostrepton scaffold, four Thr7 variants were examined, and the aqueous solubilities of these analogs are included in Table 4.1. The unmodified threonine residue is highly conserved among ribosome-binding thiopeptides and it is expected to contribute key interactions for inhibition of translation.[3, 42-43] An earlier mutagenesis effort confirmed that thiostreptons Thr7Ala, Thr7Val, and the corresponding shunt metabolites lacking an intact QA loop, SL105-1 and SL106-1 (for shunt metabolite structures, see Figure D.45), were substantially diminished in their abilities to inhibit bacterial growth (Table 4.2).[7] Consistent with their poor MIC values, the abilities of the Thr7 analogs to inhibit *in vitro* protein synthesis was also abrogated (Table 4.3). Collectively, the bacterial growth and protein synthesis inhibition assays indicate that the identity of the fourth residue within the architecture of thiostrepton is not critical for ribosome binding, but may impact other factors key to potent *in vivo* activity, such as cell membrane permeability or metabolic stability. The X-ray crystal structure of thiostrepton A bound to the large ribosomal subunit reveals a solvent-exposed Ala4 residue that does not engage in any contacts with the ribosome.[3, 7] This positioning of the fourth residue may explain the *in vitro* activity of thiostreptons presenting an assortment of modifications at this site.

4.3.5 Structural modeling of thiostrepton Ala4Cys analogs

Although the *in vitro* activity of most thiostrepton Ala4 analogs could be rationalized from structure-based knowledge of thiopeptide-ribosome interactions, it is less obvious how thiostreptons Ala4Cys F1 and F2, containing a third macrocycle, preserve their abilities to inhibit protein synthesis. To explain the apparent inconsistency between the *in vivo* and *in vitro* experiments, we modeled the *R* and *S* stereoisomers at

Ala17 α-carbon of the two Ala4Cys analogs into the 50S ribosome, adapting the reported crystal structure in which thiostrepton A is bound.[3] Figure 4.5 shows a view of thiostrepton A complexed to the ribosome and the interactions proposed between the thiostrepton Ala4Cys analogs and the ribosome. Based on these models, the core macrocycle and QA-containing loops of thiostrepton A and its analogs are expected to adopt similar overall conformations (Figures 4.5 and D.46). In thiostrepton A, the Thr7 hydroxyl group contributes to the thiopeptide fold by participating in a hydrogen bond with the quinaldic acid 9-OH.[33] This hydrogen bond appears to be maintained in the models for the Ala4Cys analogs, as the distances between the Thr7 and quinaldic acid hydroxyl groups remain within hydrogen bonding distances, at 2.8 and 2.9 Å in the *R*-form and *S*-form variants, respectively (Figure D.46).

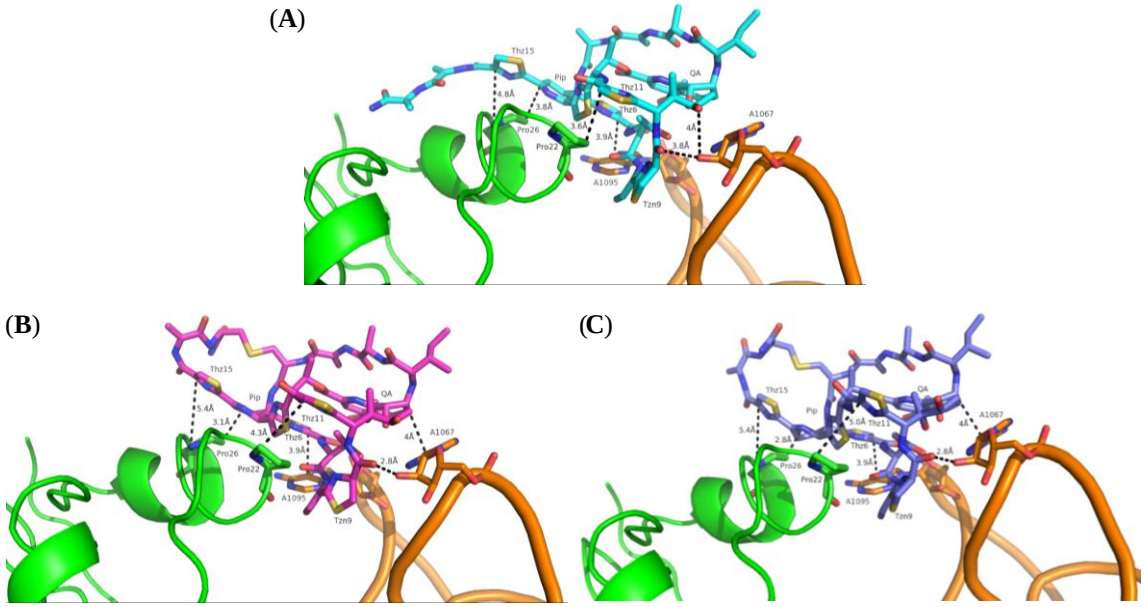

Figure 4.5. Thiostrepton A, Ala4Cys F1 and Ala4Cys F2 bound to the ribosome. (**A**) Thiostrepton A (Cyan) bound to the ribosome adapted from PDB 3CF5.[3] (**B**) Thiostrepton Ala4Cys with the *R* configuration at the α-carbon of the 17th residue (magenta) modeled into the ribosome. (**C**) Thiostrepton Ala4Cys with the *S* configuration at the α-carbon of the 17th residue (blue) modeled into the ribosome. Helices 43 and 44 of 23S rRNA are colored in orange and ribosomal protein L11 is shown in green.

In addition, Thr7 of the three thiostreptons contact the N1 of A1095 of 23S rRNA similarly (within 5 Å) in both the reported X-ray crystal structure and the modeled structures (Figure 4.5).[44] When thiostrepton A binds to the ribosome Thz11 and Thz15 approach Pro22 and Pro26 of L11, respectively, and appear to contribute hydrophobic interactions (Figure 4.5A).[3] In the structures modeled for the Ala4Cys variants, Thz11 and Thz15 move away from the two L11 prolines, while the dehydropiperidine ring (Pip) approaches Pro26 and may provide a compensating hydrophobic interaction for the complex (Figures 4.5B and 4.5C). More importantly, the carbonyl of Tzn9 in the Ala4Cys variants are now within hydrogen bonding distance (2.8 Å) to the A1067 2'-OH of 23S rRNA, an interaction not observed in the crystal structure of thiostrepton A bound to the ribosome due to the greater distance between the two groups (3.8 Å) (Figure 4.5).[3] In addition, the stacking interaction between Thz6 and A1095 as seen in the original complex is retained in the modeled structures.[3] The quinaldic acid moiety of the thiostrepton Ala4Cys analogs appears to remain close to A1067 to provide a hydrophobic interaction as reported previously for the parent thiopeptide.[3] Overall, the major binding interactions between the wild-type thiostrepton A and the ribosome are expected to be conserved in the modeled structures for the two Ala4Cys variants, in addition to a new hydrogen bond. As a result, these interactions may justify the retained *in vitro* translation inhibition efficacy of the thiostrepton Ala4Cys analogs.

4.3.6 20S proteasome inhibitory activities of the thiostrepton analogs

The 20S proteasome is a multi-subunit complex that plays a key role in eukaryotic protein degradation.[45] Different proteolytic activities (trypsin-, chymotrypsin-, and caspase-like) are conferred by three distinct types of β-subunits, and most reported

nonpeptidic molecules inhibit the chymotrypsin-like activity.[45] A prior investigation by Arndt and coworkers revealed that thiostrepton A displays 20S proteasome inhibitory properties.[46] The thiostrepton analogs described here were tested for their abilities to inhibit the 20S proteasome using fluorogenic substrates for all three proteolytic functions. One sample calculation for the IC_{50} values is included in Figure G.1 and the proteasome inhibition curves are shown in Figure G.3. Overall, the identity of the fourth residue of the thiostrepton scaffold does not appear to be absolutely critical for proteasome inhibition, since the IC_{50} values for most of the thiostrepton Ala4 analogs are comparable to that of thiostrepton A (Table 4.4).

Table 4.4. Inhibition of 20S proteasome activities by thiostrepton analogs

Compound	IC_{50} Trypsin-like [μM]	IC_{50} Chymotrypsin-like [μM]	IC_{50} Caspase-like [μM]
Thiostrepton A	0.95 ± 0.15	1.02 ± 0.12	0.59 ± 0.06
Ala4Asn	0.38 ± 0.06	0.89 ± 0.17	0.86 ± 0.14
Ala4Cys F1	1.75 ± 0.23	1.54 ± 0.18	0.32 ± 0.03
Ala4Cys F2	0.83 ± 0.05	1.38 ± 0.23	0.70 ± 0.06
Ala4Dha	2.46 ± 0.43	2.73 ± 0.20	2.43 ± 0.30
Ala4Dhb	0.29 ± 0.03	0.25 ± 0.02	0.28 ± 0.02
Ala4Gln	> 10.7[a]	4.19 ± 0.48	0.31 ± 0.02
Ala4Gly	0.41 ± 0.05	0.77 ± 0.04	0.48 ± 0.04
Ala4His	0.51 ± 0.09	0.76 ± 0.15	0.53 ± 0.03
Ala4Ile	0.24 ± 0.05	0.27 ± 0.03	0.20 ± 0.04
Ala4Leu	0.34 ± 0.04	0.53 ± 0.02	0.31 ± 0.03
Ala4Met	> 0.59[a]	> 0.59[a]	0.46 ± 0.05
Ala4Phe	0.24 ± 0.03	0.37 ± 0.09	0.27 ± 0.05
Ala4Ser	0.39 ± 0.03	1.11 ± 0.06	0.40 ± 0.06
Ala4Trp	> 0.19[a]	> 0.19[a]	> 0.19[a]
Ala4Tyr	0.25 ± 0.02	0.63 ± 0.09	0.36 ± 0.03
Ala4Val	0.59 ± 0.04	0.49 ± 0.03	0.18 ± 0.03
Thr7Ala	0.71 ± 0.07	0.57 ± 0.05	0.28 ± 0.04
SL105-1	0.77 ± 0.12	0.77 ± 0.12	0.56 ± 0.09
Thr7Val	1.33 ± 0.27	5.38 ± 0.97	1.68 ± 0.19
SL106-1	> 11[a]	6.30 ± 0.95	6.72 ± 0.40
Bortezomib	1.62 ± 0.20	0.005 ± 0.001	0.049 ± 0.003

[a]IC_{50} not determined due to solubility limitation.

The inhibitory properties of thiostreptons Ala4Met and Ala4Trp could not be fully addressed due to solubility limitations; however, the Ala4Met variant did retain anti-caspase activity (Table 4.4). Aside from these two variants, thiostrepton Ala4 analogs

bearing an unmodified side chain, with the exception of thiostrepton Ala4Gln, are associated with similar or slightly enhanced abilities to inhibit the three proteolytic activities of the proteasome. The potencies of thiostrepton Ala4Gln against the chymotrypsin and trypsin-like functions were somewhat impaired relative to the parent compound, reduced by 4-and at least 11-fold, respectively, but this analog did reveal about a 2-fold improvement in inhibition of the caspase-like activity of the proteasome (Table 4.4). Modifications introduced at the fourth residue side chain, present in the Ala4Dha, Ala4Dhb, and the Ala4Cys variants, also do not contribute to any dramatic change in proteasome inhibition, as the IC_{50} values for this subset of analogs remained within a 5-fold range relative to that of thiostrepton A (Table 4.4). Semisynthetic thiostrepton A derivatives, including those with modifications to the C-terminus and an aromatic thiazole in the core macrocycle in lieu of the more reduced thiazoline (position 9), are reported to retain their proteasome inhibitory activities, and, like the parent analog, several exhibit a bias against the caspase-like activity.[46] Likewise, our current study revealed thiostrepton Ala4 analogs also tend to demonstrate a more pronounced effect on caspase-like function. These results suggest that thiostrepton A and its analogs either adopt differing binding modes to the individual β-subunits or may instead allosterically modulate 20S proteasome activity.

The thiostrepton Thr7 variants and their two shunt metabolites were also evaluated as 20S proteasome inhibitors. Unlike its key role for ribosome binding, a residue with hydrogen bonding capability at the seventh position of thiostrepton A does not appear to be obligatory in order to disrupt proteasome function.[7] Both thiostrepton Thr7 variants retained activity against the proteasome, with the inhibitory properties of

thiostrepton Thr7Ala slightly enhanced and those of thiostrepton Thr7Val reduced relative to the wild-type metabolite (Table 4.4). Previously, it was demonstrated that a thiostrepton A derivative in which the ester bond connecting Thr12 to the QA moiety was opened *via* methanolysis resulted in a less effective proteasome inhibitor, as the IC_{50} against caspase-like activity increased over 10-fold.[46] Our current study reinforces this observation: the analogs SL105-1 and SL106-1 (structures shown in Figure D.45), lacking the intact QA loop, yet conserving thiostrepton's ester linkage between Thr12 and QA, still act as proteasome inhibitors, albeit with decreased efficacy for the Thr7Val derivative SL106-1 (Table 4.4). Thiostrepton A and siomycin A (Figure 4.1), both series *b* thiopeptides containing a QA-containing loop, are active proteasome inhibitors, whereas series *d* thiopeptides lacking this additional macrocycle, such as micrococcin P_1 and thiocillin I (Figure 4.1), have not revealed any proteasome inhibitory properties.[1, 47] It appears that the QA macrocycle is indeed important for a thiopeptide's inhibitory activity and that the proper orientation of the QA moiety may contribute to binding interactions with the proteasome, as the analogs lacking an intact QA loop do vary in their IC_{50} values. Before a comprehensive understanding of thiopeptide-based proteasome inhibition can be developed, structural studies are required to provide the molecular details into how thiostrepton A binds to the 20S proteasome and to rationalize the varied activities for the thiostrepton analogs reported thus far.

4.4 Conclusions

The realization of the ribosomal origins for thiostrepton prompted us to explore biosynthetic engineering as a way to generate thiostrepton analogs inaccessible by

semisynthetic modification alone. Saturation mutagenesis at the fourth position of the TsrA core peptide has been performed, successfully generating sixteen thiostrepton analogs. To our knowledge, this is the first report that thoroughly probed the permissiveness of the collective biosynthetic machinery toward modifications to the fourth residue in the quinaldic acid loop of a series *b* thiopeptide, substituting the parent alanine residue with the remaining 19 proteinogenic amino acid residues. The *in vitro* inhibition assays of the Ala4 variants reveal that the fourth residue of this thiopeptide is not essential for binding either the ribosome or the proteasome. The wide range of thiostrepton analogs that retain the ability to complex with the ribosome or the proteasome, including Ala4Dha, Ala4Dhb, and Ala4Ser, provide promise for coupling that engineered site to semisynthetic modification to acquire a biologically active analog with enhanced water solubility. Such a strategy could also facilitate the inclusion of an affinity tag or a fluorescent label to probe the mechanism of action, which is currently unknown, when thiostrepton A is bound to the proteasome. Modifications to the C-terminal tail region of thiostrepton A and other thiopeptides, often by conjugate addition to a dehydroalanine residue, have been utilized to increase water solubility through the introduction of polar side chains.[15, 46, 48-50] These and other semi-synthetic modifications of a thiopeptide scaffold, when introduced at an amenable position, can be broadly accepted with retained antibacterial or antimalarial potencies. The results described here support further examination of the quinaldic acid-containing macrocycle of thiostrepton A and related thiopeptides to generate novel analogs for potential clinical applications.

4.5 References

1. Bhat, U. G.; Halasi, M.; Gartel, A. L., Thiazole antibiotics target FoxM1 and induce apoptosis in human cancer cells. *PLoS One* **2009,** *4*, e5592.

2. Clough, B.; Strath, M.; Preiser, P.; Denny, P.; Wilson, I. R., Thiostrepton binds to malarial plastid rRNA. *FEBS Lett.* **1997,** *406*, 123-125.

3. Harms, J. M.; Wilson, D. N.; Schluenzen, F.; Connell, S. R.; Stachelhaus, T.; Zaborowska, Z.; Spahn, C. M. T.; Fucini, P., Translational regulation via L11: molecular switches on the ribosome turned on and off by thiostrepton and micrococcin. *Molecular cell* **2008,** *30*, 26-38.

4. McConkey, G. A.; Rogers, M. J.; McCutchan, T. F., Inhibition of *Plasmodium falciparum* protein synthesis. Targeting the plastid-like organelle with thiostrepton. *J. Biol. Chem.* **1997,** *272*, 2046-2049.

5. Bagley, M. C.; Dale, J. W.; Merritt, E. A.; Xiong, X., Thiopeptide antibiotics. *Chem. Rev.* **2005,** *105*, 685-714.

6. Li, C.; Zhang, F.; Kelly, W. L., Heterologous production of thiostrepton A and biosynthetic engineering of thiostrepton analogs. *Mol. Biosyst.* **2011,** *7*, 82-90.

7. Li, C.; Zhang, F.; Kelly, W. L., Mutagenesis of the thiostrepton precursor peptide at Thr7 impacts both biosynthesis and function. *Chem. Commun.* **2012,** *48*, 558-560.

8. Wright, F.; Bibb, M. J., Codon usage in the G+C-rich *Streptomyces* genome. *Gene* **1992,** *113*, 55-65.

9. Datsenko, K. A.; Wanner, B. L., One-step inactivation of chromosomal genes in *Escherichia coli* K-12 using PCR products. *Proc. Natl. Acad. Sci. U.S.A.* **2000,** *97*, 6640-6645.

10. Gust, B.; Challis, G. L.; Fowler, K.; Kieser, T.; Chater, K. F., PCR-targeted *Streptomyces* gene replacement identifies a protein domain needed for biosynthesis of the sesquiterpene soil odor geosmin. *Proc. Natl. Acad. Sci. U.S.A.* **2003,** *100*, 1541-1546.

11. Kieser, T.; Bibb, M. J.; Buttner, M. J.; Chater, K. F.; Hopwood, D. A., *Practical Streptomyces Genetics* The John Innes Foundation: Norwich, England, 2000.

12. Kelly, W. L.; Pan, L.; Li, C., Thiostrepton biosynthesis: Prototype for a new family of bacteriocins. *J. Am. Chem. Soc.* **2009,** *131*, 4327-4334.

13. Priestley, N. D.; Smith, T. M.; Shipley, P. R.; Floss, H. G., Studies on the biosynthesis of thiostrepton: 4-(1-hydroxyethyl)quinoline-2-carboxylate as a free intermediate on the pathway to the quinaldic acid moiety. *Bioorg. Med. Chem.* **1996,** *4*, 1135-1147.

14. Nicolaou, K. C.; Zak, M.; Safina, B. S.; Estrada, A. A.; Lee, S. H.; Nevalainen, M., Total synthesis of thiostrepton. Assembly of key building blocks and completion of the synthesis. *J. Am. Chem. Soc.* **2005,** *127*, 11176-11183.

15. Schoof, S.; Baumann, S.; Ellinger, B.; Arndt, H. D., A fluorescent probe for the 70 S-ribosomal GTPase-associated center. *ChemBioChem* **2009,** *10*, 242-245.

16. Bausch, S. L.; Poliakova, E.; Draper, D. E., Interactions of the N-terminal domain of ribosomal protein L11 with thiostrepton and rRNA. *J. Biol. Chem.* **2005,** *280*, 29956-29963.

17. Ryan, P. C.; Lu, M.; Draper, D. E., Recognition of the highly conserved GTPase center of 23 S ribosomal RNA by ribosomal protein L11 and the antibiotic thiostrepton. *J. Mol. Biol.* **1991,** *221*, 1257-1268.

18. Cousins, K. R., Computer review of ChemDraw Ultra 12.0. *J Am Chem Soc* **2011,** *133*, 8388.

19. Allinger, N. L., Conformational analysis. 130. MM2. A hydrocarbon force field utilizing V1 and V2 torsional terms. *J. Am. Chem. Soc.* **1977,** *99*, 8127-8134.

20. DeLano, W. L. *The PyMOL Molecular Graphics System*, The PyMol Molecular Graphics System, Version 1.5.0.4 Schrödinger, LLC.; DeLano Scientific, CA, USA.: **2002**.

21. Zhang, F.; Kelly, W. L., *In vivo* production of thiopeptide variants. *Methods Enzymol.* **2012,** *516*, 3-24.

22. Garg, N.; Salazar-Ocampo, L. M.; van der Donk, W. A., In vitro activity of the nisin dehydratase NisB. *Proc. Natl. Acad. Sci. U.S.A.* **2013,** *110*, 7258-7263.

23. Goto, Y.; Li, B.; Claesen, J.; Shi, Y.; Bibb, M. J.; van der Donk, W. A., Discovery of unique lanthionine synthetases reveals new mechanistic and evolutionary insights. *PLoS Biol.* **2010,** *8*, e1000339.

24. Goto, Y.; Okesli, A.; van der Donk, W. A., Mechanistic studies of Ser/Thr dehydration catalyzed by a member of the LanL lanthionine synthetase family. *Biochemistry* **2011,** *50*, 891-898.

25. Bierbaum, G.; Szekat, C.; Josten, M.; Heidrich, C.; Kempter, C.; Jung, G.; Sahl, H. G., Engineering of a novel thioether bridge and role of modified residues in the lantibiotic Pep5. *Appl. Environ. Microbiol.* **1996,** *62*, 385-392.

26. Kuipers, O. P.; Rollema, H. S.; Yap, W. M.; Boot, H. J.; Siezen, R. J.; de Vos, W. M., Engineering dehydrated amino acid residues in the antimicrobial peptide nisin. *J. Biol. Chem.* **1992,** *267*, 24340-24346.

27. Rink, R.; Wierenga, J.; Kuipers, A.; Kluskens, L. D.; Driessen, A. J.; Kuipers, O. P.; Moll, G. N., Production of dehydroamino acid-containing peptides by *Lactococcus lactis*. *Appl. Environ. Microbiol.* **2007,** *73*, 1792-1796.

28. Molloy, E. M.; Field, D.; PM, O. C.; Cotter, P. D.; Hill, C.; Ross, R. P., Saturation mutagenesis of lysine 12 leads to the identification of derivatives of nisin A with enhanced antimicrobial activity. *PLoS One* **2013,** *8*, e58530.

29. Rink, R.; Kuipers, A.; de Boef, E.; Leenhouts, K. J.; Driessen, A. J.; Moll, G. N.; Kuipers, O. P., Lantibiotic structures as guidelines for the design of peptides that can be modified by lantibiotic enzymes. *Biochemistry* **2005,** *44*, 8873-8882.

30. Puar, M. S.; Chan, T. M.; Hegde, V.; Patel, M.; Bartner, P.; Ng, K. J.; Pramanik, B. N.; MacFarlane, R. D., Sch 40832: a novel thiostrepton from *Micromonospora carbonacea*. *J. Antibiot.* **1998,** *51*, 221-224.

31. Bowers, A. A.; Acker, M. G.; Young, T. S.; Walsh, C. T., Generation of thiocillin ring size variants by prepeptide gene replacement and in vivo processing by *Bacillus cereus*. *J. Am. Chem. Soc.* **2012,** *134*, 10313-10316.

32. Chatterjee, C.; Paul, M.; Xie, L.; van der Donk, W. A., Biosynthesis and mode of action of lantibiotics. *Chem. Rev.* **2005,** *105*, 633-683.

33. Bond, C. S.; Shaw, M. P.; Alphey, M. S.; Hunter, W. N., Structure of the macrocycle thiostrepton solved using the anomalous dispersion contribution of sulfur. *Acta Crystallogr. D Biol. Crystallogr.* **2001,** *57*, 755-758.

34. Mocek, U.; Beale, J. M.; Floss, H. G., Reexamination of the ^{1}H and ^{13}C NMR spectral assignments of thiostrepton. *J. Antibiot.* **1989,** *42*, 1649-1652.

35. van de Kamp, M.; van den Hooven, H. W.; Konings, R. N.; Bierbaum, G.; Sahl, H. G.; Kuipers, O. P.; Siezen, R. J.; de Vos, W. M.; Hilbers, C. W.; van de Ven, F. J., Elucidation of the primary structure of the lantibiotic epilancin K7 from Staphylococcus epidermidis K7. Cloning and characterisation of the epilancin-K7-encoding gene and NMR analysis of mature epilancin K7. *Eur J Biochem* **1995,** *230*, 587-600.

36. Chan, W. C.; Bycroft, B. W.; Leyland, M. L.; Lian, L. Y.; Yang, J. C.; Roberts, G. C., Sequence-specific resonance assignment and conformational analysis of subtilin by 2D NMR. *FEBS Lett* **1992,** *300*, 56-62.

37. Schoof, S.; Arndt, H. D., D-cysteine occurrence in thiostrepton may not necessitate an epimerase. *Chem. Commun.* **2009**, 7113-7115.

38. Chatterjee, C.; Paul, M.; Xie, L.; van der Donk, W. A., Biosynthesis and mode of action of lantibiotics. *Chem. Rev.* **2005,** *105*, 633-683.

39. Okeley, N. M.; Zhu, Y.; van der Donk, W. A., Facile chemoselective synthesis of dehydroalanine-containing peptides. *Org. Lett.* **2000,** *2*, 3603-3606.

40. Burrage, S.; Raynham, T.; Williams, G.; Essex, J. W.; Allen, C.; Cardno, M.; Swali, V.; Bradley, M., Biomimetic synthesis of lantibiotics. *Chemistry* **2000,** *6*, 1455-1466.

41. Lipinski, C. A.; Lombardo, F.; Dominy, B. W.; Feeney, P. J., Experimental and computational approaches to estimate solubility and permeability in drug discovery and development settings. *Adv. Drug Deliv. Rev.* **2001,** *46*, 3-26.

42. Jonker, H. R.; Baumann, S.; Wolf, A.; Schoof, S.; Hiller, F.; Schulte, K. W.; Kirschner, K. N.; Schwalbe, H.; Arndt, H. D., NMR structures of thiostrepton derivatives for characterization of the ribosomal binding site. *Angew. Chem. Int. Ed. Engl.* **2011,** *50*, 3308-3312.

43. Lentzen, G.; Klinck, R.; Matassova, N.; Aboul-ela, F.; Murchie, A. I. H., Structural basis for contrasting activities of ribosome binding thiazole antibiotics. *Chemistry & biology* **2003,** *10*, 769-778.

44. Harms, J. M.; Wilson, D. N.; Schluenzen, F.; Connell, S. R.; Stachelhaus, T.; Zaborowska, Z.; Spahn, C. M.; Fucini, P., Translational regulation via L11: Molecular switches on the ribosome turned on and off by thiostrepton and micrococcin. *Mol. Cell.* **2008,** *30*, 26-38.

45. Borissenko, L.; Groll, M., 20S proteasome and its inhibitors: Crystallographic knowledge for drug development. *Chem. Rev.* **2007,** *107*, 687-717.

46. Schoof, S.; Pradel, G.; Aminake, M. N.; Ellinger, B.; Baumann, S.; Potowski, M.; Najajreh, Y.; Kirschner, M.; Arndt, H. D., Antiplasmodial thiostrepton derivatives: proteasome inhibitors with a dual mode of action. *Angew. Chem. Int. Ed. Engl.* **2010,** *49*, 3317-3321.

47. Pandit, B.; Bhat, U. G.; Gartel, A. L., Proteasome inhibitory activity of thiazole antibiotics. *Cancer Biol. Ther.* **2011,** *11*, 43-47.

48. Aminake, M. N.; Schoof, S.; Sologub, L.; Leubner, M.; Kirschner, M.; Arndt, H. D.; Pradel, G., Thiostrepton and derivatives exhibit antimalarial and gametocytocidal activity by dually targeting parasite proteasome and apicoplast. *Antimicrobial agents and chemotherapy* **2011,** *55*, 1338-1348.

49. Myers, C. L.; Hang, P. C.; Ng, G.; Yuen, J.; Honek, J. F., Semi-synthetic analogues of thiostrepton delimit the critical nature of tail region modifications in the control of protein biosynthesis and antibacterial activity. *Bioorg. Med. Chem.* **2010,** *18*, 4231-4237.

50. Naidu, B. N.; Sorenson, M. E.; Matiskella, J. D.; Li, W.; Sausker, J. B.; Zhang, Y.; Connolly, T. P.; Lam, K. S.; Bronson, J. J.; Pucci, M. J.; Yang, H.; Ueda, Y., Synthesis and antibacterial activity of nocathiacin I analogues. *Bioorg. Med. Chem. Lett.* **2006,** *16*, 3545-3549.

CHAPTER 5: SATURATION MUTAGENESIS OF TSRA ALA2 LED TO THE PRODUCTION OF THIOSTREPTON ANALOGS WITH A CONTRACTED QUINALDIC ACID-CONTAINING MACROCYCLE

From the work:

Zhang, F.; Li, C. Kelly, W. L. Saturation mutagenesis of TsrA Ala2 led to the production of thiostrepton analogs with a contracted quinaldic acid-containing macrocycle. **2014,** *In preparation.*

5.1 Introduction

Thiostrepton A (Figure 5.1), a series *b* thiopeptides, is among the thiopeptides that have exhibited antibacterial, antimalarial, and anticancer properties.[1-4] Crystallographic structural studies of thiostrepton A binding to the large ribosome have greatly enhanced researcher's understanding towards the structure-activity relationship (SAR) of this compound for its antibacterial activity.[5] In contrast, far less information is available to illustrate the detailed interactions between thiostrepton A and the 20S proteasome, or FOXM1. In order to rationally design a thiostrepton derivative capable of selectively disrupting the function of a single cellular process, whether prokaryotic or eukaryotic, it will be necessary to decipher the molecular features required to for thiostrepton A's association with each of its major biomolecular targets. Generating thiopeptide analogs could be a useful strategy to overcome not only the solubility problem but also to aid in understanding the SARs for their specific biological activities. Among these efforts, we established a platform to engineer thiostrepton A variants in *S. laurentii*.[6-7] Initially, Ala2 of the TsrA core peptide was replaced by Gly, and this successfully led to the production of a corresponding analog, thiostrepton Ala2Gly, which retained high antibacterial potency.[7] In this study, we further interrogated the promiscuity of the *tsr* biosynthetic

system toward structural modifications of the TsrA core peptide second residue via saturation mutagenesis. The resulting thiostrepton analogs were subsequently evaluated for their water solubilities, antibacterial properties, and inhibition of the 20S proteasome.

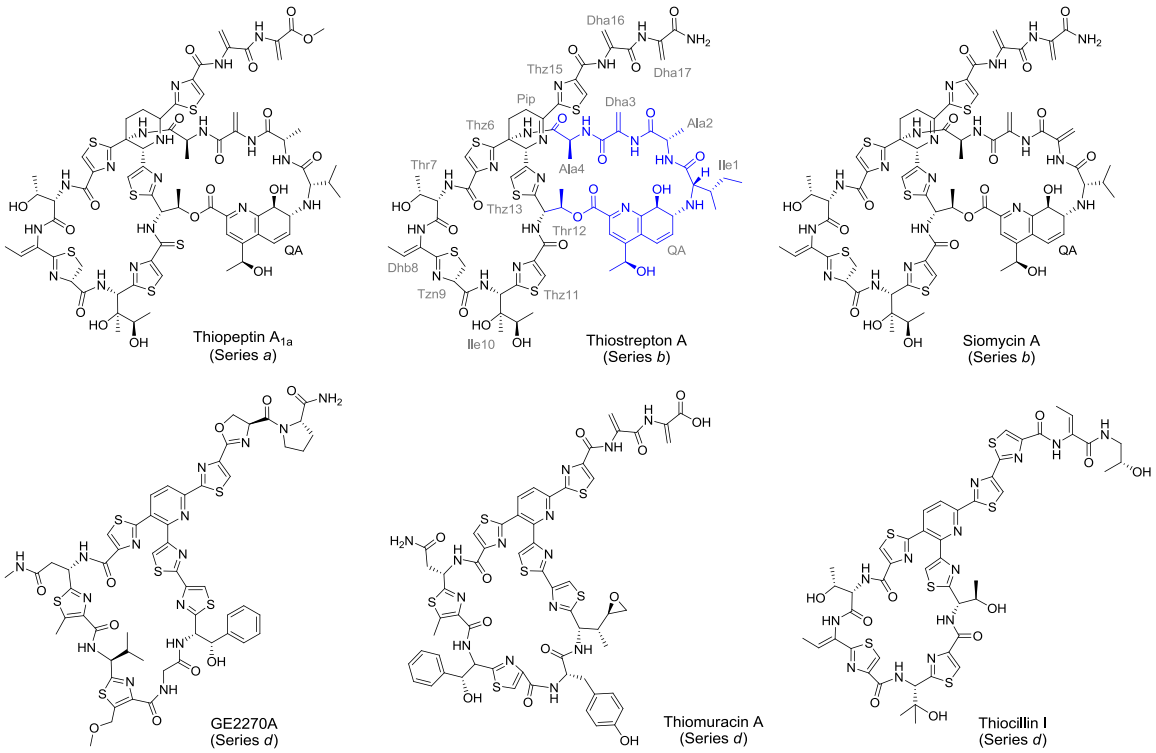

Figure 5.1. Examples of thiopeptides. The thiostrepton A residues are abbreviated using a three-letter code and labeled in blue. The quinaldic acid loop is highlighted in green.

5.2 Materials and Methods

5.2.1 General

Unless otherwise indicated, all chemicals and solvents were purchased from common vendors and used as received. Enzymes and buffers were acquired from New England Biolabs (Beverly, MA). The Wizard® Genomic DNA Purification Kit (Promega, Madison, WI) was used to isolate *Streptomyces* genomic DNA. Isolation of plasmids and fosmids from *E. coli* strains were performed using the QIAprep Spin Miniprep Kit and

DirectPrep 96 MiniPrep Kit from Qiagen (Valencia, CA). PCR products were cloned using the StrataClone Blunt PCR Cloning Kit (Agilent Technologies, La Jolla, CA). 96-well tissue culture plates and 96-well black with clear flat bottom plates were obtained from Becton Dickinson (Franklin Lakes, NJ) and Corning (Tewksbury, MA), respectively. 384-well black plates were purchased from PekinElmer (Waltham, MA). A BioTek H4 Multi-Mode Microplate Reader (Winooski, VT) was used for optical density, fluorescence and luminescence measurements. All oligonucleotides were synthesized by Integrated DNA Technologies (Coralville, IA). DNA sequencing was performed by Eurofins MWG Operon (Huntsville, AL) and sequence analysis was completed using the VectorNTI software package from Invitrogen (Carlsbad, CA).

High performance liquid chromatography (HPLC) analysis was performed on a Beckman Coulter System Gold instrument. High-resolution matrix-assisted laser desorption/ionization mass spectrometry (HR-MALDI-MS) and MALDI-MS/MS were conducted on Applied Biosystems 4700 Proteomics Analyzer at the Georgia Institute of Technology Bioanalytical Mass Spectrometry Facility. High-resolution electrospray ionization mass spectrometry (HR-ESI-MS) was performed on a Thermo LTQ-FTMS at the Emory University Mass Spectrometry Center. High performance liquid chromatography-mass spectrometry (HPLC-MS) was completed on Micromass Quattro LC at the Georgia Institute of Technology Bioanalytical Mass Spectrometry Facility using a Phenomenex Syngeri RP column (250 mm × 2 mm, 4 μm) (Torrance, CA). The column was developed at 0.25 mL/min with 20% solvent B in solvent A for 8 min followed by a gradient from 20 to 100% solvent B over 35 min (solvent A: 5% acetonitrile and 0.1% formic acid in water; solvent B: 5% water and 0.1% formic acid in

acetonitrile). NMR experiments were completed on a Bruker 500 MHz spectrometer according to standard pulse sequences supplied with the instrument at School of Chemistry and Biochemistry, Georgia Institute of Technology.

5.2.2 Bacterial strains, plasmids, and growth medium

Streptomyces laurentii ATCC 31255 (*S. laurentii*), methicillin-resistant *Staphylococcus aureus* ATCC 10537 (MRSA), vancomycin-resistant *Enterococcus faecium* ATCC 12952 (VRE), *Bacillus* sp. ATCC 27859 (*Bacillus*) and *Escherichia coli* (*E. coli*) ATCC 27856 were all purchased from American Type Culture Collection (ATCC). *E. coli* EPI300 was obtained from Epicentre® (Madison, WI). All strains, plasmids, and fosmids are itemized in Table A.1, and primers are listed in Table A.2. All *E. coli* strains were grown in Luria-Bertani liquid or solid medium with the appropriate antibiotic(s). For the selective growth of *E. coli* or *Streptomyces*, the following antibiotics and concentrations were used: apramycin (50 μg/mL), kanamycin (50 μg/mL), ampicillin (100 μg/mL), nalidixic acid (25 μg/mL), and chloramphenicol (12.5 μg/mL). MS agar and ISP3 agar were used for the intergeneric conjugation of *S. laurentii* NDS1 and sporulation of *S. laurentii* strains, respectively.[8]

5.2.3 Engineering of TsrA Ala2 variants in *S. laurentii*

All the work described in this section was performed by Dr. Chaoxuan Li. A synthetic ultramer was designed by containing a degenerate codon (NNS) at the second position of the *tsrA* core peptide-encoding region and regions homologous to fosmid int-3A100. This ultramer provided the template for amplification of mutant *tsrA* genes by polymerase chain reaction (PCR) with the primers Amp-TsrA-SP-F/R. The amplicons

were cloned into pSC-B-amp/kan, and the resulting plasmids were analyzed by DNA sequencing. Plasmids with the *tsrA* inserts containing the highest percentage of synonymous codon usage for *Streptomyces* were chosen as the template for amplification of each mutant *tsrA* gene with the primers Amp-TsrA-SP-F/R.[9] The PCR products were used to substitute the dual-marker disruption cassette in fosmid int-3A100 by PCR-targeted gene replacement in *E. coli* BW25113/pKD46.[8, 10] Fosmids were isolated from the chloramphenicol-sensitive and sucrose-tolerant *E. coli* BW25113 colonies and transformed into *E. coli* EPI300 competent cells to induce high copy numbers of the fosmids. The fosmids were digested by *Eco*RI and samples displaying the same restriction digestion pattern as the control (fosmid int-3A10) were analyzed by DNA sequencing to confirm the allelic replacement of wild-type *tsrA* by an Ala2 mutant of *tsrA*. Mutant int-A2X fosmids were first introduced into *E. coli* ET12567/pUZ8002, and then transformed into *S. laurentii* NDS1 by intergeneric conjugation.[8, 11] Apramycin-resistant colonies were confirmed by PCR using the primers SD3-F/R and DNA sequencing. The engineered *S. laurentii* strains were designated as *S. laurentii* NDS1/int-A2X, according to the introduced mutation.

5.2.4 Evaluation of thiostrepton Ala2 analog production in *S. laurentii*

Dr. Chaoxuan Li carried out the initial fermentations of all *S. laurentii* TsrA Ala2 variants. The fermentations of *S. laurentii* mutant strains were carried out in a three-step process as described previously.[12] First, 50 mL tryptic soy broth (TSB) with apramycin was inoculated with 50 µL of glycerolic mycelium stock of a *S. laurentii* mutant strain and grown at 28 °C and 220 rpm for 24 h in a 250-mL Erlenmeyer flask. Next, 500 µL of the *S. laurentii* preculture was used to inoculate 50 mL seed medium (15 g/L soybean

flour, 50 g/L glucose, 15 g/L soluble starch, pH 7.2) in a 250-mL Erlenmeyer flask. After a 48 h incubation at 28 °C and 220 rpm, 10 mL of the seed culture was used to inoculate 100 mL fermentation medium (11 g/L yeast extract, 50 g/L glucose, 15 g/L TSB, 1 g/L trace elements solution (5 g/L $CoCl_2 \cdot 6H_2O$, 0.5 g/L Na_2MoO_4, 0.5 g/L H_3BO_3, 1.0 g/L $CuSO_4 \cdot 2H_2O$, 1.0 g/L $ZnSO_4 \cdot 7H_2O$)) in a 500-mL Erlenmeyer flask. The fermentation culture was incubated at 28 °C and 220 rpm for 4 days and extracted twice with an equal volume of chloroform. The chloroform layers were pooled together and solvent was removed *in vacuo*. The solid residue was dissolved in 4 mL chloroform for HPLC and HPLC-MS analyses. HPLC analyses of the crude culture extracts were performed using a Phenomenex Luna C18(2) column (250 × 4.6 mm, 5 μm) developed with a gradient of 0 to 100% acetonitrile in water over 30 min at 1 mL/min. Absorbance was monitored at 254 nm.

5.2.5 Purification and mass spectrometry analyses of thiostrepton Ala2 analogs

S. laurentii variant culture extracts were first crystallized as previously described.[13] Briefly, the solid residue of the culture extract was dissolved in a minimum volume of chloroform and mixed with 10 volumes of *n*-hexane followed by centrifugation for 5 min at 4000 rpm (2559 × *g*) and 25 °C. The precipitate was then dissolved in a minimum volume of dichloromethane:ethanol (4:1). Diethyl ether (5 volumes) was added into the sample and the mixture was centrifuged at 4000 rpm (2559 × *g*) for 5 min at 25 °C. The solid residue was dissolved in chloroform:methanol (4:1) and further purified by semi-preparative HPLC using a Phenomenex Luna C18(2) column (250 x 10 mm, 5 μm) with water and acetonitrile, as described below, at 4.3 mL/min while monitoring absorbance at 254 nm.

Purification of thiostreptons Ala2Dha, Ala2Dhb, Ala2Met, Ala2Phe, Ala2Tyr, Ala2Ile-ΔIle1, and Ala2Val-ΔIle1 all utilized the same gradient: acetonitrile was increased from 0% to 100% in water over 30 min. Thiostreptons Ala2Ile-ΔIle1 and Ala2Val-ΔIle1 were subjected to a second round of semi-preparative HPLC purification by holding the mobile phase constant at 40% acetonitrile in water for 10 min. Purified samples were analyzed by HPLC-MS, MALDI-MS/MS, and either HR-ESI-MS or HR-MALDI-MS and stored under argon at -80 °C. Thiostreptons Ala2Dha, Ala2Dhb, Ala2Ile-ΔIle1 and Ala2Val-ΔIle1 were further analyzed by one- and two-dimensional NMR. Mass and NMR spectra are included in Appendix E and Table F.1.

5.2.6 Aqueous solubility of thiostrepton analogs

The kinetic solubilities of thiostrepton A and its analogs were measured as described previously.[14] Briefly, 1 mM DMSO stock solutions of thiostrepton A and its analogs were quantified by their absorbance at 280 nm using an extinction coefficient of 0.027 /(cm μM), assuming similar spectral properties for the compounds.[15] The solution was diluted with buffer (10 mM MOPS, pH 7.0, 5 mM $MgCl_2$, 200 mM KCl, and 5% DMSO) to a nominal concentration of 20 μM. The resulting mixture was incubated at 25 ºC for 2 h, after which time the sample was centrifuged at 14,000 rpm (18,000 × *g*) at 25 ºC for 10 min. The absorbance of the supernatant at 280 nm was used to define the solubility of a thiostrepton analog. Each analysis was performed at least in triplicate.

5.2.7 Antibacterial activity assay

Minimum inhibitory concentrations (MICs) of thiostrepton analogs against different biological indicator strains (MRSA, VRE, *Bacillus*, and *E. coli* ATCC27854) were determined using the liquid microdilution method.[7] Thiostrepton A and its analogs

were prepared in DMSO and quantified as described above. Chloramphenicol was included as the positive antibiotic control for *Bacillus* and VRE, and vancomycin was used as the positive control for MRSA. The negative control in all assays was DMSO. Cell growth was determined by comparing the optical density at 600 nm (OD_{600}) at the time of inoculation and after 18 h incubation at 37 °C. The OD_{600} difference defined growth, and the lowest concentration able to completely inhibit bacterial growth is the MIC.

5.2.8 *In vitro* transcription-translation coupled assay

In vitro transcription-translation coupled assays were completed using the *E. coli* S30 Extract System for Circular DNA and the Luciferase Assay System from Promega (Madison, WI). The experiments were performed according to the manufacturer's protocol, except that the reaction was reduced to a 10 µL volume containing 1 µL amino acid mixture, 4 µL S30 premix, 3 µL S30 *E. coli* extract, 1.25 µL nuclease-free water, 0.25 µL thiostrepton analog, and 0.5 µL pBESTLuc™ template. Thiostrepton A and its analogs were prepared in a range of concentrations in DMSO and quantified as described above. The reactions were incubated at 37 °C for 1 h, at which time 5 µL of the mixture was transferred to a well in a 96-well plate. Luciferase substrate was prepared as recommended by the manufacturer. Immediately before luminescence was measured, 50 µL of the luciferase substrate was added to each well. Relative activity was obtained by normalizing luminescence to that of a DMSO control and plotted against compound concentration. Each assay was performed in triplicate and the half maximal inhibitory concentration (IC_{50}) was calculated for each compound by fitting the data to the Hill equation using GraphPad Prism 5 (La Jolla, CA).

5.2.9 Structural modeling

The crystal structure of the thiostrepton A bound to the *Deinococcus radiodurans* (*D. radiodurans*) ribosome (PDB entry: 3CF5) was used as the template to build the *in silico* models of thiostreptons Ala2Ile-ΔIl1 and Ala2Val-ΔIle1 complexed to the ribosome.[5] Thiostrepton A interacts with helices 43 and 44 (H43/44) of *D. radiodurans* 23S rRNA and ribosomal protein L11. By visual inspection, the local complex structure, including thiostrepton A, H43/44, and L11, was extracted from the entire crystal structure and exported to ChemDraw 3D Ultra 12.0 (CambridgeSoft, Cambridge, U.K.). Thiostreptons Ala2Ile-ΔIl1 and Ala2Val-ΔIle1 were constructed in ChemDraw 3D using the crystal structure of thiostrepton A complexed to the ribosome (PDB entry: 3CF5) as the template.[16] The MM2 forcefield was used to minimize the energy of the two analogs in ChemDraw 3D, keeping the structures of H43/44 and L11 constant during this process.[17] The energy minimized structures of thiostreptons Ala2Ile-ΔIl1 and Ala2Val-ΔIle1 modeled into the local ribosome (containing H43/44 and L11) were visualized using PyMOL.[18]

5.2.10 20S Proteasome inhibition assay

Components used in the 20S proteasome inhibition assay were acquired from Enzo Life Sciences (Farmingdale, NY), including the purified human 20S proteasome and the fluorogenic substrates Boc-Leu-Arg-Arg-AMC, Suc-Leu-Leu-Val-Tyr-AMC, and Ac-Nle-Pro-Nle-Asp-AMC. The proteolytic activities of the 20S proteasome were measured using 7-amino-4-methylcoumarin (AMC)-based fluorogenic substrates: Boc-Leu-Arg-Arg-AMC for trypsin-like activity, Suc-Leu-Leu-Val-Tyr-AMC for chymotrypsin-like activity, and Ac-Nle-Pro-Nle-Asp-AMC for caspase-like activity.

Thiostrepton A and its analogs were prepared in DMSO and quantified as described above. The 20S proteasome was incubated with thiostrepton A or its analog for 15 min at 37 ºC before the addition of the fluorogenic substrate. The assay was performed in a volume of 50 µL in a 384-well plate consisting of: 5 µL thiostrepton analog at different concentrations (typically 0.15-500 µM), 10 µL 1 µg/mL 20S proteasome, 10 µL 50 µM fluorogenic substrate and 25 µL buffer (20 mM Tris-HCl, 1 mM EDTA, pH 7.5). Each analysis was performed at least in triplicate and DMSO was used as a control. Fluorescence was measured using an excitation wavelength of 360 nm and an emission wavelength of 460 nm. Emissions were recorded every 50 s for 1 h and the arbitrary fluorescence units were plotted against time for each compound to acquire the slope of the linear fit. Relative activity, obtained by normalizing the compound slope to the DMSO control slope, was plotted against compound concentration and fit to the Hill equation using GraphPad Prism 5 to calculate IC_{50}.

.

5.3 Results and Discussion

5.3.1 Generation of TsrA Ala2 mutants in *S. laurentii*

A previously developed fosmid-based engineering platform in *S. laurentii* was used as the basis for the saturation mutagenesis of TsrA Ala2 by Dr. Chaoxuan Li.[7] In this system, the core peptide-encoding region of *tsrA* in fosmid int-3A100, an *E. coli-Streptomyces* shuttle fosmid containing the entire *tsr* gene cluster, is substituted with a chloramphenicol resistance gene (chl^R) and a levansucrase-encoding gene (*sacB*).[7] A synthetic DNA ultramer was designed to incorporate the degenerate codon NNS (N refers to any nucleotide, and S refers to G or C) at the second codon of the TsrA core peptide,

providing the basis for the generation of a plasmid library of *tsrA* mutants. Amplicons of each variant *tsrA* gene were used to replace the dual-marker selection cassette in fosmid int-3A100 by λ-RED-mediated recombination.[8, 10] Dr. Chaoxuan Li introduced the mutant fosmids each separately into a *tsrA* deletion mutant of *S. laurentii* (*S. laurentii* NDS1) by intergeneric conjugation to provide 19 *S. laurentii* NDS1/int-A2X variants, including the previously constructed *S. laurentii* NDS1/int-A2G.[7] The introduced mutation is represented by the one-letter amino acid abbreviation "X" and each *S. laurentii* variant strain expresses a different version of TsrA.

5.3.2 Production and characterization of thiostrepton Ala2 analogs

Initial fermentations were performed with all *S. laurentii* TsrA Ala2 mutants and cultures were extracted with chloroform prior to analysis by Dr. Chaoxuan Li. Figure 5.2 includes the structures for anticipated thiostrepton Ala2 analogs. In the crude culture extracts of *S. laurentii* NDS1/int-A2D, A2E, A2H, A2K, A2L, A2N, A2Q, A2R and A2W, either no or only a trace amount of mature thiostrepton analogs were detected by HPLC and HPLC-MS. These results suggest that charged amino acids at physiological pH, Leu and Trp residues at the second position are either not accepted or not efficiently processed by the collective thiostrepton biosynthetic machinery. HPLC-MS analysis of the of *S. laurentii* NDS1/int-A2P crude extract did not reveal a mass consistent with thiostrepton Ala2Pro, suggesting that the conformational constraints imposed on polypeptide backbone in the TsrA Ala2Pro mutant may not be tolerated by one or more of the thiostrepton biosynthetic enzymes.

Several low-abundance metabolites with UV-visible absorption spectra similar to that of thiostrepton A and masses consistent with a mature thiostrepton Ala2Cys were

observed from the HPLC and HPLC-MS analyses of the *S. laurentii* NDS1/int-A2C culture extract. Similar results were observed in our previous study with *S. laurentii* TsrA Ala4Cys, revealing several metabolites with UV-visible absorption spectra resembling thiostrepton A.[19] Two of those analogs, thiostreptons Ala4Cys F1 and F2, were isolated and structurally characterized as lanthionine (Lan)-containing diastereomers, in which a Lan residue is formed nonenzymatically from Cys4 and Dha17 with varied configuration at the α-carbon of the 17th residue.[19] In the Ala2Cys variant, a Lan ring could also be formed which resulted in the formation of metabolites with the same mass as expected for the anticipated thiostrepton Ala2Cys. Examination of the HPLC-MS data suggested thiostrepton analogs with thiazoline residue at the second position are produced by the A2C mutant at a trace level (data not shown). It is likely that a Cys residue at the second and the fourth position of the TsrA core peptide is not well recognized by the thiostrepton cyclodehydratases and dehydrogenase as the newly introduced Cys residue is not efficiently processed to a thiazoline or thiazole group, in contrast to the fate of other Cys residues in the TsrA core peptide.[19] Initial disc diffusion antimicrobial assays with the culture extract of *S. laurentii* TsrA Ala2Cys did revealed growth inhibition against the indicator strains (*Bacillus sp.* and VRE), suggesting that active components are present in the extract (data not shown). Despite our best efforts, low titers and difficulties in separating the highly similar metabolites hindered further characterization of these analogs in this study.

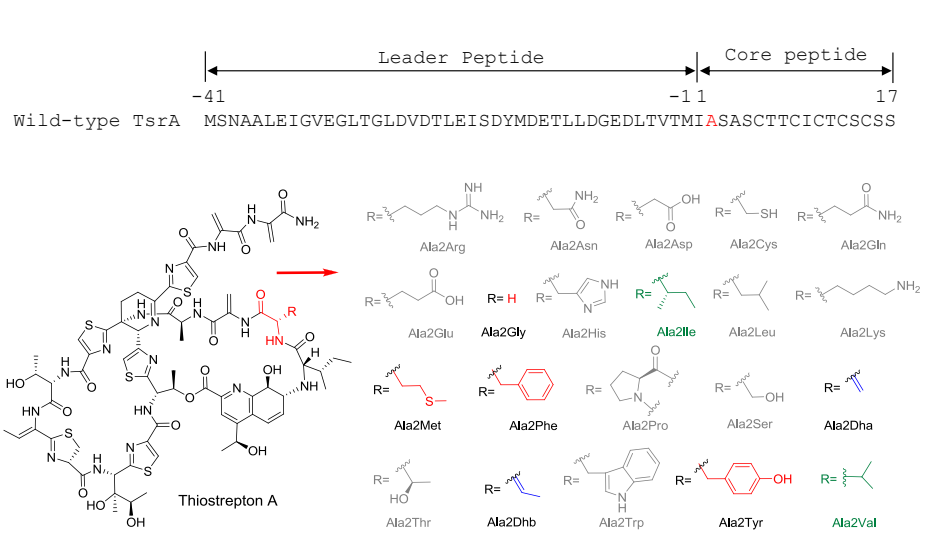

Figure 5.2. Thiostrepton A and its analogs to be generated by site-directed mutagenesis of TsrA Ala2. (**A**) Wild-type TsrA sequence with Ala2 of the core peptide highlighted in red. (**B**) Structures of thiostrepton Ala2 analogs. The analogs in grey were not observed or only produced at trace levels. The observed analogs possessing no posttranslational modification of the variant residue are highlighted in red, while the ones possessing a posttranslational modification of the variant residue are highlighted in blue. The analogs with a contracted quinaldic acid loop are shown in green.

Thiostreptons Ala2Met, Ala2Phe, and Ala2Tyr were successfully produced by the corresponding *S. laurentii* TsrA Ala2 variants (Figure 5.2).[7] These three analogs were purified by semi-preparative HPLC and their structures were verified by HR-MS and MALDI-MS/MS (Appendix E). MALDI-MS/MS of thiostrepton analogs typically leads to loss of the quinaldic acid (QA) moiety followed by the successive fragmentation of the N-terminal residues from the QA-containing macrocycle toward the dehydropiperidine ring, yielding two daughter fragments, **A** and **B**, indicative of the second residue's identity (Figure 5.3).[6, 19] Fragment **A** corresponds to the loss of QA and Ile1, while fragment **B** also lacks the second residue (-QA, -Ile1, and -Xxx2) (Figure 5.3 and Appendix E). During the MALDI-MS/MS analyses for thiostrepton Ala2Met, Ala2Phe, and Ala2Tyr, **A** was not observed, instead a fragment accounting for the cleavage of QA, Ile1 and a carbonyl group was detected (Appendix E). This new diagnostic ion together

with fragment **B** was used to deduce the chemical identity of the second residue in these three analogs.

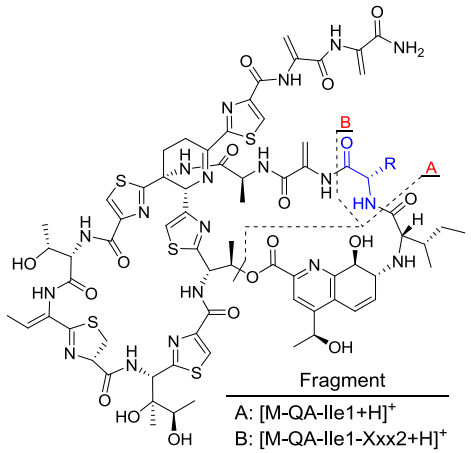

Figure 5.3. Two characteristic fragments from MALDI-MS/MS used to confirm the identify of the second residue of a thiostrepton analog.

When the culture extracts of *S. laurentii* NDS1/int-A2S and A2T were analyzed by HPLC-MS, the anticipated thiostreptons Aal2Ser and Ala2Thr analogs were not detected. Instead, the corresponding dehydrated products, thiostreptons Ala2Dha (Dha: dehydroalanine), and Ala2Dhb (Dhb: dehydrobutyrine), were observed (Figure 5.), as suggested by an 18 Da reduction in mass for each metabolite relative to the anticipated analogs. The two analogs were purified and examined by HR-MS, MALDI-MS/MS and NMR analyses (Appendix E). The diagnostic fragments **A** and **B** were identified during the MALDI-MS/MS analyses for thiostreptons Ala2Dha and Ala2Dhb (Appendix E). In the parent compound, thiostrepton A, three Dha residues and one Dhb moiety are present (Dha3, Dha16, Dha17 and Dhb8; Figure 5.1). In the NMR spectra for thiostrepton Ala2Dha, four Dha residues were instead observed (Appendix E). An additional quaternary carbon (δ_C: 134.2) and an unsaturated CH_2 (δ_C: 100.1 and δ_H: 6.27, 5.01) are indicative of a Dha residue (Table E.1). While the spectra for thiostrepton Ala2Dhb reveals new resonances for a quaternary carbon (δ_C: 128.4) and an unsaturated CH (δ_C:

119.4 and δ_H: ~5.62), characteristic of a Dhb residue (Table E.2). We recently reported that replacing Ala4 with Ser resulted in the formation of both anticipated (Ala4Ser: 93%) and dehydrated analogs (Ala4Dha: 7%), while Ala4 to Thr substitution only led to the production of the dehydrated product, Ala4Dhb.[19] In contrast to the studies with *S. laurentii* TsrA Ala4Ser and Ala4Thr, only dehydrated products were observed in the mutant strains expressing TsrA Ala2Ser and TsrA Ala2Thr, indicating that the thiostrepton dehydratase(s) may be more effective toward dehydrating a Ser residue at the second position of TsrA core peptide than the fourth position. Siomycin A, another series *b* thiopeptide (Figure 5.1), naturally harbors a Dha at the second position, whose presence suggests that the thiopeptide dehydratases may be naturally evolved to dehydrate a serine residue at this position.[20] Three enzymes (TsrC, TsrD, and TsrL) encoded in the *tsr* biosynthetic gene cluster show homology to LanB-type dehydratases responsible for the dehydration of Ser and Thr residues during biosynthesis of lanthipeptides, a separate family of RiPP metabolites.[12, 21] TsrC and TsrD, homologs to which are present in all reported thiopeptide biosynthetic systems, are proposed to install the Dha and Dhb residues during the thiopeptide maturation process, while the role of TsrL is currently unclear.[22] The lanthipeptide dehydratases can demonstrate broad substrate specificity and are often able to catalyze the dehydration of non-native Ser or Thr residues.[23-25] Likewise, a growing body of work relying upon precursor peptide engineering suggests that thiopeptide dehydratases are also somewhat promiscuous with respect to their substrate peptides.[19, 26]

For *S. laurentii* NDS1/int-A2I and int-A2V, the expected mature products, thiostreptons Ala2Ile and Ala2Val, were detected only by HPLC-MS (data not shown).

Interestingly, a major metabolite displaying UV-visible absorption spectra comparable to that of thiostrepton A was identified from HPLC analysis of the culture extracts of both mutants. These two compounds were further purified and structurally characterized by HR-MALDI-MS, MALDI-MS/MS, and NMR. MS results suggested that the Ala2Ile and Ala2Val metabolites are truncated at the N-terminus, with the Ile1l residue lacking in the structures (Figure 5.4 and Appendix E). In MALDI-MS/MS spectra of both thiostrepton analogs, a fragment that is 233 Da less than the parent ion was detected, indicative of the presence of an N-terminus-linked quinaldic acid moiety (Appendix E). NMR analyses were performed to verify the structures proposed for thiostreptons Ala2Ile-ΔIle1 and Ala2Val-ΔIle1. As expected for both analogs, the resonances corresponding to Ile1 were absent (Appendix E).

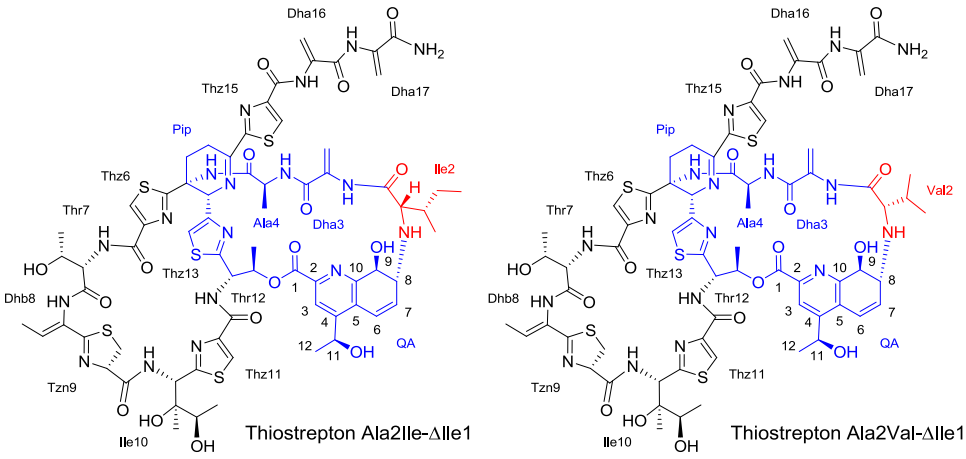

Figure 5.4. Structures of thiostreptons Ala2Ile-ΔIle1 and Ala2Val-ΔIle1. The quinaldic acid loop is highlighted in blue and the mutated residue is shown in red. The numbering system used for the quinaldic acid residue is labeled in black.

In both ΔIle1 variants, the chemical shifts corresponding to QA-8 and QA-9 appeared in the upfield region ($\delta_{C\text{-}8}$: ~62.8; $\delta_{H\text{-}8}$: ~3.45 and $\delta_{C\text{-}9}$: ~73.8; $\delta_{H\text{-}9}$: ~4.52), resembled the resonances observed for other thiostrepton analogs bearing an intact QA macrocycle (Tables E.3 and E.4).[6-7, 19, 27] For thiostrepton Ala2Val-ΔIle, an HMBC

correlation was observed between the α-proton of Val2 and the C-8 of the QA moiety, confirming further a covalent link between the engineered Val2 residue and the quinaldic acid (Appendix E). During the late stages of thiostrepton A maturation, the Thr12 β-hydroxyl is acylated with the QA derivative, 4-(1-hydroxyethyl)quinoline-2-carboxylic acid (HEQ).[13] Next, it is expected that the HEQ ligand is epoxygenated at C-8 and C-9 (Figure 5.4).[13] Peptidolysis of the leader peptide, either before or after attachment and modification of the quinaldic acid moiety, deprotects the primary amine of the core peptide N terminus, permitting a nucleophilic attack of the epoxy group, and forms the second macrocycle that distinguishes thiostrepton and the series *b* thiopeptides.[6, 28-29] Similar to Ile1 in wild-type thiostrepton A, Ile2 and Val2 confer branched, hydrophobic side chains. A trace amount of thiostrepton Ala2Leu-ΔIle1 was also observed in the culture extract of *S. laurentii* NDS1/A2L, however, only by HPLC-MS (data not shown). Our observation suggests that the identity of the first residue that is ultimately incorporated into a mature thiostrepton analog may be important for the recognition by the peptidase or protease. It is likely that the peptidase or protease may bind to the late-stage intermediate during thiostrepton A biosynthesis, pinpoint the branched, hydrophobic amino acid residue at the core peptide second position, and cleave the leader peptide plus Ile1. The newly freed N-terminal amine of the second residue would attack the quinaldic acid epoxide and result in the formation of a thiostrepton analog with a contracted quinaldic acid macrocycle, containing only three residues at the N-terminus. This hypothesis is supported by the naturally observed Val1 in Siomycin A (series *b*) and thiopeptin $A1_a$ (series *a*) (Figure 5.1).[20, 30] The presence of a Val or Ile residue at the N-terminus of a native thiopeptide indicates that the peptidase and the additional thiopeptide

posttranslational modification enzymes may have higher specificity toward these two amino acids in comparison to a Leu residue at the first position. This would explain the robust production of thiostreptons Ala2Ile-ΔIle1 and Ala2Val-ΔIle1, in contrast to the trace level of thiostrepton Ala2Leu-ΔIle1 that is only detected by HPLC-MS. The identity of this peptidase, however, is unclear. A gene for a functional peptidase is not readily identifiable in either the *tsr* or the *sio* biosynthetic locus.[12, 31] A non-specific peptidase or protease encoded elsewhere on the genome of *S. laurentii* may instead execute leader peptide cleavage.[12] Once the peptidase is identified, further biochemical and structural studies with this enzyme would permit detailed understanding of how the leader peptide is removed. This knowledge will aid in the design of thiostrepton analogs with either expanded or contracted quinaldic acid loop, if the thiostrepton posttranslational system would collectively tolerate the new precursor peptide variant.

Table 5.1. Summary of water solubility of thiostrepton analogs

Compound	Water solubility (μM)
Thiostrepton A	8.10 ± 0.24
Ala2Dha	4.14 ± 0.28
Ala2Dhb	11.10 ± 0.27
Ala2Gly	16.79 ± 0.60
Ala2Ile-ΔIle1	10.18 ± 0.36
Ala2Met	13.62 ± 0.38
Ala2Phe	4.71 ± 0.13
Ala2Tyr	0.92 ± 0.10
Ala2Val-ΔIle1	3.28 ± 0.22

In total, eight thiostrepton Ala2 analogs were isolated during this saturation mutagenesis study. The thiostrepton Ala2 analogs were further measured for their kinetic aqueous solubility, a parameter commonly assessed in the prescreening process of drug development (Table 5.1).[32] All analogs displayed similar solubilities compared to that of thiostrepton A (within 3-fold range), with the exception of the Ala2Tyr variant, which suffers a 9-fold impairment in solubility due to the newly introduced non-polar, aromatic

side chain. The titer of each analog was used to estimate the tolerance level of the collective thiostrepton A biosynthetic pathway toward the mutated residue at the second position (Table F.2). In comparison to thiostrepton A production (115 mg/L), introducing a serine residue at the second position is highly preferred by the biosynthetic machinery and the newly introduced serine was further dehydrated to provide thiostrepton Ala2Dha (301 mg/L). Siomycin A has a structure highly similar to that of thiostrepton A, differing only at positions 1 and 2 (Val1 and Dha2) (Figure 5.1).[20] The presence of Dha2 in siomycin A suggests that the dehydratase(s) may have a natural tendency to dehydrate a serine residue at this position. Further alignment of the LanB-type dehydratases TsrC and SioJ from the *sio* locus reveals 76% identity and 81% similarity between these two enzymes, while TsrD demonstrates 77% identity and 87% similarity to SioK.[12, 31] In contrast, the identities and similarities between TsrC or TsrD and its respective homologs from the nosiheptide and thiocillin biosynthetic pathways (both lacking the Dha2 residue) are greatly reduced (<34% for identities and <48% for similarities).[33-34] The high homologies between the dehydratases from the thiostrepton A and siomycin biosynthetic pathways suggest that TsrC and TsrD may favor a Ser residue at the TsrA core peptide second position which may account for the nearly 3-fold increase in the titer of Ala2Dha variant relative to that of wild-type metabolite. Substituting Ala2 with Thr is also well-recognized as thiostrepton Ala2Dhb is produced at about 39 mg/L. Replacing Ala2 with Ile and Val did permit robust production of the N-terminal truncated thiostrepton analogs (34 mg/L for thiostrepton Ala2Ile-ΔIle1 and 51 mg/L for thiostrepton Ala2Ile-ΔIle1). The production of thiostrepton Ala2Gly is less efficient (19 ± 3 mg/L) and replacing Ala2 with residues containing linear or aromatic side chains may not be favored by the *tsr*

maturation system as the titers of thiostreptons Ala2Met, Ala2Phe, and Ala2Tyr are significantly reduced to less than 4 mg/L. The second residue of the TsrA core peptide is closely located to the leader peptide and introducing a variant residue at this position may affect the correct folding of a mutant TsrA. This would render the TsrA Ala2 variant less favored by the enzymes involved in the maturation of a thiostrepton analog, thus accounting for the moderate restrict of the biosynthetic system toward modifications at the second position, in contrast to the highly mutable TsrA Ala4.[19]

5.3.3 Antibacterial activities of thiostrepton analogs

A microbroth dilution method was used to determine the antibacterial activities of the isolated thiostrepton Ala2 analogs against three indicator strains of *Staphylococcous*, *Bacillus*, and *Enterococcus*.[6-7] Most of the thiostrepton Ala2 analogs showed either comparable or modestly reduced ability to inhibit the growth of these test strains relative to thiostrepton A, which provided MIC values ranging from 0.012 to 0.025 μg/mL (Table 5.2). The antibacterial activities of thiostreptons Ala2Dhb and Ala2Tyr did decrease up to 20-fold, resulting in MIC values ranging from 0.1 to 0.3 μg/mL (Table 5.2). Thiostreptons Ala2Ile-ΔIle1 and Ala2Val-ΔIle1, however, lost their abilities to inhibit bacterial growth in the concentration range tested (MIC >5.0 μg/mL, Table 5.2). Consistent with thiopeptides' selective activity against Gram-positive bacteria, none of Ala2 analogs were able to inhibit the growth of *E. coli* ATCC 27856 (Data not shown).[7] Two explanations can be provided for the inactive thiostreptons Ala2Ile-ΔIle1 and Ala2Val-ΔIle1. First, the ΔIle1 analogs cannot bind the ribosome. An alternative explanation for the loss of inhibitory activities is that the analogs are unable to reach the ribosome.

Table 5.2. MIC values of thiostrepton analogs

Compound	MIC[a] (μg/mL)		
	MRSA[b]	VRE[c]	*Bacillus*[d]
Thiostrepton A	0.012	0.012	0.025
Ala2Dha	0.010	0.008	0.042
Ala2Dhb	0.11	0.11	0.11
Ala2Gly	0.023	0.019	0.19
Ala2Ile-ΔIle1	>5.0	>5.0	>5.0
Ala2Met	0.014	0.007	0.086
Ala2Phe	0.022	0.011	0.087
Ala2Tyr	0.22	0.11	0.27
Ala2Val-ΔIle1	>5.0	>5.0	>5.0
Vancomycin	0.39	ND[e]	ND
Chloramphenicol	ND	3.9	0.98

[a] Minimum inhibitory concentration.
[b] *Staphylococcus aureus* ATCC 10537.
[c] *Enterococcus faecium* ATCC 12952.
[d] *Bacillus* sp. ATCC 27859.
[e] Not determined.

A coupled *in vitro* transcription-translation assay was therefore employed to directly assess the abilities of the thiostrepton Ala2 variants to inhibit protein synthesis and the translation inhibition curves are shown in Figure G.4. Under these conditions, the activity observed for thiostrepton A was consistent with previously reported value.[35] The half maximal inhibitory concentrations (IC_{50}) obtained for most thiostrepton Ala2 analogs are comparable to that for thiostrepton A, with an exception that thiostrepton Ala2Ile-ΔIle1 demonstrate more than a ten-fold increase (Table 5.3). The IC_{50} for thiostrepton Ala2Val-ΔIle1 was not determined due to the solubility limitation. However, thiostrepton Ala2Val-ΔIle1 was speculated to have comparable inhibitory activity as thiostrepton Ala2Ile-ΔIle1 based on their extremely similar structures. Thiostreptons Ala2Dhb and Ala2Tyr, having up to 20-fold reduction in their efficacy toward inhibiting bacterial growth in liquid culture, however, demonstrated equivalent abilities to inhibit *in vitro* protein synthesis as thiostrepton A (Tables 5.2 and 5.3). The results observed for thiostreptons Ala2Dhb and Ala2Tyr suggested that off-target factors may account for their reduced *in vivo* activities, such as, cell permeability or metabolite stability.

Table 5.3. *In vitro* translation inhibition by thiostrepton analogs

Compound	IC_{50} (μM)
Thiostrepton A	0.63 ± 0.01
Ala2Dha	0.58 ± 0.03
Ala2Dhb	0.35 ± 0.04
Ala2Gly	0.46 ± 0.05
Ala2Ile-ΔIle1	8.1 ± 1.0
Ala2Met	0.33 ± 0.03
Ala2Phe	0.34 ± 0.02
Ala2Tyr	0.58 ± 0.08
Ala2Val-ΔIle1	>3.28[a]

[a] IC_{50} not determined due to solubility limitation.

Till now, only Ala or Dha is observed at the second position of all reported series *a* and *b* thiopeptides, which inhibit protein synthesis by interacting with the ribosome.[36] Our results here expanded the chemical entities of the second position to other hydrophobic residues (Dha, Dhb, Met, Phe, and Tyr) and demonstrated that those analogs retained their *in vitro* potency to inhibit protein synthesis. Overall, the MIC data for the analogs generated in this study are in line with their IC_{50} values. This observation is consistent with the X-ray crystal structure of thiostrepton A bound to the ribosome revealing a solvent-exposed Ala2 residue.[5] Even though only limited thiostrepton Ala2 analogs were produced from current saturation mutagenesis study, our results do suggest that the second position of the TsrA core peptide could tolerate further modifications without affecting the abilities of the analogs to complex with the 50S ribosome. In contrast, the size of the quinaldic acid-containing macrocycle does matter for thiostrepton A's antibacterial potency as indicated by the reduced *in vivo* and *in vitro* inhibitory activities of thiostreptons Ala2Ile-ΔIle1 and Ala2Val-ΔIle1 (Tables 5.2 and 5.3).

5.3.4 Structural modeling of the N-terminus truncated thiostrepton analogs

To further examine the diminished ribosome-inhibiting capabilities of the two analogs harboring a contracted QA loop, both thiostreptons Ala2Ile-ΔIle1 and Ala2Val-

ΔIle1 were modeled into the 50S ribosome, using the crystal structure of thiostrepton A bound to the ribosome as the template.[5] Partial views of thiostrepton A bound to the ribosome and the modeled complexes of the two ΔIle1 analogs and the ribosome are depicted in Figure 5.5. In thiostrepton A, an intramolecular hydrogen bond between the Thr7 hydroxyl group and the 9-OH of the quinaldic acid moiety stabilizes the three-dimensional conformation (Figure E.36).[37] In both ΔIle1 thiostrepton variants, the distances between the aforementioned two oxygen groups are 3.2 Å preserving this key internal hydrogen bond and suggesting that these analogs and thiostrepton A adopt similar overall folds (Figure E.36). The quinaldic acid moieties in the two modeled complexes remain close to A1067, as is observed in the thiostrepton A complex, and likely contribute favorable hydrophobic interactions.[5] In the crystal structure of thiostrepton A bound to the ribosome, Thz15 approaches Pro26 of L11 (within 3.4 Å) and Thz11 sits above Pro22 (within 3.6 Å), providing additional hydrophobic interactions (Figure 5.5A).[5] In the structures modeled for the two ΔIle1 analogs bound to the ribosome, Thz15 similarly approaches Pro26 (3.7 Å), however, Thz11 is unable to interact with Pro22 due to the greater distance (4.8 Å) (Figures 5.5B and 5.5C). In addition, the distance between Thz6 and A1095 of 23S rRNA in the reported structure (3.7 Å) is elongated to 4.2 Å in the models.[5] 7 In the crystal structure of thiostrepton A bound to the ribosome, the Tzn9 carbonyl is 3.7 Å away from the 2'-OH of A1067 (Figure 5.5A).[5] In the two models, this distance is reduced to 3.3 Å, permitting a new hydrogen-bonding interaction (Figure 5.5).

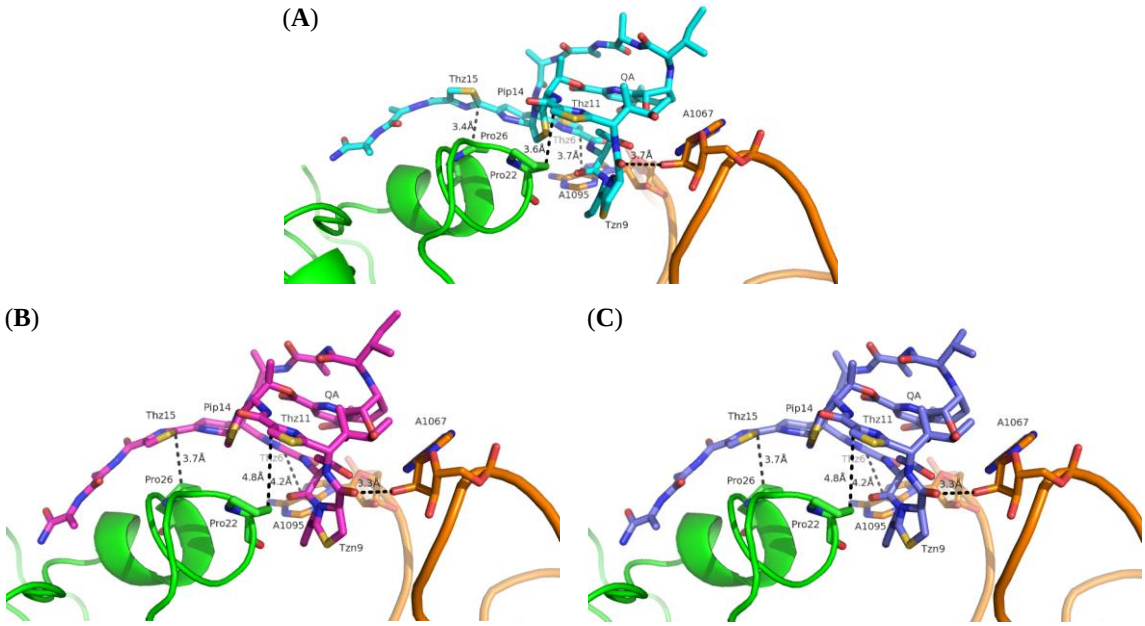

Figure 5.5. Thiostrepton A, Ala2Ile-ΔIle1 and Ala2Val-ΔIle1 bound to the 50S ribosome. (**A**) Thiostrepton A (Cyan) bound to the ribosome adapted from PDB 3CF5.[5] (**B**) Model of thiostrepton Ala2Ile-ΔIle1 (magenta) bound to the ribosome. (**C**) Model of thiostrepton Ala2Val-ΔIle1 (blue) bound to the ribosome. Helices 43 and 44 of 23S rRNA are colored in orange and ribosomal protein L11 is shown in green.

It therefore appears only the hydrophobic interaction between Thz15 and Pro26 is conserved in the models. The new hydrogen-bond would contribute to the binding of the two ΔIle1 analogs to the ribosome, however, may not be enough to completely compensate the loss of other hydrophobic interactions. This may explain the reduced inhibitory activities against *in vitro* protein synthesis. Besides the weakened interactions between the two ΔIle analogs and the ribosome, off-target effects, such as an inability of the analogs to reach the ribosome or instability of the analogs, may collectively account for the dramatically reduced potencies of thiostreptons Ala2Ile-ΔIle1 and Ala2Val-ΔIle1 against *in vivo* bacterial growth.

5.3.5 20S proteasome inhibitory activities of thiostrepton analogs

Previously, the Arndt group reported that thiostrepton A and some derivatives are active 20S proteasome inhibitors, which partially accounts for the thiopeptide's antimalarial activity.[38-39] Three fluorogenic substrates were individually used to test for inhibition of trypsin-, chymotrypsin-, and caspase-like proteolytic functions of the proteasome by the analogs generated in this study. The proteasome inhibition curves are shown in Figure G.5. Many of thiostrepton Ala2 analogs isolated and assessed here revealed IC_{50} values analogous to those of thiostrepton A (Table 5.4). The presence of an aromatic side chain in thiostreptons Ala2Phe and Ala2Tyr did cause an improvement (3-5 fold) in inhibiting the trypsin-like activity of the proteasome. The longer, linear side chain introduced by thiostrepton Ala2Met likely contributed to enhanced potency against all three proteolytic activities of the proteasome, an effect most pronounced for the trypsin-like function, by 10-fold. The efficacy of thiostrepton Ala2Dhb toward chymotrypsin-like activity of the proteasome was slightly reduced (3 fold) in comparison to that of thiostrepton A. Thiostreptons Ala2Ile-ΔIle1 and Ala2Val-ΔIle1 retained their inhibitory activities against the proteasome, albeit slightly reduced. The ΔIle1 analogs inhibition of the chymotrypsin-like function was most perturbed (up to 6 fold). Earlier studies with thiostrepton analogs lacking an intact QA loop revealed that those thiopeptides are less active proteasome inhibitors, suggesting that a closed QA macrocycle is likely to be important for thiostreptons' potency against the proteasome.[19, 39] Our current results extend the understanding about the significance of the QA loop, indicating that the ability of a thiostrepton analog to interfere with proteasome's function may not be critically sensitive to the size of the QA-containing macrocycle. Nonetheless,

with a contracted QA loop, the thiostrepton analog may adopt a slightly differed conformation which in turn reduces the binding affinity of a thiopeptide to the proteasome, as demonstrated by thiostreptons Ala2Ile-ΔIle1 and Ala2Val-ΔIle1.

Table 5.4. 20S Proteasome inhibitory activities of thiostrepton analogs

Compound	IC_{50}, [μM] Trypsin-like	IC_{50}, [μM] Chymotrypsin-like	IC_{50}, [μM] Caspase-like
Thiostrepton A	0.95 ± 0.15	1.0 ± 0.1	0.59 ± 0.06
Ala2Dha	0.71 ± 0.07	0.99 ± 0.01	0.51 ± 0.03
Ala2Dhb	1.3 ± 0.2	3.1 ± 0.3	0.92 ± 0.06
Ala2Gly	1.2 ± 0.1	0.76 ± 0.12	0.37 ± 0.04
Ala2Ile-ΔIle1	2.1 ± 0.4	6.3 ± 0.4	1.6 ± 0.3
Ala2Met	0.09 ± 0.01	0.62 ± 0.01	0.14 ± 0.01
Ala2Phe	0.18 ± 0.02	0.96 ± 0.03	0.46 ± 0.04
Ala2Tyr	0.34 ± 0.03	>0.92[a]	0.58 ± 0.09
Ala2Val-ΔIle1	0.84 ± 0.04	3.9 ± 0.2	1.2 ± 0.04
Bortezomib	1.6 ± 0.2	0.005 ± 0.001	0.049 ± 0.003

[a] IC_{50} not determined due to solubility limitation.

It appears that the second residue of thiostrepton may not necessarily be a decisive factor in its ability to obstruct 20S proteasome activity. We note, however, that only eight thiostrepton Ala2 analogs, all harboring a hydrophobic residue at the variable residue. Additional studies are necessary to determine whether or not polar functional groups at the second position retain their capacities as proteasome inhibitors. Thiostrepton analogs generated previously by semi-synthetically modifying the C-terminus with alkyl chains or oxidizing the ninth thiazoline to a thiazole all retained their inhibitory activities against the proteasome, often demonstrating varied potencies against the caspase-like and chymotrypsin-like functions.[39] Diverse effectiveness against individual proteolytic activities was also observed for all Ala2 analogs. It is possible that either different thiostrepton binding sites may exist in the proteasome β subunits or allosteric interactions occurring to influence proteasome activity. Structural information is required to fully articulate the nature by which thiostrepton A engages the proteasome,

and to offer a firmer explanation for the various thiostrepton analog activities reported to date.

5.4 Conclusions

We have probed the tolerance of the thiostrepton biosynthetic pathway toward proteinogenic amino acid residues at the second position of TsrA core peptide by saturation mutagenesis. In total, eight thiostrepton Ala2 analogs were isolated, including the two analogs with a contracted quinaldic acid loop resulting from ΔIle1. Our results suggest that the thiostrepton A biosynthetic machinery is moderately permissive toward chemical substitutions at the second position. Most polar residues and a Pro at the second position are not effectively processed to the corresponding mature thiostrepton analog. Production of thiostreptons Ala2Ile1-ΔIle1 and Ala2Val-ΔIle1 suggest that the thiostrepton A biosynthetic system accepts an Ile or Val residue at the second position and efficiently converted them to late-stage intermediate. Additionally, Ile2 and Val2 are recognized by the protease or peptidase as new cleavage site, resulting in the formation of the two analogs with a shorten quinaldic acid-containing loop. This information could contribute to the design of thiostrepton analogs with either expanded or contracted quinaldic acid macrocycle if the thiostrepton posttranslational system would collectively tolerate the new precursor peptide variant. In all series *a* and *b* thiopeptides reported thus far, only Ala and Dha appear at the second position in the four amino acid-quinaldic acid macrocycle. Herein, we have expanded the chemical entities observed at this position to include other hydrophobic residues. The nature of the second residue of thiostrepton may not be absolutely critical for either the antibacterial or proteasome inhibitory properties of

a series *b* thiopeptide. To further test our hypothesis on the importance of the second residue for thiostrepton's antibacterial and proteasome inhibitory activities, additional analogs harboring polar functional groups would need to be accessed. These analogs have potentials in solving the water solubility issue associated with thiopeptides while retaining their potent biological activities, as exemplified by the encouraging results from nocathiacin studies.[40-41] One opportunity to provide thiostrepton analogs with hydrophilic ligands would be to utilize thiostreptons Ala2Dha or Ala2Dhb as a starting substrate, adapting previously reported semi-synthetic strategies.[38, 40-42] Prior to this work, majority of the efforts toward generating a thiostrepton analog relied on semi-synthetic derivatization and were unable to access the analogs with a contracted quinaldic acid-containing loop. Our current study expanded the thiostrepton scaffold and introduced new handles for semisynthetic work, supporting future engineering of novel thiostrepton Ala2 analogs.

5.5 References

1. Bhat, U. G.; Halasi, M.; Gartel, A. L., Thiazole antibiotics target FoxM1 and induce apoptosis in human cancer cells. *PLoS One* **2009,** *4*, e5592.

2. Clough, B.; Strath, M.; Preiser, P.; Denny, P.; Wilson, I. R., Thiostrepton binds to malarial plastid rRNA. *FEBS Lett.* **1997,** *406*, 123-125.

3. Harms, J. M.; Wilson, D. N.; Schluenzen, F.; Connell, S. R.; Stachelhaus, T.; Zaborowska, Z.; Spahn, C. M. T.; Fucini, P., Translational regulation via L11: molecular switches on the ribosome turned on and off by thiostrepton and micrococcin. *Molecular cell* **2008,** *30*, 26-38.

4. McConkey, G. A.; Rogers, M. J.; McCutchan, T. F., Inhibition of *Plasmodium falciparum* protein synthesis. Targeting the plastid-like organelle with thiostrepton. *J. Biol. Chem.* **1997,** *272*, 2046-2049.

5. Harms, J. M.; Wilson, D. N.; Schluenzen, F.; Connell, S. R.; Stachelhaus, T.; Zaborowska, Z.; Spahn, C. M.; Fucini, P., Translational regulation via L11: Molecular switches on the ribosome turned on and off by thiostrepton and micrococcin. *Mol. Cell.* **2008,** *30*, 26-38.

6. Li, C.; Zhang, F.; Kelly, W. L., Mutagenesis of the thiostrepton precursor peptide at Thr7 impacts both biosynthesis and function. *Chem. Commun.* **2012,** *48*, 558-560.

7. Li, C.; Zhang, F.; Kelly, W. L., Heterologous production of thiostrepton A and biosynthetic engineering of thiostrepton analogs. *Mol. BioSyst.* **2011,** *7*, 82-90.

8. Gust, B.; Challis, G. L.; Fowler, K.; Kieser, T.; Chater, K. F., PCR-targeted *Streptomyces* gene replacement identifies a protein domain needed for biosynthesis of the sesquiterpene soil odor geosmin. *Proc. Natl. Acad. Sci. U.S.A.* **2003,** *100*, 1541-1546.

9. Wright, F.; Bibb, M. J., Codon usage in the G+C-rich *Streptomyces* genome. *Gene* **1992,** *113*, 55-65.

10. Datsenko, K. A.; Wanner, B. L., One-step inactivation of chromosomal genes in *Escherichia coli* K-12 using PCR products. *Proc. Natl. Acad. Sci. U.S.A.* **2000,** *97*, 6640-6645.

11. Kieser, T. B., M. J.; Buttner, M. J.; Chater, K. F.; Hopwood, D. A. , *Practical Streptomyces Genetics*. John Innes Foundation: Norwich, UK, 2000.

12. Kelly, W. L.; Pan, L.; Li, C., Thiostrepton biosynthesis: Prototype for a new family of bacteriocins. *J. Am. Chem. Soc.* **2009,** *131*, 4327-4334.

13. Priestley, N. D.; Smith, T. M.; Shipley, P. R.; Floss, H. G., Studies on the biosynthesis of thiostrepton: 4-(1-hydroxyethyl)quinoline-2-carboxylate as a free intermediate on the pathway to the quinaldic acid moiety. *Bioorg. Med. Chem.* **1996,** *4*, 1135-1147.

14. Bausch, S. L.; Poliakova, E.; Draper, D. E., Interactions of the N-terminal domain of ribosomal protein L11 with thiostrepton and rRNA. *J. Biol. Chem.* **2005,** *280*, 29956-29963.

15. Ryan, P. C.; Lu, M.; Draper, D. E., Recognition of the highly conserved GTPase center of 23S ribosomal RNA by ribosomal protein L11 and the antibiotic thiostrepton. *J. Mol. Biol.* **1991,** *221*, 1257-1268.

16. Cousins, K. R., Computer review of ChemDraw Ultra 12.0. *J. Am. Chem. Soc.* **2011,** *133*, 8388.

17. Allinger, N. L., Conformational analysis. 130. MM2. A hydrocarbon force field utilizing V1 and V2 torsional terms. *J. Am. Chem. Soc.* **1977,** *99*, 8127-8134.

18. DeLano, W. L. *The PyMOL Molecular Graphics System*, The PyMol Molecular Graphics System, Version 1.5.0.4 Schrödinger, LLC.; DeLano Scientific, CA, USA.: **2002**.

19. Zhang, F.; Kelly, W. L., Saturation mutagenesis of TsrA Ala4 unveils a highly mutable residue of thiostrepton A. *Submitted* **2014**.

20. Tori, K.; Tokura, K.; Okabe, K.; Ebata, M.; Otsuka, H.; Lukacs, G., Carbon-13 NMR studies of peptide antibiotics, thiostrepton and siomycin A: the structure relationship. *Tetrahedron Letters* **1976,** *17*, 185-188.

21. Garg, N.; Salazar-Ocampo, L. M.; van der Donk, W. A., In vitro activity of the nisin dehydratase NisB. *Proc. Natl. Acad. Sci. U.S.A.* **2013,** *110*, 7258-7263.

22. Zhang, F.; Kelly, W. L., *In vivo* production of thiopeptide variants. *Methods Enzymol.* **2012,** *516*, 3-24.

23. Kuipers, O. P.; Rollema, H. S.; Yap, W. M.; Boot, H. J.; Siezen, R. J.; de Vos, W. M., Engineering dehydrated amino acid residues in the antimicrobial peptide nisin. *J. Biol. Chem.* **1992,** *267*, 24340-24346.

24. Bierbaum, G.; Szekat, C.; Josten, M.; Heidrich, C.; Kempter, C.; Jung, G.; Sahl, H. G., Engineering of a novel thioether bridge and role of modified residues in the lantibiotic Pep5. *Appl. Environ. Microbiol.* **1996,** *62*, 385-392.

25. Rink, R.; Wierenga, J.; Kuipers, A.; Kluskens, L. D.; Driessen, A. J.; Kuipers, O. P.; Moll, G. N., Production of dehydroamino acid-containing peptides by *Lactococcus lactis*. *Appl. Environ. Microbiol.* **2007,** *73*, 1792-1796.

26. Bowers, A. A.; Acker, M. G.; Young, T. S.; Walsh, C. T., Generation of thiocillin ring size variants by prepeptide gene replacement and in vivo processing by *Bacillus cereus*. *J. Am. Chem. Soc.* **2012,** *134*, 10313-10316.

27. Mocek, U.; Beale, J. M.; Floss, H. G., Reexamination of the ^{1}H and ^{13}C NMR spectral assignments of thiostrepton. *J. Antibiot.* **1989,** *42*, 1649-1652.

28. Mocek, U.; Zeng, Z.; O'Hagan, D.; Zhou, P.; Fan, L. D. G.; Beale, J. M.; Floss, H. G., Biosynthesis of the modified peptide antibiotic thiostrepton in *Streptomyces azureus* and *Streptomyces laurentii*. *J. Am. Chem. Soc.* **1993,** *115*, 7992-8001.

29. Mocek, U.; Knaggs, A. R.; Tsuchiya, R.; Nguyen, T.; Beale, J. M.; Floss, H. G., Biosynthesis of the modified peptide antibiotic nosiheptide in *Streptomyces actuosus*. *J. Am. Chem. Soc.* **1993,** *115*, 7557-7568.

30. Hensens, O. D.; Albers-Schönberg, G., Total structure of the peptide antibiotic components of thiopeptin by ^{1}H and ^{13}C NMR spectroscopy. *Tetrahedron Lett.* **1978,** *19*, 3649-3652.

31. Liao, R.; Duan, L.; Lei, C.; Pan, H.; Ding, Y.; Zhang, Q.; Chen, D.; Shen, B.; Yu, Y.; Liu, W., Thiopeptide biosynthesis featuring ribosomally synthesized precursor peptides and conserved posttranslational modifications. *Chem. Biol.* **2009,** *16*, 141-147.

32. Lipinski, C. A.; Lombardo, F.; Dominy, B. W.; Feeney, P. J., Experimental and computational approaches to estimate solubility and permeability in drug discovery and development settings. *Adv. Drug Deliv. Rev.* **2001,** *46*, 3-26.

33. Wieland Brown, L. C.; Acker, M. G.; Clardy, J.; Walsh, C. T.; Fischbach, M. A., Thirteen posttranslational modifications convert a 14-residue peptide into the antibiotic thiocillin. *Proc. Natl. Acad. Sci. U. S. A.* **2009,** *106*, 2549-2553.

34. Yu, Y.; Duan, L.; Zhang, Q.; Liao, R.; Ding, Y.; Pan, H.; Wendt-Pienkowski, E.; Tang, G.; Shen, B.; Liu, W., Nosiheptide biosynthesis featuring a unique indole side ring formation on the characteristic thiopeptide framework. *ACS Chem. Biol.* **2009,** *4*, 855-864.

35. Jonker, H. R. A.; Baumann, S.; Wolf, A.; Schoof, S.; Hiller, F.; Schulte, K. W.; Kirschner, K. N.; Schwalbe, H.; Arndt, H.-D., NMR structures of thiostrepton derivatives for characterization of the ribosomal binding site. *Angew. Chem. Int. Ed. Engl.* **2011,** *50*, 3308-3312.

36. Bagley, M. C.; Dale, J. W.; Merritt, E. A.; Xiong, X., Thiopeptide antibiotics. *Chem. Rev.* **2005,** *105*, 685-714.

37. Bond, C. S.; Shaw, M. P.; Alphey, M. S.; Hunter, W. N., Structure of the macrocycle thiostrepton solved using the anomalous dispersion contribution of sulfur. *Acta Crystallogr. D Biol. Crystallogr.* **2001,** *57*, 755-758.

38. Aminake, M. N.; Schoof, S.; Sologub, L.; Leubner, M.; Kirschner, M.; Arndt, H.-D.; Pradel, G., Thiostrepton and derivatives exhibit antimalarial and gametocytocidal activity by dually targeting parasite proteasome and apicoplast. *Antimicrob. Agents Chemother.* **2011,** *55*, 1338-1348.

39. Schoof, S.; Pradel, G.; Aminake, M. N.; Ellinger, B.; Baumann, S.; Potowski, M.; Najajreh, Y.; Kirschner, M.; Arndt, H.-D., Antiplasmodial thiostrepton derivatives: Proteasome inhibitors with a dual mode of action. *Angew. Chem. Int. Ed. Engl.* **2010,** *49*, 3317-3321.

40. Naidu, B. N.; Sorenson, M. E.; Bronson, J. J.; Pucci, M. J.; Clark, J. M.; Ueda, Y., Synthesis, in vitro, and in vivo antibacterial activity of nocathiacin I thiol-Michael adducts. *Bioorg. Med. Chem. Lett.* **2005,** *15*, 2069-2072.

41. Naidu, B. N.; Sorenson, M. E.; Zhang, Y.; Kim, O. K.; Matiskella, J. D.; Wichtowski, J. A.; Connolly, T. P.; Li, W.; Lam, K. S.; Bronson, J. J.; Pucci, M. J.; Clark, J. M.; Ueda, Y., Nocathiacin I analogues: synthesis, in vitro and in vivo biological activity of novel semi-synthetic thiazolyl peptide antibiotics. *Bioorg. Med. Chem. Lett.* **2004,** *14*, 5573-5577.

42. Hegde, N. S.; Sanders, D. A.; Rodriguez, R.; Balasubramanian, S., The transcription factor FOXM1 is a cellular target of the natural product thiostrepton. *Nat. Chem.* **2011,** *3*, 725-731.

CHAPTER 6: CONCLUSIONS AND OUTLOOK

The realization of the ribosomally-synthesized peptide origins for thiostrepton prompted us to explore biosynthetic engineering as a way to generate thiostrepton analogs that are inaccessible by semisynthetic modification alone. Due to the difficulties in the genetic manipulation of *S. laurentii*, a methodology to heterologously produce thiostrepton A was originally designed. The production of thiostrepton A from the non-cognate hosts, however, did not permit robust production of thiostrepton A. Genetic manipulations of the thiostrepton A biosynthetic gene cluster likely will generate biosynthetic intermediates or analogs produced at levels lower than the wild-type thiopeptide, and such metabolites may easily escape the detection limits if using the heterologous hosts developed here. Therefore, the same strategy toward the engineering of thiostrepton variants in the native thiostrepton-producing bacterium, *S. laurentii*, was pursued.

The introduction of a fosmid used in the heterologous production of thiostrepton A into *S. laurentii* NDS1, a *tsrA* deletion mutant, permitted restoration of thiostrepton A production to that of the wild-type level. The fosmid was then engineered to enable the replacement of wild-type *tsrA*. Three residues: Ala2, Ala4 and Thr7 were targeted for initial round of mutagenesis, since none are expected to be directly involved in a potentially critical transformation in precursor peptide processing. Introduction of a fosmid encoding either TsrA Ala2Gly or Ala4Gly into *S. laurentii* NDS1 led to the successful production of the respective thiostrepton variants, with retained antibacterial activities. In contrast, thiostrepton Thr7Gly was not detected in culture extract of the

corresponding *S. laurentii* variant. This initial study laid the groundwork for more radical substitutions at each of the three unmodified residues in thiostrepton A.

The seventh residue of thiostrepton A is predicted to be critical for the metabolite's antibacterial activity. Prior effort toward generating thiostrepton Thr7Gly was not successful. It was therefore uncertain whether or not variants of Thr7 could be successfully generated and used to probe the importance of this residue in antibacterial activity. The Thr7 residue was then targeted with additional modifications. However, we successfully generated two thiostrepton Thr7 analogs, Thr7Ala and Thr7Val. As predicted by the crystal structure of thiostrepton A bound to the ribosome, the antibacterial activity of thiostrepton Thr7Ala was indeed greatly impaired. Furthermore, the identification of the shunt metabolite SL105-1 grants insight into the late stages maturation of a thiostrepton. The production of SL105-1 suggests that epoxidation of 4-(1-hydroxyethyl)quinolone-2-carboxylic acid and subsequent quinaldic acid loop closure occur later in the biosynthesis of thiostrepton A.

Successful production of the bioactive thiostrepton Ala4Gly encouraged us to more thoroughly probe the range of amino acid residues tolerated at the fourth position of the TsrA core peptide by the saturation mutagenesis of Ala4. This work generated sixteen thiostrepton analogs. To our knowledge, this is the first report that thoroughly probed the permissiveness of the collective biosynthetic machinery toward modifications to the fourth residue in the quinaldic acid loop of a series *b* thiopeptide, substituting the parent alanine residue with the remaining 19 proteinogenic amino acid residues. The *in vitro* inhibition assays of the Ala4 variants reveal that the fourth residue of this thiopeptide is not essential for binding either the ribosome or the proteasome.

Similarly, the tolerance of the thiostrepton biosynthetic pathway toward proteinogenic amino acid residues at the second position of TsrA core peptide was also probed by saturation mutagenesis. In total, eight thiostrepton Ala2 analogs were isolated, including the two analogs with a contracted quinaldic acid loop resulting from ΔIle1. Our results suggest that the thiostrepton A biosynthetic machinery is moderately permissive toward chemical substitutions at the second position. Production of thiostreptons Ala2Ile1-ΔIle1 and Ala2Val-ΔIle1 suggest that the thiostrepton A biosynthetic system accepts an Ile or Val residue at the second position and efficiently converted them to late-stage intermediate. Additionally, Ile2 and Val2 are recognized by the protease or peptidase as new cleavage site, resulting in the formation of the two analogs with a shorten quinaldic acid-containing loop. In all series *a* and *b* thiopeptides reported thus far, only Ala and Dha appear at the second position in the four amino acid-quinaldic acid macrocycle. Herein, we have expanded the chemical entities observed at this position to include other hydrophobic residues. The nature of the second residue of thiostrepton may not be absolutely critical for either the antibacterial or proteasome inhibitory properties of a series *b* thiopeptide.

The wide range of thiostrepton analogs that retain the ability to complex with the ribosome or the proteasome, including Ala2Dha, Ala2Dhb, Ala4Dha, Ala4Dhb, and Ala4Ser, provide promise for coupling an engineered thiopeptide with semisynthetic modification to acquire a biologically active analog with enhanced water solubility. Such a strategy could also facilitate the inclusion of cross-linking functional group or a fluorescent label to probe the mechanism of action when thiostrepton A is bound to the proteasome, which is currently unknown. Modifications to the C-terminal tail region of

thiostrepton A and other thiopeptides, often by conjugate addition to a dehydroalanine residue, have been utilized to increase water solubility through the introduction of polar side chains.[1-5] Similar and other types of semi-synthetic modifications of a thiopeptide scaffold, when introduced at an amenable position, can be broadly accepted with retained antibacterial or antimalarial potency. To further test our hypothesis on the importance of the second residue for thiostrepton's antibacterial and proteasome inhibitory activities, additional analogs harboring polar functional groups would need to be accessed. The information obtained from thiostrepton Ala2Ile1-ΔIle1 and Ala2Val-ΔIle1 could facilitate the design of thiostrepton analogs with either expanded or contracted quinaldic acid-containing loop if the thiostrepton posttranslational system would collectively tolerate the new precursor peptide variant.

The established biosynthetic engineering platform permits *in vivo* production of thiostrepton variants in a relatively efficient fashion. The thiostrepton analogs and shunt metabolites obtained from these studies provided useful insights into the late maturation process of thiostrepton A, in addition to the importance of TsrA core peptide second and fourth residues for the thiopeptide's antibacterial and 20S proteasome inhibitory activities. The results described here support further examination of the quinaldic acid-containing macrocycle of thiostrepton and related thiopeptides to generate novel analogs. The library of thiostrepton analogs can be used to interrogate the thiopeptide structure-activity relationships and may be useful to address the bioavailability issues plaguing these otherwise promising lead molecules.

References:

1. Aminake, M. N.; Schoof, S.; Sologub, L.; Leubner, M.; Kirschner, M.; Arndt, H. D.; Pradel, G., Thiostrepton and derivatives exhibit antimalarial and gametocytocidal activity by dually targeting parasite proteasome and apicoplast. *Antimicrob. Agents Chemother.* **2011,** *55*, 1338-1348.

2. Myers, C. L.; Hang, P. C.; Ng, G.; Yuen, J.; Honek, J. F., Semi-synthetic analogues of thiostrepton delimit the critical nature of tail region modifications in the control of protein biosynthesis and antibacterial activity. *Bioorg. Med. Chem.* **2010,** *18*, 4231-4237.

3. Naidu, B. N.; Sorenson, M. E.; Matiskella, J. D.; Li, W.; Sausker, J. B.; Zhang, Y.; Connolly, T. P.; Lam, K. S.; Bronson, J. J.; Pucci, M. J.; Yang, H.; Ueda, Y., Synthesis and antibacterial activity of nocathiacin I analogues. *Bioorg. Med. Chem. Lett.* **2006,** *16*, 3545-3549.

4. Schoof, S.; Baumann, S.; Ellinger, B.; Arndt, H.-D., A fluorescent probe for the 70S-ribosomal GTPase-associated center. *ChemBioChem* **2009,** *10*, 242-245.

5. Schoof, S.; Pradel, G.; Aminake, M. N.; Ellinger, B.; Baumann, S.; Potowski, M.; Najajreh, Y.; Kirschner, M.; Arndt, H.-D., Antiplasmodial thiostrepton derivatives: Proteasome inhibitors with a dual mode of action. *Angew. Chem. Int. Ed. Engl.* **2010,** *49*, 3317-3321.

APPENDIX A: STRAINS, FOSMIDS, PLASMIDS, AND PRIMERS USED IN THIS STUDY

Table A.1. Strains, plasmids and fosmids used in these studies

Strain/Plasmids/Fosmids	Description	Reference or source
***Streptomyces* strains**		
S. laurentii ATCC 31255	Wild-type, thiostrepton producer	ATCC
S. actuosus ATCC 25421	Wild-type, nosiheptide producer	ATCC
S. lividans TK24	A common host for *Streptomyces* gene expression and manipulation	[1]
S. coelicolor CH999	A common host for *Streptomyces* gene expression and manipulation	[2]
S. actuosus FZ1	*S. actuosus* containing int-3A10	[3]
S. actuosus FZ2	*S. actuosus* containing int-pCC1FOS	[3]
S. lividans FZ1	*S. lividans* containing int-3A10	[3]
S. lividans FZ2	*S. lividans* containing int-pCC1FOS	[3]
S. laurentii NDS1*	*S. laurentii* containing an in-frame deletion of *tsrA*	[3]
S. laurentii NDS1/int-3A10*	*S. laurentii* NDS1 containing int-3A10 (wild-type *tsrA*)	[3]
S. laurentii NDS1/int-3A101*	*S. laurentii* NDS1 containing int-3A101 (*tsrA* A2G)	[3]
S. laurentii NDS1/int-3A102*	*S. laurentii* NDS1 containing int-3A102 (*tsrA* A4G)	[3]
S. laurentii NDS1/int-3A103*	*S. laurentii* NDS1 containing int-3A103 (*tsrA* T7G)	[3]
S. laurentii NDS1/int-3A104*	*S. laurentii* NDS1 containing int-3A104 (*tsrA* T7S)	[4]
S. laurentii NDS1/int-3A105*	*S. laurentii* NDS1 containing int-3A105 (*tsrA* T7A)	[4]
S. laurentii NDS1/int-3A106*	*S. laurentii* NDS1 containing int-3A106 (*tsrA* T7V)	[4]
S. laurentii NDS1/int-A2C*	*S. laurentii* NDS1 containing int-A2C	[5]
S. laurentii NDS1/int-A2D*	*S. laurentii* NDS1 containing int-A2D	[5]
S. laurentii NDS1/int-A2E*	*S. laurentii* NDS1 containing int-A2E	[5]
S. laurentii NDS1/int-A2F*	*S. laurentii* NDS1 containing int-A2F	[5]
S. laurentii NDS1/int-A2H*	*S. laurentii* NDS1 containing int-A2H	[5]
S. laurentii NDS1/int-A2I*	*S. laurentii* NDS1 containing int-A2I	[5]
S. laurentii NDS1/int-A2K*	*S. laurentii* NDS1 containing int-A2K	[5]
S. laurentii NDS1/int-A2L*	*S. laurentii* NDS1 containing int-A2L	[5]
S. laurentii NDS1/int-A2M*	*S. laurentii* NDS1 containing int-A2M	[5]
S. laurentii NDS1/int-A2N*	*S. laurentii* NDS1 containing int-A2N	[5]
S. laurentii NDS1/int-A2P*	*S. laurentii* NDS1 containing int-A2P	[5]
S. laurentii NDS1/int-A2Q*	*S. laurentii* NDS1 containing int-A2Q	[5]
S. laurentii NDS1/int-A2R*	*S. laurentii* NDS1 containing int-A2R	[5]
S. laurentii NDS1/int-A2S*	*S. laurentii* NDS1 containing int-A2S	[5]
S. laurentii NDS1/int-A2T*	*S. laurentii* NDS1 containing int-A2T	[5]
S. laurentii NDS1/int-A2V*	*S. laurentii* NDS1 containing int-A2V	[5]
S. laurentii NDS1/int-A2W*	*S. laurentii* NDS1 containing int-A2W	[5]
S. laurentii NDS1/int-A2Y*	*S. laurentii* NDS1 containing int-A2Y	[5]
S. laurentii NDS1/int-A4C	*S. laurentii* NDS1 containing int-A4C	[6]
S. laurentii NDS1/int-A4D	*S. laurentii* NDS1 containing int-A4D	[6]
S. laurentii NDS1/int-A4E	*S. laurentii* NDS1 containing int-A4E	[6]
S. laurentii NDS1/int-A4F	*S. laurentii* NDS1 containing int-A4F	[6]
S. laurentii NDS1/int-A4H	*S. laurentii* NDS1 containing int-A4H	[6]
S. laurentii NDS1/int-A4I	*S. laurentii* NDS1 containing int-A4I	[6]

S. laurentii NDS1/int-A4K	*S. laurentii* NDS1 containing int-A4K	[6]
S. laurentii NDS1/int-A4L	*S. laurentii* NDS1 containing int-A4L	[6]
S. laurentii NDS1/int-A4M	*S. laurentii* NDS1 containing int-A4M	[6]
S. laurentii NDS1/int-A4N	*S. laurentii* NDS1 containing int-A4N	[6]
S. laurentii NDS1/int-A4P	*S. laurentii* NDS1 containing int-A4P	[6]
S. laurentii NDS1/int-A4Q	*S. laurentii* NDS1 containing int-A4Q	[6]
S. laurentii NDS1/int-A4R	*S. laurentii* NDS1 containing int-A4R	[6]
S. laurentii NDS1/int-A4S	*S. laurentii* NDS1 containing int-A4S	[6]
S. laurentii NDS1/int-A4T	*S. laurentii* NDS1 containing int-A4T	[6]
S. laurentii NDS1/int-A4V	*S. laurentii* NDS1 containing int-A4V	[6]
S. laurentii NDS1/int-A4W	*S. laurentii* NDS1 containing int-A4W	[6]
S. laurentii NDS1/int-A4Y	*S. laurentii* NDS1 containing int-A4Y	[6]
***E. coli* strains**		
EPI 300	Host for inducing high copy number of a fosmid	Epicentre®
BW25113/pKD46	Host for PCR-targeted disruption of a gene from a fosmid or plasmid	[7]
ET12567/pUZ8002	Host for conjugation with *Streptomyces* species	[8]
Strains used for antibacterial assays		
Bacillus sp. ATCC 27859	Wild-type	ATCC
Escherichia coli ATCC 27856	Wild-type	ATCC
Staphylococcus aureus ATCC 10537	Methicillin-resistant	ATCC
Enterococcus faecium ATCC 12952	Vancomycin-resistant	ATCC
Plasmids		
pCC1FOS	Fosmid used for genomic library construction	Epicentre®
pSC-B-amp/kan	A routine vector from StrataClone Blunt PCR Cloning Kit, for cloning blunt-end PCR product	Agilent Technologies
pSET152	An integrative plasmid containing the apramycin resistance gene and all essential genes for the conjugal transfer and integration into a streptomycete chromosome	[9]
pSE34	Plasmid containing the thiostrepton resistance gene	Pfizer
pIJ778	A plasmid containing the spectinomycin/ streptomycin resistance cassette	[8]
pEX100T	Plasmid containing *sacB* gene	ATCC
JA3A10	Fosmid containing the *tsr* biosynthetic gene cluster	[10]
pJP11*	pCR4-Blunt vector harboring a 1.8 kb fragment PCR amplified from *S. laurentii* genomic DNA, which contains the 0.2 kb *tsrA* gene and its two flanking 0.8 kb region	[10]
int-pCC1FOS	A fosmid containing all essential genes for the conjugal transfer and integration into a streptomycete chromosome	[3]
int-3A10	A fosmid containing the entire *tsr* gene cluster and all essential genes for the conjugal transfer and integration into a streptomycete chromosome	[3]
pLeft*	pSC-B-amp/kan vector harboring the	[3]

pRight*	1022 nt sequence upstream of *tsrA* pSC-B-amp/kan vector harboring the	3
pLR*	1003 nt sequence downstream of *tsrA* pLeft containing a 1 kb insert from the *Nde*I-*Sbf*I digestion of pRight	3
pGM160HK*	A derivative of pGM160K[10] in which a 1.6 kb *Hind*III-digested fragment was deleted	3
pGM160HKss*	A derivative of pGM160HK, in which the ampicillin resistance gene was replaced by the spectinomycin-streptomycin resistance cassette. It is a conjugal and temperature-sensitive *E. coli-Streptomyces* shuttle vector	3
pNDS1*	pGM160HKss containing a 2 kb insert from *Hind*III digestion of pLR	3
pDC1*	Vector pSC-B-amp/kan containing a 0.9 kb *chl*^{R} gene	3
pDC2*	Vector pSC-B-amp/kan containing a 1.8 kb *sacB* gene amplified from pEX100T with primers: SacB-F and SacB-R	3
pDC3*	Plasmid containing the dual-marker cassette (*chl*^{R} and *sacB*)	3
pCL61*	Plasmid containing the *tsrA* variant encoding the Ala2Gly mutation	3
pCL62*	Plasmid containing the *tsrA* variant encoding the Ala4Gly mutation	3
pCL63*	Plasmid containing the *tsrA* variant encoding the Thr7Gly mutation	3
pCL64*	Plasmid containing the *tsrA* variant encoding the Thr7Ser mutation	4
pCL65*	Plasmid containing the *tsrA* variant encoding the Thr7Ala mutation	4
pCL66*	Plasmid containing the *tsrA* variant encoding the Thr7Val mutation	4
pA2C*	pSC-B-amp/kan containing the *tsrA* variant encoding the Ala2Cys mutation	5
pA2D*	pSC-B-amp/kan containing the *tsrA* variant encoding the Ala2Asp mutation	5
pA2E*	pSC-B-amp/kan containing the *tsrA* variant encoding the Ala2Glu mutation	5
pA2F*	pSC-B-amp/kan containing the *tsrA* variant encoding the Ala2Phe mutation	5
pA2H*	pSC-B-amp/kan containing the *tsrA* variant encoding the Ala2His mutation	5
pA2I*	pSC-B-amp/kan containing the *tsrA* variant encoding the Ala2Ile mutation	5
pA2K*	pSC-B-amp/kan containing the *tsrA* variant encoding the Ala2Lys mutation	5
pA2L*	pSC-B-amp/kan containing the *tsrA* variant encoding the Ala2Leu mutation	5
pA2M*	pSC-B-amp/kan containing the *tsrA* variant encoding the Ala2Met mutation	5
pA2N*	pSC-B-amp/kan containing the *tsrA* variant encoding the Ala2Asn mutation	5
pA2P*	pSC-B-amp/kan containing the *tsrA* variant encoding the Ala2Pro mutation	5

pA2Q*	pSC-B-amp/kan containing the *tsrA* variant encoding the Ala2Gln mutation	5
pA2R*	pSC-B-amp/kan containing the *tsrA* variant encoding the Ala2Arg mutation	5
pA2S*	pSC-B-amp/kan containing the *tsrA* variant encoding the Ala2Ser mutation	5
pA2T*	pSC-B-amp/kan containing the *tsrA* variant encoding the Ala2Thr mutation	5
pA2V*	pSC-B-amp/kan containing the *tsrA* variant encoding the Ala2Val mutation	5
pA2W*	pSC-B-amp/kan containing the *tsrA* variant encoding the Ala2Trp mutation	5
pA2Y*	pSC-B-amp/kan containing the *tsrA* variant encoding the Ala2Tyr mutation	5
pA4C	pSC-B-amp/kan containing the *tsrA* variant encoding the Ala4Cys mutation	6
pA4D	pSC-B-amp/kan containing the *tsrA* variant encoding the Ala4Asp mutation	6
pA4E	pSC-B-amp/kan containing the *tsrA* variant encoding the Ala4Glu mutation	6
pA4F	pSC-B-amp/kan containing the *tsrA* variant encoding the Ala4Phe mutation	6
pA4H	pSC-B-amp/kan containing the *tsrA* variant encoding the Ala4His mutation	6
pA4I	pSC-B-amp/kan containing the *tsrA* variant encoding the Ala4Ile mutation	6
pA4K	pSC-B-amp/kan containing the *tsrA* variant encoding the Ala4Lys mutation	6
pA4L	pSC-B-amp/kan containing the *tsrA* variant encoding the Ala4Leu mutation	6
pA4M	pSC-B-amp/kan containing the *tsrA* variant encoding the Ala4Met mutation	6
pA4N	pSC-B-amp/kan containing the *tsrA* variant encoding the Ala4Asn mutation	6
pA4P	pSC-B-amp/kan containing the *tsrA* variant encoding the Ala4Pro mutation	6
pA4Q	pSC-B-amp/kan containing the *tsrA* variant encoding the Ala4Gln mutation	6
pA4R	pSC-B-amp/kan containing the *tsrA* variant encoding the Ala4Arg mutation	6
pA4S	pSC-B-amp/kan containing the *tsrA* variant encoding the Ala4Ser mutation	6
pA4T	pSC-B-amp/kan containing the *tsrA* variant encoding the Ala4Thr mutation	6
pA4V	pSC-B-amp/kan containing the *tsrA* variant encoding the Ala4Val mutation	6
pA4W	pSC-B-amp/kan containing the *tsrA* variant encoding the Ala4Trp mutation	6
pA4Y	pSC-B-amp/kan containing the *tsrA* variant encoding the Ala4Tyr mutation	6
Fosmids		
int-3A100*	Derived from int-3A10. *tsrA* is replaced by *chl*^{R}*-sacB* cassette	3
int-3A101*	Derived from int-3A100. The *chl*^{R}*-sacB* cassette is replaced by the *tsrA* variant	3

	encoding the Ala2Gly mutation	
int-3A102*	Derived from int-3A100. The *chl*^{R}-*sacB* cassette is replaced by the *tsrA* variant encoding the Ala4Gly mutation	3
int-3A103*	Derived from int-3A100. The *chl*^{R}-*sacB* cassette is replaced by the *tsrA* variant encoding the Thr7Gly mutation	3
int-3A104*	Derived from int-3A100. The *chl*^{R}-*sacB* cassette is replaced by the *tsrA* variant encoding the Thr7Ser mutation	4
int-3A105*	Derived from int-3A100. The *chl*^{R}-*sacB* cassette is replaced by the *tsrA* variant encoding the Thr7Ala mutation	4
int-3A106*	Derived from int-3A100. The *chl*^{R}-*sacB* cassette is replaced by the *tsrA* variant encoding the Thr7Val mutation	4
int-A2C*	Derived from int-3A100. The *chl*^{R}-*sacB* cassette is replaced by the *tsrA* variant encoding the Ala2Cys mutation	5
int-A2D*	Derived from int-3A100. The *chl*^{R}-*sacB* cassette is replaced by the *tsrA* variant encoding the Ala2Asp mutation	5
int-A2E*	Derived from int-3A100. The *chl*^{R}-*sacB* cassette is replaced by the *tsrA* variant encoding the Ala2Glu mutation	5
int-A2F*	Derived from int-3A100. The *chl*^{R}-*sacB* cassette is replaced by the *tsrA* variant encoding the Ala2Phe mutation	5
int-A2H*	Derived from int-3A100. The *chl*^{R}-*sacB* cassette is replaced by the *tsrA* variant encoding the Ala2His mutation	5
int-A2I*	Derived from int-3A100. The *chl*^{R}-*sacB* cassette is replaced by the *tsrA* variant encoding the Ala2Ile mutation	5
int-A2K*	Derived from int-3A100. The *chl*^{R}-*sacB* cassette is replaced by the *tsrA* variant encoding the Ala2Lys mutation	5
int-A2L*	Derived from int-3A100. The *chl*^{R}-*sacB* cassette is replaced by the *tsrA* variant encoding the Ala2Leu mutation	5
int-A2M*	Derived from int-3A100. The *chl*^{R}-*sacB* cassette is replaced by the *tsrA* variant encoding the Ala2Met mutation	5
int-A2N*	Derived from int-3A100. The *chl*^{R}-*sacB* cassette is replaced by the *tsrA* variant encoding the Ala2Asn mutation	5
int-A2P*	Derived from int-3A100. The *chl*^{R}-*sacB* cassette is replaced by the *tsrA* variant encoding the Ala2Pro mutation	5
int-A2Q*	Derived from int-3A100. The *chl*^{R}-*sacB* cassette is replaced by the *tsrA* variant encoding the Ala2Gln mutation	5
int-A2R*	Derived from int-3A100. The *chl*^{R}-*sacB* cassette is replaced by the *tsrA* variant encoding the Ala2Arg mutation	5
int-A2S*	Derived from int-3A100. The *chl*^{R}-*sacB*	5

	cassette is replaced by the *tsrA* variant encoding the Ala2Ser mutation	
int-A2T*	Derived from int-3A100. The *chl*^{R}-*sacB* cassette is replaced by the *tsrA* variant encoding the Ala2Thr mutation	5
int-A2V*	Derived from int-3A100. The *chl*^{R}-*sacB* cassette is replaced by the *tsrA* variant encoding the Ala2Val mutation	5
int-A2W*	Derived from int-3A100. The *chl*^{R}-*sacB* cassette is replaced by the *tsrA* variant encoding the Ala2Trp mutation	5
int-A2Y*	Derived from int-3A100. The *chl*^{R}-*sacB* cassette is replaced by the *tsrA* variant encoding the Ala2Tyr mutation	5
int-A4C	Derived from int-3A100. The *chl*^{R}-*sacB* cassette is replaced by the *tsrA* variant encoding the Ala4Cys mutation	6
int-A4D	Derived from int-3A100. The *chl*^{R}-*sacB* cassette is replaced by the *tsrA* variant encoding the Ala4Asp mutation	6
int-A4E	Derived from int-3A100. The *chl*^{R}-*sacB* cassette is replaced by the *tsrA* variant encoding the Ala4Glu mutation	6
int-A4F	Derived from int-3A100. The *chl*^{R}-*sacB* cassette is replaced by the *tsrA* variant encoding the Ala4Phe mutation	6
int-A4H	Derived from int-3A100. The *chl*^{R}-*sacB* cassette is replaced by the *tsrA* variant encoding the Ala4His mutation	6
int-A4I	Derived from int-3A100. The *chl*^{R}-*sacB* cassette is replaced by the *tsrA* variant encoding the Ala4Ile mutation	6
int-A4K	Derived from int-3A100. The *chl*^{R}-*sacB* cassette is replaced by the *tsrA* variant encoding the Ala4Lys mutation	6
int-A4L	Derived from int-3A100. The *chl*^{R}-*sacB* cassette is replaced by the *tsrA* variant encoding the Ala4Leu mutation	6
int-A4M	Derived from int-3A100. The *chl*^{R}-*sacB* cassette is replaced by the *tsrA* variant encoding the Ala4Met mutation	6
int-A4N	Derived from int-3A100. The *chl*^{R}-*sacB* cassette is replaced by the *tsrA* variant encoding the Ala4Asn mutation	6
int-A4P	Derived from int-3A100. The *chl*^{R}-*sacB* cassette is replaced by the *tsrA* variant encoding the Ala4Pro mutation	6
int-A4Q	Derived from int-3A100. The *chl*^{R}-*sacB* cassette is replaced by the *tsrA* variant encoding the Ala4Gln mutation	6
int-A4R	Derived from int-3A100. The *chl*^{R}-*sacB* cassette is replaced by the *tsrA* variant encoding the Ala4Arg mutation	6
int-A4S	Derived from int-3A100. The *chl*^{R}-*sacB* cassette is replaced by the *tsrA* variant encoding the Ala4Ser mutation	6

int-A4T	Derived from int-3A100. The *chl*^{R}-*sacB* cassette is replaced by the *tsrA* variant encoding the Ala4Thr mutation	6
int-A4V	Derived from int-3A100. The *chl*^{R}-*sacB* cassette is replaced by the *tsrA* variant encoding the Ala4Val mutation	6
int-A4W	Derived from int-3A100. The *chl*^{R}-*sacB* cassette is replaced by the *tsrA* variant encoding the Ala4Trp mutation	6
int-A4Y	Derived from int-3A100. The *chl*^{R}-*sacB* cassette is replaced by the *tsrA* variant encoding the Ala4Tyr mutation	6

* These strains, fosmids and plasmids were generated by Dr. Chaoxuan Li.

Table A.2. Primers used in these studies

Primer	Sequence	Description
CTSR1-F	5'-TTTGAGTTATCGAGATTTTCAGGAGCTAAGG AAGCTAAAGCGGTGGTTTTTTTGTTTGCAAGC-3'	Primers for the replacement of *chl*^{R} in pCC1FOS, or fosmids based on it, with genes *aac(3)IV*, *int*, *attP* and *oriT* amplified from pSET152. pSET152 sequence is underlined.
CTSR1-R	5'-ACCAGGCGTTTAAGGGCACCAATAACTGCC TTAAAAAAACCGATGCAAAGTGCCGATCA-3'	
CTSR2-F	5'-GCGGTGGTTTTTTTGTTTGCAAGC-3'	Primers for the confirmation of int-pCC1FOS and int-3A10.
CTSR2-R	5'-CCGATGCAAAGTGCCGATCA-3'	
CTSR3-F	5'- GCGGTGGTTTTTTTGTTTGCAAGC-3'	Primers for the confirmation of int-pCC1FOS and int-3A10.
CTSR3-R	5'- CTACGGAAGGAGCTGTGGAC-3'	
TSRK-F	5'-CCGATGCAAAGTGCCGATCA-3'	Primers for the amplification of *tsrK*.
TSRK-R	5'-TCGCTCGAGGCGCAGCACCTTGCC-3'	
TSRV-F	5'-TGCTGCATATGACGGGAGTCACCGAACCG-3'	Primers for the amplification of *tsrV*.
TSRV-R	5'-TTCCTCGAGTCAGTCTCCCGGCGCCTC-3'	
TSRN-F	5'-AGTATTCATATGACCGCCCCCGCGCTCCCGC TC-3'	Primers for the amplification of *tsrN*.
TSRN-R	5'-ACCCTCGAGTCAGACGGCGAGCCGCCGTT C-3'	
DTSR1-F	5'-AAGCTTGTGAGGGTCACCACGGATCC-3'	Primers for the amplification of the region upstream of *tsrA*. Underlined regions are the restriction sites of *Hind*III, *Nde*I and *Sbf*I.
DTSR1-R	5'-CCTGCAGGCATATGCTCCAGGGCGGCATTGCT CAT-3'	
DTSR2-F	5'-CATATGTGAGGTAACACCCGGCGCGGA-3'	Primers for the amplification of the region downstream of *tsrA*. Underlined regions are restriction sites of *Hind*III, *Nde*I and *Sbf*I.
DTSR2-R	5'-CCTGCAGGAAGCTTGCTCCAGGTCCGCGACGC CG-3'	
DTSR3-F	5'-ATCGTGTTGGGCTTGACG-3'	Primers used to confirm the construction of *S. laurentii* NDS1.
DTSR3-R	5'-CGCGGTGCAATAGGACAT-3'.	
Chl-F	5'-ATTCCGGGGATCCGTCGACCAGATCT*GCCGCTC CATGAGCTTATCG*-3'	Primers for the amplification of *chl*^{R} from pCC1FOS. Underlined regions are restriction sites of *Bgl*II, *Nde*I and *Sbf*I. pCC1FOS sequence is italicized.
Chl-R	5'-CCTGCAGGCATATG*AATTACGCCCCGCCCTGCC*-3'	
SacB-F	5'-CATATG*AACTTTATGCCCATGCAACAG*-3'	Primers for the amplification of *sacB* gene from pEX100T. Underlined regions are restriction sites of *Bgl*II, *Nde*I and *Sbf*I. pEX100T sequence is italicized.
SacB-R	5'-CCTGCAGGTGTAGGCTGGAGCTGCTTCAGATCT*G AGAGTGCACCATAATCGGC*-3'	
AmpSS-F	*5'-CCAATGCTTAATCAGTGAGGCACCTATCTCAGCGATC T*GGGAATAGGAACTTCATGAGC-3'	Primers for the amplification of the spectinomycin-streptomycin resistance cassette from pIJ778 to replace ampicillin resistance gene in pGM160HK. Underlined regions are sequence of pIJ778. pGM160HK sequence is in italics.
AmpSS-R	5'-*ATGAGTATTCAACATTTCCGTGTCGCCCTTATTCCCTT T*GAAGTTCCCGCCAGCCTCGC-3'	
DC1-F	5'-ATTCCGGGGATCCGTCGACCAGATCTGCCG CTCCATGAGCTTATCG-3'	Primers for the amplification of *chl*^{R} from pCC1FOS. The *Sbf*I and *Nde*I restriction sites are underlined and in italics, respectively.
DC1-R	5'-CCTGCAGG*CATATG*AATTACGCCCCGCCCTG CC-3'	
DC2-F	5'-*CATATG*AACTTTATGCCCATGCAACAG-3'	Primers for the amplification of *sacB* from pEX100T. The *Sbf*I and *Nde*I restriction sites are underlined and in italics, respectively.
DC2-R	5'-CCTGCAGGTGTAGGCTGGAGCTGCTTCAGA TCTGAGAGTGCACCATAATCGGC-3'	
A2G-F	5'-GTCACGATGATCGGCTCCGCCTCCTGC-3'	Primers to generate TsrA Ala2Gly.
A2G-R	5'-GCAGGAGGCGGAGCCGATCATCGTGAC-3'	
A4G-F	5'-GATGATCGCGTCCGGCTCCTGCACCACC-3'	Primers to generate TsrA Ala4Gly.
A4G-R	5'-GGTGGTGCAGGAGCCGGACGCGATCATC-3'	
T7G-F	5'-GTCCGCCTCCTGCGGCACCTGCATCTGC-3'	Primers to generate TsrA Thr7Gly.

T7G-R	5’-GCAGATGCAGGTGCCGCAGGAGGCGGAC-3’	
T7S-F T7S-R	5’-GTCCGCCTCCTGCTCCACCTGCATCTGC-3’ 5’-GCAGATGCAGGTGGAGCAGGAGGCGGAC-3’	Primers to generate TsrA Thr7Ser.
T7A-F T7A-R	5’-GTCCGCC TCCTGCGGCACCTGCATCTGC-3’ 5’-GCAGATGCAGGTGCCGCAGGAGGCGGAC-3’	Primers to generate TsrA Thr7Ala.
T7V-F T7V-R	5’-ACTACATGGACGAGACGCTGCTC-3’ 5’-CAGGTCCGGCGGGCGGGGA-3’	Primers for amplification of chemically synthesized ultramer T7V.
T7V	5’-ACTACATGGACGAGACGCTGCTCGACGGTG AGGACCTGACCGTCACGATGATCGCGTCCGCCTCCT GCGTCACCTGCATCTGCACCTGCAGCTGCAGCTCCTG AGGTAACACCCGGCGCGGAGGACTGTTCCTCCCCGC CCGCCGGACCTG-3’	Chemically synthesized ultramer to generate TsrA Thr7Val.
A2X	5’-ACTACATGGACGAGACGCTGCTCGACGGTG AGGACCTGACCGTCACGATGATC<u>NNS</u>TCCGCCTCCTG CACCACCTGCATCTGCACCTGCAGCTGCAGCTCCTGA GGTAACACCCGGCGCGGAGGACTGTTCCTCCCCGCC CGCCGGACCTG-3’	Chemically synthesized ultramer to generate TsrA Ala2 mutants. Underlined degenerate codon encodes the amino acid at the 2nd position of the TsrA core peptide.
A4X	5’-ACTACATGGACGAGACGCTGCTCGACGGTG AGGACCTGACCGTCACGATGATCGCGTCC<u>NNS</u>TCCT GCACCACCTGCATCTGCACCTGCAGCTGCAGCTCCTG AGGTAACACCCGGCGCGGAGGACTGTTCCTCCCCGC CCGCCGGACCTG-3’	Chemically synthesized ultramer to generate TsrA Ala4 mutants. Underlined degenerate codon encodes the amino acid at the 4th position of the TsrA core peptide.
SD1-F SD1-R	5’-<u>GCGCGATCGACGCGACCGCAGACTTGCCGA AAGGTTGTG</u>ATTCCGGGGATCCGTCGACC-3’ 5’-<u>GGCGGGGAGGAACAGTCCTCCGCGCCGGGT GTTACCTCA</u>TGTAGGCTGGAGCTGCTTC-3’	Primers for the disruption of *tsrA* in int-3A10. The underlined regions are homologous to *tsrA*.
SD2-F SD2-R	5’-GCGCGATCGACGCGACCGCAG-3’ 5’-GGCGGGGAGGAACAGTCCTCC-3’	Primers used in the amplification of *tsrA* variants from plasmid templates.
SD3-F SD3-R	5’-ATCGTGTTGGGCTTGACG-3’ 5’-CGCGGTGCAATAGGACAT-3’	Primers used in DNA sequencing to confirm int-3A10 derived fosmid variants.

References:

1. Hopwood, D. A.; Hintermann, G.; Kieser, T.; Wright, H. M., Integrated DNA sequences in three streptomycetes form related autonomous plasmids after transfer to *Streptomyces lividans*. *Plasmid* **1984,** *11*, 1-16.

2. Ziermann, R.; Betlach, M. C., Recombinant polyketide synthesis in *Streptomyces*: engineering of improved host strains. *BioTechniques* **1999,** *26*, 106-110.

3. Li, C.; Zhang, F.; Kelly, W. L., Heterologous production of thiostrepton A and biosynthetic engineering of thiostrepton analogs. *Mol. BioSyst.* **2011,** *7*, 82-90.

4. Li, C.; Zhang, F.; Kelly, W. L., Mutagenesis of the thiostrepton precursor peptide at Thr7 impacts both biosynthesis and function. *Chem. Commun.* **2012,** *48*, 558-560.

5. Zhang, F. L., C.; Kelly, W. L., Saturation mutagenesis of the Ala2 residue of TsrA in *Streptomyces laurentii*. *In preparation* **2014**.

6. Zhang, F.; Kelly, W. L., Saturation mutagenesis of TsrA Ala4 unveils a highly mutable residue of thiostrepton A. *Submitted* **2014**.

7. Datsenko, K. A.; Wanner, B. L., One-step inactivation of chromosomal genes in *Escherichia coli* K-12 using PCR products. *Proc. Natl. Acad. Sci. U.S.A.* **2000,** *97*, 6640-6645.

8. Gust, B.; Challis, G. L.; Fowler, K.; Kieser, T.; Chater, K. F., PCR-targeted *Streptomyces* gene replacement identifies a protein domain needed for biosynthesis of the sesquiterpene soil odor geosmin. *Proc. Natl. Acad. Sci. U.S.A.* **2003,** *100*, 1541-1546.

9. Bierman, M.; Logan, R.; O'Brien, K.; Seno, E. T.; Rao, R. N.; Schoner, B. E., Plasmid cloning vectors for the conjugal transfer of DNA from *Escherichia coli* to *Streptomyces spp*. *Gene* **1992,** *116*, 43-49.

10. Kelly, W. L.; Pan, L.; Li, C., Thiostrepton biosynthesis: Prototype for a new family of bacteriocins. *J. Am. Chem. Soc.* **2009,** *131*, 4327-4334.

APPENDIX B: SPECTRAL DATA FOR THIOSTREPTON A FROM CHAPTER 2

Figure B.1. HPLC-MS of culture extracts from *S. actuosus* FZ1 and *S. actuosus* FZ2.

(**A**) HPLC-MS of the culture extract from *S. actuosus* FZ1. (*1*) Chromatogram extracted for *m*/*z* 833 $[M+2H]^{2+}$ from *S. actuosus* FZ1. (*2*) Mass spectrum of thiostrepton A from *S. actuosus* FZ1 eluting at t_R = 27.8 min.

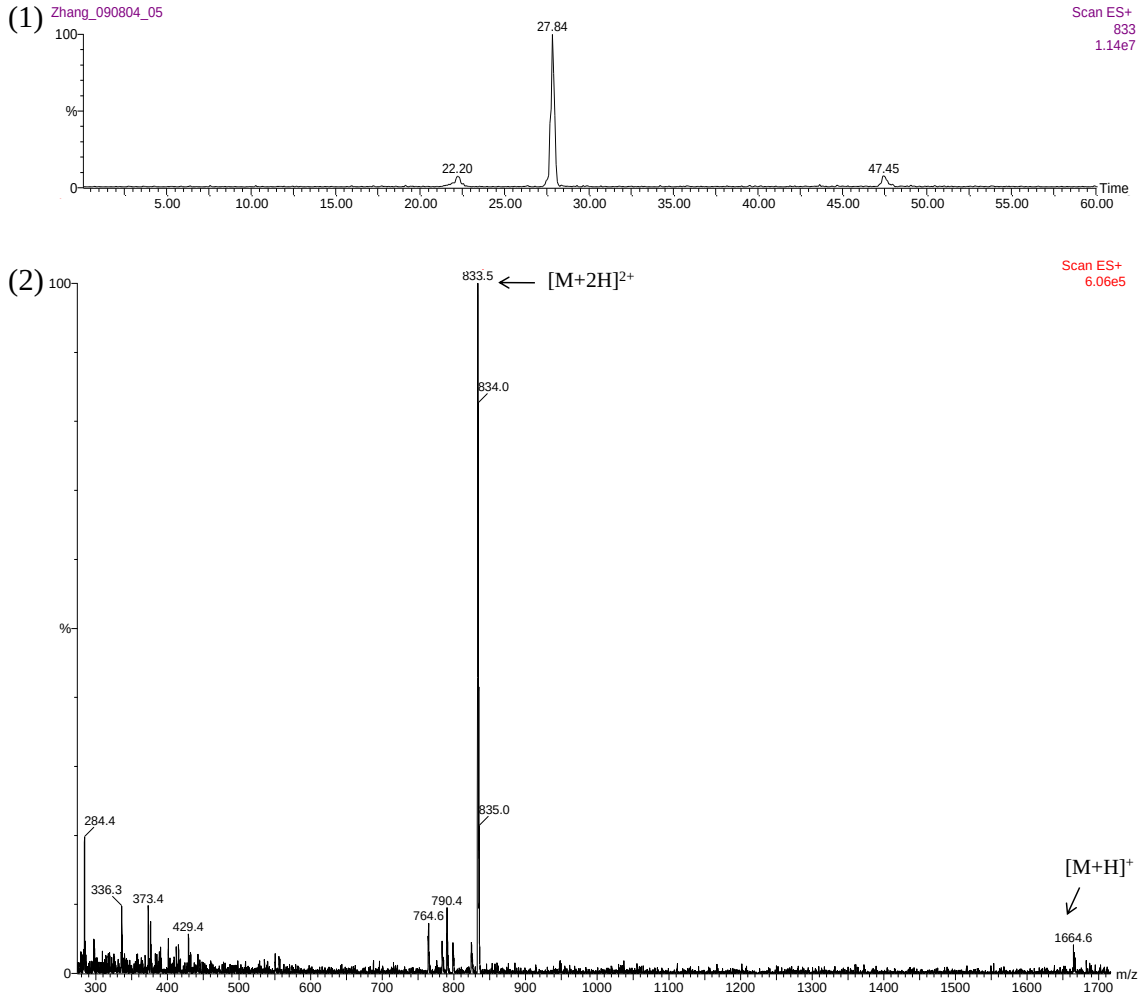

(**B**) HPLC-MS chromatogram extracted for *m*/*z* 833 $[M+2H]^{2+}$ from the *S. actuosus* FZ2 culture extract.

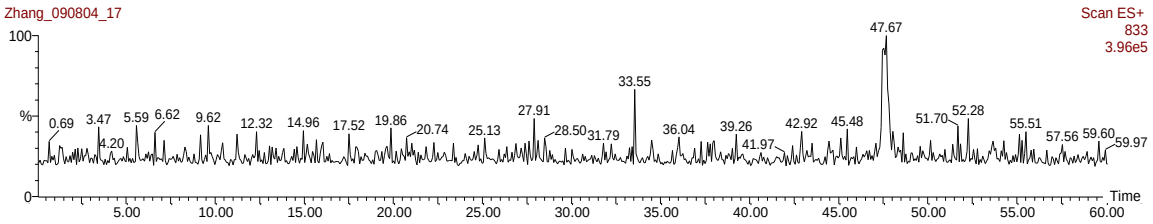

Figure B.2. HPLC-MS of culture extracts from *S. lividans* FZ1 and *S. lividans* FZ2.

(**A**) HPLC-MS of the culture extract from *S. lividans* FZ1. (*1*) HPLC-MS chromatogram extracted for *m*/*z* 833 $[M+2H]^{2+}$ from *S. lividans* FZ1. (*2*) Mass spectrum of thiostrepton A from *S. lividans* FZ1 eluting at t_R = 27.8 min.

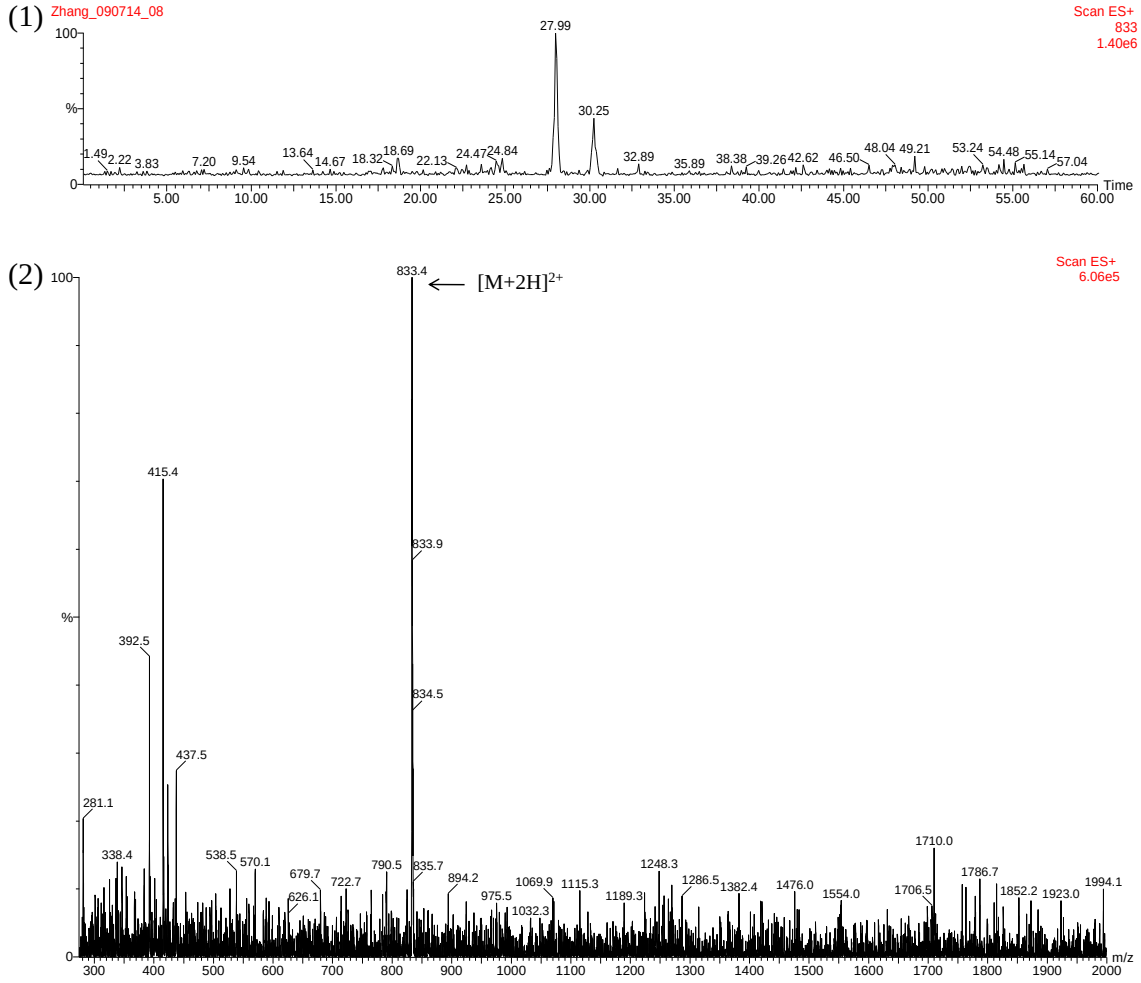

(**B**) HPLC-MS chromatogram extracted for *m*/*z* 833 $[M+2H]^{2+}$ from the *S. lividans* FZ2 culture extract.

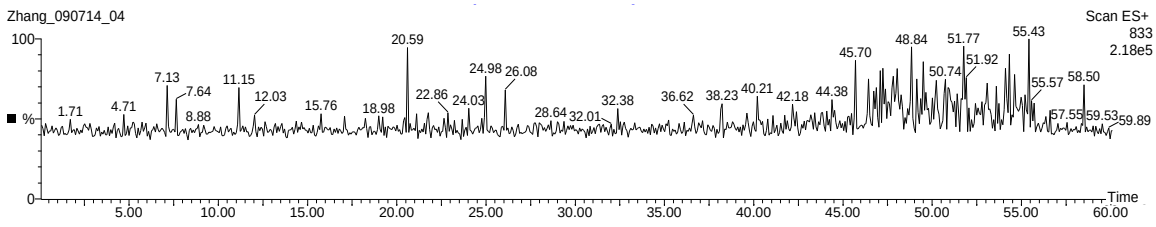

APPENDIX C: SUPPORTING FIGURES AND SPECTRAL DATA FOR COMPOUNDS FROM CHAPTER 3

Figure C.1. Structure of and numbering system used for thiostrepton Ala2Gly.

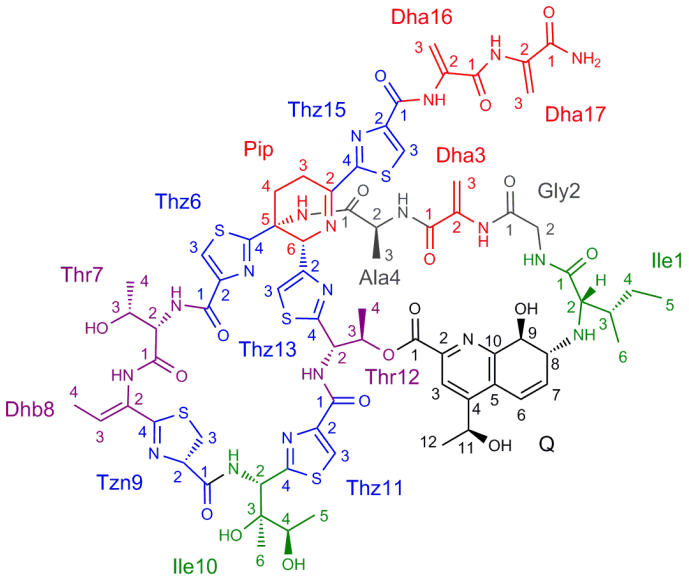

Figure C.2. HPLC-MS of thiostrepton Ala2Gly isolated from *S. laurentii* NDS1 int-3A101.

(**A**) Total ion chromatogram of thiostrepton Ala2Gly.

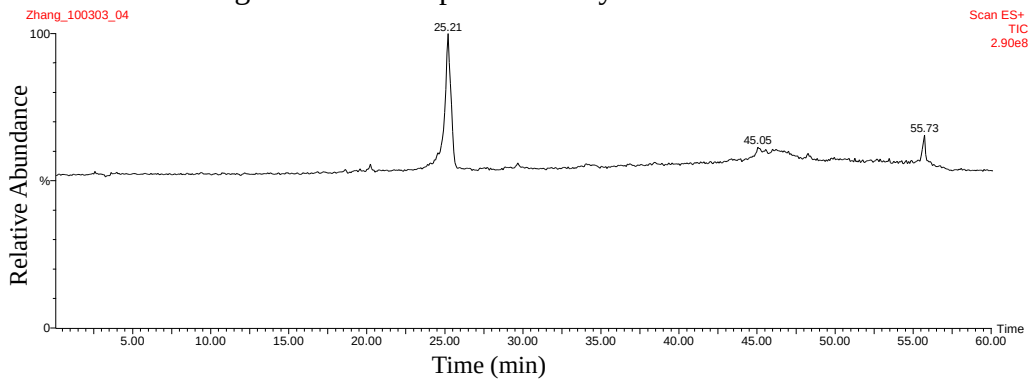

(**B**) Chromatogram extracted for *m*/*z* 826 of thiostrepton Ala2Gly.

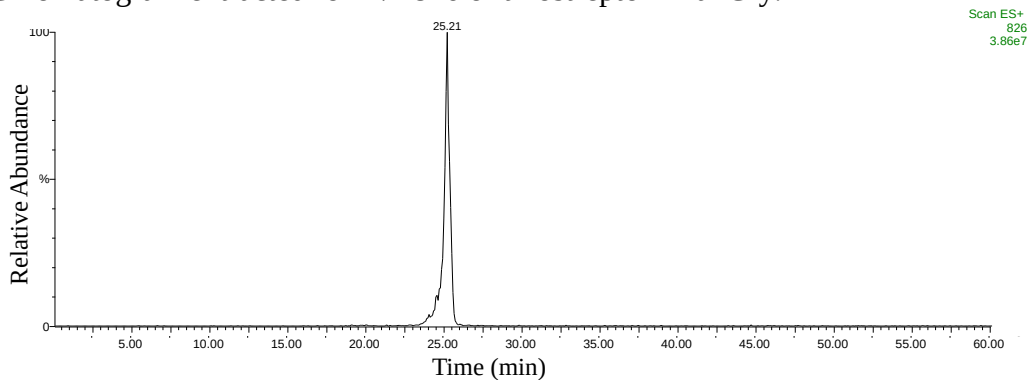

(**C**) Mass spectrum of thiostrepton Ala2Gly eluting at t_R = 25.2 min.

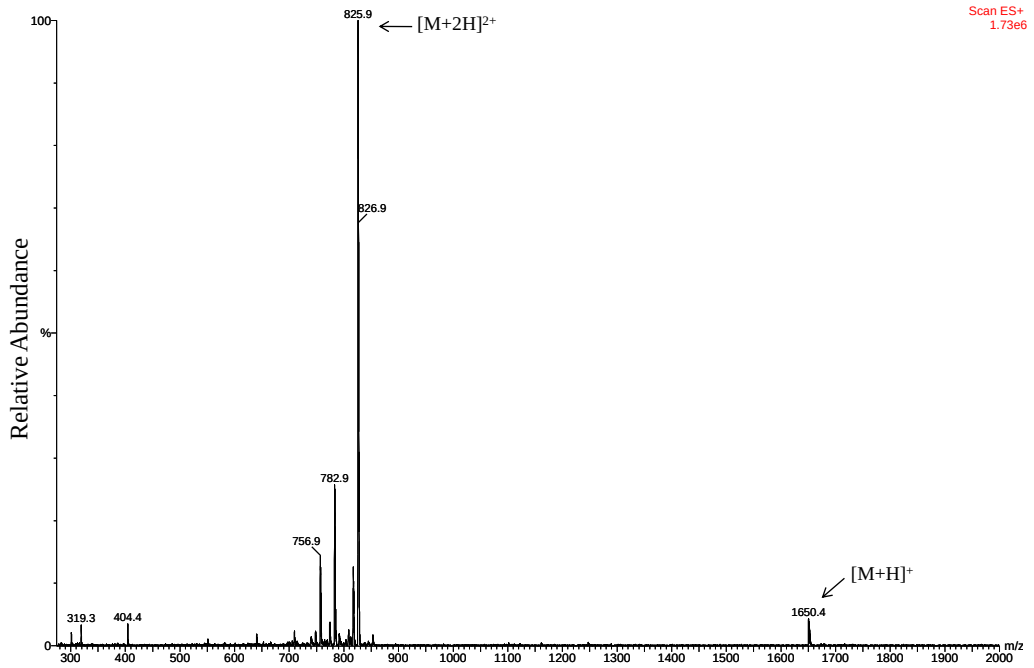

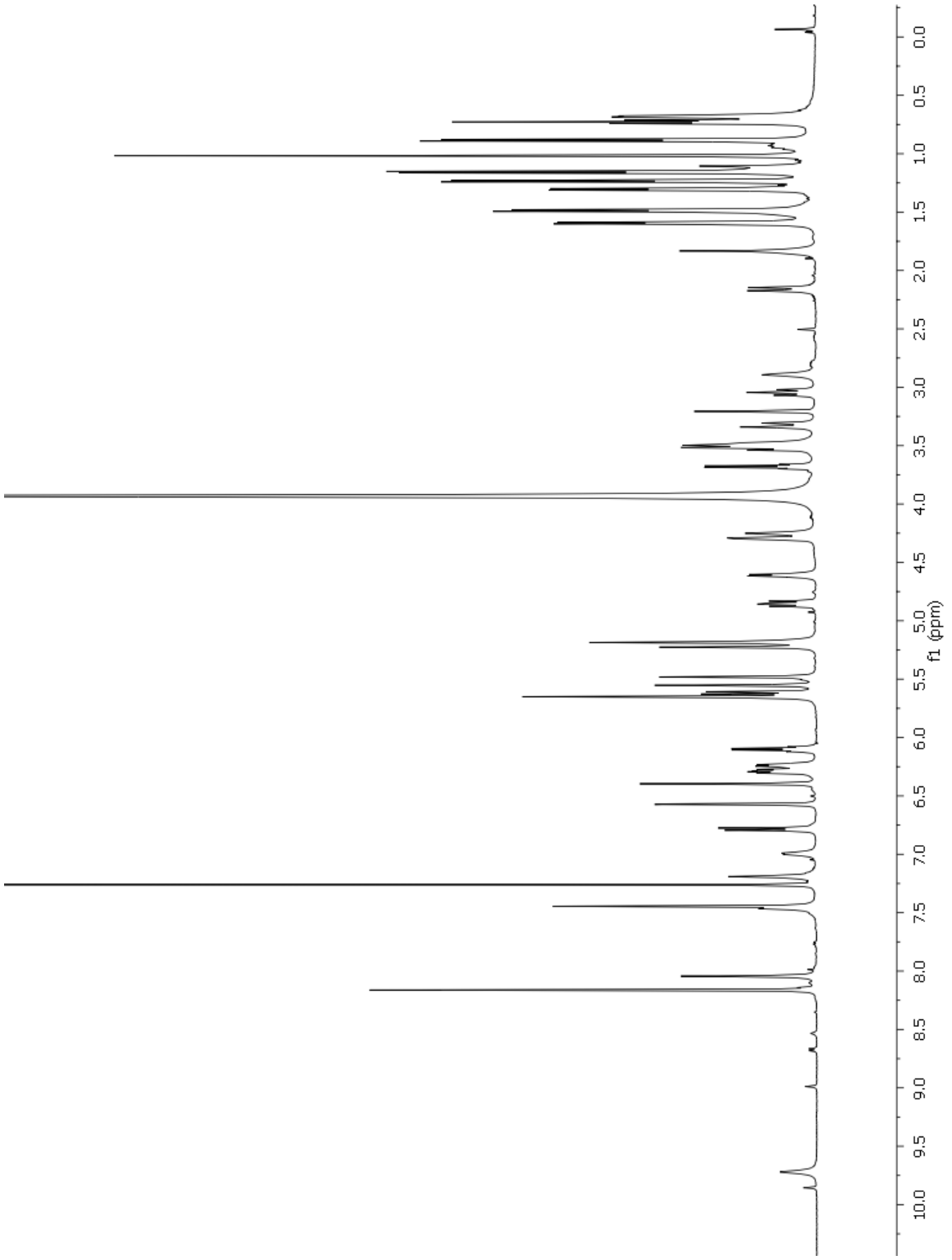

Figure C.3. ^{1}H NMR spectrum of thiostrepton Ala2Gly (500 MHz, $CDCl_3$-CD_3OD 4:1, 25 °C).

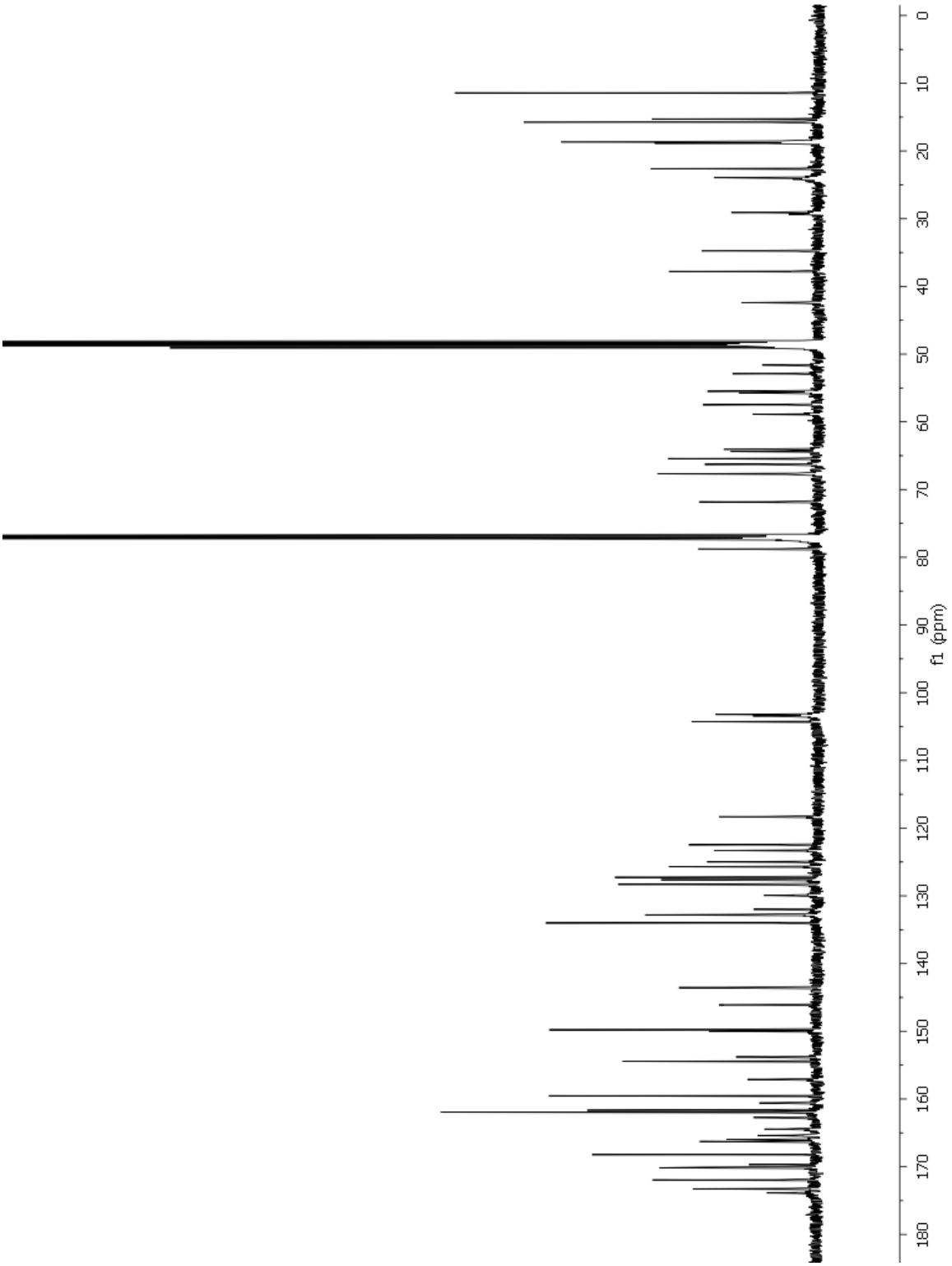

Figure C.4. ^{13}C NMR spectrum of thiostrepton Ala2Gly (125 MHz, $CDCl_3$-CD_3OD 4:1, 25 °C).

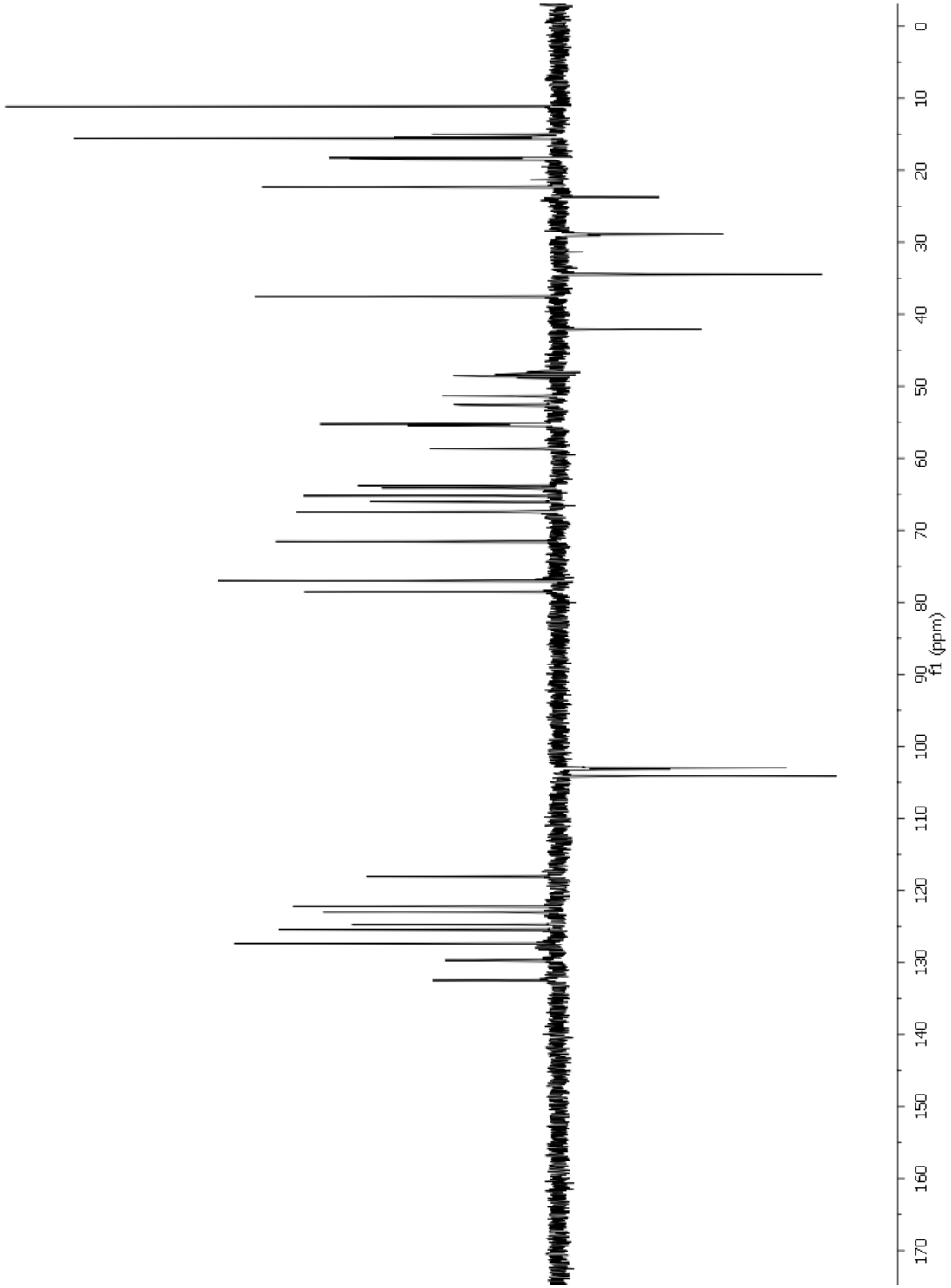

Figure C.5. DEPT-135 NMR spectrum of thiostrepton Ala2Gly (125 MHz, $CDCl_3$-CD_3OD 4:1, 25 °C).

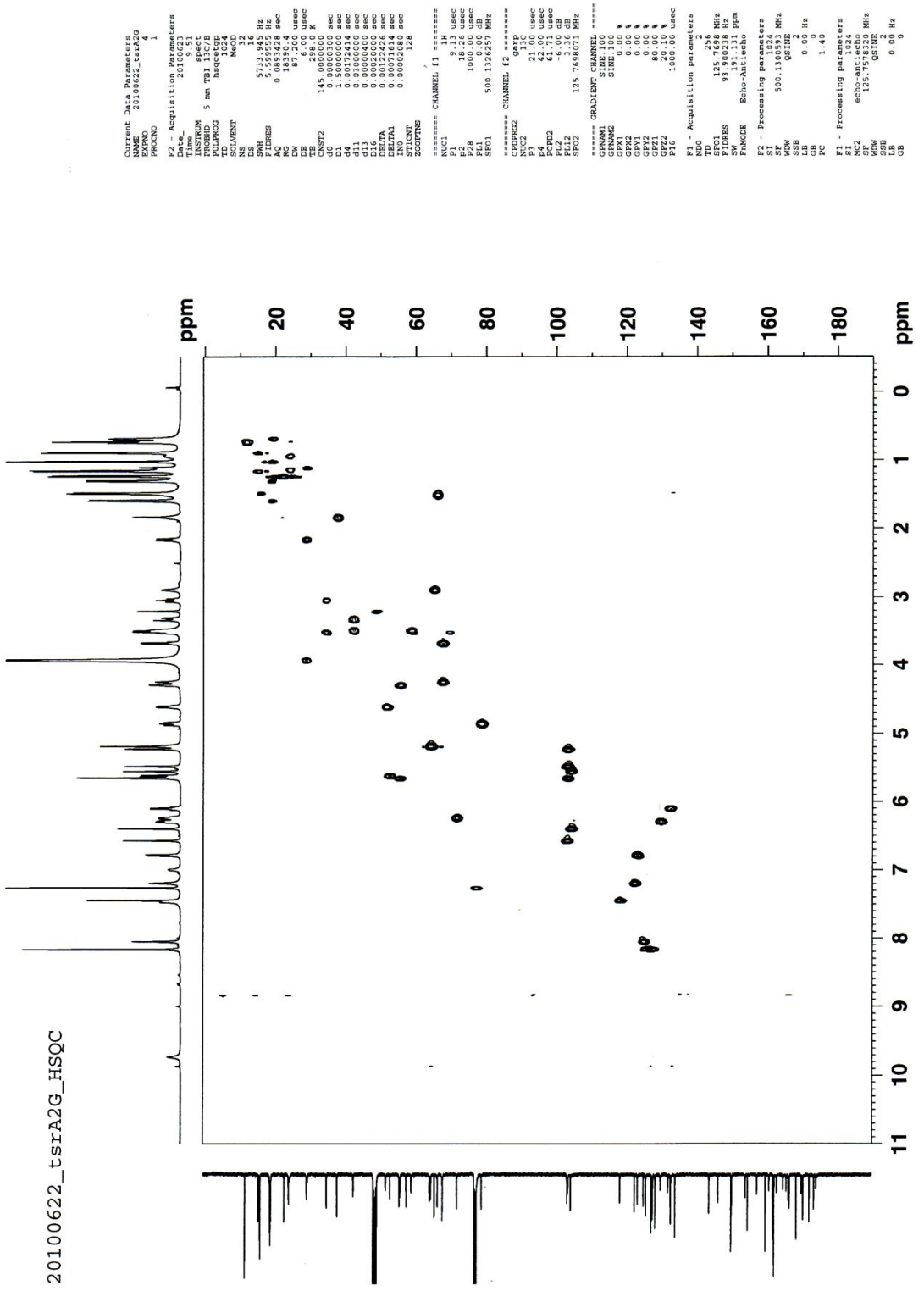

Figure C.6. gHSQC spectrum of thiostrepton Ala2Gly (500 MHz, $CDCl_3$-CD_3OD 4:1, 25 °C).

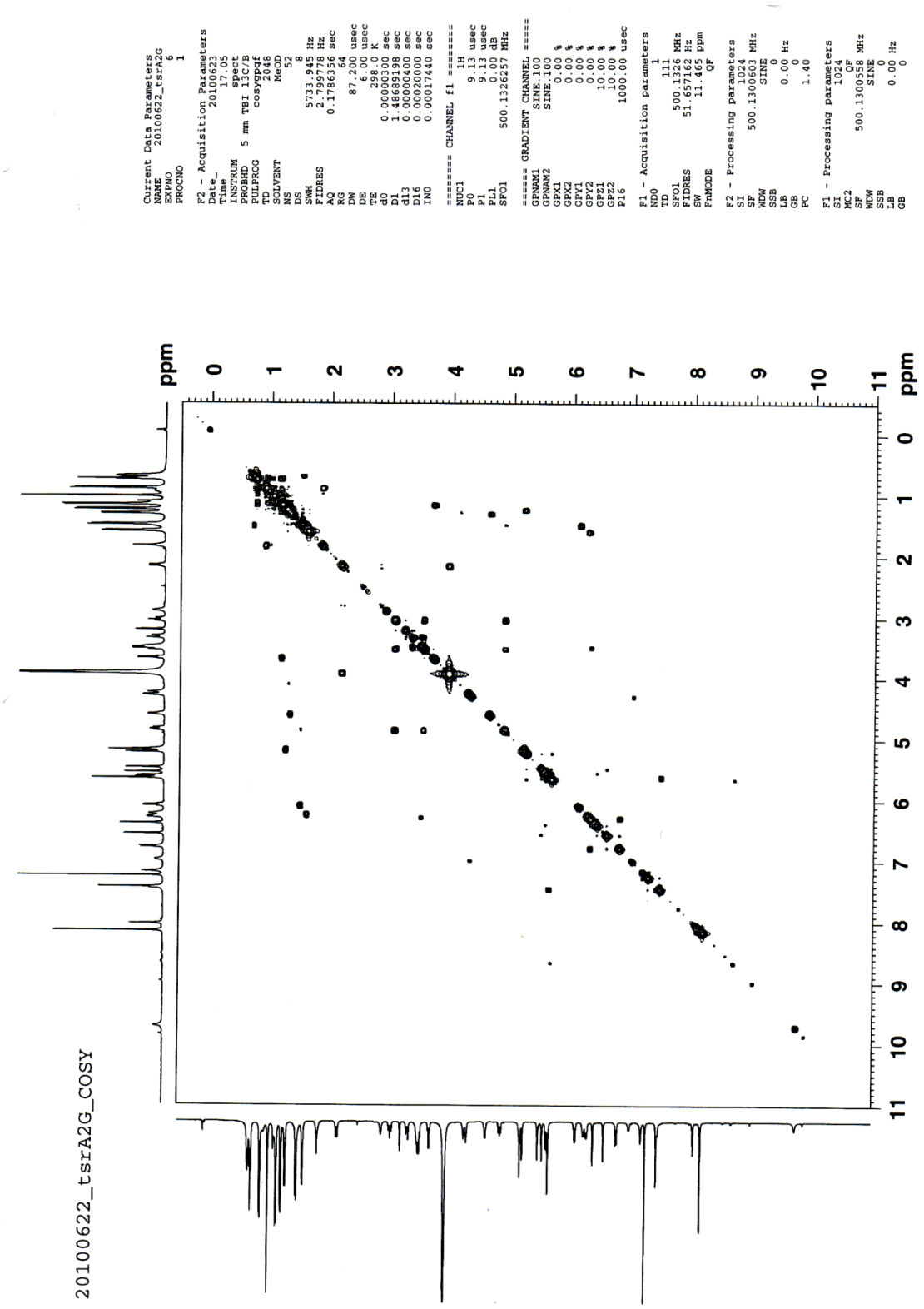

Figure C.7. gCOSY spectrum of thiostrepton Ala2Gly (500 MHz, $CDCl_3$-CD_3OD 4:1, 25 °C).

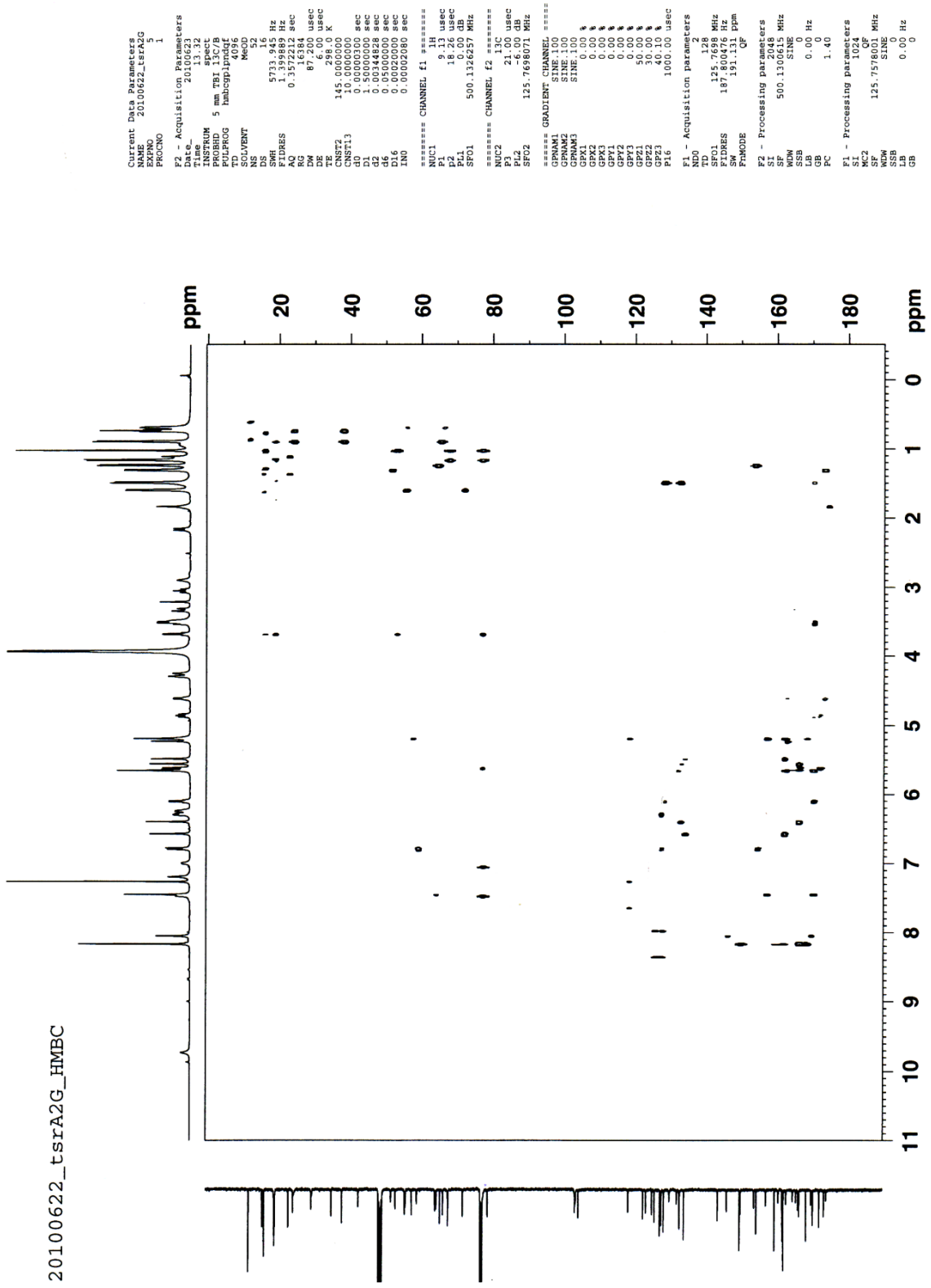

Figure C.8. gHMBC spectrum of thiostrepton Ala2Gly (500 MHz, $CDCl_3$-CD_3OD 4:1, 25 °C).

Table C.1. ^{1}H and ^{13}C NMR assignments of thiostrepton Ala2Gly

Position	δ_C [ppm]; mult	δ_H [ppm] (mult, J in Hz)	HMBC[a]	COSY[b]
Ile1				
Ile1-1	173.9; C q			
Ile1-2	65.4; CH	2.89 (s)		
Ile1-3	37.8; CH	1.83 (m)	Ile1-1	Ile1-6, Ile1-4-H_B
Ile1-4	23.9; CH_2	H_A: 1.16-1.15 (m)		Ile1-4-H_A, Ile1-5
		H_B: 0.93 (m)		Ile1-3, Ile1-4-H_B, Ile1-5
Ile1-5	11.4; CH_3	0.73 (t, 7.3)	Ile1-3, Ile1-4	Ile1-4-H_A, Ile1-4-H_B
Ile1-6	15.3; CH_3	0.88 (d, 6.9)	Ile1-2, Ile1-3, Ile1-4	Ile1-3
Gly2				
Gly2-1	164.4; C q			
Gly2-2	42.4; CH_2	H_A: 3.55-3.46 (m)		Gly2-2-H_B
		H_B: 3.33 (d, 17.2)	Gly2-1	Gly2-2-H_A
Dha3				
Dha3-1	162.7; C q			
Dha3-2	132.0; C q			
Dha3-3	103.4; CH_2	H_A: 5.65 (s)	Dha3-1, Dha3-2	Dha3-3-H_B
		H_B: 5.23 (bs)	Dha3-1	Dha3-3-H_A
Ala4				
Ala4-1	173.3; C q			
Ala4-2	51.6; CH	4.61 (q, 6.2)	Dha3-1, Ala4-1	Ala4-3
Ala4-3	18.6; CH_3	1.30 (d, 6.4)	Ala4-1, Ala4-2	Ala4-2
Pip				
Pip-2	162.0; C q			
Pip-3	23.9; CH_2	2.82-2.77 (m)		Pip-4-H_B
Pip-4	29.1; CH_2	H_A: 3.95[c],		Pip-4-H_B
		H_B: 2.16 (d, 13.1)		Pip-4-H_A, Pip-3
Pip-5	57.5; C q			
Pip-6	64.1; CH	5.19 (s)	Pip-2, Pip-5, Thz13-2, Thz13-3, Thz15-4	
Thz6				
Thz6-1	161.7; C q			
Thz6-2	146.1; C q			
Thz6-3	125.0; CH	8.04 (s)	Thz6-2, Thz6-4	
Thz6-4	169.7; C q			
Thr7				
Thr7-1	165.4; C q			
Thr7-2	55.7; CH	4.29 (d, 3.0)	Thz6-1	Thr7-3, Thr7-NH
Thr7-3	66.3; CH	1.53-1.45 (m)		Thr7-4
Thr7-4	18.9; CH_3	0.68 (d, 4.7)	Thr7-2, Thr7-3	Thr7-3
Thr7-NH[d]		7.00 (d, 6.2)		Thr7-2
Dhb8				
Dhb8-2	128.3; C q			
Dhb8-3	132.7; CH	6.10 (q, 6.9)	Dhb8-2, Tzn9-4	Dhb8-4
Dhb8-4	15.7; CH_3	1.49 (d, 7.0)	Dhb8-2, Dhb8-3, Tzn9-4	Dhb8-3
Tzn9				
Tzn9-1	172.0; C q			
Tzn9-2	78.8; CH	4.85 (dd, 12.3, 9.4)	Tzn9-1, Tzn9-4	Tzn9-3-H_A, Tzn9-3-H_B
Tzn9-3	34.8; CH_2	H_A: 3.55-3.46 (m)	Tzn9-2, Tzn9-4	Tzn9-2, Tzn9-3-H_B,
		H_B: 3.04 (t, 12.1)	Tzn9-1, Tzn9-2	Tzn9-2, Tzn9-3-H_A
Tzn9-4	170.2; C q			
Ile10				
Ile10-2	52.9; CH	5.62 (d, 9.9)	Tzn9-1, Ile10-3, Thz11-4	Ile10-NH
Ile10-3	77.2; C q			
Ile10-4	67.7; CH	3.68 (q, 6.4)	Ile10-2, Ile10-3, Ile10-5, Ile10-6	Ile10-5
Ile10-5	15.3; CH_3	1.16 (d, 6.4)	Ile10-3, Ile10-4, Ile10-6	Ile10-4
Ile10-6	18.7; CH_3	1.02 (s)	Ile10-2, Ile10-3, Ile10-4, Ile10-5	
Ile10-NH[d]		7.48-7.43 (m)		Ile10-2
Thz11				
Thz11-1	161.7; C q			
Thz11-2	150.0; C q			
Thz11-3	125.7; CH	8.16 (s)	Thz11-1, Thz11-2, Thz11-4	
Thz11-4	166.3; C q			

Position	δ_C [ppm]; mult	δ_H [ppm] (mult, J in Hz)	HMBC[a]	COSY[b]
Thr12				
Thr12-2	55.5; CH	5.65 (s)	Thz11-1, Thz13-4	Thr12-NH
Thr12-3	71.8; CH	6.24 (m)	Q-1	Thr12-4
Thr12-4	18.7; CH_3	1.59 (d, 6.4)	Thr12-2, Thr12-3	Thr12-3
Thr12-NH[d]		8.67 (d, 8.8)		Thr12-2
Thz13				
Thz13-2	157.1; C q			
Thz13-3	118.3; CH	7.44 (s)	Pip-6, Thz13-2, Thz13-4	
Thz13-4	170.1; C q			
Thz15				
Thz15-1	159.5; C q			
Thz15-2	149.8; C q			
Thz15-3	127.6; CH	8.16 (s)	Thz15-1, Thz15-2, Thz15-4	
Thz15-4	168.2; C q			
Dha16				
Dha16-1	161.9; C q			
Dha16-2	134.0; C q			
Dha16-3	103.2; CH_2	H_A: 6.57 (d, 1.8)	Dha16-1, Dha16-2	Dha16-3-H_B
		H_B: 5.48 (d, 1.7)	Dha16-1, Dha16-2	Dha16-3-H_A
Dha17				
Dha17-1	166.0; C q			
Dha17-2	132.8; C q			
Dha17-3	104.3; CH_2	H_A: 6.40 (s)	Dha17-1, Dha17-2	Dha17-3-H_B
		H_B: 5.55 (s)	Dha17-1, Dha17-2	Dha17-3-H_A
Q				
Q-1	160.6; C q			
Q-2	143.6; C q			
Q-3	122.5; CH	7.19 (s)	Q-5	
Q-4	153.8; C q			
Q-5	127.3; C q			
Q-6	123.3; CH	6.78 (d, 9.9)	Q-5, Q-8, Q-10	Q-7
Q-7	129.9; CH	6.29 (dd, 9.5, 5.7)	Q-5	Q-6, Q-8
Q-8	58.9; CH	3.55-3.46 (m)		Q-7
Q-9	67.7; CH	4.25 (s)		
Q-10	154.4; C q			
Q-11	64.4; CH	5.21-5.15 (m)		Q-12
Q-12	22.6; CH_3	1.23 (d, 6.6)	Q-4, Q-11	Q-11

[a] HMBC correlations are from the proton to the indicated carbon.
[b] COSY correlations are from the proton to the proton attached to the indicated position.
[c] The δ of this resonance was determined by HSQC due to overlap with the methanol-d_4 peak.
[d] Only those amide resonances demonstrating COSY correlations to neighboring protons were assigned.

Figure C.9. Structure of and numbering system used for thiostrepton Ala4Gly.

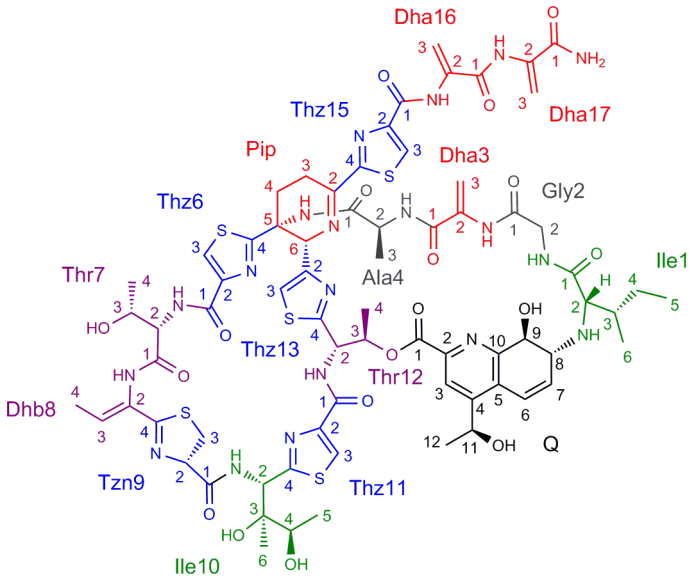

Figure C.10. HPLC-MS of thiostrepton Ala4Gly isolated from *S. laurentii* NDS1 int-3A102.

(**A**) Total ion chromatogram of thiostrepton Ala4Gly.

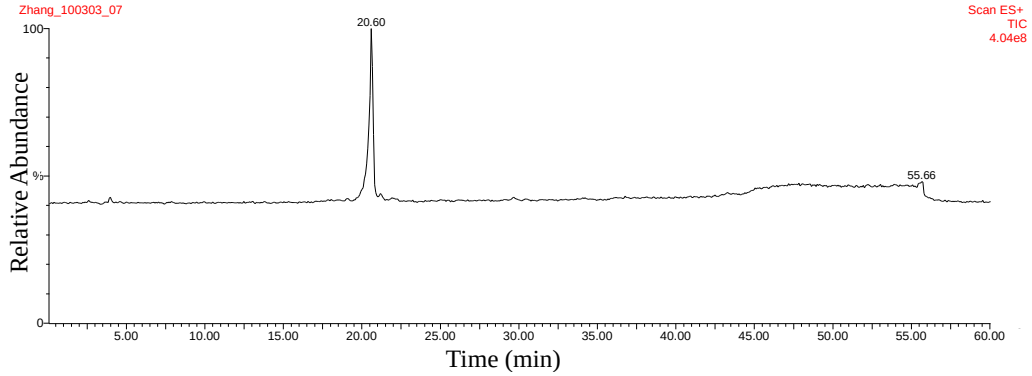

(**B**) Chromatogram extracted for *m*/*z* 826 for thiostrepton Ala4Gly.

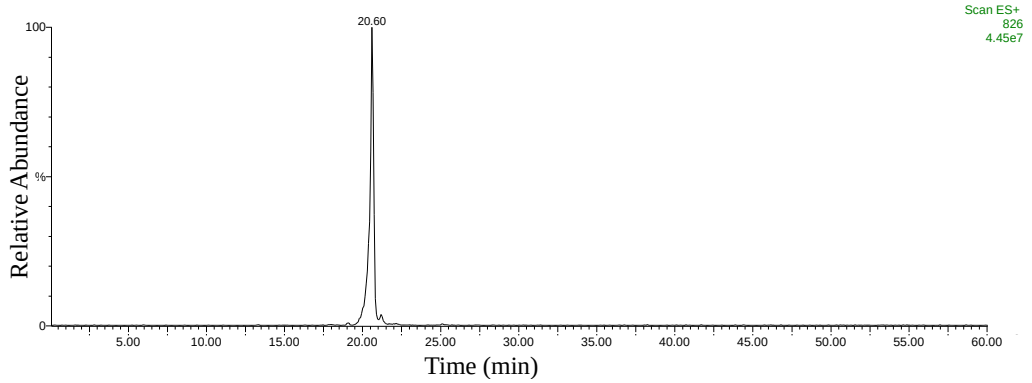

(**C**) Mass spectrum of thiostrepton Ala4Gly eluting at t_R = 20.6 min.

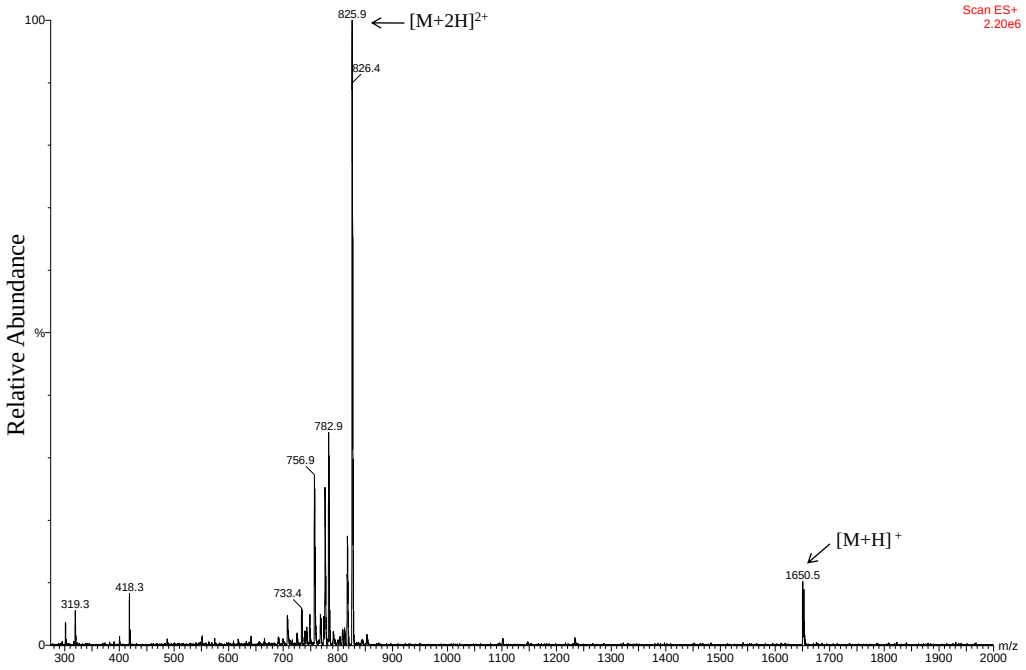

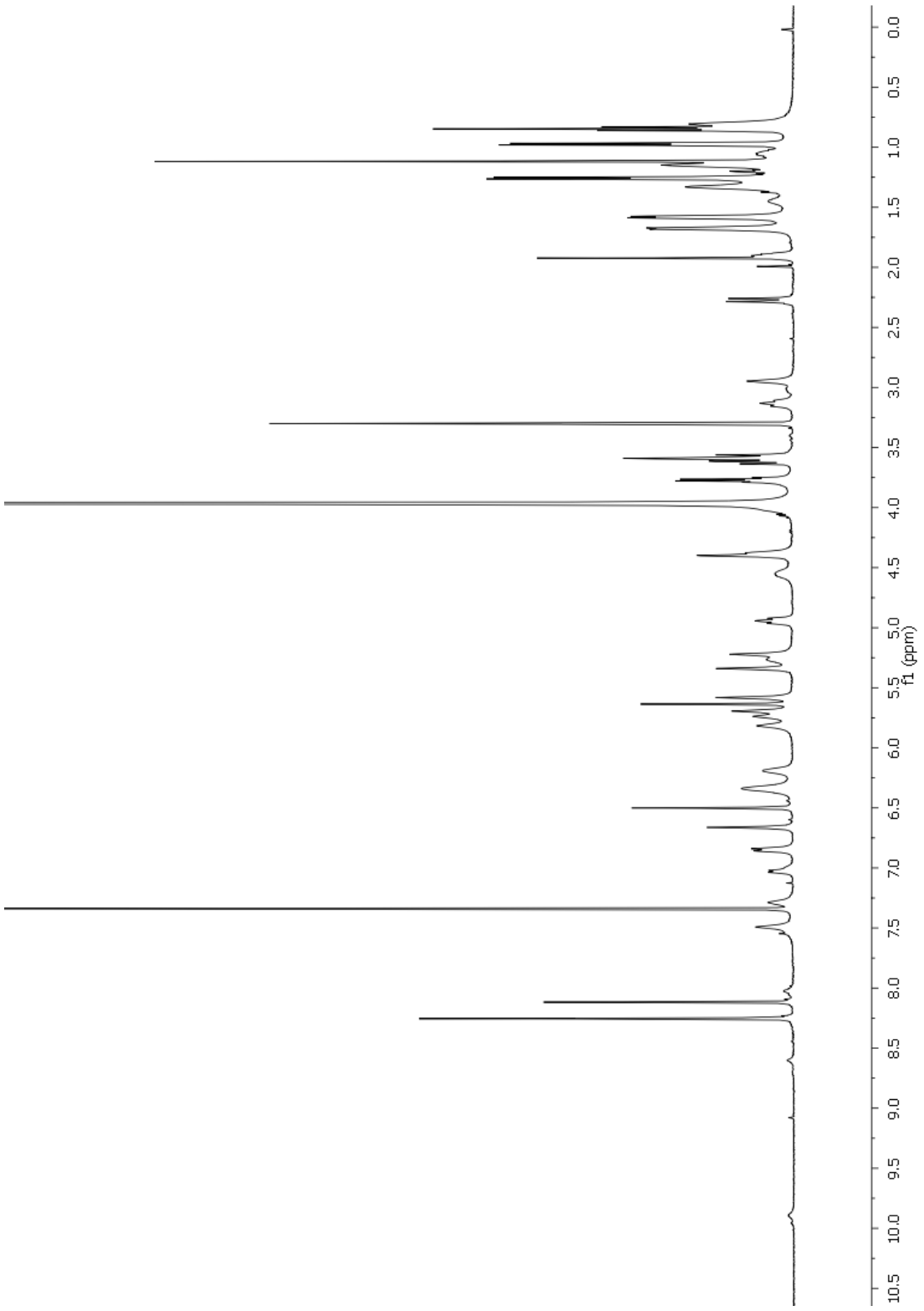

Figure C.11. ^{1}H NMR spectrum of thiostrepton Ala4Gly (500 MHz, $CDCl_3$-CD_3OD 4:1, 25 °C).

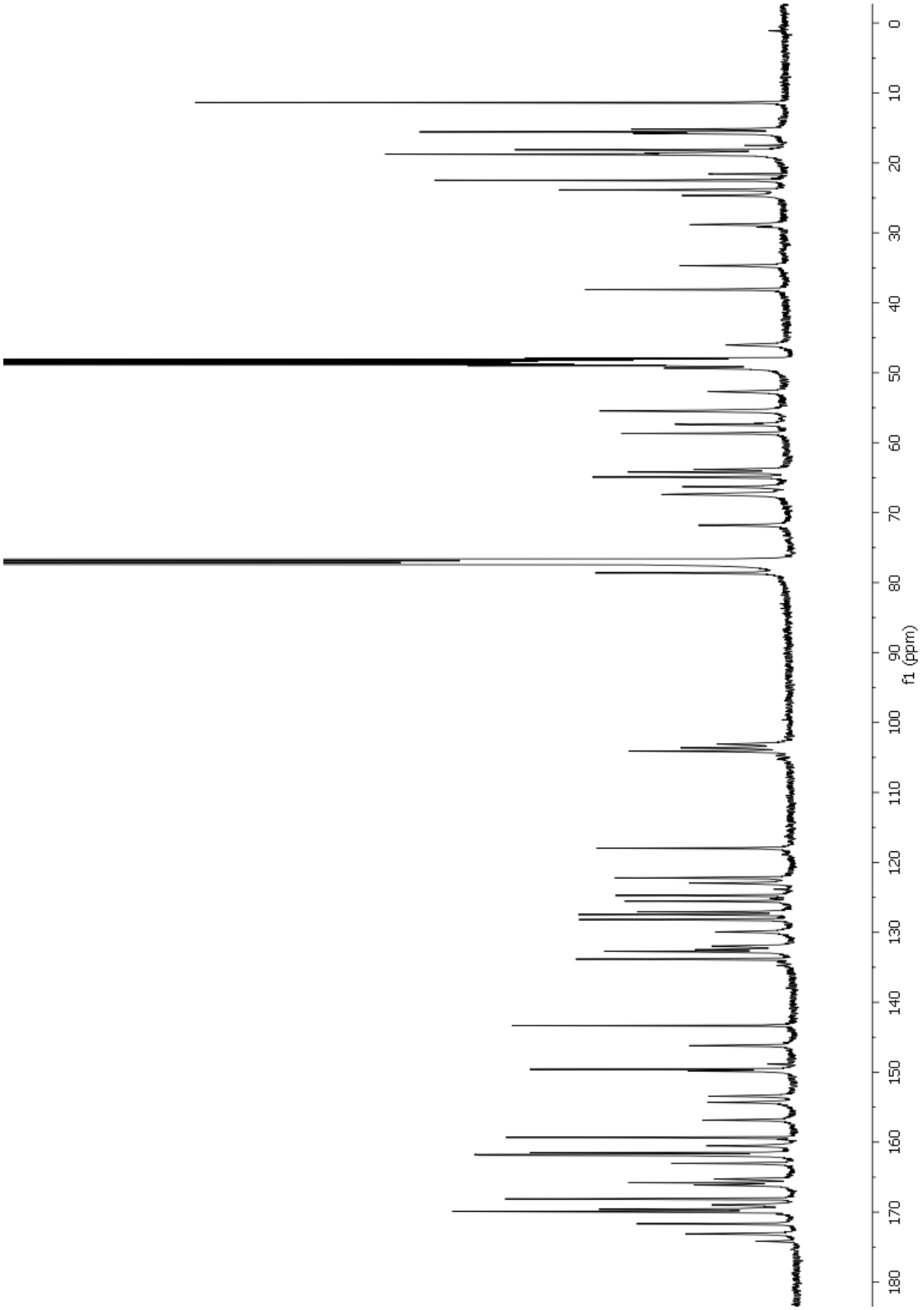

Figure C.12. ^{13}C NMR spectrum of thiostrepton Ala4Gly (125 MHz, $CDCl_3$-CD_3OD 4:1, 25 °C).

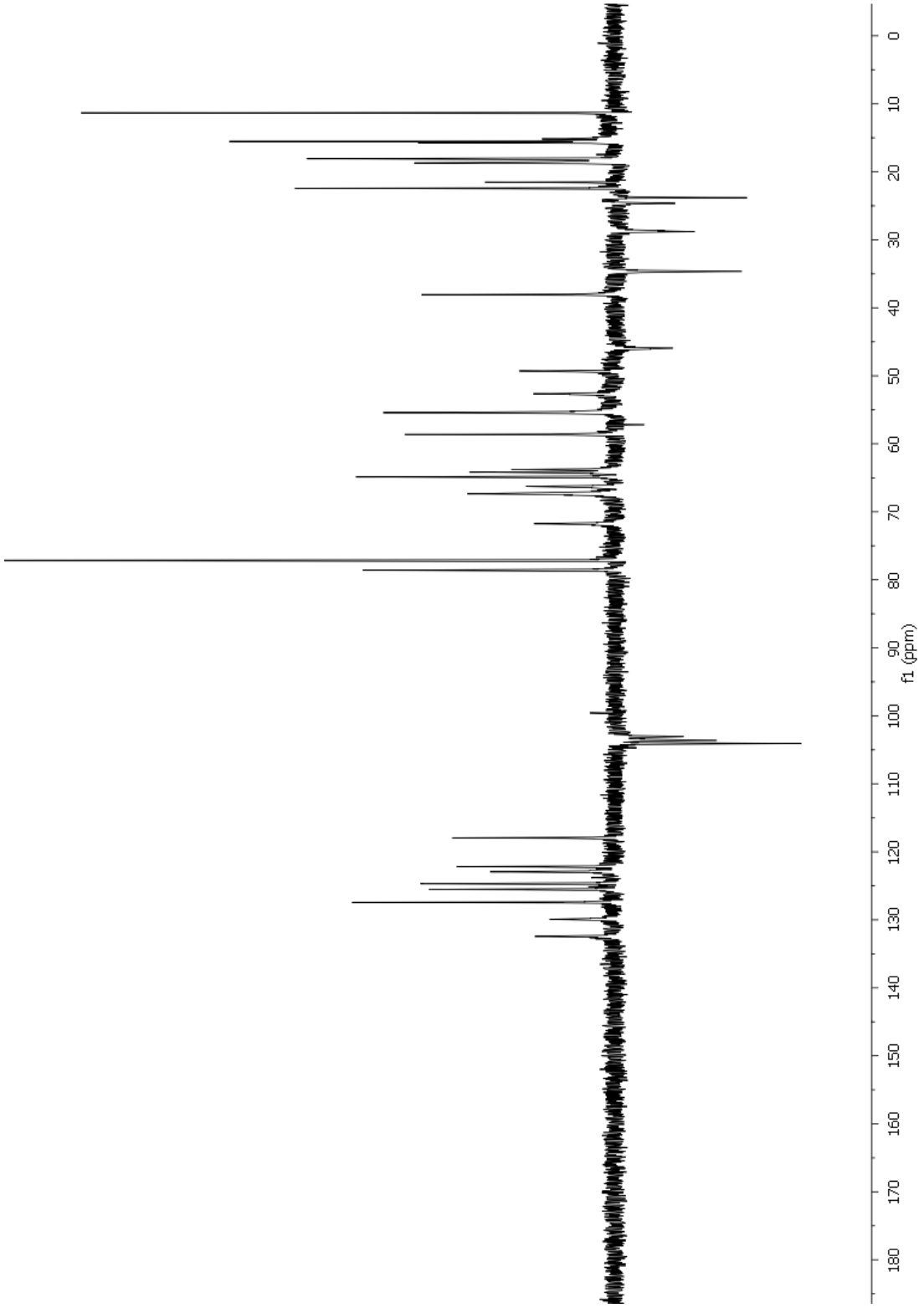

Figure C.13. DEPT-135 NMR spectrum of thiostrepton Ala4Gly (125 MHz, $CDCl_3$-CD_3OD 4:1, 25 °C).

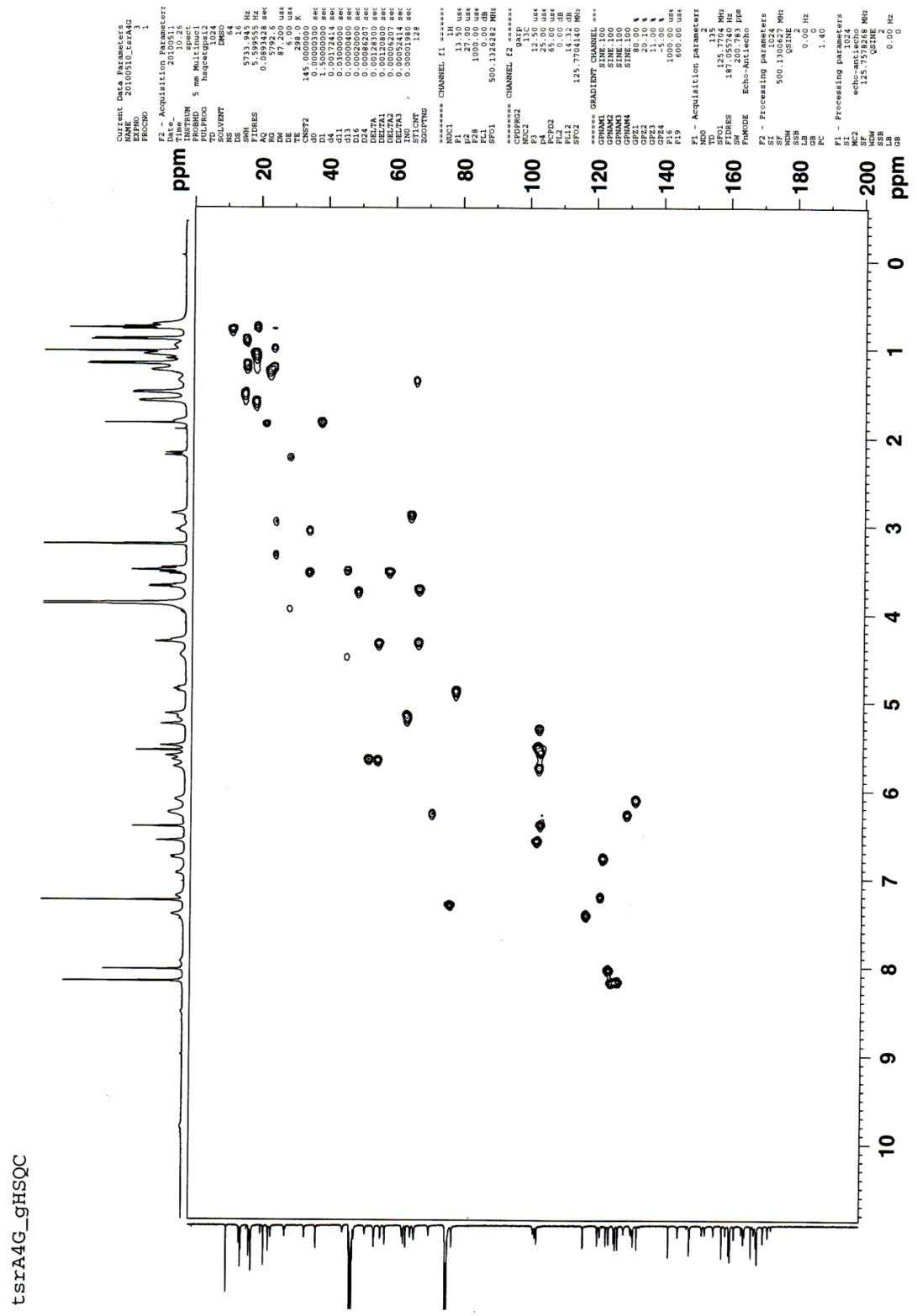

Figure C.14. gHSQC spectrum of thiostrepton Ala4Gly (500 MHz, CDCl3-CD3OD 4:1, 25 °C).

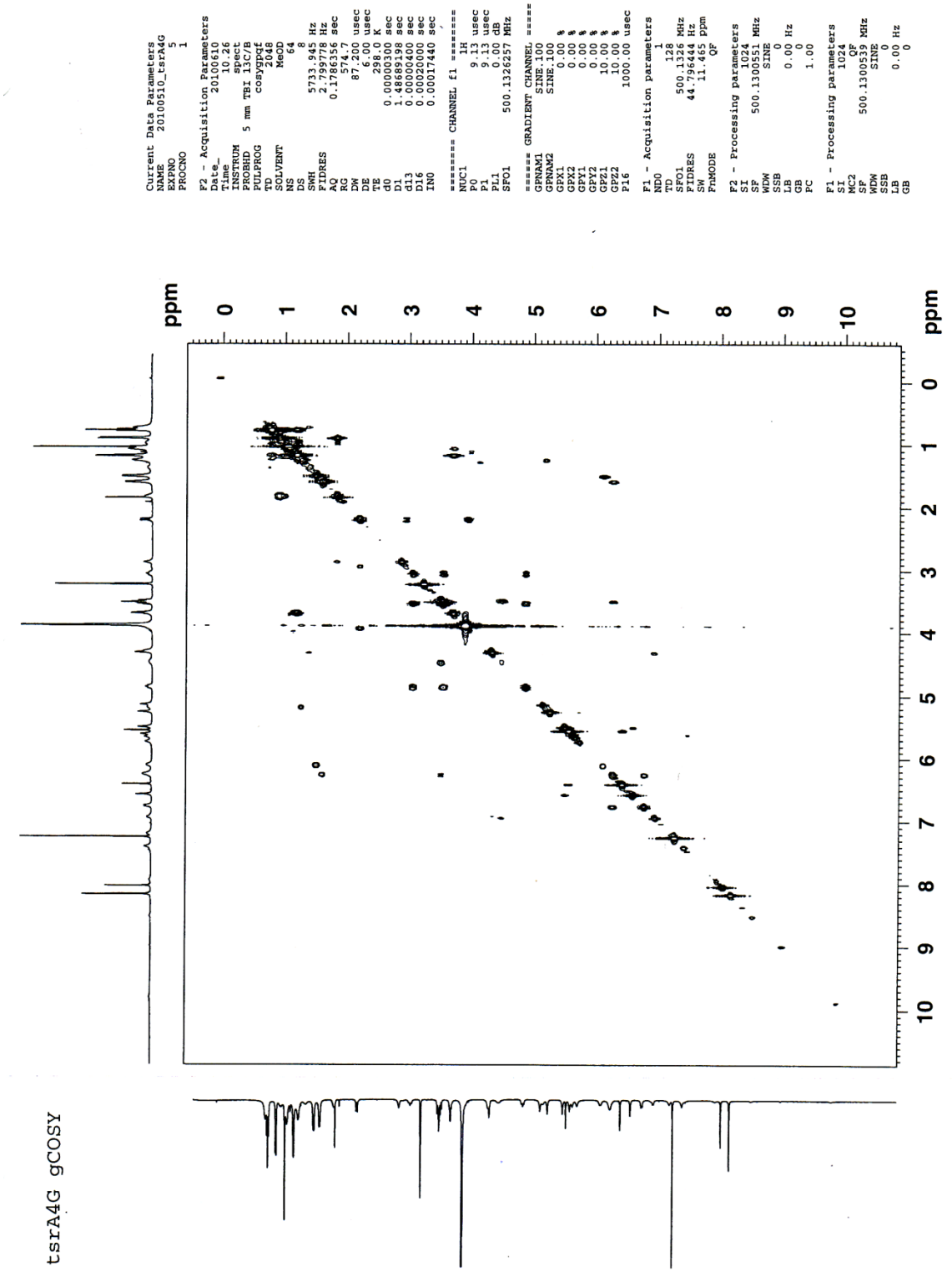

Figure C.15. gCOSY spectrum of thiostrepton Ala4Gly (500 MHz, $CDCl_3$-CD_3OD 4:1, 25 °C).

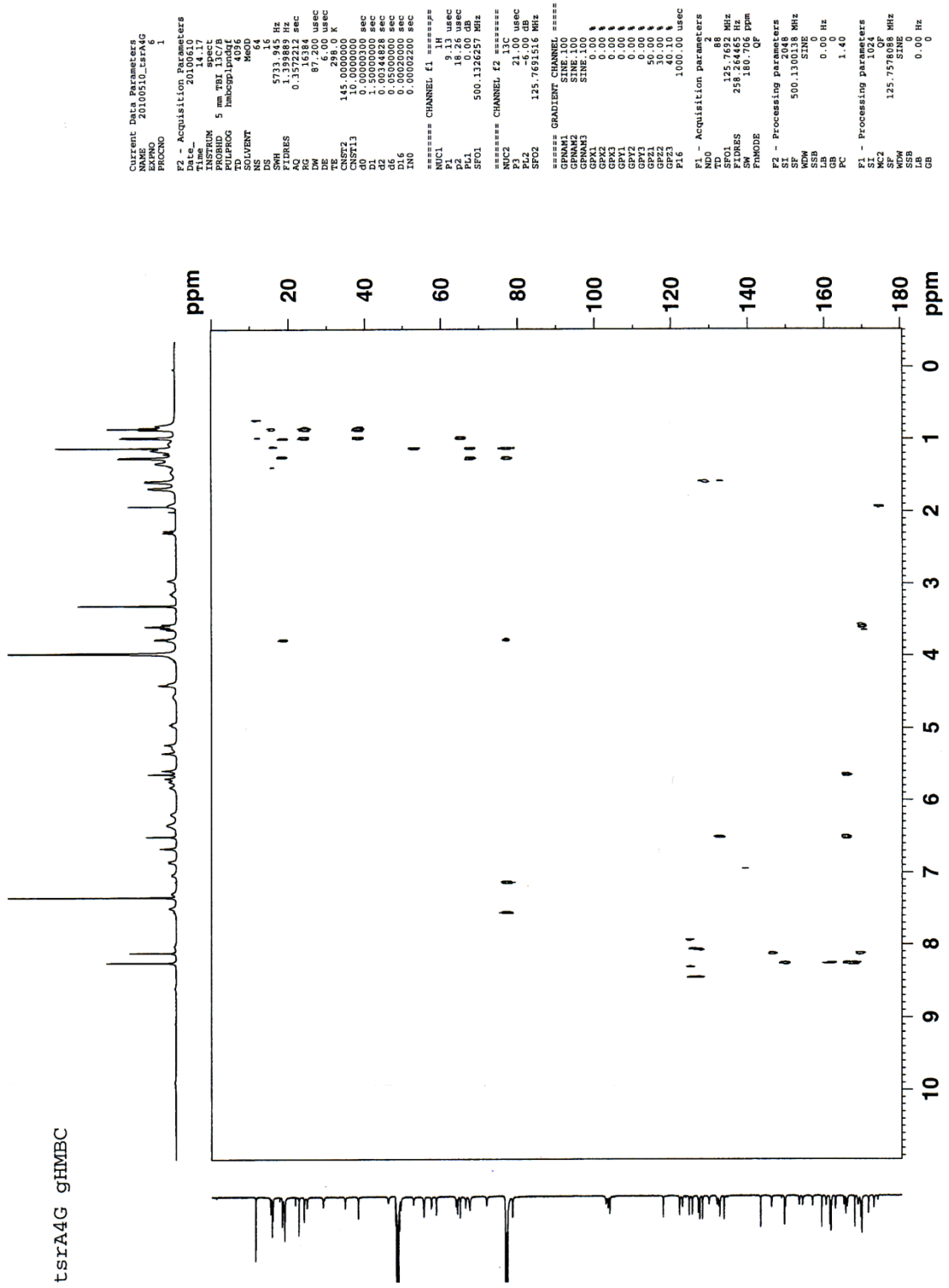

Figure C.16. gHMBC spectrum of thiostrepton Ala4Gly (500 MHz, $CDCl_3$-CD_3OD 4:1, 25 °C).

Table C.2. ^{1}H and ^{13}C NMR assignments of thiostrepton Ala4Gly

Position	δ_C [ppm]; mult	δ_H [ppm] (mult, J in Hz)	HMBC[a]	COSY[b]
Ile1				
Ile1-1	174.1; C q			
Ile1-2	64.9; CH	2.87 (s)		Ile1-3
Ile1-3	38.1; CH	1.83 (m)	Ile1-1	Ile1-4-H_B, Ile1-6
Ile1-4	23.9; CH_2	H_A: 1.18-1.17 (m)		Ile1-4-H_B, Ile1-5
		H_B: 0.97 (m)		Ile1-3, Ile1-4-H_A, Ile1-5
Ile1-5	11.4; CH_3	0.77 (t, 7.3)	Ile1-3, Ile1-4, Ile1-6	Ile1-4-H_A, Ile1-4-H_B
Ile1-6	15.6; CH_3	0.90 (d, 6.9)	Ile1-1, Ile1-2, Ile1-3, Ile1-4, Ile1-5	Ile1-3
Ala2				
Ala2-1	168.9; C q			
Ala2-2	49.3; CH	3.69 (q, 6.3)		Ala2-3
Ala2-3	18.6; CH_3	1.07 (br)		Ala2-2
Dha3				
Dha3-1	163.0; C q			
Dha3-2	132.0; C q			
Dha3-3	103.6; CH_2	H_A: 5.74 (s)		
		H_B: 5.26 (s)		Dha3-3- H_A
Gly4				
Gly4-1	173.1; C q			
Gly4-2	46.0; CH_2	H_A: 4.47 (br)		Gly4-2-H_B
		H_B: 3.56-3.48 (m)		Gly4-2-H_A
Gly4-NH[d]		6.95 (d, 8.2)		Gly4-2-H_A
Pip				
Pip-2	161.6; C q			
Pip-3	24.7; CH_2	H_A: 3.34-3.30 (m)		
		H_B: 2.94 (m)		Pip-4-H_B
Pip-4	28.8; CH_2	H_A: 4.00-3.93 (m)[c]		Pip-4-H_B
		H_B: 2.21-2.18 (m)		Pip-4-H_A, Pip-3-H_B
Pip-5	57.4; C q			
Pip-6	63.8; CH	5.14 (s)		
Thz6				
Thz6-1	161.9; C q	Thz6-1		
Thz6-2	146.2; C q			
Thz6-3	124.7; CH	8.04 (s)	Thz6-2, Thz6-4	
Thz6-4	169.6; C q			
Thr7				
Thr7-1	165.3; C q			
Thr7-2	55.5; CH	4.32 (d, 2.6)		Thr7-3
Thr7-3	66.3; CH	1.37 (br)		Thr7-4
Thr7-4	18.8; CH_3	0.73 (br s)		Thr7-3
Dhb8				
Dhb8-2	128.2; C q			
Dhb8-3	132.5; CH	6.11 (s)		Dhb8-4
Dhb8-4	15.2; CH_3	1.50 (d, 6.4)	Dhb8-2, Dhb8-3	Dhb8-3
Tzn9				
Tzn9-1	171.7; C q			
Tzn9-2	78.6; CH	4.86 (t, 10.7)		Tzn9-3-H_A, Tzn9-3-H_B
Tzn9-3	34.7; CH_2	H_A: 3.56-3.48 (m)	Tzn9-4	Tzn9-2, Tzn9-3-H_B
		H_B: 3.06 (t, 11.2)		Tzn9-2, Tzn9-3-H_A
Tzn9-4	169.9; C q			
Ile10				
Ile10-2	52.7; CH	5.61 (s)		
Ile10-3	77.2; C q			
Ile10-4	67.4; CH	3.69 (q, 6.3)	Ile10-3, Ile10-6	Ile10-5
Ile10-5	15.7; CH_3	1.18 (d, 6.4)	Ile10-3, Ile10-4, Ile10-6	Ile10-4
Ile10-6	18.1; CH_3	1.04 (s)	Ile10-2, Ile10-C3, Ile10-4, Ile10-5	
Thz11				
Thz11-1	159.3; C q			
Thz11-2	149.8; C q			
Thz11-3	125.5; CH	8.18 (s)	Thz11-2, Thz11-4	
Thz11-4	168.1; C q			

Position	δ_C [ppm]; mult	δ_H [ppm] (mult, J in Hz)	HMBC[a]	COSY[b]
Thr12				
Thr12-2	55.5; CH	5.66 (s)		
Thr12-3	71.8; CH	6.26 (s)		Thr12-4
Thr12-4	18.8; CH_3	1.60 (d, 5.6)		Thr12-3
Thz13				
Thz13-2	156.8; C q			
Thz13-3	118.0; CH	7.41 (s)		
Thz13-4	170.0; C q			
Thz15				
Thz15-1	161.5; C q			
Thz15-2	149.6; C q			
Thz15-3	127.5; CH	8.17 (s)	Thz15-1, Thz15-C2, Thz15-C4	
Thz15-4	166.1; C q			
Dha16				
Dha16-1	161.7; C q			
Dha16-2	133.8; C q			
Dha16-3	103.1; CH_2	H_A: 6.58 (s)		Dha3-16- H_B
		H_B: 5.50 (s)		Dha3-16- H_A
Dha17				
Dha17-1	165.7; C q			
Dha17-2	132.7; C q			
Dha17-3	104.1; CH_2	H_A: 6.42 (s)	Dha17-1, Dha17-2	Dha3-17- H_B
		H_B: 5.56 (s)	Dha17-1	Dha3-17- H_A
Q				
Q-1	160.5; C q			
Q-2	143.3; C q			
Q-3	122.2; CH	7.21 (s)		
Q-4	153.4; C q			
Q-5	127.1; C q			
Q-6	123.0; CH	6.77 (d, 9.7)		Q-7
Q-7	129.9; CH	6.26 (s)		Q-6, Q-8
Q-8	58.7; CH	3.56-3.48 (m)		Q-7
Q-9	67.4; CH	4.30 (m)		Q-9-OH
Q-10	154.3; C q			
Q-11	64.2; CH	5.19 (br)		Q-12
Q-12	22.5; CH_3	1.25 (br)		Q-11
Q-9-OH		6.95 (d, 8.2)		Q-9

[a] HMBC correlations are from the proton to the indicated carbon.
[b] COSY correlations are from the proton to the proton attached to the indicated position.
[c] The δ of this resonance was determined by HSQC due to overlap with the methanol-d_4 peak.
[d] Only this amide resonance demonstrating COSY correlation to neighboring proton was assigned.

Figure C.17. HPLC and UV-Vis absorption spectra from the TsrA Thr7Ala-expressing fermentation extract. (**A**) HPLC analysis of *S. laurentii* NDS1 int-3A105 (TsrA Thr7Ala) culture extract. (**B**) UV-Vis absorption spectrum of SL105-1 **B** (t_R = 16.9 min). (**C**) UV-Vis absorption spectrum of thiostrepton Thr7Ala **A** (t_R = 18.3 min).

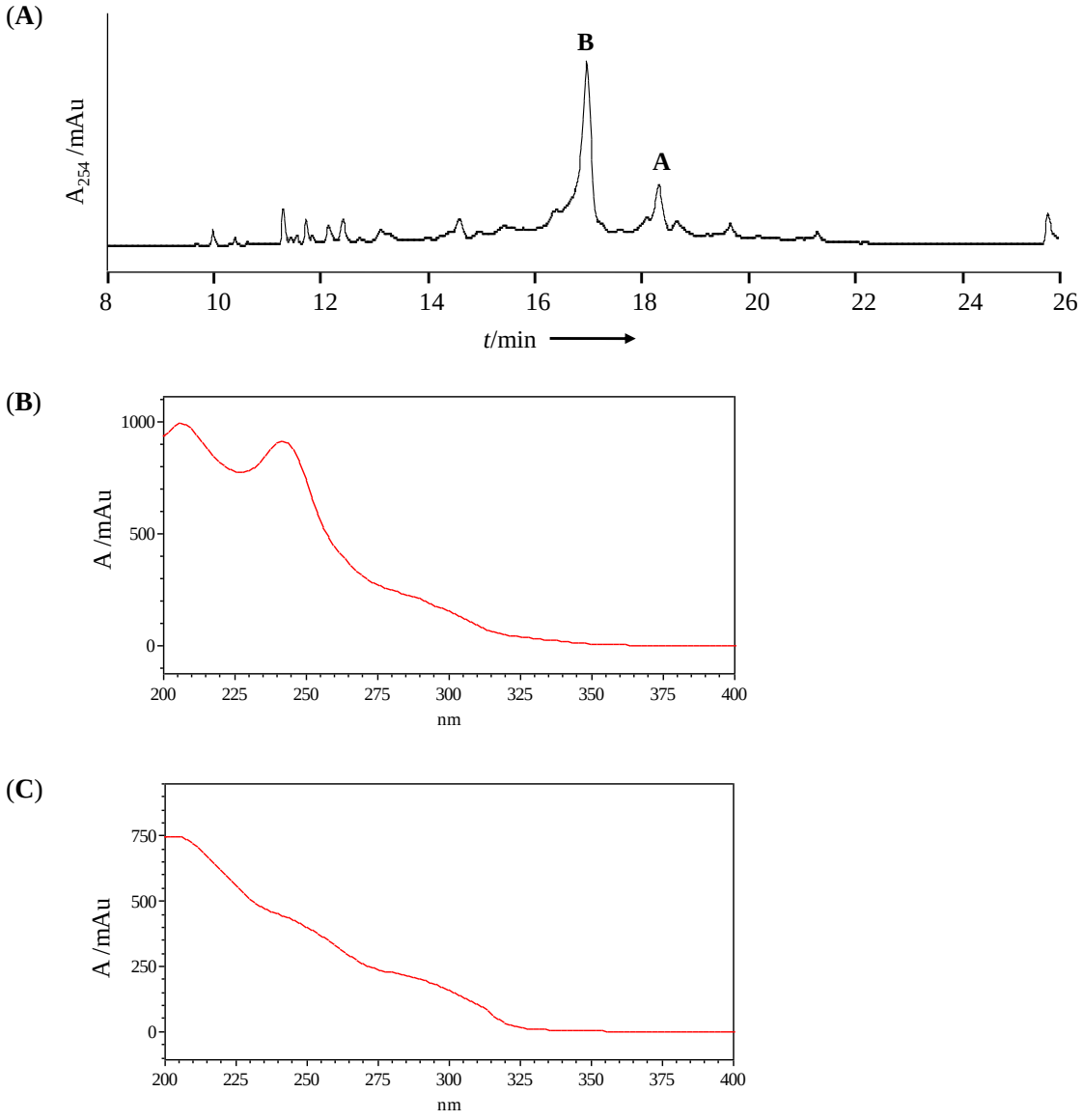

Figure C.18. Structure of and numbering system used for thiostrepton Thr7Ala.

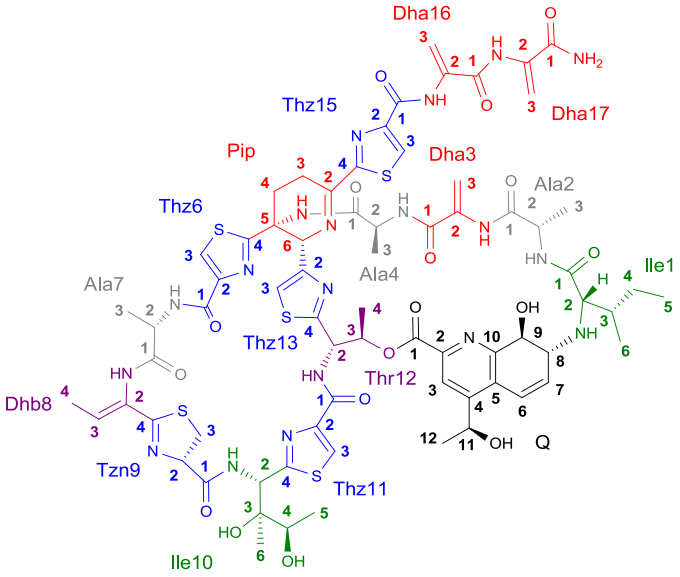

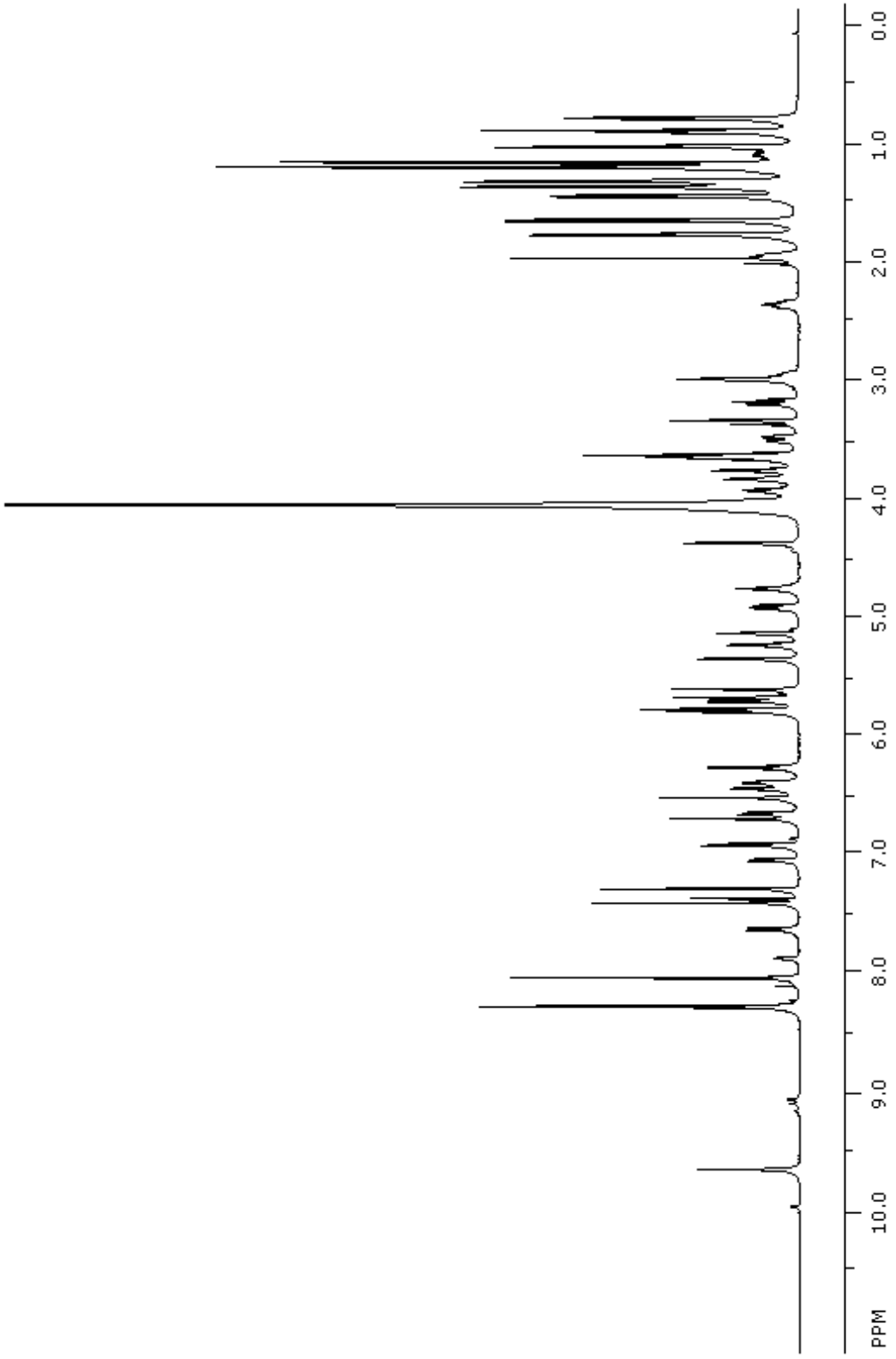

Figure C.19. ^{1}H NMR spectrum of thiostrepton Thr7Ala (500 MHz, $CDCl_3$-CD_3OD 4:1, 25 °C).

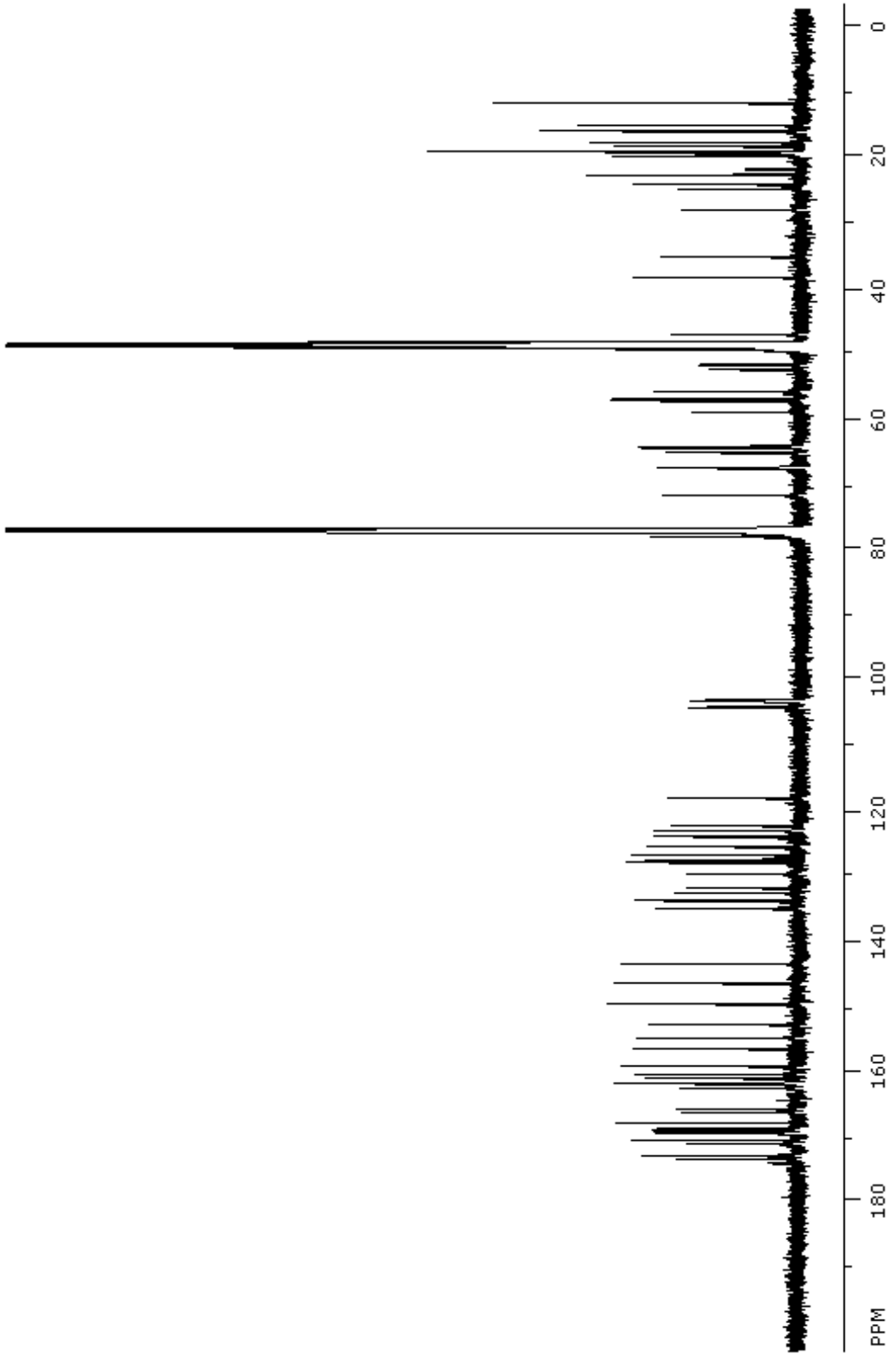

Figure C.20. ^{13}C NMR spectrum of thiostrepton Thr7Ala (125 MHz, $CDCl_3$-CD_3OD 4:1, 25 °C).

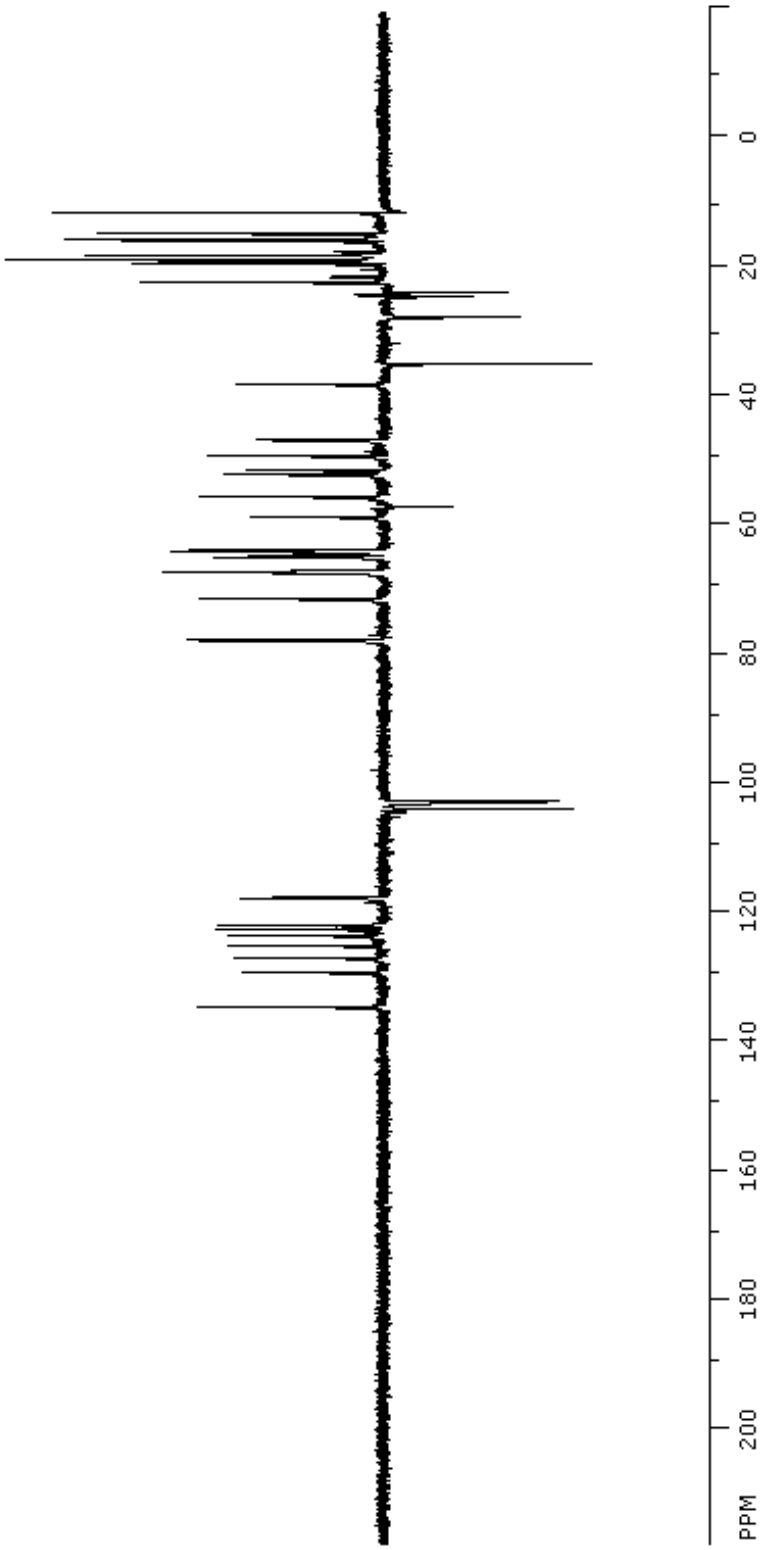

Figure C.21. DEPT-135 NMR spectrum of thiostrepton Thr7Ala (125 MHz, $CDCl_3$-CD_3OD 4:1, 25 °C).

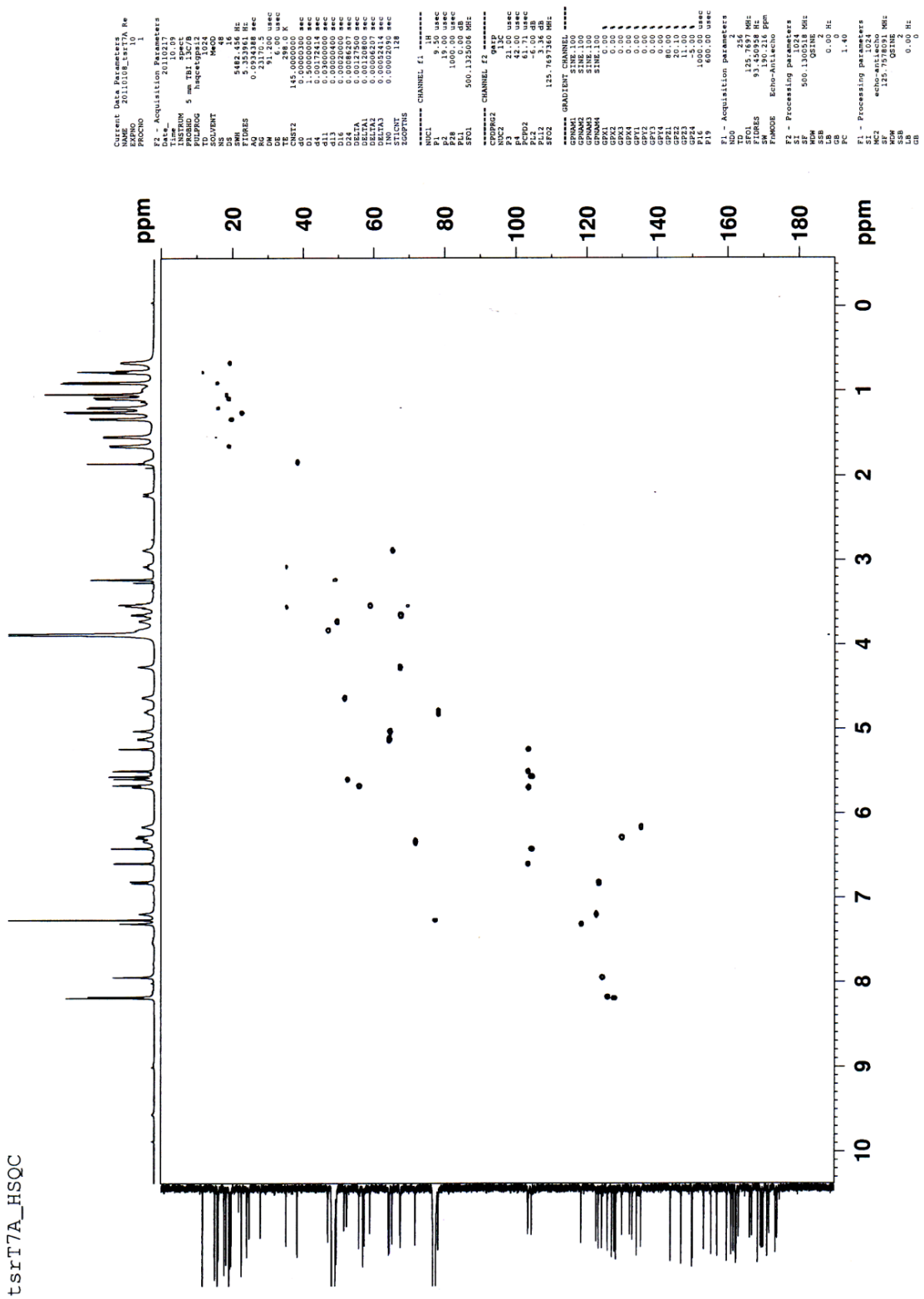

Figure C.22. gHSQC spectrum of thiostrepton Thr7Ala (500 MHz, $CDCl_3$-CD_3OD 4:1, 25 °C).

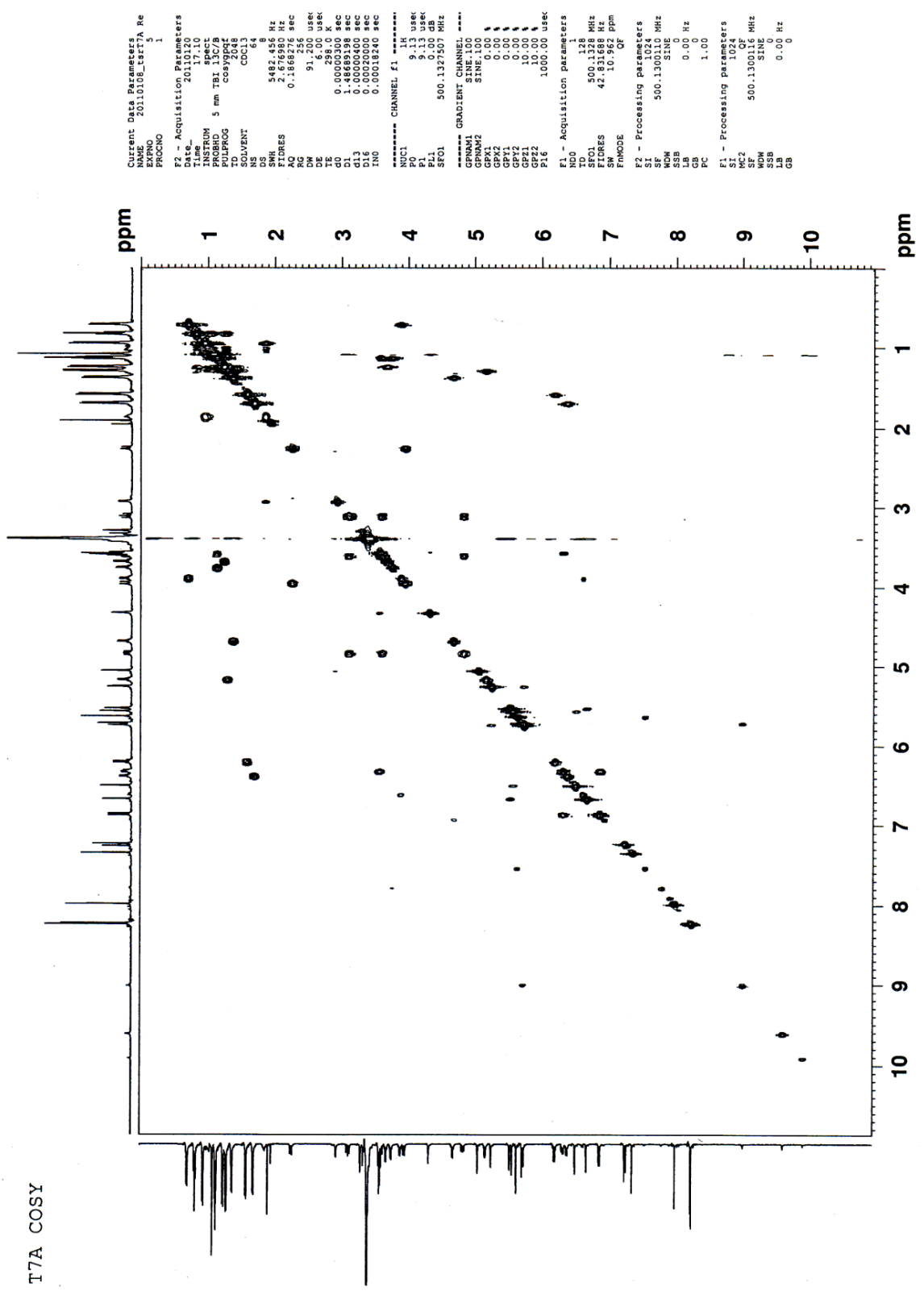

Figure C.23. gCOSY spectrum of thiostrepton Thr7Ala (500 MHz, $CDCl_3$-CD_3OD 4:1, 25 °C).

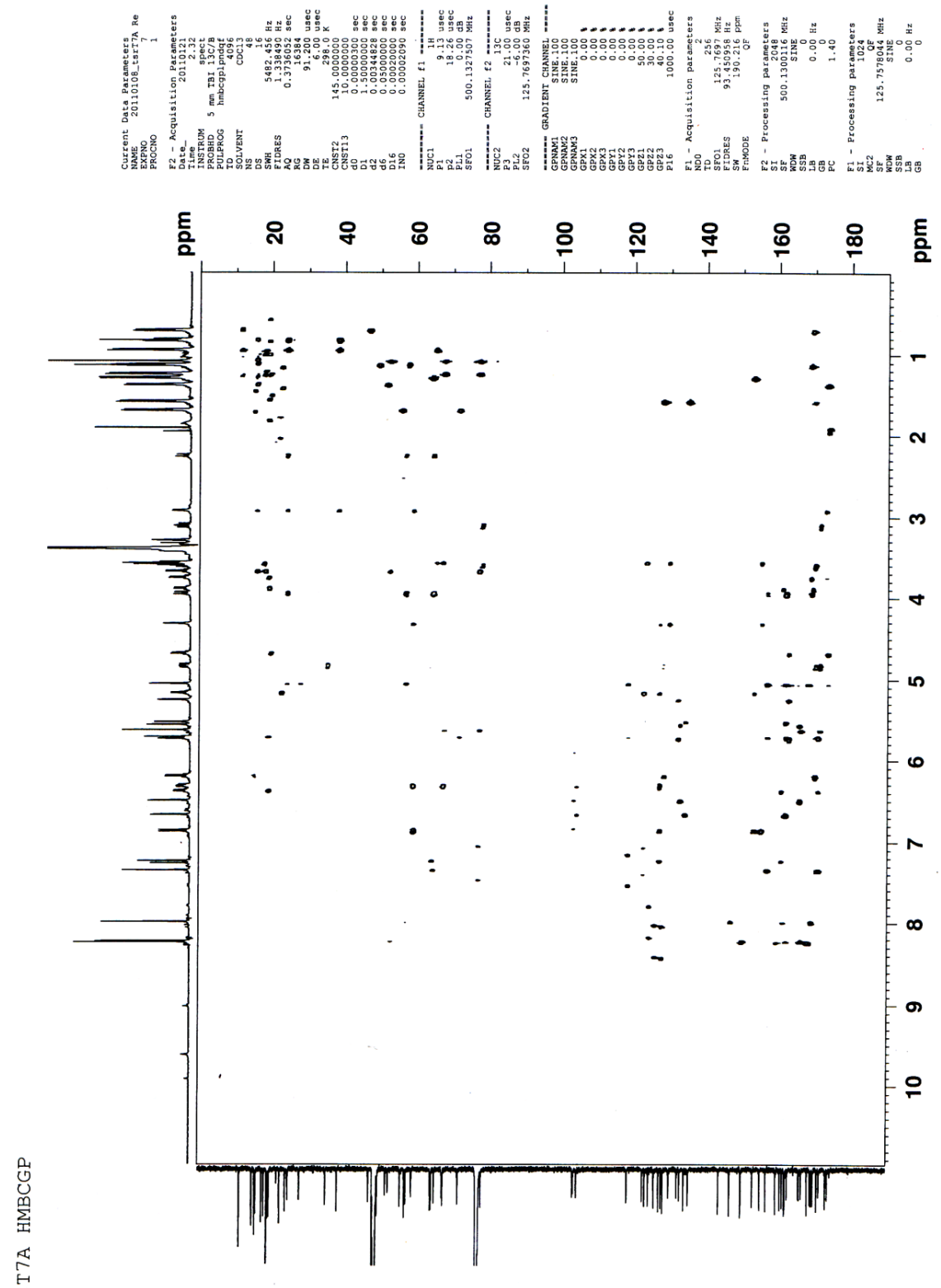

Figure C.24. gHMBC spectrum of thiostrepton Thr7Ala (500 MHz, $CDCl_3$-CD_3OD 4:1, 25 °C).

Table C.3. ^{1}H and ^{13}C NMR assignments of thiostrepton Thr7Ala

Position	δ_C [ppm]; mult	δ_H [ppm]; (mult, J in Hz)	HMBC[a]	COSY[b]
Ile1				
Ile1-1	173.1; C q			
Ile1-2	65.2; CH	2.92 (d, 4.0)	Ile1-1, Ile1-3, Ile1-4, Ile1-6, Q8	Ile1-3
Ile1-3	38.2; CH	1.88-1.82 (m)		Ile1-4-H_B, Ile1-6
Ile1-4	23.9; CH_2	H_A: 1.32-1.26 (m)	Ile1-5, Ile1-6	Ile1-4-H_B, Ile1-5
		H_B: 1.04-0.98 (m)	Ile-5, Ile1-6	Ile1-3, Ile1-4-H_A, Ile1-5
Ile1-5	11.4; CH_3	0.82 (t, 7.3)	Ile1-3, Ile1-4	Ile1-4-H_A, Ile1-4-H_B
Ile1-6	15.7; CH_3	0.94 (d, 6.9)	Ile1-2, Ile1-3, Ile1-4	Ile1-3
Ala2				
Ala2-1	169.0; C q			
Ala2-2	49.4; CH	3.75 (q, 6.8)	Ile1-1, Ala2-1, Ala2-3	Ala2-3
Ala2-3	18.9; CH_3	1.13 (d, 6.7)	Ala2-1, Ala2-2	Ala2-2
Ala2-NH[d]		7.79 (d, 5.9)		Ala2-2
Dha3				
Dha3-1	162.8; C q			
Dha3-2	132.1; C q			
Dha3-3	103.4; CH_2	H_A: 5.74 (d, 2.0)	Dha3-1, Dha3-2	Dha3-3-H_B
		H_B: 5.25 (d, 2.0)	Dha3-1, Dha3-2	Dha3-3-H_A
Ala4				
Ala4-1	173.7; C q			
Ala4-2	51.6; CH	4.68 (q, 6.6)	Dha3-1Ala4-1, Ala4-3	Ala4-3
Ala4-3	19.5; CH_3	1.37 (d, 6.7)	Ala4-1, Ala4-2	Ala4-2
Ala4-NH[d]		6.93 (d, 7.6)		Ala4-2
Pip				
Pip-2	162.2; C q			
Pip-3	23.9; CH_2	H_A: 3.63-3.55 (m)		
		H_B: 2.89-2.85 (m)		Pip-4-H_B
Pip-4	27.8; CH_2	H_A: 3.95 (m)	Pip-2, Pip-3, Pip-5, Pip-6, Thz6-4, Thz13-2	Pip-4-H_B
		H_B: 2.25 (m)	Pip-3, Pip-5, Pip-6	Pip-4-H_A, Pip-3-H_B
Pip-5	56.9; C q			
Pip-6	64.4; CH	5.05 (s)	Ala4-1, Pip-2, Pip-3, Pip-4, Pip-5, Thz13-2, Thz13-3, Thz15-4	
Thz6				
Thz6-1	161.4; C q			
Thz6-2	146.8; C q			
Thz6-3	124.2; CH	7.99 (s)	Thz6-1, Thz6-2, Thz6-4	
Thz6-4	169.2; C q			
Ala7				
Ala7-1	169.6; C q			
Ala7-2	47.0; CH	3.89 (q, 7.0)	Thz6-1, Ala7-1, Ala7-3	Ala7-3, Ala7-NH
Ala7-3	19.1; CH_3	0.70 (d, 7.2)	Ala7-1, Ala7-2	Ala7-2
Ala7-NH[d]		6.61 (d, 9.5)		Ala7-2
Dhb8				
Dhb8-2	128.2; C q			
Dhb8-3	135.2; CH	6.20 (q, 7.0)	Dhb8-2, Dhb8-4, Tzn9-4	Dhb8-4
Dhb8-4	14.9; CH_3	1.58 (d, 7.0)	Dhb8-2, Dhb8-3, Tzn9-4	Dhb8-3
Tzn9				
Tzn9-1	171.4; C q			
Tzn9-2	78.1; CH	4.83 (dd, 13.1, 8.9)	Dhb8-2, Tzn9-1, Tzn9-3, Tzn9-4	Tzn9-3-H_A, Tzn9-3-H_B
Tzn9-3	35.1; CH_2	H_A: 3.63-3.55 (m)	Tzn9-2, Tzn9-4	Tzn9-2, Tzn9-3-H_B
		H_B: 3.11 (dd, 13.1, 11.6)	Tzn9-1, Tzn9-2	Tzn9-2, Tzn9-3-H_A
Tzn9-4	169.8; C q			
Ile10				
Ile10-2	52.4; CH	5.63 (s)	Tzn9-1, Ile10-3, Ile10-4, Thz11-4	Ile10-NH
Ile10-3	77.0[c]			
Ile10-4	67.6; CH	3.68 (q, 6.4)	Ile10-2, Ile10-3, Ile10-5, Ile10-6	Ile10-5
Ile10-5	15.9; CH_3	1.24 (d, 6.4)	Ile10-3, Ile10-4, Ile10-6	Ile10-4
Ile10-6	18.1; CH_3	1.08 (s)	Ile10-2, Ile10-3, Ile10-4	
Ile10-NH[d]		7.54 (d, 9.6)		Ile10-2

Position	δ_C [ppm]; mult	δ_H [ppm]; (mult, J in Hz)	HMBC[a]	COSY[b]
Thz11				
Thz11-1	162.1; C q			
Thz11-2	150.0; C q			
Thz11-3	125.8; CH	8.22 (s)	Ile10-2, Thz11-1, Thz11-2, Thz11-4	
Thz11-4	166.5; C q			
Thr12				
Thr12-2	55.8; CH	5.72 (s)	Thz11-1, Thr12-3, Thr12-4, Thz13-2, Thz13-3, Thz13-4	Thr12-NH
Thr12-3	71.7; CH	6.38 (q, 6.6)	Thr12-4, Thz13-4, Q-1	Thr12-4
Thr12-4	18.9; CH_3	1.69 (d, 6.6)	Thr12-2, Thr12-3	Thr12-3
Thr12-NH[d]		9.01 (d, 7.6)		Thr12-2
Thz13				
Thz13-2	156.8; C q			
Thz13-3	118.3; CH	7.35 (s)	Pip-6, Thz13-2, Thz13-4	
Thz13-4	170.8; C q			
Thz15				
Thz15-1	159.5; C q			
Thz15-2	149.8; C q			
Thz15-3	127.7; CH	8.25 (s)	Thz15-1, Thz15-2, Thz15-4	
Thz15-4	168.2; C q			
Dha16				
Dha16-1	162.0; C q			
Dha16-2	134.0; C q			
Dha16-3	103.2; CH_2	H_A: 6.67 (d, 2.3)	Dha16-1, Dha16-2	Dha16-3-H_B
		H_B: 5.53 (d, 2.4)	Dha16-1, Dha16-2	Dha16-3-H_A
Dha17				
Dha17-1	166.0; C q			
Dha17-2	132.8; C q			
Dha17-3	104.3; CH_2	H_A: 6.50 (d, 1.9)	Dha17-1, Dha17-2	Dha17-3-H_B
		H_B: 5.57 (d, 1.9)	Dha17-1, Dha17-2	Dha17-3-H_A
Q				
Q-1	160.8; C q			
Q-2	143.7; C q			
Q-3	122.5; CH	7.22 (s)	Q-1, Q-5, Q-11	
Q-4	153.1; C q			
Q-5	127.0; C q			
Q-6	123.2; CH	6.86 (d, 10.1)	Q-4, Q-5, Q-8, Q-10	Q-7
Q-7	129.9; CH	6.32 (dd, 9.7, 5.5)	Q-5, Q-8, Q-9	Q-6, Q-8
Q-8	58.9; CH	3.63-3.55 (m)	Q-6, Q-7, Q-9, Q-10	Q-7, Q-9
Q-9	67.4; CH	4.32 (s)	Q-5, Q-7, Q-8, Q-10	Q-8
Q-10	155.1; C q			
Q-11	64.2; CH	5.17 (q, 6.5)	Q-3, Q-4, Q-5, Q-12	Q-12
Q-12	22.4; CH_3	1.29 (d, 6.6)	Q-4, Q-11	Q-11

[a] HMBC correlations are from the proton to the indicated carbon.
[b] COSY correlations are from the proton to the proton attached to the indicated position.
[c] The δ of this resonance was determined by HMBC due to overlap with the $CDCl_3$ peak.
[d] Only those amide resonances demonstrating COSY correlations to neighboring protons were assigned.

APPENDIX D: SUPPORTING FIGURES AND SPECTRAL DATA FOR COMPOUNDS FROM CHAPTER 4

Figure D.1. MS analysis of thiostrepton Ala4Asn isolated from *S. laurentii* NDS1/int-A4N.

(**A**) HPLC-MS analysis. (1) Chromatogram extracted for *m/z* 854.3, the calculated $[M+2H]^{2+}$ ion of thiostrepton Ala4Asn. (2) Total ion chromatogram.

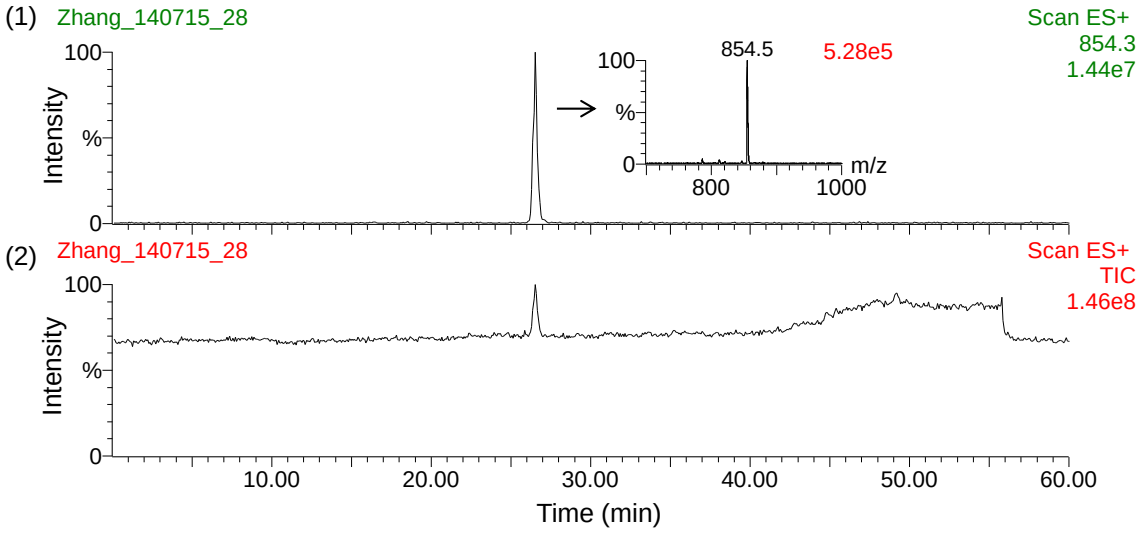

(**B**) MALDI MS spectrum of thiostrepton Ala4Asn.

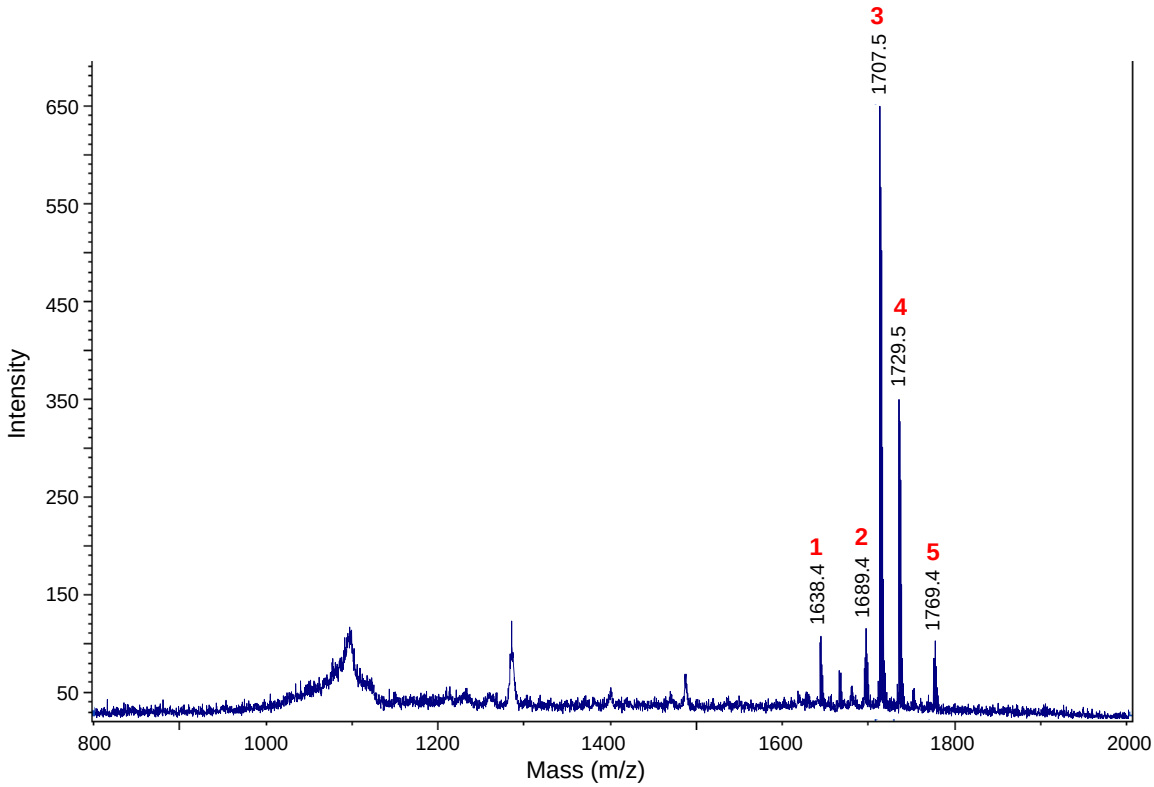

(**C**) MALDI MS/MS of parent ion *m/z* 1707.5.

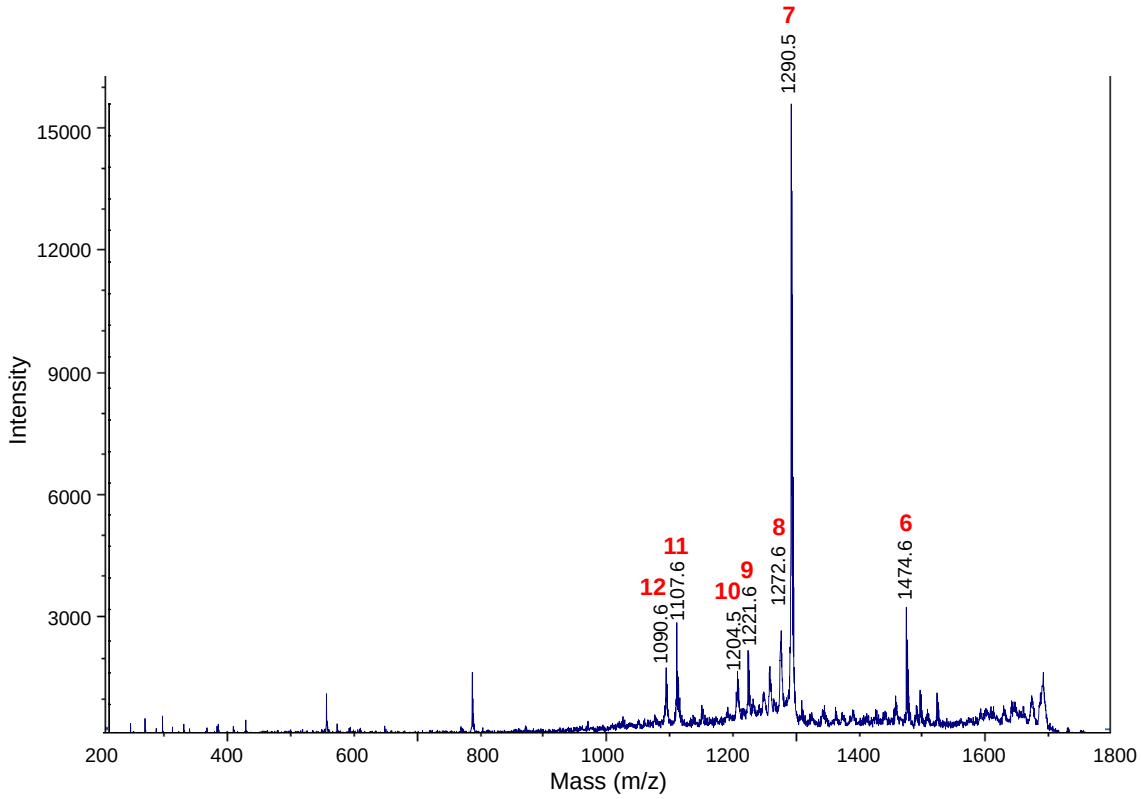

(**D**) Table and structure showing key ions and fragments in the MALDI MS and MS/MS of thiostrepton Ala4Asn.

Fragment	Expected	Observed
1. M+H$^+$-Dha17 (*in situ* truncation)	1638.5	1638.4
2. M-H_2O+H$^+$	1689.5	1689.4
3. M+H$^+$ (Parent ion)	1707.5	1707.5
4. M+Na$^+$	1729.5	1729.5
5. M+Cu$^+$	1769.4	1769.4
6. M-QA+H$^+$	1474.4	1474.6
7. M-QA-Ile1-Ala2+H$^+$	1290.3	1290.5
8. M-QA-Ile1-Ala2-H_2O+H$^+$	1272.3	1272.6
9. M-QA-Ile1-Ala2-Dha3+H$^+$	1221.3	1221.6
10. M-QA-Ile1-Ala2-Dha3-OH+H$^+$	1204.3	1204.5
11. M-QA-Ile1-Ala2-Dha3-Asn4+H$^+$	1107.3	1107.6
12. M-QA-Ile1-Ala2-Dha3-Asn4-OH+H$^+$	1090.2	1090.6

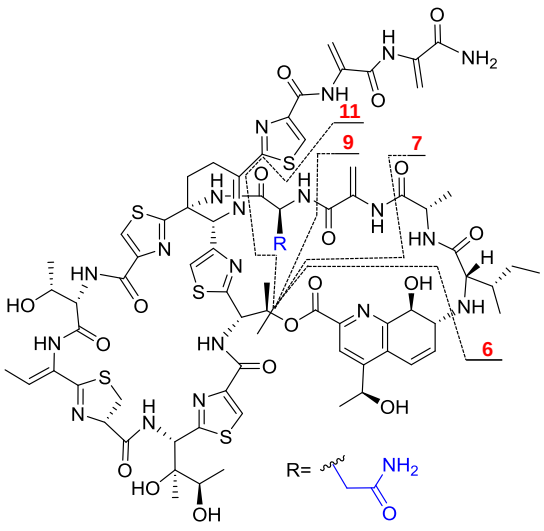

Figure D.2. HPLC-MS analysis of the C-terminal truncation reactions of thiostrepton A, thiostrepton Ala4Asn, thiostrepton Ala4Cys F1, and thiostrepton Ala4Cys F2.

(**A**) **The C-terminal truncation reaction of thiostrepton A.** The left panel includes the HPLC-MS analysis of the reaction mixture at t = 0 h and the right panel includes the reaction mixture at t = 24 h.
(**1**) Chromatogram extracted for the calculated $[M+2H]^{2+}$ *m/z* of 763.7 for thiostrepton A having lost Dha16 and Dha17. (**2**) Chromatogram extracted for the calculated $[M+2H]^{2+}$ *m/z* of 798.2 for thiostrepton A having lost Dha17. (**3**) Chromatogram extracted for the calculated $[M+2H]^{2+}$ *m/z* of 832.8 for thiostrepton A. (**4**) Total ion chromatogram.

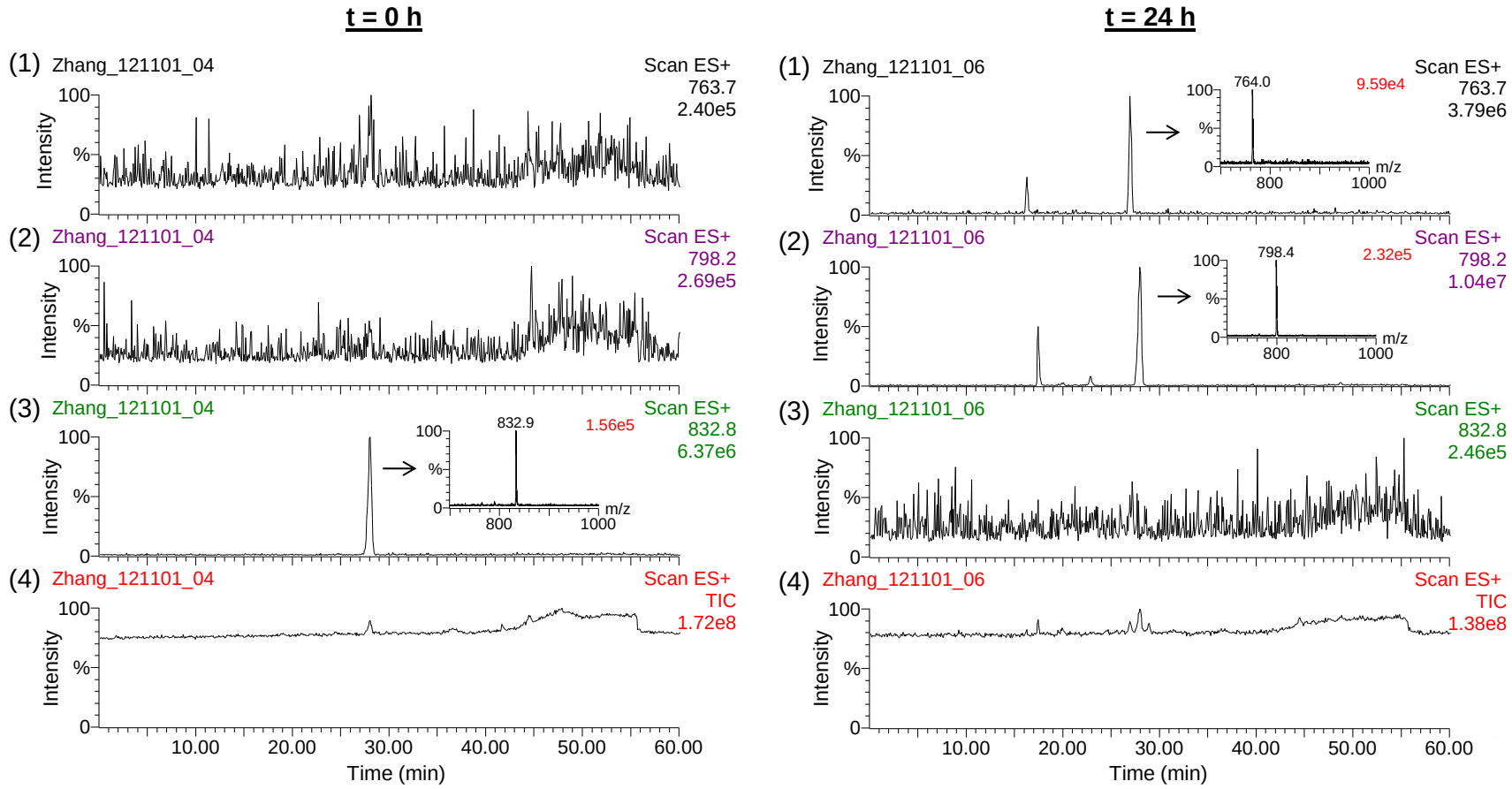

(**B**) **The C-terminal truncation reaction of thiostrepton Ala4Asn.** The left panel includes the HPLC-MS analysis of the reaction mixture at t = 0 h and the right panel includes the reaction mixture at t = 24 h.
(**1**) Chromatogram extracted for the calculated $[M+2H]^{2+}$ *m/z* of 785.2 for thiostrepton Ala4Asn having lost Dha16 and Dha17. (**2**) Chromatogram extracted for the calculated $[M+2H]^{2+}$ *m/z* of 819.7 for thiostrepton Ala4Asn having lost Dha17. (**3**) Chromatogram extracted for the calculated $[M+2H]^{2+}$ *m/z* of 854.3for thiostrepton Ala4Asn. (**4**) Total ion chromatogram.

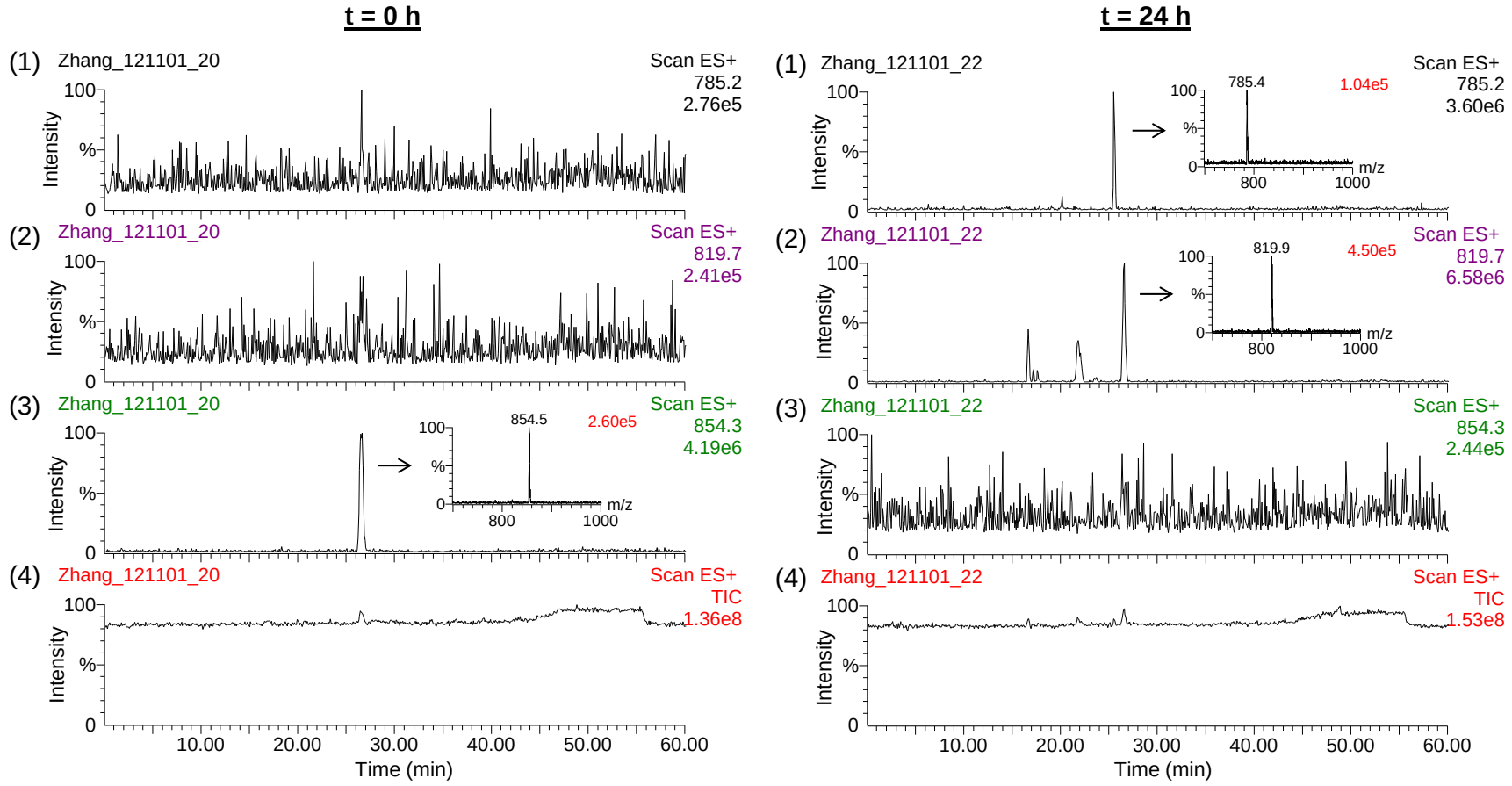

(**C**) **The C-terminal truncation reaction of thiostrepton Ala4Cys F1.** The left panel includes the HPLC-MS analysis of the reaction mixture at t = 0 h and the right panel includes the reaction mixture at t = 24 h.
(**1**) Chromatogram extracted for *m/z* of 885.3, the calculated $[M+2H]^{2+}$ ion of the thiostrepton Ala4Cys F1-Et_2NH adduct. (**2**) Chromatogram extracted the calculated $[M+2H]^{2+}$ *m/z* of 779.7 for thiostrepton Ala4Cys F1 having lost Dha16 and Dha17. (**3**) Chromatogram extracted for the calculated $[M+2H]^{2+}$ *m/z* of 814.2 for thiostrepton Ala4Cys F1 having lost Dha17. (**4**) Chromatogram extracted for the calculated $[M+2H]^{2+}$ *m/z* of 848.7 for thiostrepton Ala4Cys F1. (**5**) Total ion chromatogram.

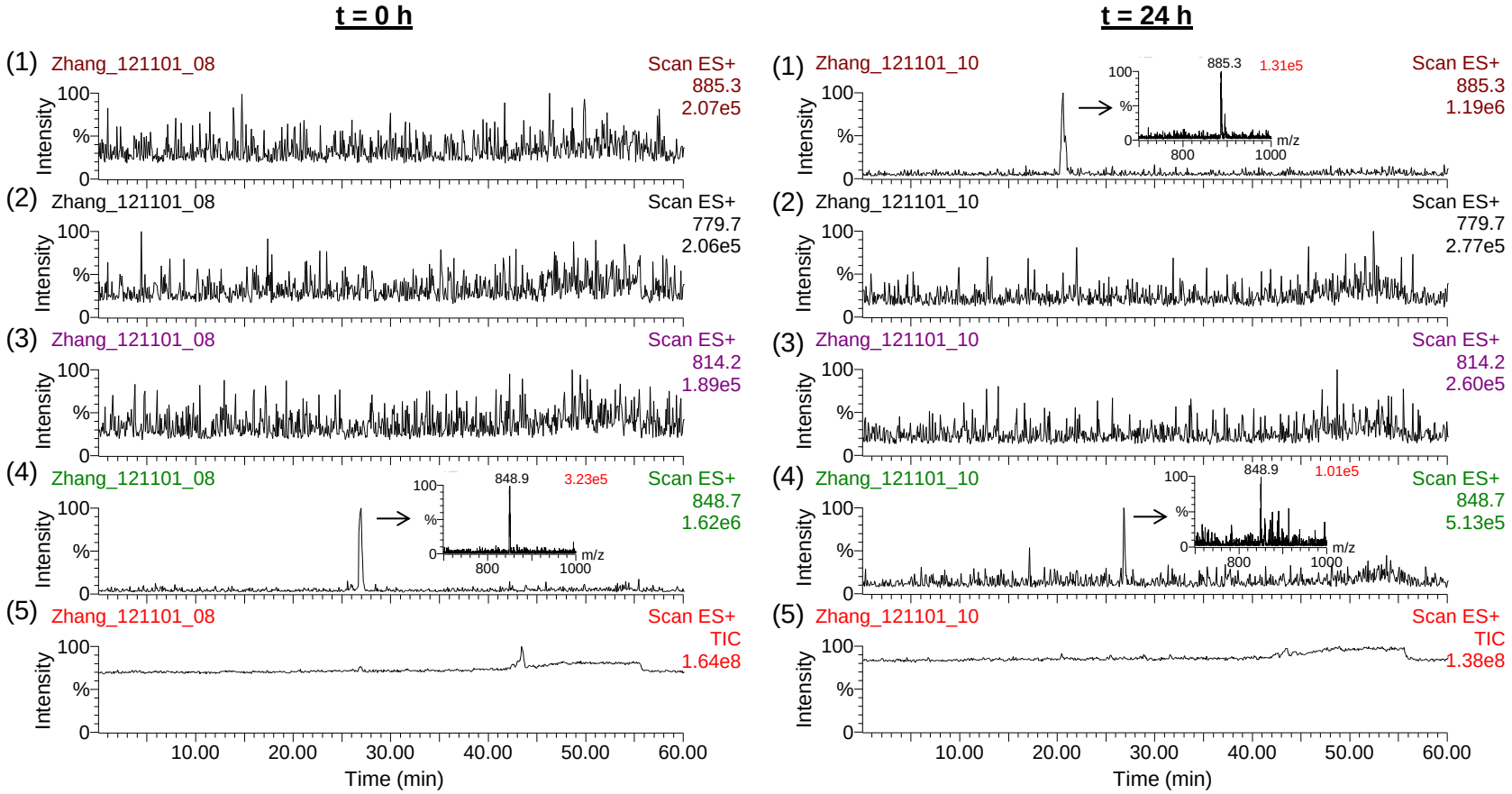

(**D**) **The C-terminal truncation reaction of thiostrepton Ala4Cys F2.** The left panel includes the HPLC-MS analysis of the reaction mixture at t = 0 h and the right panel includes the reaction mixture at t = 24 h.
(**1**) Chromatogram extracted for *m/z* of 885.3, the calculated $[M+2H]^{2+}$ ion of the thiostrepton Ala4Cys F2-Et_2NH adduct. (**2**) Chromatogram extracted for the calculated $[M+2H]^{2+}$ *m/z* of 779.7 for thiostrepton Ala4Cys F2 having lost Dha16 and Dha17. (**3**) Chromatogram extracted for the calculated $[M+2H]^{2+}$ *m/z* of 814.2 for thiostrepton Ala4Cys F2 having lost Dha17. (**4**) Chromatogram extracted for the calculated $[M+2H]^{2+}$ *m/z* of 848.7 for thiostrepton Ala4Cys F2. (**5**) Total ion chromatogram.

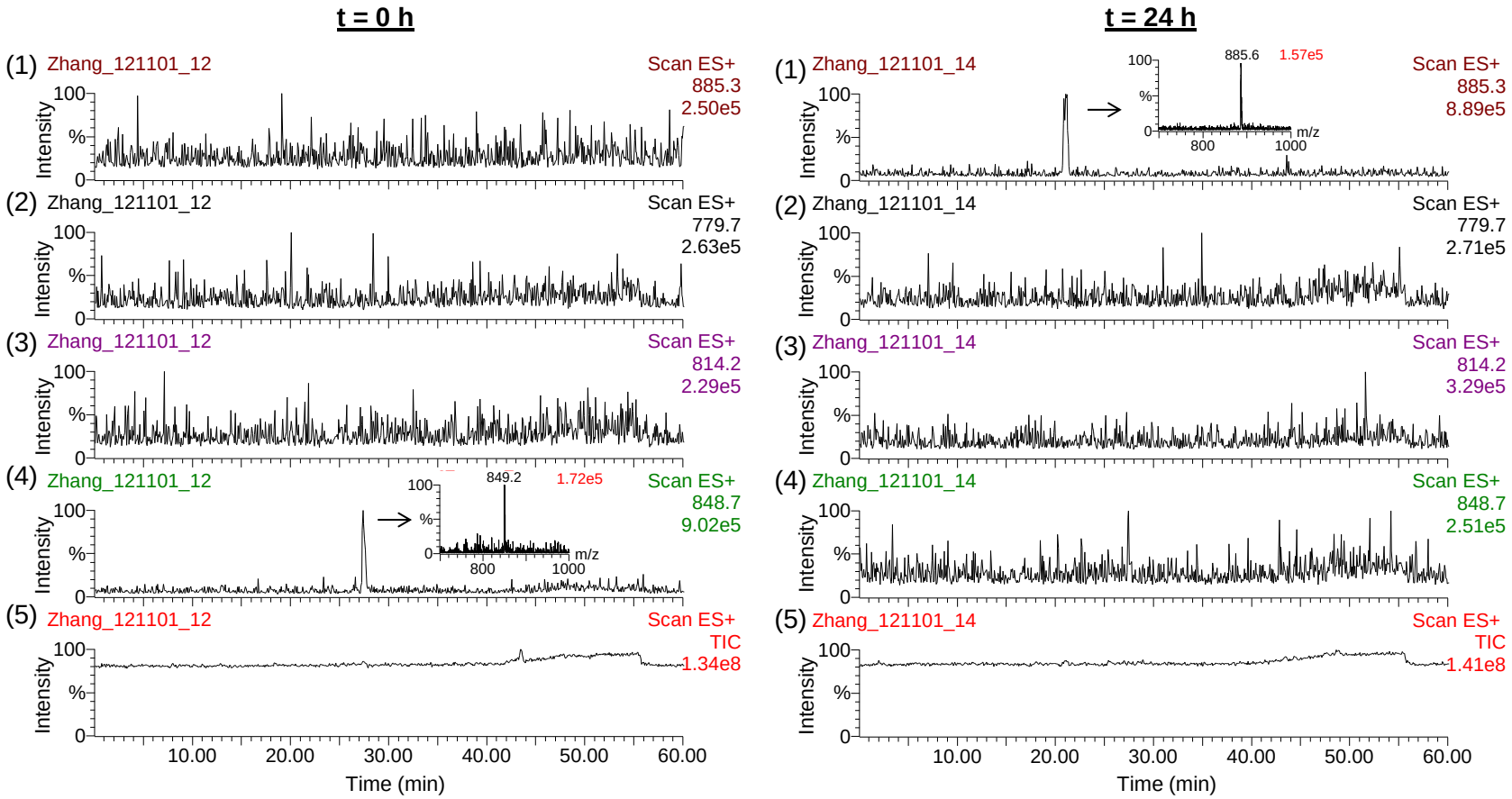

Figure D.3. MS analysis of thiostrepton Ala4Cys F1 isolated from *S. laurentii* NDS1/int-A4C.

(**A**) HPLC-MS analysis. (1) Chromatogram extracted for *m/z* 848.7, the calculated $[M+2H]^{2+}$ ion of thiostrepton Ala4Cys F1. (2) Total ion chromatogram.

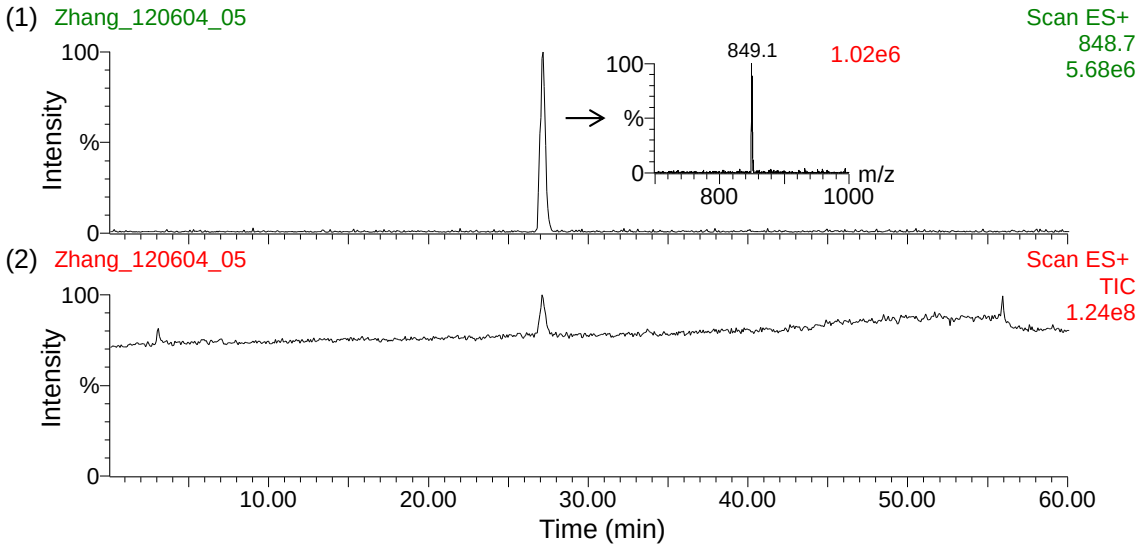

(**B**) MALDI MS spectrum of thiostrepton Ala4Cys F1. (Peaks labeled with * are internal standards. Angiotensin II: $[M+H]^+$ 1046.5; Angiotensin I: $[M+H]^+$ 1296.7; $[Glu^1]$-Fibrinopeptide B $[M+H]^+$ 1570.7. This MALDI MS analysis was performed on Bruker® Autoflex and internal standards were used as general protocol for this instrument.)

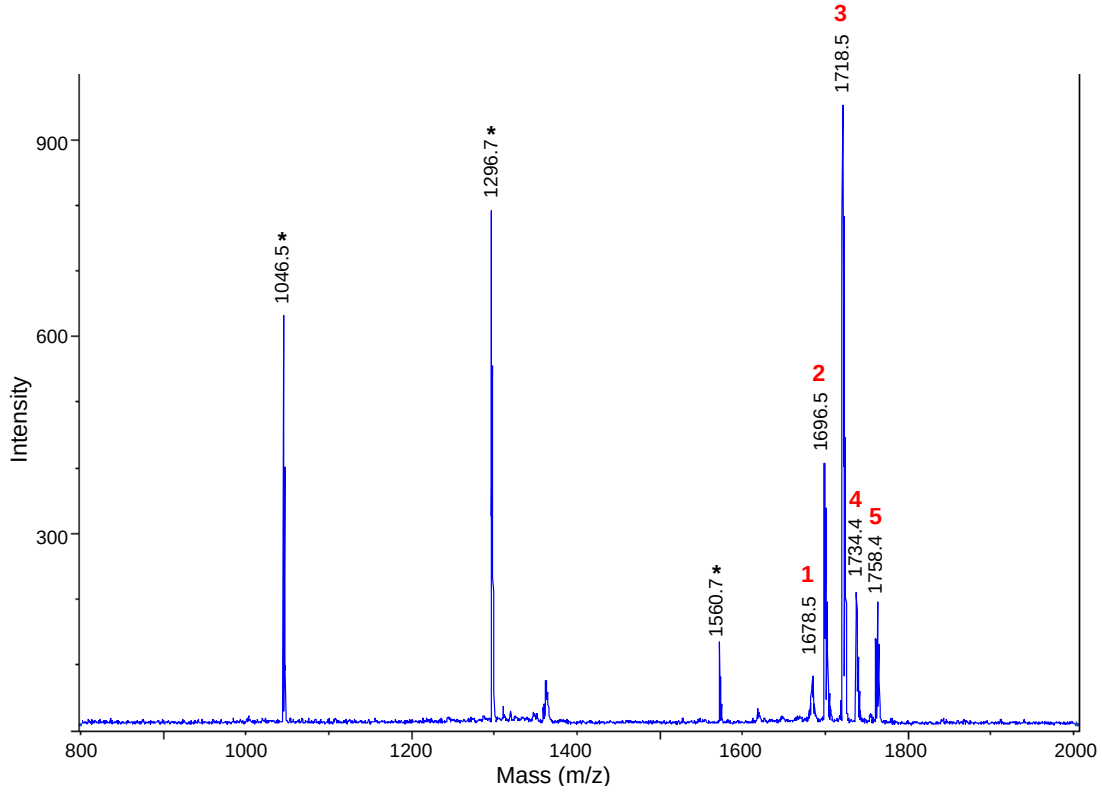

(**C**) MALDI MS/MS of parent ion *m/z* 1696.5.

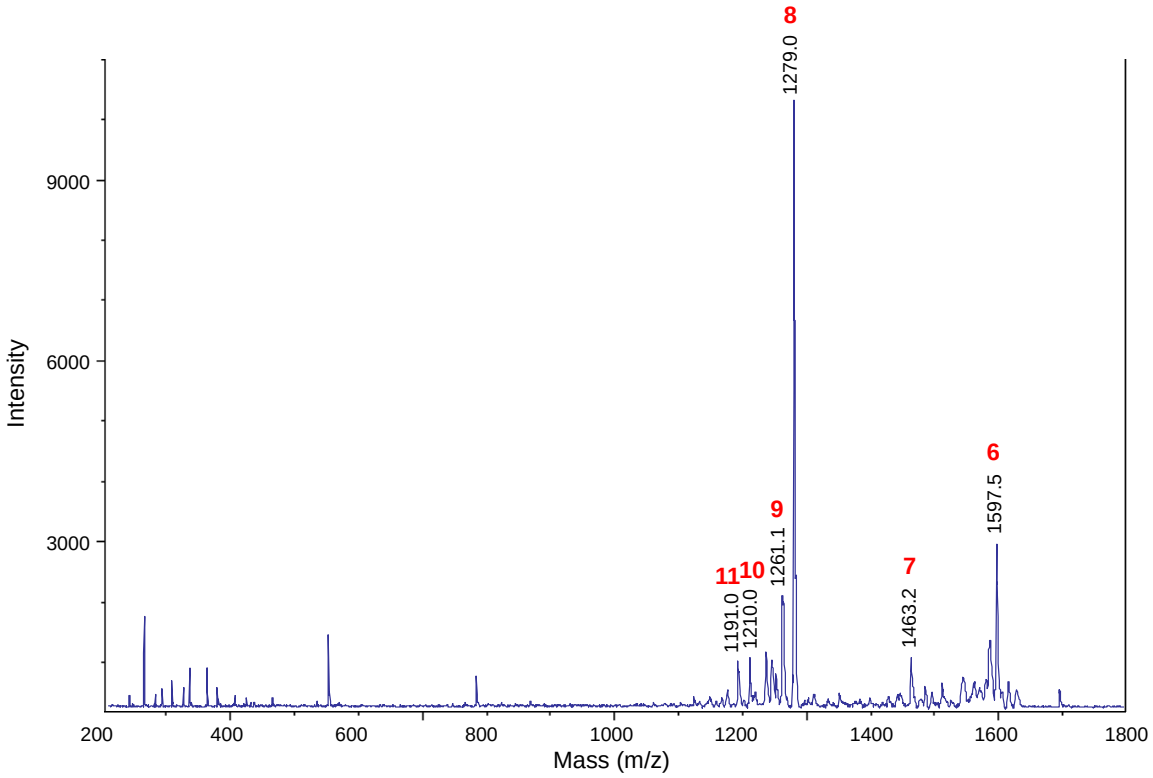

(**D**) Table and structure showing key ions and fragments in the MALDI MS and MS/MS of thiostrepton Ala4Cys F1.

Fragment	Expected	Observed
1. M-H_2O+H^+	1678.5	1678.5
2. M+H^+ (Parent ion)	1696.5	1696.5
3. M+Na^+	1718.5	1718.5
4. M+K^+	1734.4	1734.4
5. M+Cu^+	1758.4	1758.5
6. M-Ala2-CO+H^+	1597.4	1597.5
7. M-QA+H^+	1463.4	1463.2
8. M-QA-Ile1-Ala2+H^+	1279.3	1279.0
9. M-QA-Ile1-Ala2-H_2O+H^+	1261.3	1261.1
10. M-QA-Ile1-Ala2-Dha3+H^+	1210.3	1210.0
11. M-QA-Ile1-Ala2-Dha3-H-H_2O+H^+	1191.2	1191.0

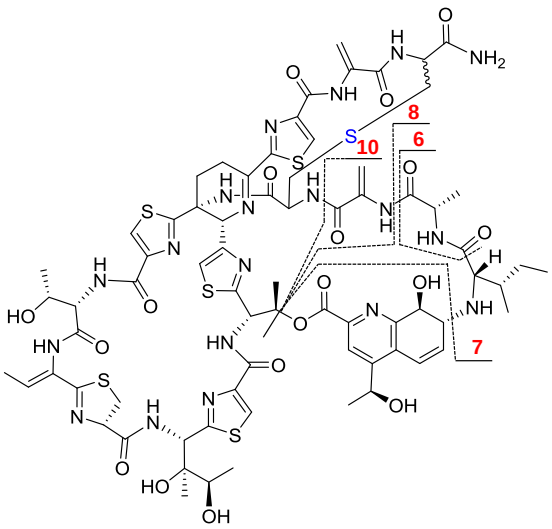

Figure D.4. Structure and numbering system used for thiostreptons Ala4Cys F1 and F2.

Thiostrepton Ala4Cys F1 and F2 are proposed to be diastereomers differing in configuration at the α-carbon of Ala17, however, their absolute configurations were not determined.

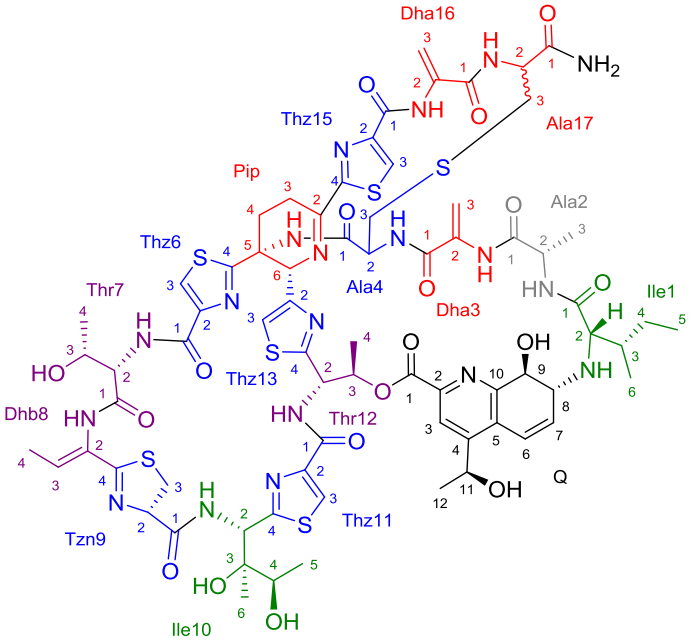

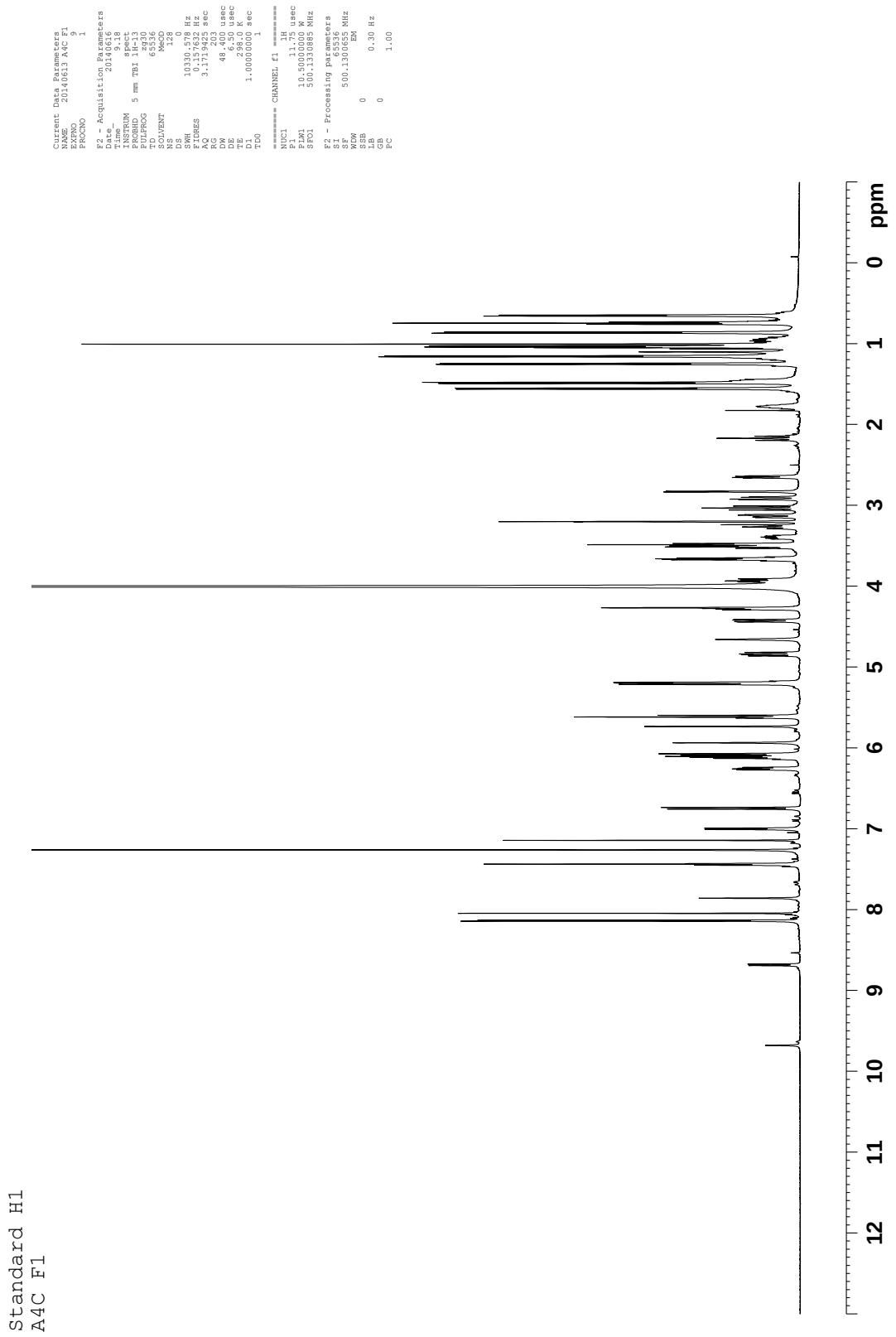

Figure D.5. ^{1}H NMR spectrum of thiostrepton Ala4Cys F1 (500 MHz, $CDCl_3$-CD_3OD 4:1, 25 °C).

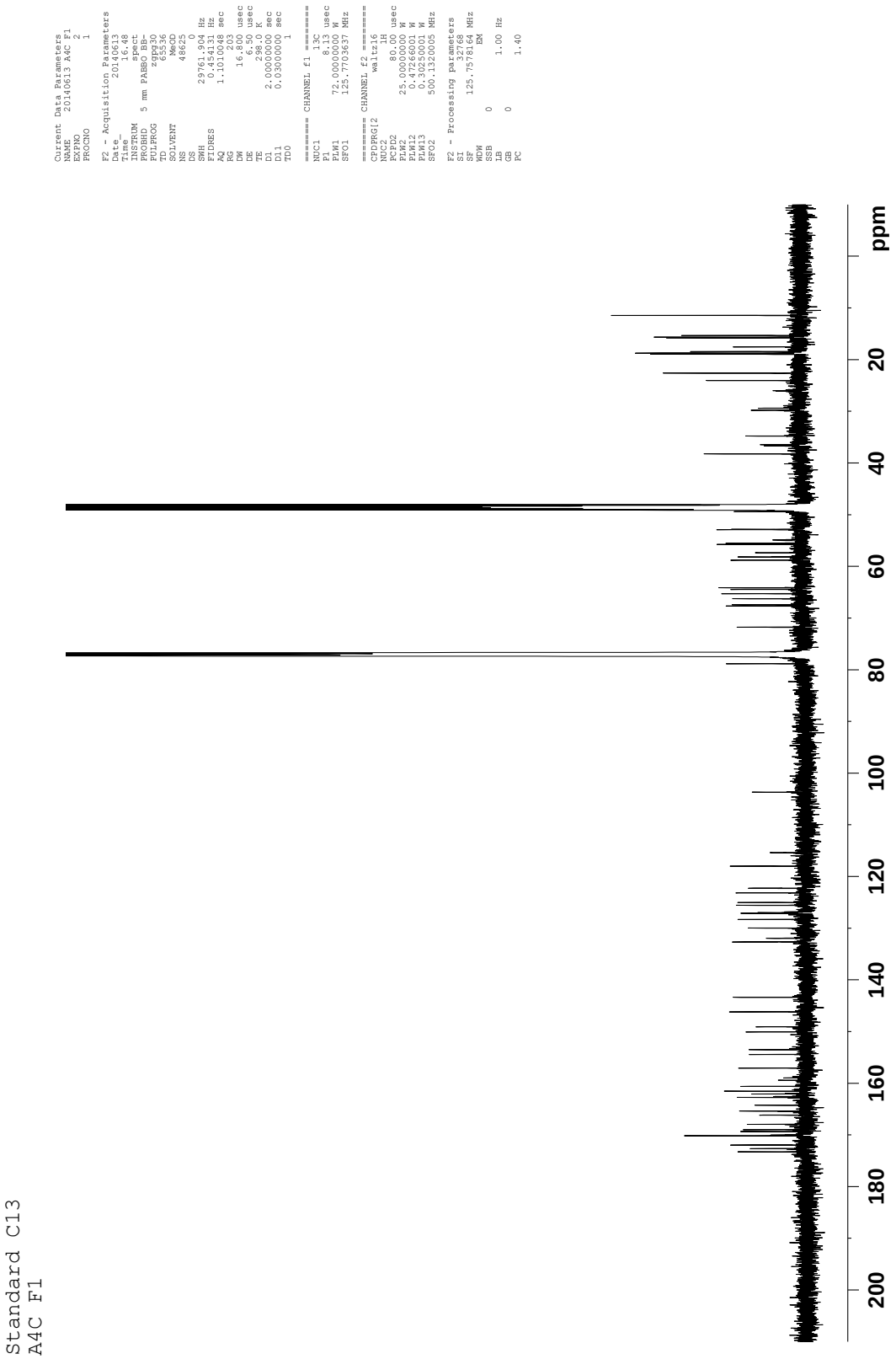

Figure D.6. ^{13}C NMR spectrum of thiostrepton Ala4Cys F1 (125 MHz, $CDCl_3$-CD_3OD 4:1, 25 °C).

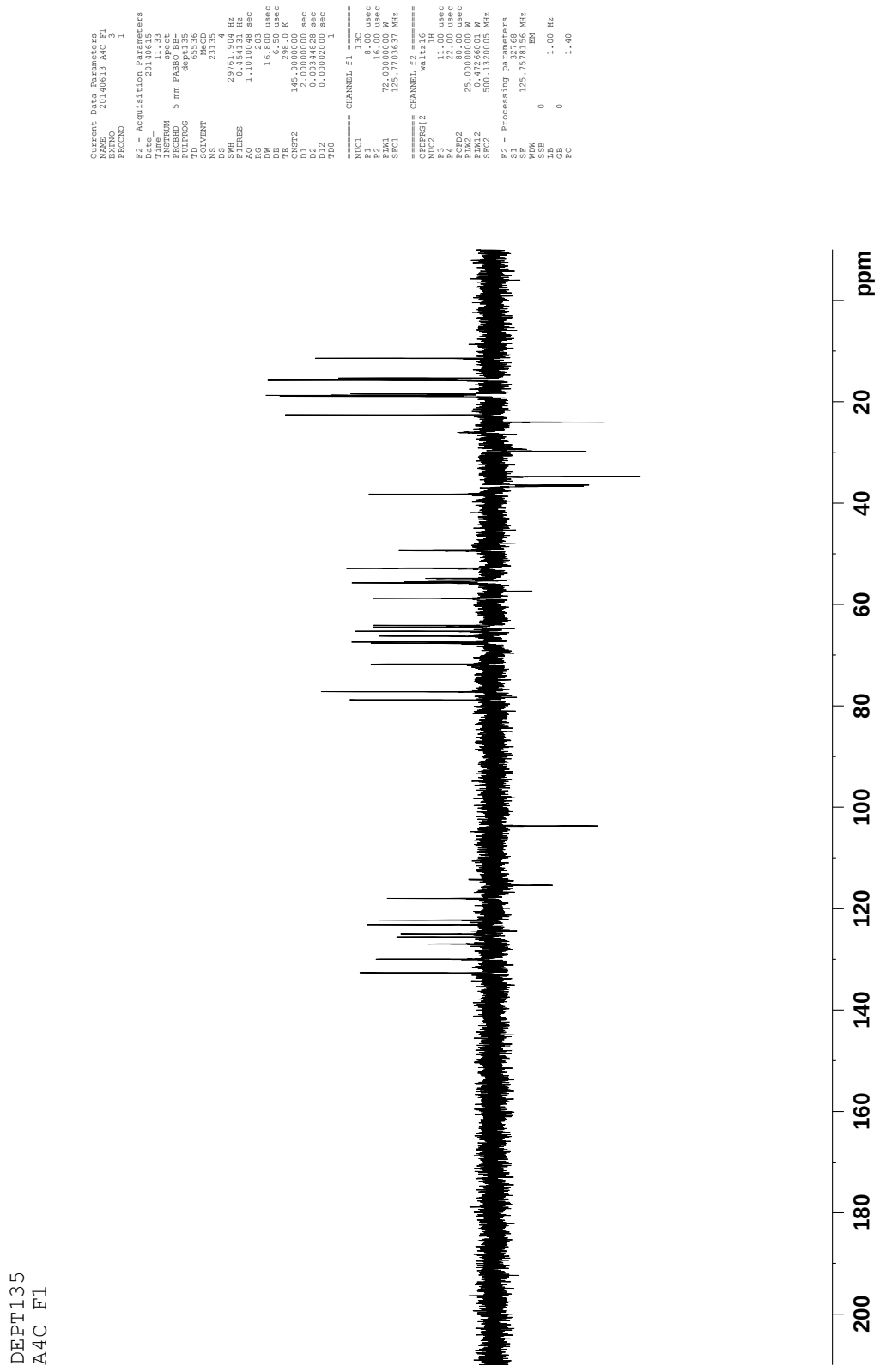

Figure D.7. DEPT-135 NMR spectrum of thiostrepton Ala4Cys F1 (125 MHz, $CDCl_3$-CD_3OD 4:1, 25 °C).

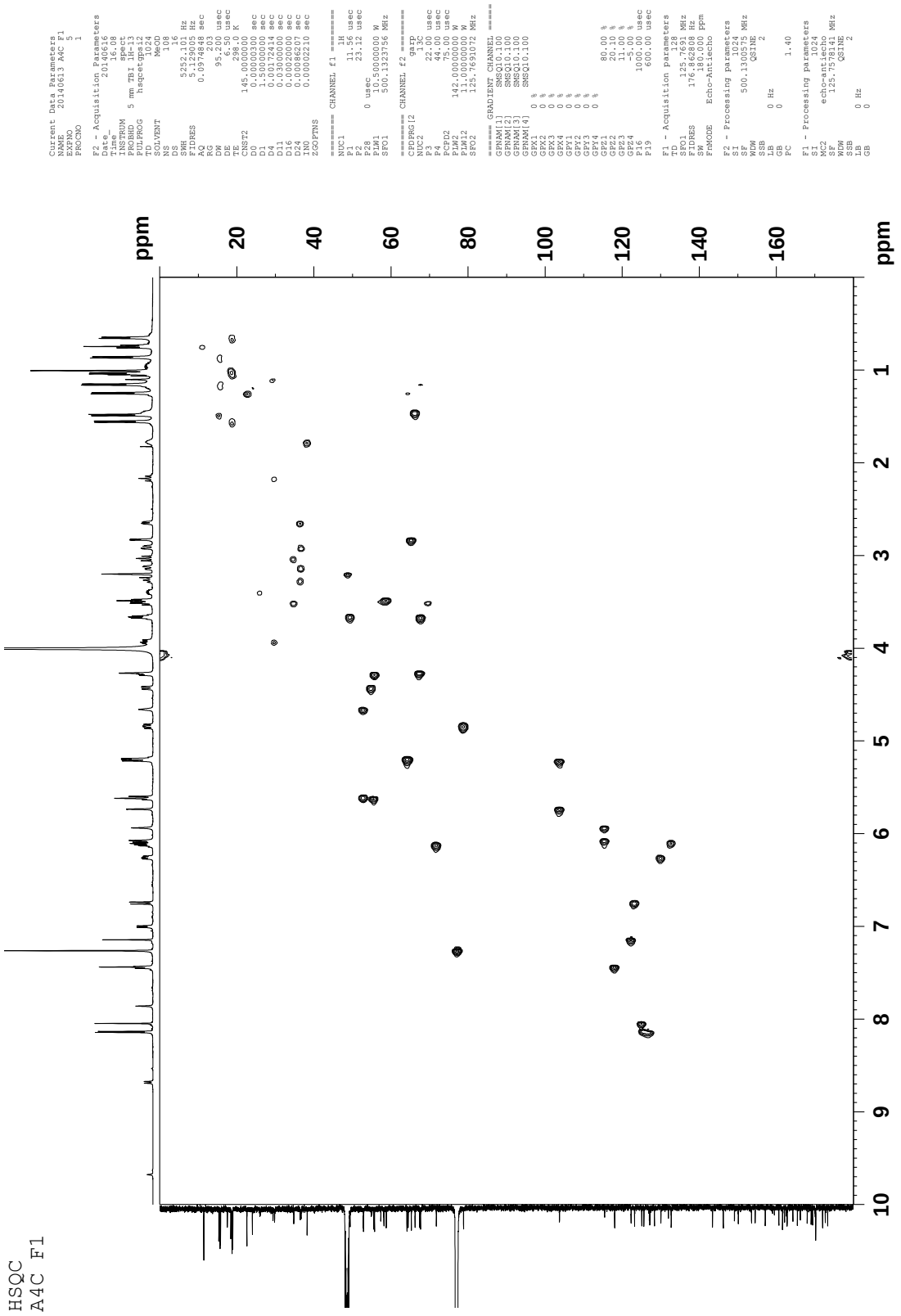

Figure D.8. gHSQC spectrum of thiostrepton Ala4Cys F1 (500 MHz, $CDCl_3$-CD_3OD 4:1, 25 °C).

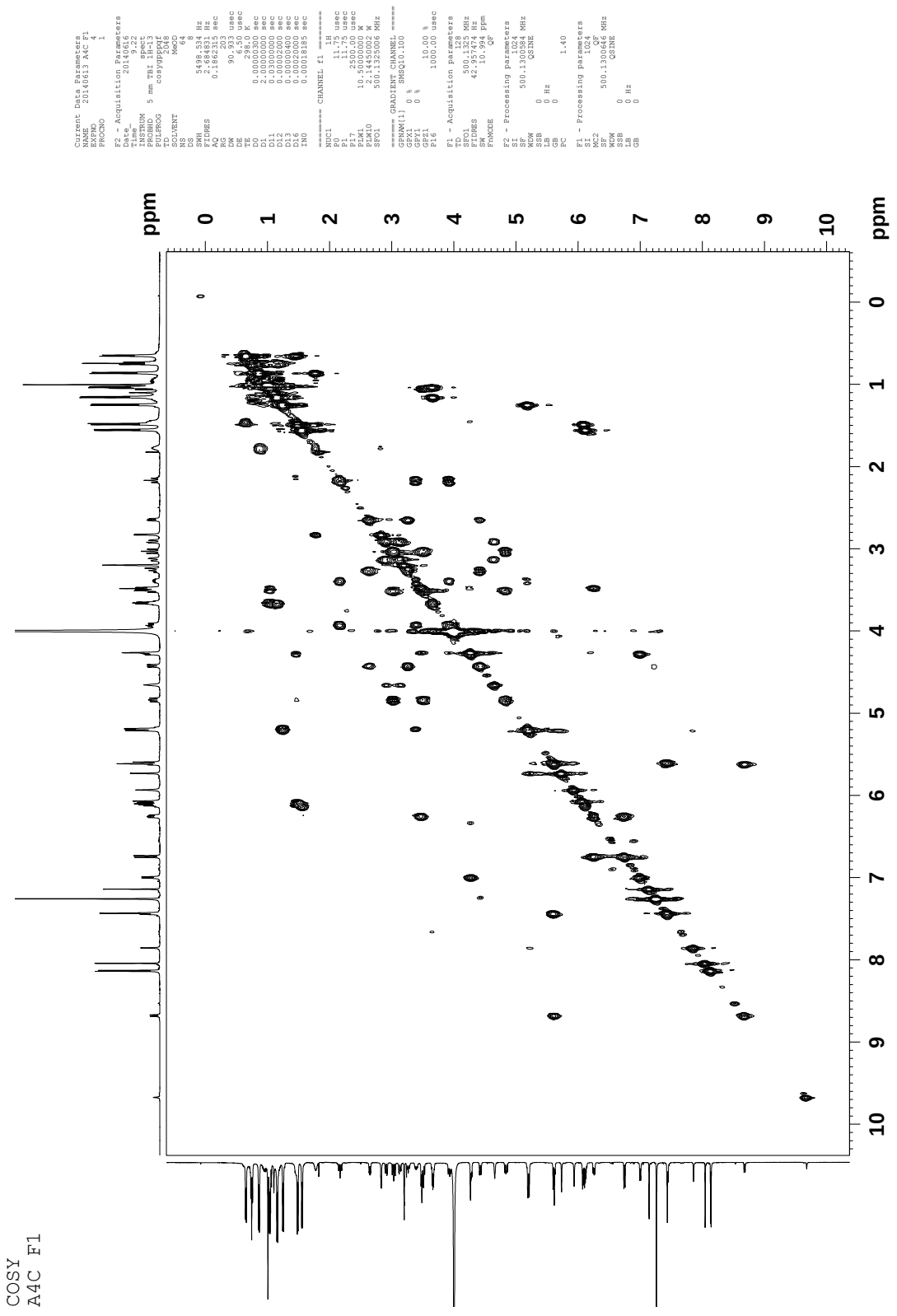

Figure D.9. gCOSY spectrum of thiostrepton Ala4Cys F1 (500 MHz, $CDCl_3$-CD_3OD 4:1, 25 °C).

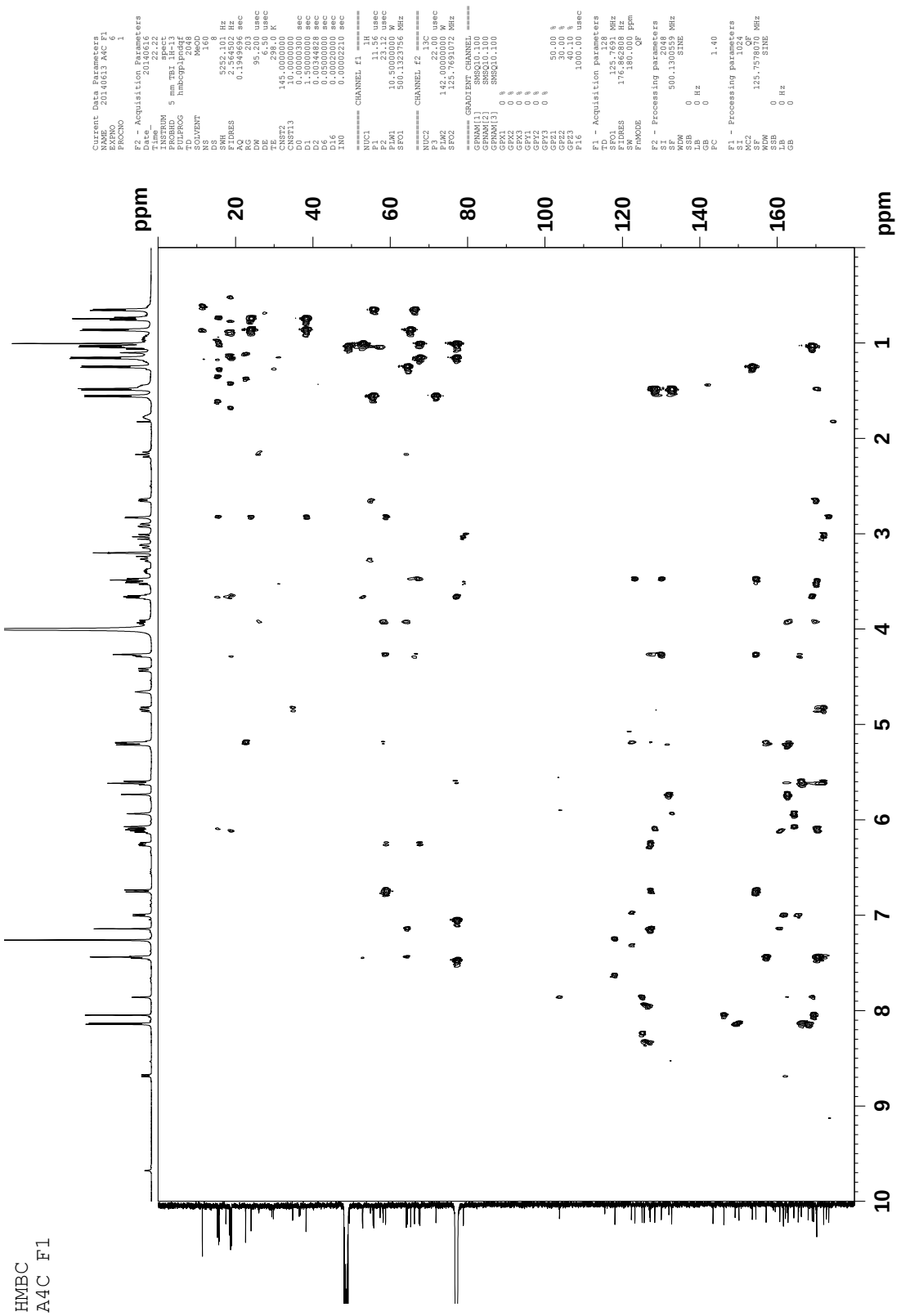

Figure D.10. gHMBC spectrum of thiostrepton Ala4Cys F1 (500 MHz, $CDCl_3$-CD_3OD 4:1, 25 °C).

Table D.1. ^{1}H and ^{13}C NMR assignments of thiostrepton Ala4Cys F1

Position	δ_C [ppm]; mult	δ_H [ppm]; (mult, J in Hz)	HMBC[a]	COSY[b]
Ile1				
Ile1-1	173.3; C q			
Ile1-2	65.3; CH	2.83 (d, 4.4)	Ile1-1; Ile1-3; Ile1-4; Ile1-6; Q-8	Ile1-3
Ile1-3	38.2; CH	1.82-1.74 (m)		Ile1-6
Ile1-4	24.0; CH_2	H_A: 1.22-1.16 (m)	Ile1-5; Ile1-6	Ile1-4-H_B; Ile1-5
		H_B: 0.99-0.90 (m)	Ile1-3; Ile1-5; Ile1-6	Ile1-4-H_A; Ile1-5
Ile1-5	11.4; CH_3	0.75 (t, 7.4)	Ile1-3; Ile1-6	Ile1-4-H_A; Ile1-4-H_B
Ile1-6	15.6; CH_3	0.86 (d, 6.9)	Ile1-2; Ile1-3; Ile1-5	Ile1-3
Ala2				
Ala2-1	169.0; C q			
Ala2-2	49.4; CH	3.70-3.63 (m)	Ala2-1; Ala2-3	Ala2-3
Ala2-3	18.7; CH_3	1.03 (d, 6.7)	Ala2-1; Ala2-2	Ala2-2
Dha3				
Dha3-1	162.6; C q			
Dha3-2	131.9; C q			
Dha3-3	103.7; CH_2	H_A: 5.73 (d, 1.7)	Dha3-1; Dha3-2	Dha3-3-H_B
		H_B: 5.21 (br s)	Dha3-1; Dha3-2	Dha3-3-H_A
Dha3-NH[d]		7.86 (s)	Ala2-1	
Ala4				
Ala4-1	170.1; C q			
Ala4-2	54.9; CH	4.43 (dd, 11.7, 3.3)		Ala4-3-H_A; Ala4-3-H_B
Ala4-3	36.5; CH_2	H_A: 3.27 (t, 11.2)	Ala4-2	Ala4-2; Ala4-3-H_B
		H_B: 2.65 (dd, 10.0, 3.1)	Ala4-1; Ala4-2	Ala4-2; Ala4-3-H_A
Pip				
Pip-2	162.8; C q			
Pip-3	26.0; CH_2	H_A: 3.42-3.36 (m)		Pip-3-H_B; Pip-4-H_A; Pip-4-H_B; Pip-6
		H_B: 3.07-3.00 (m)		Pip-3-H_A; Pip-4-H_B
Pip-4	29.8; CH_2	H_A: 3.96-3.90 (m)	Ala4-1; Pip-2; Pip-3; Pip-5; Pip-6	Pip-3-H_A; Pip-4-H_B
		H_B: 2.20-2.13 (m)		Pip-3-H_A; Pip-3-H_B; Pip-4-H_A
Pip-5	58.2; C q			
Pip-6	64.1; CH	5.21-5.18 (m)	Pip-2; Thz13-2	Pip-3-H_A
Thz6				
Thz6-1	161.6; C q			
Thz6-2	146.2; C q			
Thz6-3	125.0; CH	8.05 (s)	Thz6-2; Thz6-4	
Thz6-4	169.4 ; C q			
Thr7				
Thr7-1	165.4; C q			
Thr7-2	55.7; CH	4.28 (dd, 8.2, 4.2)	Thr7-1; Thr7-3	Thr7-3; Thr7-NH
Thr7-3	66.3; CH	1.49-1.42 (m)	Thr7-1; Thr7-4	Thr7-4
Thr7-4	18.9; CH_3	0.65 (d, 6.2)	Thr7-2; Thr7-3	Thr7-3
Thr7-NH[d]		7.00 (d, 7.5)	Thz6-1; Thr7-1	Thr7-2
Dhb8				
Dhb8-2	128.3; C q			
Dhb8-3	132.7; CH	6.10 (q, 7.0)	Dhb8-2; Tzn9-4	Dhb8-4
Dhb8-4	15.3; CH_3	1.49 (d, 7.1)	Dhb8-2; Dhb8-3; Tzn9-4	Dhb8-3
Tzn9				
Tzn9-1	172.0; C q			
Tzn9-2	78.8; CH	4.84 (dd, 12.9, 9.0)	Tzn9-1; Tzn9-3; Tzn9-4	Tzn9-3-H_A; Tzn9-3-H_B
Tzn9-3	34.8; CH_2	H_A: 3.51 (dd, 12.6, 9.9)	Tzn9-2; Tzn9-4	Tzn9-2; Tzn9-3-H_B
		H_B: 3.03 (t, 12.3)	Tzn9-1; Tzn9-2	Tzn9-2; Tzn9-3-H_A
Tzn9-4	170.2; C q			
Ile10				
Ile10-2	52.8; CH	5.61 (d, 10.1)	Tzn9-1; Ile10-3; Thz11-4	Ile10-NH
Ile10-3	77.0[c]; C q			
Ile10-4	67.7; CH	3.70-3.63 (m)	Ile10-2; Ile10-3; Ile10-5; Ile10-6	Ile10-5
Ile10-5	15.8; CH_3	1.16 (d, 6.4)	Ile10-3; Ile10-4; Ile10-6	Ile10-4

Position	δ_C [ppm]; mult	δ_H [ppm]; (mult, J in Hz)	HMBC[a]	COSY[b]
Ile10-6	18.4; CH_3	1.01 (s)	Ile10-2; Ile10-3; Ile10-4; Ile10-5	
Ile10-NH[d]		7.44 (d, 9.8)		Ile10-2
Thz11				
Thz11-1	162.1; C q			
Thz11-2	150.1; C q			
Thz11-3	125.6; CH	8.13 (s)	Thz11-2; Thz11-4	
Thz11-4	166.2; C q			
Thr12				
Thr12-2	55.5; CH	5.62 (d, 7.2)	Thz11-1; Thz13-2; Thz13-4	Thr12-NH
Thr12-3	71.8; CH	6.14 (q, 7.3)	Thr12-4; Thz13-4; Q-1	Thr12-4
Thr12-4	18.7; CH_3	1.57 (d, 6.6)	Thr12-2; Thr12-3	Thr12-3
Thr12-NH[d]		8.68 (d, 8.8)		Thr12-2
Thz13				
Thz13-2	157.1; C q			
Thz13-3	118.0; CH	7.44 (s)	Pip-6; Thz13-2; Thz13-4	
Thz13-4	170.2; C q			
Thz15				
Thz15-1	159.4; C q			
Thz15-2	149.1; C q			
Thz15-3	127.0; CH	8.14 (s)	Thz15-2; Thz15-4	
Thz15-4	168.0; C q			
Dha16				
Dha16-1	164.3; C q			
Dha16-2	132.7; C q			
Dha16-3	115.4; CH_2	H_A: 6.07 (br s)	Dha16-1	Dha16-3-H_B
		H_B: 5.94 (br s)	Dha16-1; Dha16-2	Dha16-3-H_A
Ala17				
Ala17-1	170.0; C q			
Ala17-2	54.9; CH	4.66 (t, 3.8)		Ala17-3-H_A; Ala17-3-H_B
Ala17-3	36.5; CH_2	H_A: 3.13 (dd, 14.6, 3.7)		Ala17-2; Ala17-3-H_B
		H_B: 2.91 (dd, 14.6, 3.5)		Ala17-2; Ala17-3-H_A
Q				
Q-1	160.6; C q			
Q-2	143.4; C q			
Q-3	122.3; CH	7.14 (s)	Q-1; Q-5; Q-11	
Q-4	153.5; C q			
Q-5	127.1; C q			
Q-6	123.2; CH	6.75 (d, 10.1)	Q-5; Q-8; Q-10	Q-7
Q-7	130.0; CH	6.25 (dd, 9.4, 5.5)	Q-5; Q-8; Q-9	Q-6; Q-8
Q-8	58.8; CH	3.51-3.46 (m)	Ile1-2; Q-6; Q-7; Q-9; Q-10	Q-7
Q-9	67.4; CH	4.27 (br s)	Q-5; Q-7; Q-8; Q-10	Q-8
Q-10	154.4; C q			
Q-11	64.4; CH	5.21-5.18 (m)	Q-3; Q-12	Q-12
Q-12	22.6; CH_3	1.25 (d, 6.6)	Q-4; Q-11	Q-11

[a] HMBC correlations are from the proton to the indicated carbon.
[b] COSY correlations are from the proton to the proton attached to the indicated position.
[c] The δ of this resonance was determined by HMBC due to overlap with the $CDCl_3$ resonance.
[d] Only those amide resonances demonstrating COSY or HMBC correlations to neighboring protons or carbons, respectively, were assigned.

Figure D.11. MS analysis of thiostrepton Ala4Cys F2 isolated from *S. laurentii* NDS1/int-A4C.

(**A**) HPLC-MS analysis. (1) Chromatogram extracted for *m/z* 848.7, the calculated $[M+2H]^{2+}$ ion of thiostrepton Ala4Cys F2. (2) Total ion chromatogram.

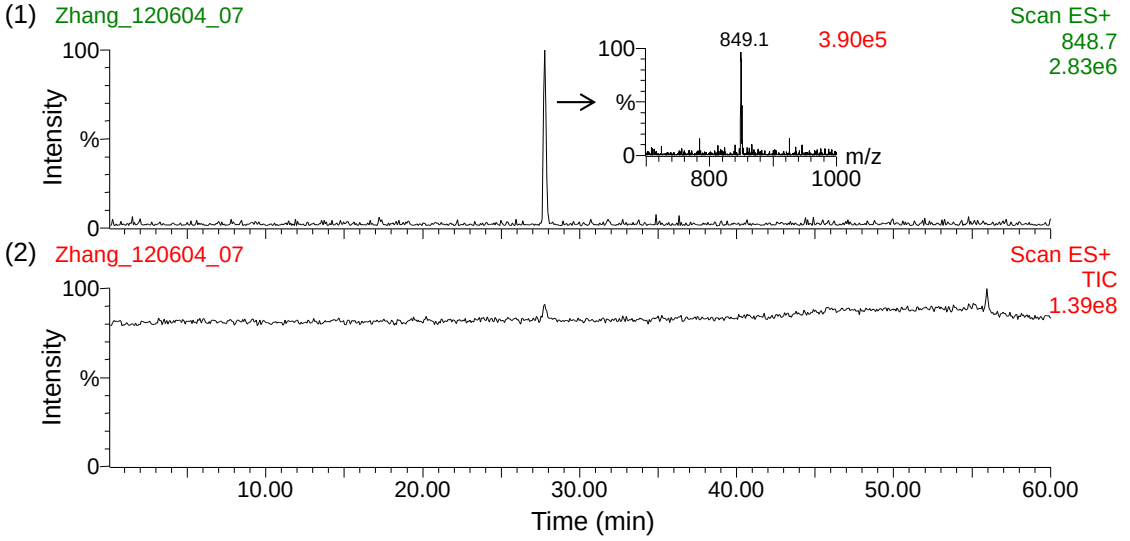

(**B**) MALDI MS spectrum of thiostrepton Ala4Cys F2. (Peaks labeled with * are internal standards. Angiotensin II: $[M+H]^+$ 1046.5; Angiotensin I: $[M+H]^+$ 1296.7; $[Glu^1]$-Fibrinopeptide B $[M+H]^+$ 1570.7. This MALDI MS analysis was performed on Bruker® Autoflex and internal standards were used as general protocol for this instrument.)

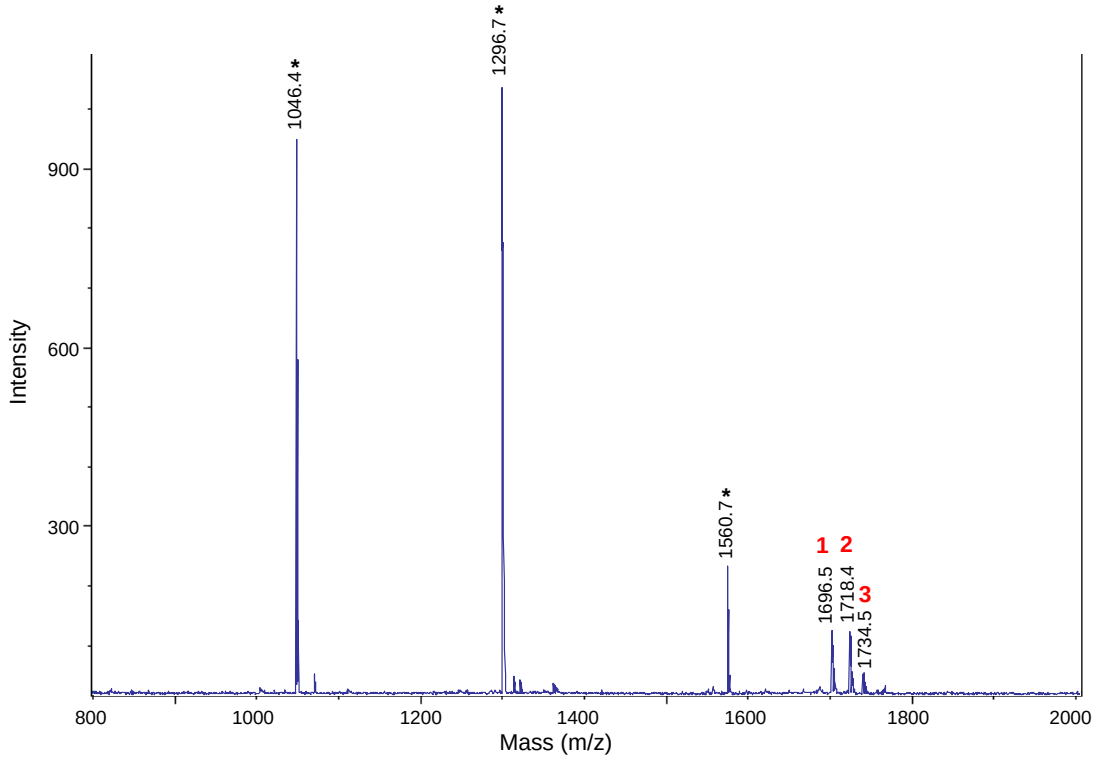

(**C**) MALDI MS/MS of parent ion *m/z* 1696.5.

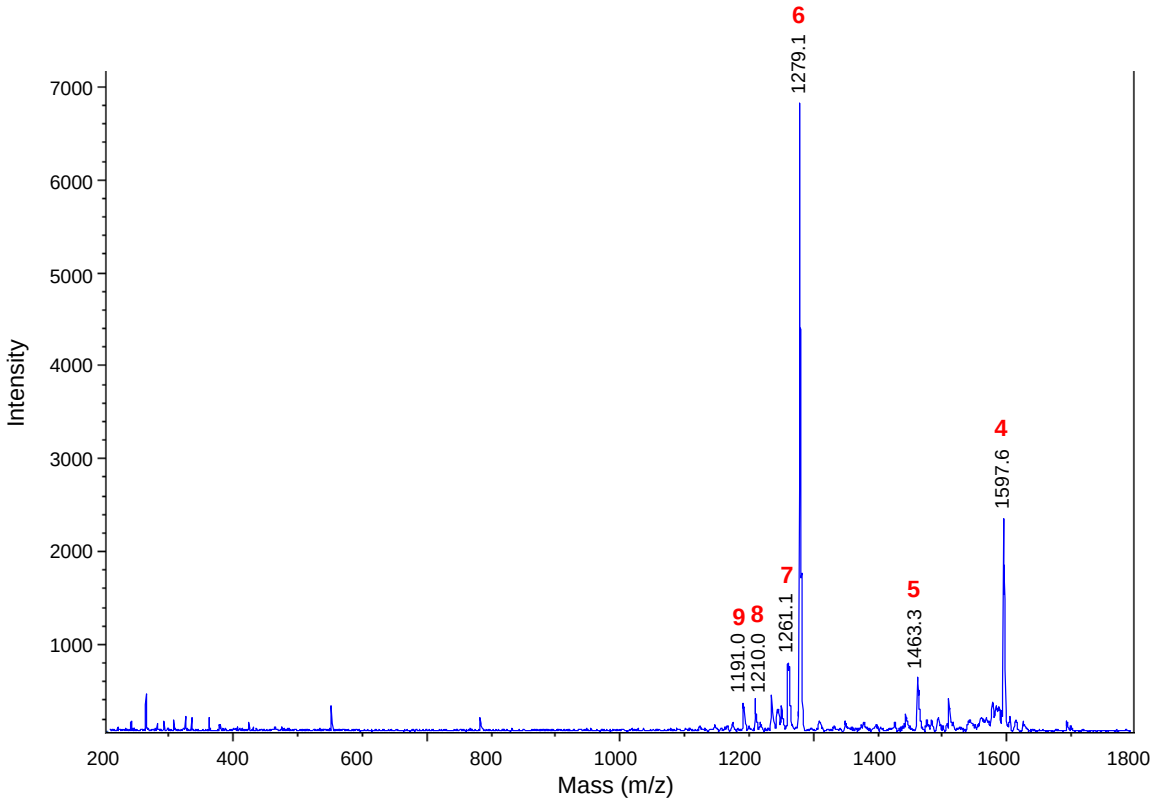

(**D**) Table and structure showing key ions and fragments in the MALDI MS and MS/MS of thiostrepton Ala4Cys F2.

Fragment	Expected	Observed
1. $M+H^+$ (Parent ion)	1696.5	1696.5
2. $M+Na^+$	1718.5	1718.4
3. $M+K^+$	1734.4	1734.5
4. M-Ala2-CO+H^+	1597.4	1597.6
5. M-QA+H^+	1463.4	1463.3
6. M-QA-Ile1-Ala2+H^+	1279.3	1279.1
7. M-QA-Ile1-Ala2-H_2O+H^+	1261.3	1261.1
8. M-QA-Ile1-Ala2-Dha3+H^+	1210.3	1210.0
9. M-QA-Ile1-Ala2-Dha3-H-H_2O+H^+	1191.2	1191.0

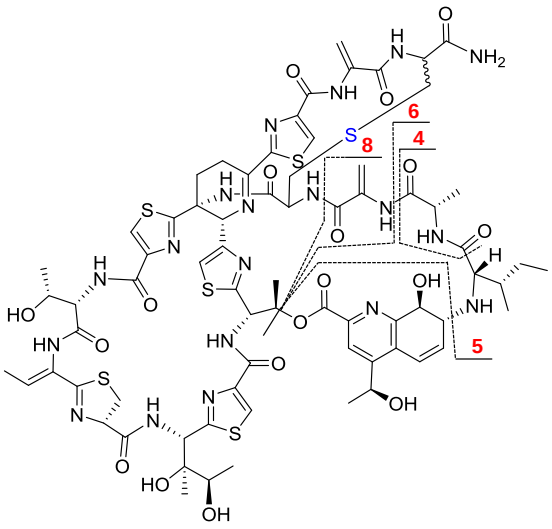

Figure D.12. Structure and numbering system used for thiostreptons Ala4Cys F1 and F2.

Thiostrepton Ala4Cys F1 and F2 are proposed to be diastereomers differing in configuration at the α-carbon of Ala17, however, their absolute configurations were not determined.

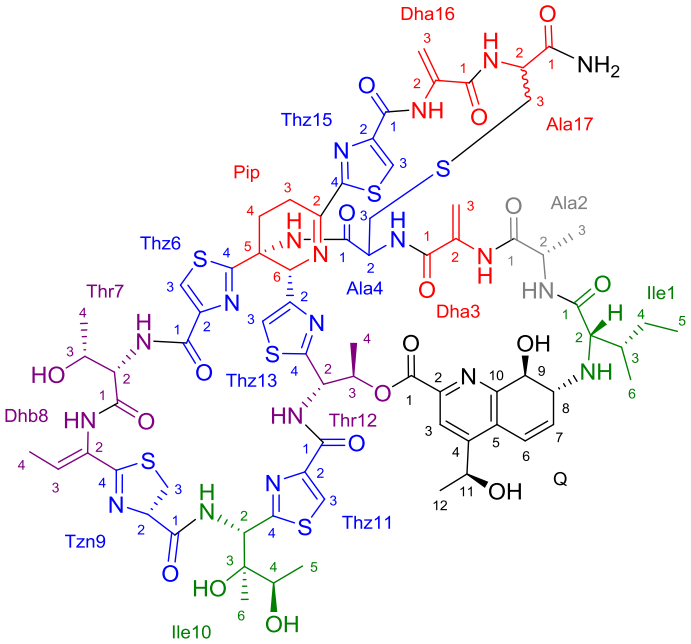

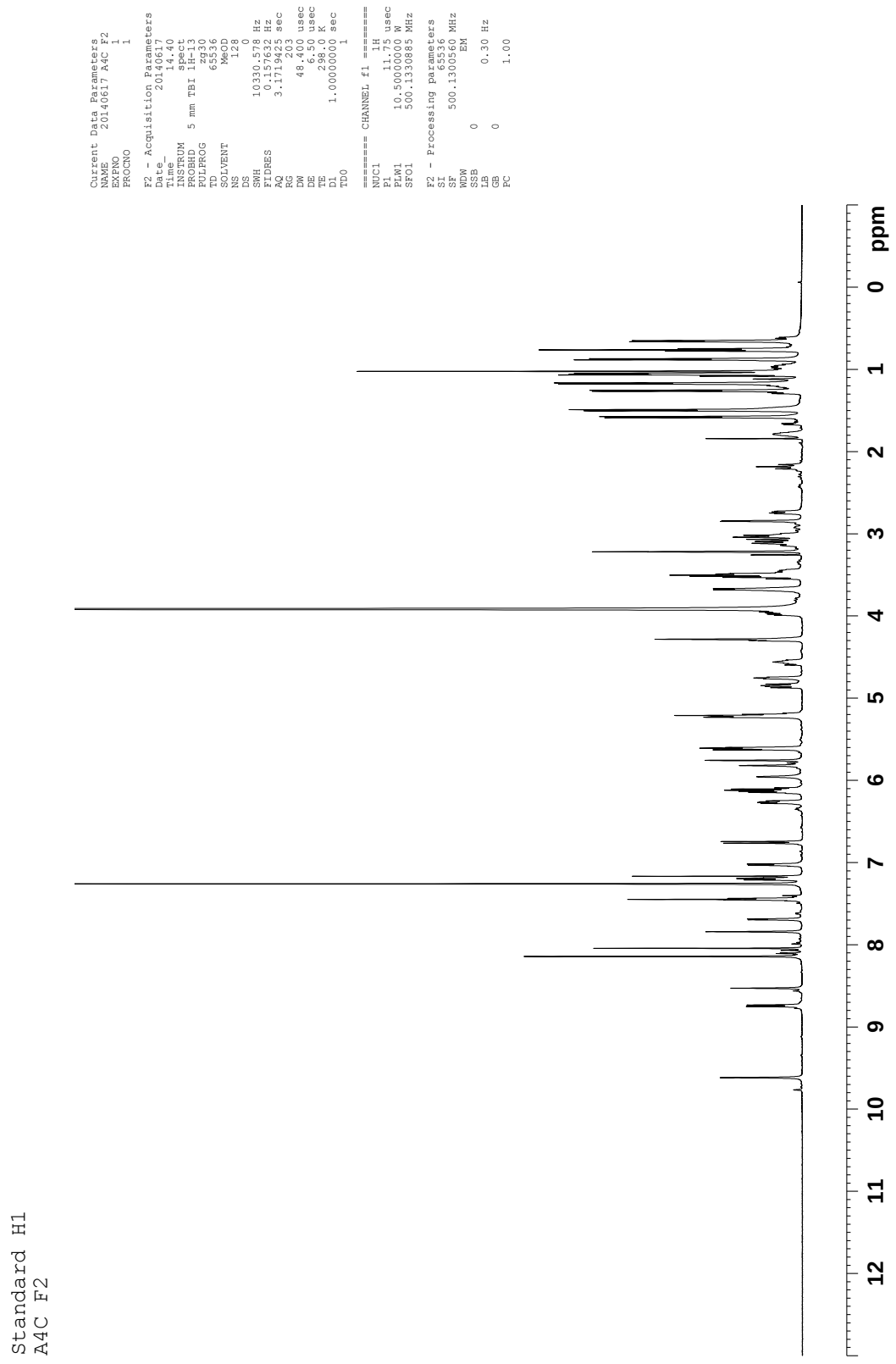

Figure D.13. ^{1}H NMR spectrum of thiostrepton Ala4Cys F2 (500 MHz, $CDCl_3$-CD_3OD 4:1, 25 °C).

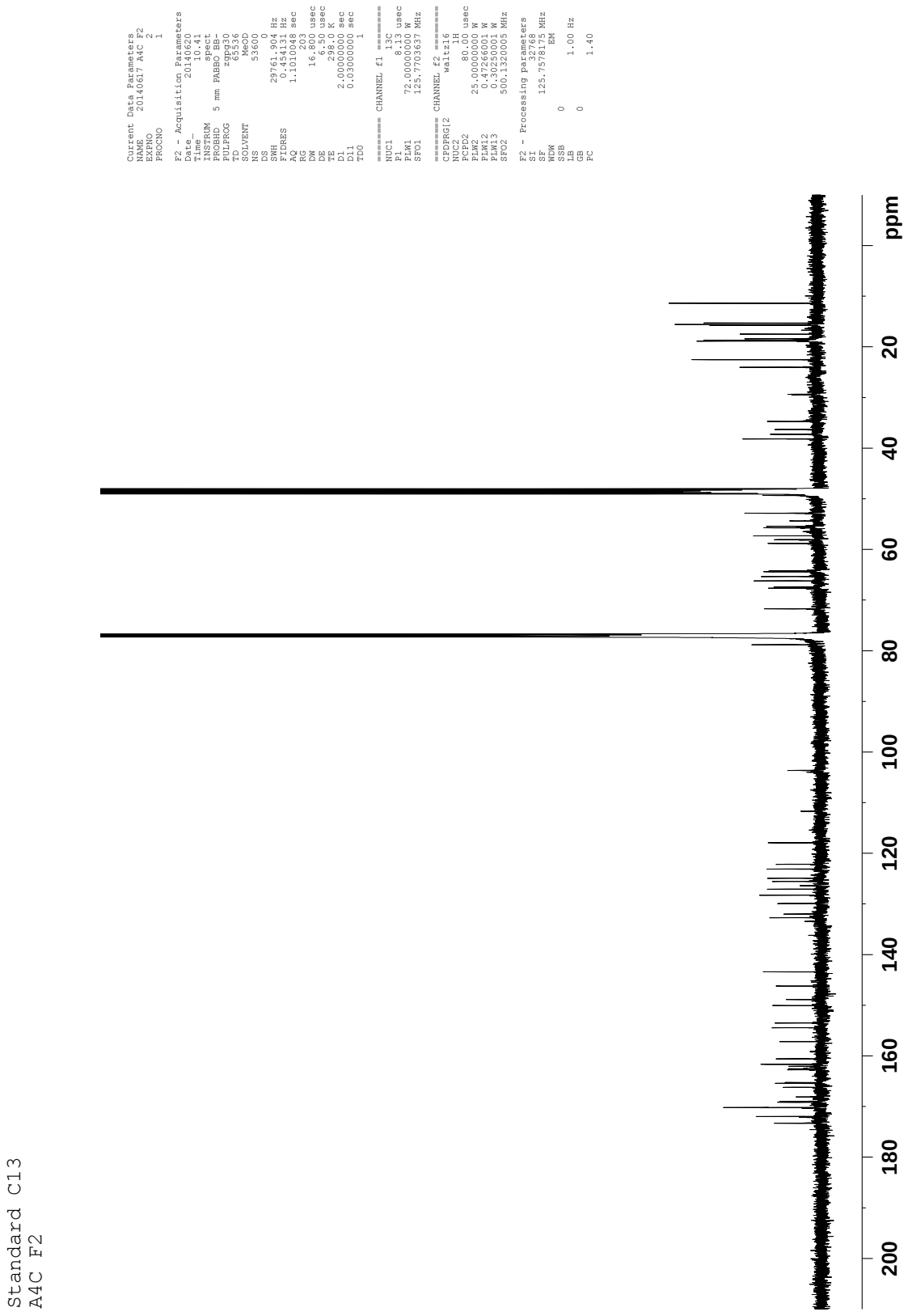

Figure D.14. ^{13}C NMR spectrum of thiostrepton Ala4Cys F2 (125 MHz, $CDCl_3$-CD_3OD 4:1, 25 °C).

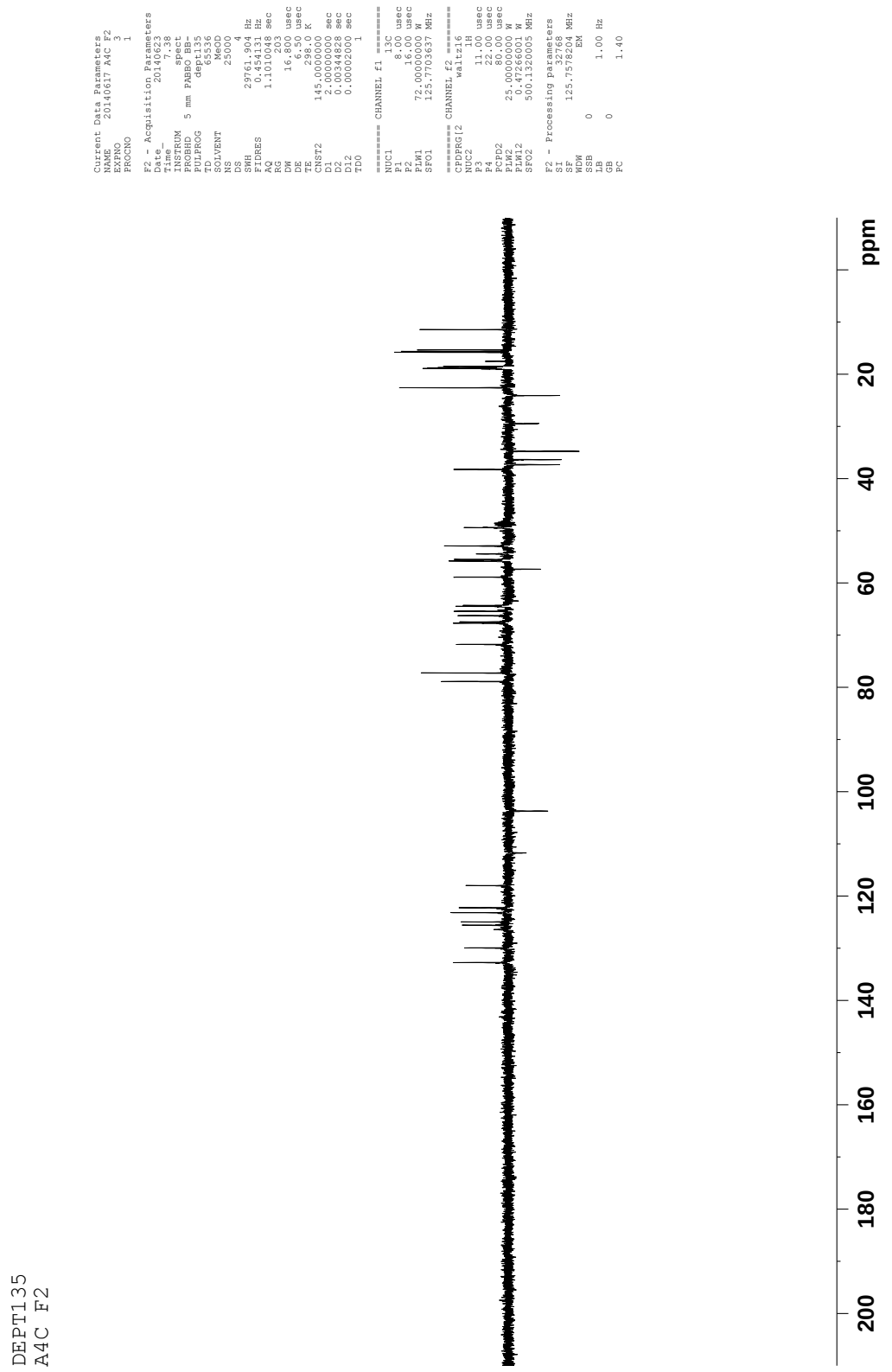

Figure D.15. DEPT-135 NMR spectrum of thiostrepton Ala4Cys F2 (125 MHz, $CDCl_3$-CD_3OD 4:1, 25 °C).

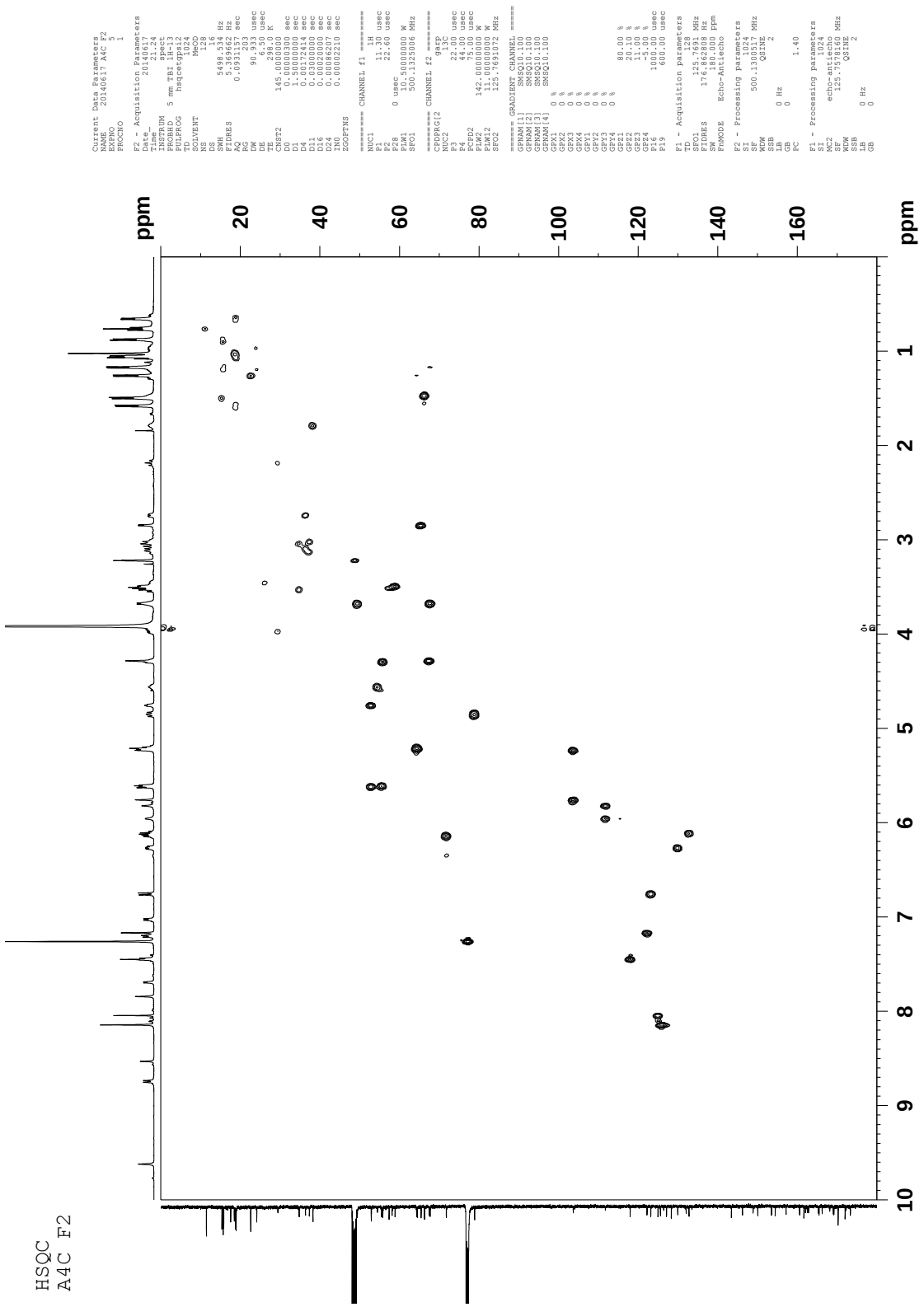

Figure D.16. gHSQC spectrum of thiostrepton Ala4Cys F2 (500 MHz, $CDCl_3$-CD_3OD 4:1, 25 °C).

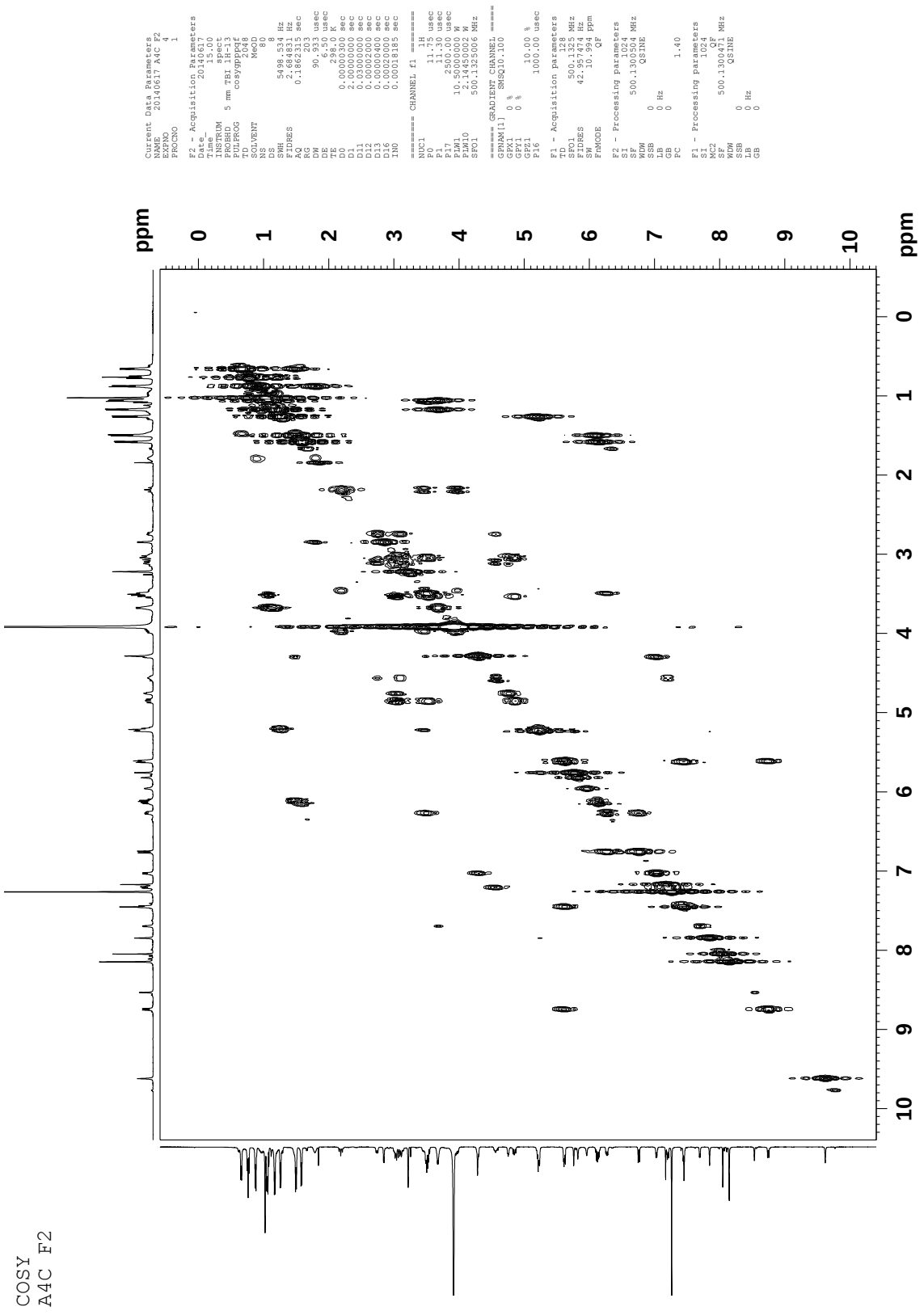

Figure D.17. gCOSY spectrum of thiostrepton Ala4Cys F2 (500 MHz, $CDCl_3$-CD_3OD 4:1, 25 °C).

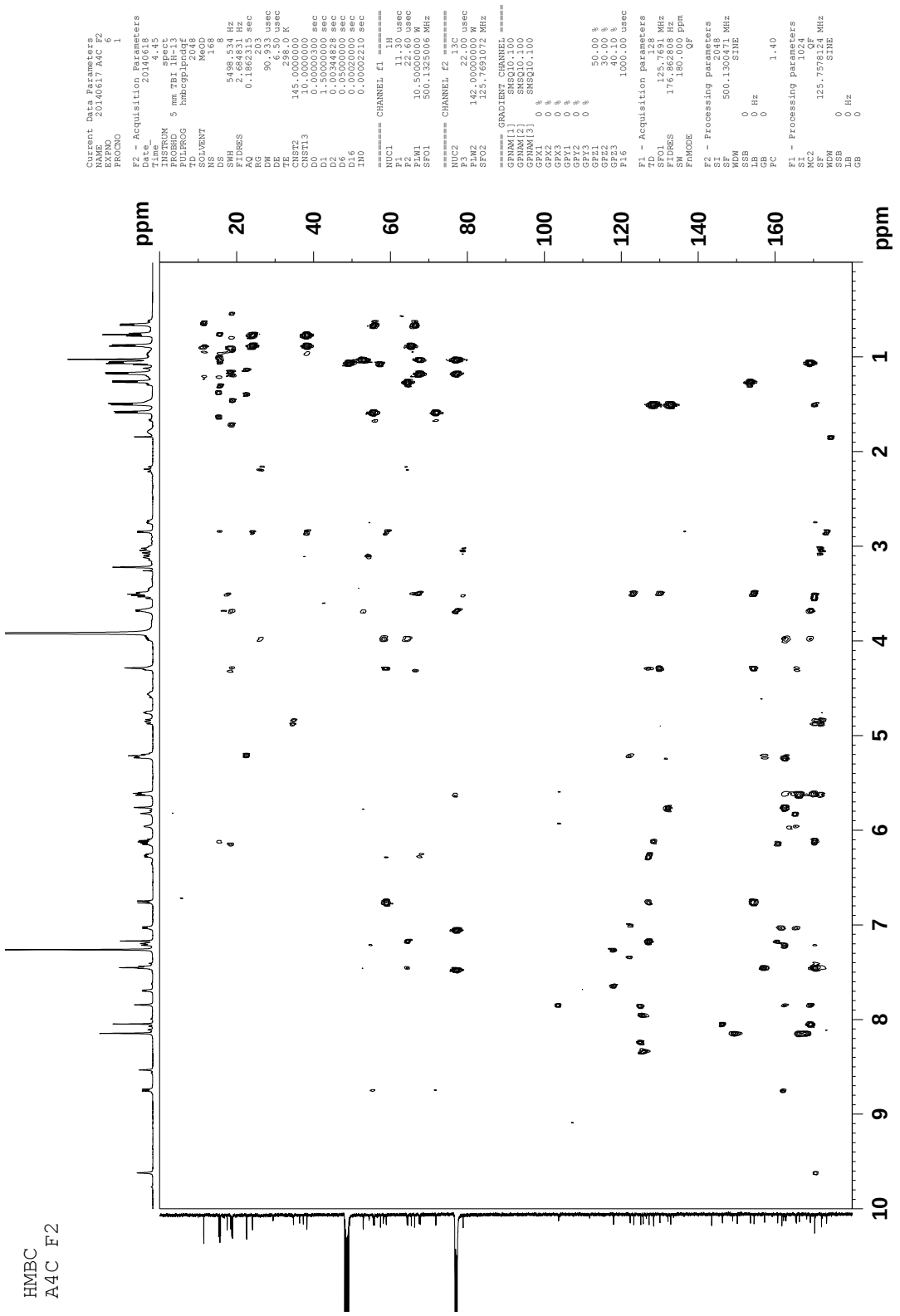

Figure D.18. gHMBC spectrum of thiostrepton Ala4Cys F2 (500 MHz, $CDCl_3$-CD_3OD 4:1, 25 °C).

Table D.2. ^{1}H and ^{13}C NMR assignments of thiostrepton Ala4Cys F2

Position	δ_C [ppm]; mult	δ_H [ppm]; (mult, J in Hz)	HMBC[a]	COSY[b]
Ile1				
Ile1-1	173.3; C q			
Ile1-2	65.4; CH	2.85 (d, 4.4)	Ile1-1;Ile1-3; Ile1-4; Ile1-6; Q-8	Ile1-3
Ile1-3	38.2; CH	1.83-1.75 (m)		Ile1-2; Ile1-4-H_B; Ile1-6
Ile1-4	24.1; CH_2	H_A: 1.24-1.19 (m)	Ile1-2; Ile1-3; Ile1-5; Ile1-6	Ile1-3; Ile1-4-H_B; Ile1-5
		H_B: 1.10-0.92 (m)	Ile1-2; Ile1-3; Ile1-6	Ile1-3; Ile1-4-H_A; Ile1-5
Ile1-5	11.4; CH_3	0.76 (t, 7.3)	Ile1-3; Ile1-4; Ile1-6	Ile1-4-H_A; Ile1-4-H_B
Ile1-6	15.6; CH_3	0.88 (d, 6.9)	Ile1-2; Ile1-3; Ile1-4	Ile1-3
Ile1-NH[d]		8.11 (d, 2.8)	Ile-1	
Ala2				
Ala2-1	169.1; C q			
Ala2-2	49.4; CH	3.71-3.64 (m)	Ala2-1; Ala2-3	Ala2-3; Ala2-NH
Ala2-3	18.7; CH_3	1.05 (d, 6.7)	Ala2-1; Ala2-2	Ala2-2
Ala2-NH[d]		7.70 (d, 5.3)		Ala2-2
Dha3				
Dha3-1	162.5; C q			
Dha3-2	132.0; C q			
Dha3-3	103.7; CH_2	H_A: 5.76 (d, 1.9)	Dha3-1; Dha3-2	Dha3-3-H_B
		H_B: 5.23 (br s)	Dha3-1; Dha3-2	Dha3-3-H_A
Dha3-NH[d]		7.84 (s)	Ala2-1; Dha3-1; Dha3-3	
Ala4				
Ala4-1	170.2; C q			
Ala4-2	54.4; CH	4.59-4.52 (m)		Ala4-3-H_A; Ala4-3-H_B; Ala4-NH
Ala4-3	36.3; CH_2	H_A: 3.13-3.08 (m)	Ala4-2; Ala17-3	Ala4-2; Ala4-3-H_B
		H_B: 2.74 (dd, 10.9, 4.1)	Ala4-1; Ala4-2	Ala4-2; Ala4-3-H_A
Ala4-NH[d]		7.20 (d, 8.3)	Dha3-1; Ala4-2	Ala4-2
Pip				
Pip-2	162.7; C q			
Pip-3	26.2; CH_2	H_A: 3.48-3.43 (m)		Pip-4-H_A; Pip-4-H_B; Pip-6
		H_B: 2.99-2.86 (m)		
Pip-4	29.4; CH_2	H_A: 4.00-3.94 (m)	Pip-2; Pip-3; Pip-5; Pip-6; Thz6-4; Thz13-2	Pip-3-H_A; Pip-4-H_B
		H_B: 2.22-2.14 (m)	Pip-3	Pip-3-H_A; Pip-3-H_B; Pip-4-H_A
Pip-5	58.1; C q			
Pip-6	64.3; CH	5.23-5.17 (m)	Pip-2; Thz13-2	Pip-3-H_A
Pip-NH[d]		9.62 (s)	Ala4-1	
Thz6				
Thz6-1	161.7; C q			
Thz6-2	146.2; C q			
Thz6-3	125.0; CH	8.04 (s)	Thz6-2; Thz6-4	
Thz6-4	169.0; C q			
Thr7				
Thr7-1	165.4; C q			
Thr7-2	55.8; CH	4.31-4.25 (m)	Thr7-1; Thr7-3; Thr7-4	Thr7-3; Thr7-NH
Thr7-3	66.2; CH	1.50-1.45 (m)	Thr7-4	Thr7-2; Thr7-4
Thr7-4	18.9; CH_3	0.66 (d, 6.1)	Thr7-2; Thr7-3	Thr7-3
Thr7-NH[d]		7.03 (d, 7.5)	Thz6-1; Thr7-1; Thr7-2	Thr7-2
Dhb8				
Dhb8-2	128.3; C q			
Dhb8-3	132.7; CH	6.11 (q, 6.8)	Dhb8-2; Dhb8-4; Tzn9-4	Dhb8-4
Dhb8-4	15.3; CH_3	1.50 (d, 7.0)	Dhb8-2; Dhb8-3; Tzn9-4	Dhb8-3
Tzn9				
Tzn9-1	172.1; C q			
Tzn9-2	78.9; CH	4.85 (dd, 12.8, 9.0)	Tzn9-1; Tzn9-3; Tzn9-4	Tzn9-3-H_A; Tzn9-3-H_B
Tzn9-3	34.7; CH_2	H_A: 3.56-3.51 (m)	Tzn9-2; Tzn9-4	Tzn9-2; Tzn9-3-H_B
		H_B: 3.08-3.01 (m)	Tzn9-1; Tzn9-2	Tzn9-2; Tzn9-3-H_A
Tzn9-4	170.2; C q			

Position	δ_C [ppm]; mult	δ_H [ppm]; (mult, J in Hz)	HMBC[a]	COSY[b]
Ile10				
Ile10-2	52.9; CH	5.62 (d, 9.9)	Tzn9-1; Ile10-3; Thz11-4	Ile10-NH
Ile10-3	77.0[c]; C q			
Ile10-4	67.7; CH	3.71-3.64 (m)	Ile10-2; Ile10-3; Ile10-5; Ile10-6	Ile10-5
Ile10-5	15.8; CH_3	1.17 (d, 6.4)	Ile10-3; Ile10-4; Ile10-6	Ile10-4
Ile10-6	18.4; CH_3	1.02 (s)	Ile10-2; Ile10-3; Ile10-4; Ile10-5	
Ile10-NH		7.45 (d, 9.5)	Tzn9-1; Ile10-2; Ile10-3	Ile10-2
Thz11				
Thz11-1	162.5; C q			
Thz11-2	148.9; C q			
Thz11-3	125.6; CH	8.14 (s)	Thz11-2; Thz11-4	
Thz11-4	166.2; C q			
Thr12				
Thr12-2	55.5; CH	5.61 (d, 8.6)	Thz11-1; Thz13-4	Thr12-NH
Thr12-3	71.7; CH	6.14 (q, 6.4)	Thr12-4; Q-1	Thr12-4
Thr12-4	18.7; CH_3	1.58 (d, 6.6)	Thr12-2; Thr12-3	Thr12-3
Thr12-NH		8.74 (d, 8.8)		Thr12-2
Thz13				
Thz13-2	157.2; C q			
Thz13-3	117.9; CH	7.45 (s)	Pip-6; Thz13-2; Thz13-4	
Thz13-4	170.2; C q			
Thz15				
Thz15-1	159.2; C q			
Thz15-2	150.0; C q			
Thz15-3	126.4; CH	8.14 (s)	Thz15-2; Thz15-4	
Thz15-4	168.1; C q			
Dha16				
Dha16-1	165.2; C q			
Dha16-2	133.5; C q			
Dha16-3	111.7; CH_2	H_A: 5.96 (d, 2.6)	Dha16-1; Dha16-2	Dha16-3-H_B
		H_B: 5.82 (br s)	Dha16-1	Dha16-3-H_A
Ala17				
Ala17-1	172.0; C q			
Ala17-2	52.9; CH	4.75 (t, 4.7)	Ala17-1	Ala17-3-H_A; Ala17-3-H_B
Ala17-3	37.3; CH_2	H_A: 3.16-3.10 (m)	Ala17-1; Ala17-2	Ala17-2; Ala17-3-H_B
		H_B: 3.05-2.99 (m)	Ala17-1; Ala17-2	Ala17-2; Ala17-3-H_A
Q				
Q-1	160.6; C q			
Q-2	143.4; C q			
Q-3	122.2; CH	7.17 (s)	Q-1; Q-5; Q-11	
Q-4	153.5; C q			
Q-5	127.1; C q			
Q-6	123.1; CH	6.76 (d, 10.1)	Q-5; Q-8; Q-10	Q-7
Q-7	129.9; CH	6.27 (dd, 9.5, 5.2)	Q-5; Q-8; Q-9	Q-6; Q-8
Q-8	58.8; CH	3.51-3.48 (m)	Ile1-2; Q-6; Q-7; Q-9; Q-10	Q-7
Q-9	67.4; CH	4.28 (s)	Q-5; Q-7; Q-8; Q-10	Q-8
Q-10	154.4; C q			
Q-11	64.4; CH	5.23-5.17 (m)	Q-3; Q-5; Q-12	Q-12
Q-12	22.6; CH_3	1.26 (d, 6.6)	Q-4; Q-11	Q-11

[a] HMBC correlations are from the proton to the indicated carbon.
[b] COSY correlations are from the proton to the proton attached to the indicated position.
[c] The δ of this resonance was determined by HMBC due to overlap with the $CDCl_3$ resonance.
[d] Only those amide resonances demonstrating COSY or HMBC correlations to neighboring protons or carbons, respectively, were assigned.

Figure D.19. MS analysis of thiostrepton Ala4Dha isolated from *S. laurentii* NDS1/int-A4S.

(**A**) HPLC-MS analysis. (1) Chromatogram extracted for *m/z* 831.7, the calculated $[M+2H]^{2+}$ ion of thiostrepton Ala4Dha. (2) Total ion chromatogram.

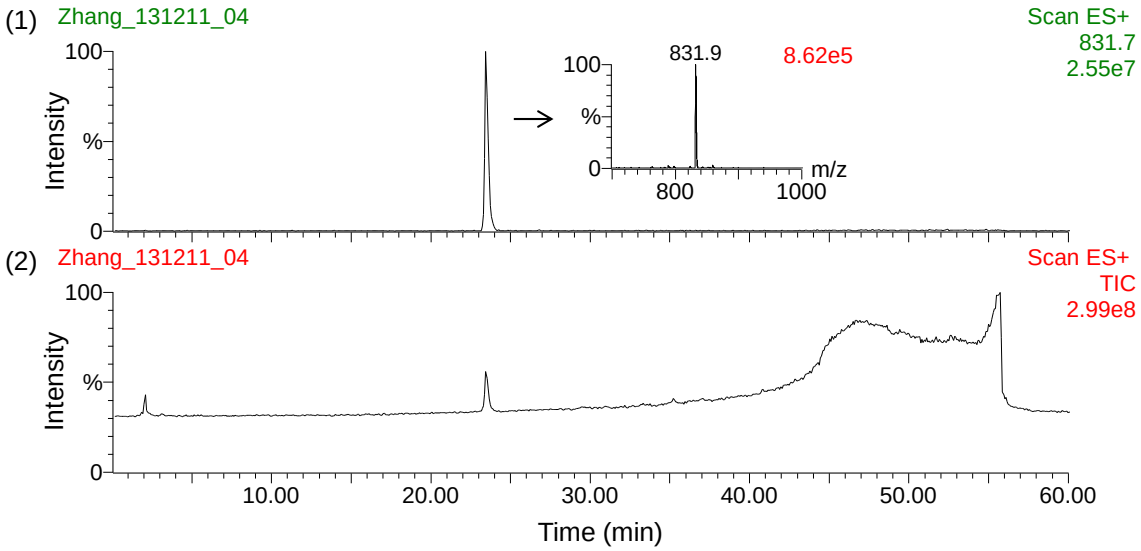

(**B**) MALDI MS spectrum of thiostrepton Ala4Dha.

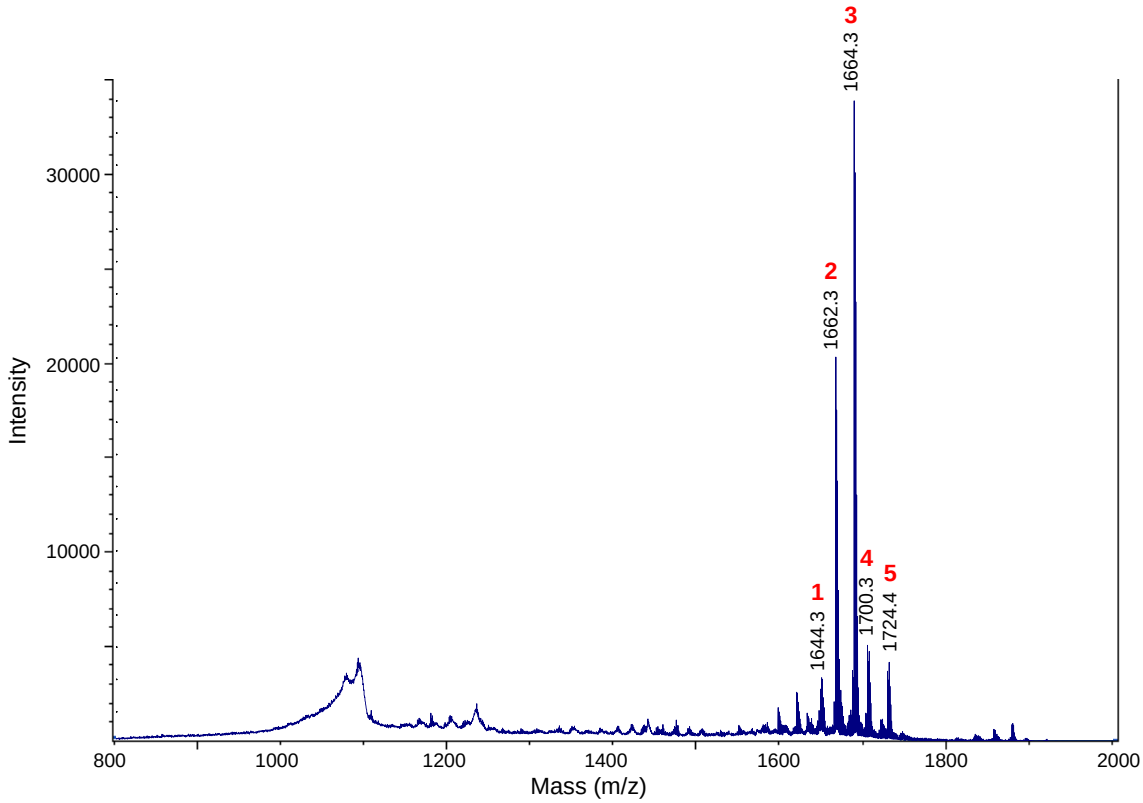

(**C**) MALDI MS/MS of parent ion *m/z* 1662.3.

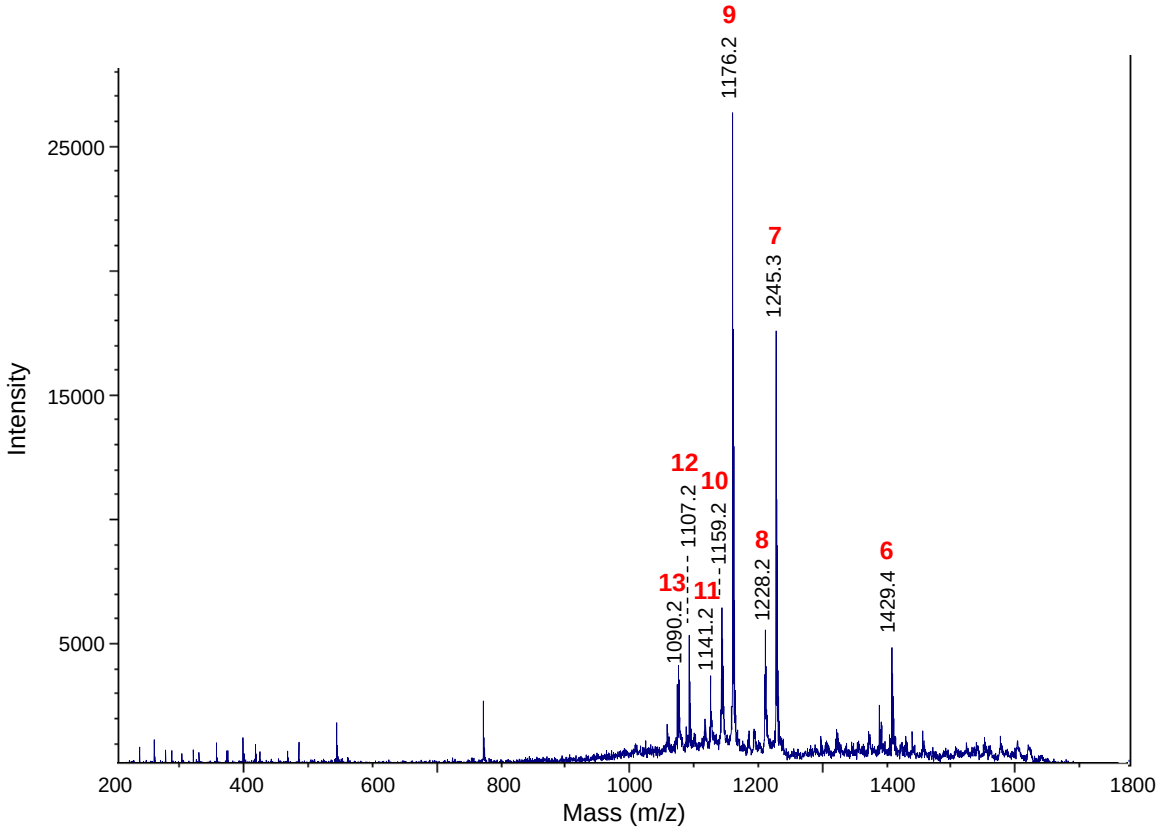

(**D**) Table and structure showing key ions and fragments in the MALDI MS and MS/MS of thiostrepton Ala4Dha.

Fragment	Expected	Observed
1. M-H_2O+H^+	1644.5	1644.3
2. M+H^+ (Parent ion)	1662.5	1662.3
3. M+Na^+	1684.5	1684.3
4. M+K^+	1700.4	1700.3
5. M+Cu^+	1724.4	1724.4
6. M-QA+H^+	1429.4	1429.4
7. M-QA-Ile1-Ala2+H^+	1245.3	1245.3
8. M-QA-Ile1-Ala2-OH+H^+	1228.3	1228.2
9. M-QA-Ile1-Ala2-Dha3+H^+	1176.3	1176.2
10. M-QA-Ile1-Ala2-Dha3-OH+H^+	1159.3	1159.2
11. M-QA-Ile1-Ala2-Dha3-H_2O-OH+H^+	1141.3	1141.2
12. M-QA-Ile1-Ala2-Dha3-Dha4+H^+	1107.3	1107.2
13. M-QA-Ile1-Ala2-Dha3-Dha4-OH+H^+	1090.2	1090.2

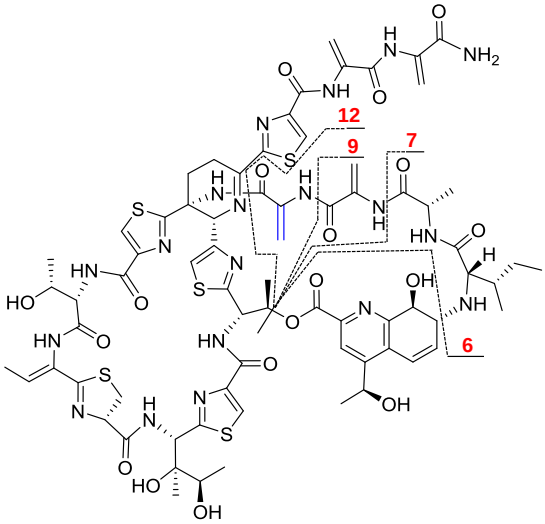

Figure D.20. Structure and numbering system used for thiostrepton Ala4Dha.

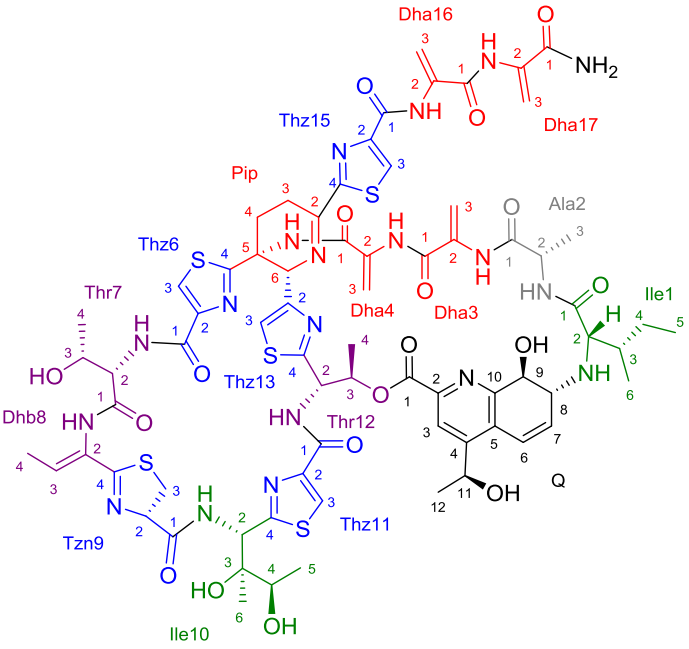

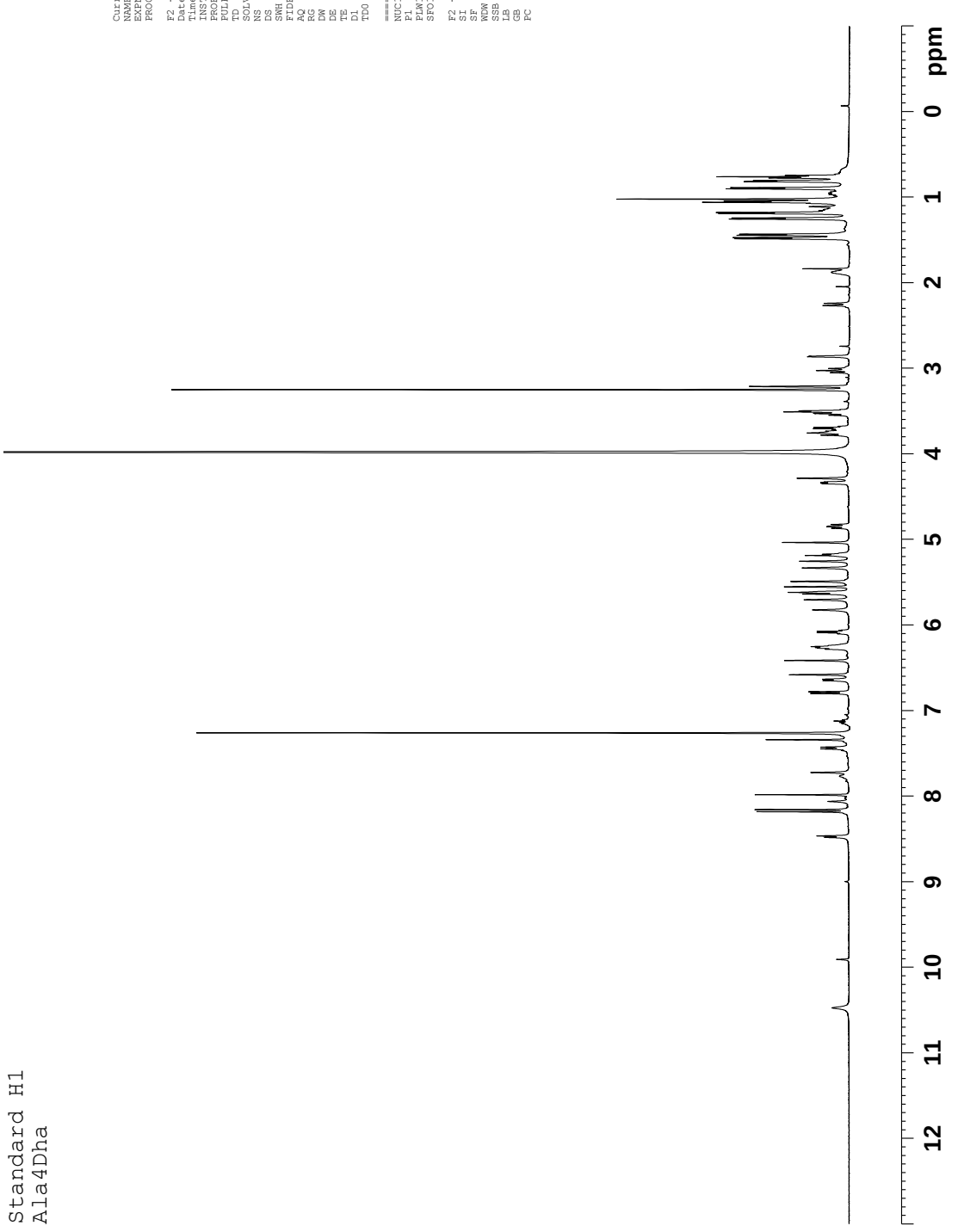

Figure D.21. ^{1}H NMR spectrum of thiostrepton Ala4Dha (500 MHz, $CDCl_3$-CD_3OD 4:1, 25 °C).

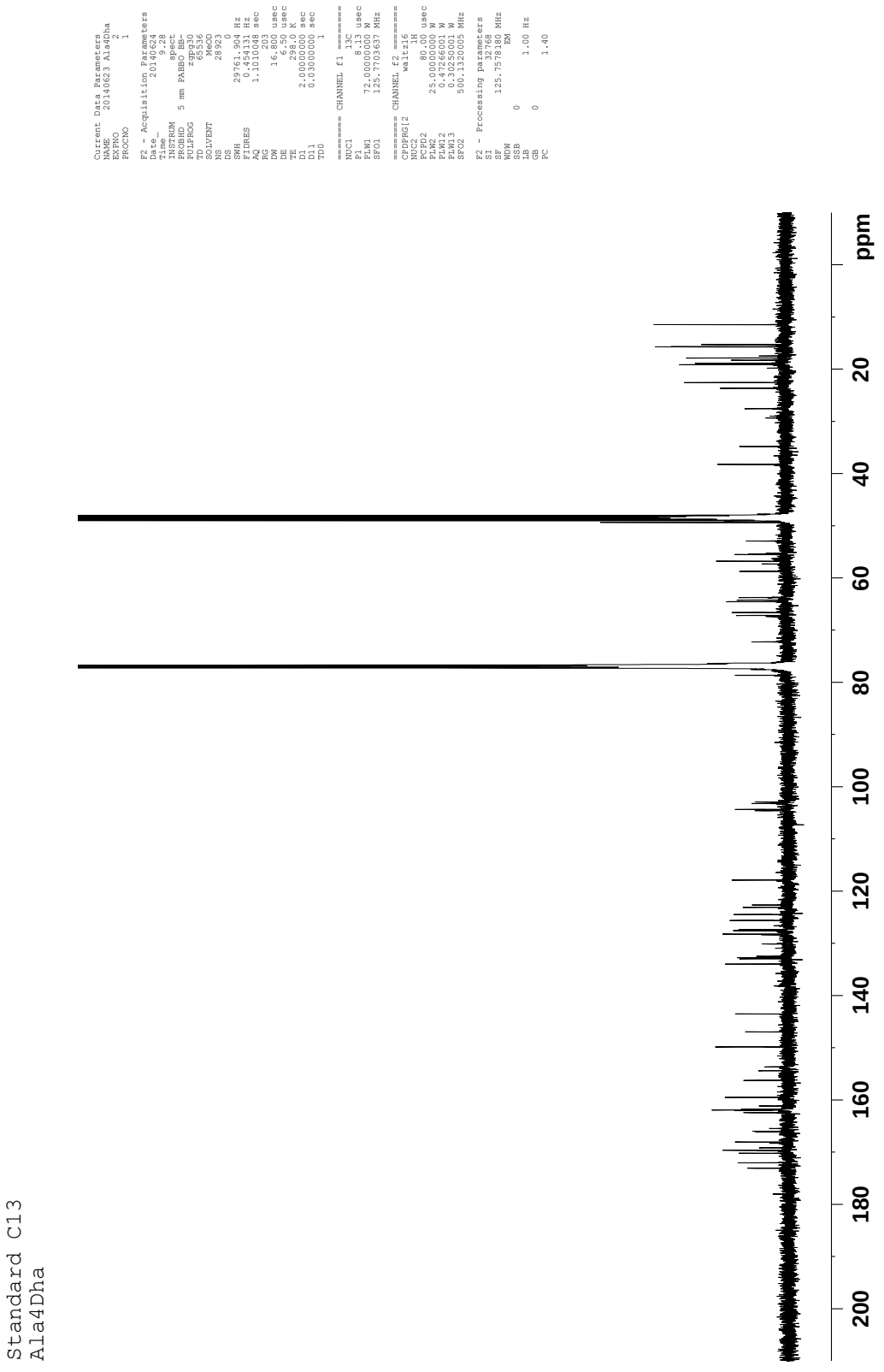

Figure D.22. ^{13}C NMR spectrum of thiostrepton Ala4Dha (125 MHz, $CDCl_3$-CD_3OD 4:1, 25 °C).

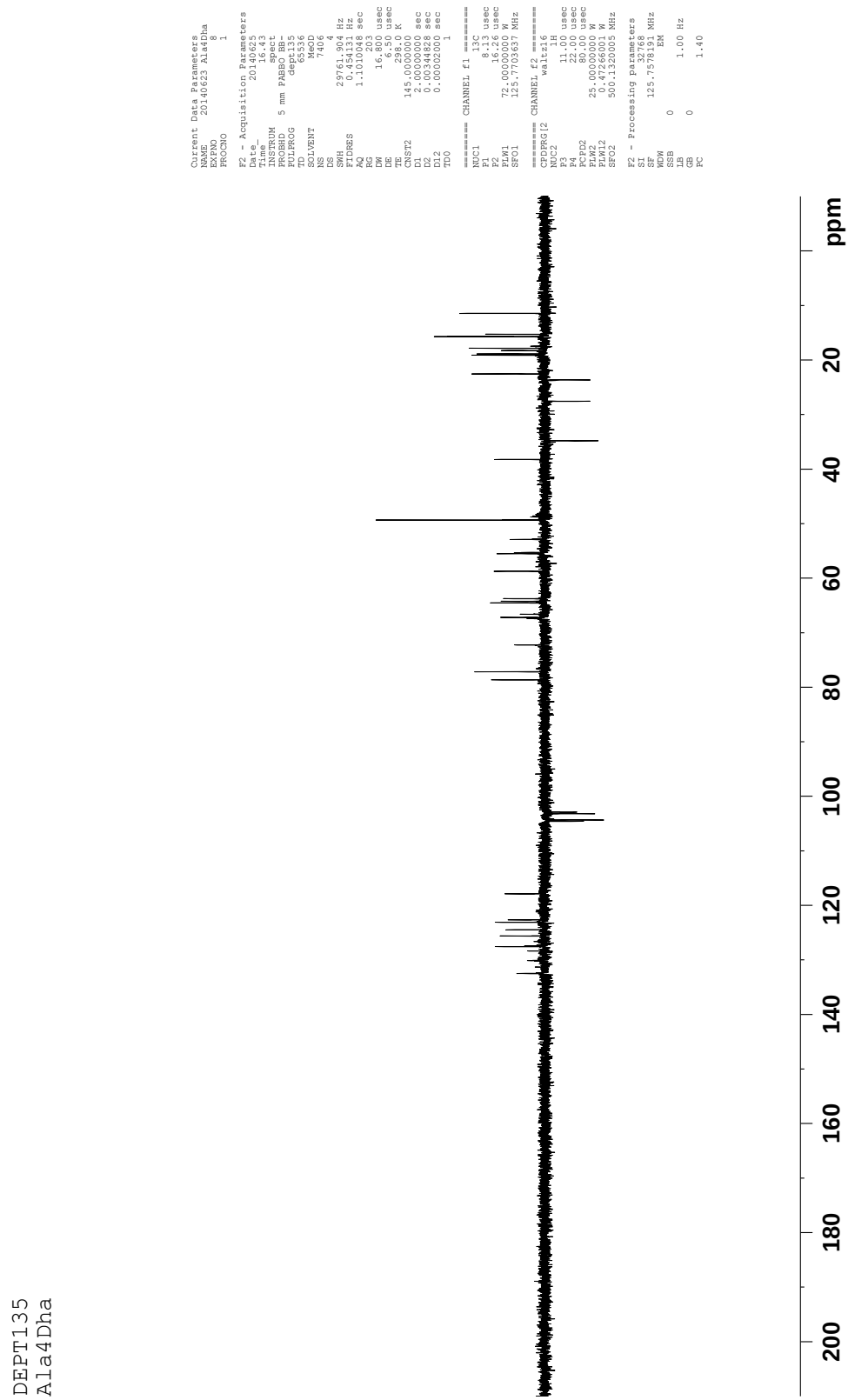

Figure D.23. DEPT-135 NMR spectrum of thiostrepton Ala4Dha (125 MHz, $CDCl_3$-CD_3OD 4:1, 25 °C).

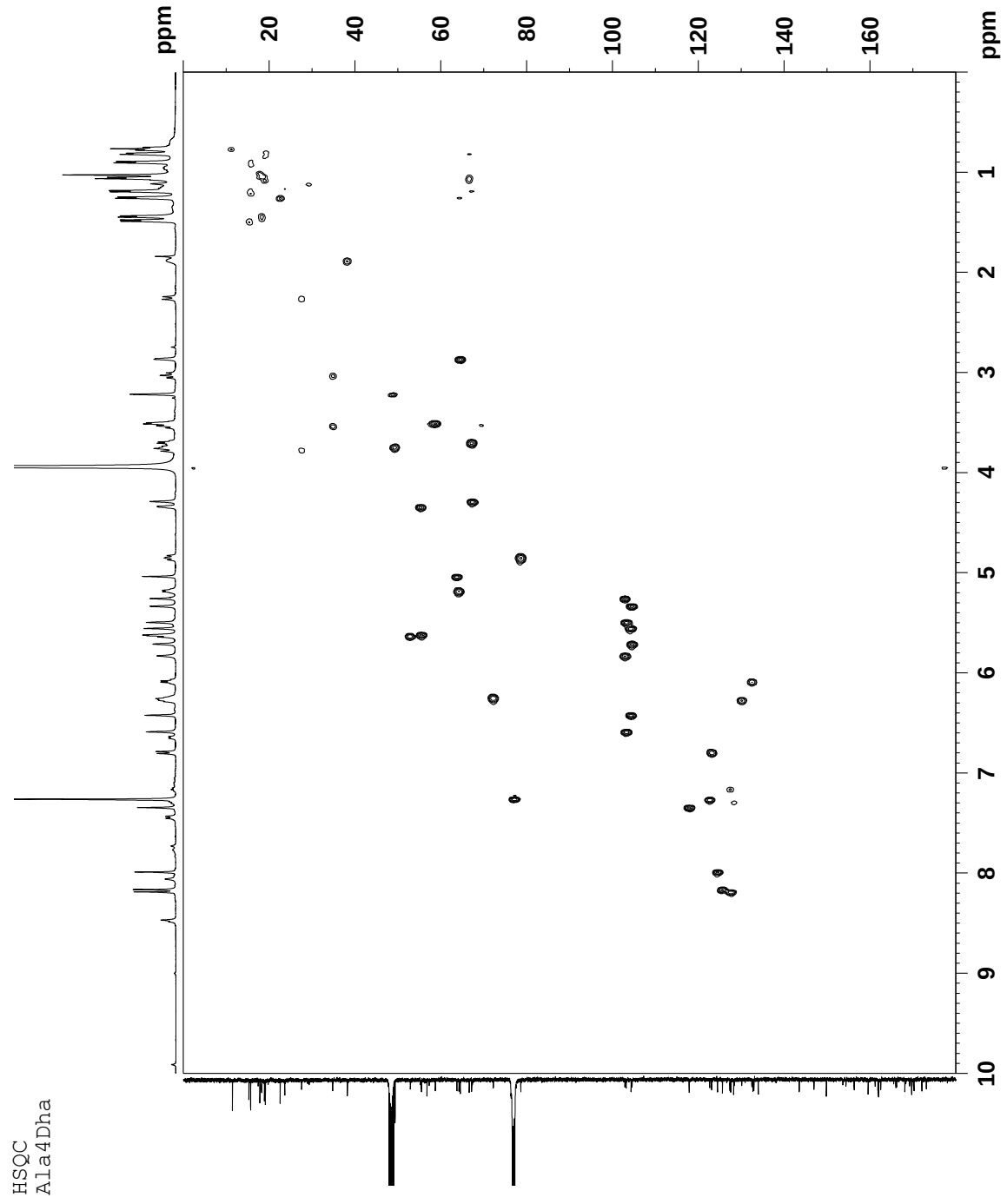

Figure D.24. gHSQC spectrum of thiostrepton Ala4Dha (500 MHz, $CDCl_3$-CD_3OD 4:1, 25 °C).

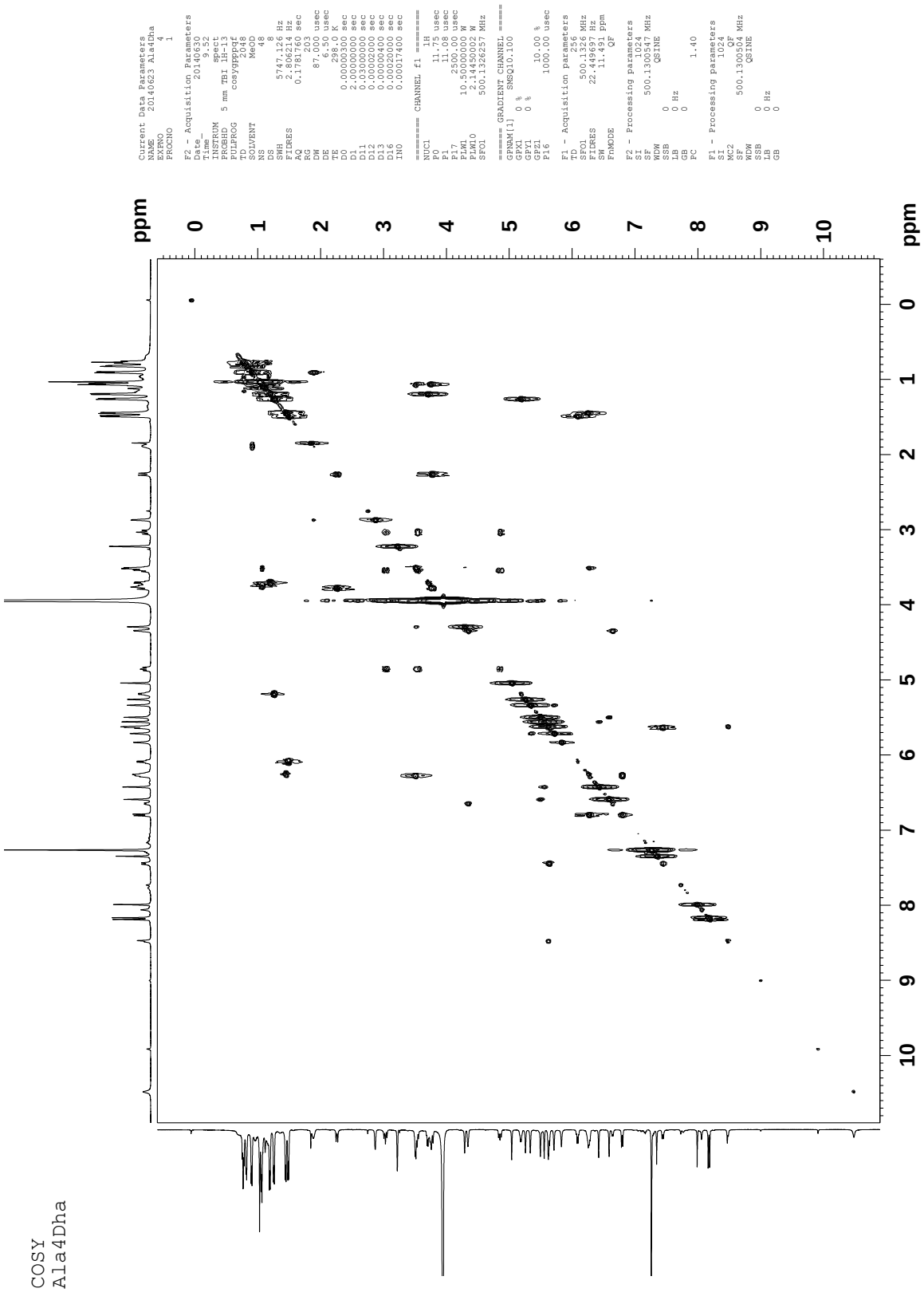

Figure D.25. gCOSY spectrum of thiostrepton Ala4Dha (500 MHz, $CDCl_3$-CD_3OD 4:1, 25 °C).

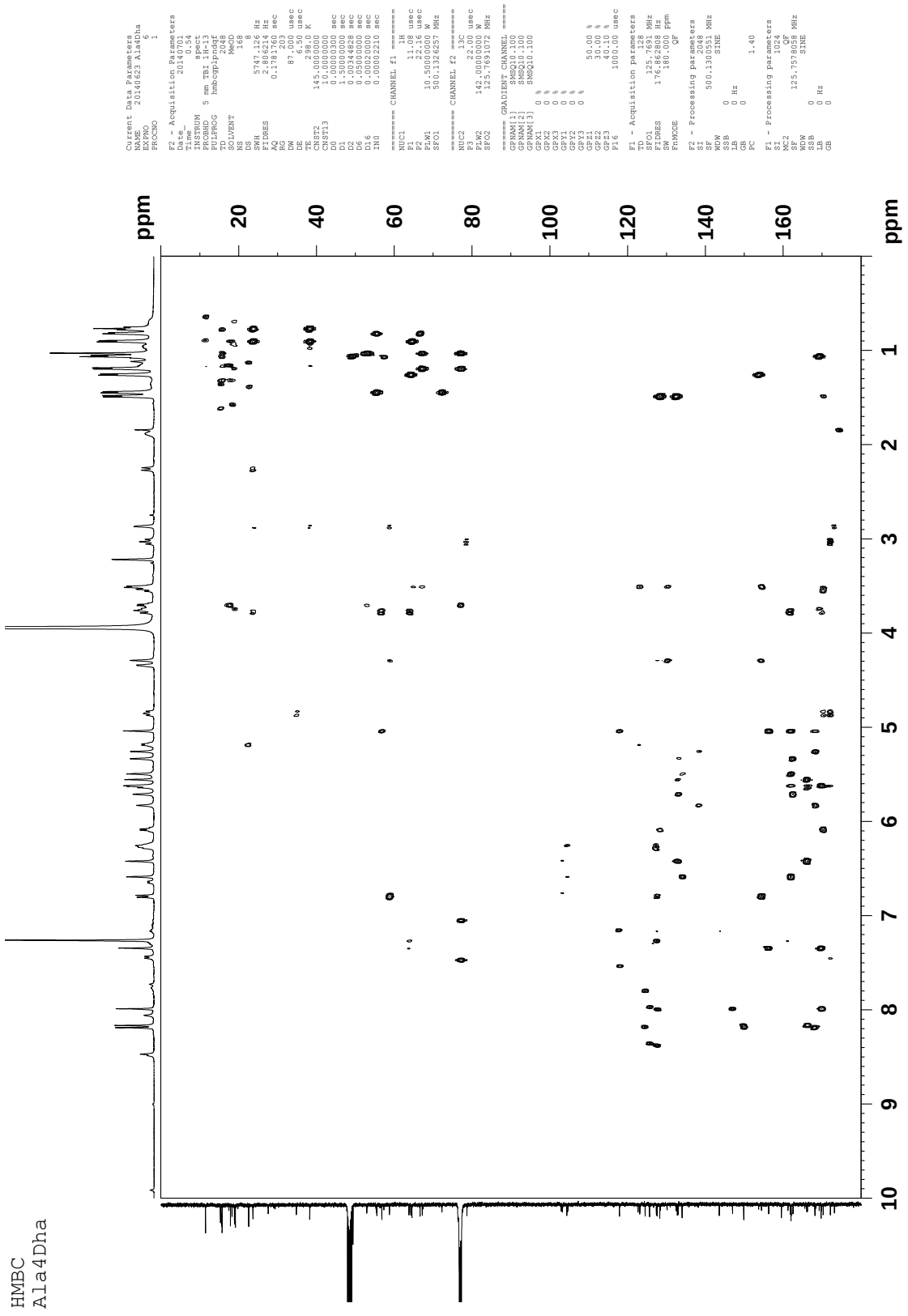

Figure D.26. gHMBC spectrum of thiostrepton Ala4Dha (500 MHz, $CDCl_3$-CD_3OD 4:1, 25 °C).

Table D.3. ^{1}H and ^{13}C NMR assignments of thiostrepton Ala4Dha

Position	δ_C [ppm]; mult	δ_H [ppm]; (mult, J in Hz)	HMBC[a]	COSY[b]
Ile1				
Ile1-1	173.1; C q			
Ile1-2	64.6; CH	2.86 (d, 3.3)	Ile1-1; Ile1-3; Ile1-4; Ile1-6; Q-8	Ile1-3
Ile1-3	38.3; CH	1.91-1.84 (m)		Ile1-2; Ile1-6
Ile1-4	23.7; CH_2	H_A: 1.18-1.14 (m)	Ile1-5; Ile1-6	Ile1-4-H_B; Ile1-5
		H_B: 0.99-0.93 (m)	Ile1-3; Ile1-5; Ile1-6	Ile1-3; Ile1-4-H_A; Ile1-5
Ile1-5	11.5; CH_3	0.76 (t, 7.3)	Ile1-3; Ile1-4; Ile1-6	Ile1-4-H_A; Ile1-4-H_B
Ile1-6	15.8; CH_3	0.90 (d, 6.8)	Ile1-2; Ile1-3; Ile1-4; Ile1-5	Ile1-3
Ala2				
Ala2-1	169.2; C q			
Ala2-2	49.4; CH	3.80-3.73 (m)	Ala2-1; Ala2-3	Ala2-3
Ala2-3	18.9; CH_3	1.05 (d, 6.6)	Ala2-1; Ala2-2	Ala2-2
Dha3				
Dha3-1	162.5; C q			
Dha3-2	133.0; C q			
Dha3-3	104.6; CH_2	H_A: 5.70 (br s)	Dha3-1; Dha3-2	Dha3-3-H_B
		H_B: 5.33 (br s)	Dha3-1; Dha3-2	Dha3-3-H_A
Dha4				
Dha4-1	168.3; C q			
Dha4-2	138.2; C q			
Dha4-3	102.9; CH_2	H_A: 5.82 (br s)	Dha4-1; Dha4-2	
		H_B: 5.25 (br s)	Dha4-1; Dha4-2	
Pip				
Pip-2	161.8; C q			
Pip-3	23.8; CH_2	H_A: 3.56-3.48 (m)		
		H_B: 3.06-2.99 (m)		
Pip-4	27.6; CH_2	H_A: 3.80-3.73 (m)	Pip-2; Pip-3; Pip-5; Pip-6; Thz6-4	Pip-4-H_B
		H_B: 2.28-2.22 (m)		Pip-4-H_A
Pip-5	56.8; C q			
Pip-6	63.8; CH	5.03 (s)	Ala4-1; Pip-2; Pip-3; Thz13-2; Thz15-4	
Thz6				
Thz6-1	162.0; C q			
Thz6-2	147.0; C q			
Thz6-3	124.5; CH	7.98 (s)	Thz6-1; Thz6-2; Thz6-4	
Thz6-4	169.8; C q			
Thr7				
Thr7-1	165.5; C q			
Thr7-2	55.4; CH	4.34 (dd, 9.3, 1.8)	Thr7-1; Thr7-3	Thr7-3; Thr7-NH
Thr7-3	66.7; CH	1.07-1.04 (m)		
Thr7-4	19.2; CH_3	0.81 (d, 5.9)	Thr7-2; Thr7-3	Thr7-3
Thr7-NH[d]		6.64 (d, 8.1)		Thr7-2
Dhb8				
Dhb8-2	128.3; C q			
Dhb8-3	132.5; CH	6.08 (q, 7.0)	Dhb8-2; Dhb8-4; Tzn9-4	Dhb8-4
Dhb8-4	15.3; CH_3	1.48 (d, 6.9)	Dhb8-2; Dhb8-3; Tzn9-4	Dhb8-3
Tzn9				
Tzn9-1	172.1; C q			
Tzn9-2	78.7; CH	4.85 (dd, 12.6, 9.2)	Tzn9-1; Tzn9-3; Tzn9-4	Tzn9-3-H_A; Tzn9-3-H_B
Tzn9-3	34.8; CH_2	H_A: 3.57-3.51 (m)	Tzn9-2; Tzn9-4	Tzn9-2; Tzn9-3-H_B
		H_B: 3.03 (t, 12.3)	Tzn9-1; Tzn9-2	Tzn9-2; Tzn9-3-H_A
Tzn9-4	170.2; C q			
Ile10				
Ile10-2	52.9; CH	5.63 (d, 6.9)	Tzn9-1; Ile10-3; Thz11-4	Ile10-NH
Ile10-3	77.0[c]; C q			
Ile10-4	67.2; CH	3.70 (q, 6.2)	Ile10-2; Ile10-3; Ile10-5; Ile10-6	Ile10-5
Ile10-5	15.7; CH_3	1.18 (d, 6.3)	Ile10-3; Ile10-4	Ile10-4
Ile10-6	17.9; CH_3	1.02 (s)	Ile10-2; Ile10-3; Ile10-4; Ile10-5	Ile10-5
Ile10-NH[d]		7.44 (d, 10.0)		Ile10-2

Position	δ_C [ppm]; mult	δ_H [ppm]; (mult, J in Hz)	HMBC[a]	COSY[b]
Thz11				
Thz11-1	162.0; C q			
Thz11-2	149.9; C q			
Thz11-3	125.6; CH	8.16 (s)	Thz11-2; Thz11-4	
Thz11-4	166.2; C q			
Thr12				
Thr12-2	55.4; CH	5.62 (d, 8.1)	Thz11-1; Thr12-4; Thz13-4	Thr12-3; Thr12-NH
Thr12-3	72.3; CH	6.26-6.21 (m)		Thr12-4
Thr12-4	18.3; CH_3	1.44 (d, 6.5)	Thr12-2; Thr12-3	Thr12-3
Thr12-NH[d]		8.47 (d, 8.5)		Thr12-2
Thz13				
Thz13-2	156.3; C q			
Thz13-3	117.9; CH	7.34 (s)	Pip-6; Thz13-2; Thz13-4	
Thz13-4	169.7; C q			
Thz15				
Thz15-1	159.5; C q			
Thz15-2	149.9; C q			
Thz15-3	127.6; CH	8.18 (s)	Thz15-1; Thz15-2; Thz15-4	
Thz15-4	168.1; C q			
Dha16				
Dha16-1	162.0; C q			
Dha16-2	134.0; C q			
Dha16-3	103.2; CH_2	H_A: 6.58 (d, 1.1)	Dha16-1; Dha16-2	Dha16-3-H_B
		H_B: 5.49 (d, 2.0)	Dha16-1; Dha16-2	Dha16-3-H_A
Dha17				
Dha17-1	166.0; C q			
Dha17-2	132.8; C q			
Dha17-3	104.4; CH_2	H_A: 6.41 (d, 1.1)	Dha17-1; Dha17-2	Dha17-3-H_B
		H_B: 5.56 (d, 1.5)	Dha17-1; Dha17-2	Dha17-3-H_A
Q				
Q-1	161.2; C q			
Q-2	143.6; C q			
Q-3[c]	122.7; CH	7.26 (s)	Q-1; Q-5; Q-11	
Q-4	153.7; C q			
Q-5	127.4; C q			
Q-6	123.1; CH	6.79 (d, 9.9)	Q-5; Q-8; Q-10	Q-7
Q-7	130.2; CH	6.27 (dd, 9.1, 5.8)	Q-5; Q-8; Q-9	Q-6; Q-8
Q-8	58.8; CH	3.54-3.48 (m)	Ile1-2; Q-6; Q-7; Q-9; Q-10	Q-7; Q-9
Q-9	67.4; CH	4.28 (br s)	Q-5; Q-7; Q-8; Q-10	Q-8
Q-10	154.4; C q			
Q-11	64.3; CH	5.18 (q, 6.4)	Q-3; Q-5; Q-12	Q-12
Q-12	22.6; CH_3	1.25 (d, 6.5)	Q-4; Q-11	Q-11

[a] HMBC correlations are from the proton to the indicated carbon.
[b] COSY correlations are from the proton to the proton attached to the indicated position.
[c] The δ of this resonance was determined either by HMBC or HSQC due to overlap with the $CDCl_3$ resonance.
[d] Only those amide resonances demonstrating COSY correlations to neighboring protons were assigned.

Figure D.27. MS analysis of thiostrepton Ala4Dhb isolated from *S. laurentii* NDS1/int-A4T.

(**A**) HPLC-MS analysis. (1) Chromatogram extracted for *m*/*z* 838.8, the calculated $[M+2H]^{2+}$ ion of thiostrepton Ala4Dhb. (2) Total ion chromatogram.

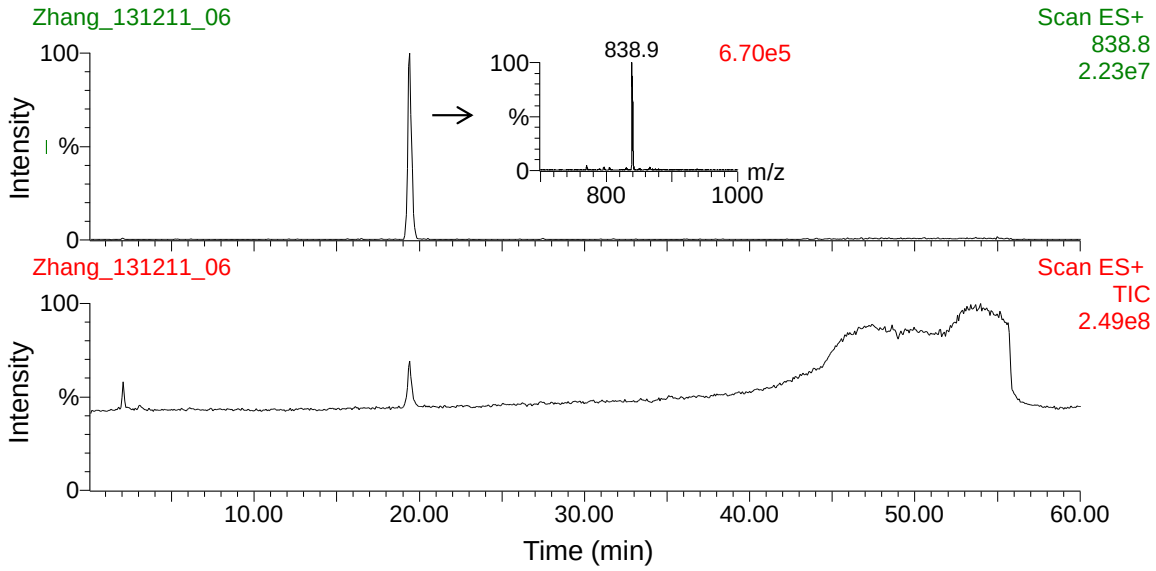

(**B**) MALDI MS spectrum of thiostrepton Ala4Dhb.

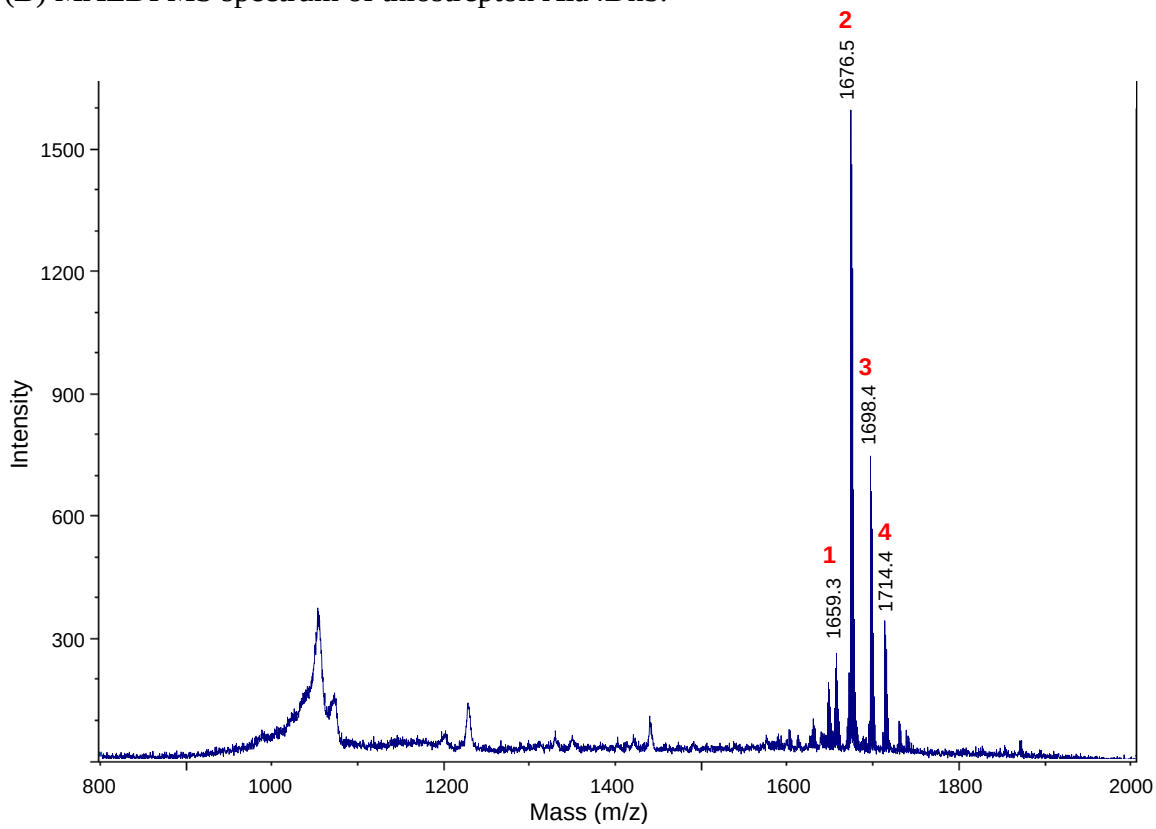

(**C**) MALDI MS/MS of parent ion *m/z* 1676.5.

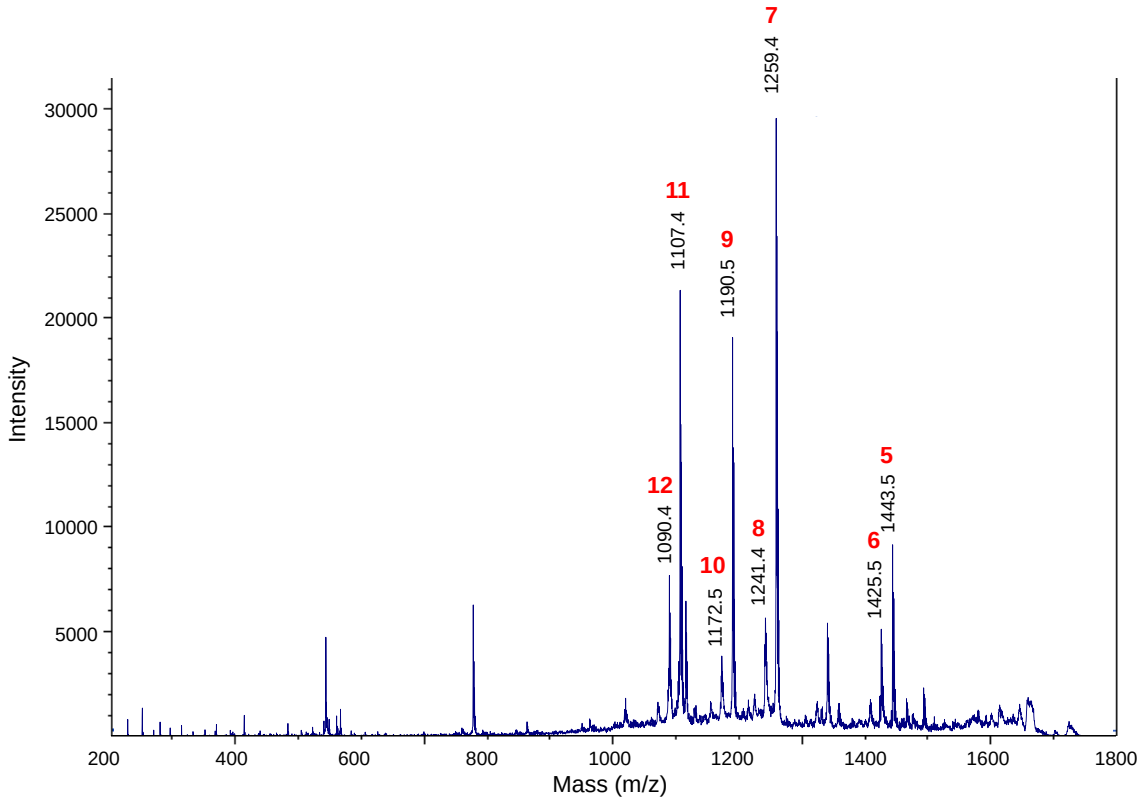

(**D**) Table and structure showing key ions and fragments in the MALDI MS and MS/MS of thiostrepton Ala4Dhb.

Fragment	Expected	Observed
1. M-OH+H$^+$	1659.5	1659.3
2. M+H$^+$ (Parent ion)	1676.5	1676.5
3. M+Na$^+$	1698.5	1698.4
4. M+K$^+$	1714.5	1714.4
5. M-QA+H$^+$	1443.4	1443.5
6. M-QA-H_2O+H$^+$	1425.4	1425.5
7. M-QA-Ile1-Ala2+H$^+$	1259.3	1259.4
8. M-QA-Ile1-Ala2-H_2O+H$^+$	1241.3	1241.4
9. M-QA-Ile1-Ala2-Dha3+H$^+$	1190.3	1190.5
10. M-QA-Ile1-Ala2-Dha3-H_2O+H$^+$	1172.3	1172.5
11. M-QA-Ile1-Ala2-Dha3-Dhb4+H$^+$	1107.3	1107.4
12. M-QA-Ile1-Ala2-Dha3-Dhb4-OH+H$^+$	1090.2	1090.4

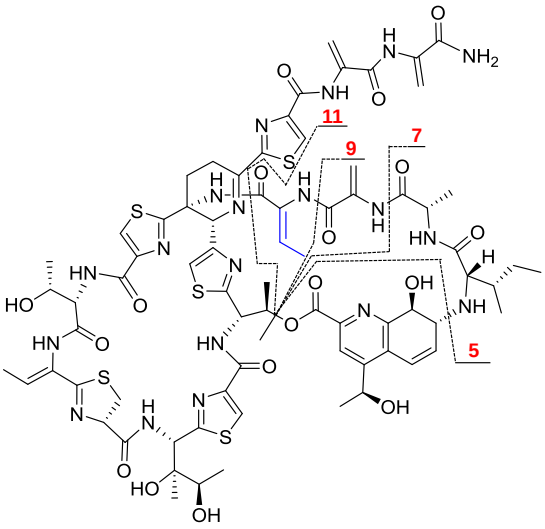

Figure D.28. Structure and numbering system used for thiostrepton Ala4Dhb.

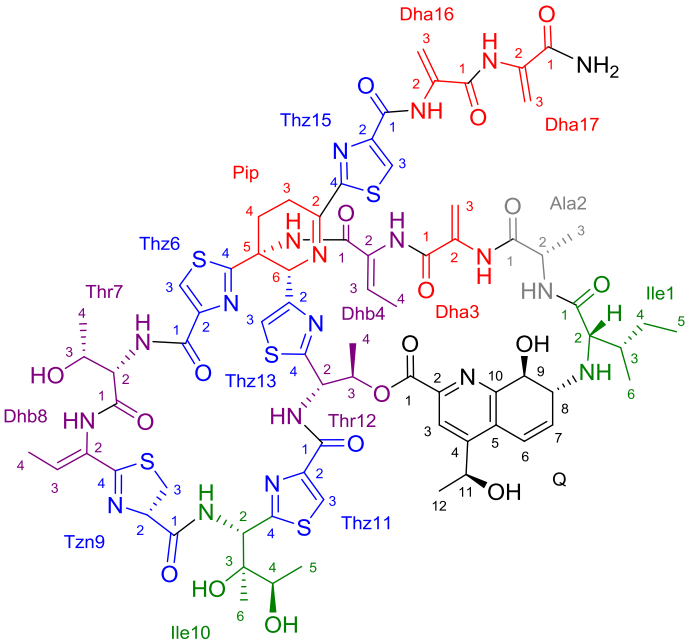

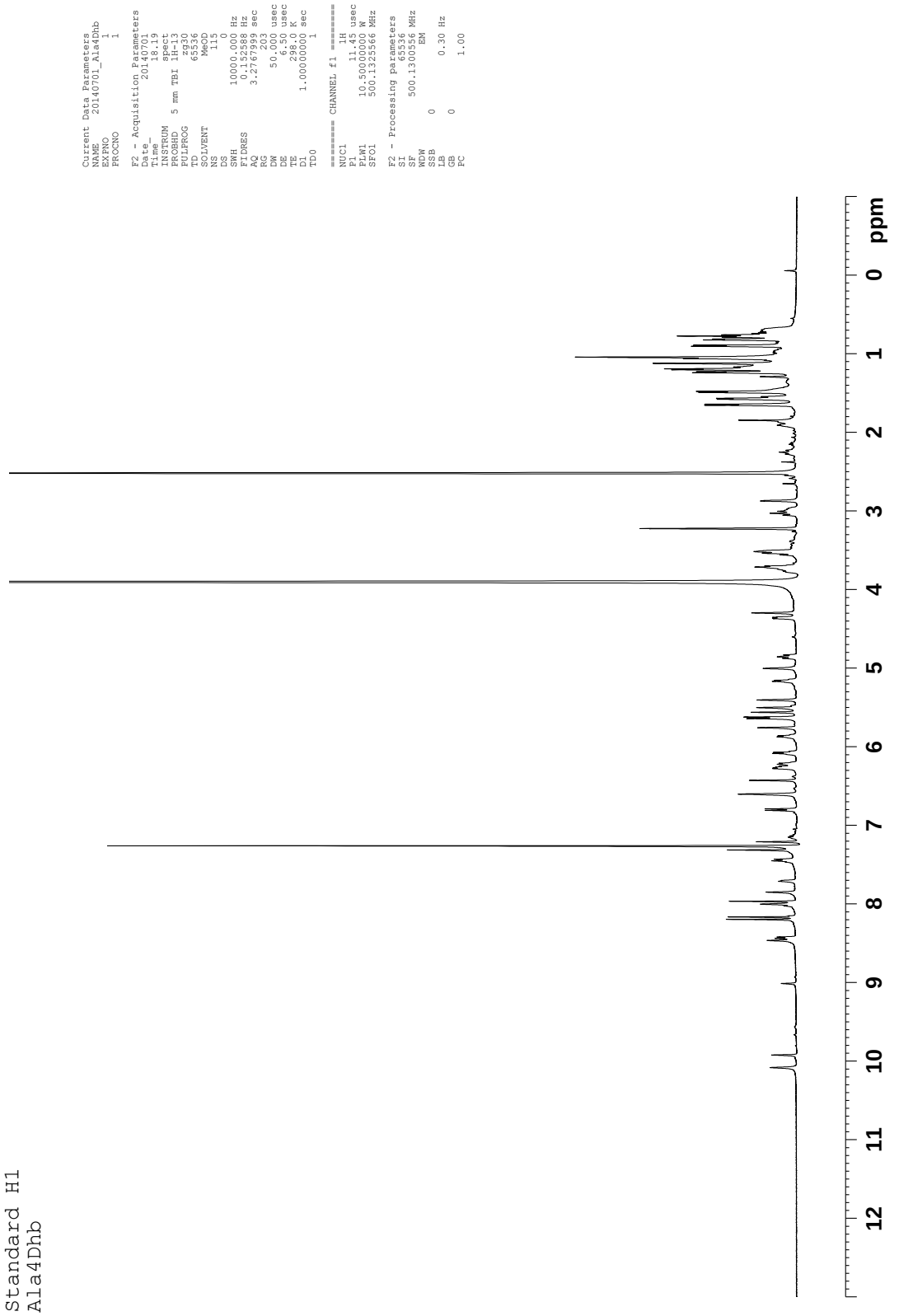

Figure D.29. ^{1}H NMR spectrum of thiostrepton Ala4Dhb (500 MHz, $CDCl_3$-CD_3OD 4:1, 25 °C).

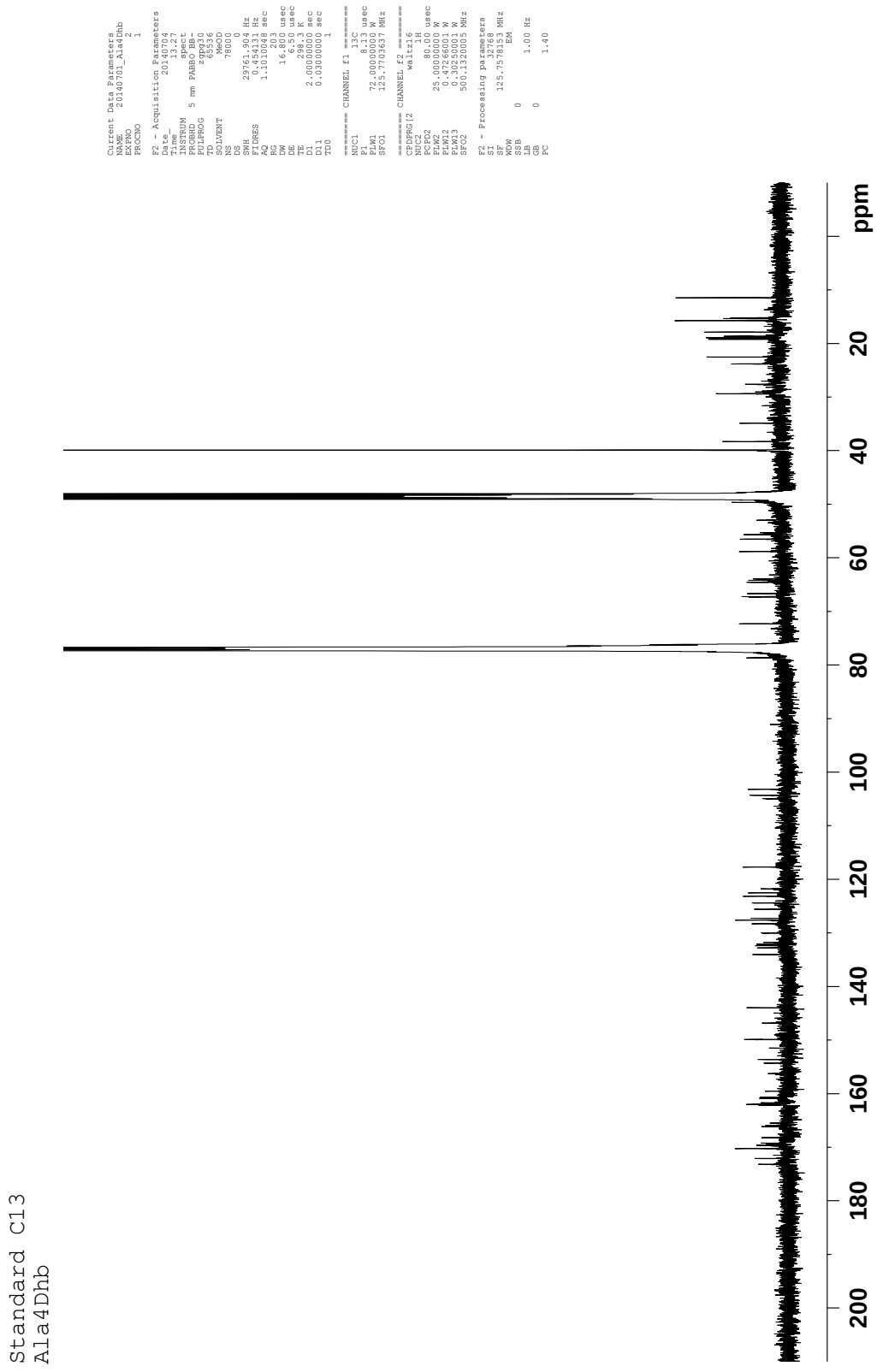

Figure D.30. ^{13}C NMR spectrum of thiostrepton Ala4Dhb (125 MHz, $CDCl_3$-CD_3OD 4:1, 25 °C).

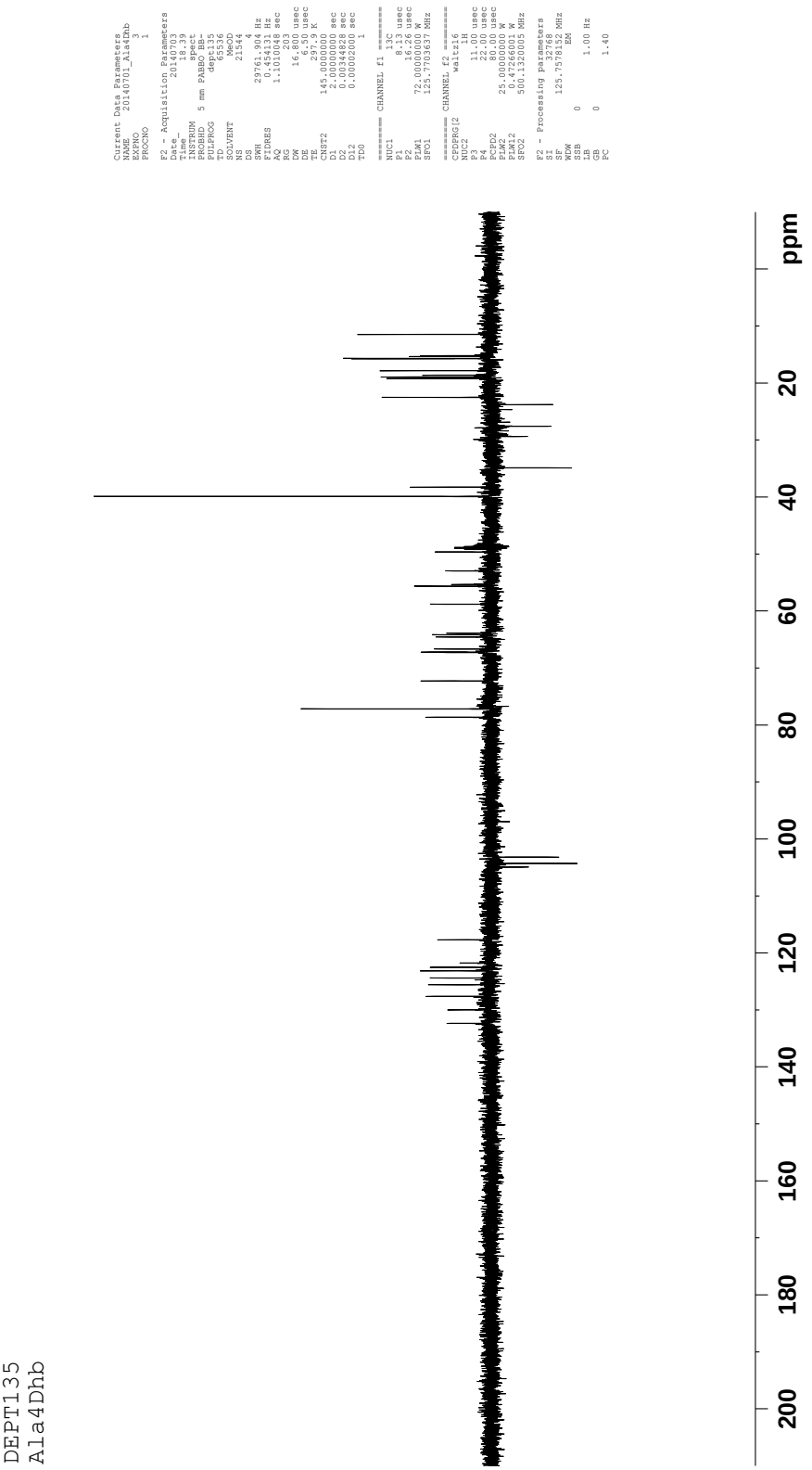

Figure D.31. DEPT-135 NMR spectrum of thiostrepton Ala4Dhb (125 MHz, $CDCl_3$-CD_3OD 4:1, 25 °C).

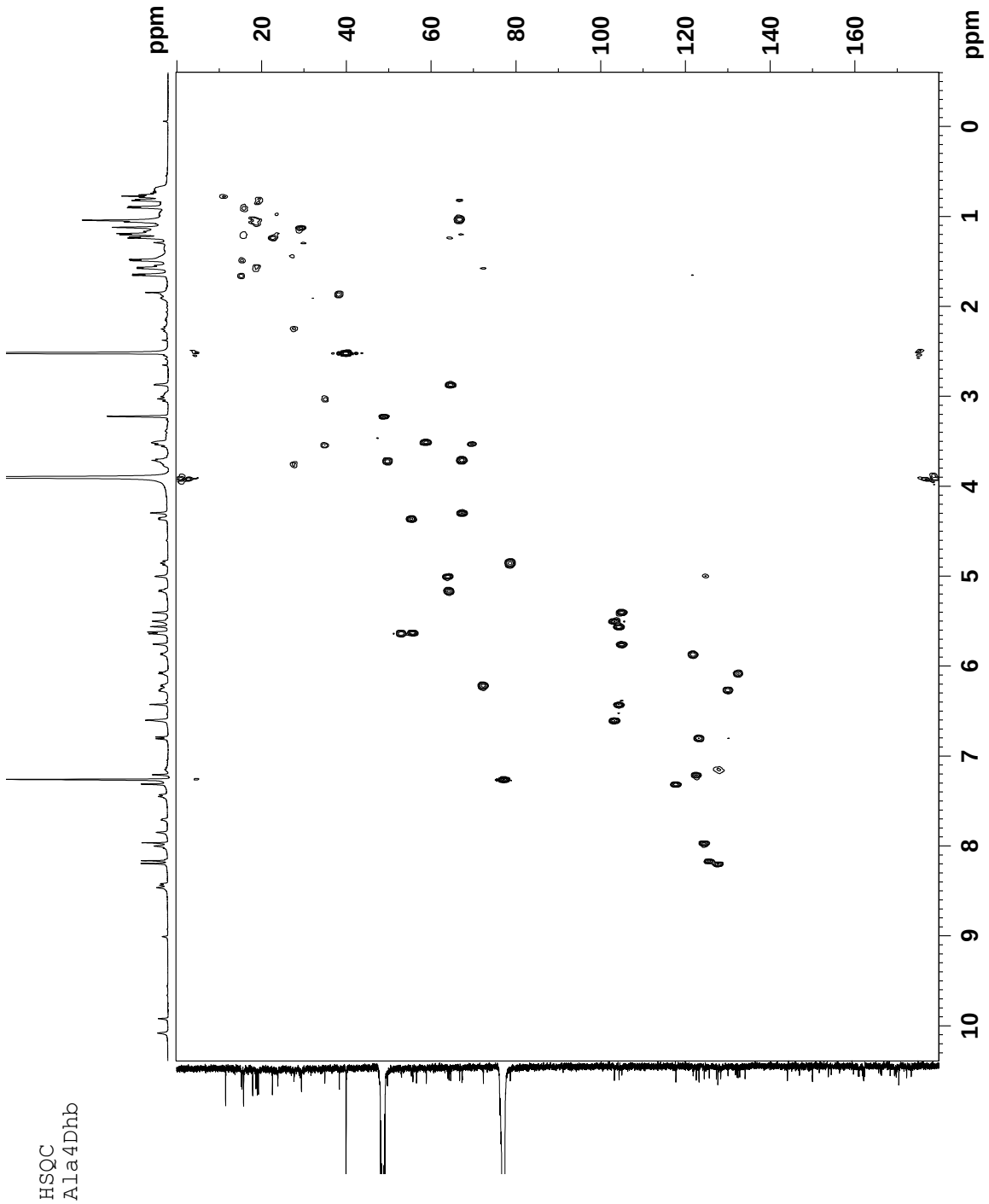

Figure D.32. gHSQC spectrum of thiostrepton Ala4Dhb (500 MHz, $CDCl_3$-CD_3OD 4:1, 25 °C).

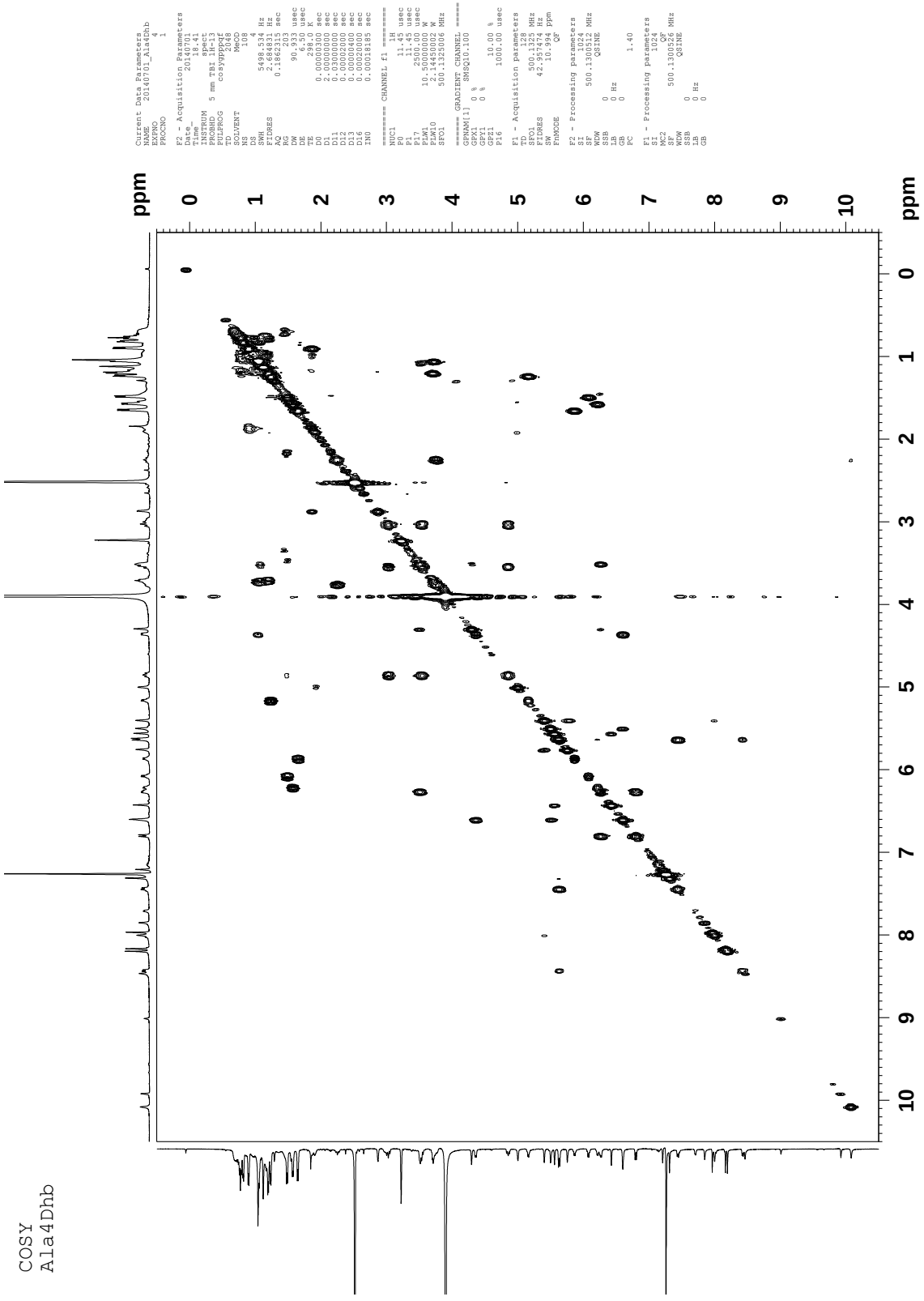

Figure D.33. gCOSY spectrum of thiostrepton Ala4Dhb (500 MHz, $CDCl_3$-CD_3OD 4:1, 25 °C).

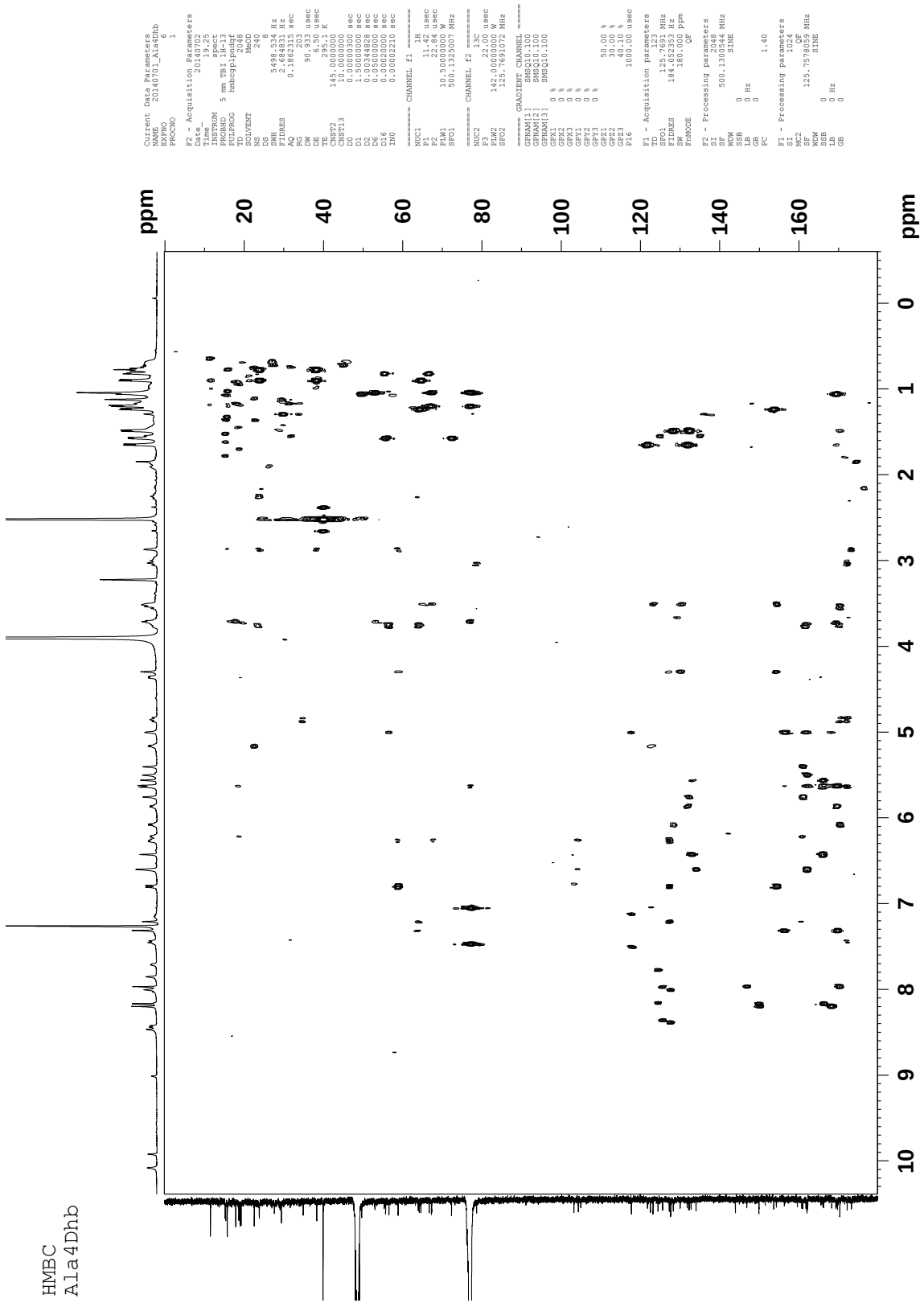

Figure D.34. gHMBC spectrum of thiostrepton Ala4Dhb (500 MHz, $CDCl_3$-CD_3OD 4:1, 25 °C).

Table D.4. ^{1}H and ^{13}C NMR assignments of thiostrepton Ala4Dhb

Position	δ_C [ppm]; mult	δ_H [ppm]; (mult, J in Hz)	HMBC[a]	COSY[b]
Ile1				
Ile1-1	173.2; C q			
Ile1-2	64.6; CH	2.87 (d, 3.4)	Ile1-1; Ile1-3; Ile1-4; Ile1-6; Q-8	Ile1-3
Ile1-3	38.3; CH	1.88-1.83 (m)		Ile1-2; Ile-4-H_A; Ile1-4-H_B; Ile1-6
Ile1-4	23.8; CH_2	H_A: 1.20-1.16 (m)	Ile1-5; Ile1-6	Ile1-3; Ile1-4-H_B; Ile1-5
		H_B: 1.01-0.92 (m)	Ile1-5	Ile1-3; Ile1-4-H_A; Ile1-5
Ile1-5	11.5; CH_3	0.77 (t, 7.3)	Ile1-3; Ile1-4; Ile1-6	Ile1-4-H_A; Ile1-4-H_B
Ile1-6	15.7; CH_3	0.90 (d, 6.8)	Ile1-2; Ile1-3; Ile1-4; Ile1-5	Ile1-3
Ala2				
Ala2-1	169.3; C q			
Ala2-2	49.7; CH	3.75-3.68 (m)	Ala2-1	Ala2-3
Ala2-3	18.9; CH_3	1.05 (d, 6.9)	Ala2-1; Ala2-2	Ala2-2
Dha3				
Dha3-1	160.9; C q			
Dha3-2	132.2; C q			
Dha3-3	105.0; CH_2	H_A: 5.76 (br s)	Dha3-1; Dha3-2	Dha3-3-H_B
		H_B: 5.41 (br s)	Dha3-1; Dha3-2	Dha3-3-H_A
Dhb4				
Dhb4-1	169.4; C q			
Dhb4-2	131.8; C q			
Dhb4-3	121.8; CH	5.87 (q, 6.8)	Dhb4-1	Dhb4-4
Dhb4-4	15.2; CH_3	1.65 (d, 6.8)	Dhb4-1; Dhb4-2; Dhb4-3	Dhb4-3
Pip				
Pip-2	161.7; C q			
Pip-3	23.8; CH_2	H_A: 3.42-3.37 (m)		Pip-4-H_B
		H_B: 3.00-2.95 (m)		Pip-4-H_A; Pip-4-H_B
Pip-4	27.6; CH_2	H_A: 3.80-3.73 (m)	Pip-2; Pip-3; Pip-5; Pip-6; Thz6-4	Pip-3-H_B; Pip-4-H_B
		H_B: 2.30-2.22 (m)	Pip-3; Pip-6	Pip-3-H_A; Pip-4-H_A; Pip-3-H_B
Pip-5	56.5; C q			
Pip-6	63.9; CH	5.00 (br s)	Pip-2; Thz13-2	
Thz6				
Thz6-1	162.2; C q			
Thz6-2	146.8; C q			
Thz6-3	124.4; CH	7.97 (s)	Thz6-2, Thz6-4	
Thz6-4	170.3; C q			
Thr7				
Thr7-1	165.5; C q			
Thr7-2	55.3; CH	4.36 (dd, 7.9, 3.1)	Thr7-1; Thr7-3	Thr7-3; Thr7-NH
Thr7-3	66.7; CH	1.08-1.01 (m)		Thr7-2; Thr7-4
Thr7-4	19.2; CH_3	0.82 (d, 5.8)	Thr7-2; Thr7-3	Thr7-3
Thr7-NH[d]		6.63-6.58 (m)		Thr7-2
Dhb8				
Dhb8-2	128.3; C q			
Dhb8-3	132.4; CH	6.08 (q, 6.7)	Tzn9-4	Dhb8-4
Dhb8-4	15.4; CH_3	1.49 (d, 6.9)	Dhb8-2; Dhb8-3; Tzn9-4	Dhb8-3
Tzn9				
Tzn9-1	172.1; C q			
Tzn9-2	78.7; CH	4.85 (dd, 12.8, 9.2)	Tzn9-1; Tzn9-4	Tzn9-3-H_A; Tzn9-3-H_B
Tzn9-3	34.9; CH_2	H_A: 3.57-3.52 (m)	Tzn9-2; Tzn9-4	Tzn9-2; Tzn9-3-H_B
		H_B: 3.03 (t, 12.4)	Tzn9-1; Tzn9-2	Tzn9-2; Tzn9-3-H_A
Tzn9-4	170.3; C q			
Ile10				
Ile10-2	53.0; CH	5.63 (d, 9.8)	Tzn9-1; Ile10-3; Thz11-4	Ile10-NH
Ile10-3	77.0[c]; C q			
Ile10-4	67.3; CH	3.75-3.68 (m)	Ile10-2; Ile10-3; Ile10-5; Ile10-6	Ile10-5
Ile10-5	15.7; CH_3	1.20 (d, 6.3)	Ile10-3; Ile10-4	Ile10-4
Ile10-6	17.9; CH_3	1.04 (s)	Ile10-2; Ile10-3; Ile10-4; Ile10-5	
Ile10-NH[d]		7.44 (d, 9.8)		Ile10-2

Position	δ_C [ppm]; mult	δ_H [ppm]; (mult, J in Hz)	HMBC[a]	COSY[b]
Thz11				
Thz11-1	161.9; C q			
Thz11-2	149.9; C q			
Thz11-3	125.6; CH	8.17 (s)	Thz11-1; Thz11-2; Thz11-4	
Thz11-4	166.2; C q			
Thr12				
Thr12-2	55.7; CH	5.63 (d, 9.8)	Thz11-1; Thr12-4; Thz13-2; Thz13-	Thr12-3; Thr12-NH
Thr12-3	72.3; CH	6.22 (q, 6.8)		Thr12-2; Thr12-4
Thr12-4	18.6; CH_3	1.57 (d, 6.2)	Thr12-2; Thr12-3	Thr12-3
Thr12-NH[d]		8.43 (d, 8.6)		Thr12-2
Thz13				
Thz13-2	156.3; C q			
Thz13-3	117.8; CH	7.31 (s)	Pip-6; Thz13-2; Thz13-4	
Thz13-4	169.7; C q			
Thz15				
Thz15-1	159.6; C q			
Thz15-2	150.0; C q			
Thz15-3	127.6; CH	8.20 (s)	Thz15-1; Thz15-2; Thz15-4	
Thz15-4	168.2; C q			
Dha16				
Dha16-1	162.0; C q			
Dha16-2	134.0; C q			
Dha16-3	103.2; CH_2	H_A: 6.53 (br s)	Dha16-1; Dha16-2	Dha16-3-H_B
		H_B: 5.50 (br s)	Dha16-1; Dha16-2	Dha16-3-H_A
Dha17				
Dha17-1	166.0; C q			
Dha17-2	132.8; C q			
Dha17-3	104.3; CH_2	H_A: 6.43 (br s)	Dha17-1; Dha17-2	Dha17-3-H_B
		H_B: 5.56 (br s)	Dha17-1; Dha17-2	Dha17-3-H_A
Q				
Q-1	160.7; C q			
Q-2	144.0; C q			
Q-3	122.5; CH	7.21 (s)	Q-1; Q-5; Q-11	
Q-4	153.7; C q			
Q-5	127.3; C q			
Q-6	123.2; CH	6.80 (d, 9.9)	Q-5; Q-8; Q-10	Q-7
Q-7	130.0; CH	6.26 (dd, 9.2, 5.6)	Q-5; Q-8; Q-9	Q-6; Q-8
Q-8	58.8; CH	3.54-3.48 (m)	Ile1-2; Q-9; Q-10	Q-7; Q-9
Q-9	67.4; CH	4.30 (br s)		Q-8
Q-10	154.3; C q			
Q-11	64.2; CH	5.16 (q, 5.8)	Q-12	Q-12
Q-12	22.5; CH_3	1.23 (d, 6.4)	Q-4, Q-11	Q-11

[a] HMBC correlations are from the proton to the indicated carbon.
[b] COSY correlations are from the proton to the proton attached to the indicated position.
[c] The δ of this resonance was determined by HMBC due to overlap with the $CDCl_3$ resonance.
[d] Only those amide resonances demonstrating COSY correlations to neighboring protons were assigned.

Figure D.35. MS analysis of thiostrepton Ala4Gln isolated from *S. laurentii* NDS1/int-A4Q.

(**A**) HPLC-MS analysis. (1) Chromatogram extracted for *m*/*z* 861.3, the calculated $[M+2H]^{2+}$ ion of thiostrepton Ala4Gln. (2) Total ion chromatogram.

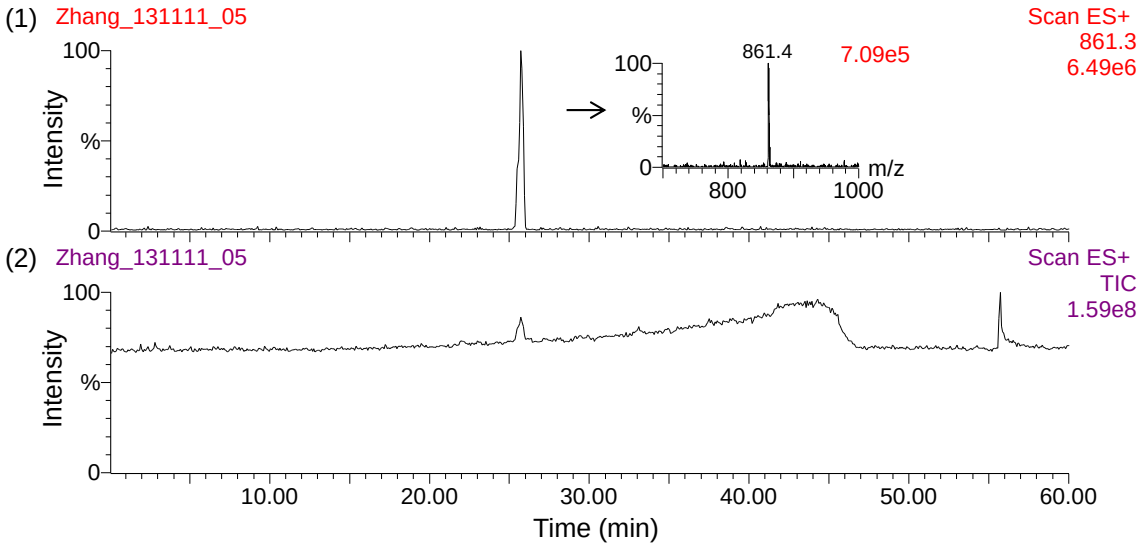

(**B**) MALDI MS spectrum of thiostrepton Ala4Gln.

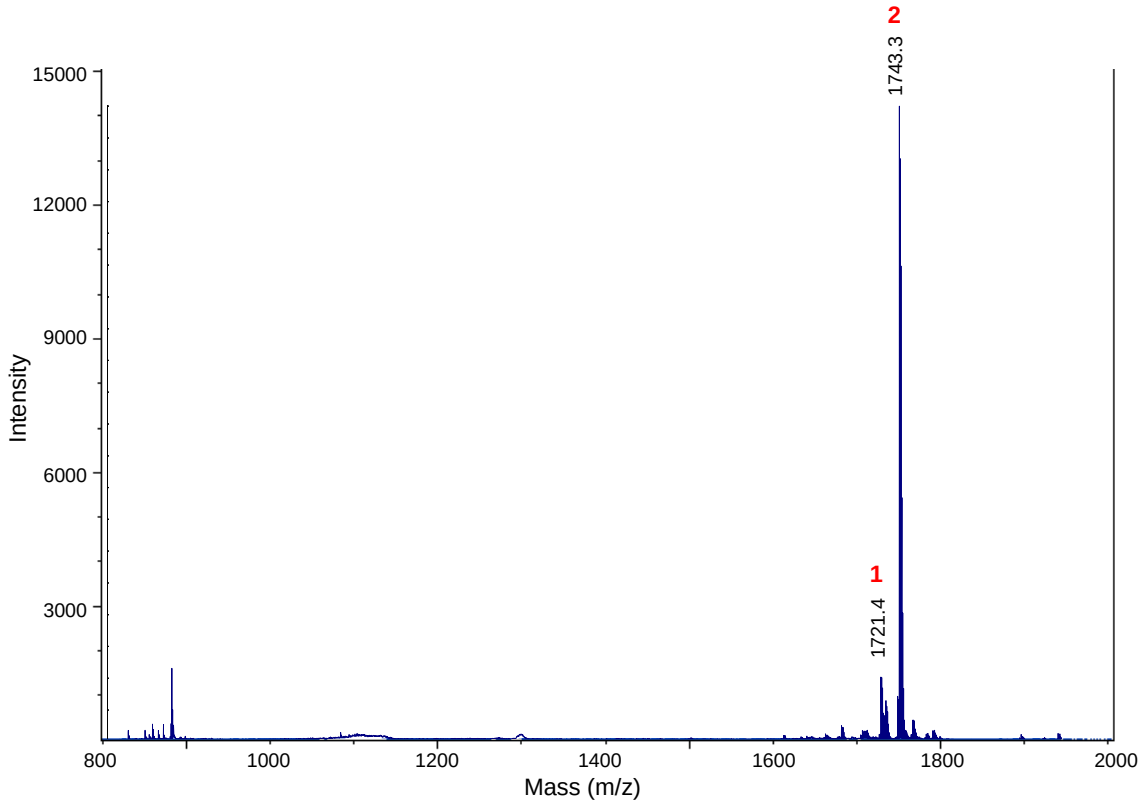

(**C**) MALDI MS/MS of parent ion *m/z* 1721.4.

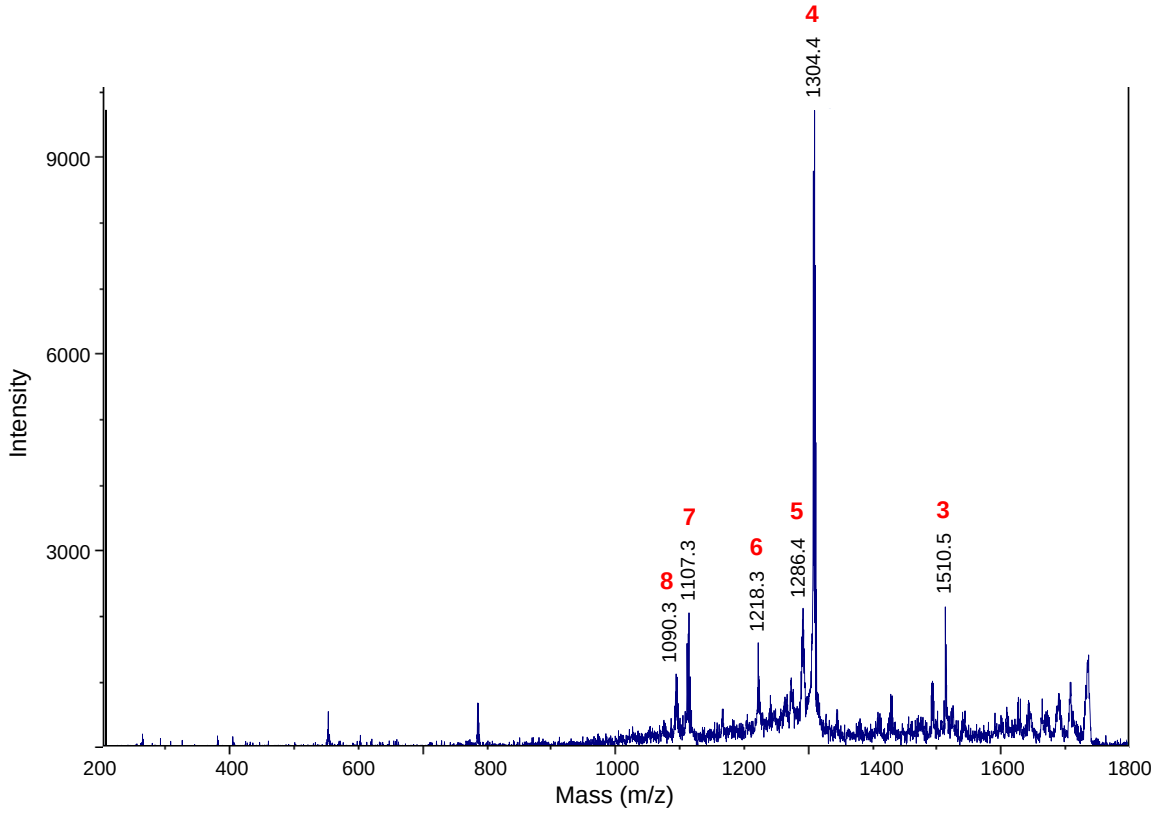

(**D**) Table and structure showing key ions and fragments in the MALDI MS and MS/MS of thiostrepton Ala4Gln.

Fragment	Expected	Observed
1. $M+H^+$ (Parent ion)	1721.5	1721.4
2. $M+Na^+$	1743.5	1743.3
3. M-Dha16-Dha17-NH_2-C_4H_9+H^+	1510.4	1510.5
4. M-QA-Ile1-Ala2+H^+	1304.3	1304.4
5. M-QA-Ile1-Ala2-H_2O+H^+	1286.3	1286.4
6. M-QA-Ile1-Ala2-Dha3-OH+H^+	1218.3	1218.3
7. M-QA-Ile1-Ala2-Dha3-Gln4+H^+	1107.3	1107.3
8. M-QA-Ile1-Ala2-Dha3-Gln4-OH+H^+	1090.2	1090.3

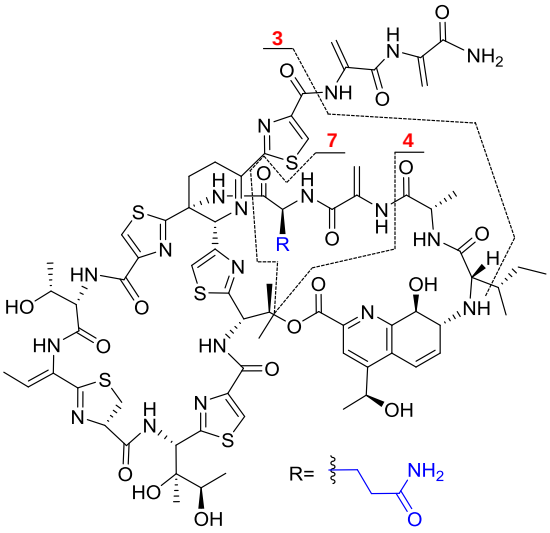

Figure D.36. MS analysis of thiostrepton Ala4His isolated from *S. laurentii* NDS1/int-A4H.

(**A**) HPLC-MS analysis. (1) Chromatogram extracted for *m/z* 865.8, the calculated $[M+2H]^{2+}$ ion of thiostrepton Ala4His. (2) Total ion chromatogram.

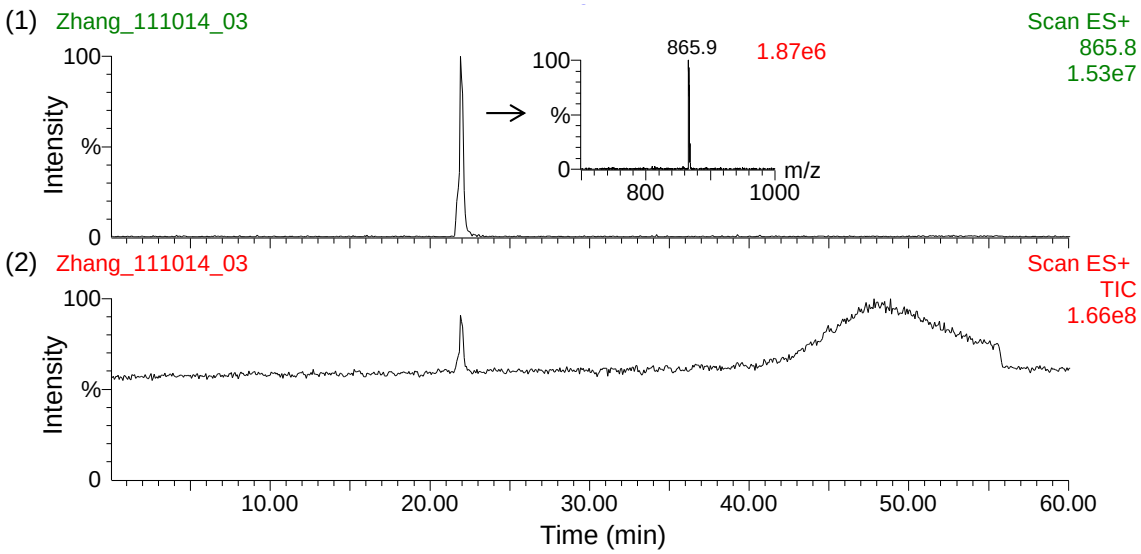

(**B**) MALDI MS spectrum of thiostrepton Ala4His.

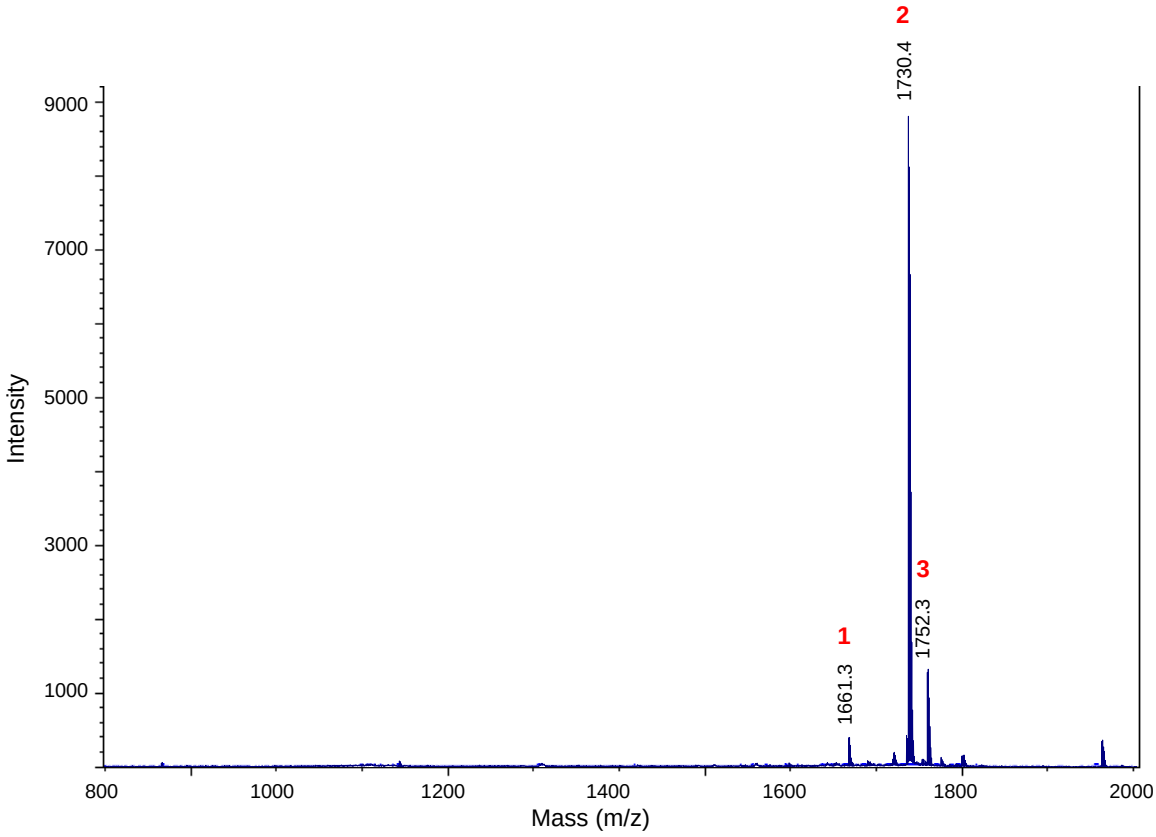

(**C**) MALDI MS/MS of parent ion *m/z* 1730.4.

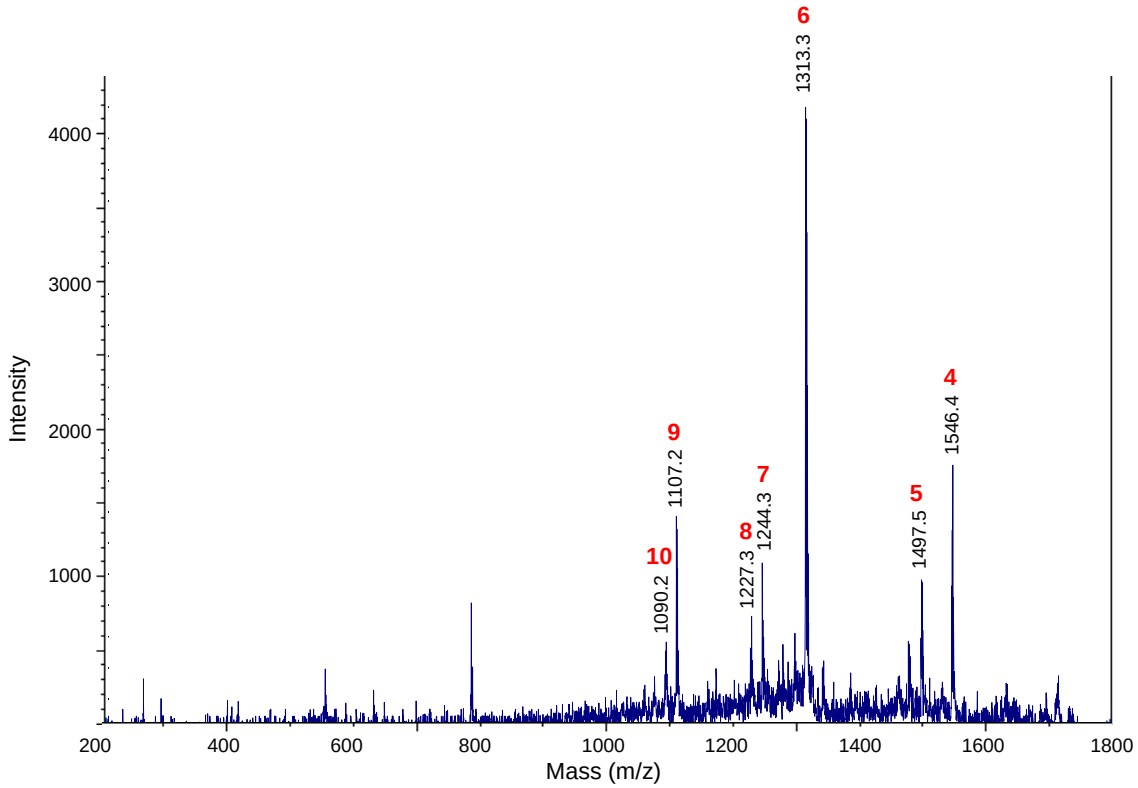

(**D**) Table and structure showing key ions and fragments in the MALDI MS and MS/MS of thiostrepton Ala4His.

Fragment	Expected	Observed
1. M+H$^+$-Dha17 (*in situ* truncation)	1661.5	1661.3
2. M+H$^+$ (Parent ion)	1730.5	1730.4
3. M+Na$^+$	1752.5	1752.3
4. M-Ile1-Ala2+H$^+$	1546.4	1546.4
5. M-QA+H$^+$	1497.5	1497.5
6. M-QA-Ile1-Ala2+H$^+$	1313.3	1313.3
7. M-QA-Ile1-Ala2-Dha3+H$^+$	1244.3	1244.3
8. M-QA-Ile1-Ala2-Dha3-OH+H$^+$	1227.3	1227.3
9. M-QA-Ile1-Ala2-Dha3-His4+H$^+$	1107.3	1107.2
10. M-QA-Ile1-Ala2-Dha3-His4-H_2O+H$^+$	1090.2	1090.2

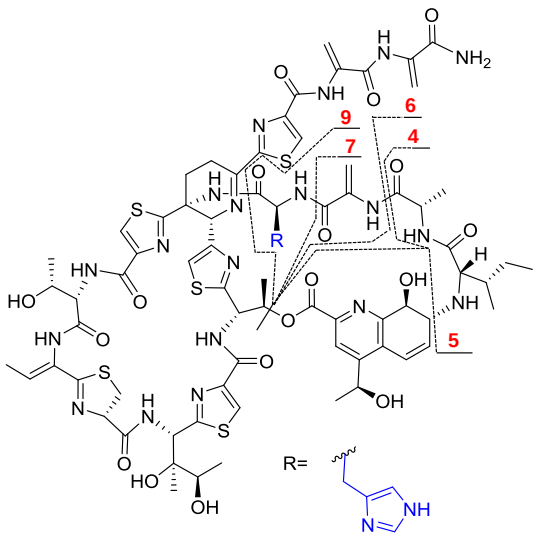

Figure D.37. MS analysis of thiostrepton Ala4Ile isolated from *S. laurentii* NDS1/int-A4I.

(**A**) HPLC-MS analysis. (1) Chromatogram extracted for *m/z* 853.8, the calculated $[M+2H]^{2+}$ ion of thiostrepton Ala4Ile. (2) Total ion chromatogram.

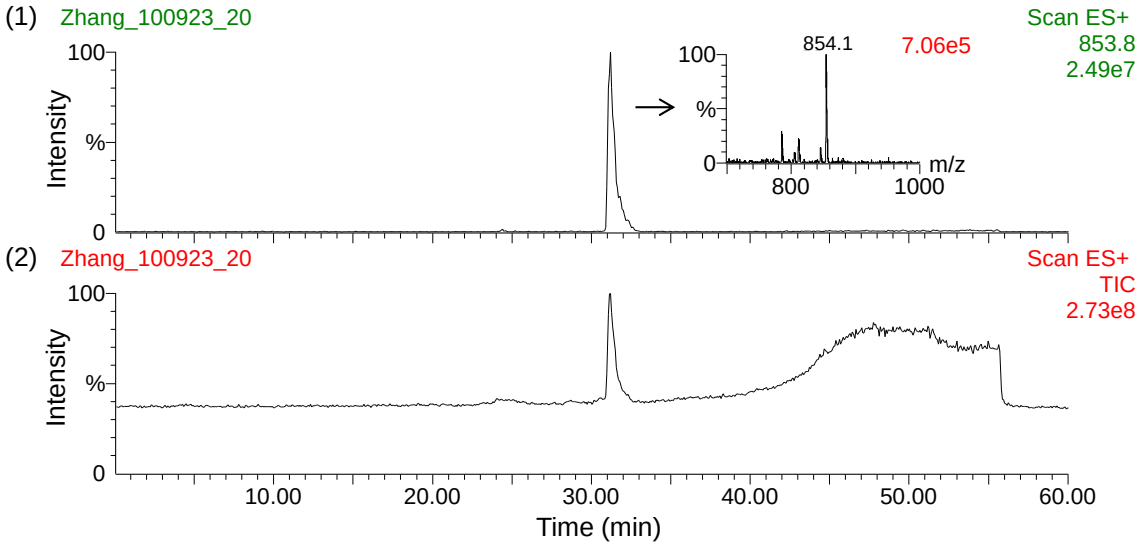

(**B**) MALDI MS spectrum of thiostrepton Ala4Ile.

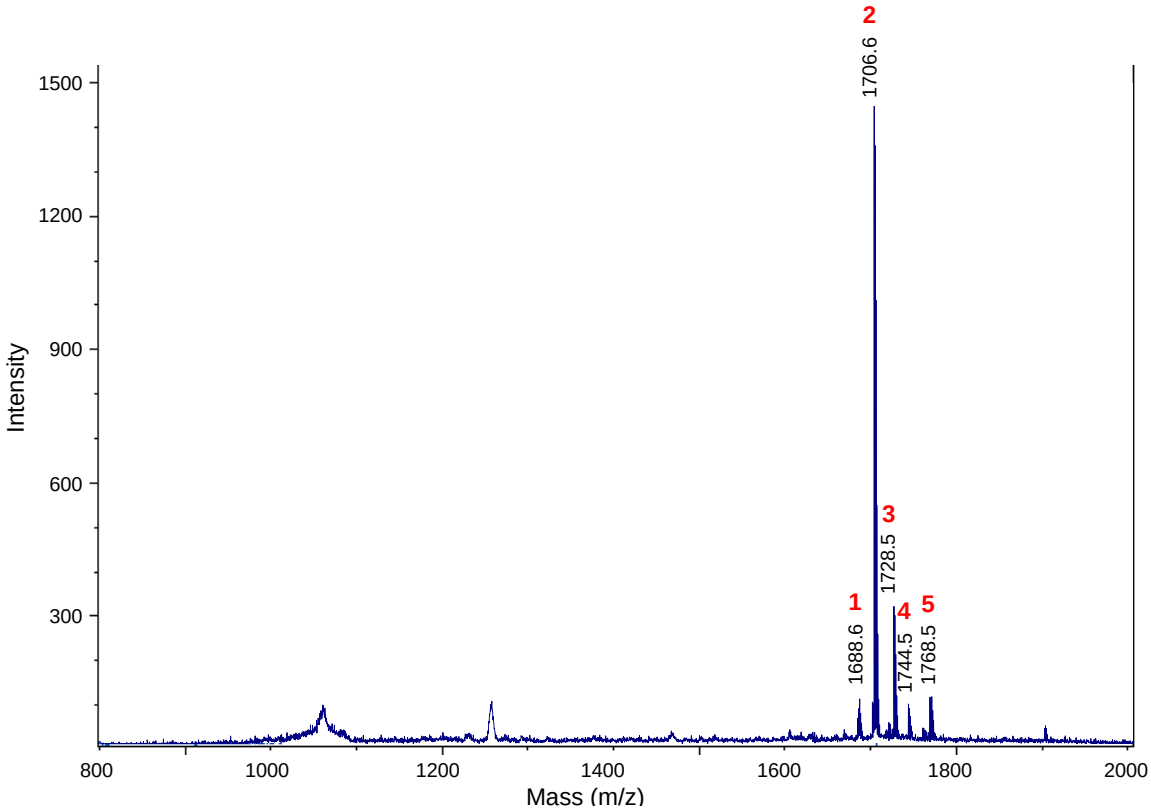

(**C**) MALDI MS/MS of parent ion *m/z* 1706.6.

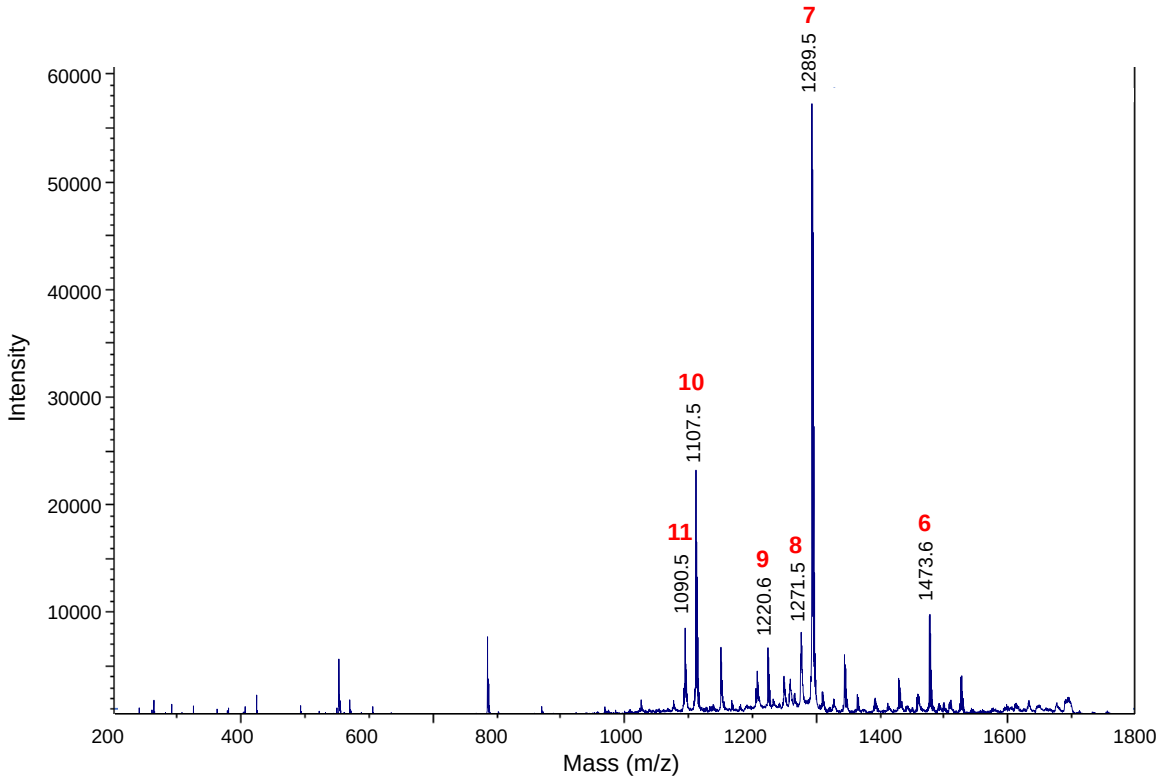

(**D**) Table and structure showing key ions and fragments in the MALDI MS and MS/MS of thiostrepton Ala4Ile.

Fragment	Expected	Observed
1. M-H_2O+H^+	1688.5	1688.6
2. M+H^+ (Parent ion)	1706.5	1706.6
3. M+Na^+	1728.5	1728.5
4. M+K^+	1744.5	1744.5
5. M+Cu^+	1768.5	1768.5
6. M-QA+H^+	1473.5	1473.6
7. M-QA-Ile1-Ala2+H^+	1289.4	1289.5
8. M-QA-Ile1-Ala2-H_2O+H^+	1271.3	1271.5
9. M-QA-Ile1-Ala2-Dha3+H^+	1220.3	1220.6
10. M-QA-Ile1-Ala2-Dha3-Ile4+H^+	1107.3	1107.5
11. M-QA-Ile1-Ala2-Dha3-Ile4-OH+H^+	1090.2	1090.5

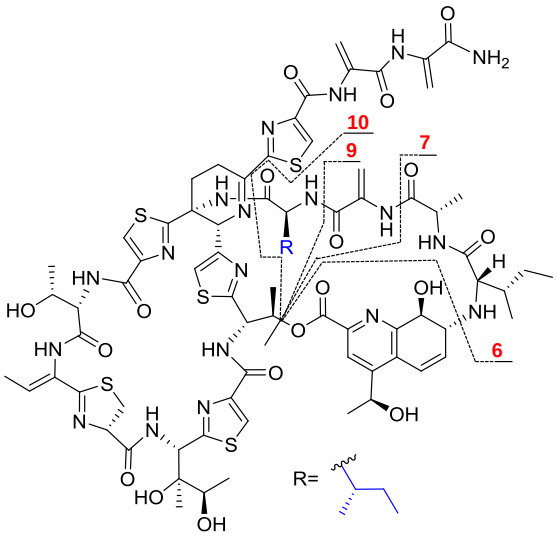

Figure D.38. MS analysis of thiostrepton Ala4Leu isolated from *S. laurentii* NDS1/int-A4L.

(**A**) HPLC-MS analysis. (1) Chromatogram extracted for *m*/*z* 853.8, the calculated $[M+2H]^{2+}$ ion of thiostrepton Ala4Leu. (2) Total ion chromatogram.

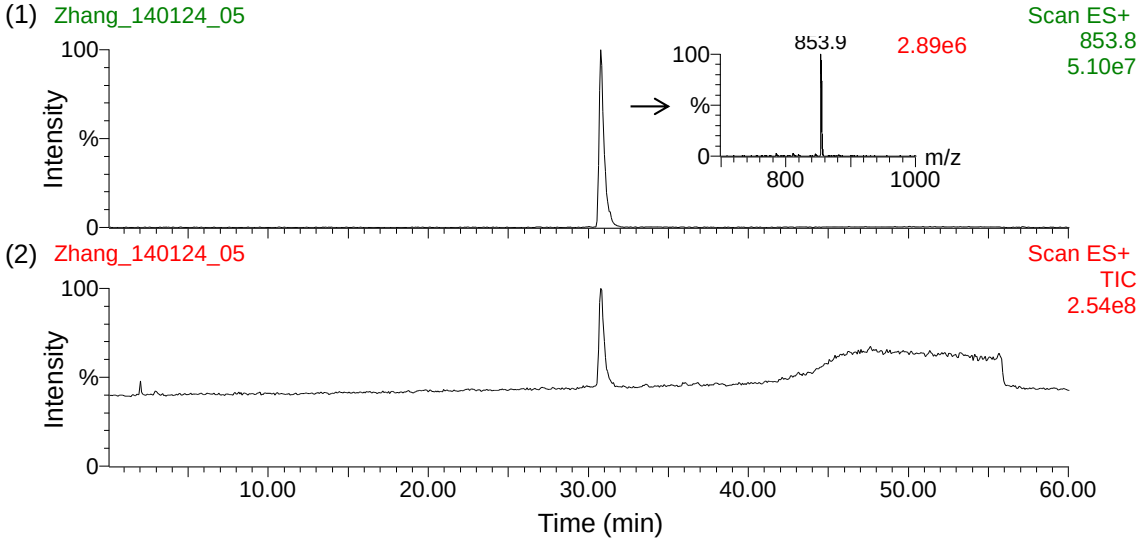

(**B**) MALDI MS spectrum of thiostrepton Ala4Leu.

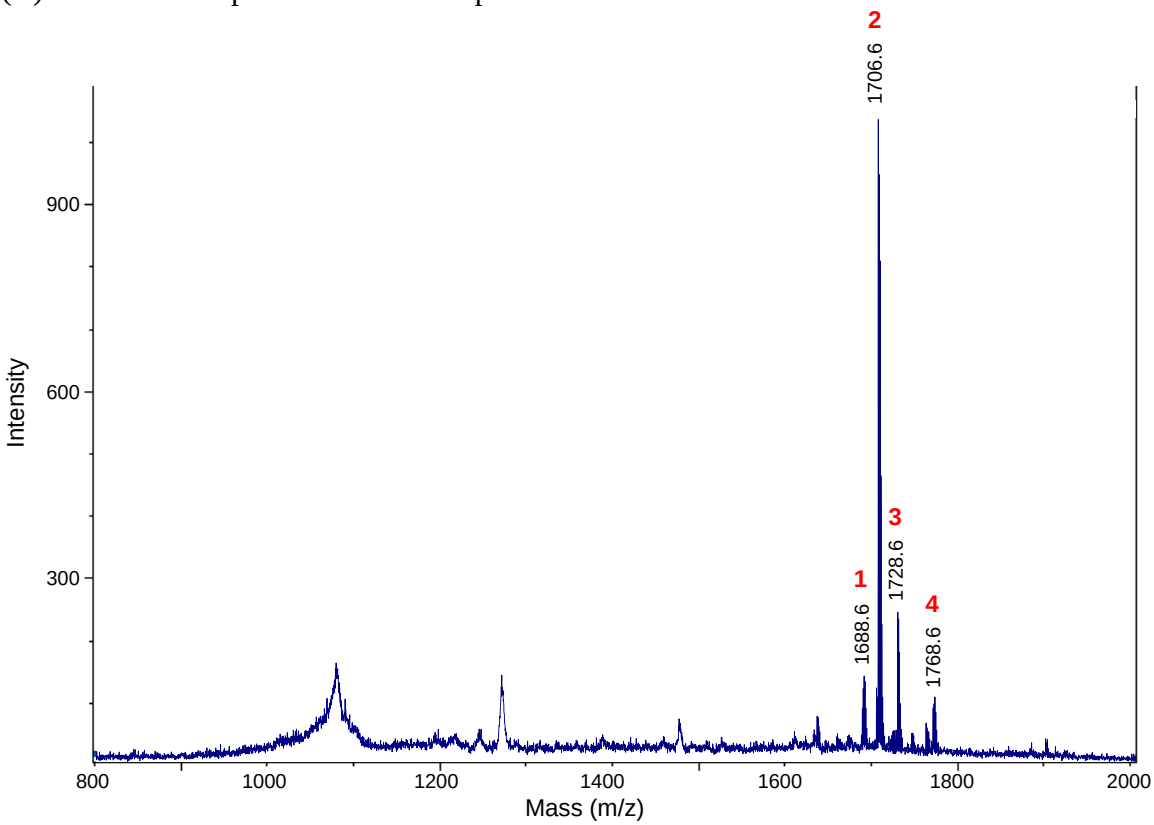

(**C**) MALDI MS/MS of parent ion *m/z* 1706.6.

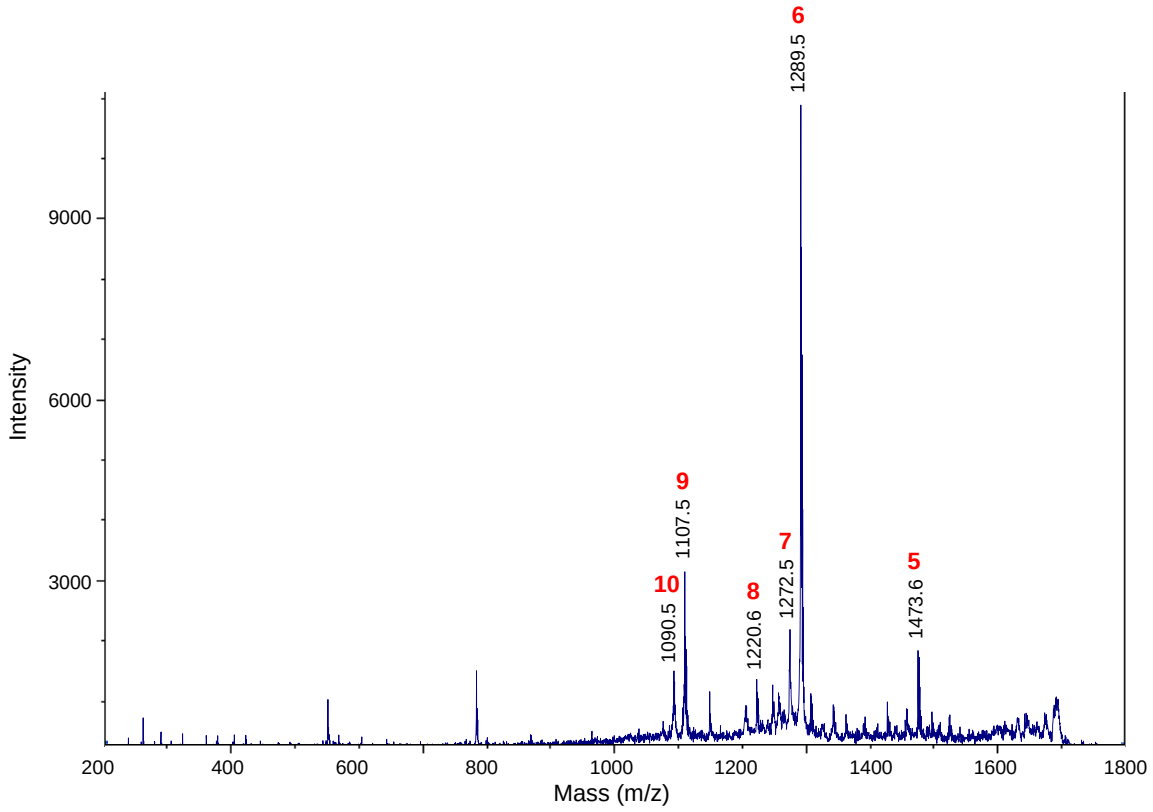

(**D)** Table and structure showing key ions and fragments in the MALDI MS and MS/MS of thiostrepton Ala4Leu.

Fragment	Expected	Observed
1. M-H_2O+H^+	1688.5	1688.6
2. M+H^+ (Parent ion)	1706.5	1706.6
3. M+Na^+	1728.5	1728.6
4. M+Cu^+	1768.5	1768.6
5. M-QA+H^+	1473.5	1473.6
6. M-QA-Ile1-Ala2+H^+	1289.4	1289.5
7. M-QA-Ile1-Ala2-OH+H^+	1272.4	1272.5
8. M-QA-Ile1-Ala2-Dha3+H^+	1220.3	1220.6
9. M-QA-Ile1-Ala2-Dha3-Leu4+H^+	1107.3	1107.5
10. M-QA-Ile1-Ala2-Dha3-Leu4-OH+H^+	1090.2	1090.5

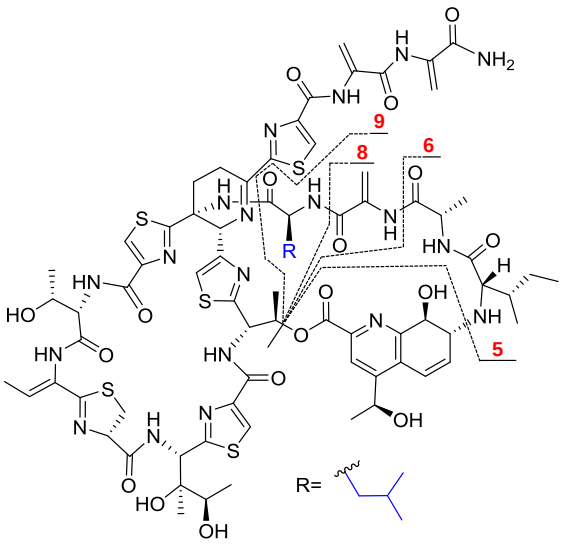

Figure D.39. MS analysis of thiostrepton Ala4Met isolated from *S. laurentii* NDS1/int-A4M.

(**A**) HPLC-MS analysis. (1) Chromatogram extracted for *m*/*z* 862.8, the calculated $[M+2H]^{2+}$ ion of thiostrepton Ala4Met. (2) Total ion chromatogram.

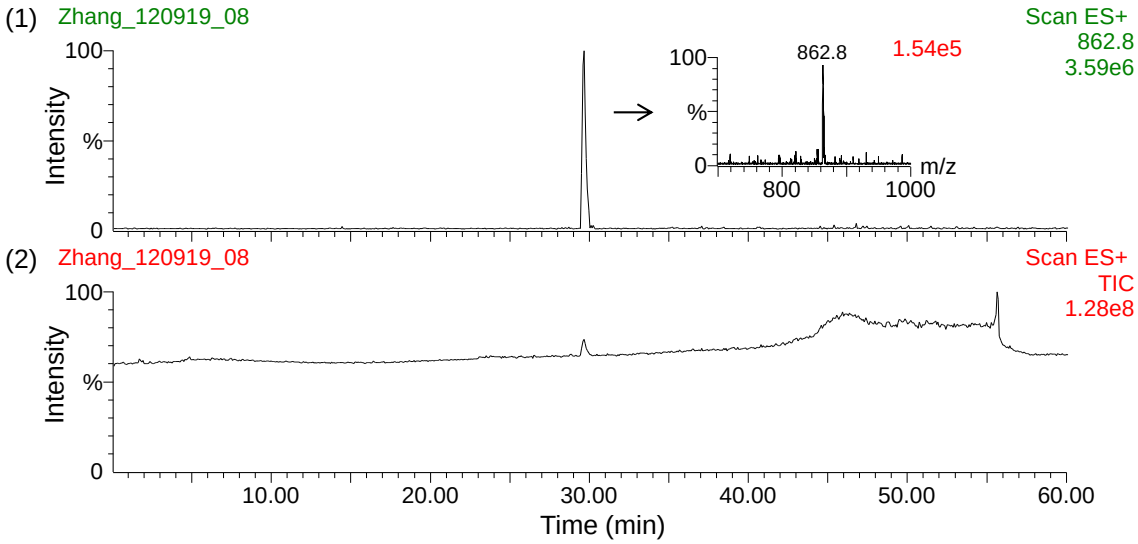

(**B**) MALDI MS spectrum of thiostrepton Ala4Met.

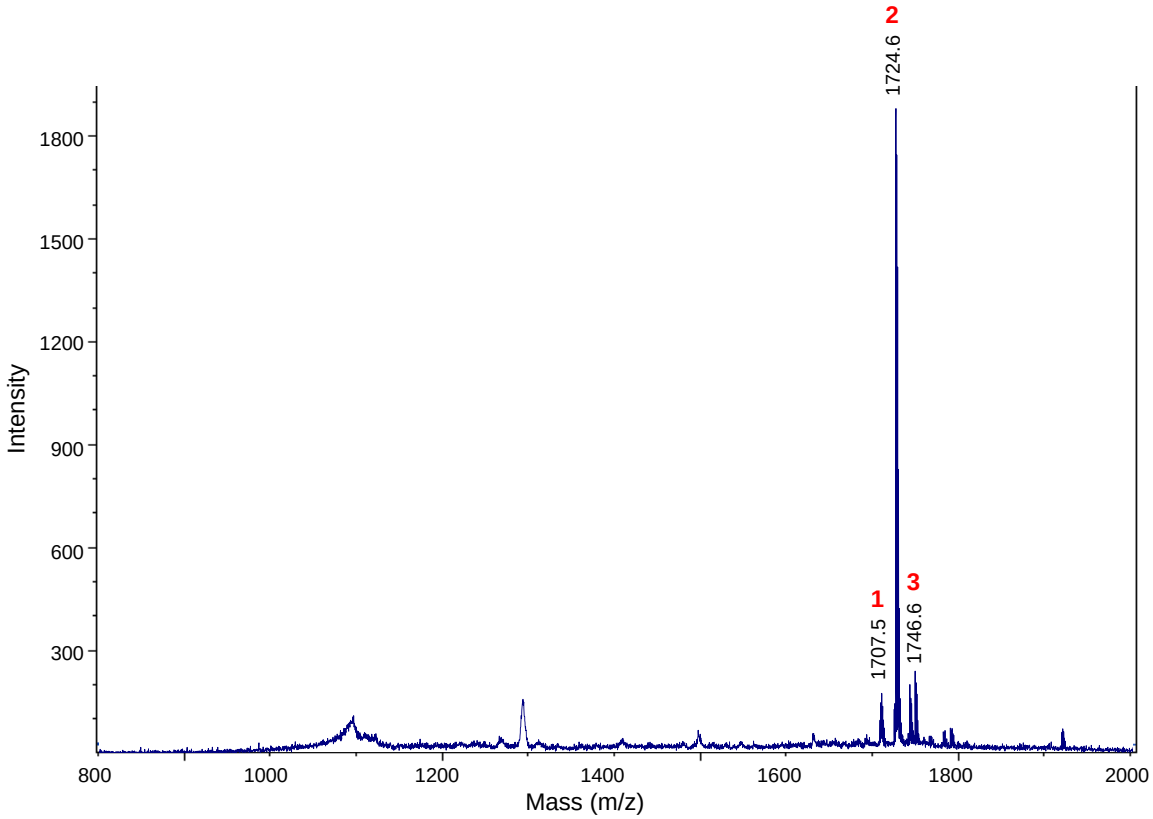

(**C**) MALDI MS/MS of parent ion *m/z* 1724.6.

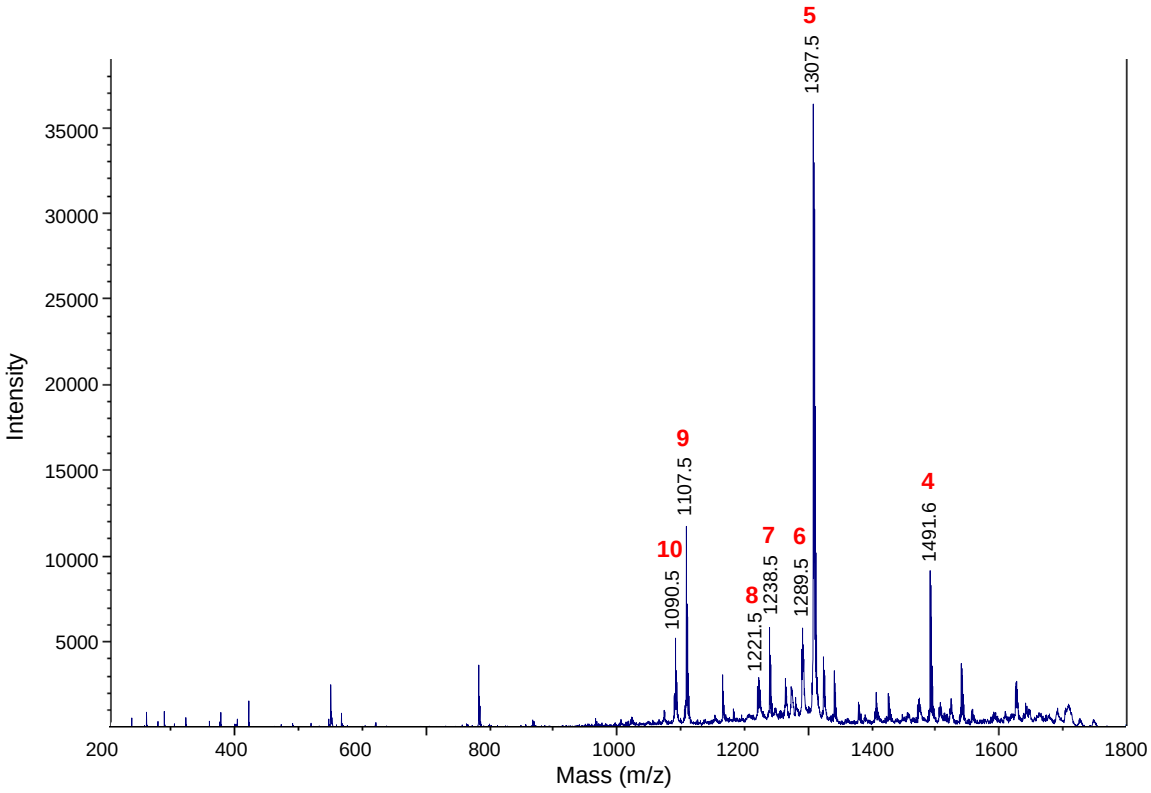

(**D**) Table and structure showing key ions and fragments in the MALDI MS and MS/MS of thiostrepton Ala4Met.

Fragment	Expected	Observed
1. M-OH+H$^+$	1707.5	1707.5
2. M+H$^+$ (Parent ion)	1724.5	1724.6
3. M+Na$^+$	1746.5	1746.6
4. M-QA+H$^+$	1491.4	1491.6
5. M-QA-Ile1-Ala2+H$^+$	1307.3	1307.5
6. M-QA-Ile1-Ala2-H_2O+H$^+$	1289.3	1289.5
7. M-QA-Ile1-Ala2-Dha3+H$^+$	1238.3	1238.5
8. M-QA-Ile1-Ala2-Dha3-OH+H$^+$	1221.3	1221.5
9. M-QA-Ile1-Ala2-Dha3-Met4+H$^+$	1107.3	1107.5
10. M-QA-Ile1-Ala2-Dha3-Met4-OH+H$^+$	1090.2	1090.5

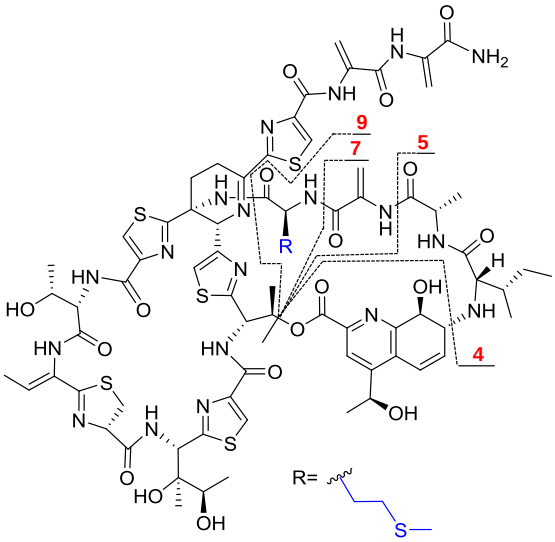

Figure D.40. MS analysis of thiostrepton Ala4Phe isolated from *S. laurentii* NDS1/int-A4F.

(**A**) HPLC-MS analysis. (1) Chromatogram extracted for *m/z* 870.8, the calculated $[M+2H]^{2+}$ ion of thiostrepton Ala4Phe. (2) Total ion chromatogram.

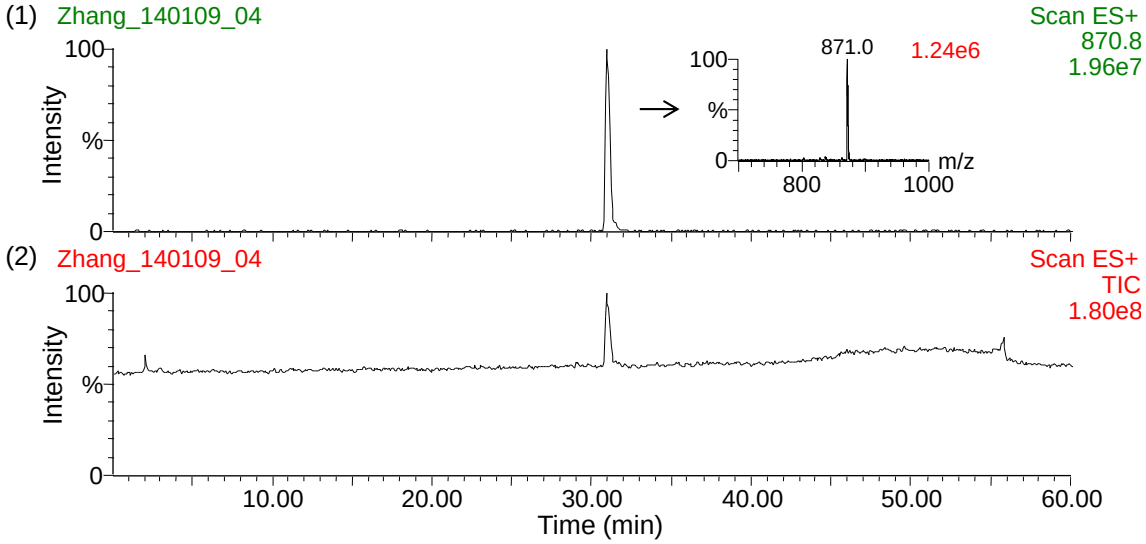

(**B**) MALDI MS spectrum of thiostrepton Ala4Phe.

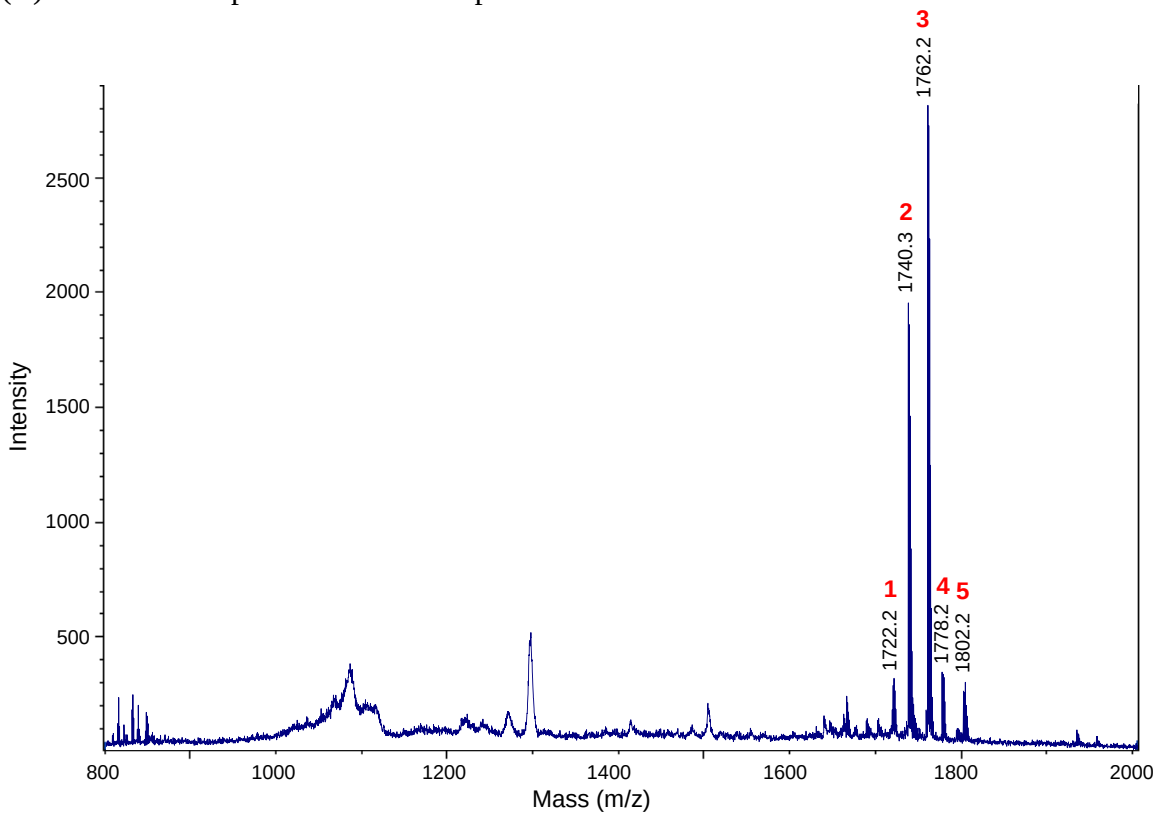

(**C**) MALDI MS/MS of parent ion *m/z* 1740.3.

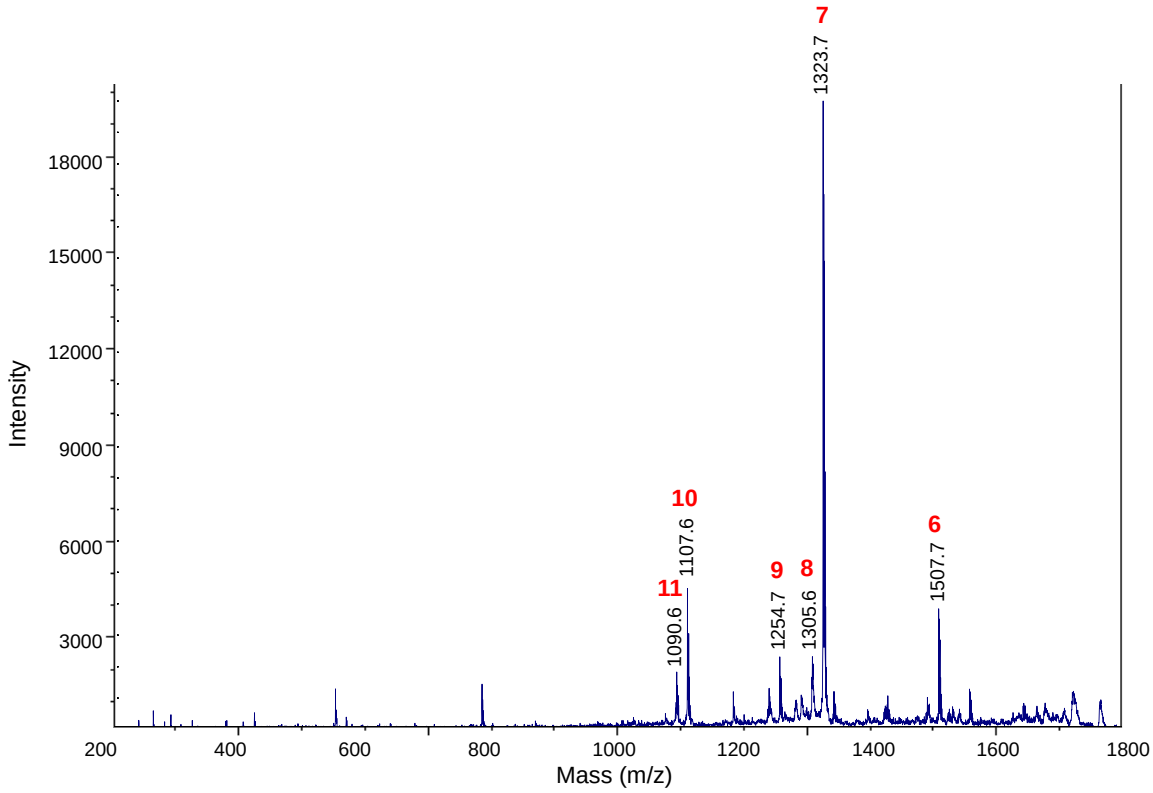

(**D**) Table and structure showing key ions and fragments in the MALDI MS and MS/MS of thiostrepton Ala4Phe.

Fragment	Expected	Observed
1. M-H_2O+H^+	1722.5	1722.2
2. M+H^+ (Parent ion)	1740.5	1740.3
3. M+Na^+	1762.5	1762.2
4. M+K^+	1778.5	1778.2
5. M+Cu^+	1802.5	1802.2
6. M-QA+H^+	1507.5	1507.7
7. M-QA-Ile1-Ala2+H^+	1323.3	1323.7
8. M-QA-Ile1-Ala2-H_2O+H^+	1305.3	1305.6
9. M-QA-Ile1-Ala2-Dha3+H^+	1254.3	1254.7
10. M-QA-Ile1-Ala2-Dha3-Phe4+H^+	1107.3	1107.6
11. M-QA-Ile1-Ala2-Dha3-Phe4-OH+H^+	1090.2	1090.6

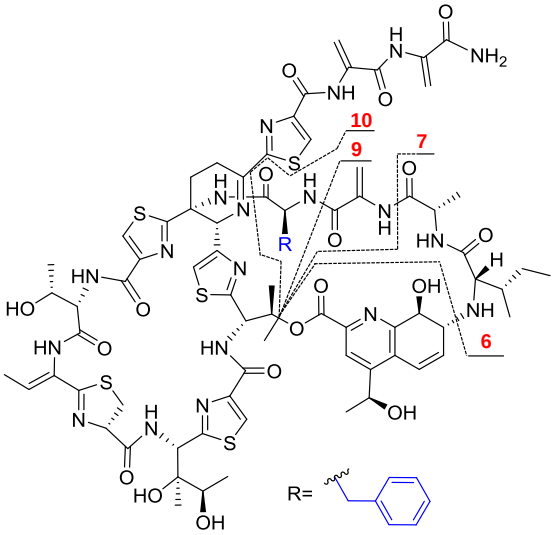

Figure D.41. MS analysis of thiostrepton Ala4Ser isolated from *S. laurentii* NDS1/int-A4S.

(**A**) HPLC-MS analysis. (1) Chromatogram extracted for *m/z* 840.8, the calculated $[M+2H]^{2+}$ ion of thiostrepton Ala4Ser. (2) Total ion chromatogram.

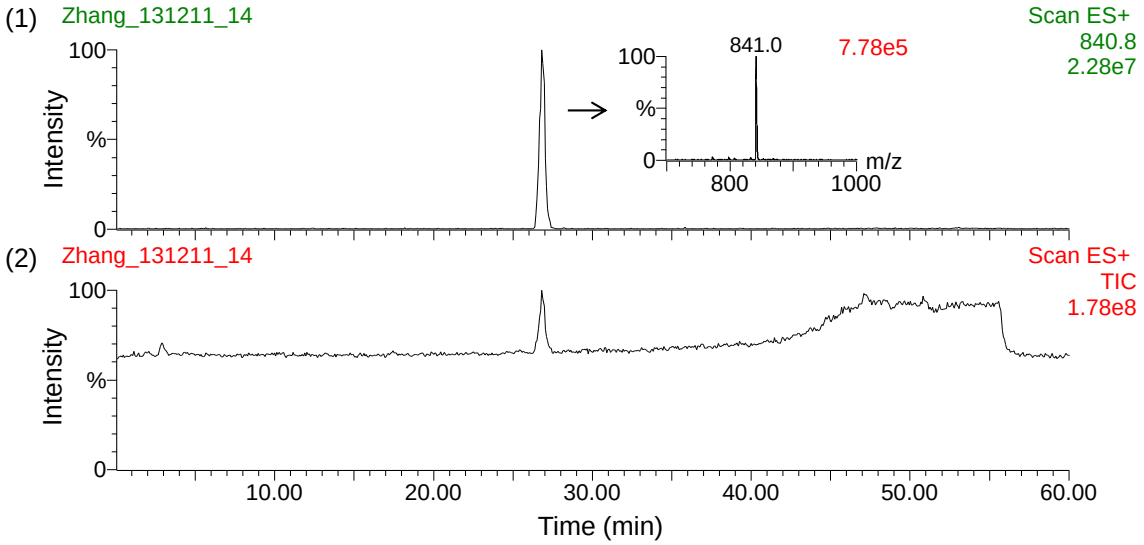

(**B**) MALDI MS spectrum of thiostrepton Ala4Ser.

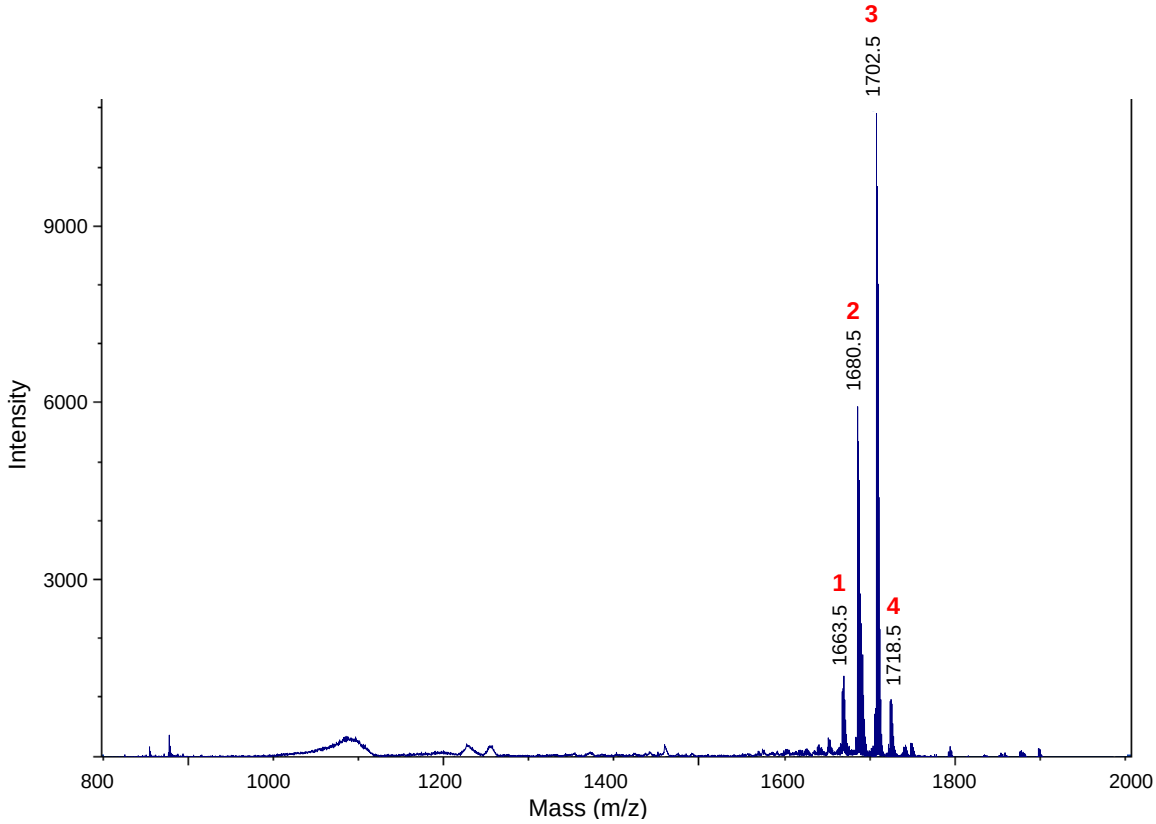

(**C**) MALDI MS/MS of parent ion *m/z* 1680.5.

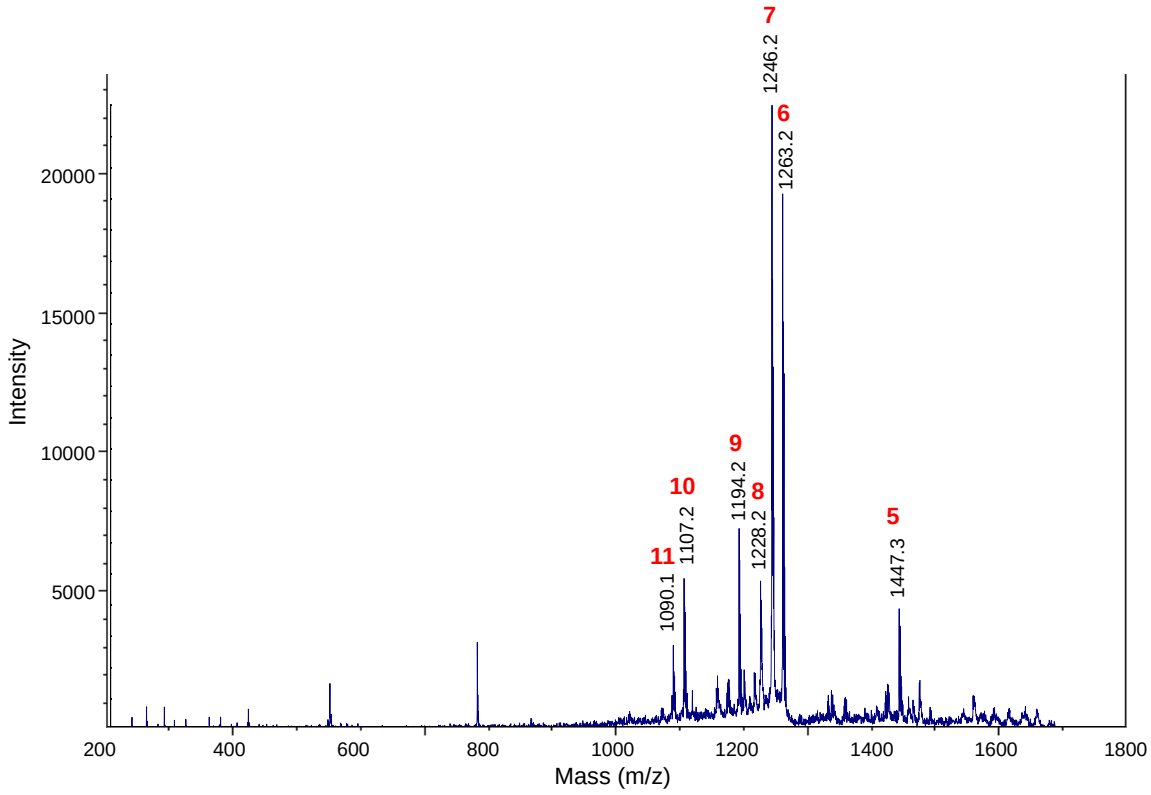

(**D**) Table and structure showing key ions and fragments in the MALDI MS and MS/MS of thiostrepton Ala4Ser.

Fragment	Expected	Observed
1. M-OH+H$^+$	1663.5	1663.5
2. M+H$^+$ (Parent ion)	1680.5	1680.5
3. M+Na$^+$	1702.5	1702.5
4. M+K$^+$	1718.5	1718.5
5. M-QA+H$^+$	1447.4	1447.3
6. M-QA-Ile1-Ala2+H$^+$	1263.3	1263.2
7. M-QA-Ile1-Ala2-OH+H$^+$	1246.3	1246.2
8. M-QA-Ile1-Ala2-OH-H_2O+H$^+$	1228.3	1228.2
9. M-QA-Ile1-Ala2-Dha3+H$^+$	1194.3	1194.2
10. M-QA-Ile1-Ala2-Dha3-Ser4+H$^+$	1107.3	1107.2
11. M-QA-Ile1-Ala2-Dha3-Ser4-OH+H$^+$	1090.2	1090.1

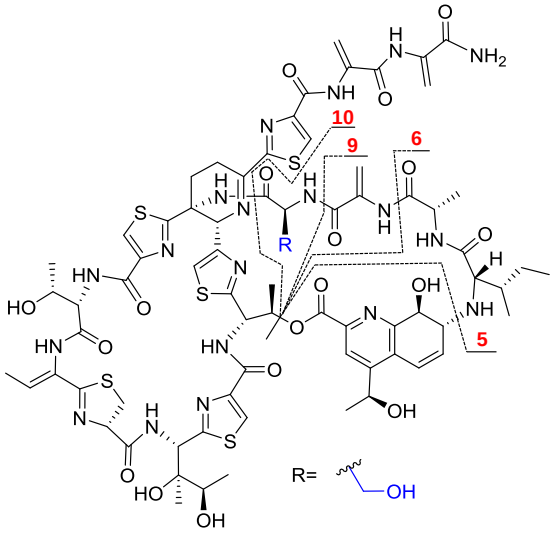

Figure D.42. MS analysis of thiostrepton Ala4Trp isolated from *S. laurentii* NDS1/int-A4W.

(**A**) HPLC-MS analysis. (1) Chromatogram extracted for *m/z* 890.3, the calculated $[M+2H]^{2+}$ ion of thiostrepton Ala4Trp. (2) Total ion chromatogram.

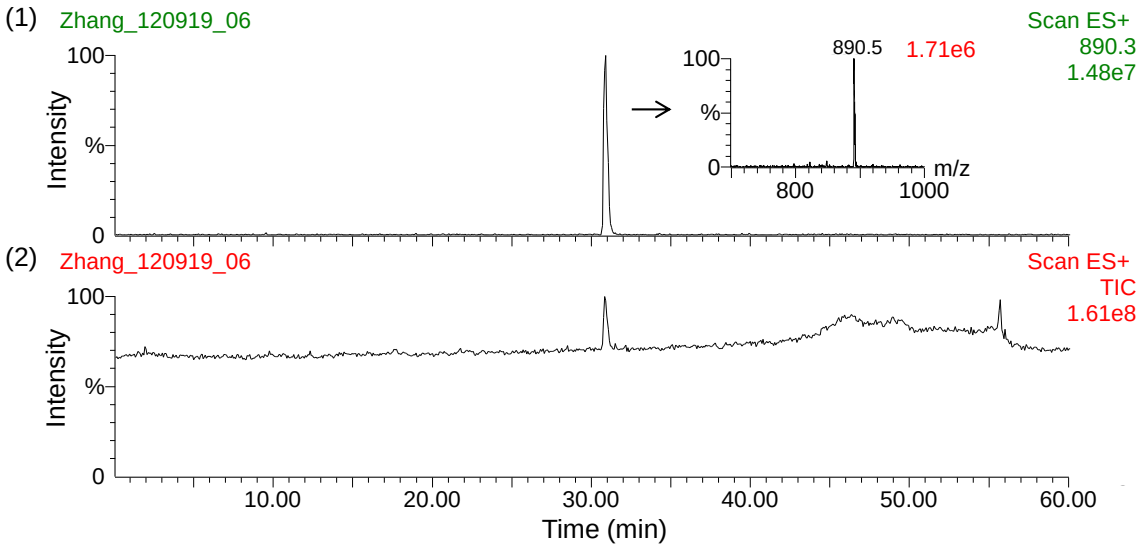

(**B**) MALDI MS spectrum of thiostrepton Ala4Trp.

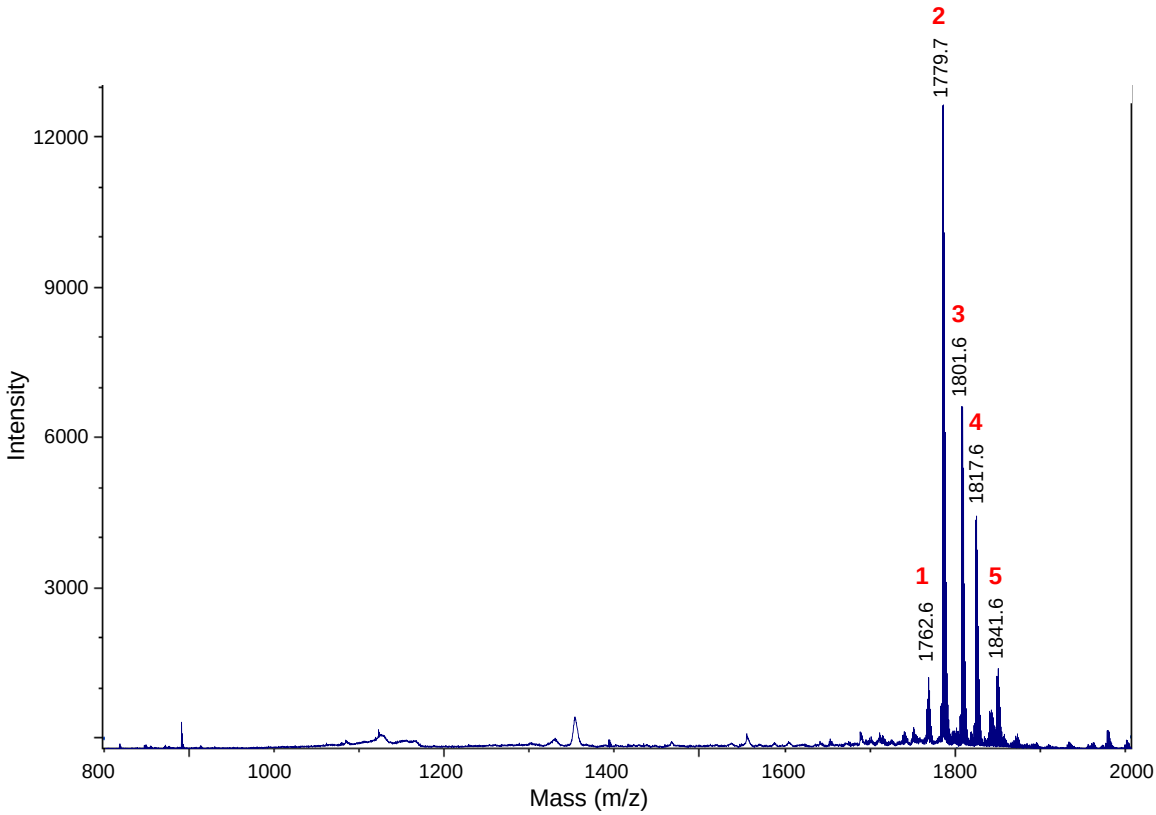

(**C**) MALDI MS/MS of parent ion *m/z* 1779.7.

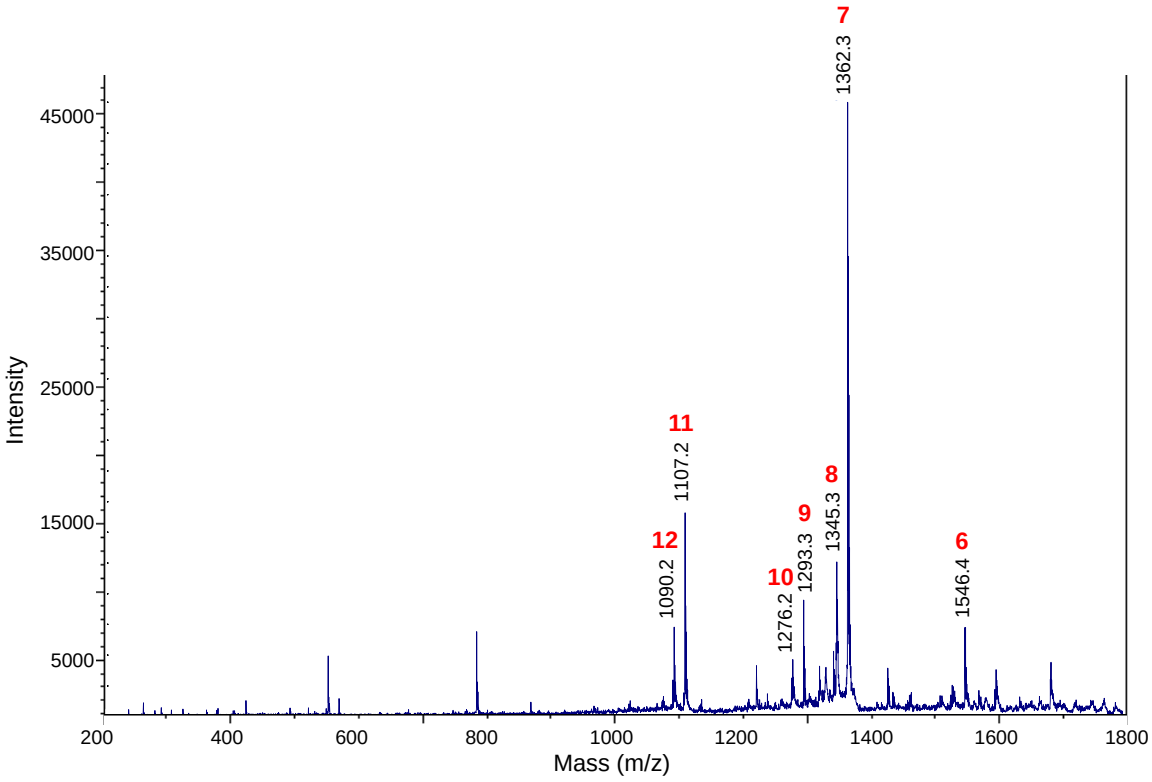

(**D**) Table and structure showing key ions and fragments in the MALDI MS and MS/MS of thiostrepton Ala4Trp.

Fragment	Expected	Observed
1. M-OH+H$^+$	1762.5	1762.6
2. M+H$^+$ (Parent ion)	1779.5	1779.7
3. M+Na$^+$	1801.5	1801.6
4. M+K$^+$	1817.5	1817.6
5. M+Cu$^+$	1841.5	1841.6
6. M-QA+H$^+$	1546.5	1546.4
7. M-QA-Ile1-Ala2+H$^+$	1362.4	1362.3
8 M-QA-Ile1-Ala2-OH+H$^+$	1345.3	1345.3
9. M-QA-Ile1-Ala2-Dha3+H$^+$	1293.3	1293.3
10. M-QA-Ile1-Ala2-Dha3-OH+H$^+$	1276.3	1276.2
11. M-QA-Ile1-Ala2-Dha3-Trp4+H$^+$	1107.3	1107.2
12. M-QA-Ile1-Ala2-Dha3-Trp4-OH+H$^+$	1090.2	1090.2

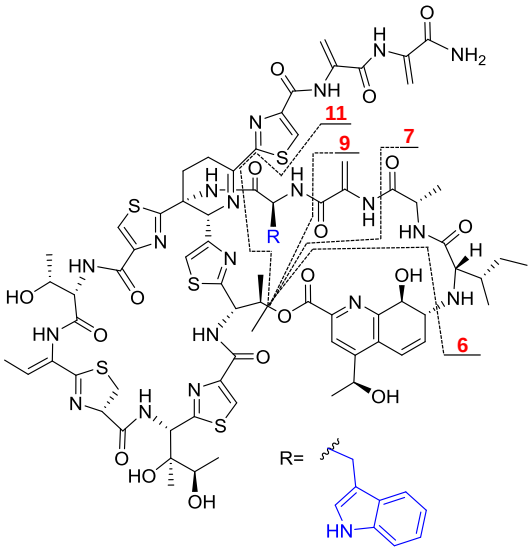

Figure D.43. MS analysis of thiostrepton Ala4Tyr isolated from *S. laurentii* NDS1/int-A4Y.

(**A**) HPLC-MS analysis. (1) Chromatogram extracted for *m/z* 878.8, the calculated $[M+2H]^{2+}$ ion of thiostrepton Ala4Tyr. (2) Total ion chromatogram

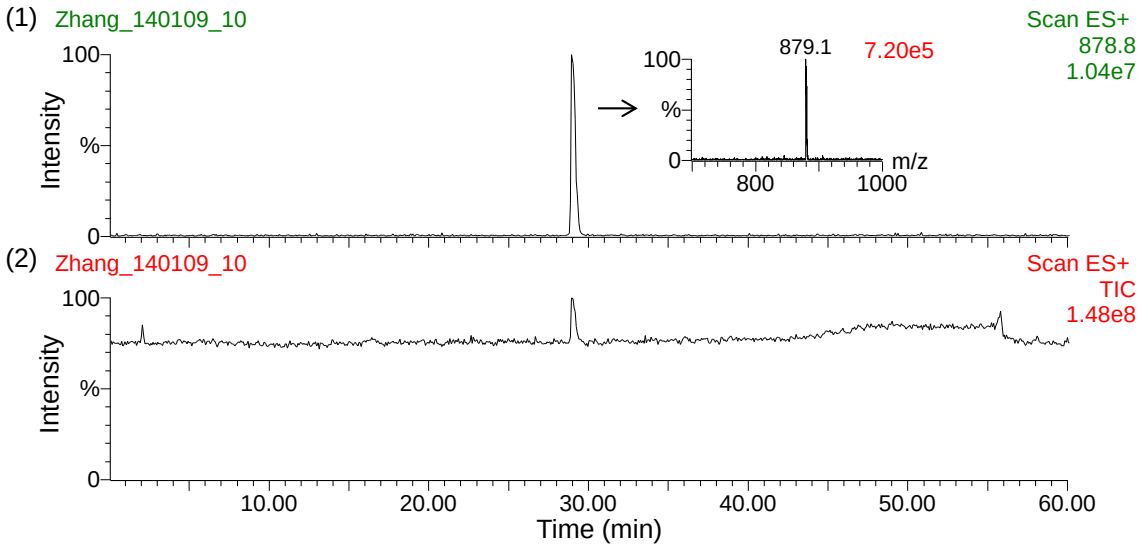

(**B**) MALDI MS spectrum of thiostrepton Ala4Tyr.

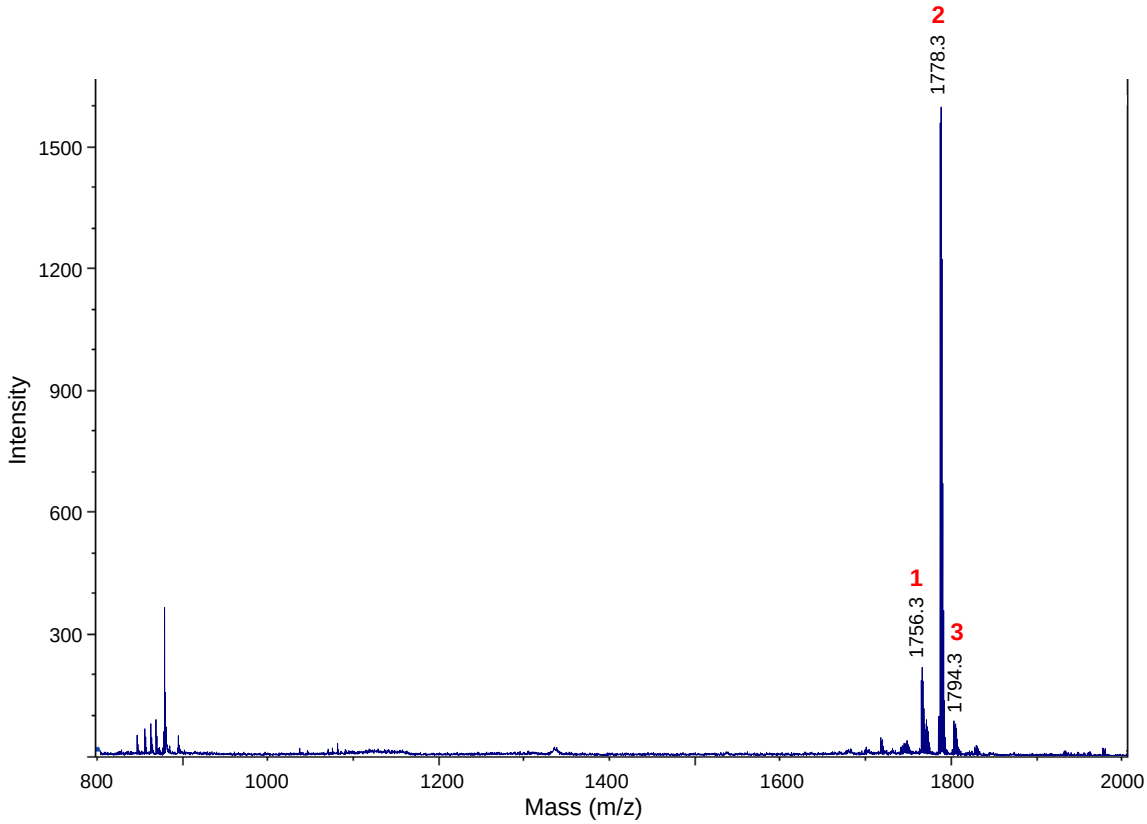

(**C**) MALDI MS/MS of parent ion *m/z* 1756.5.

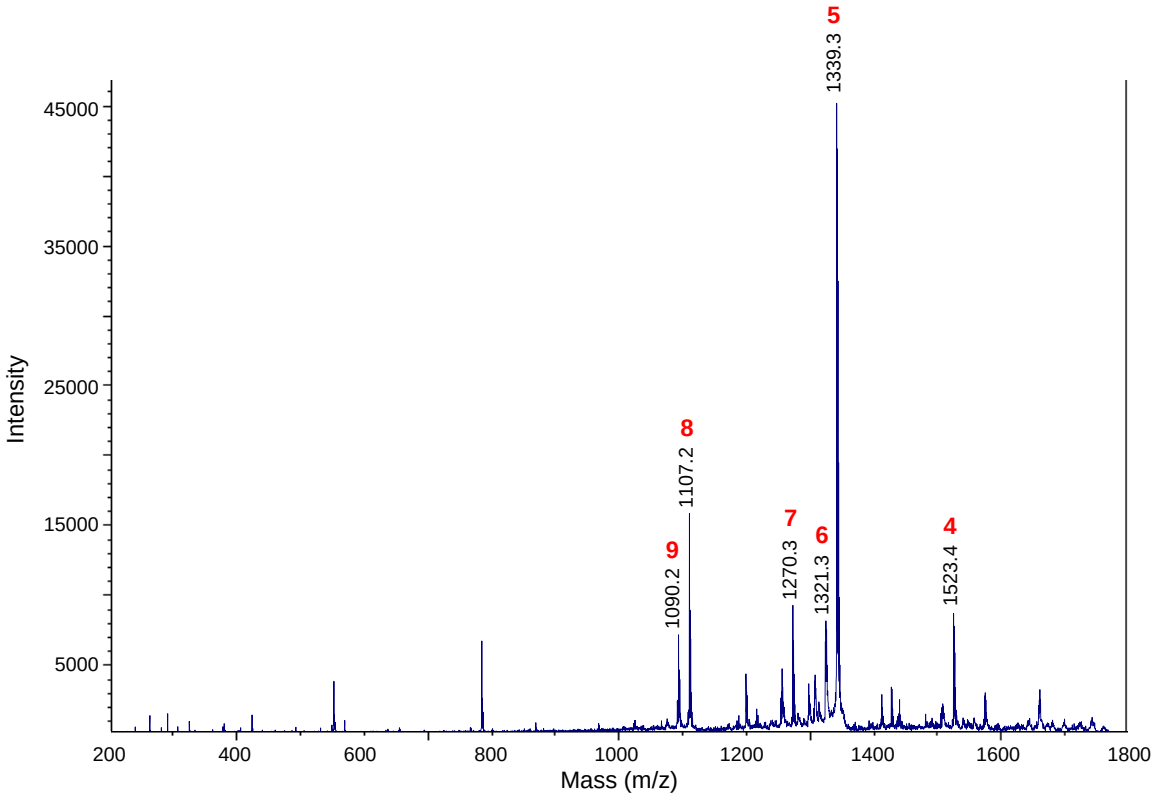

(**D**) Table and structure showing key ions and fragments in the MALDI MS and MS/MS of thiostrepton Ala4Tyr.

Fragment	Expected	Observed
1. $M+H^+$ (Parent ion)	1756.5	1756.3
2. $M+Na^+$	1778.5	1778.3
3. $M+K^+$	1794.5	1794.3
4. M-QA+H^+	1523.5	1523.4
5. M-QA-Ile1-Ala2+H^+	1339.3	1339.3
6. M-QA-Ile1-Ala2-H_2O+H^+	1321.3	1321.3
7. M-QA-Ile1-Ala2-Dha3+H^+	1270.3	1270.3
8. M-QA-Ile1-Ala2-Dha3-Tyr4+H^+	1107.3	1107.2
9. M-QA-Ile1-Ala2-Dha3-Tyr4-OH+H^+	1090.2	1090.2

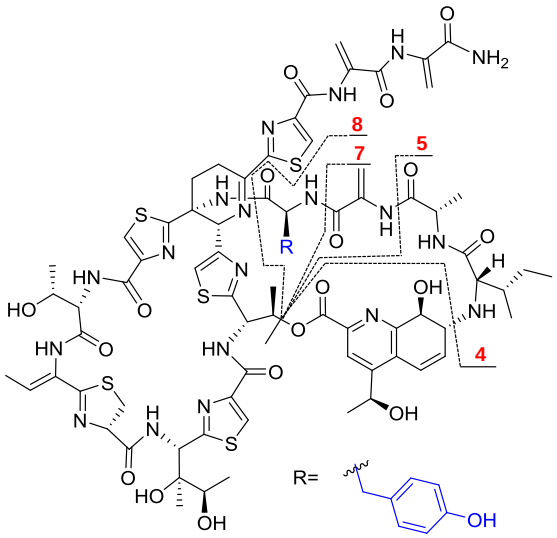

Figure D.44. MS analysis of thiostrepton Ala4Val isolated from *S. laurentii* NDS1/int-A4V.

(**A**) HPLC-MS analysis. (1) Chromatogram extracted for *m*/*z* 846.8, the calculated $[M+2H]^{2+}$ ion of thiostrepton Ala4Val. (2) Total ion chromatogram.

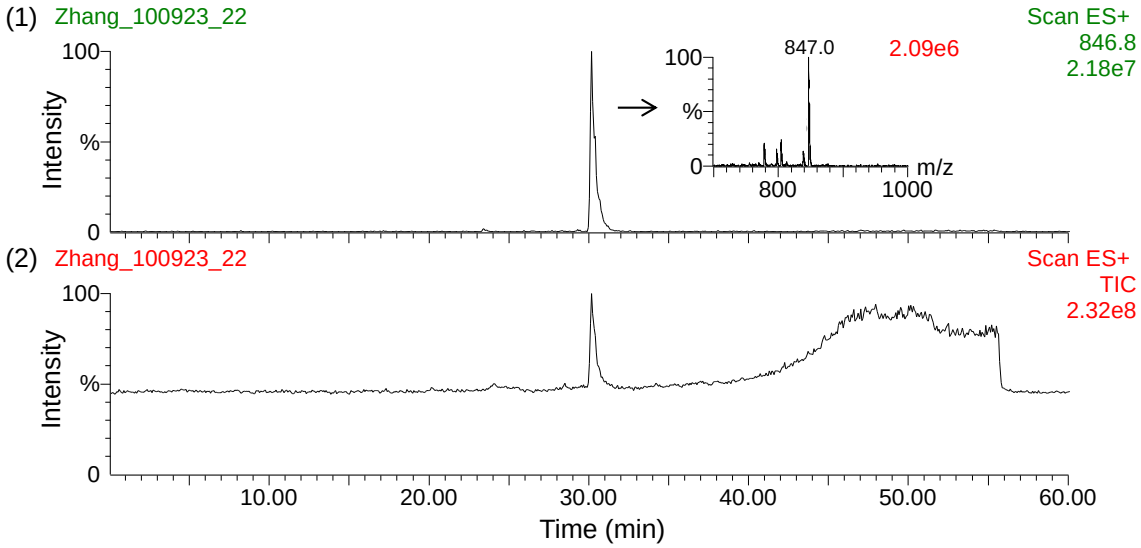

(**B**) MALDI MS spectrum of thiostrepton Ala4Val.

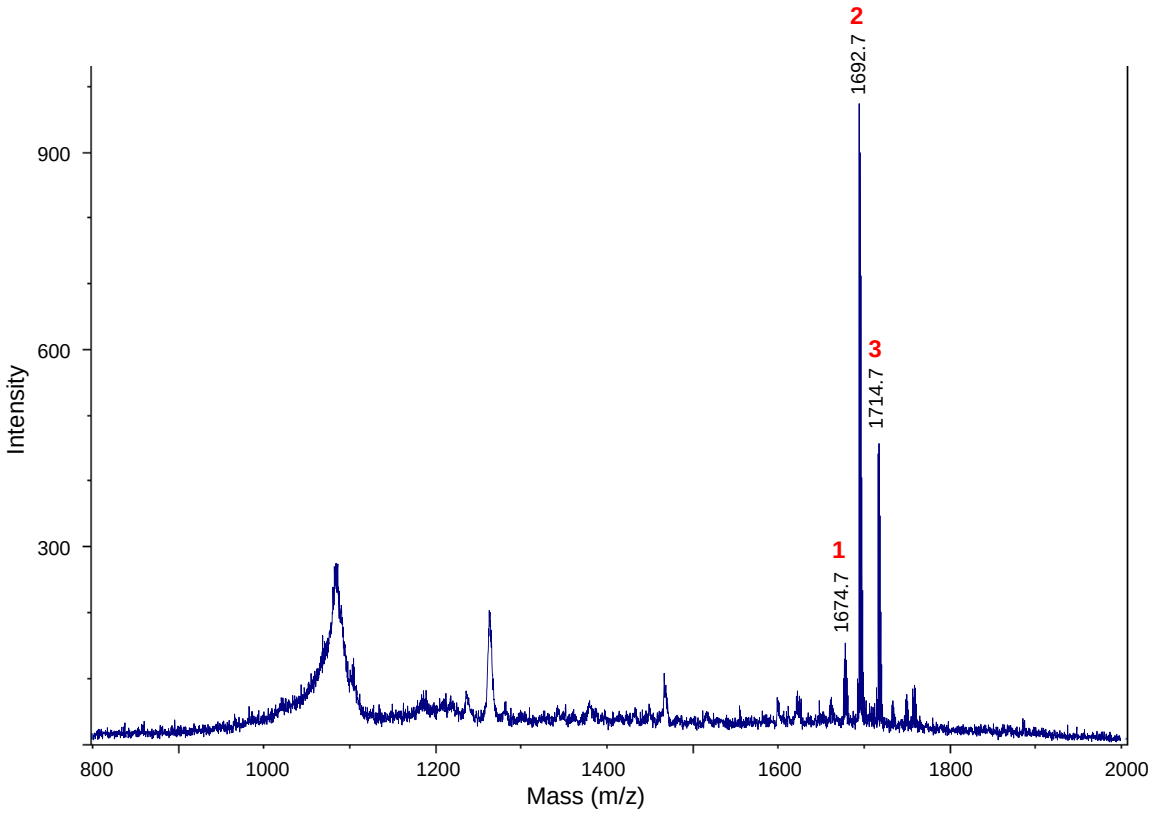

(**C**) MALDI MS/MS of parent ion *m/z* 1692.7.

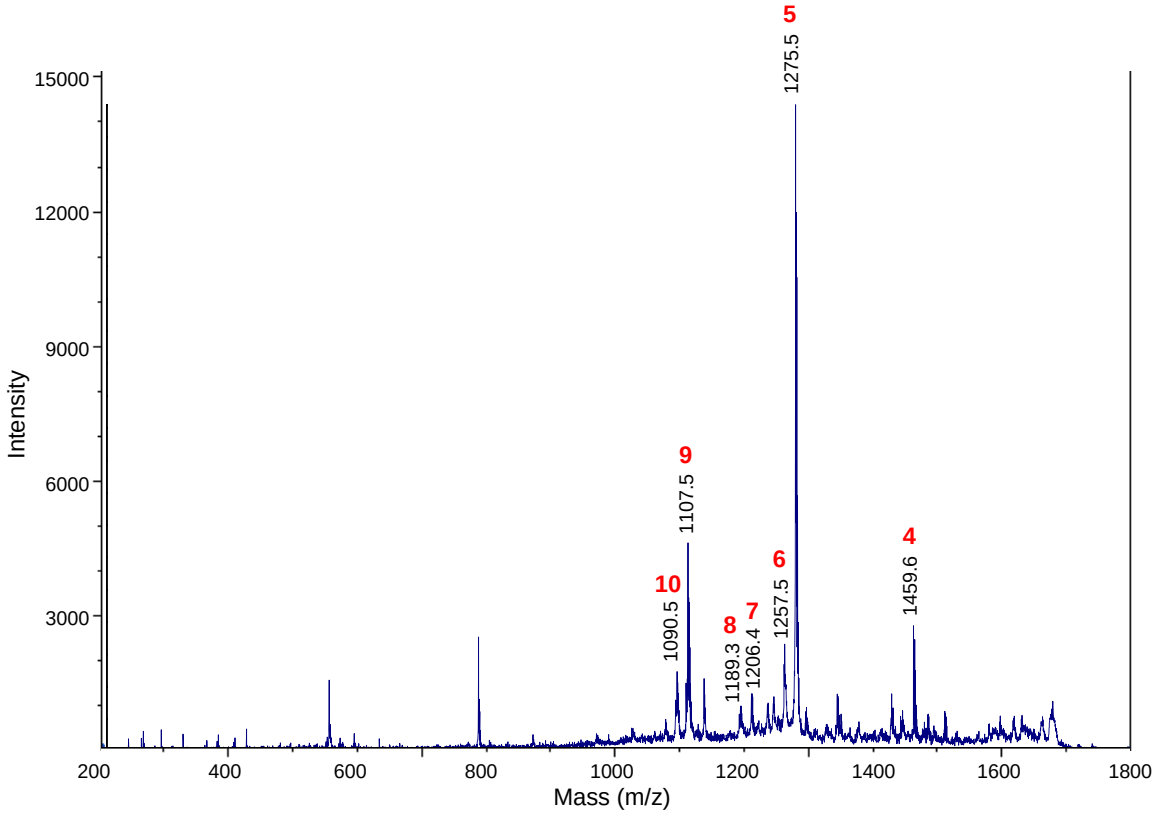

(**D**) Table and structure showing key ions and fragments in the MALDI MS and MS/MS of thiostrepton Ala4Val.

Fragment	Expected	Observed
1. M-H_2O+H^+	1674.5	1674.7
2. M+H^+ (Parent ion)	1692.5	1692.7
3. M+Na^+	1714.5	1714.7
4. M-QA+H^+	1459.5	1459.6
5. M-QA-Ile1-Ala2+H^+	1275.3	1275.5
6. M-QA-Ile1-Ala2-H_2O+H^+	1257.3	1257.5
7. M-QA-Ile1-Ala2-Dha3+H^+	1206.3	1206.4
8. M-QA-Ile1-Ala2-Dha3-OH+H^+	1189.3	1189.3
9. M-QA-Ile1-Ala2-Dha3-Val4+H^+	1107.3	1107.5
10. M-QA-Ile1-Ala2-Dha3-Val4-OH+H^+	1090.2	1090.5

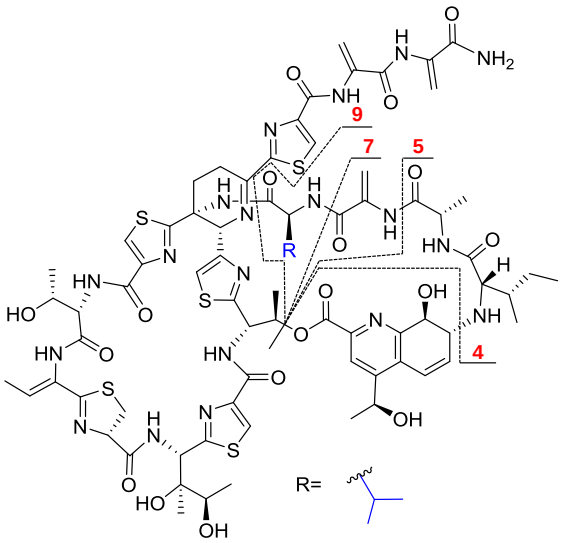

Figure D.45. Structures of SL105-1 and SL106-1.

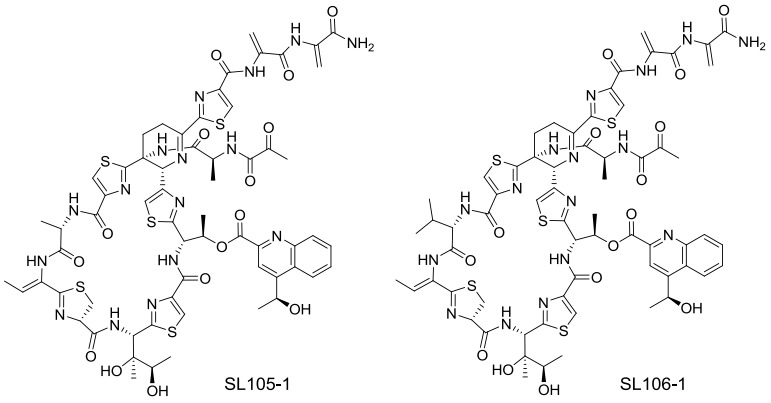

Figure D.46. Thiostrepton A, Ala4Cys F1 and F2 bound to the ribosome.
Measurements of the distances between Thr7 and quinaldic acid hydroxyl groups in thiostrepton A, thiostrepton Ala4Cys F1 and F2. (**A**) Thiostrepton A (Cyan) bound to the ribosome adapted from PDB 3CF5.[1] (**B**) Thiostrepton Ala4Cys with the *R* configuration at the α-carbon of the 17th residue (magenta) modeled into the ribosome. (**C**) Thiostrepton Ala4Cys with the *S* configuration at the α-carbon of the 17th residue (blue) modeled into the ribosome. Helices 43 and 44 of 23S rRNA are colored in orange and the ribosomal protein L11 is shown in green.

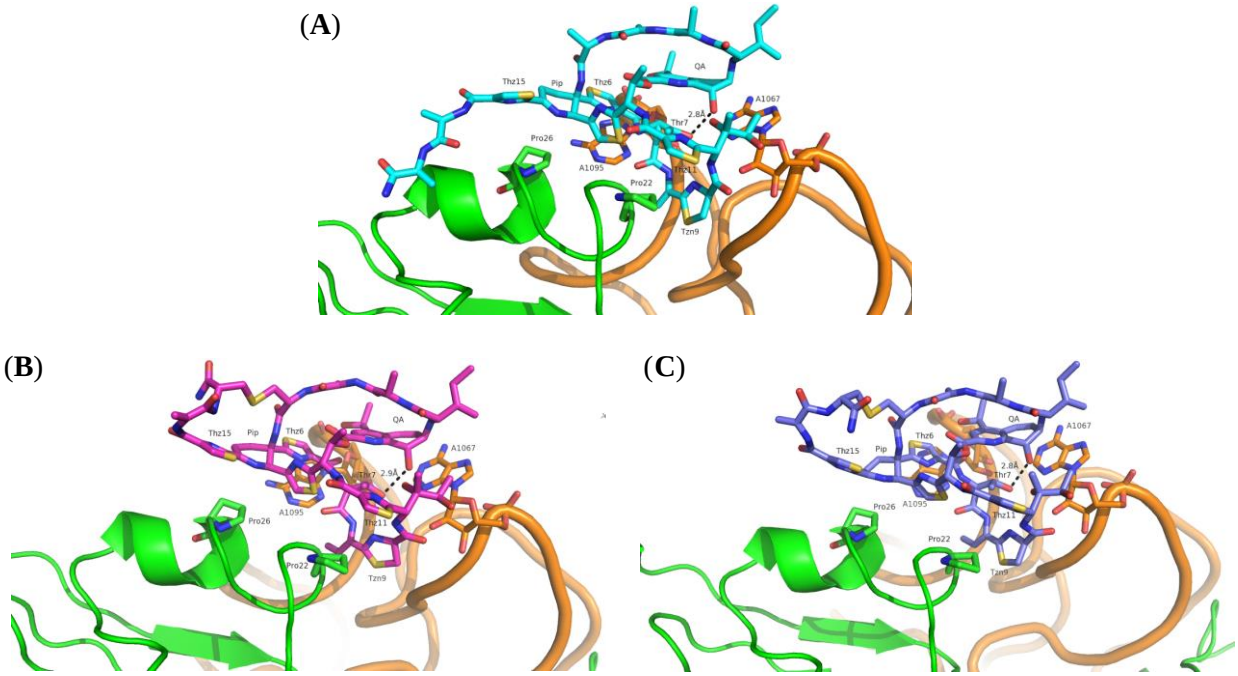

Reference:

1. Harms, J. M.; Wilson, D. N.; Schluenzen, F.; Connell, S. R.; Stachelhaus, T.; Zaborowska, Z.; Spahn, C. M.; Fucini, P., Translational regulation via L11: Molecular switches on the ribosome turned on and off by thiostrepton and micrococcin. *Mol. Cell.* **2008,** *30*, 26-38.

APPENDIX E: SUPPORTING FIGURES AND SPECTRAL DATA FOR COMPOUNDS FROM CHAPTER 5

Figure E.1. MS analysis of thiostrepton Ala2Dha isolated from *S. laurentii* NDS1/int-A2S.

(**A**) HPLC-MS analysis. (1) Chromatogram extracted for *m/z* 831.7, the calculated $[M+2H]^{2+}$ ion of thiostrepton Ala2Dha. (2) Total ion chromatogram.

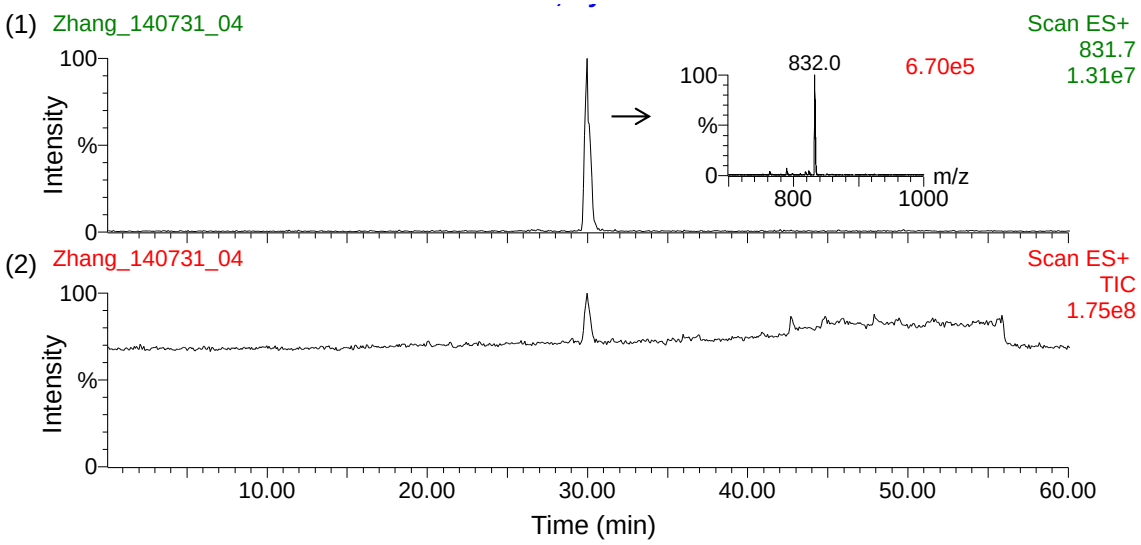

(**B**) MALDI MS spectrum of thiostrepton Ala2Dha.

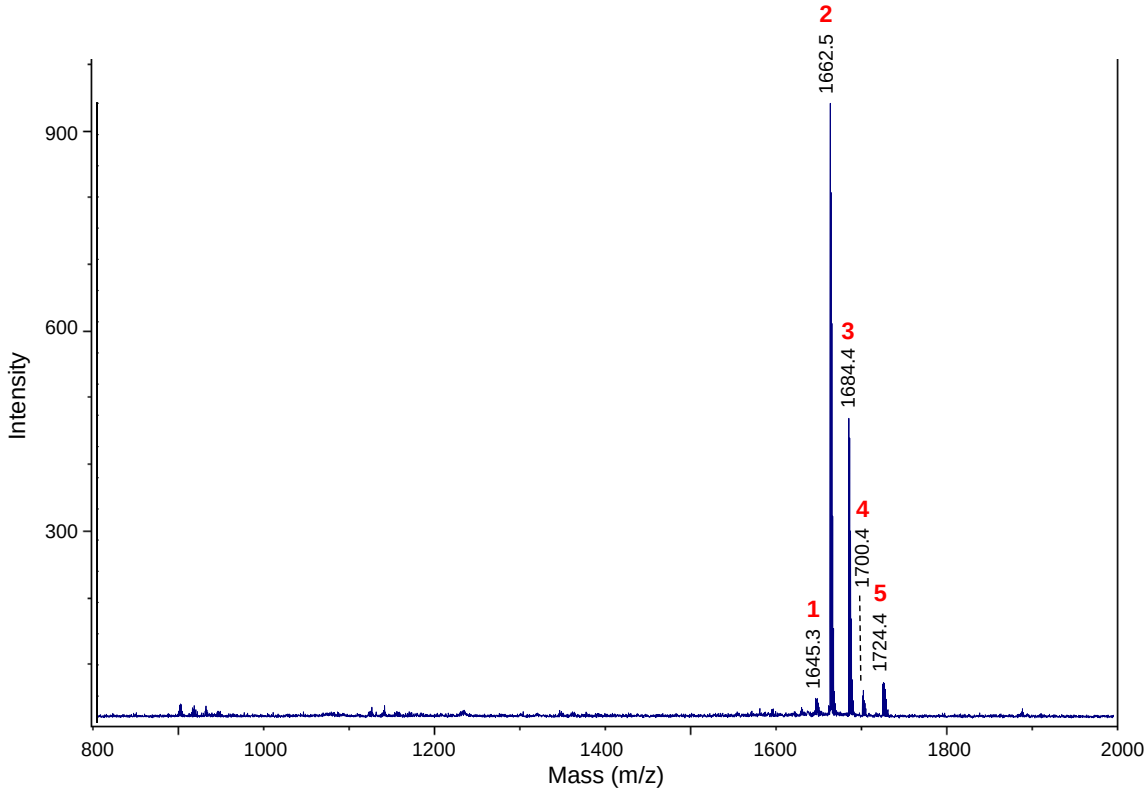

(**C**) MALDI MS/MS of parent ion *m/z* 1662.5.

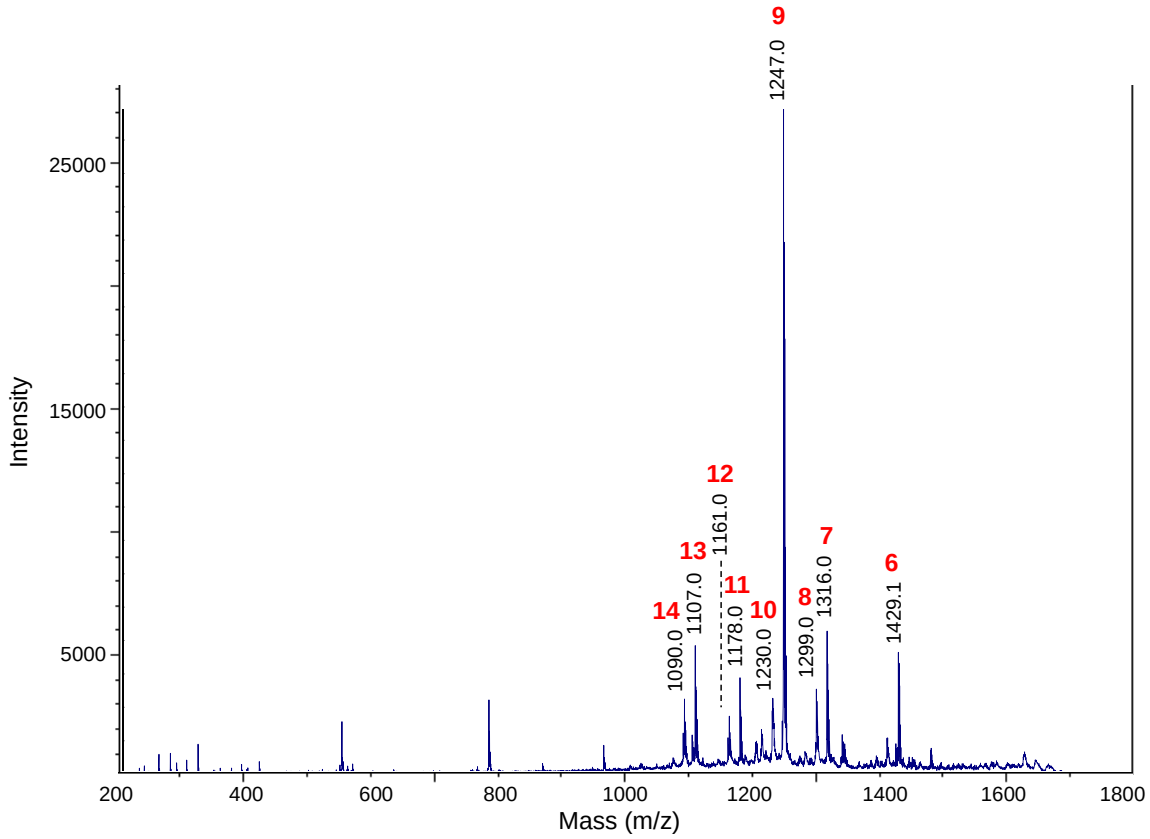

(**D**) Table and structure showing key ions and fragments in the MALDI MS and MS/MS of thiostrepton Ala2Dha.

Fragment	Expected	Observed
1. M-OH+H$^+$	1645.5	1645.3
2. M+H$^+$ (Parent ion)	1662.5	1662.5
3. M+Na$^+$	1684.5	1684.4
4. M+K$^+$	1700.4	1700.4
5. M+Cu$^+$	1724.4	1724.4
6. M-QA+H$^+$	1429.4	1429.1
7. M-QA-Ile1+H$^+$	1316.3	1316.0
8. M-QA-Ile1-OH+H$^+$	1299.3	1299.0
9. M-QA-Ile1-Dha2+H$^+$	1247.3	1247.0
10. M-QA-Ile1-Dha2-OH+H$^+$	1230.3	1230.0
11. M-QA-Ile1-Dha2-Dha3+H$^+$	1178.3	1178.0
12. M-QA-Ile1-Dha2-Dha3-OH+H$^+$	1161.3	1161.0
13. M-QA-Ile1-Dhaa2-Dha3-Dha4+H$^+$	1107.3	1107.0
14. M-QA-Ile1-Dha2-Dha3-Alaa4-OH+H$^+$	1090.2	1090.0

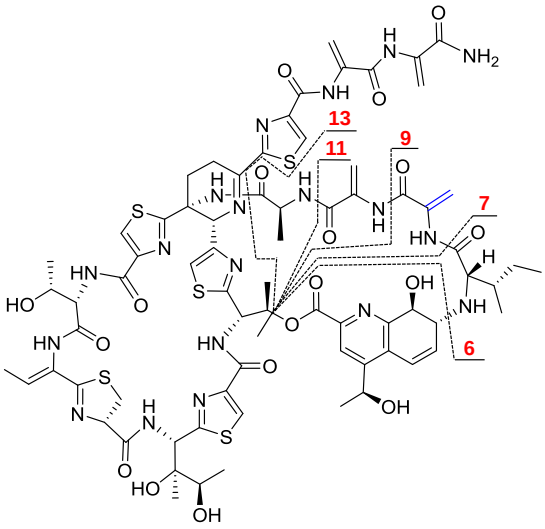

Figure E.2. Structure and numbering system used for thiostrepton Ala2Dha.

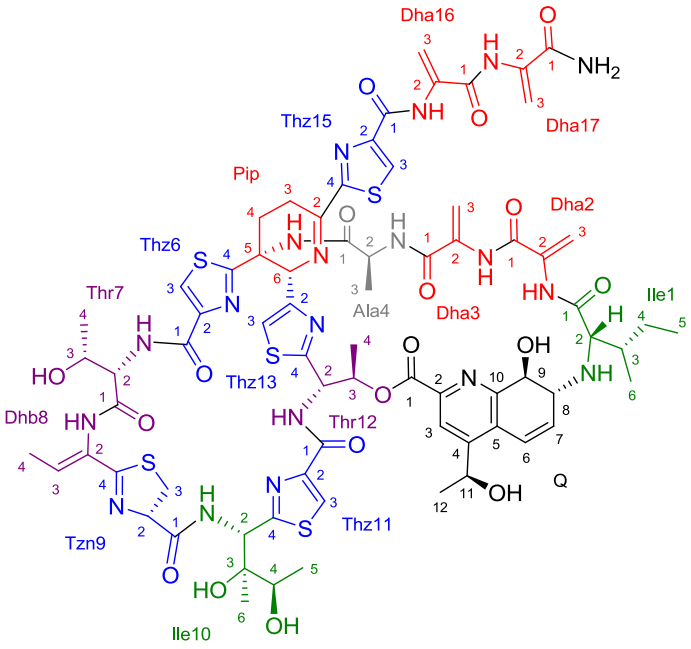

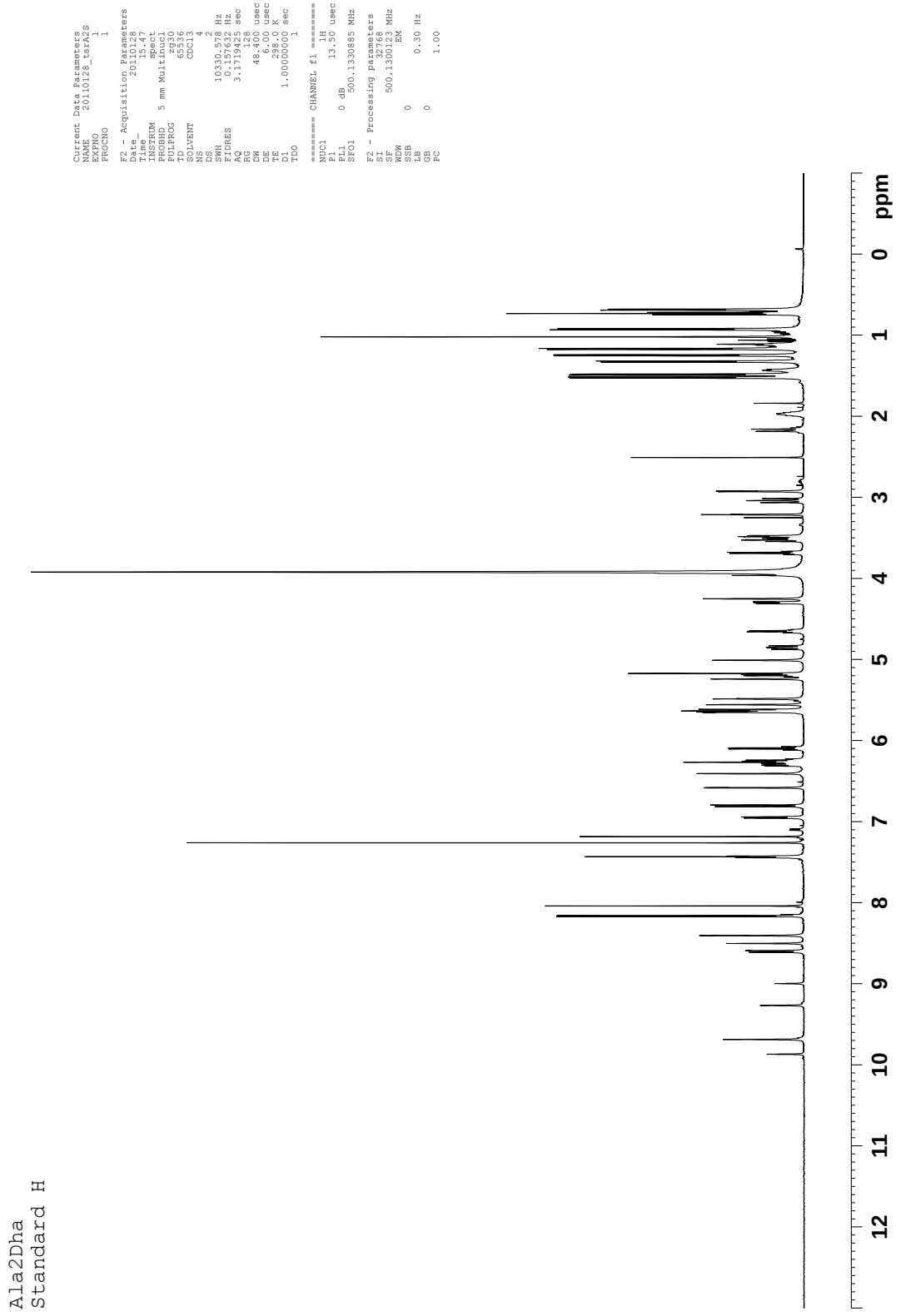

Figure E.3. ^{1}H NMR spectrum of thiostrepton Ala2Dha (500 MHz, $CDCl_3$-CD_3OD 4:1, 25 °C).

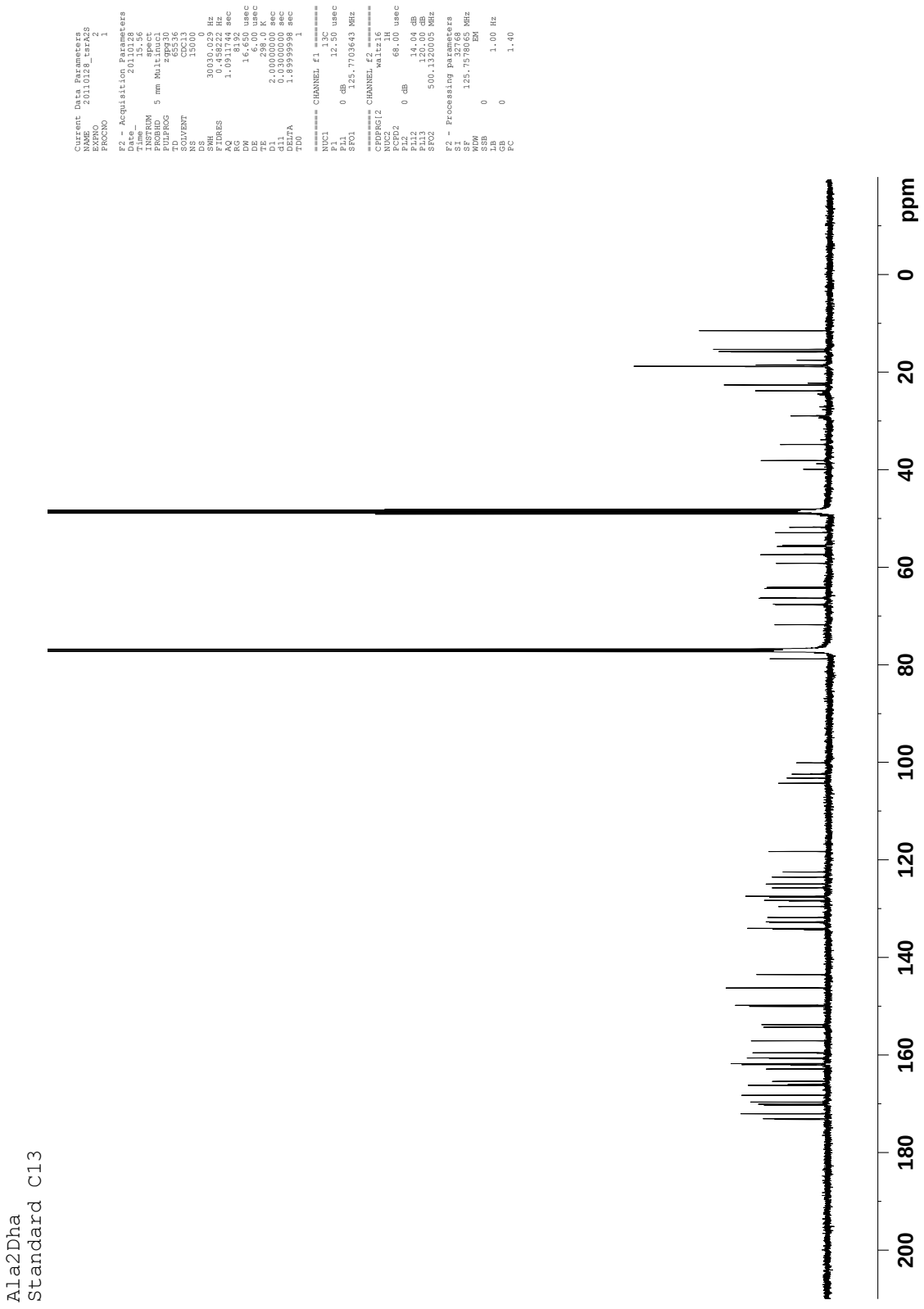

Figure E.4. ^{13}C NMR spectrum of thiostrepton Ala2Dha (125 MHz, $CDCl_3$-CD_3OD 4:1, 25 °C).

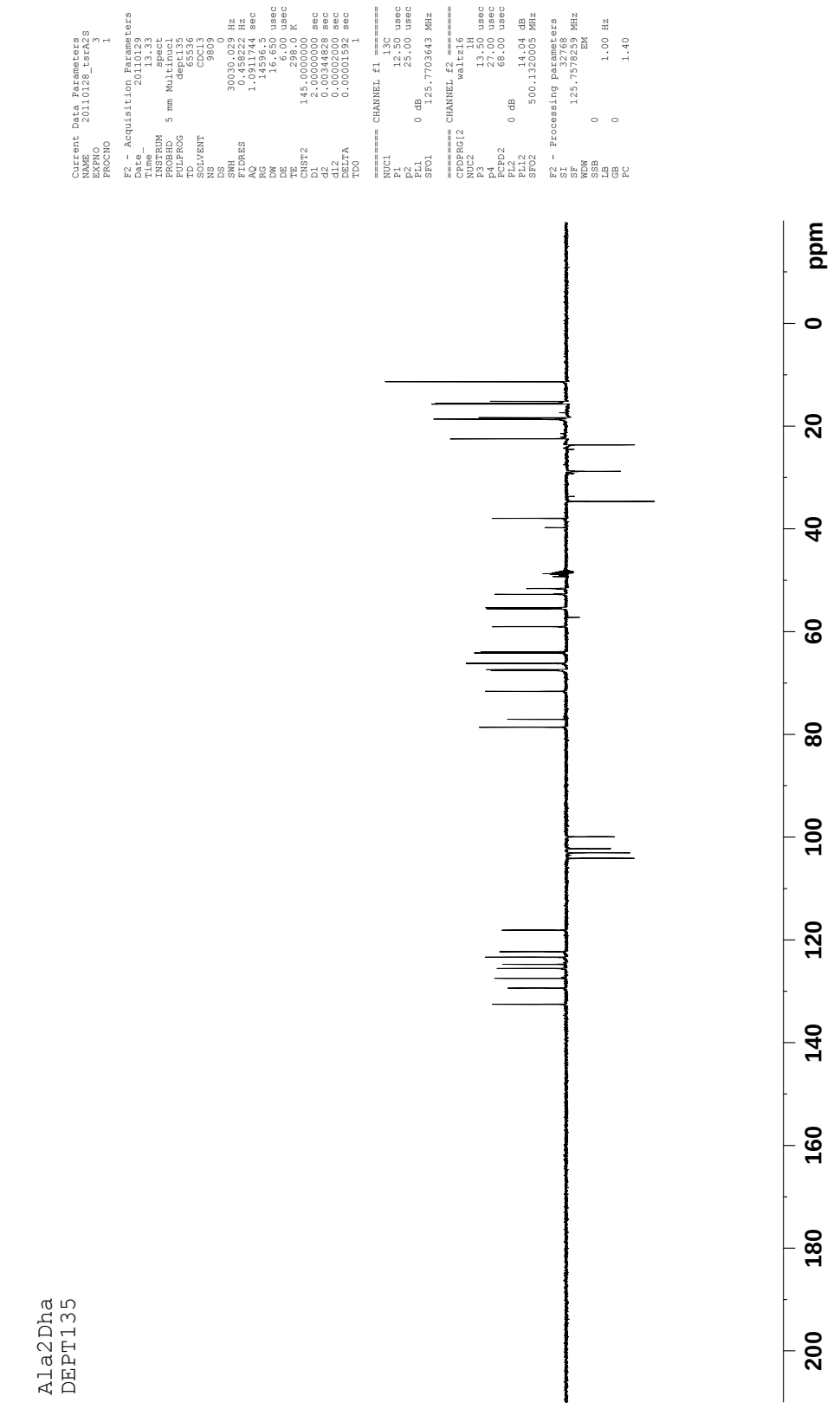

Figure E.5. DEPT-135 NMR spectrum of thiostrepton Ala2Dha (125 MHz, $CDCl_3$-CD_3OD 4:1, 25 °C).

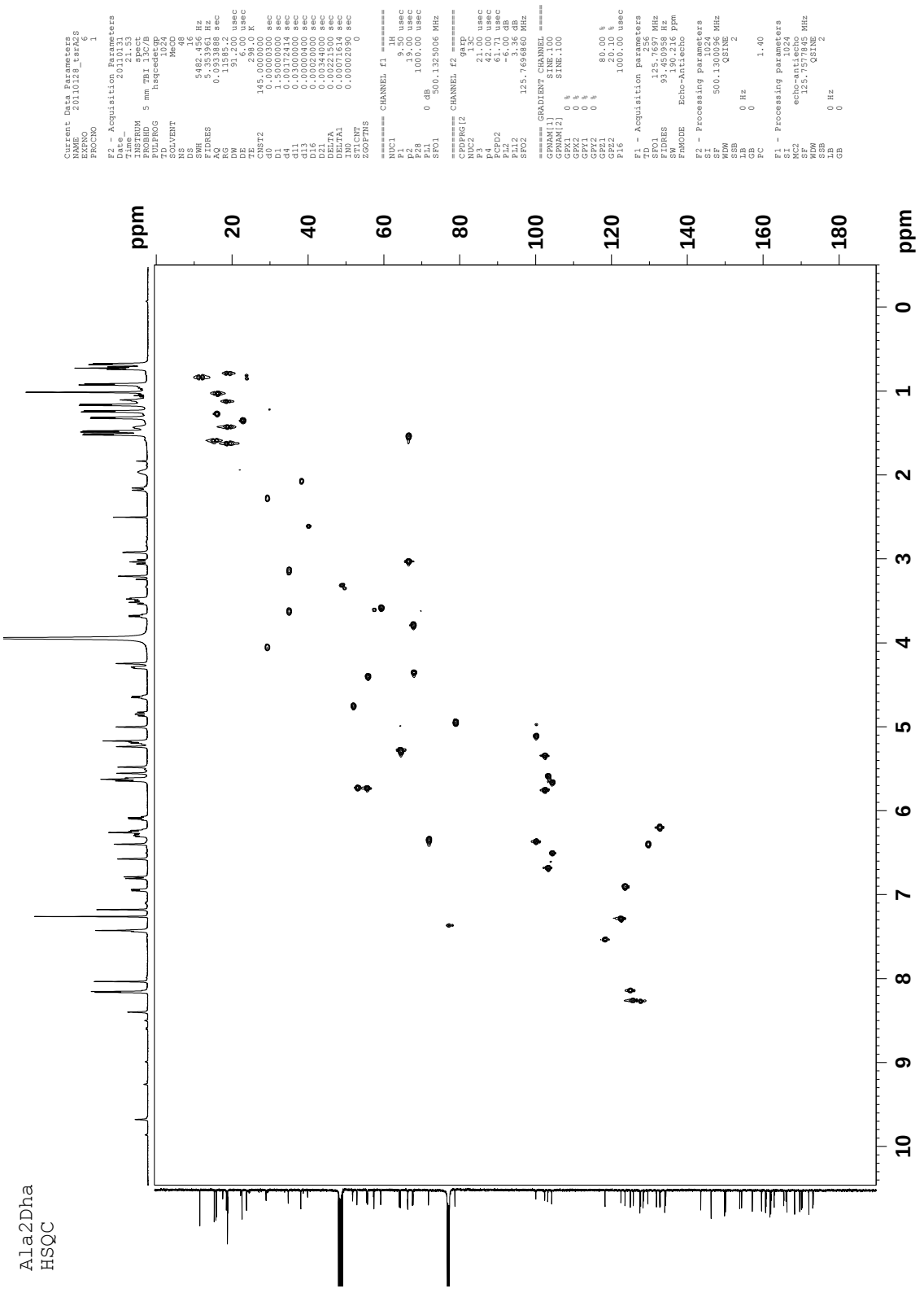

Figure E.6. gHSQC spectrum of thiostrepton Ala2Dha (500 MHz, $CDCl_3$-CD_3OD 4:1, 25 °C).

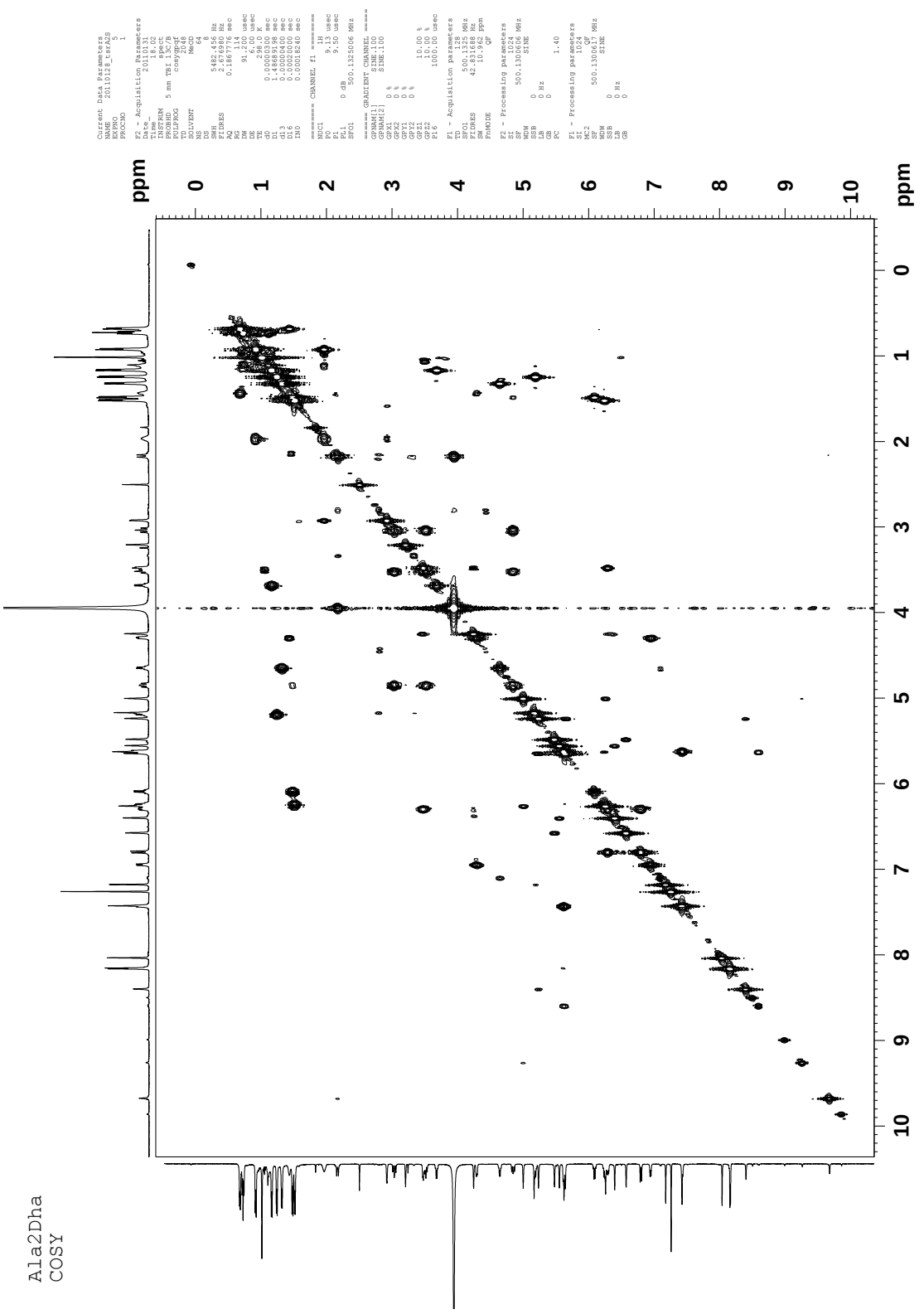

Figure E.7. gCOSY spectrum of thiostrepton Ala2Dha (500 MHz, $CDCl_3$-CD_3OD 4:1, 25 °C).

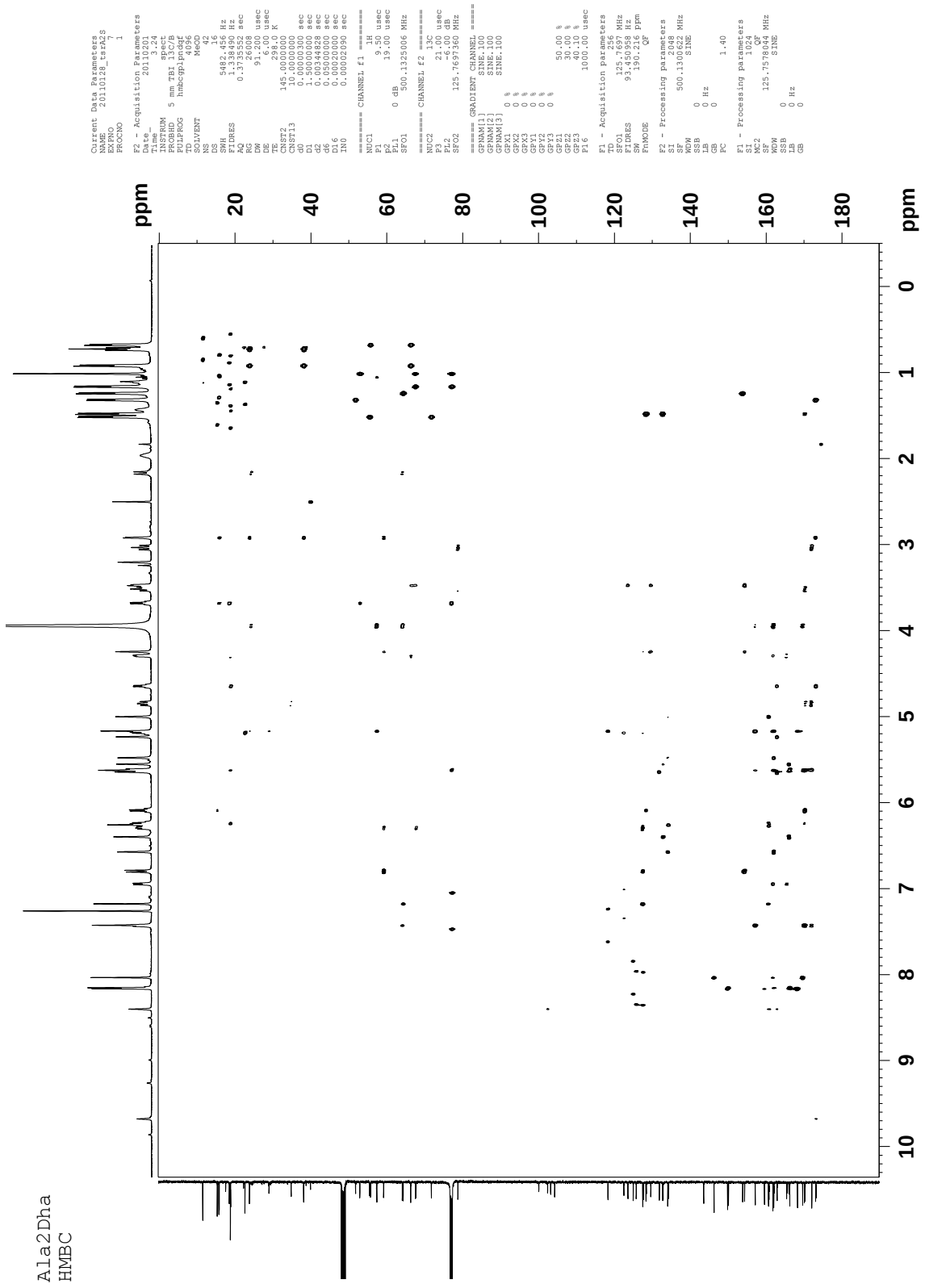

Figure E.8. gHMBC spectrum of thiostrepton Ala2Dha (500 MHz, $CDCl_3$-CD_3OD 4:1, 25 °C).

Table E.1. ^{1}H and ^{13}C NMR assignments of thiostrepton Ala2Dha

Position	δ_C [ppm]; mult	δ_H [ppm]; (mult, J in Hz)	HMBC[a]	COSY[b]
Ile1				
Ile1-1	173.0; C q			
Ile1-2	66.3; CH	2.93 (d, 3.8)	Ile1-1; Ile1-3; Ile-4; Ile1-6; Q8	Ile1-3
Ile1-3	38.1; CH	2.00-1.94 (m)		Ile1-2; Ile1-4-H_A; Ile1-4-H_B; Ile1-6
Ile1-4	23.8; CH_2	H_A: 1.14-1.10 (m)	Ile1-5	Ile1-3; Ile1-4-H_B; Ile1-5
		H_B: 0.99-0.94 (m)		Ile1-3, Ile1-4-H_A; Ile1-5
Ile1-5	11.5; CH_3	0.73 (t, 7.1)	Ile1-3; Ile1-4	Ile1-4-H_A; Ile1-4-H_B
Ile1-6	15.7; CH_3	0.92 (d, 6.9)	Ile1-2; Ile1-3; Ile1-4	Ile1-3
Dha2				
Dha2-1	160.7; C q			
Dha2-2	134.2; C q			
Dha2-3	100.1;	H_A: 6.27 (br s)	Dha2-1; Dha2-2	Dha2-3-H_B
	CH_2	H_B: 5.01 (d, 1.4)	Dha2-1; Dha2-2	Dha2-3-H_A
Dha3				
Dha3-1	162.8; C q			
Dha3-2	131.8; C q			
Dha3-3	102.4;	H_A: 5.65 (d, 2.2)	Dha3-1; Dha3-2	Dha3-3-H_B
	CH_2	H_B: 5.24 (br s)	Dha3-1	Dha3-3-H_A; Dha3-NH
Dha3-NH[d]		8.40 (s)	Dha2-1; Dha3-1; Dha3-3	Dha3-3-H_B
Ala4				
Ala4-1	173.1; C q			
Ala4-2	51.8; CH	4.65 (q, 6.6)	Dha3-1; Ala4-1; Ala4-3	Ala4-3; Ala4-NH
Ala4-3	18.8; CH_3	1.32 (d, 6.7)	Ala4-1; Ala4-2	Ala4-2
Ala4-NH[d]		7.10 (d, 8.2)		Ala4-2
Pip				
Pip-2	161.9; C q			
Pip-3	24.5; CH_2	H_A: 3.36-3.32 (m)		Pip-4-H_B
		H_B: 2.83-2.77 (m)		Pip-4-H_A; Pip-4-H_B
Pip-4	28.9; CH_2	H_A: 3.95 (m)	Pip-2; Pip-3; Pip-5; Pip-6; Thz6-4; Thz13-2	Pip-4-H_B
		H_B: 2.17 (m)	Pip-3; Pip-6	Pip-3-H_A; Pip-4-H_A; Pip-3-H_B
Pip-5	57.3; C q			
Pip-6	64.1; CH	5.17 (s)	Pip-2; Pip-4; Pip-5; Thz13-2; Thz13-3; Thz15-4	Pip-3-H_A; Pip-3-H_B
Thz6				
Thz6-1	161.7; C q			
Thz6-2	146.2; C q			
Thz6-3	124.9; CH	8.04 (s)	Thz6-1; Thz6-2; Thz6-4	
Thz6-4	169.6; C q			
Thr7				
Thr7-1	165.4; C q			
Thr7-2	55.7; CH	4.30 (dd, 7.7, 3.6)	Thz6-1; Thr7-1; Thr7-3; Thr7-4	Thr7-3; Thr7-NH
Thr7-3	66.3; CH	1.46-1.40 (m)	Thr7-4	Thr7-2; Thr7-4
Thr7-4	18.8; CH_3	0.68 (d, 6.3)	Thr7-2; Thr7-3	Thr7-3
Thr7-NH[d]		6.95 (d, 7.6)	Thz6-1; Thr7-1	Thr7-2
Dhb8				
Dhb8-2	128.3; C q			
Dhb8-3	132.7; CH	6.10 (q, 7.0)	Dhb8-2; Dhb8-4; Tzn9-4	Dhb8-4
Dhb8-4	15.3; CH_3	1.48 (d, 7.3)	Dhb8-2; Dhb8-3; Tzn9-4	Dhb8-3
Tzn9				
Tzn9-1	172.0; C q			
Tzn9-2	78.8; CH	4.85 (dd, 12.8, 9.0)	Tzn9-1; Tzn9-3; Tzn9-4	Tzn9-3-H_A; Tzn9-3-H_B
Tzn9-3	34.8; CH_2	H_A: 3.52 (dd, 11.2, 9.0)	Tzn9-2; Tzn9-4	Tzn9-2; Tzn9-3-H_B
		H_B: 3.04 (dd, 12.8, 11.5)	Tzn9-1; Tzn9-2	Tzn9-2; Tzn9-3-H_A
Tzn9-4	170.2; C q			
Ile10				
Ile10-2	52.9; CH	5.62 (d, 5.1)	Tzn9-1; Ile10-3; Thz11-4	Ile10-NH
Ile10-3	77.1[c]; C q			
Ile10-4	67.6; CH	3.68 (q, 6.4)	Ile10-2; Ile10-3; Ile10-5; Ile10-6	Ile10-5
Ile10-5	15.8; CH_3	1.17 (d, 6.3)	Ile10-3; Ile10-4	Ile10-4
Ile10-6	18.5; CH_3	1.02 (s)	Ile10-2; Ile10-3; Ile10-4	
Ile10-NH[d]		7.43 (d, 9.8)	Tzn9-1	Ile10-2

Position	δ_C [ppm]; mult	δ_H [ppm]; (mult, J in Hz)	HMBC[a]	COSY[b]
Thz11				
Thz11-1	162.0; C q			
Thz11-2	150.0; C q			
Thz11-3	125.7; CH	8.16 (s)	Thz11-1; Thz11-2; Thz11-4	
Thz11-4	166.2; C q			
Thr12				
Thr12-2	55.5; CH	5.64 (d, 4.1)	Thz11-1; Thr12-4; Thz13-2; Thz13-4	Thr12-3, Thr12-NH
Thr12-3	71.8; CH	6.25 (q, 6.7)	Thr12-4; Thz13-4; Q-1	Thr12-2, Thr12-4
Thr12-4	18.8; CH_3	1.52 (d, 6.3)	Thr12-2; Thr12-3	Thr12-3
Thr12-NH[d]		8.60 (d, 8.9)		Thr12-2
Thz13				
Thz13-2	157.1; C q			
Thz13-3	118.3; CH	7.43 (s)	Pip-6; Thz13-2; Thz13-4	
Thz13-4	170.0; C q			
Thz15				
Thz15-1	159.5; C q			
Thz15-2	149.8; C q			
Thz15-3	127.6; CH	8.17 (s)	Thz15-1; Thz15-2; Thz15-4	
Thz15-4	168.2; C q			
Dha16				
Dha16-1	162.0; C q			
Dha16-2	134.0; C q			
Dha16-3	103.2; CH_2	H_A: 6.58 (d, 2.2)	Dha16-1; Dha16-2	Dha16-3-H_B
		H_B: 5.48 (d, 2.2)	Dha16-1; Dha16-2	Dha16-3-H_A
Dha17				
Dha17-1	166.0; C q			
Dha17-2	132.8; C q			
Dha17-3	104.3; CH_2	H_A: 6.41 (d, 1.2)	Dha17-1; Dha17-2	Dha17-3-H_B
		H_B: 5.56 (d, 1.6)	Dha17-1; Dha17-2	Dha17-3-H_A
Q				
Q-1	160.6; C q			
Q-2	143.5; C q			
Q-3	122.5; CH	7.18 (s)	Q-1; Q-5; Q-11	
Q-4	153.8; C q			
Q-5	127.4; C q			
Q-6	123.5; CH	6.80 (d, 10.1)	Q-5; Q-8; Q-10	Q-7
Q-7	129.5; CH	6.30 (dd, 9.8, 5.7)	Q-5; Q-8; Q-9	Q-6; Q-8; Q-9
Q-8	59.2; CH	3.48 (dd, 5.9, 1.8)	Q-6; Q-7; Q-9; Q-10; Ile1-2	Q-7; Q-9
Q-9	67.7; CH	4.25 (s)	Q-5; Q-7; Q-8; Q-10	Q-7; Q-8
Q-10	154.3; C q			
Q-11	64.3; CH	5.19 (q, 6.6)	Q-3; Q-5; Q-12	Q-12
Q-12	22.6; CH_3	1.25 (d, 6.6)	Q-4; Q-11	Q-11

[a] HMBC correlations are from the proton to the indicated carbon.
[b] COSY correlations are from the proton to the proton attached to the indicated position.
[c] The δ of this resonance was determined by HMBC due to overlap with the $CDCl_3$ resonance.
[d] Only those amide resonances demonstrating COSY correlations to neighboring protons were assigned.

Figure E.9. MS analysis of thiostrepton Ala2Dhb isolated from *S. laurentii* NDS1/int-A2T.

(**A**) HPLC-MS analysis. (1) Chromatogram extracted for *m*/*z* 838.8, the calculated $[M+2H]^{2+}$ ion of thiostrepton Ala2Dhb. (2) Total ion chromatogram.

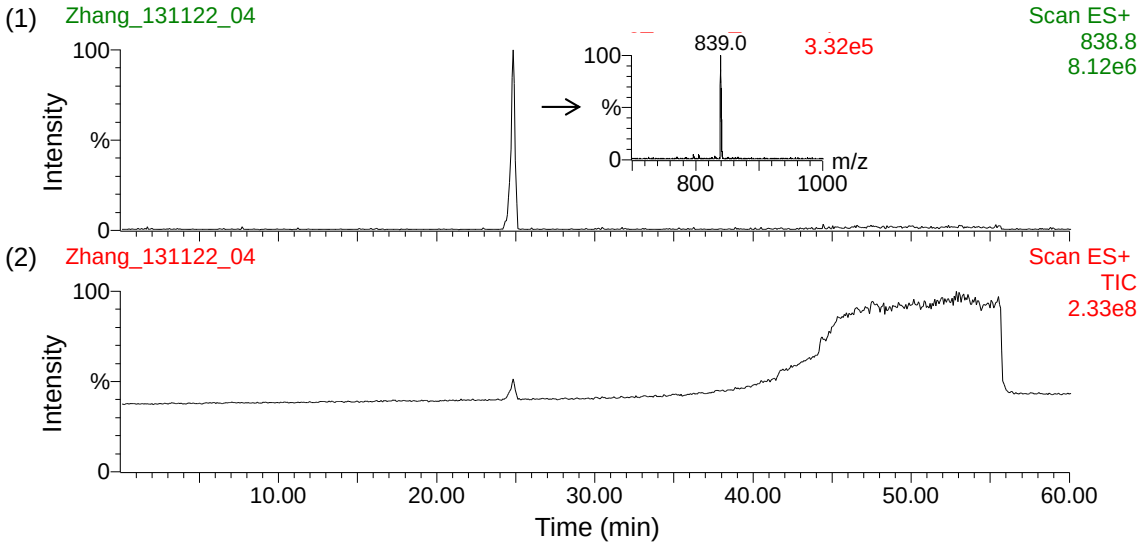

(**B**) MALDI MS spectrum of thiostrepton Ala2Dhb.

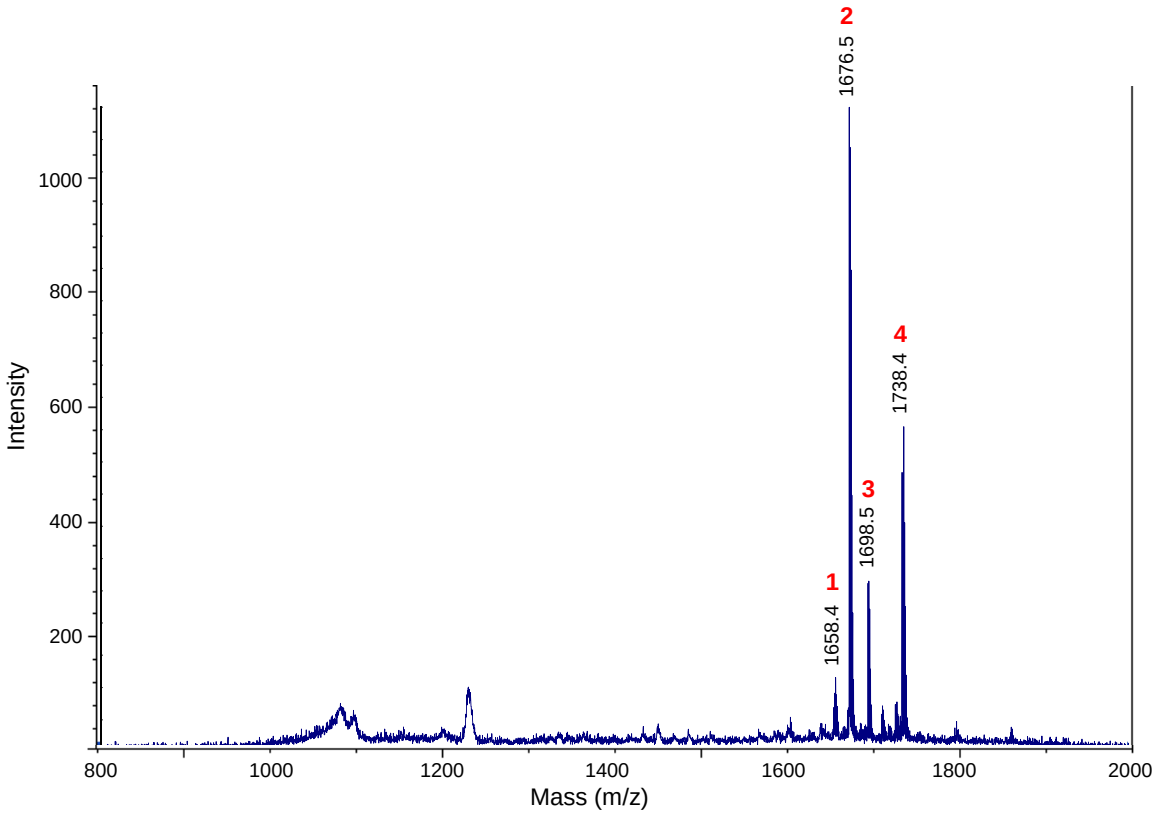

(**C**) MALDI MS/MS of parent ion *m/z* 1676.5.

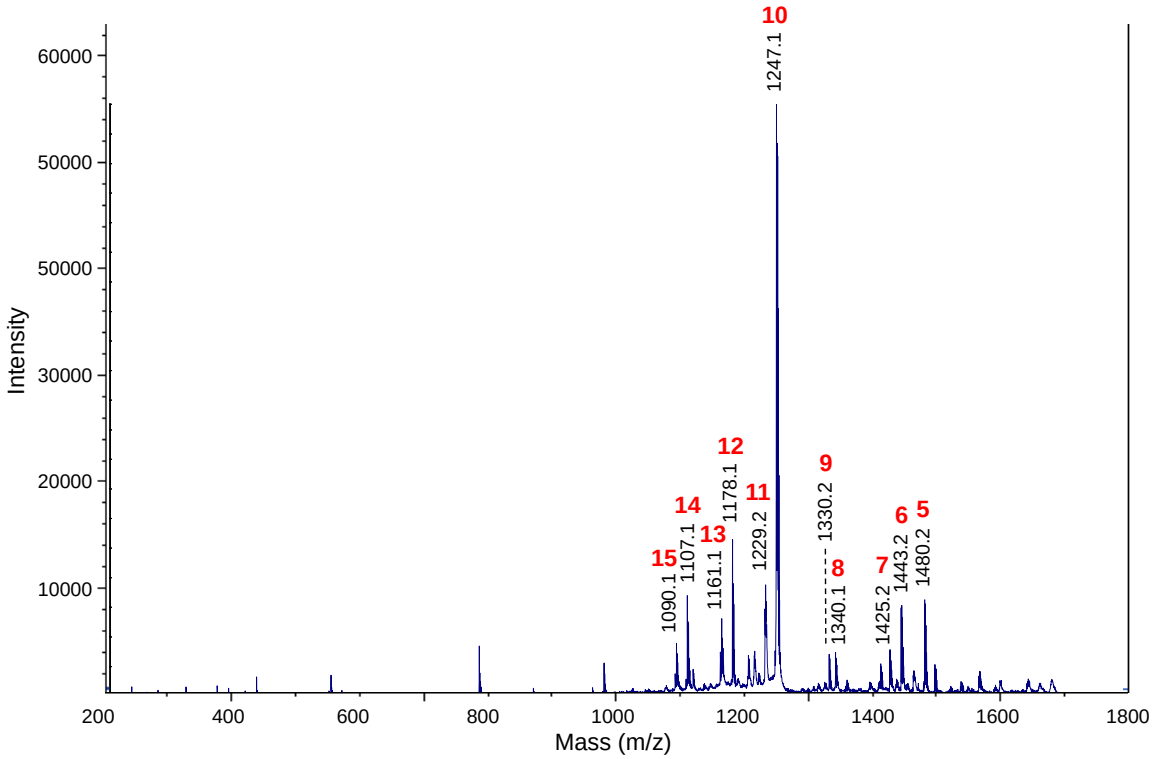

(**D**) Table and structure showing key ions and fragments in the MALDI MS and MS/MS of thiostrepton Ala2Dhb.

Fragment	Expected	Observed
1. M-H_2O+H^+	1658.5	1658.4
2. M+H^+ (Parent ion)	1676.5	1676.5
3. M+Na^+	1698.5	1698.5
4. M+Cu^+	1738.4	1738.4
5. M-Ile1-Dhb2+H^+	1480.4	1480.2
6. M-QA+H^+	1443.4	1443.2
7. M-QA-H_2O+H^+	1425.4	1425.2
8. M-Ile1-Dhb2-Dha3-Ala4+H^+	1340.3	1340.1
9. M-QA-Ile1+H^+	1330.3	1330.2
10. M-QA-Ile1-Dhb2+H^+	1247.3	1247.1
11. M-QA-Ile1-Dhb2-H_2O+H^+	1229.3	1229.2
12. M-QA-Ile1-Dhb-Dha3+H^+	1178.3	1178.1
13. M-QA-Ile1-Dhb2-Dha3-OH+H^+	1161.3	1161.1
14. M-QA-Ile1-Dhb2-Dha3-Ala4+H^+	1107.3	1107.1
15. M-QA-Ile1-Dhb2-Dha3-Ala4-OH+H^+	1090.2	1090.1

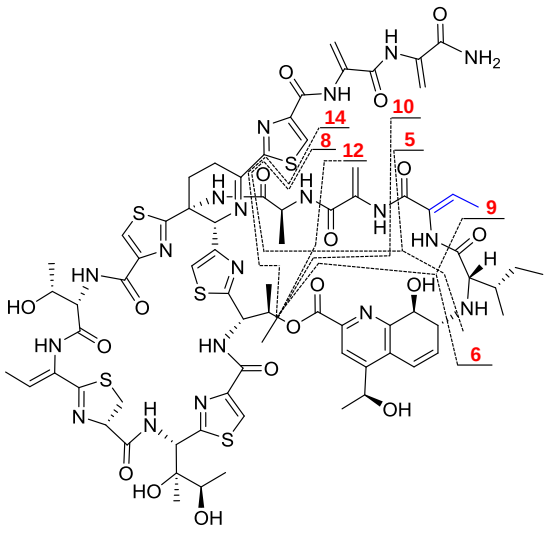

Figure E.10. Structure and numbering system used for thiostrepton Ala2Dhb.

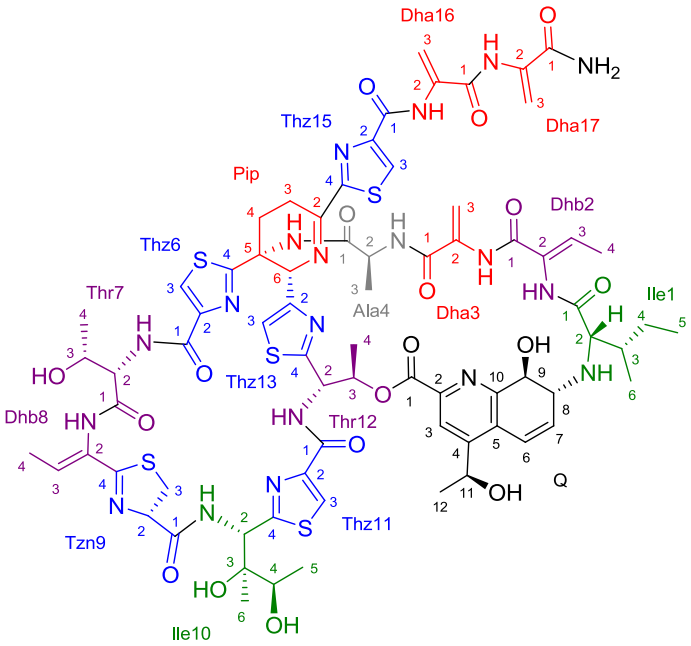

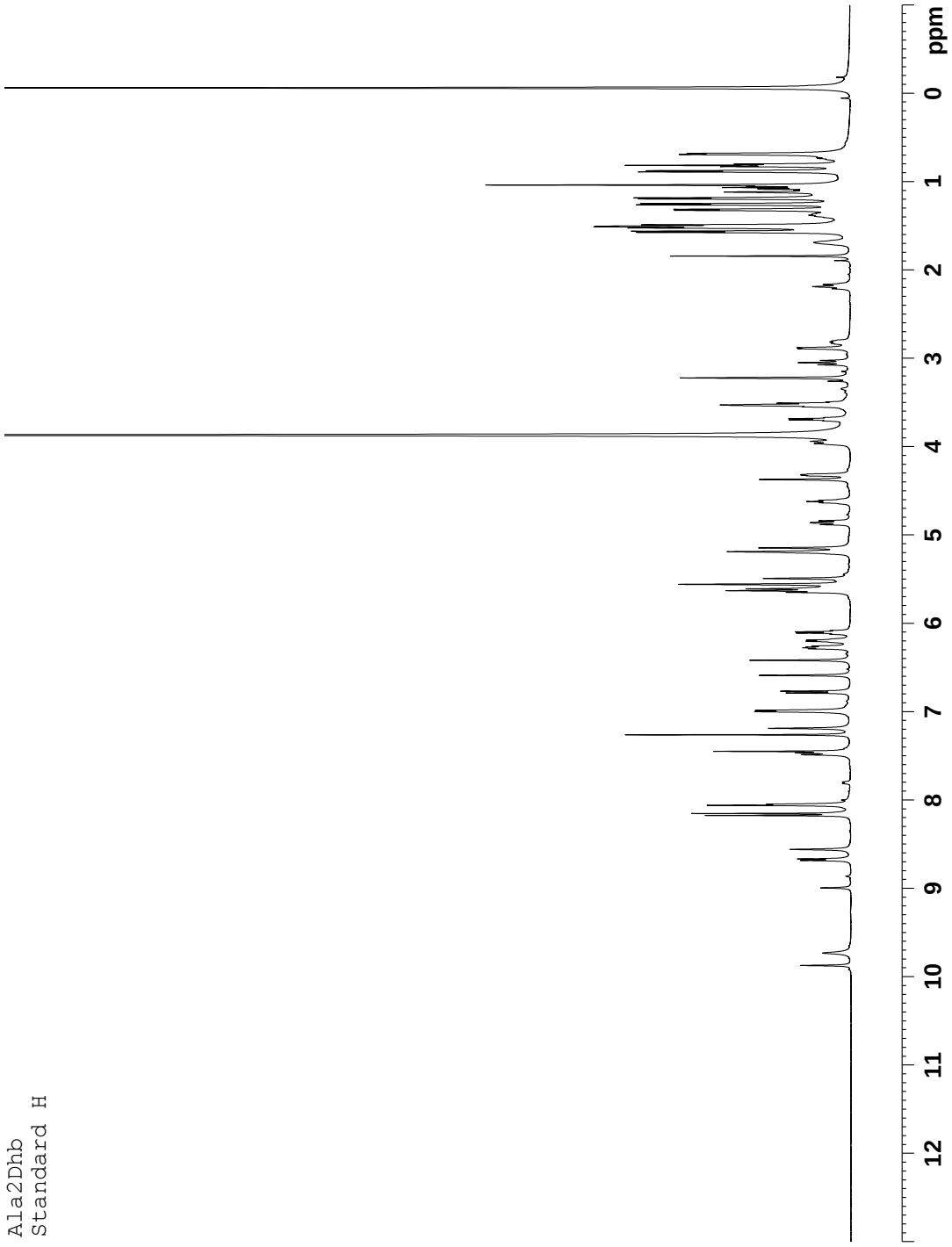

Figure E.11. ^{1}H NMR spectrum of thiostrepton Ala2Dhb (500 MHz, $CDCl_3$-CD_3OD 4:1, 25 °C).

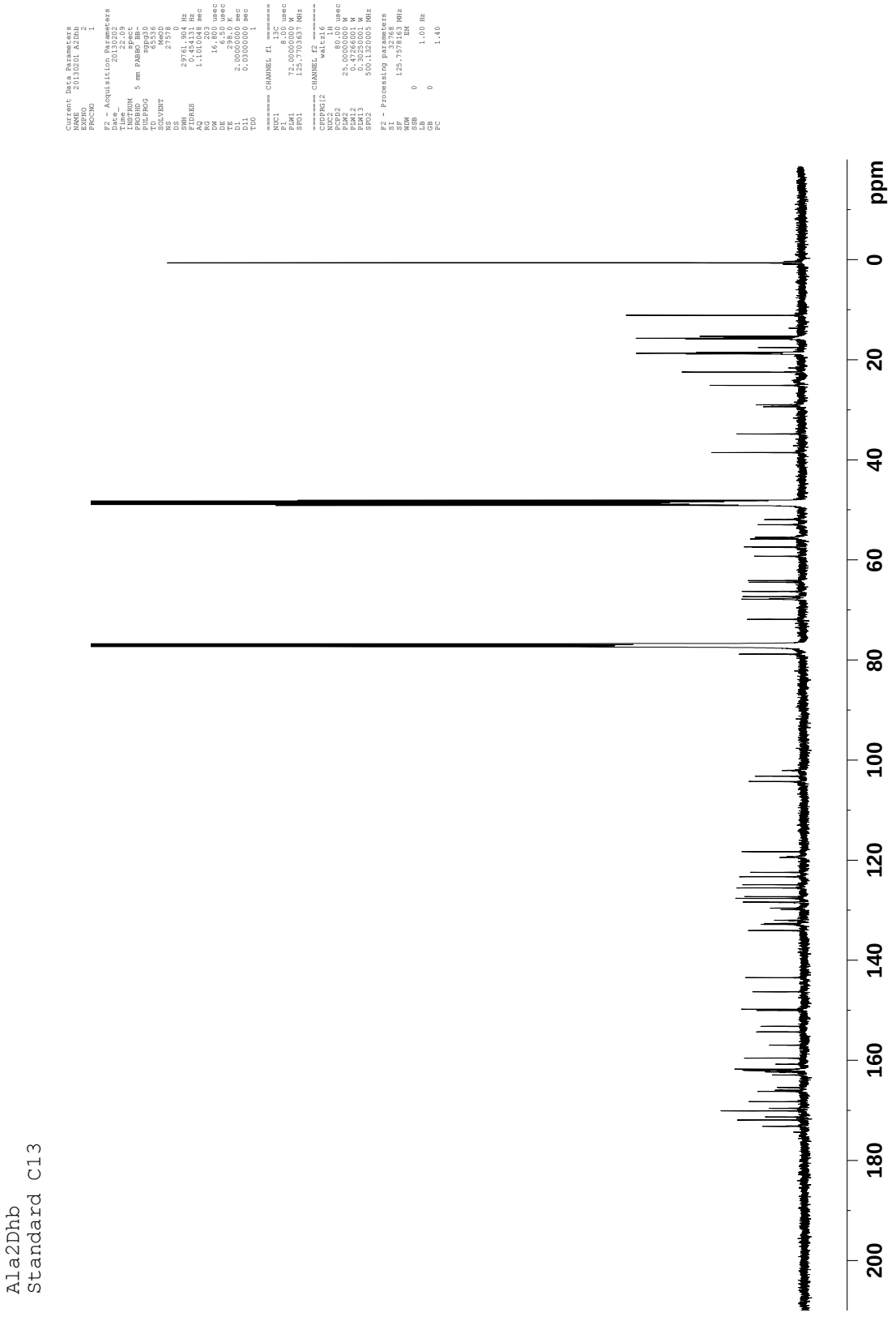

Figure E.12. ^{13}C NMR spectrum of thiostrepton Ala2Dhb (125 MHz, $CDCl_3$-CD_3OD 4:1, 25 °C).

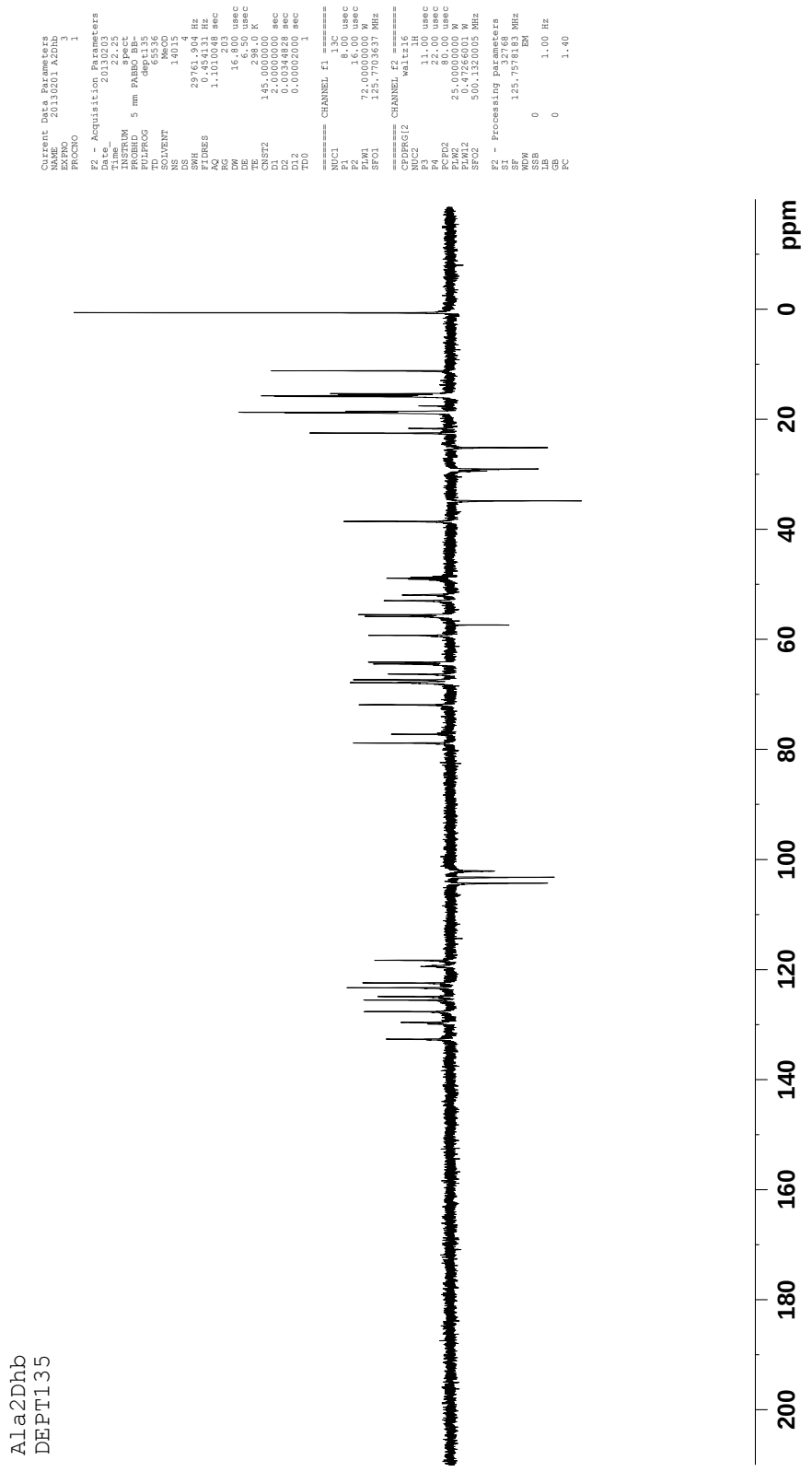

Figure E.13. DEPT-135 NMR spectrum of thiostrepton Ala2Dhb (125 MHz, $CDCl_3$-CD_3OD 4:1, 25 °C).

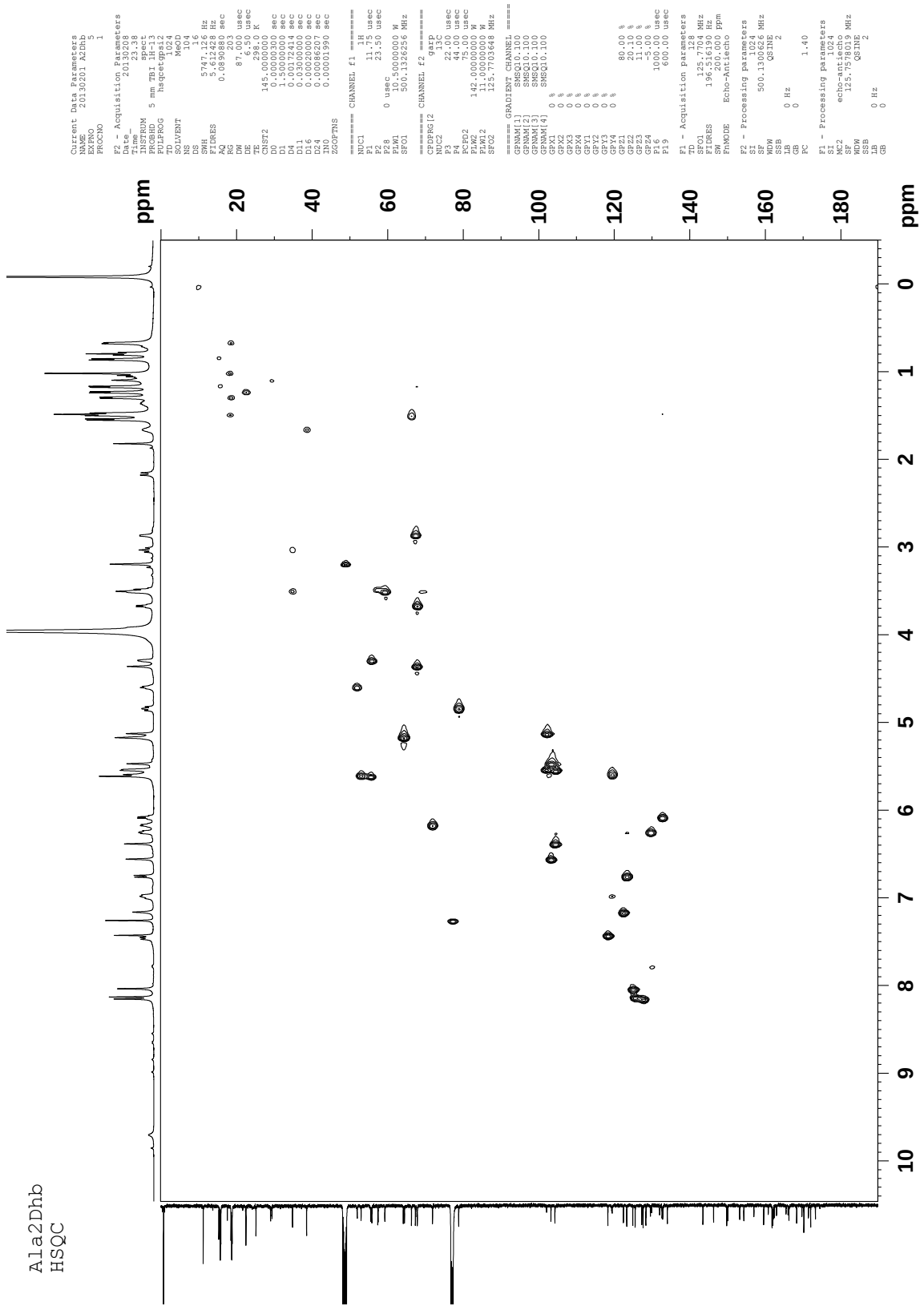

Figure E.14. gHSQC spectrum of thiostrepton Ala2Dhb (500 MHz, $CDCl_3$-CD_3OD 4:1, 25 °C).

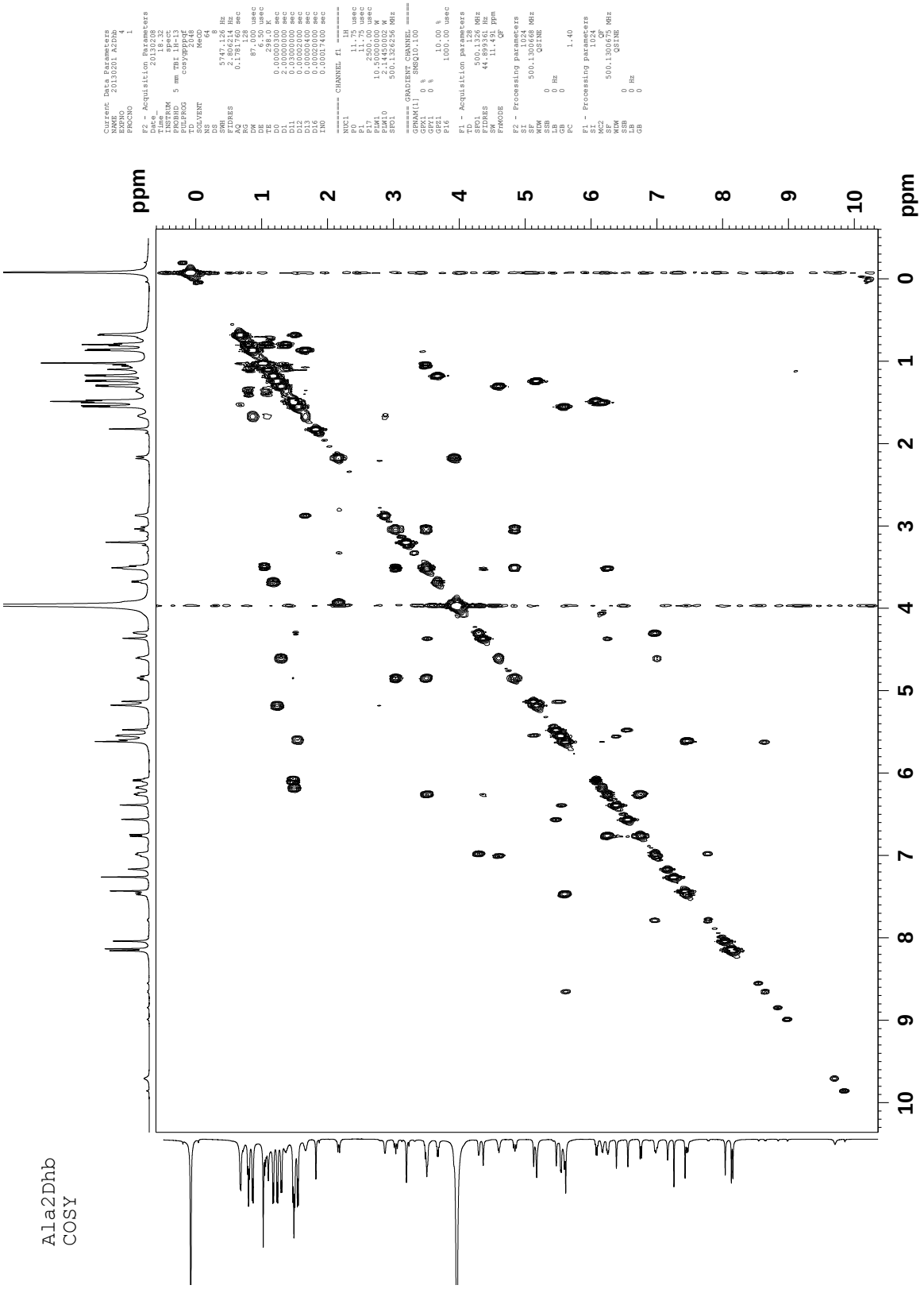

Figure E.15. gCOSY spectrum of thiostrepton Ala2Dhb (500 MHz, $CDCl_3$-CD_3OD 4:1, 25 °C).

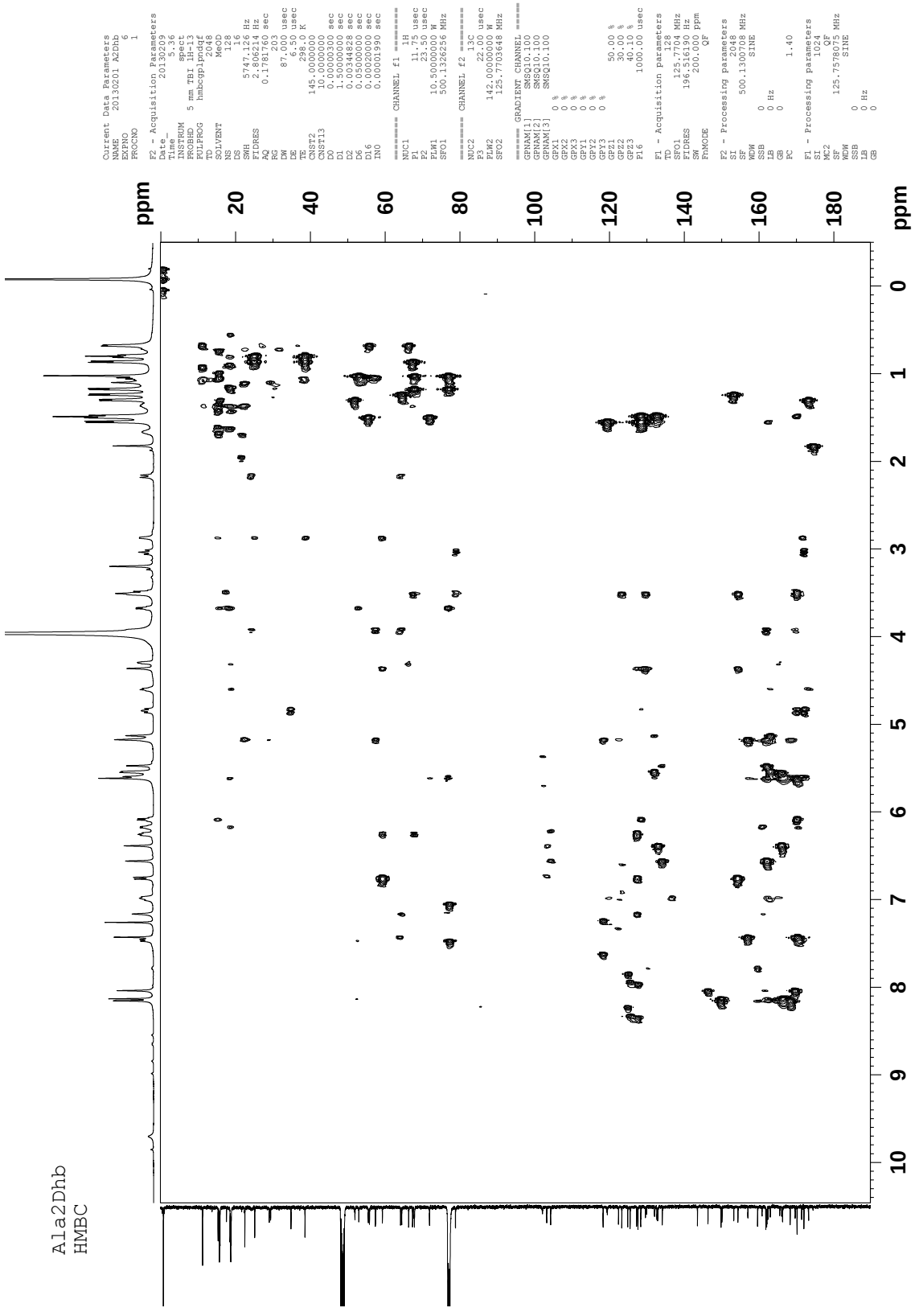

Figure E.16. gHMBC spectrum of thiostrepton Ala2Dhb (500 MHz, $CDCl_3$-CD_3OD 4:1, 25 °C).

Table E.2. ^{1}H and ^{13}C NMR assignments of thiostrepton Ala2Dhb

Position	δ_C [ppm]; mult	δ_H [ppm]; (mult, J in Hz)	HMBC[a]	COSY[b]
Ile1				
Ile1-1	171.3; C q			
Ile1-2	67.3; CH	2.87 (d, 4.1)	Ile1-1; Ile1-3; Ile1-4; Ile1-6; Q-8	Ile1-3
Ile1-3	38.5; CH	1.70-1.63 (m)	Ile1-6	Ile1-2; Ile1-4-H_A; Ile1-4-H_B; Ile1-6
Ile1-4	25.1; CH_2	H_A: 1.41-1.33 (m)	Ile1-2; Ile1-5; Ile1-6	Ile1-3; Ile1-4-H_B; Ile1-5
		H_B: 1.12-1.07 (m)	Ile1-2; Ile1-3; Ile1-5; Ile1-6	Ile1-3; Ile1-4-H_A; Ile1-5
Ile1-5	11.2; CH_3	0.80 (t, 6.9)	Ile1-3; Ile1-4	Ile1-4-H_A; Ile1-4-H_B
Ile1-6	15.3; CH_3	0.86 (d, 6.7)	Ile1-2; Ile1-3; Ile1-4	Ile1-3
Dhb2				
Dhb2-1	162.1; C q			
Dhb2-2	128.4; C q			
Dhb2-3	119.4; CH	5.64-5.60 (m)	Dhb2-1; Dhb2-4	Dhb2-4
Dhb2-4	18.5; CH_3	1.55 (d, 7.0)	Dhb2-1; Dhb2-2; Dhb2-3	Dhb2-3
Dhb2-NH[d]		7.02-6.94 (m)	Dha2-1; Dhb2-3	
Dha3				
Dha3-1	163.0; C q			
Dha3-2	132.0; C q			
Dha3-3	102.1; CH_2	H_A: 5.54 (s)	Dha3-1; Dha3-2	Dha3-3-H_B
		H_B: 5.13 (s)	Dha3-1; Dha3-2	Dha3-3-H_A
Ala4				
Ala4-1	173.2; C q			
Ala4-2	51.9; CH	4.60 (q, 6.0)	Dha3-1; Ala4-1; Ala4-3	Ala4-3; Ala4-NH
Ala4-3	18.8; CH_3	1.30 (d, 6.2)	Ala4-1; Ala4-2	Ala4-2
Ala4-NH[d]		7.02-6.94 (m)		Ala4-2
Pip				
Pip-2	161.9; C q			
Pip-3	24.1; CH_2	H_A: 3.34-3.30 (m)		Pip-4-H_B
		H_B: 2.83-2.76 (m)		Pip-4-H_A; Pip-4-H_B
Pip-4	29.0; CH_2	H_A: 3.94-3.87 (m)	Pip-2; Pip-3; Pip-5; Pip-6; Thz6-4	Pip-4-H_B
		H_B: 2.21-2.12 (m)	Pip-3; Pip-6	Pip-3-H_A; Pip-3-H_B; Pip-4-H_A
Pip-5	57.5; C q			
Pip-6	64.1; CH	5.17 (br s)	Pip-2; Pip-4; Pip-5; Thz13-2; Thz13-3; Thz15-4	Pip-3-H_B
Thz6				
Thz6-1	161.8; C q			
Thz6-2	146.3; C q			
Thz6-3	124.9; CH	7.98 (s)	Thz6-1; Thz6-2; Thz6-4	
Thz6-4	169.6; C q			
Thr7				
Thr7-1	165.5; C q			
Thr7-2	55.8; CH	4.32-4.27 (m)	Thr7-3; Thr7-4	Thr7-3; Thr7-NH
Thr7-3	66.3; CH	1.52-1.45 (m)	Thr7-2	Thr7-4
Thr7-4	18.7; CH_3	0.68 (d, 5.5)	Thr7-2; Thr7-3	Thr7-3
Thr7-NH[d]		7.02-6.94 (m)	Thr7-1	Thr7-2
Dhb8				
Dhb8-2	128.4; C q			
Dhb8-3	132.6; CH	6.08 (q, 6.6)	Dhb8-2; Dhb8-4; Tzn9-4	Dhb8-4
Dhb8-4	15.3; CH_3	1.48 (d, 7.8)	Dhb8-2; Dhb8-3; Tzn9-4	Dhb8-3
Tzn9				
Tzn9-1	172.0; C q			
Tzn9-2	78.8; CH	4.84 (dd, 11.8, 9.8)	Dhb8-2; Tzn9-1; Tzn9-3; Tzn9-4	Tzn9-3-H_A; Tzn9-3-H_B
Tzn9-3	34.8; CH_2	H_A: 3.54-3.46 (m)	Tzn9-2; Tzn9-4	Tzn9-2; Tzn9-3-H_B
		H_B: 3.03 (t, 12.1)	Tzn9-1; Tzn9-2	Tzn9-2; Tzn9-3-H_A
Tzn9-4	170.1; C q			
Ile10				
Ile10-2	52.9; CH	5.59 (s)	Ile10-3; Thz11-4	Ile10-NH
Ile10-3	77.2[c]; C q			
Ile10-4	67.8; CH	3.67 (q, 6.3)	Ile10-2; Ile10-3; Ile10-5; Ile10-6	Ile10-5
Ile10-5	15.7; CH_3	1.17 (d, 6.2)	Ile10-3; Ile10-4; Ile10-6	Ile10-4
Ile10-6	18.5; CH_3	1.02 (s)	Ile10-2; Ile10-3; Ile10-4	
Ile10-NH[d]		7.46 (d, 9.8)		Ile10-2

Position	δ_C [ppm]; mult	δ_H [ppm]; (mult, J in Hz)	HMBC[a]	COSY[b]
Thz11				
Thz11-1	162.4; C q			
Thz11-2	150.0; C q			
Thz11-3	125.5; CH	8.13 (s)	Thz11-1; Thz11-2; Thz11-4	
Thz11-4	166.2; C q			
Thr12				
Thr12-2	55.5; CH	5.62 (s)	Thr12-3; Thr12-4; Thz13-2; Thz13-4	Thr12-3; Thr12-NH
Thr12-3	71.9; CH	6.17 (q, 6.2)	Thr12-4; Thz13-4; Q-1	Thr12-4
Thr12-4	18.7; CH_3	1.49 (d, 7.4)	Thr12-2; Thr12-3	Thr12-3
Thr12-NH[d]		8.65 (d, 9.1)		Thr12-2
Thz13				
Thz13-2	157.0; C q			
Thz13-3	118.3; CH	7.43 (s)	Pip-6; Thz13-2; Thz13-4	
Thz13-4	170.1; C q			
Thz15				
Thz15-1	159.6; C q			
Thz15-2	149.8; C q			
Thz15-3	127.6; CH	8.15 (s)	Thz15-1; Thz15-2; Thz15-4	
Thz15-4	168.3; C q			
Dha16				
Dha16-1	162.0; C q			
Dha16-2	134.0; C q			
Dha16-3	103.2; CH_2	H_A: 6.56 (s) H_B: 5.47 (s)	Dha16-1; Dha16-2 Dha16-1; Dha16-2	Dha16-3-H_B Dha16-3-H_A
Dha17				
Dha17-1	166.0; C q			
Dha17-2	132.8; C q			
Dha17-3	104.3; CH_2	H_A: 6.39 (s) H_B: 5.55 (s)	Dha17-1; Dha17-2 Dha17-1; Dha17-2	Dha17-3-H_B Dha17-3-H_A
Q				
Q-1	160.8; C q			
Q-2	143.5; C q			
Q-3	122.4; CH	7.16 (s)	Q-1; Q-5; Q-11	
Q-4	153.2; C q			
Q-5	127.3; C q			
Q-6	123.3; CH	6.76 (d, 9.9)	Q-5; Q-8; Q-10	Q-7
Q-7	129.6; CH	6.25 (dd, 9.0, 5.8)	Q-5; Q-8; Q-9	Q-6; Q-8; Q-9
Q-8	59.2; CH	3.54-3.46 (m)	Ile1-2; Q-6; Q-7; Q-9; Q-10	Q-7; Q-9
Q-9	67.7; CH	4.36 (s)	Q-5; Q-7; Q-8; Q-10	Q-7; Q-8
Q-10	154.3; C q			
Q-11	64.4; CH	5.17 (br s)	Q-3; Q-12	Q-12
Q-12	22.5; CH_3	1.24 (d, 6.4)	Q-4; Q-11	Q-11

[a] HMBC correlations are from the proton to the indicated carbon.
[b] COSY correlations are from the proton to the proton attached to the indicated position.
[c] The δ of this resonance was determined by HMBC due to overlap with the $CDCl_3$ resonance.
[d] Only those amide resonances demonstrating either HMBC or COSY correlations to neighboring carbons or protons, respectively, were assigned.

Figure E.17. MS analysis of thiostrepton Ala2Ile-ΔIle1 isolated from *S. laurentii* NDS1/int-A2I.

(**A**) HPLC-MS analysis. (1) Chromatogram extracted for *m/z* 797.2, the calculated $[M+2H]^{2+}$ ion of thiostrepton Ala2Ile-ΔIle1. (2) Total ion chromatogram.

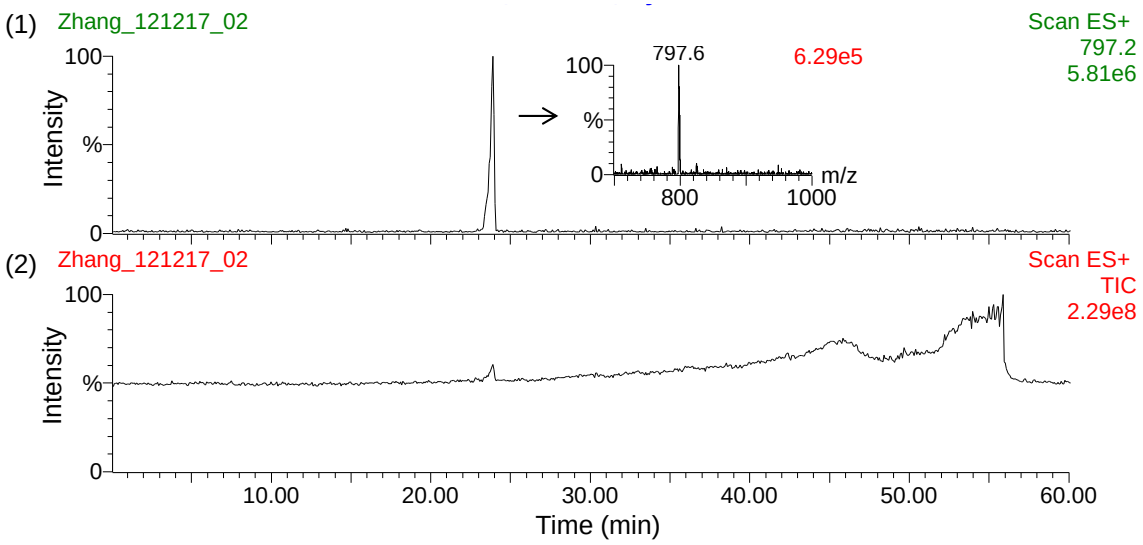

(**B**) MALDI MS spectrum of thiostrepton Ala2Ile-ΔIle1.

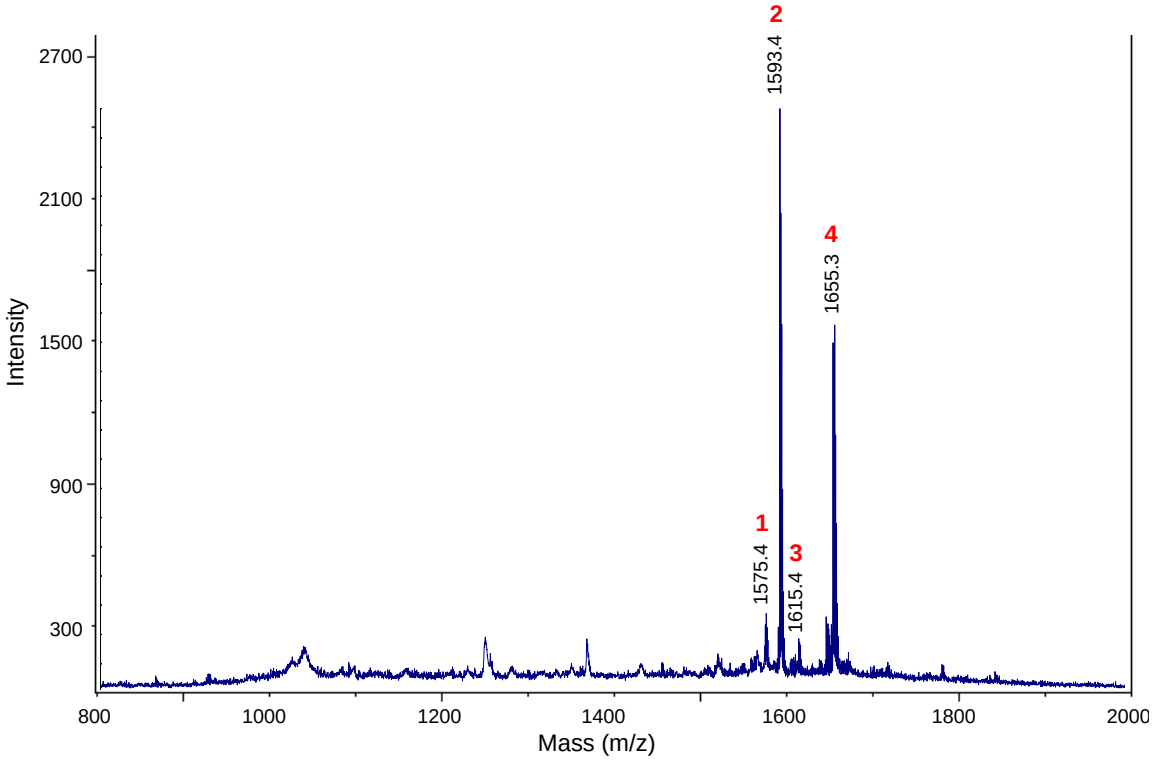

(**C**) MALDI MS/MS of parent ion *m/z* 1593.4.

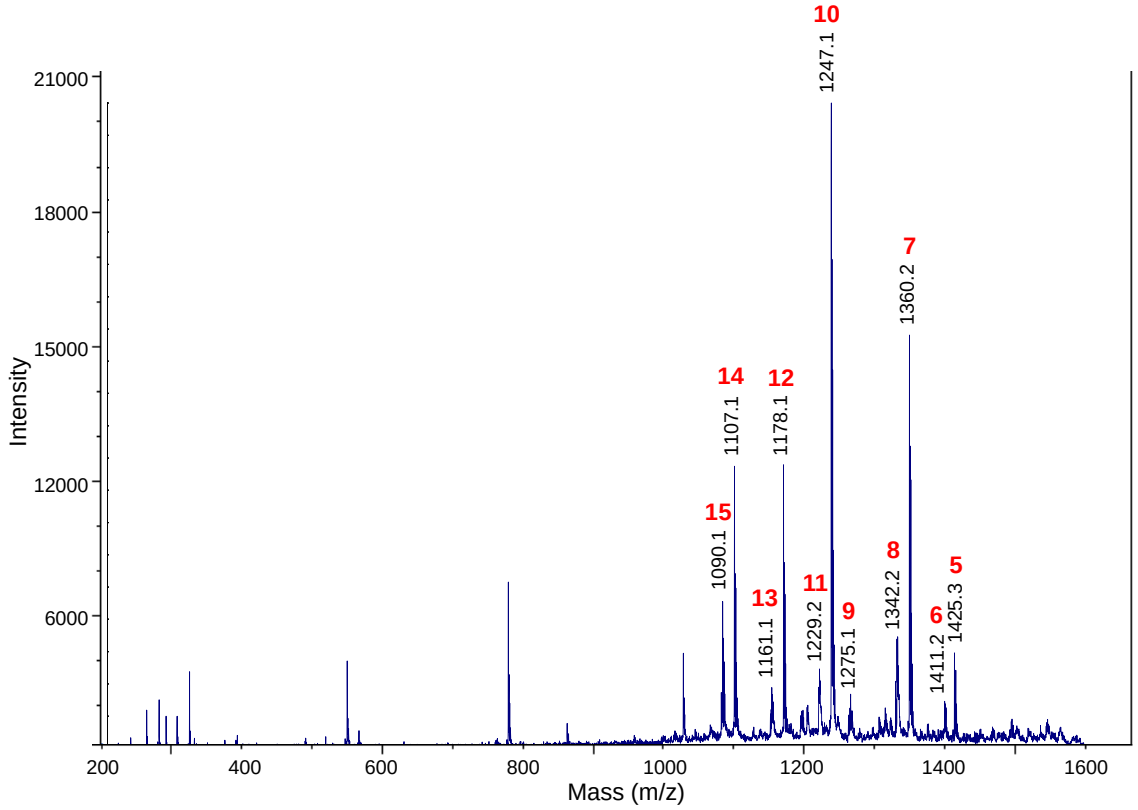

(**D**) Table and structure showing key ions and fragments in the MALDI MS and MS/MS of thiostrepton Ala2Ile-ΔIle1.

Fragment	Expected	Observed
1. M-H_2O+H^+	1575.5	1575.4
2. M+H^+ (Parent ion)	1593.5	1593.4
3. M+Na^+	1615.4	1615.4
4. M+Cu^+	1655.4	1655.3
5. M-Dhb8-Tzn9+H^+	1425.4	1425.3
6. M-Ile2-Dha3+H^+	1411.4	1411.2
7. M-QA+H^+	1360.4	1360.2
8. M-QA-H_2O+H^+	1342.4	1342.2
9. M-QA-(Ile2-CO)+H^+	1275.3	1275.1
10. M-QA-Ile2+H^+	1247.3	1247.1
11. M-QA-Ile2-H_2O+H^+	1229.3	1229.2
12. M-QA-Ile2-Dha3+H^+	1178.3	1178.1
13. M-QA-Ile2-Dha3-OH+H^+	1161.3	1161.1
14. M-QA-Ile2-Dha3-Ala4+H^+	1107.3	1107.1
15. M-QA-Ile2-Dha3-Ala4-OH+H^+	1090.2	1090.1

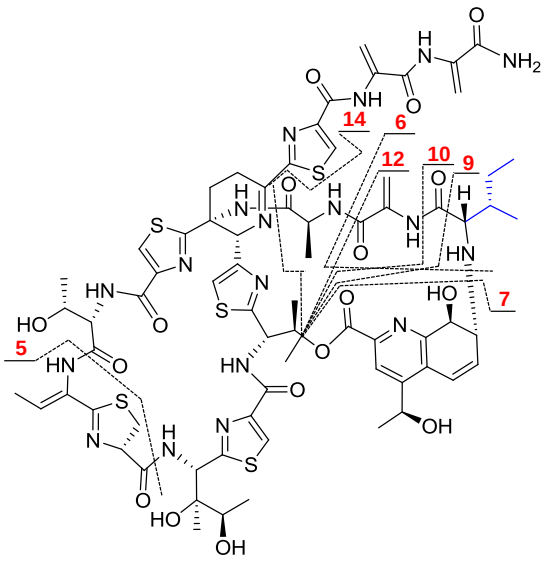

Figure E.18. Structure and numbering system used for thiostrepton Ala2Ile-ΔIle1.

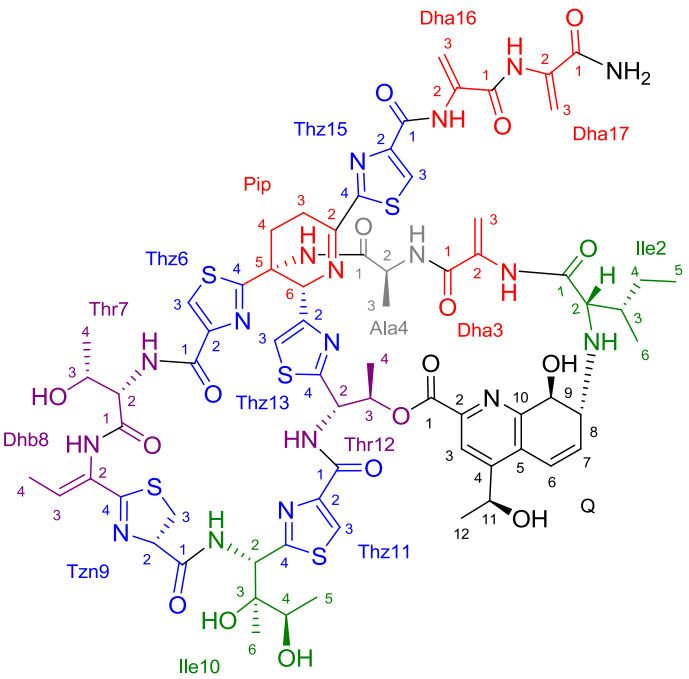

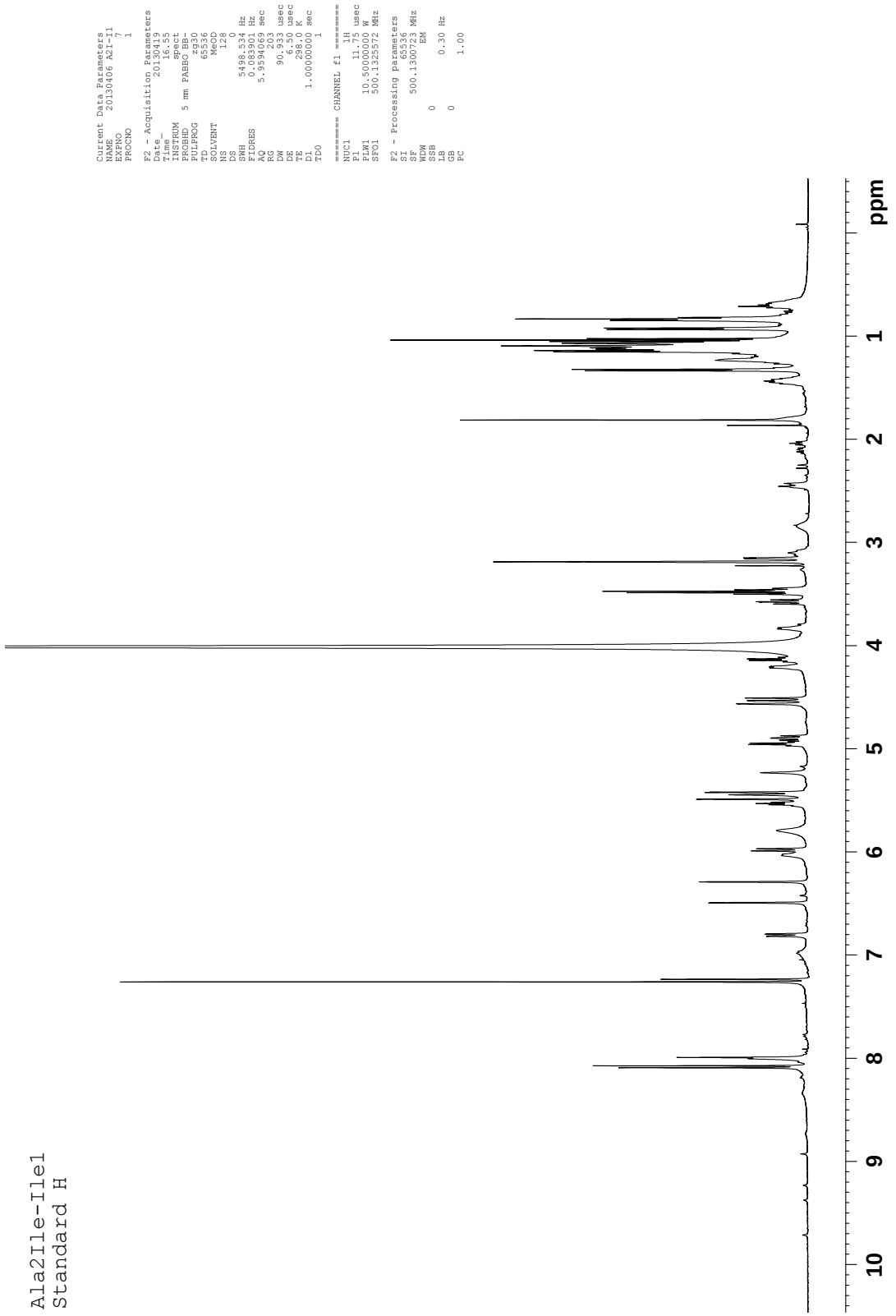

Figure E.19. ^{1}H NMR spectrum of thiostrepton Ala2Ile-ΔIle1 (500 MHz, $CDCl_3$-CD_3OD 4:1, 25 °C).

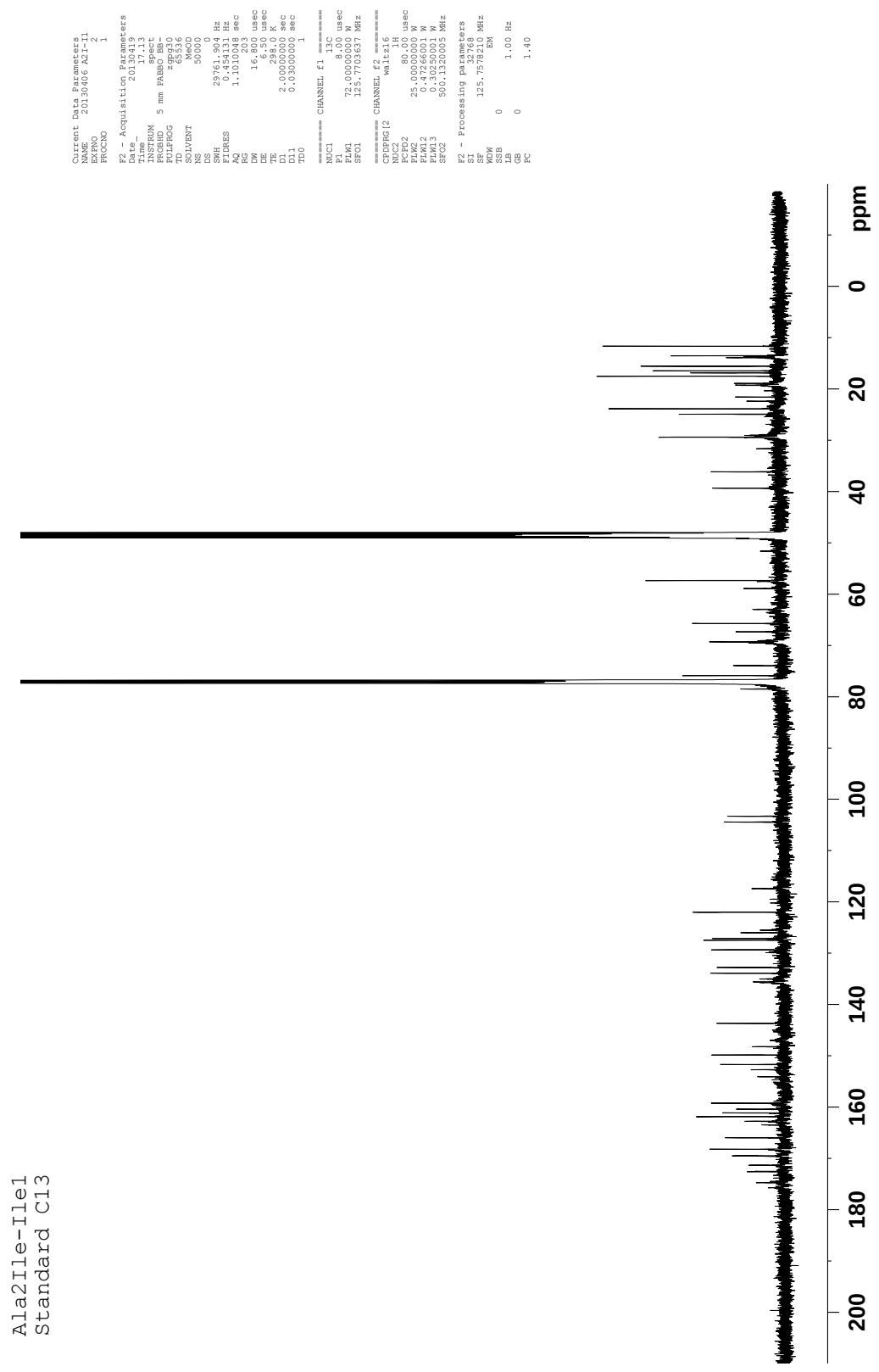

Figure E.20. ^{13}C NMR spectrum of thiostrepton Ala2Ile-ΔIle1 (125 MHz, $CDCl_3$-CD_3OD 4:1, 25 °C).

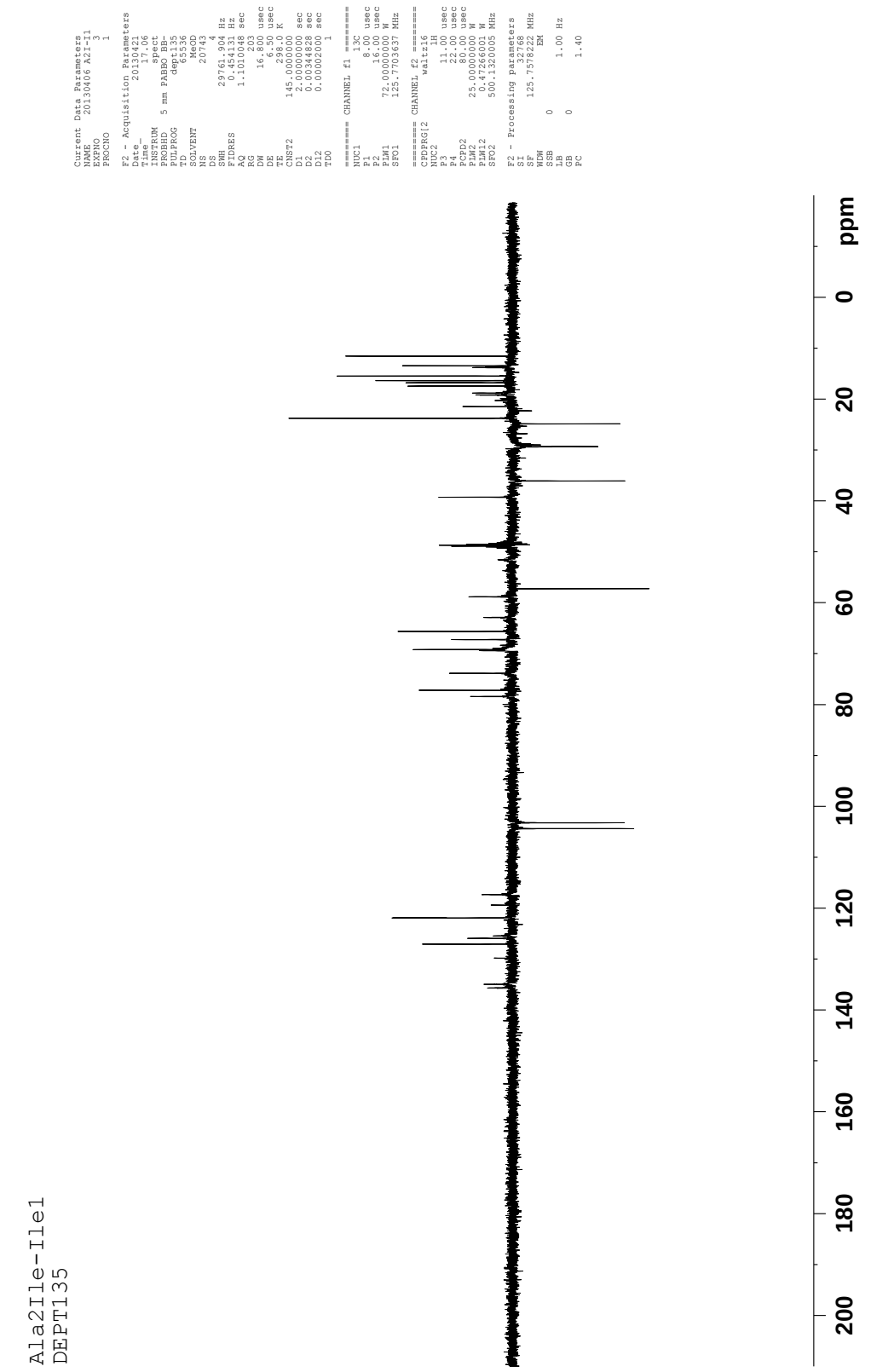

Figure E.21. DEPT-135 NMR spectrum of thiostrepton Ala2Ile-ΔIle1 (125 MHz, $CDCl_3$-CD_3OD 4:1, 25 °C).

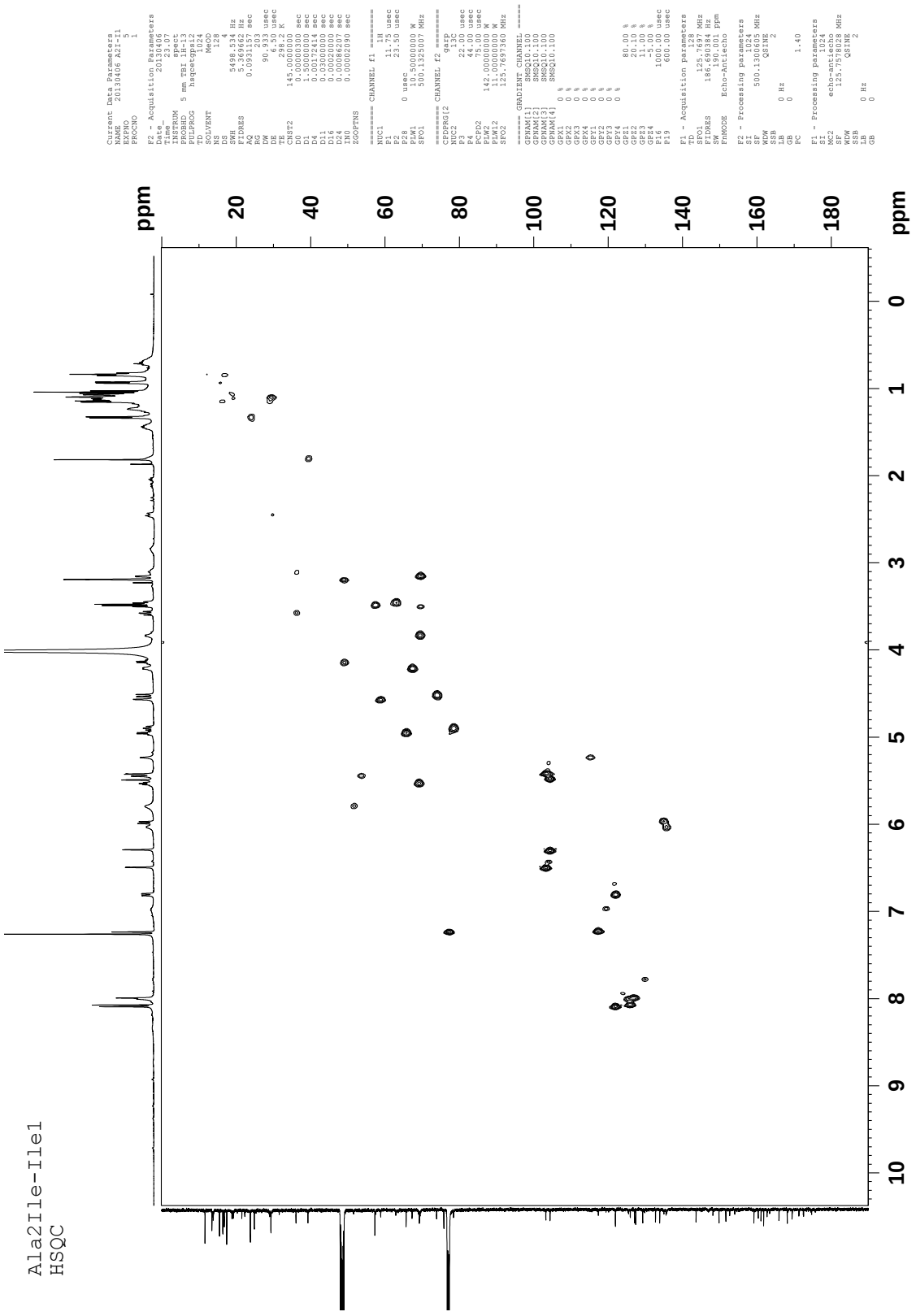

Figure E.22. gHSQC NMR spectrum of thiostrepton Ala2Ile-ΔIle1 (500 MHz, $CDCl_3$-CD_3OD 4:1, 25 °C).

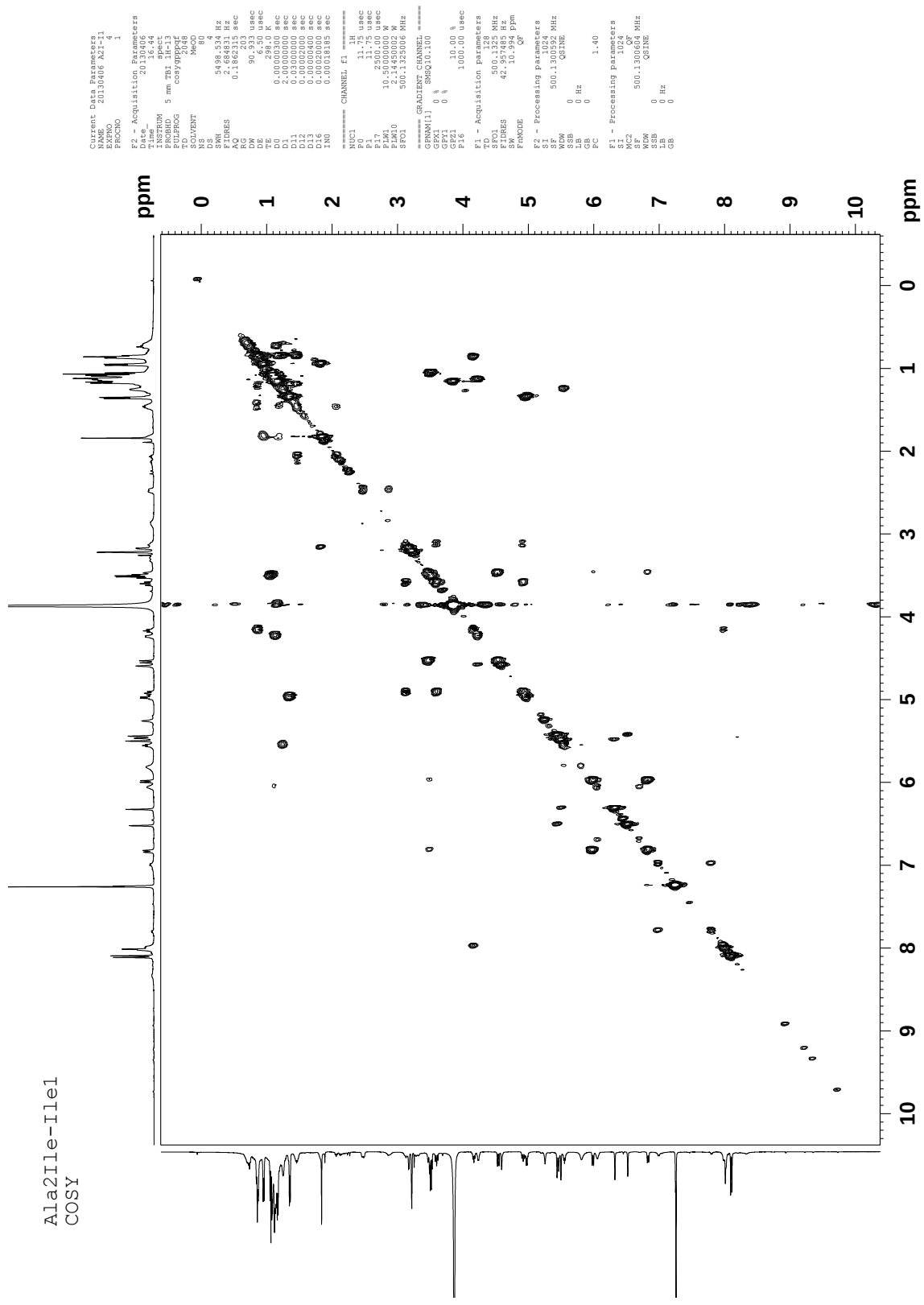

Figure E.23. gCOSY NMR spectrum of thiostrepton Ala2Ile-ΔIle1 (125 MHz, $CDCl_3$-CD_3OD 4:1, 25 °C).

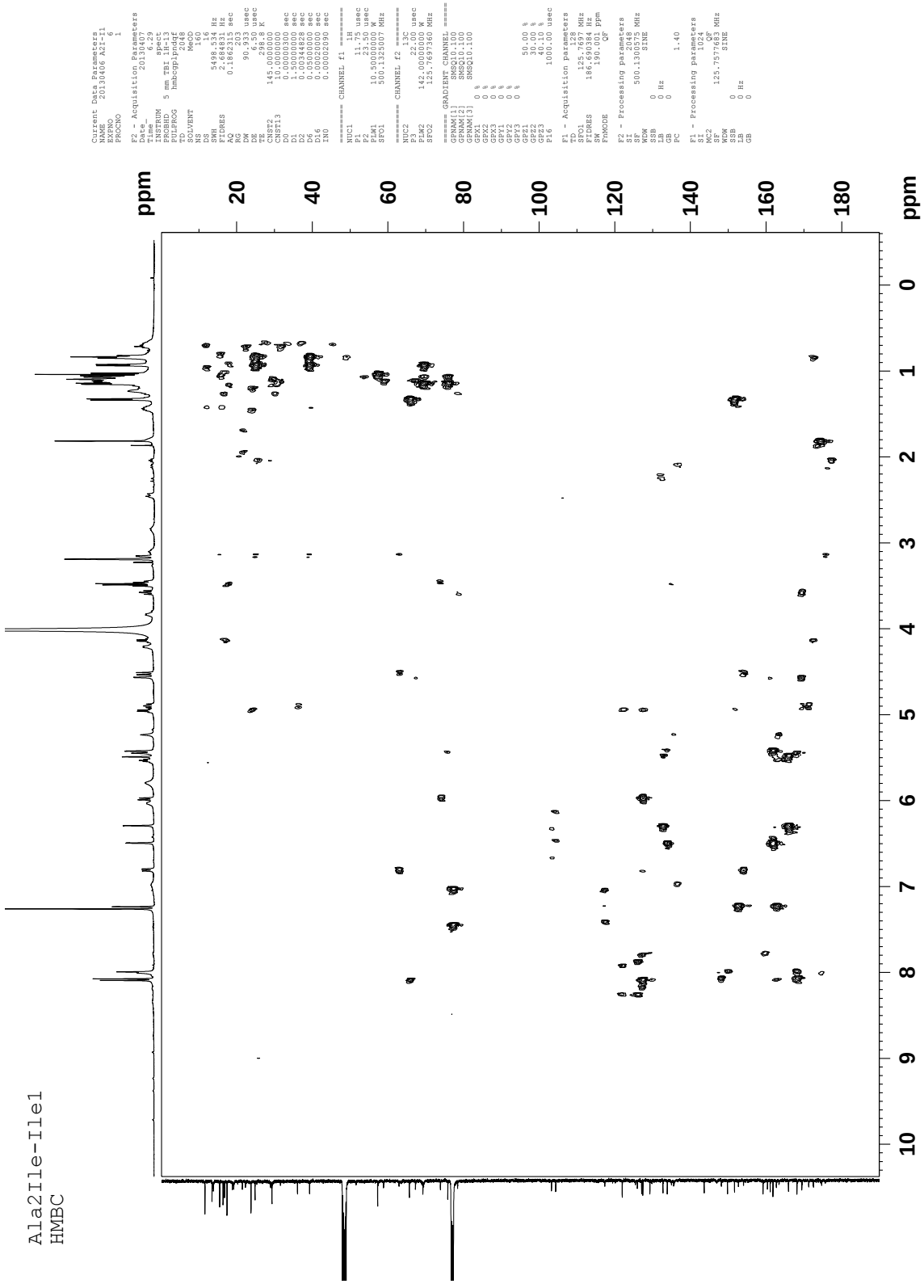

Figure E.24. gHMBC NMR spectrum of thiostrepton Ala2Ile-ΔIle1 (125 MHz, $CDCl_3$-CD_3OD 4:1, 25 °C).

Table E.3. ^{1}H and ^{13}C NMR assignments of thiostrepton Ala2Ile-ΔIle1

Position	δ_C [ppm]; mult	δ_H [ppm]; (mult, J in Hz)	HMBC[a]	COSY[b]
Ile2				
Ile2-1	174.7; C q			
Ile2-2	69.4; CH	3.15 (d, 3.8)	Ile2-3; Ile2-4; Ile2-6	Ile2-3
Ile2-3	39.3; CH	1.82-1.78 (m)	Ile2-1	Ile2-2; Ile2-4-H_A; Ile2-4-H_B; Ile2-6
Ile2-4	24.9; CH_2	H_A: 1.48-1.39 (m)	Ile2-3; Ile2-5; Ile2-6	Ile2-3; Ile2-4-H_B; Ile2-5
		H_B: 1.21-1.16 (m)	Ile2-2	Ile2-3; Ile2-4-H_A; Ile2-5
Ile2-5	11.6; CH_3	0.83 (t, 7.3)	Ile2-3; Ile2-4; Ile2-6	Ile2-4-H_A; Ile2-4-H_B
Ile2-6	15.5; CH_3	0.93 (d, 6.9)	Ile2-2; Ile2-3; Ile2-4; Ile2-5	Ile2-3
Dha3				
Dha3-1	163.4; C q			
Dha3-2	135.6; C q			
Dha3-3	115.2; CH_2	H_A: 5.79 (br s)		
		H_B: 5.23 (br s)	Dha3-1; Dha3-2	
Ala4				
Ala4-1	172.5; C q			
Ala4-2	49.3; CH	4.14 (q, 7.4)	Ala4-1; Ala4-3	Ala4-3
Ala4-3	16.8; CH_3	0.84 (d, 7.3)	Ala4-1; Ala4-2	Ala4-2
Pip				
Pip-2	159.2; C q			
Pip-3	22.3; CH_2	H_A: 3.50-3.40 (m)		Pip-3-H_B; Pip-4-H_B
		H_B: 2.89-2.80 (m)		Pip-4-H_B
Pip-4	29.3; CH_2	H_A: 3.86-3.80 (m)		
		H_B: 2.48-2.42 (m)		Pip-3-H_A; Pip-3-H_B
Pip-5	57.5; C q			
Pip-6	63.6; CH	5.23 (br s)		
Thz6				
Thz6-1	161.1; C q			
Thz6-2	149.8; C q			
Thz6-3	127.1; CH	7.99 (s)	Thz6-2; Thz6-4	
Thz6-4	168.2; C q			
Thr7				
Thr7-1	169.5; C q			
Thr7-2	58.8; CH	4.56 (d, 2.0)	Thz6-1; Thr7-1; Thr7-3	Thr7-3
Thr7-3	67.3; CH	4.23-4.18 (m)		Thr7-2; Thr7-4
Thr7-4	19.2; CH_3	1.12 (d, 6.0)	Thr7-2; Thr7-3	Thr7-3
Dhb8				
Dhb8-2	127.4; C q			
Dhb8-3	135.7; CH	6.08-6.03 (m)	Dhb8-2	Dhb8-4
Dhb8-4	19.2; CH_3	1.13-1.09 (m)		
Tzn9				
Tzn9-1	171.3; C q			
Tzn9-2	78.4; CH	4.90 (dd, 11.4, 9.8)	Tzn9-1; Tzn9-3; Tzn9-4	Tzn9-3-H_A; Tzn9-3-H_B
Tzn9-3	36.1; CH_2	H_A: 3.58 (dd, 11.1; 9.2)	Tzn9-2; Tzn9-4	Tzn9-2; Tzn9-3-H_B
		H_B: 3.10 (t, 12.0)		Tzn9-2; Tzn9-3-H_A
Tzn9-4	169.5; C q			
Ile10				
Ile10-2	53.7; CH	5.45 (s)	Ile10-3; Thz11-4	
Ile10-3	75.8; C q			
Ile10-4	69.3; CH	3.86-3.80 (m)		Ile10-5
Ile10-5	16.4; CH_3	1.15 (d, 6.5)	Ile10-3; Ile10-4	Ile10-4
Ile10-6	18.8; CH_3	1.07 (s)	Ile10-2; Ile10-3; Ile10-4; Ile10-5	
Thz11				
Thz11-1	162.7; C q			
Thz11-2	149.8; C q			
Thz11-3	121.9; CH	8.09 (s)	Thz11-1; Thz11-4	
Thz11-4	168.3; C q			
Thr12				
Thr12-2	51.6; CH	5.79 (br s)		Thr12-3
Thr12-3	69.3; CH	5.53 (pentet, 6.1)	Q-1	Thr12-2; Thr12-4
Thr12-4	13.8; CH_3	1.26-1.21 (m)		Thr12-3

Position	δ_C [ppm]; mult	δ_H [ppm]; (mult, J in Hz)	HMBC[a]	COSY[b]
Thz13				
Thz13-2	159.2; C q			
Thz13-3	125.5; CH	8.00 (s)	Thz13-4	
Thz13-4	168.2; C q			
Thz15				
Thz15-1	160.4; C q			
Thz15-2	148.2; C q			
Thz15-3	126.0; CH	8.07 (s)	Thz15-2; Thz15-4	
Thz15-4	168.3; C q			
Dha16				
Dha16-1	161.8; C q			
Dha16-2	133.9; C q			
Dha16-3	103.2; CH_2	H_A: 6.49 (d, 2.2)	Dha16-1; Dha16-2	Dha16-3-H_B
		H_B: 5.42 (d, 2.1)	Dha16-1; Dha16-2	Dha16-3-H_A
Dha17				
Dha17-1	165.9; C q			
Dha17-2	132.7; C q			
Dha17-3	104.4; CH_2	H_A: 6.29 (d, 1.4)	Dha17-1; Dha17-2	Dha17-3-H_B
		H_B: 5.49 (d, 1.3)	Dha17-1; Dha17-2	Dha17-3-H_A
Q				
Q-1	162.7; C q			
Q-2	152.7; C q			
Q-3	117.4; CH	7.23 (s)	Q-1; Q-2; Q-10	
Q-4	151.7; C q			
Q-5	127.4; C q			
Q-6	122.0; CH	6.81 (dd, 10.1,2.3)	Q-5; Q-8; Q-10	Q-7; Q-8
Q-7	135.0 CH	5.98 (m)	Q-5; Q-9	Q-6; Q-8
Q-8	62.9; CH	3.50-3.40 (m)	Q-7; Q-9	Q-6; Q-7; Q-9
Q-9	73.9; CH	4.52 (d, 12.4)	Q-8; Q-10	Q-8
Q-10	154.0; C q			
Q-11	65.7; CH	4.95 (q, 6.5)	Q-4; Q-5; Q-6; Q-12	Q-12
Q-12	23.8; CH_3	1.33 (d, 6.6)	Q-4; Q-11	Q-11

[a] HMBC correlations are from the proton to the indicated carbon.
[b] COSY correlations are from the proton to the proton attached to the indicated position.

Figure E.25. MS analysis of thiostrepton Ala2Met isolated from *S. laurentii* NDS1/int-A2M.

(**A**) HPLC-MS analysis. (1) Chromatogram extracted for *m/z* 862.8, the calculated $[M+2H]^{2+}$ ion of thiostrepton Ala2Met. (2) Total ion chromatogram.

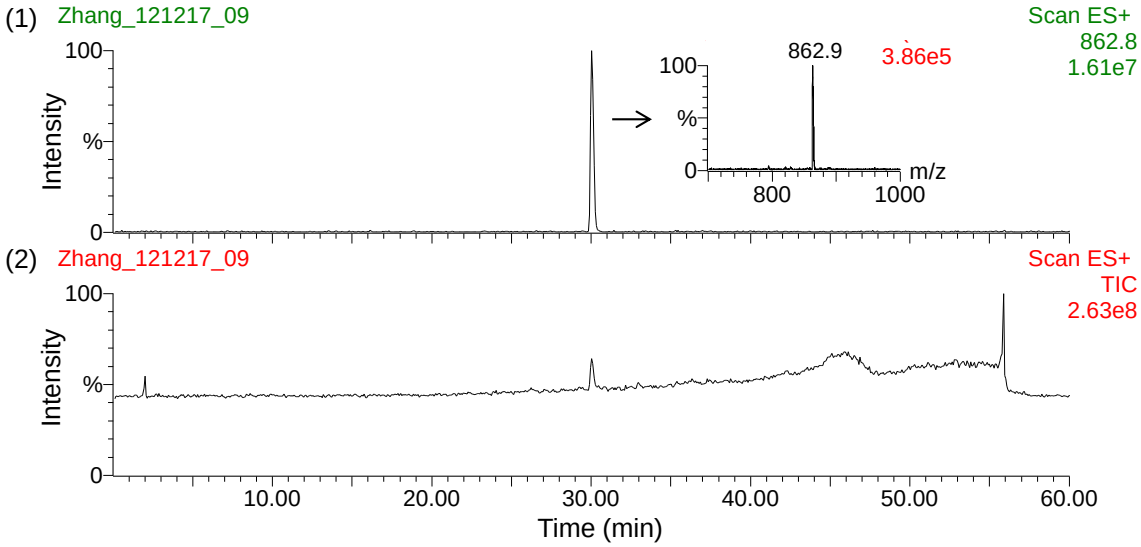

(**B**) MALDI MS spectrum of thiostrepton Ala2Met.

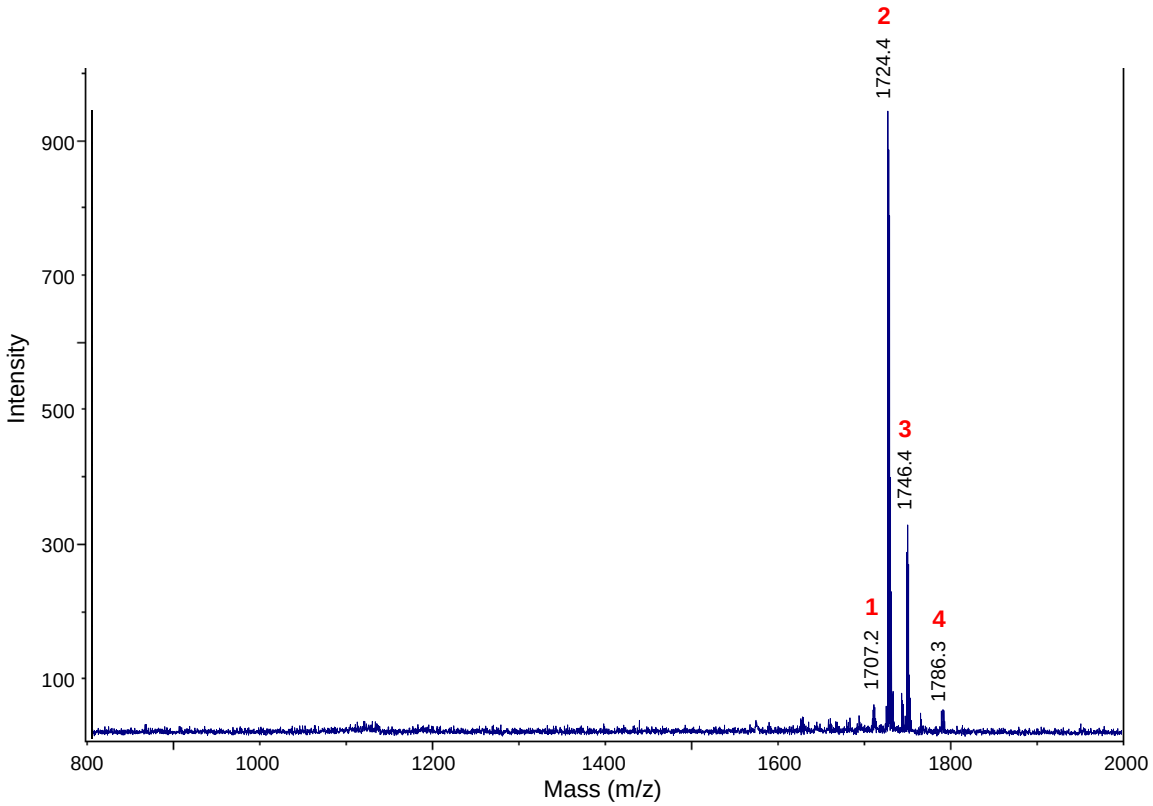

(**C**) MALDI MS/MS of parent ion *m/z* 1724.4.

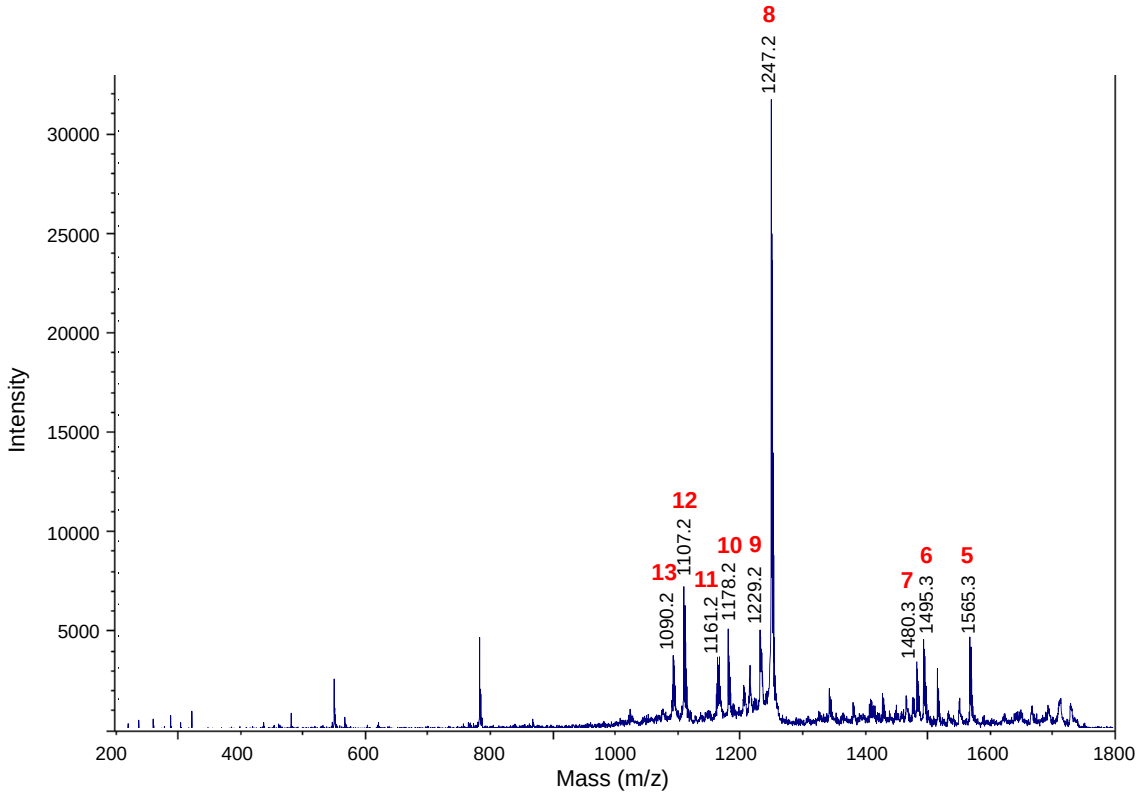

(**D**) Table and structure showing key ions and fragments in the MALDI MS and MS/MS of thiostrepton Ala2Met.

Fragment	Expected	Observed
1. M-OH+H$^+$	1707.5	1707.2
2. M+H$^+$ (Parent ion)	1724.5	1724.4
3. M+Na$^+$	1746.5	1746.4
4. M+Cu$^+$	1786.4	1786.3
5. M-Met2-CO+H$^+$	1565.5	1565.3
6. M-(Ile1-NH)-Met2+H$^+$	1495.4	1495.3
7. M-Ile1-Met2+H$^+$	1480.4	1480.3
8. M-QA-Ile1-Met2+H$^+$	1247.3	1247.2
9. M-QA-Ile1-Met2-H_2O+H$^+$	1229.3	1229.2
10. M-QA-Ile1-Met2-Dha3+H$^+$	1178.3	1178.2
11. M-QA-Ile1-Met-Dha3-OH+H$^+$	1161.3	1161.2
12. M-QA-Ile1-Met2-Dha3-Ala4+H$^+$	1107.3	1107.2
13. M-QA-Ile1-Met2-Dha3-Ala4-OH+H$^+$	1090.2	1090.2

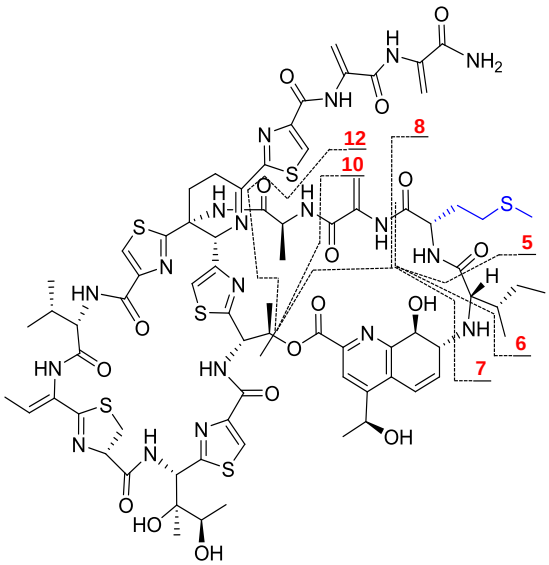

Figure E.26. MS analysis of thiostrepton Ala2Phe isolated from *S. laurentii* NDS1/int-A2F.

(**A**) HPLC-MS analysis. (1) Chromatogram extracted for *m/z* 870.8, the calculated $[M+2H]^{2+}$ ion of thiostrepton Ala2Phe. (2) Total ion chromatogram.

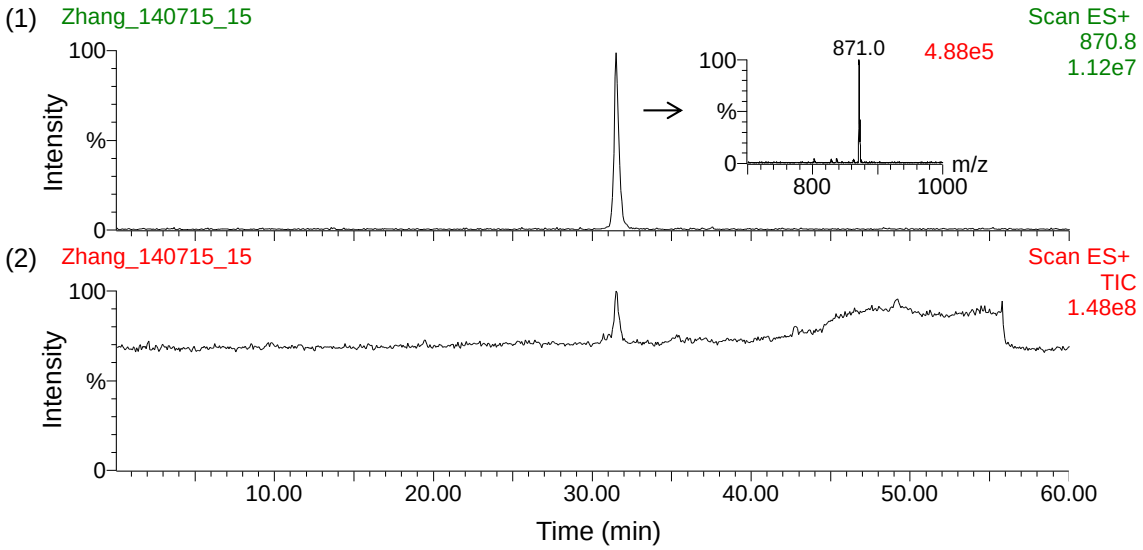

(**B**) MALDI MS spectrum of thiostrepton Ala2Phe.

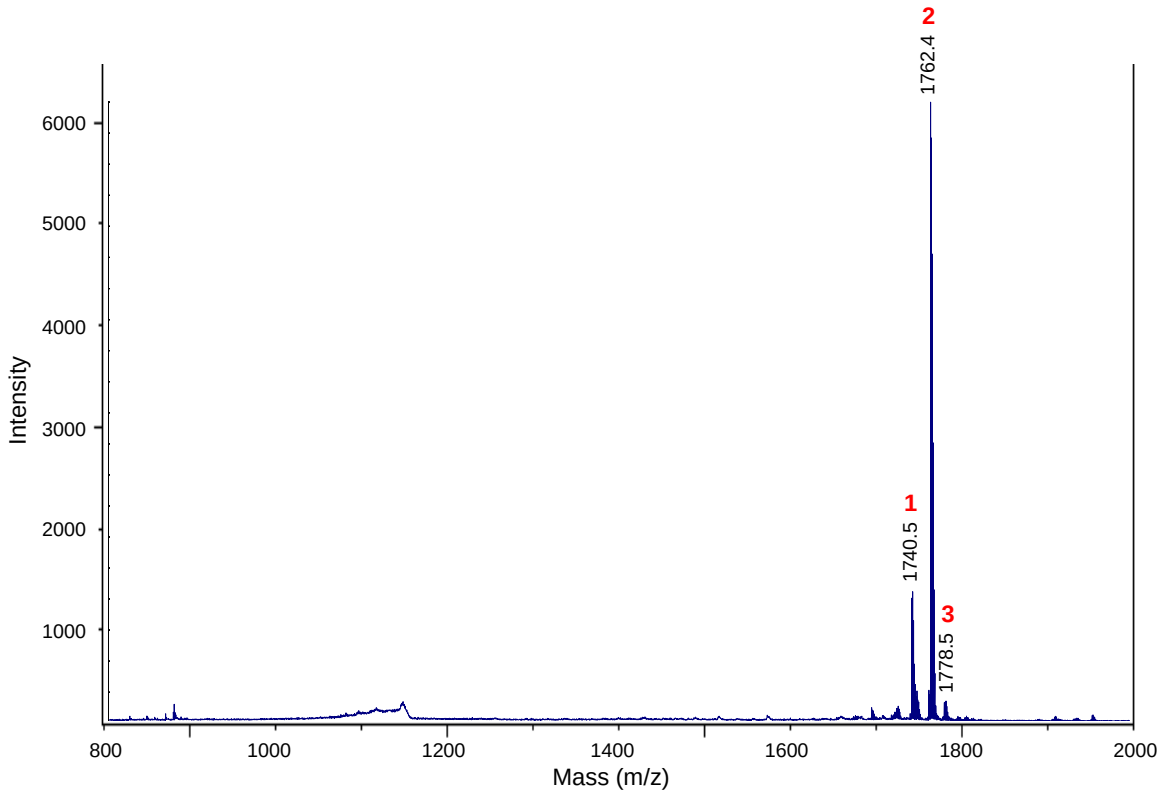

(**C**) MALDI MS/MS of parent ion *m/z* 1740.5.

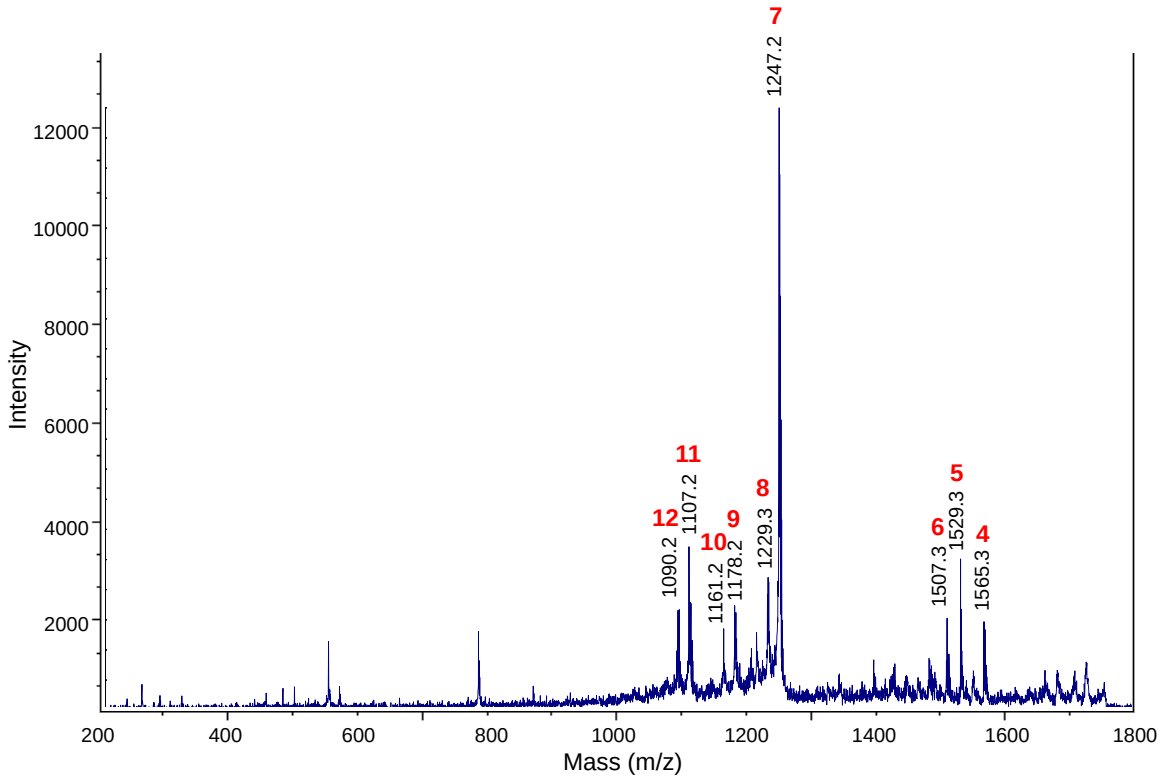

(**D**) Table and structure showing key ions and fragments in the MALDI MS and MS/MS of thiostrepton Ala2Phe.

Fragment	Expected	Observed
1. $M+H^+$ (Parent ion)	1740.5	1740.5
2. $M+Na^+$	1762.5	1762.4
3. $M+K^+$	1778.5	1778.5
4. M-Phe2-CO+H^+	1565.5	1565.3
5. M-Dhb8-Tzn9-CO-NH+H^+	1529.5	1529.3
6. M-QA+H^+	1507.5	1507.3
7. M-QA-Ile1-Phe2+H^+	1247.3	1247.2
8. M-QA-Ile1-Phe2-H_2O+H^+	1229.3	1229.3
9. M-QA-Ile1-Phe2-Dha3+H^+	1178.3	1178.2
10. M-QA-Ile1-Phe2-Dha3-OH+H^+	1161.3	1161.2
11. M-QA-Ile1-Phe2-Dha3-Phe4+H^+	1107.3	1107.2
12. M-QA-Ile1-Phe2-Dha3-Ala4-OH+H^+	1090.2	1090.2

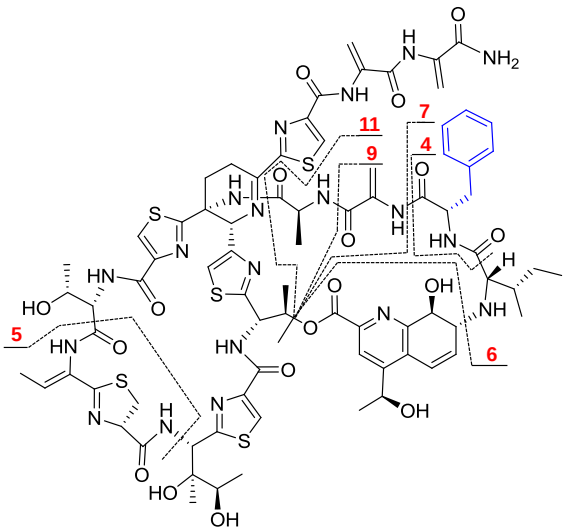

Figure E.27. MS analysis of thiostrepton Ala2Tyr isolated from *S. laurentii* NDS1/int-A2Y.

(**A**) HPLC-MS analysis. (1) Chromatogram extracted for *m/z* 878.8, the calculated $[M+2H]^{2+}$ ion of thiostrepton Ala2Tyr. (2) Total ion chromatogram

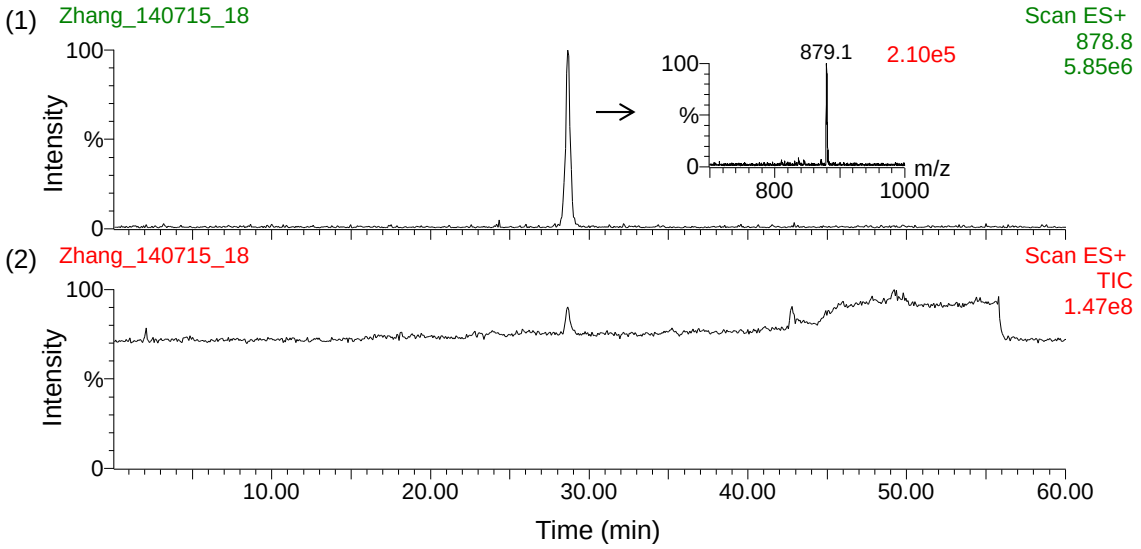

(**B**) MALDI MS spectrum of thiostrepton Ala2Tyr.

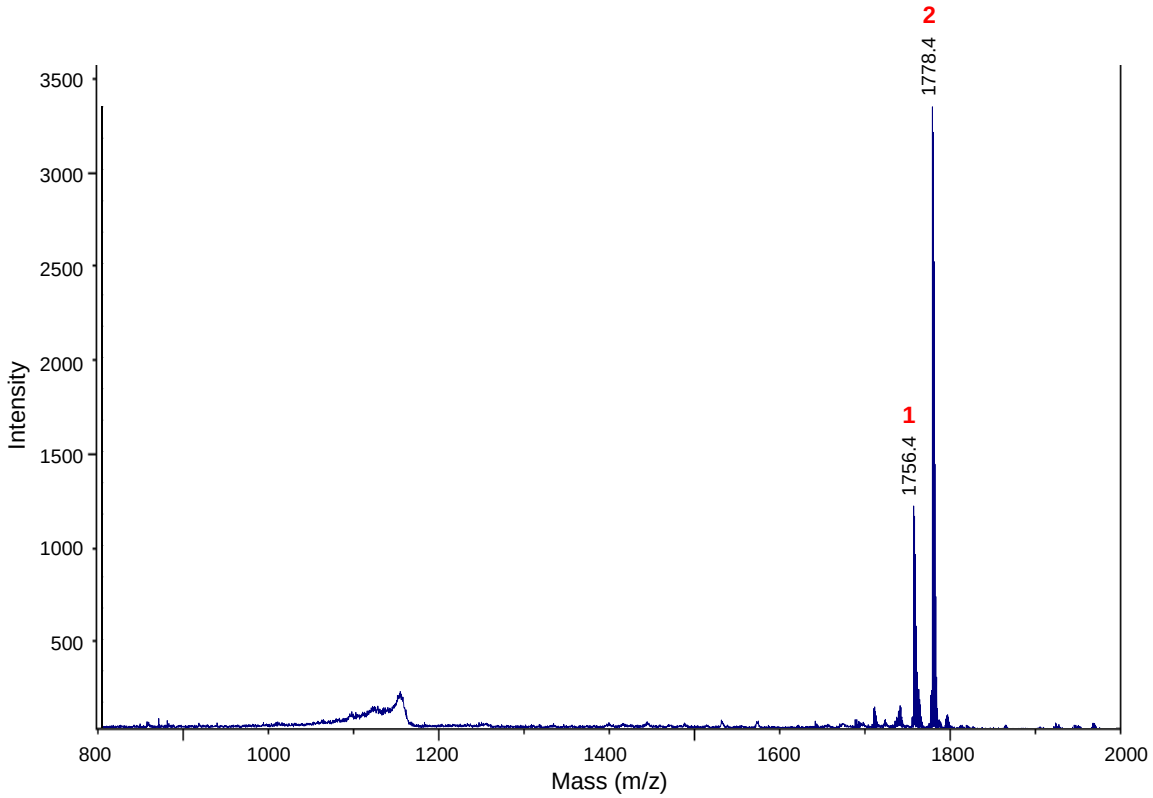

(**C**) MALDI MS/MS of parent ion *m/z* 1756.4.

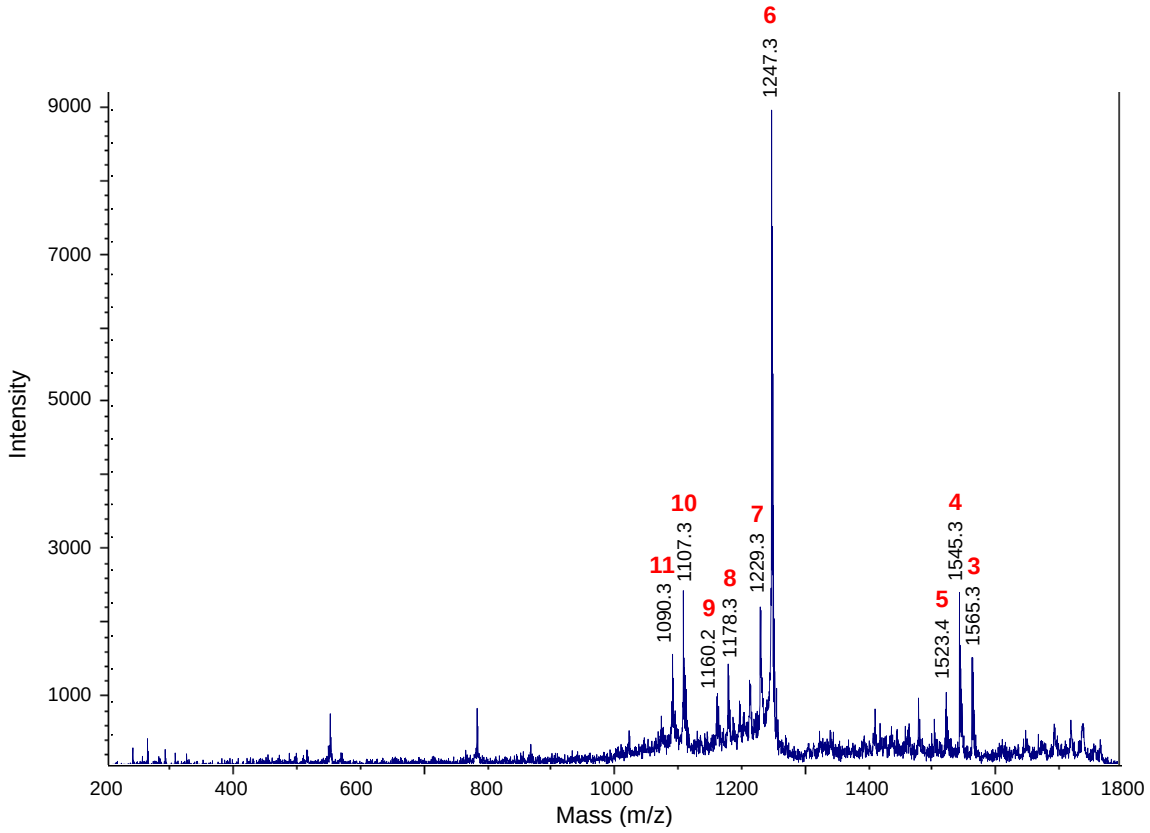

(**D**) Table and structure showing key ions and fragments in the MALDI MS and MS/MS of thiostrepton Ala2Tyr.

Fragment	Expected	Observed
1. $M+H^+$ (Parent ion)	1756.5	1756.4
2. $M+Na^+$	1778.5	1778.4
3. M-Tyr2-CO+H^+	1565.5	1565.3
4. M-Dhb8-Tzn9-CO-NH+H^+	1545.5	1545.3
5. M-QA+H^+	1523.5	1523.4
6. M-QA-Ile1-Tyr2+H^+	1247.3	1247.3
7. M-QA-Ile1-Tyr2-H_2O+H^+	1229.3	1229.3
8. M-QA-Ile1-Tyr2-Dha3+H^+	1178.3	1178.3
9. M-QA-Ile1-Tyr2-Dha3-H_2O+H^+	1160.3	1160.2
10. M-QA-Ile1-Tyr2-Dha3-Ala4+H^+	1107.3	1107.3
11. M-QA-Ile1-Tyr2-Dha3-Ala4-OH+H^+	1090.3	1090.3

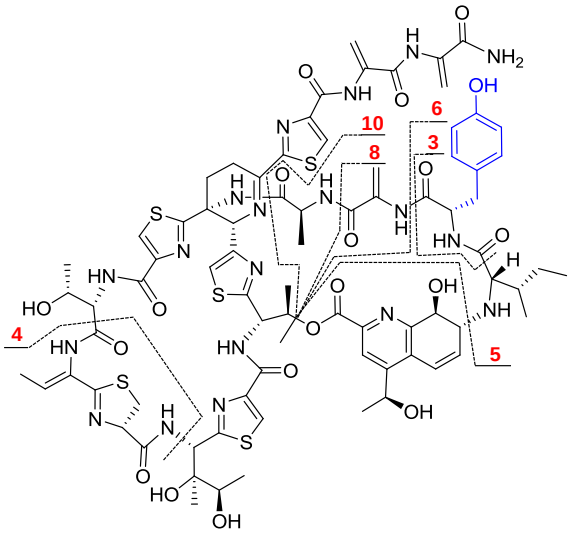

Figure E.28. MS analysis of thiostrepton Ala2Val-ΔIle1 isolated from *S. laurentii* NDS1/int-A2V.

(**A**) HPLC-MS analysis. (1) Chromatogram extracted for *m/z* 790.2, the calculated $[M+2H]^{2+}$ ion of thiostrepton Ala2Val-ΔIle1. (2) Total ion chromatogram.

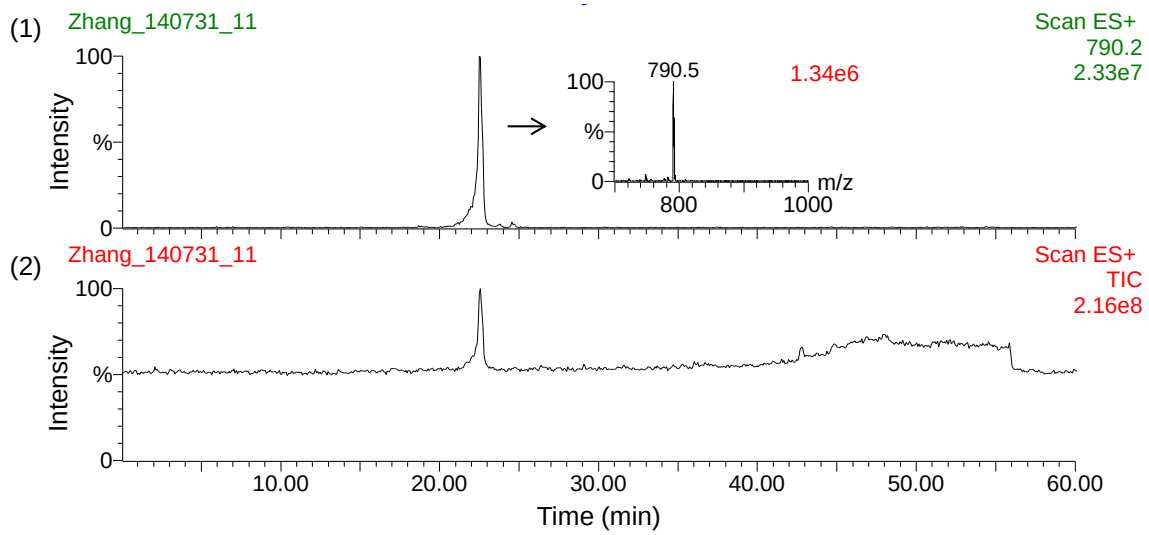

(**B**) MALDI MS spectrum of thiostrepton Ala2Val-ΔIle1.

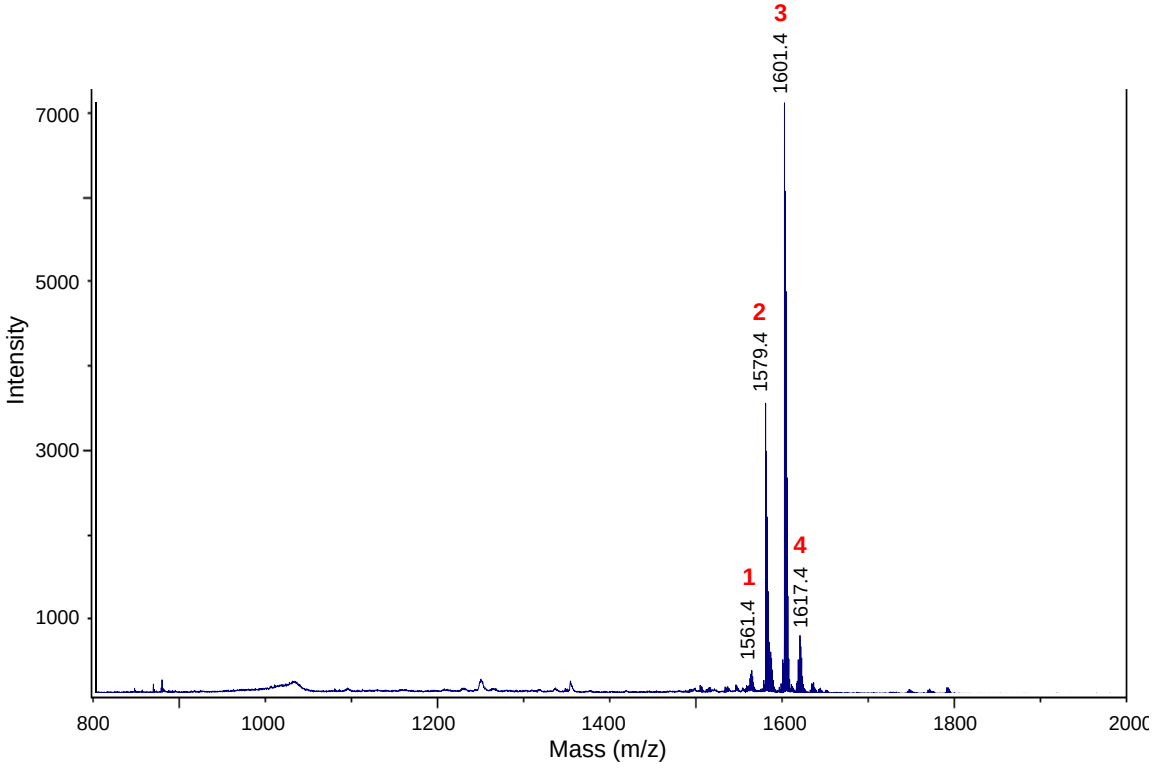

(**C**) MALDI MS/MS of parent ion *m/z* 1579.4.

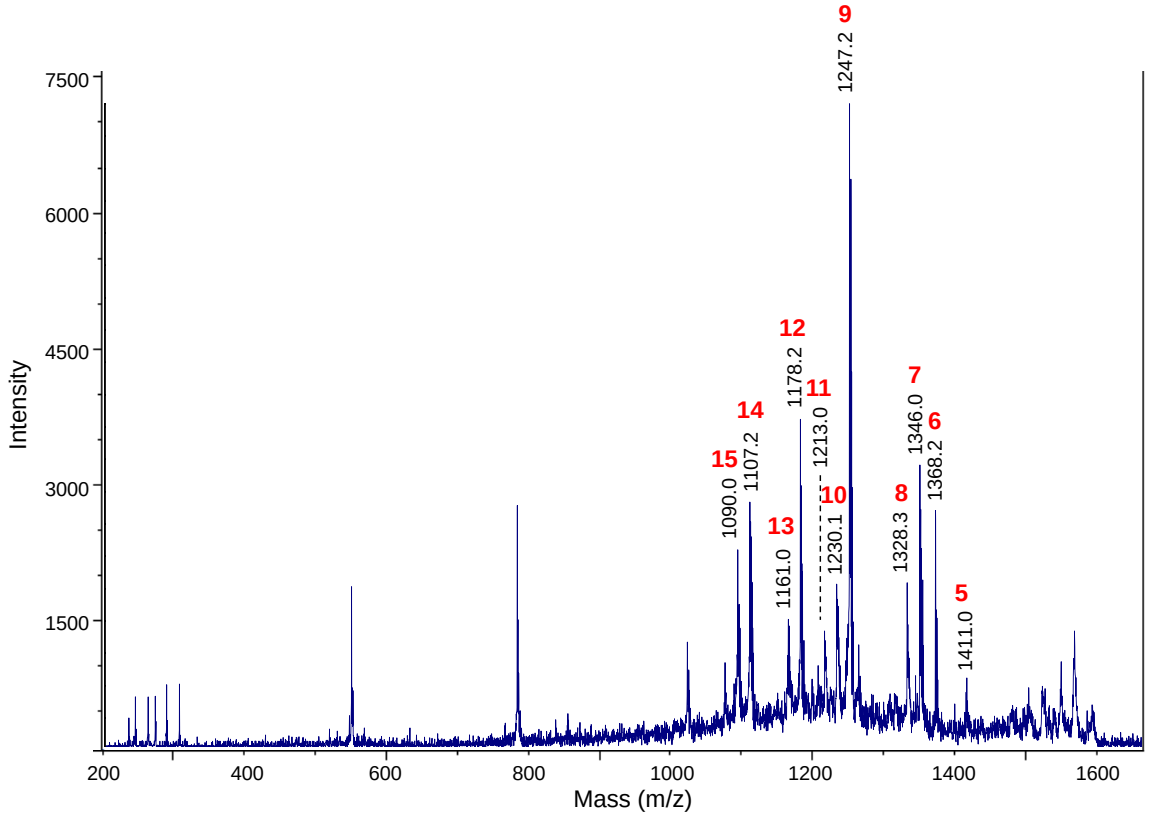

(**D**) Table and structure showing key ions and fragments in the MALDI MS and MS/MS of thiostrepton Ala2Val-ΔIle1.

Fragment	Expected	Observed
1. M-H_2O+H^+	1561.4	1561.4
2. M+H^+ (Parent ion)	1579.4	1579.4
3. M+Na^+	1601.4	1601.4
4. M+K^+	1617.4	1617.4
5. M-Dhb8-Tzn9+H^+	1411.4	1411.0
6. M-Val2-Dha3-(Ala4-CO)+H^+	1368.3	1368.2
7. M-QA+H^+	1346.4	1346.3
8. M-QA-H_2O+H^+	1328.4	1328.3
9. M-QA-Val2+H^+	1247.3	1247.2
10. M-QA-Val2-OH+H^+	1230.3	1230.1
11. M-QA-Val2-OH-OH+H^+	1213.3	1213.0
12. M-QA-Val2-Dha3+H^+	1178.3	1178.2
13. M-QA-Val2-Dha3-OH+H^+	1161.3	1161.0
14. M-QA-Val2-Dha3-Ala4+H^+	1107.3	1107.2
15. M-QA-Val2-Dha3-Ala4-OH+H^+	1090.2	1090.0

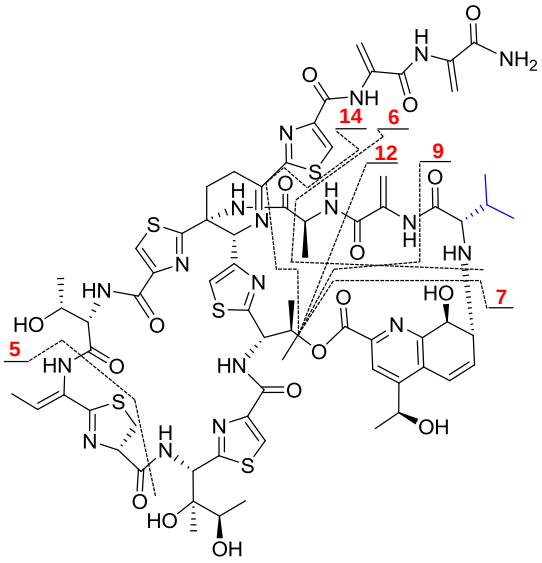

Figure E.29. Structure and numbering system used for thiostrepton Ala2Val-ΔIle1.

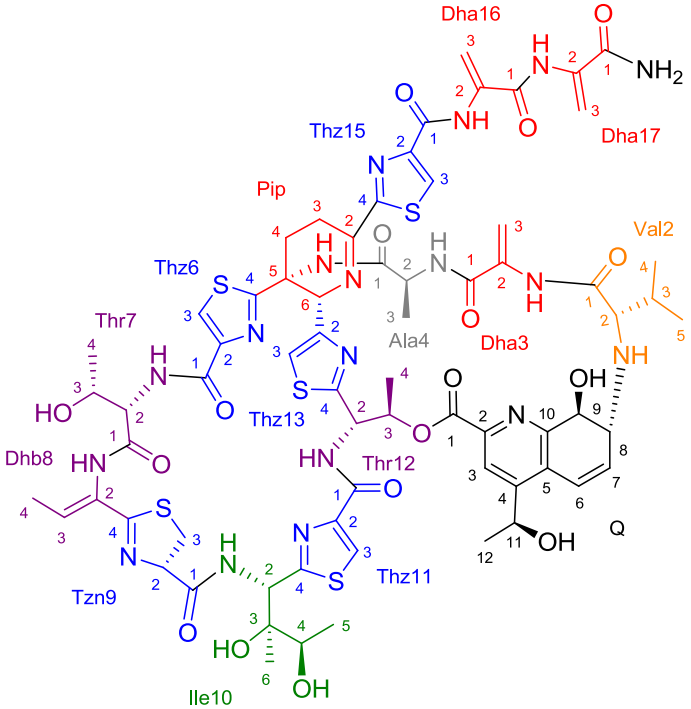

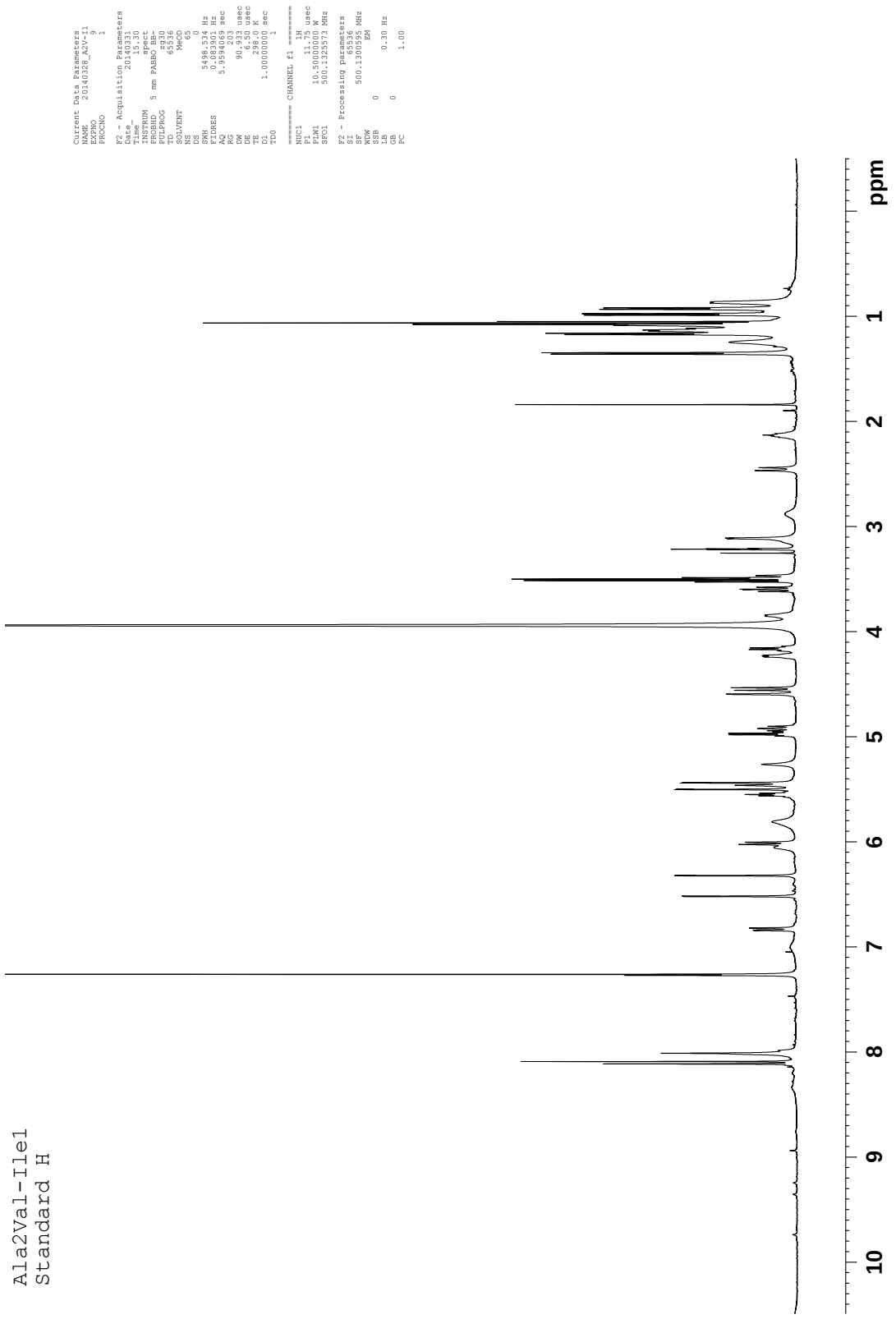

Figure E.30. ^{1}H NMR spectrum of thiostrepton Ala2Val-ΔIle1 (500 MHz, $CDCl_3$-CD_3OD 4:1, 25 °C).

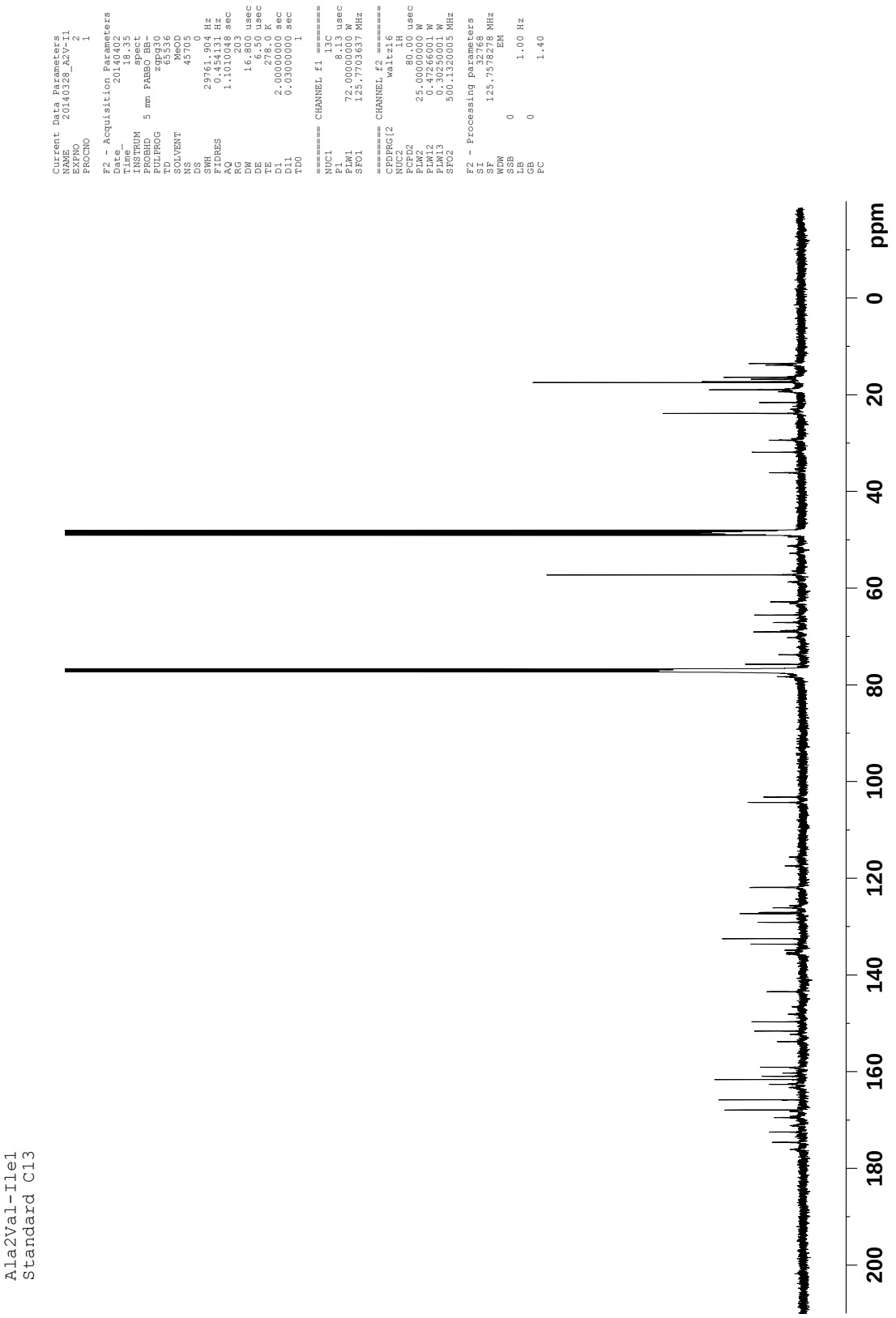

Figure E.31. ^{13}C NMR spectrum of thiostrepton Ala2Val-ΔIle1 (125 MHz, $CDCl_3$-CD_3OD 4:1, 25 °C).

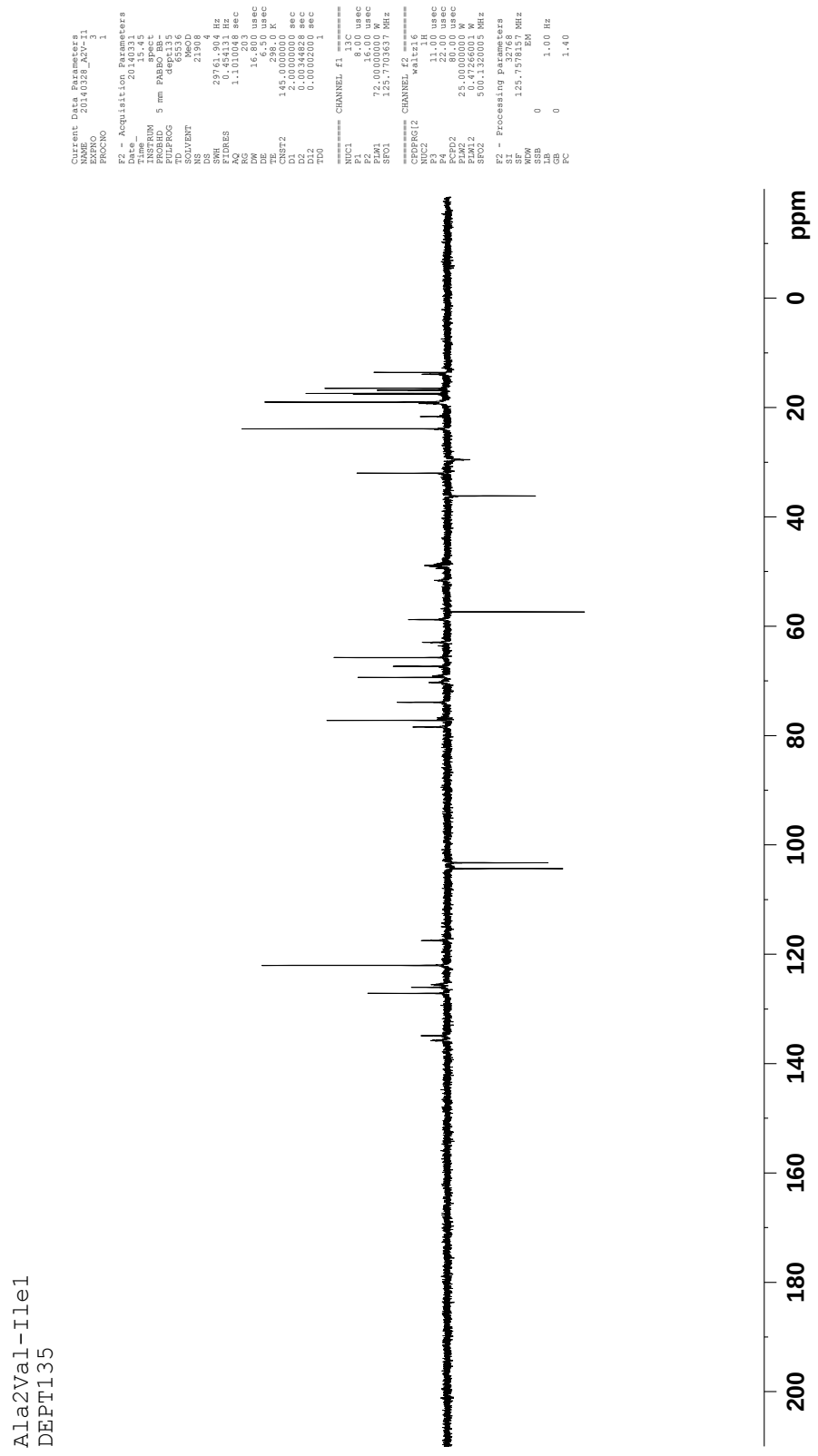

Figure E.32. DEPT-135 NMR spectrum of thiostrepton Ala2Val-ΔIle1 (125 MHz, $CDCl_3$-CD_3OD 4:1, 25 °C).

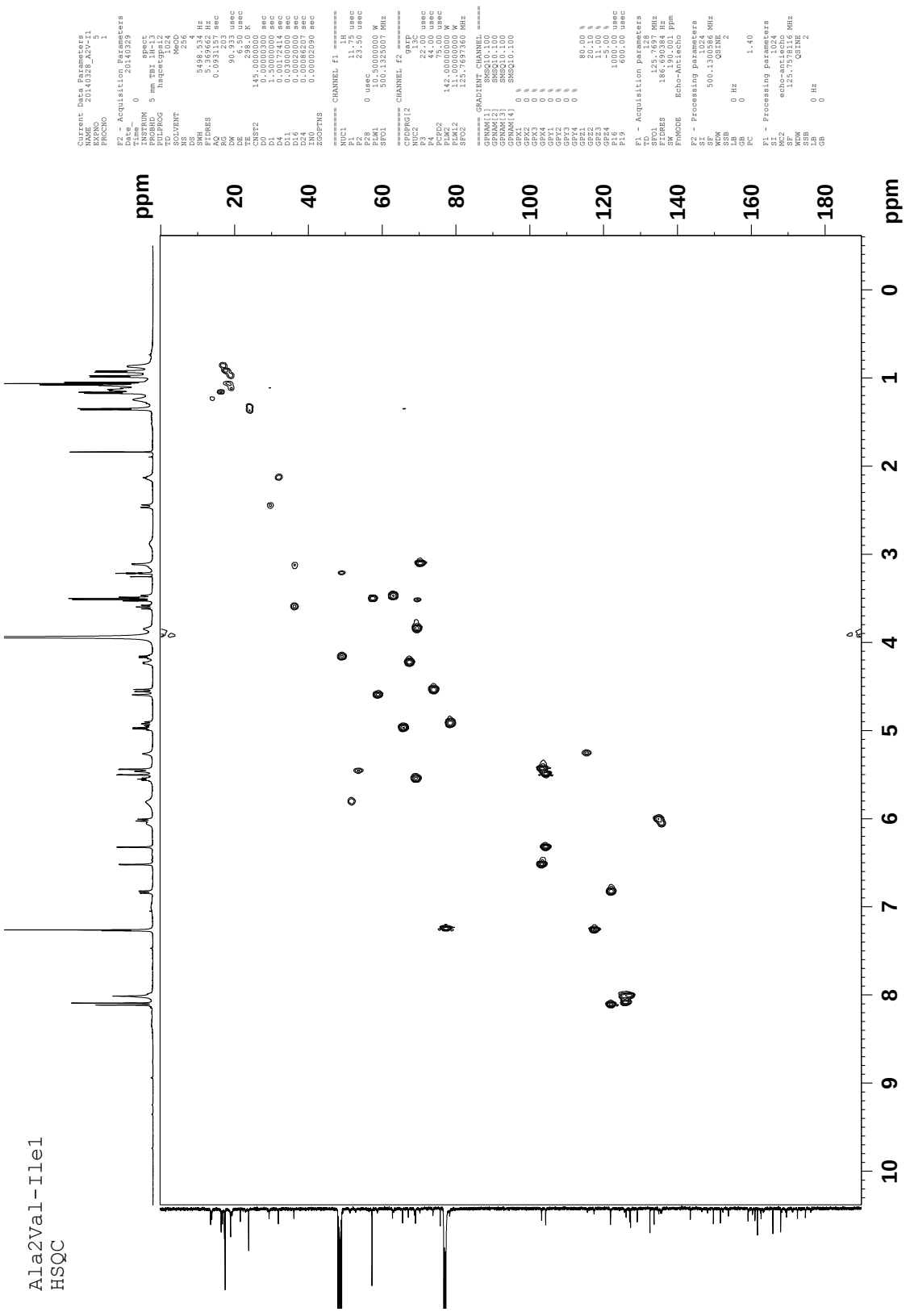

Figure E.33. gHSQC NMR spectrum of thiostrepton Ala2Val-ΔIle1 (500 MHz, $CDCl_3$-CD_3OD 4:1, 25 °C).

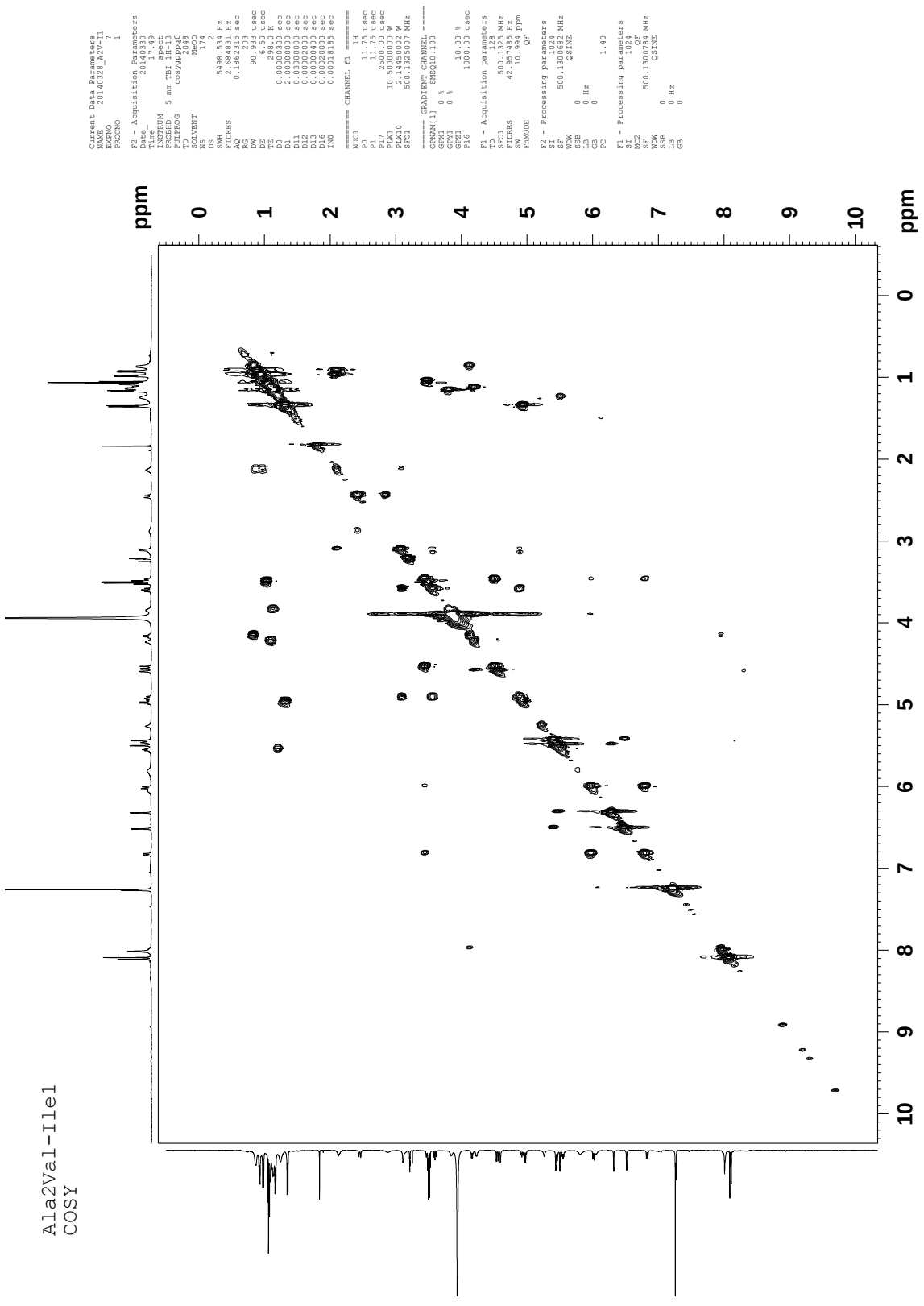

Figure E.34. gCOSY NMR spectrum of thiostrepton Ala2Val-ΔIle1 (125 MHz, $CDCl_3$-CD_3OD 4:1, 25 °C).

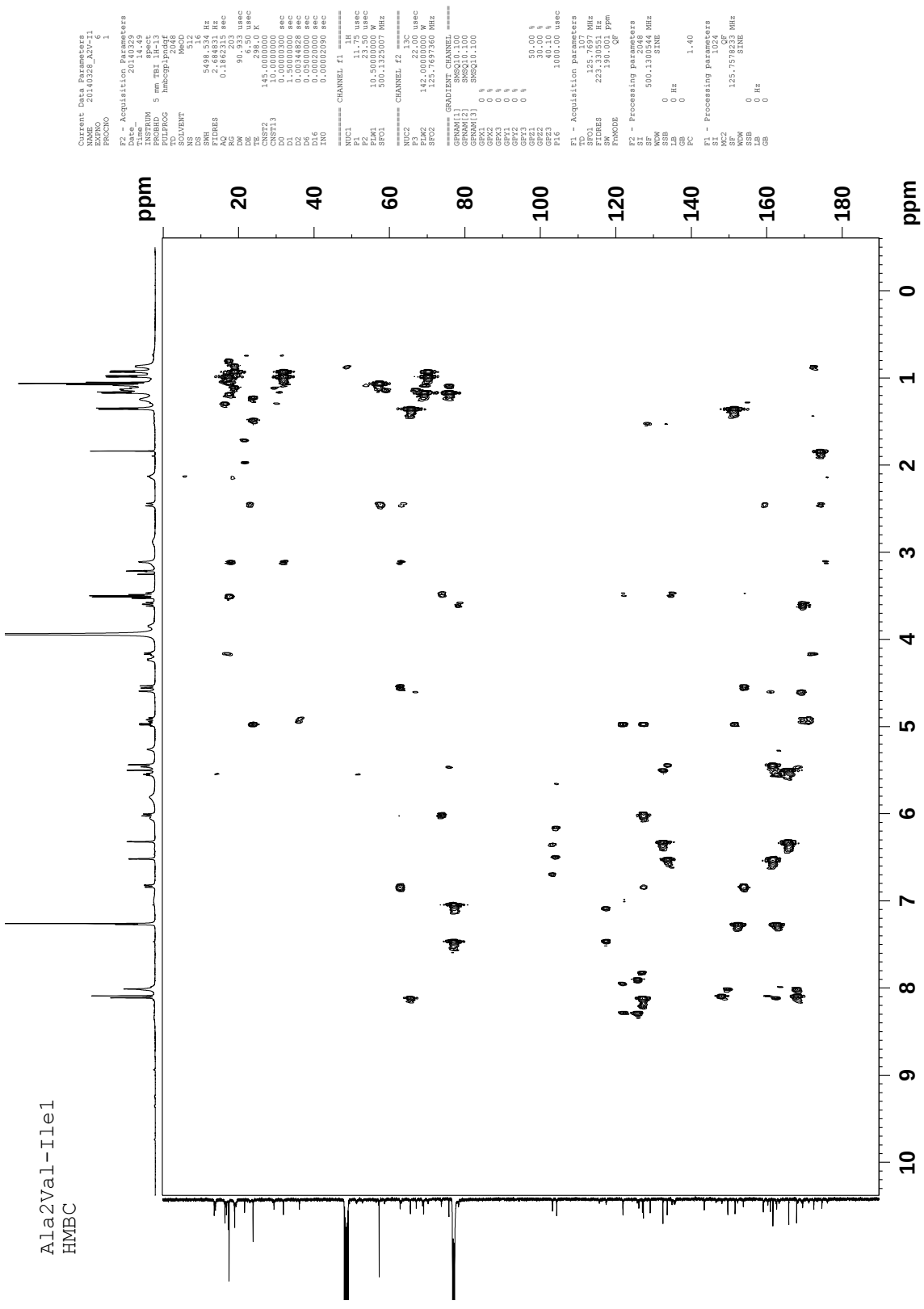

Figure E.35. gHMBC NMR spectrum of thiostrepton Ala2Val-ΔIle1 (125 MHz, $CDCl_3$-CD_3OD 4:1, 25 °C).

Table E.4. ^{1}H and ^{13}C NMR assignments of thiostrepton Ala2Val-ΔIle1

Position	δ_C [ppm]; mult	δ_H [ppm]; (mult, J in Hz)	HMBC[a]	COSY[b]
Val2				
Val2-1	176.1; C q			
Val2-2	70.2; CH	3.11 (d, 3.6)	Val2-1; Val2-3; Val2-4_B; Q-8	Val2-3
Val2-3	31.9; CH	2.17-2.09 (m)	Val2-1	Val2-2; Val2-4_A; Val2-4_B
Val2-4_A	19.3; CH_3	0.98 (d, 6.9)	Val2-2; Val2-3; Val2-4_B	Val2-3
Val2-4_B	17.5; CH_3	0.92 (d, 6.9)	Val2-2; Val2-3; Val2-4_A	Val2-3
Dha3				
Dha3-1	163.3; C q			
Dha3-2	135.4; C q			
Dha3-3	115.6; CH_2	H_A: 5.81 (br s)		
		H_B: 5.26 (br s)	Dha3-1	
Ala4				
Ala4-1	172.5; C q			
Ala4-2	49.4; CH	4.16 (q, 7.3)	Ala4-1; Ala4-3	Ala4-3
Ala4-3	16.8; CH_3	0.87 (d, 5.8)	Ala4-1; Ala4-2	Ala4-2
Pip				
Pip-2	159.1; C q			
Pip-3	23.0; CH_2	H_A: 3.53-3.48 (m)		
		H_B: 2.92-2.83 (m)		Pip-4-H_B
Pip-4	29.4; CH_2	H_A: 3.88-3.81 (m)		
		H_B: 2.47-2.42 (m)	Pip-2; Pip-3; Pip-5; Pip-6	Pip-3-H_B
Pip-5	57.3; C q			
Pip-6	63.1; CH	5.26 (br s)		
Thz6				
Thz6-1	161.0; C q			
Thz6-2	149.7; C q			
Thz6-3	127.1; CH	8.01 (s)	Thz6-2; Thz6-4	
Thz6-4	167.9; C q			
Thr7				
Thr7-1	169.5; C q			
Thr7-2	58.7; CH	4.59 (d, 2.0)	Thz6-1; Thr7-1; Thr7-3	Thr7-3
Thr7-3	67.1; CH	4.26-4.20 (m)		Thr7-2; Thr7-4
Thr7-4	19.3; CH_3	1.13 (d, 5.5)	Thr7-2; Thr7-3	Thr7-3
Dhb8				
Dhb8-2	127.3; C q			
Dhb8-3	135.7; CH	6.08-6.03 (m)	Dhb8-2	Dhb8-4
Dhb8-4	19.0; CH_3	1.13-1.09 (m)		
Tzn9				
Tzn9-1	171.2; C q			
Tzn9-2	78.3; CH	4.92 (dd, 11.5, 9.6)	Tzn9-1; Tzn9-3; Tzn9-4	Tzn9-3-H_A; Tzn9-3-H_B
Tzn9-3	36.1; CH_2	H_A: 3.60 (dd, 11.2; 9.1)	Tzn9-1; Tzn9-2; Tzn9-4	Tzn9-2; Tzn9-3-H_B
		H_B: 3.17-3.12 (m)		Tzn9-2; Tzn9-3-H_A
Tzn9-4	169.5; C q			
Ile10				
Ile10-2	52.8; CH	5.46 (s)	Ile10-3; Thz11-4	
Ile10-3	75.8; C q			
Ile10-4	69.0; CH	3.88-3.81 (m)		Ile10-5
Ile10-5	16.4; CH_3	1.17 (d, 6.5)	Ile10-3; Ile10-4	Ile10-4
Ile10-6	19.0; CH_3	1.08 (s)	Ile10-3; Ile10-4	
Thz11				
Thz11-1	162.6; C q			
Thz11-2	149.7; C q			
Thz11-3	121.9; CH	8.11 (s)	Thz11-1; Thz11-2; Thz11-4	
Thz11-4	168.2; C q			
Thr12				
Thr12-2	51.3; CH	5.84-5.77 (m)		Thr12-3
Thr12-3	69.0; CH	5.55 (pentet, 6.0)	Thz11-1; Thr12-2; Thr12-4; Q-1	Thr12-2; Thr12-4
Thr12-4	13.9; CH_3	1.28-1.21 (m)		Thr12-3

Position	δ_C [ppm]; mult	δ_H [ppm]; (mult, J in Hz)	HMBC[a]	COSY[b]
Thz13				
Thz13-2	159.1; C q			
Thz13-3	125.7; CH	8.01 (s)	Thz13-4	
Thz13-4	167.9; C q			
Thz15				
Thz15-1	160.3; C q			
Thz15-2	148.1; C q			
Thz15-3	126.1; CH	8.09 (s)	Thz15-1; Thz15-2; Thz15-4	
Thz15-4	168.2; C q			
Dha16				
Dha16-1	161.6; C q			
Dha16-2	133.6; C q			
Dha16-3	103.2; CH_2	H_A: 6.52 (d, 2.3)	Dha16-1; Dha16-2	Dha16-3-H_B
		H_B: 5.44 (d, 2.3)	Dha16-1; Dha16-2	Dha16-3-H_A
Dha17				
Dha17-1	165.8; C q			
Dha17-2	132.5; C q			
Dha17-3	104.3; CH_2	H_A: 6.32 (d, 1.7)	Dha17-1; Dha17-2	Dha17-3-H_B
		H_B: 5.50 (d, 1.7)	Dha17-1; Dha17-2	Dha17-3-H_A
Q				
Q-1	162.6; C q			
Q-2	151.6; C q			
Q-3	117.4; CH	7.27 (s)	Q-1; Q-2; Q-4; Q-10	
Q-4	152.3; C q			
Q-5	127.3; C q			
Q-6	121.9; CH	6.83 (dd, 10.2; 2.5)	Q-5; Q-8; Q-10	Q-7; Q-8
Q-7	134.9; CH	6.01 (m)	Q-5; Q-8; Q-9	Q-6; Q-8
Q-8	62.8; CH	3.50-3.45 (m)	Q-6; Q-7; Q-9; Q-10	Q-6; Q-7; Q-9
Q-9	73.8; CH	4.54 (d, 12.3)	Q-8; Q-10	Q-8
Q-10	153.8; C q			
Q-11	65.6; CH	4.97 (q, 6.5)	Q-2; Q-5; Q-6; Q-12	Q-12
Q-12	23.9; CH_3	1.35 (d, 6.6)	Q-4; Q-11	Q-11

[a] HMBC correlations are from the proton to the indicated carbon.
[b] COSY correlations are from the proton to the proton attached to the indicated position.

Figure E.36. Thiostrepton A, Ala2Ile-ΔIle1 and Ala2Val-ΔIle1 bound to the ribosome. Measurements of the distances between Thr7 and quinaldic acid hydroxyl groups in thiostrepton A, thiostrepton Ala2Ile-ΔIle1 and Ala2Val-ΔIle1. (**A**) Thiostrepton A (Cyan) bound to the ribosome adapted from PDB 3CF5.[1] (**B**) Model of thiostrepton Ala2Ile-ΔIle1 (magenta) bound to the ribosome. (**C**) Model of thiostrepton Ala2Val-ΔIle1 (blue) bound to the ribosome. Helices 43 and 44 of 23S rRNA are colored in orange and ribosomal protein L11 is shown in green.

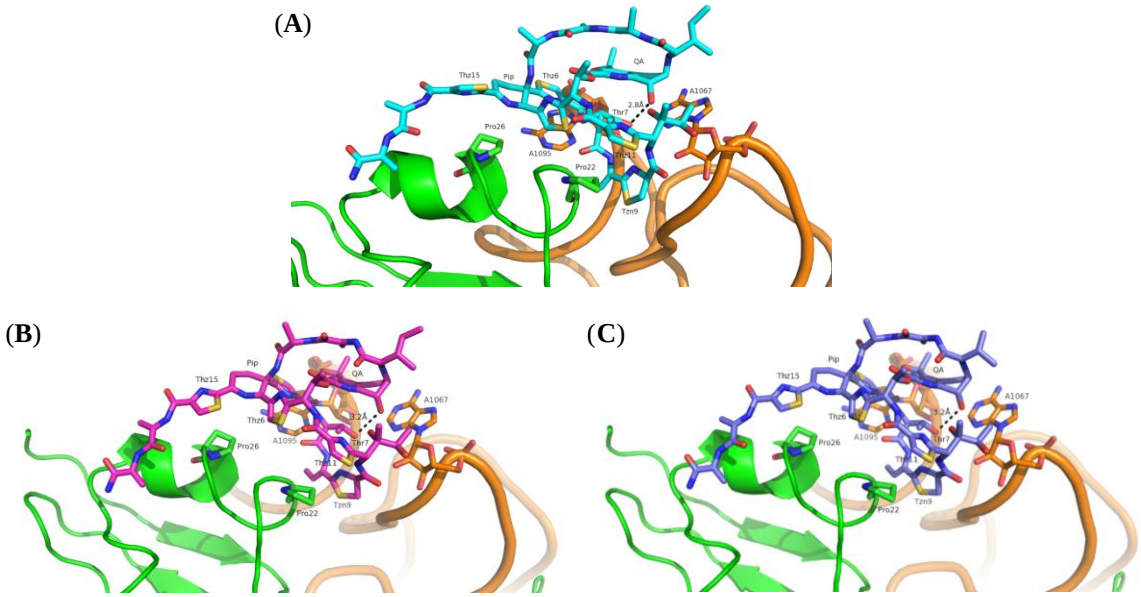

Reference:

1. Harms, J. M.; Wilson, D. N.; Schluenzen, F.; Connell, S. R.; Stachelhaus, T.; Zaborowska, Z.; Spahn, C. M.; Fucini, P., Translational regulation via L11: Molecular switches on the ribosome turned on and off by thiostrepton and micrococcin. *Mol. Cell.* **2008,** *30*, 26-38.

APPENDIX F: HR-MS AND TITERS OF THIOSTREPTON ANALOGS

Table F.1. Summary of HR-MS results of thiostrepton analogs

Thiostrepton variant	Analysis	Molecular formula	Calculated $[M+Na]^+$	Observed $[M+H]^+$
Thiostrepton Ala2Dha	HR-ESI-MS	$C_{72}H_{83}N_{19}O_{18}S_5$	1684.4665	1684.4718
Thiostrepton Ala2Gly	HR-ESI-MS	$C_{71}H_{83}O_{18}N_{19}S_5$	1672.4670	1672.4689
Thiostrepton Ala4Gly	HR-ESI-MS	$C_{71}H_{83}O_{18}N_{19}S_5$	1672.4670	1672.4664
Thiostrepton Thr7Val	HR-ESI-MS	$C_{73}H_{87}N_{19}O_{17}S_5$	1684.5029	1684.5087

Thiostrepton variant	Analysis	Molecular formula	Calculated $[M+H]^+$	Observed $[M+H]^+$
SL105-1	HR-MALDI-MS	$C_{62}H_{66}N_{16}O_{15}S_5$	1435.3575	1435.3618
SL106-1	HR-MALDI-MS	$C_{64}H_{70}N_{16}O_{15}S_5$	1463.3888	1463.3890
Thiostrepton Ala2Dhb	HR-MALDI-MS	$C_{73}H_{85}N_{19}O_{18}S_5$	1676.5002	1676.5043
Thiostrepton Ala2Ile-ΔIle1	HR-MALDI-MS	$C_{69}H_{80}N_{18}O_{17}S_5$	1593.4631	1593.4673
Thiostrepton Ala2Met	HR-MALDI-MS	$C_{74}H_{89}N_{19}O_{18}S_6$	1724.5036	1724.4999
Thiostrepton Ala2Phe	HR-MALDI-MS	$C_{78}H_{89}N_{19}O_{18}S_5$	1740.5315	1740.5244
Thiostrepton Ala2Tyr	HR-MALDI-MS	$C_{78}H_{89}N_{19}O_{19}S_5$	1756.5264	1756.5267
Thiostrepton Ala2Val-ΔIle1	HR-MALDI-MS	$C_{68}H_{78}N_{18}O_{17}S_5$	1579.4474	1579.4519
Thiostrepton Ala4Asn	HR-MALDI-MS	$C_{73}H_{86}N_{20}O_{19}S_5$	1707.5060	1707.5106
Thiostrepton Ala4Cys F1	HR-MALDI-MS	$C_{72}H_{85}N_{19}O_{18}S_6$	1696.4723	1696.4725
Thiostrepton Ala4Cys F2	HR-MALDI-MS	$C_{72}H_{85}N_{19}O_{18}S_6$	1696.4723	1696.4704
Thiostrepton Ala4Dha	HR-MALDI-MS	$C_{72}H_{83}N_{19}O_{18}S_5$	1662.4845	1662.4830
Thiostrepton Ala4Dhb	HR-ESI-MS	$C_{73}H_{85}N_{19}O_{18}S_5$	1676.5002	1676.5064
Thiostrepton Ala4Gln	HR-MALDI-MS	$C_{74}H_{88}N_{20}O_{19}S_5$	1721.5217	1721.5255
Thiostrepton Ala4His	HR-MALDI-MS	$C_{75}H_{87}N_{21}O_{18}S_5$	1730.5220	1730.5193
Thiostrepton Ala4Ile	HR-ESI-MS	$C_{75}H_{91}N_{19}O_{18}S_5$	1706.5471	1706.5460
Thiostrepton Ala4Leu	HR-ESI-MS	$C_{75}H_{91}N_{19}O_{18}S_5$	1706.5471	1706.5550
Thiostrepton Ala4Met	HR-ESI-MS	$C_{74}H_{89}N_{19}O_{18}S_6$	1724.5036	1724.5088
Thiostrepton Ala4Phe	HR-MALDI-MS	$C_{78}H_{89}N_{19}O_{18}S_5$	1740.5315	1740.5394
Thiostrepton Ala4Ser	HR-MALDI-MS	$C_{72}H_{85}N_{19}O_{19}S_5$	1680.4951	1680.5016
Thiostrepton Ala4Trp	HR-MALDI-MS	$C_{80}H_{90}N_{20}O_{18}S_5$	1779.5424	1779.5558
Thiostrepton Ala4Tyr	HR-MALDI-MS	$C_{78}H_{89}N_{19}O_{19}S_5$	1756.5264	1756.5343
Thiostrepton Ala4Val	HR-ESI-MS	$C_{74}H_{89}N_{19}O_{18}S_5$	1692.5315	1692.5348
Thiostrepton Thr7Ala	HR-MALDI-MS	$C_{71}H_{83}N_{19}O_{17}S_5$	1634.4896	1634.4906

Table F.2. Titers of thiostrepton analogs

Fermentation of each *S. laurentii* variant strain was carried out in two sets of triplicate. The yields of all thiostrepton analogs were quantified by HPLC against a standard calibration curve of thiostrepton A assuming similar spectral properties for each derivative.

Compound	Titer (mg/L)
Thiostrepton A	115 ± 35
Ala2Dha	301 ± 7
Ala2Dhb	39 ± 9
Ala2Gly	19 ± 3
Ala2Ile-ΔIle1	34 ± 4
Ala2Met	3.1 ± 0.2
Ala2Phe	2.5 ± 0.6
Ala2Tyr	1.7 ± 0.6
Ala2Val-ΔIle1	51 ± 16
Ala4Asn	41.5 ± 11.5
Ala4Cys F1	4.9 ± 1.4
Ala4Cys F2	5.3 ± 1.2
Ala4Dha	41.9 ± 12.3
Ala4Dhb	24.7 ± 4.8
Ala4Gln	3.8 ± 0.5
Ala4Gly	19.2 ± 4.6
Ala4His	4.7 ± 0.9
Ala4Ile	47.0 ± 24.5
Ala4Leu	90.6 ± 39.5
Ala4Met	82.0 ± 10.8
Ala4Phe	4.7 ± 2.1
Ala4Ser	3.0 ± 1.2
Ala4Trp	3.1 ± 1.5
Ala4Tyr	4.4 ± 2.6
Ala4Val	86.3 ± 17.9

APPENDIX G: ONE SAMPLE CALCULATION FOR IC_{50} VALUES AND IC_{50} FIT CURVES

Figure G.1. One sample calculation for IC_{50} values.

Here is showing the calculation of thiostrepton Ala2Met's IC_{50} value against the proteasome chymotrypsin-like function.

Fluorescence was measured using an excitation wavelength of 360 nm and an emission wavelength of 460 nm. Emissions were documented every 50 s for 1 h and the arbitrary fluorescence units (AFU) were plotted against time for each compound to acquire the slope of the linear fit.

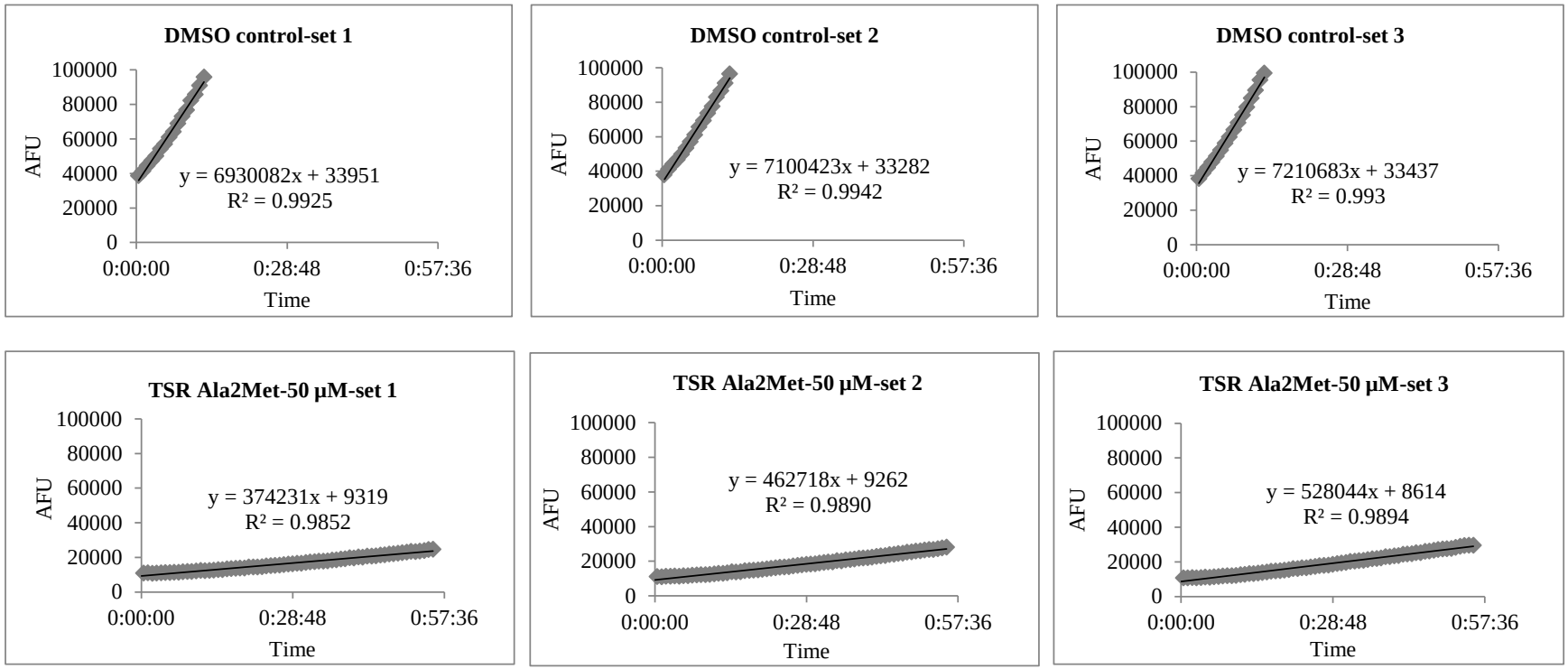

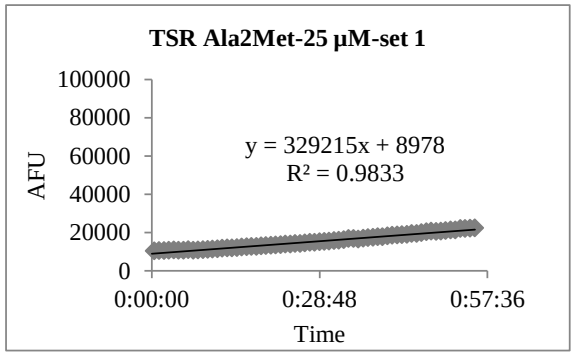
TSR Ala2Met-25 µM-set 1
100000
80000
60000
40000
20000
0
AFU
y = 329215x + 8978
R² = 0.9833
0:00:00
0:28:48
0:57:36
Time

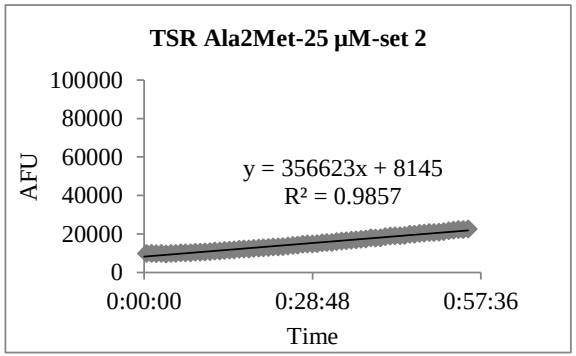
TSR Ala2Met-25 µM-set 2
100000
80000
60000
40000
20000
0
AFU
y = 356623x + 8145
R² = 0.9857
0:00:00
0:28:48
0:57:36
Time

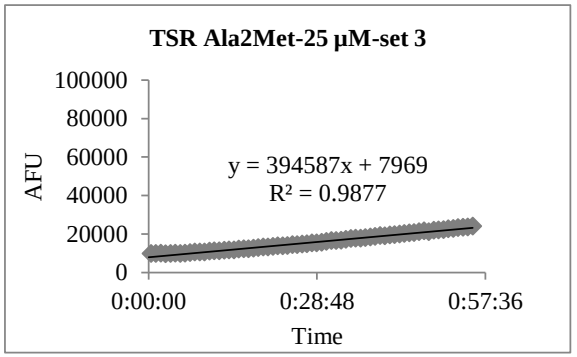
TSR Ala2Met-25 µM-set 3
100000
80000
60000
40000
20000
0
AFU
y = 394587x + 7969
R² = 0.9877
0:00:00
0:28:48
0:57:36
Time

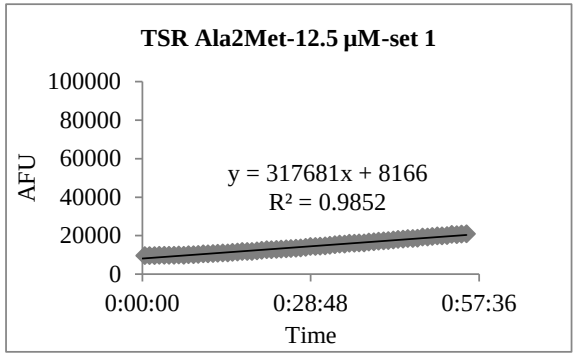
TSR Ala2Met-12.5 µM-set 1
100000
80000
60000
40000
20000
0
AFU
y = 317681x + 8166
R² = 0.9852
0:00:00
0:28:48
0:57:36
Time

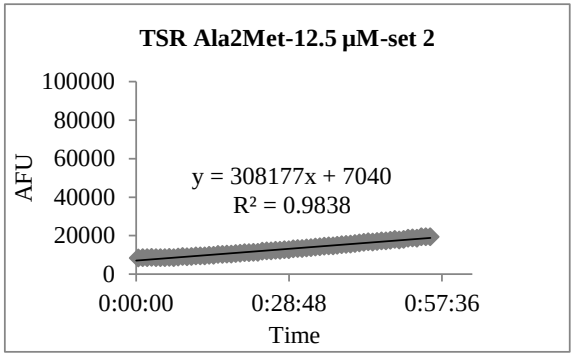
TSR Ala2Met-12.5 µM-set 2
100000
80000
60000
40000
20000
0
AFU
y = 308177x + 7040
R² = 0.9838
0:00:00
0:28:48
0:57:36
Time

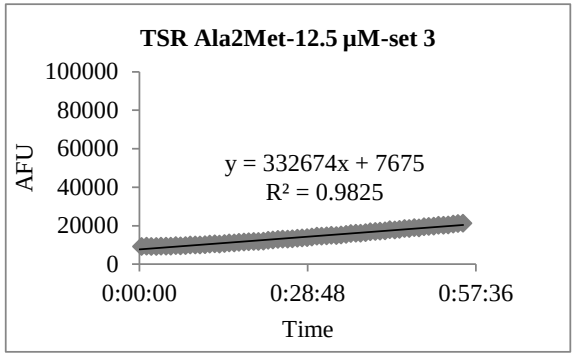
TSR Ala2Met-12.5 µM-set 3
100000
80000
60000
40000
20000
0
AFU
y = 332674x + 7675
R² = 0.9825
0:00:00
0:28:48
0:57:36
Time

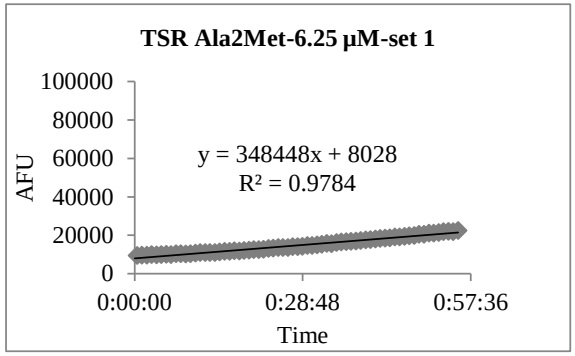
TSR Ala2Met-6.25 µM-set 1
100000
80000
60000
40000
20000
0
AFU
y = 348448x + 8028
R² = 0.9784
0:00:00
0:28:48
0:57:36
Time

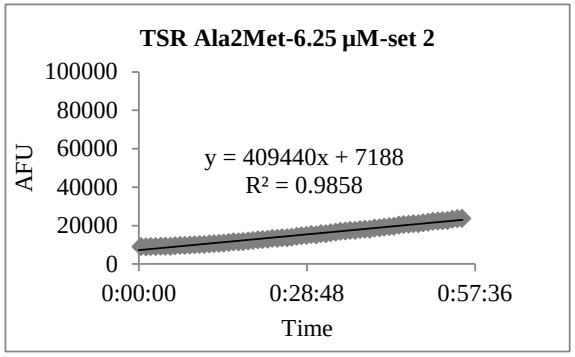
TSR Ala2Met-6.25 µM-set 2
100000
80000
60000
40000
20000
0
AFU
y = 409440x + 7188
R² = 0.9858
0:00:00
0:28:48
0:57:36
Time

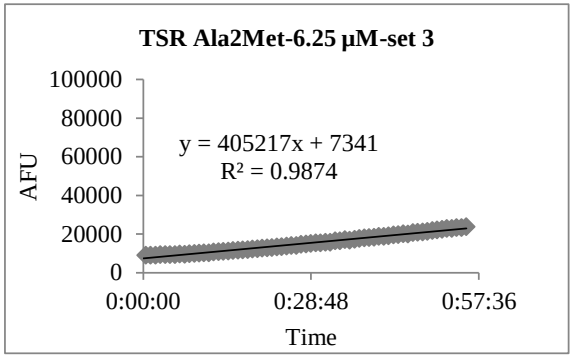
TSR Ala2Met-6.25 µM-set 3
100000
80000
60000
40000
20000
0
AFU
y = 405217x + 7341
R² = 0.9874
0:00:00
0:28:48
0:57:36
Time

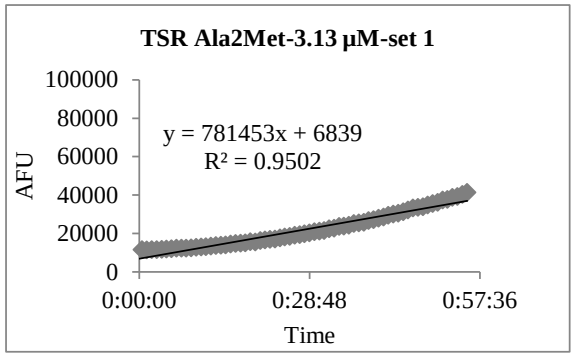
TSR Ala2Met-3.13 µM-set 1
y = 781453x + 6839
R² = 0.9502
AFU
Time
100000
80000
60000
40000
20000
0
0:00:00
0:28:48
0:57:36

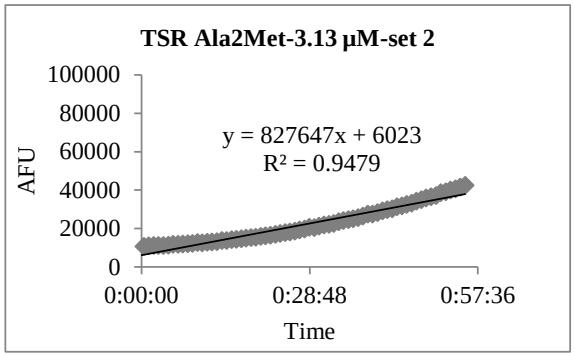
TSR Ala2Met-3.13 µM-set 2
y = 827647x + 6023
R² = 0.9479
AFU
Time
100000
80000
60000
40000
20000
0
0:00:00
0:28:48
0:57:36

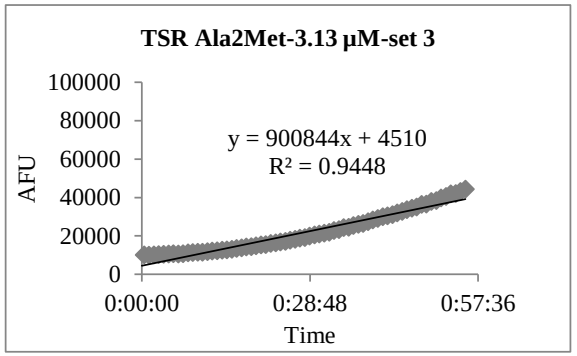
TSR Ala2Met-3.13 µM-set 3
y = 900844x + 4510
R² = 0.9448
AFU
Time
100000
80000
60000
40000
20000
0
0:00:00
0:28:48
0:57:36

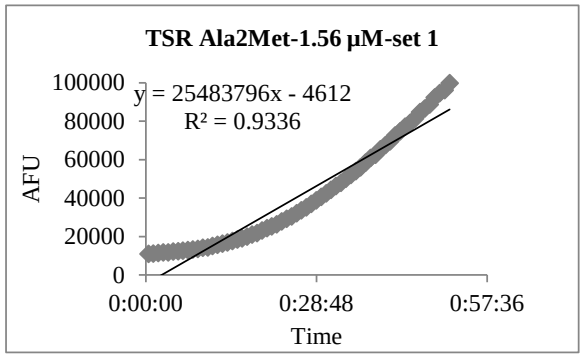
TSR Ala2Met-1.56 µM-set 1
y = 25483796x - 4612
R² = 0.9336
AFU
Time
100000
80000
60000
40000
20000
0
0:00:00
0:28:48
0:57:36

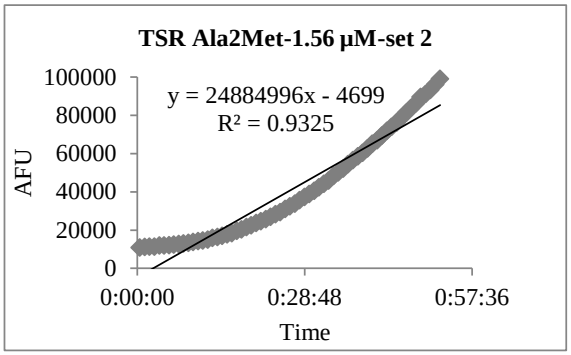
TSR Ala2Met-1.56 µM-set 2
y = 24884996x - 4699
R² = 0.9325
AFU
Time
100000
80000
60000
40000
20000
0
0:00:00
0:28:48
0:57:36

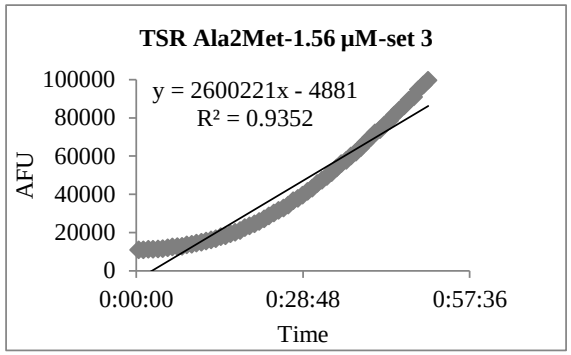
TSR Ala2Met-1.56 µM-set 3
y = 2600221x - 4881
R² = 0.9352
AFU
Time
100000
80000
60000
40000
20000
0
0:00:00
0:28:48
0:57:36

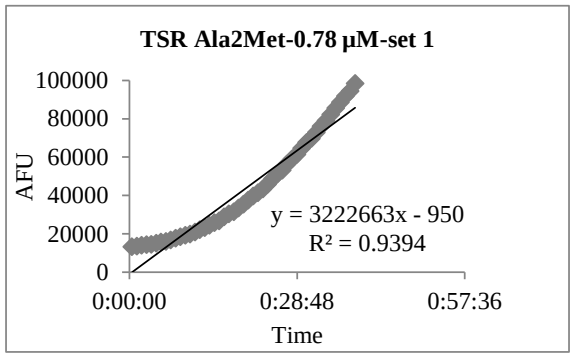
TSR Ala2Met-0.78 µM-set 1
y = 3222663x - 950
R² = 0.9394
AFU
Time
100000
80000
60000
40000
20000
0
0:00:00
0:28:48
0:57:36

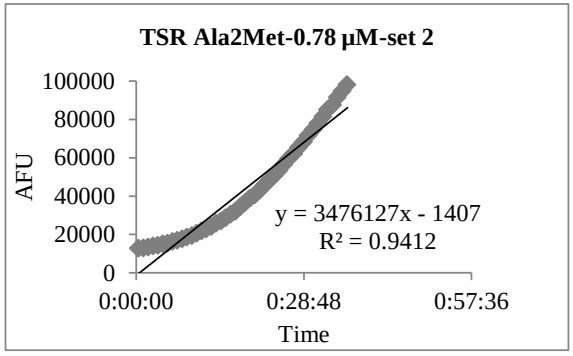
TSR Ala2Met-0.78 µM-set 2
y = 3476127x - 1407
R² = 0.9412
AFU
Time
100000
80000
60000
40000
20000
0
0:00:00
0:28:48
0:57:36

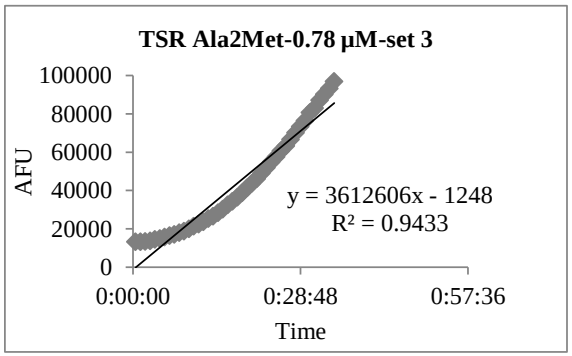
TSR Ala2Met-0.78 µM-set 3
y = 3612606x - 1248
R² = 0.9433
AFU
Time
100000
80000
60000
40000
20000
0
0:00:00
0:28:48
0:57:36

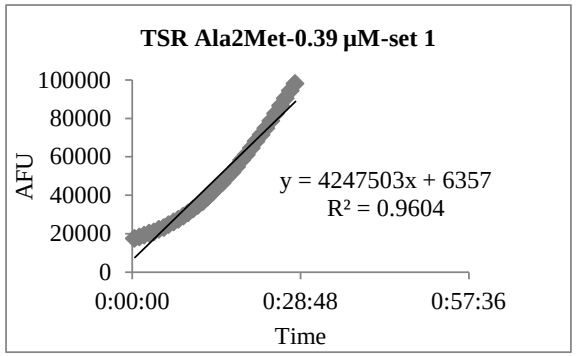
TSR Ala2Met-0.39 µM-set 1
AFU
100000
80000
60000
40000
20000
0
y = 4247503x + 6357
R² = 0.9604
0:00:00
0:28:48
0:57:36
Time

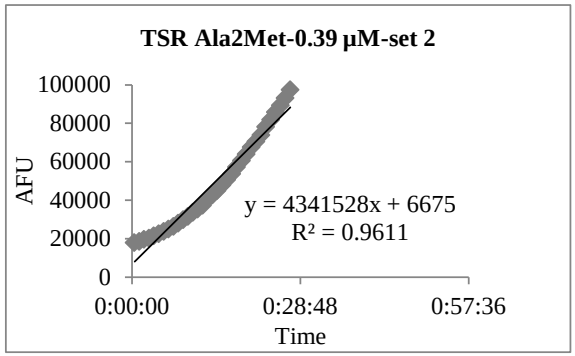
TSR Ala2Met-0.39 µM-set 2
AFU
100000
80000
60000
40000
20000
0
y = 4341528x + 6675
R² = 0.9611
0:00:00
0:28:48
0:57:36
Time

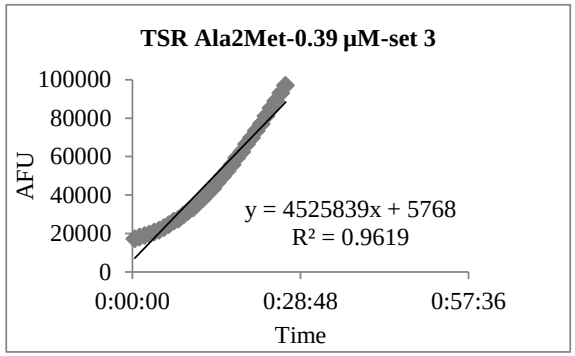
TSR Ala2Met-0.39 µM-set 3
AFU
100000
80000
60000
40000
20000
0
y = 4525839x + 5768
R² = 0.9619
0:00:00
0:28:48
0:57:36
Time

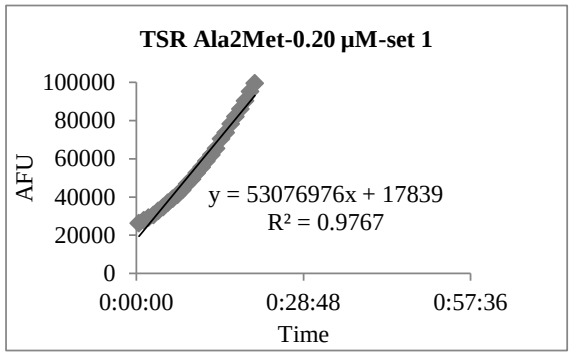
TSR Ala2Met-0.20 µM-set 1
AFU
100000
80000
60000
40000
20000
0
y = 53076976x + 17839
R² = 0.9767
0:00:00
0:28:48
0:57:36
Time

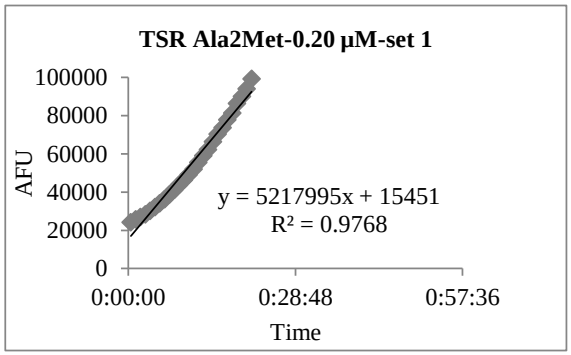
TSR Ala2Met-0.20 µM-set 1
AFU
100000
80000
60000
40000
20000
0
y = 5217995x + 15451
R² = 0.9768
0:00:00
0:28:48
0:57:36
Time

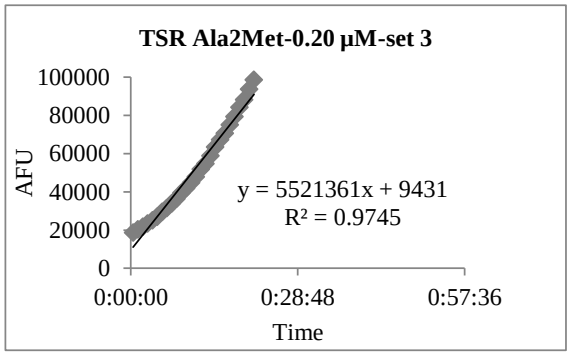
TSR Ala2Met-0.20 µM-set 3
AFU
100000
80000
60000
40000
20000
0
y = 5521361x + 9431
R² = 0.9745
0:00:00
0:28:48
0:57:36
Time

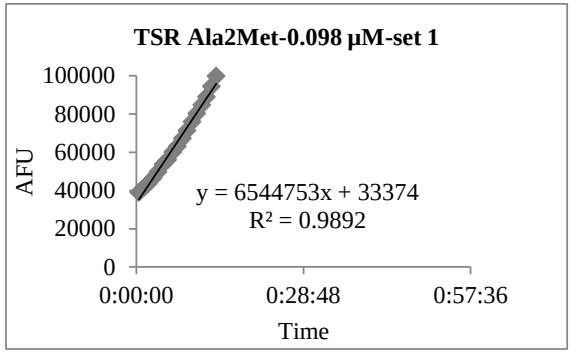
TSR Ala2Met-0.098 µM-set 1
AFU
100000
80000
60000
40000
20000
0
y = 6544753x + 33374
R² = 0.9892
0:00:00
0:28:48
0:57:36
Time

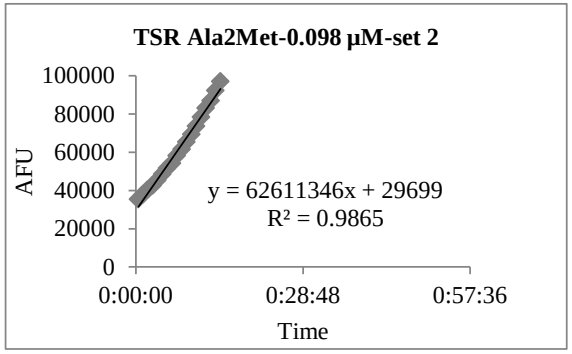
TSR Ala2Met-0.098 µM-set 2
AFU
100000
80000
60000
40000
20000
0
y = 62611346x + 29699
R² = 0.9865
0:00:00
0:28:48
0:57:36
Time

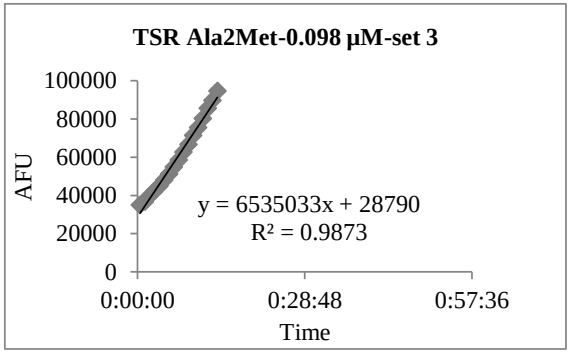
TSR Ala2Met-0.098 µM-set 3
AFU
100000
80000
60000
40000
20000
0
y = 6535033x + 28790
R² = 0.9873
0:00:00
0:28:48
0:57:36
Time

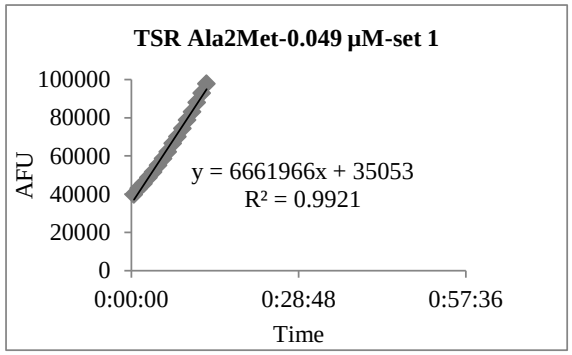
TSR Ala2Met-0.049 µM-set 1
AFU
100000
80000
60000
40000
20000
0
y = 6661966x + 35053
R² = 0.9921
0:00:00
0:28:48
0:57:36
Time

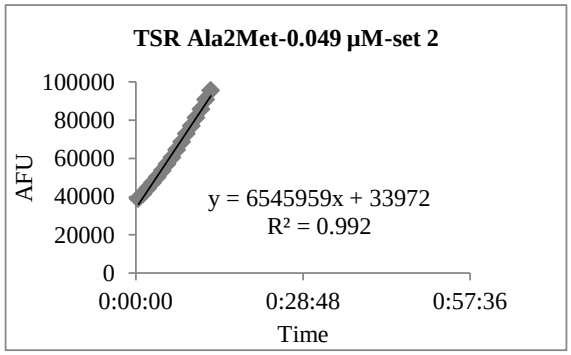
TSR Ala2Met-0.049 µM-set 2
AFU
100000
80000
60000
40000
20000
0
y = 6545959x + 33972
R² = 0.992
0:00:00
0:28:48
0:57:36
Time

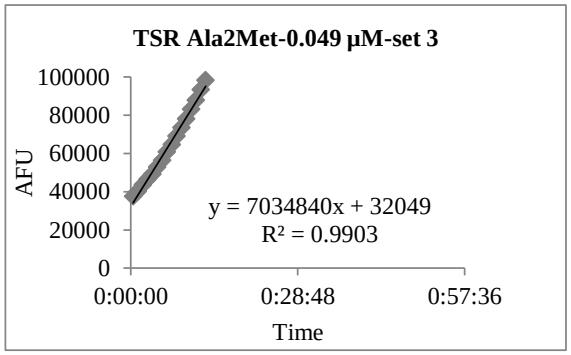
TSR Ala2Met-0.049 µM-set 3
AFU
100000
80000
60000
40000
20000
0
y = 7034840x + 32049
R² = 0.9903
0:00:00
0:28:48
0:57:36
Time

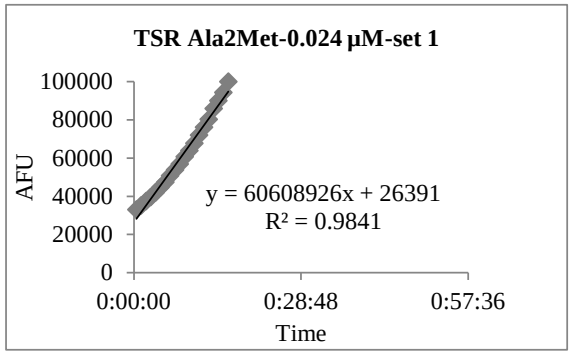
TSR Ala2Met-0.024 µM-set 1
AFU
100000
80000
60000
40000
20000
0
y = 60608926x + 26391
R² = 0.9841
0:00:00
0:28:48
0:57:36
Time

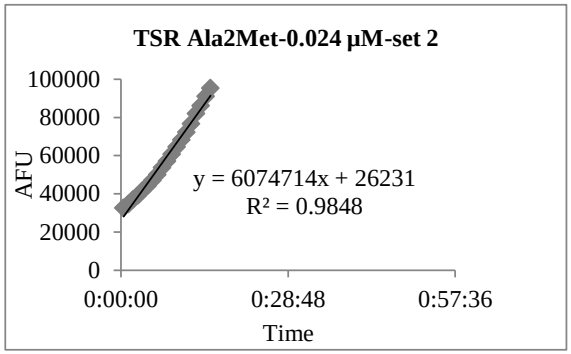
TSR Ala2Met-0.024 µM-set 2
AFU
100000
80000
60000
40000
20000
0
y = 6074714x + 26231
R² = 0.9848
0:00:00
0:28:48
0:57:36
Time

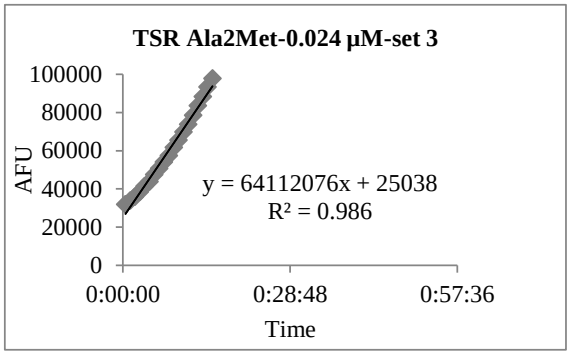
TSR Ala2Met-0.024 µM-set 3
AFU
100000
80000
60000
40000
20000
0
y = 64112076x + 25038
R² = 0.986
0:00:00
0:28:48
0:57:36
Time

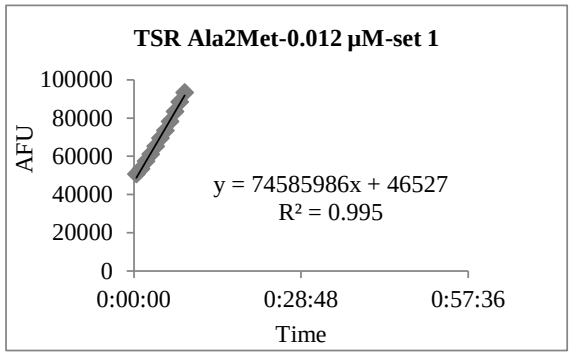
TSR Ala2Met-0.012 µM-set 1
AFU
100000
80000
60000
40000
20000
0
y = 74585986x + 46527
R² = 0.995
0:00:00
0:28:48
0:57:36
Time

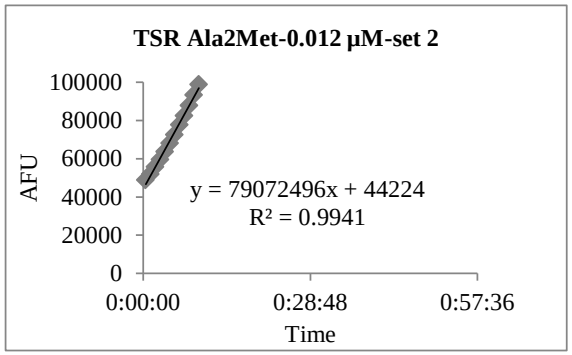
TSR Ala2Met-0.012 µM-set 2
AFU
100000
80000
60000
40000
20000
0
y = 79072496x + 44224
R² = 0.9941
0:00:00
0:28:48
0:57:36
Time

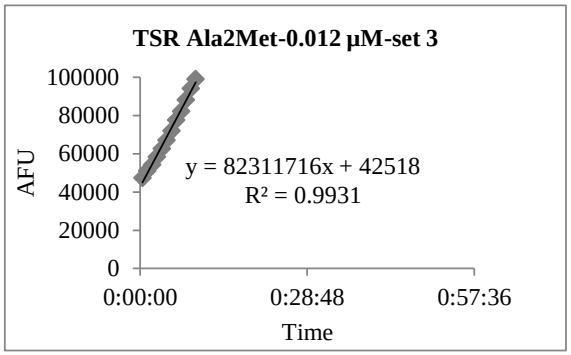
TSR Ala2Met-0.012 µM-set 3
AFU
100000
80000
60000
40000
20000
0
y = 82311716x + 42518
R² = 0.9931
0:00:00
0:28:48
0:57:36
Time

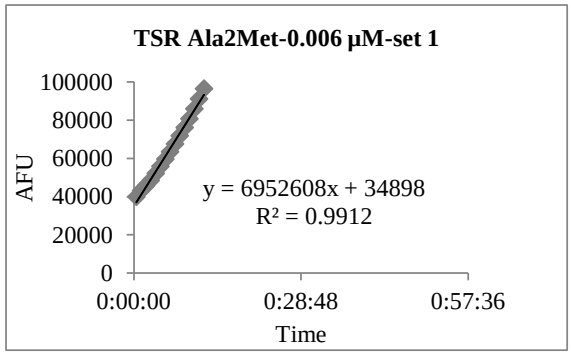
TSR Ala2Met-0.006 µM-set 1
AFU
100000
80000
60000
40000
20000
0
y = 6952608x + 34898
R² = 0.9912
0:00:00
0:28:48
0:57:36
Time

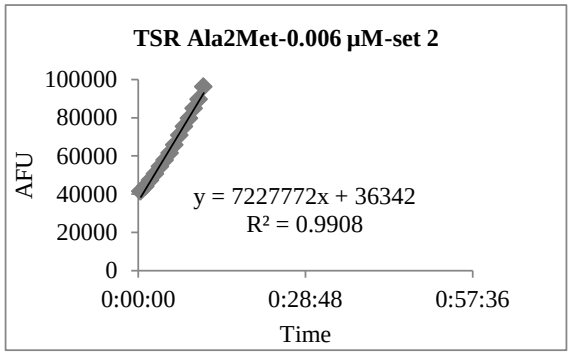
TSR Ala2Met-0.006 µM-set 2
AFU
100000
80000
60000
40000
20000
0
y = 7227772x + 36342
R² = 0.9908
0:00:00
0:28:48
0:57:36
Time

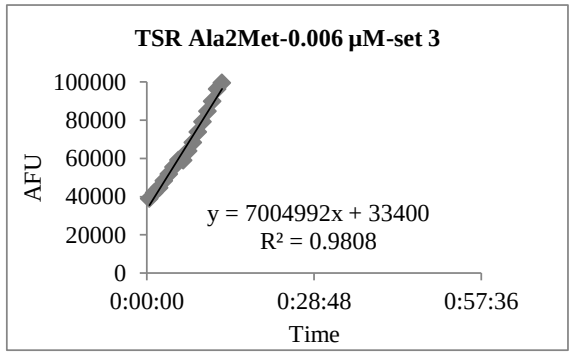
TSR Ala2Met-0.006 µM-set 3
AFU
100000
80000
60000
40000
20000
0
y = 7004992x + 33400
R² = 0.9808
0:00:00
0:28:48
0:57:36
Time

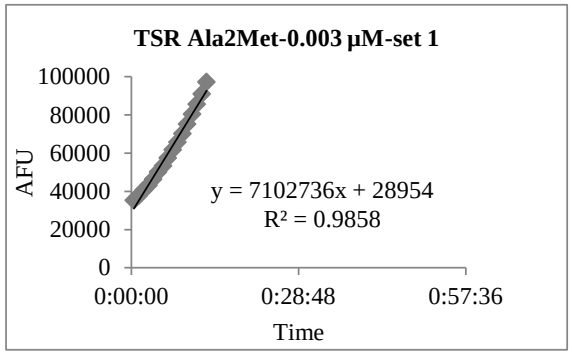
TSR Ala2Met-0.003 µM-set 1
AFU
100000
80000
60000
40000
20000
0
y = 7102736x + 28954
R² = 0.9858
0:00:00
0:28:48
0:57:36
Time

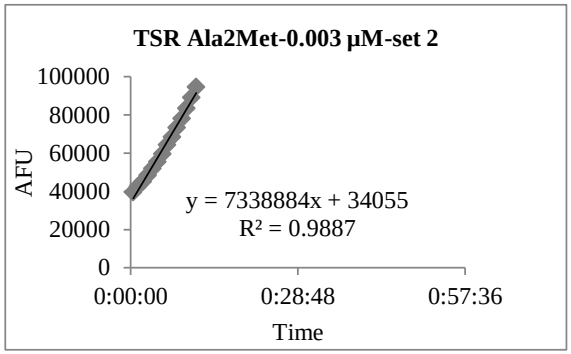
TSR Ala2Met-0.003 µM-set 2
AFU
100000
80000
60000
40000
20000
0
y = 7338884x + 34055
R² = 0.9887
0:00:00
0:28:48
0:57:36
Time

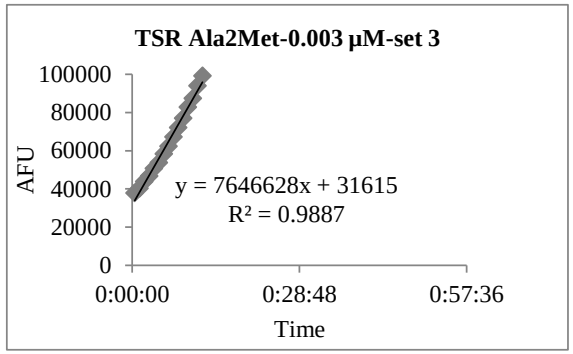
TSR Ala2Met-0.003 µM-set 3
AFU
100000
80000
60000
40000
20000
0
y = 7646628x + 31615
R² = 0.9887
0:00:00
0:28:48
0:57:36
Time

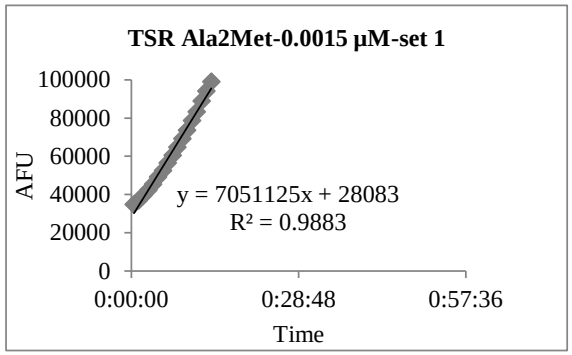
TSR Ala2Met-0.0015 µM-set 1
AFU
100000
80000
60000
40000
20000
0
y = 7051125x + 28083
R² = 0.9883
0:00:00
0:28:48
0:57:36
Time

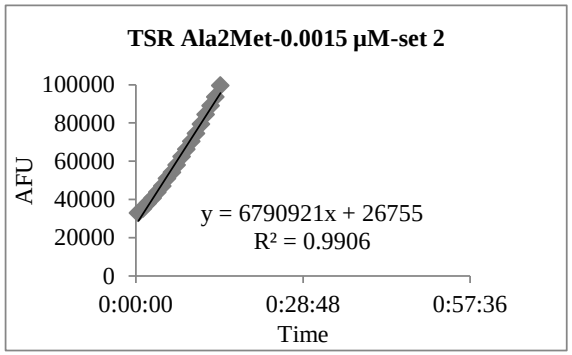
TSR Ala2Met-0.0015 µM-set 2
AFU
100000
80000
60000
40000
20000
0
y = 6790921x + 26755
R² = 0.9906
0:00:00
0:28:48
0:57:36
Time

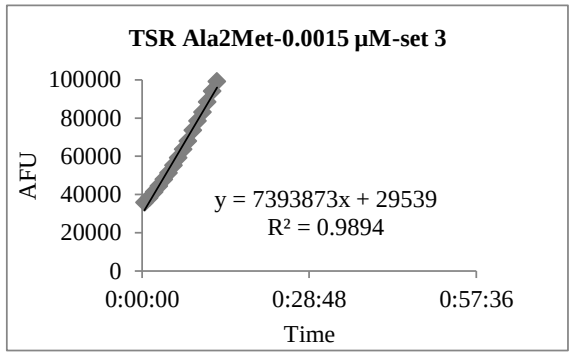
TSR Ala2Met-0.0015 µM-set 3
AFU
100000
80000
60000
40000
20000
0
y = 7393873x + 29539
R² = 0.9894
0:00:00
0:28:48
0:57:36
Time

Relative activity was obtained by normalizing the compound slope to the DMSO control slope.

	Slope (Set 1)	Slope (Set 2)	Slope (Set 3)	Average DMSO slope
DMSO Control	6930082	7100423	7210683	7080396

TSR Ala2Met Concentration (µM)	Slope (Set 1)	Slope (Set 2)	Slope (Set 3)	Average DMSO slope	Relative activity %; (Set 1)	Relative activity %; (Set 2)	Relative activity %; (Set 3)
50	374231	462718	528044	7080396	5.2855	6.5352	7.4578
25	329215	356623	394587	7080396	4.6497	5.0368	5.5730
12.5	317681	308177	332674	7080396	4.4868	4.3525	4.6985
6.25	348448	409440	405217	7080396	4.9213	5.7827	5.7231
3.13	781453	827647	900844	7080396	11.0369	11.6893	12.7231
1.56	2548379	2488499	2600221	7080396	35.9920	35.1463	36.7242
0.78	3222663	3476127	3612606	7080396	45.5153	49.0951	51.0227
0.39	4247503	4341528	4525839	7080396	59.9896	61.3176	63.9207
0.2	5307697	5217995	5521361	7080396	74.9633	73.6964	77.9810
0.098	6544753	6261134	6535033	7080396	92.4348	88.4292	92.2976
0.049	6661966	6545959	7034840	7080396	94.0903	92.4519	99.3566
0.024	6060892	6074714	6411207	7080396	85.6010	85.7962	90.5487
0.012	7458598	7907249	8231171	7080396	105.3415	111.6781	116.2530
0.006	6952608	7227772	7004992	7080396	98.1952	102.0815	98.9350
0.003	7102736	7338884	7646628	7080396	100.3155	103.6508	107.9972
0.0015	7051125	6790921	7393873	7080396	99.5866	95.9116	104.4274

Relative activity was plotted against compound concentration and fit to the Hill equation using GraphPad Prism 5 to calculate IC_{50}.

TSR Ala2Met Concentration (μM)	Relative activity %; (Set 1)	Relative activity %; (Set 2)	Relative activity %; (Set 3)
50	5.2855	6.5352	7.4578
25	4.6497	5.0368	5.5730
12.5	4.4868	4.3525	4.6985
6.25	4.9213	5.7827	5.7231
3.13	11.0369	11.6893	12.7231
1.56	35.9920	35.1463	36.7242
0.78	45.5153	49.0951	51.0227
0.39	59.9896	61.3176	63.9207
0.20	74.9633	73.6964	77.9810
0.098	92.4348	88.4292	92.2976
0.049	94.0903	92.4519	99.3566
0.024	85.6010	85.7962	90.5487
0.012	105.3415	111.6781	116.2530
0.006	98.1952	102.0815	98.9350
0.003	100.3155	103.6508	107.9972
0.0015	99.5866	95.9116	104.4274

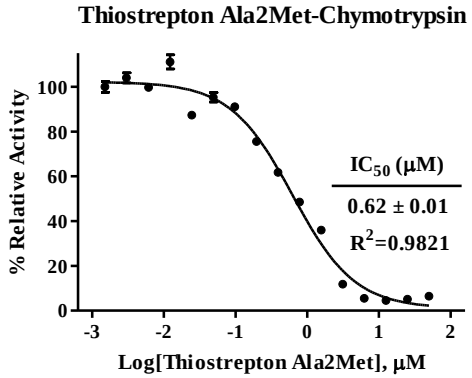

Figure G.2. *In vitro* translation inhibition curves for compounds from chapter 4.

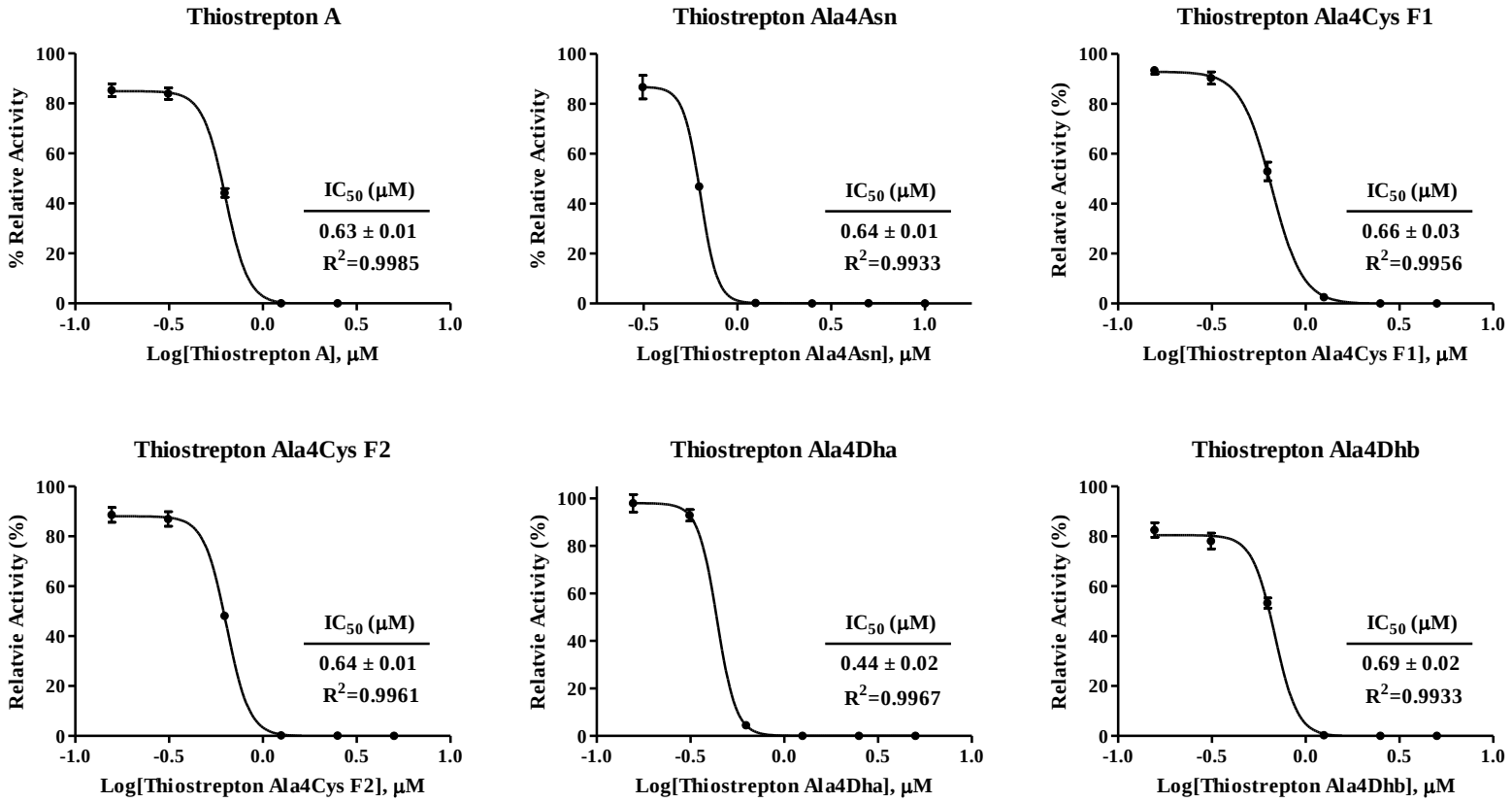

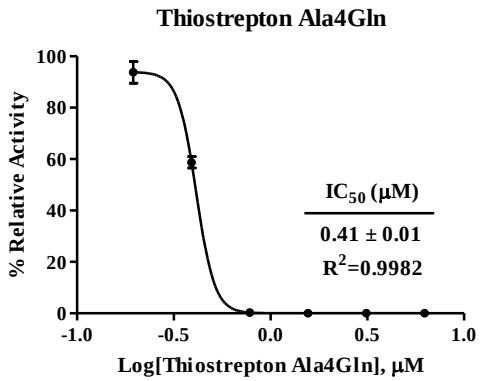
Thiostrepton Ala4Gln
% Relative Activity
100
80
60
40
20
0
-1.0
-0.5
0.0
0.5
1.0
Log[Thiostrepton Ala4Gln], µM
IC50 (µM)
0.41 ± 0.01
R2=0.9982

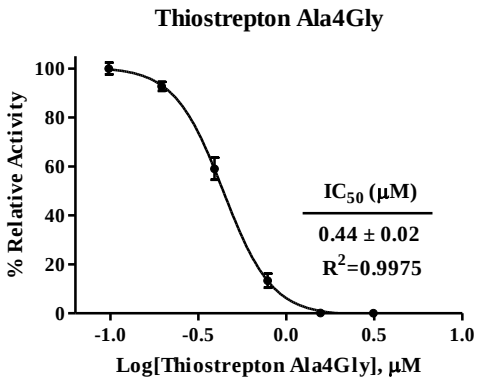
Thiostrepton Ala4Gly
% Relative Activity
100
80
60
40
20
0
-1.0
-0.5
0.0
0.5
1.0
Log[Thiostrepton Ala4Gly], µM
IC50 (µM)
0.44 ± 0.02
R2=0.9975

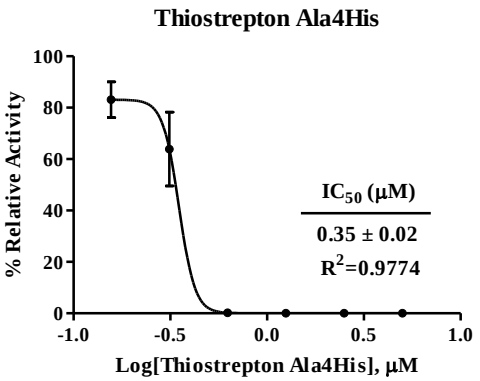
Thiostrepton Ala4His
% Relative Activity
100
80
60
40
20
0
-1.0
-0.5
0.0
0.5
1.0
Log[Thiostrepton Ala4His], µM
IC50 (µM)
0.35 ± 0.02
R2=0.9774

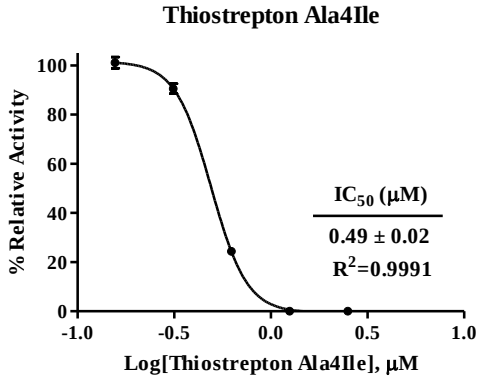
Thiostrepton Ala4Ile
% Relative Activity
100
80
60
40
20
0
-1.0
-0.5
0.0
0.5
1.0
Log[Thiostrepton Ala4Ile], µM
IC50 (µM)
0.49 ± 0.02
R2=0.9991

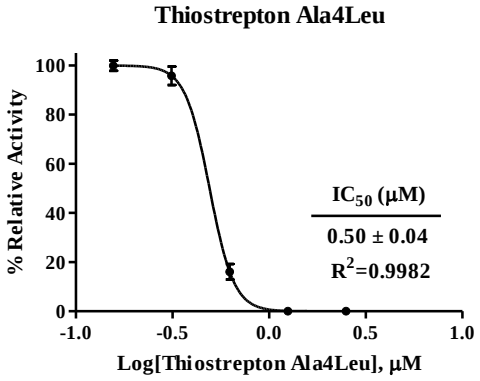
Thiostrepton Ala4Leu
% Relative Activity
100
80
60
40
20
0
-1.0
-0.5
0.0
0.5
1.0
Log[Thiostrepton Ala4Leu], µM
IC50 (µM)
0.50 ± 0.04
R2=0.9982

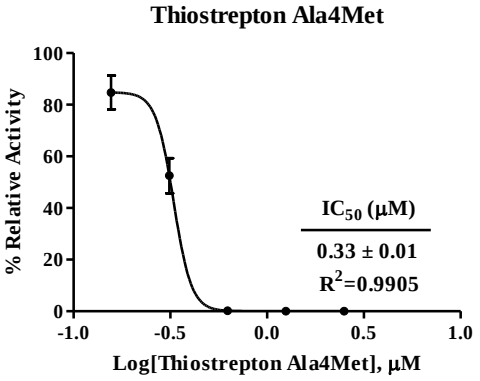
Thiostrepton Ala4Met
% Relative Activity
100
80
60
40
20
0
-1.0
-0.5
0.0
0.5
1.0
Log[Thiostrepton Ala4Met], µM
IC50 (µM)
0.33 ± 0.01
R2=0.9905

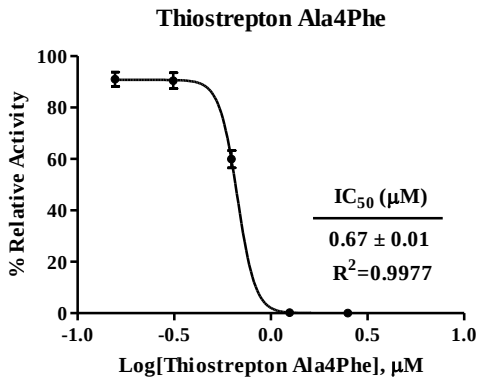
Thiostrepton Ala4Phe
% Relative Activity
100
80
60
40
20
0
-1.0
-0.5
0.0
0.5
1.0
Log[Thiostrepton Ala4Phe], µM
IC50 (µM)
0.67 ± 0.01
R2=0.9977

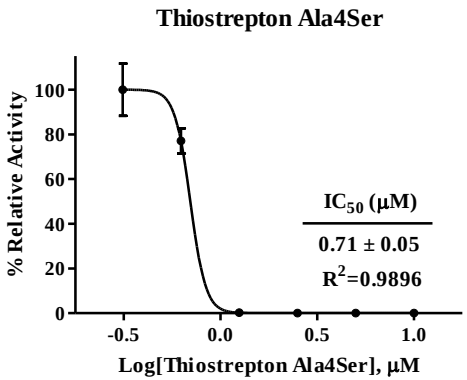
Thiostrepton Ala4Ser
% Relative Activity
100
80
60
40
20
0
-0.5
0.0
0.5
1.0
Log[Thiostrepton Ala4Ser], µM
IC50 (µM)
0.71 ± 0.05
R2=0.9896

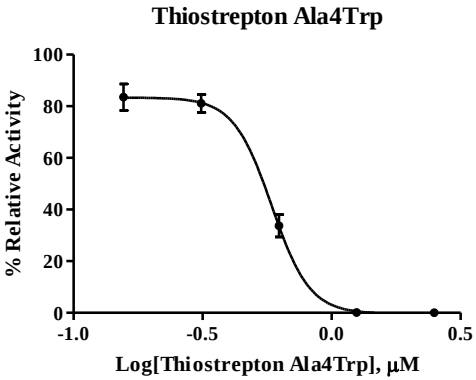
Thiostrepton Ala4Trp
% Relative Activity
100
80
60
40
20
0
-1.0
-0.5
0.0
0.5
Log[Thiostrepton Ala4Trp], µM

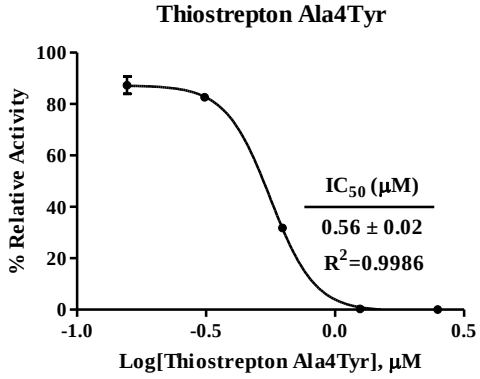
Thiostrepton Ala4Tyr
% Relative Activity
100
80
60
40
20
0
-1.0
-0.5
0.0
0.5
Log[Thiostrepton Ala4Tyr], µM
IC50 (µM)
0.56 ± 0.02
R2=0.9986

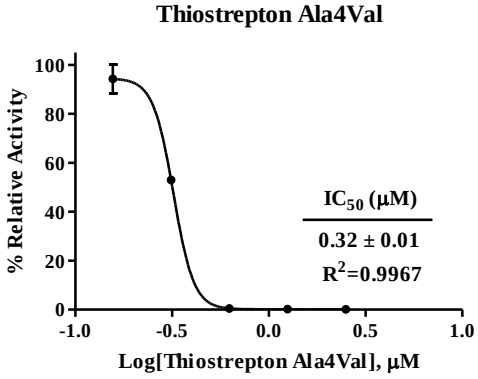
Thiostrepton Ala4Val
% Relative Activity
100
80
60
40
20
0
-1.0
-0.5
0.0
0.5
1.0
Log[Thiostrepton Ala4Val], µM
IC50 (µM)
0.32 ± 0.01
R2=0.9967

Figure G.3. 20S proteasome inhibition curves for compounds from chapter 4.

Thiostrepton A

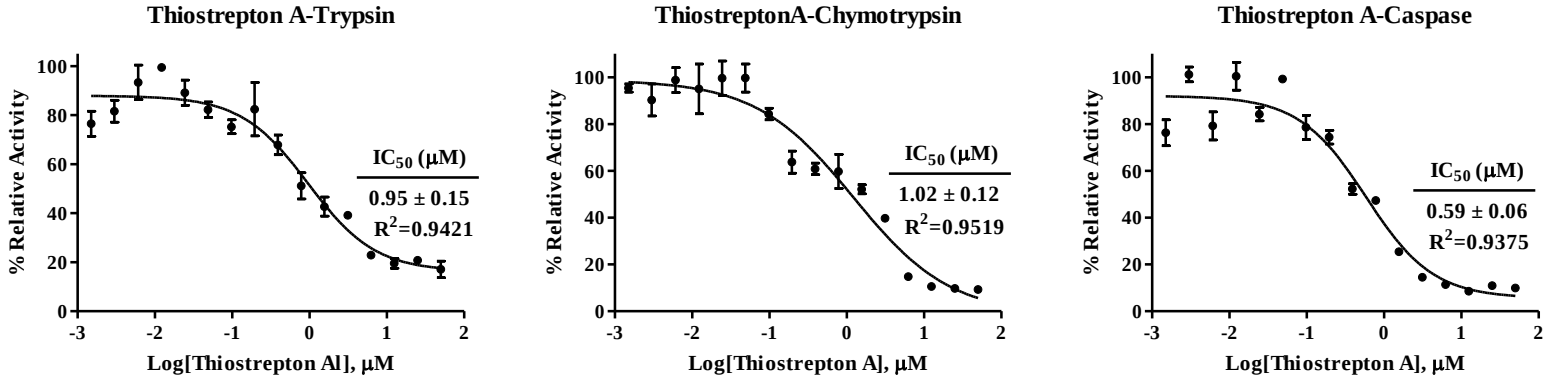

Bortezomib

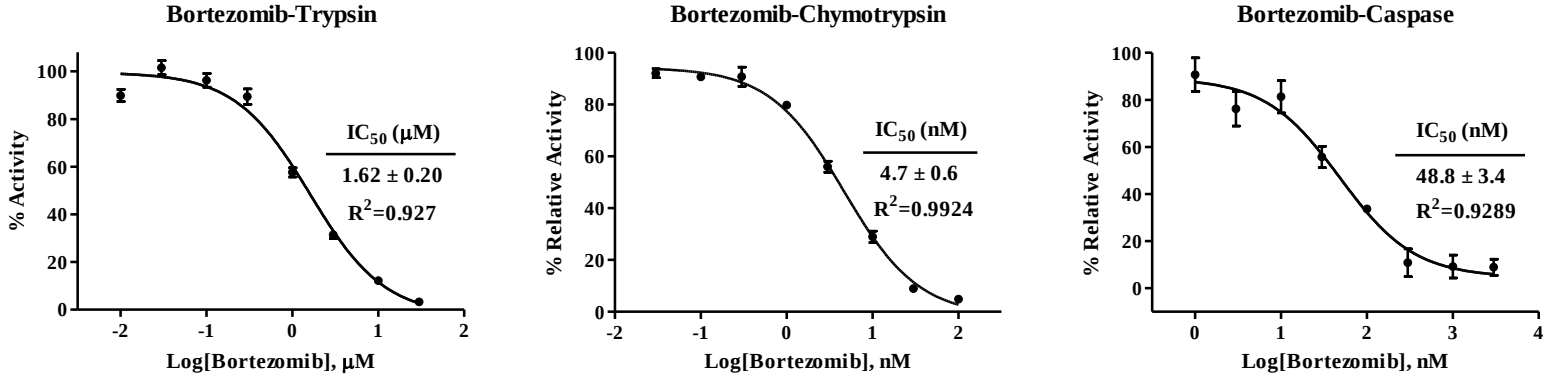

Thiostrepton Ala4Asn

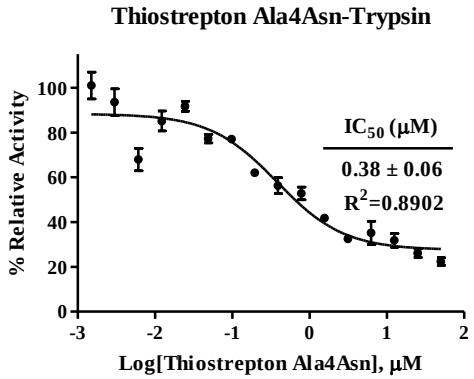

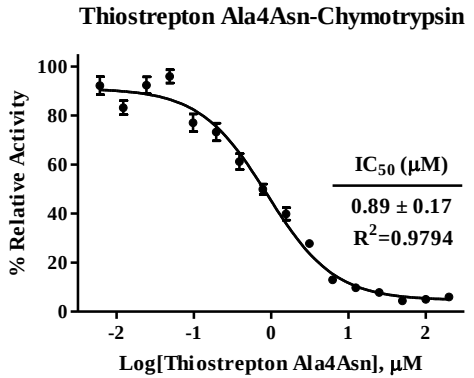

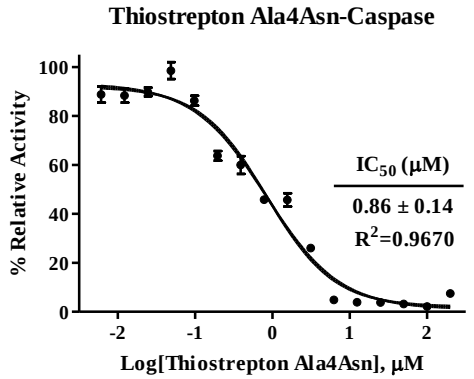

Thiostrepton Ala4Cys F1

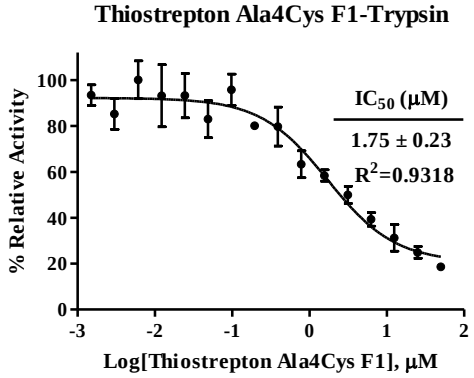

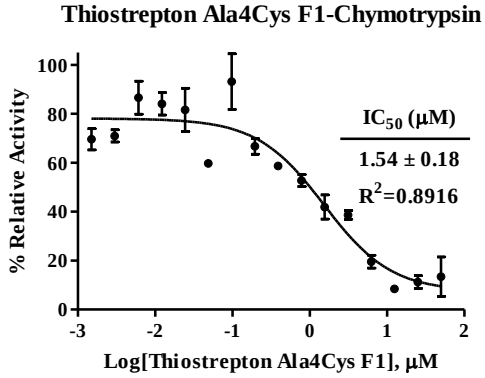

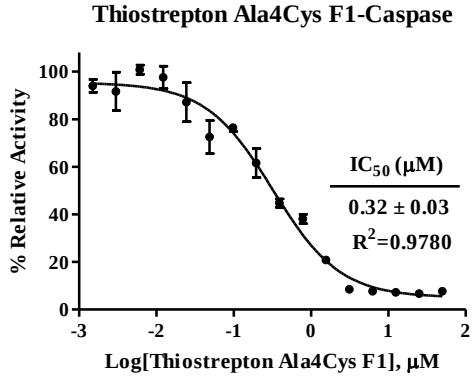

Thiostrepton Ala4Cys F2

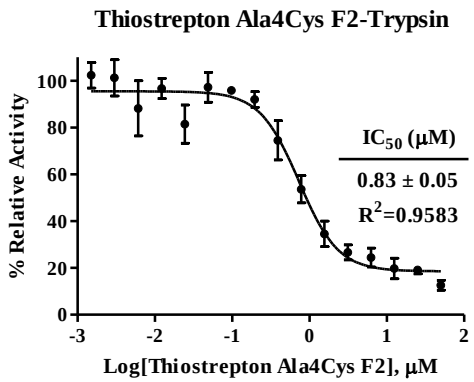

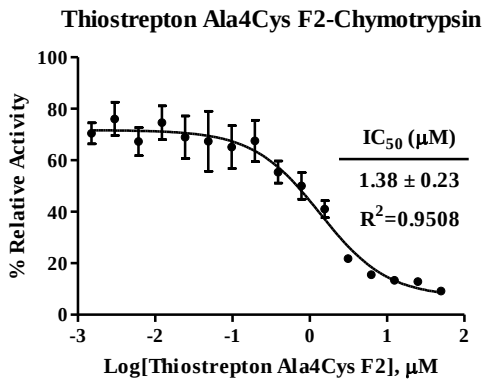

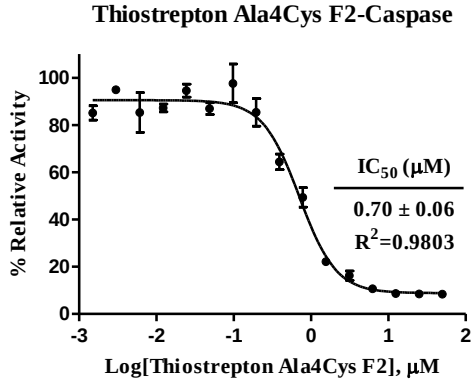

Thiostrepton Ala4Dha

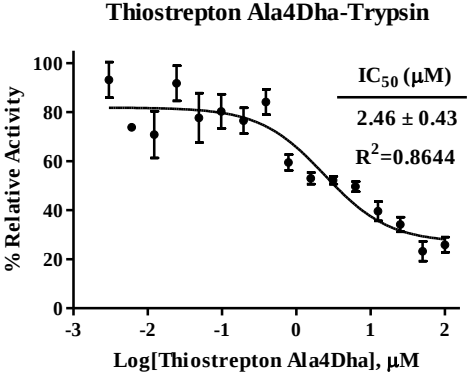

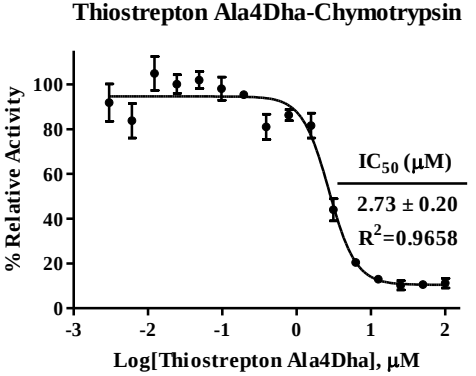

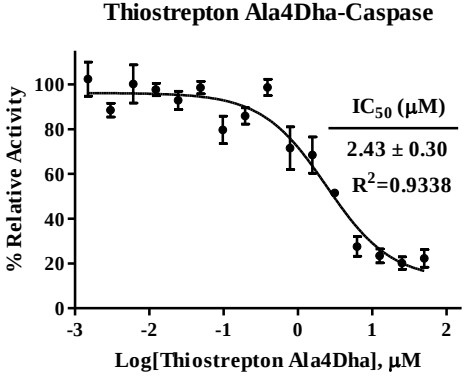

Thiostrepton Ala4Dhb

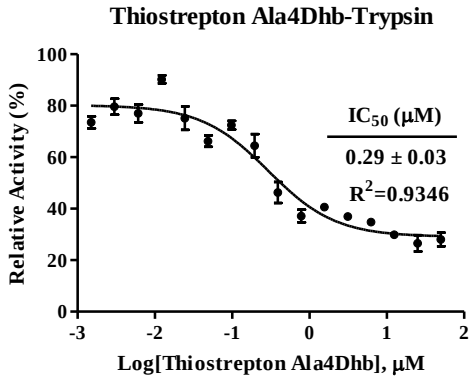

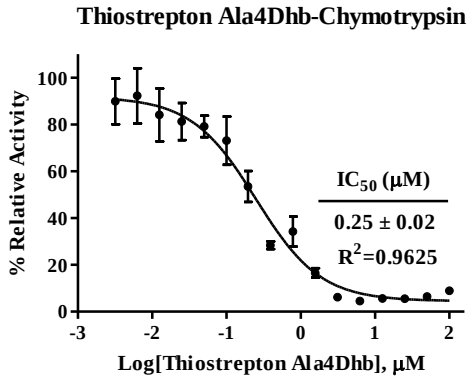

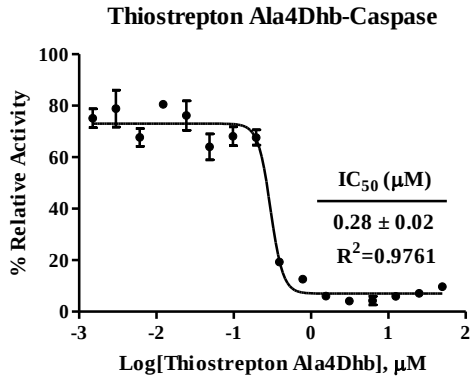

Thiostrepton Ala4Gln

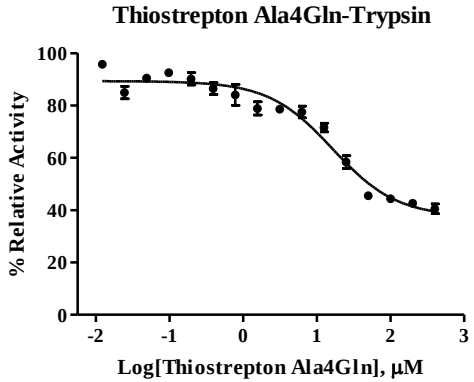

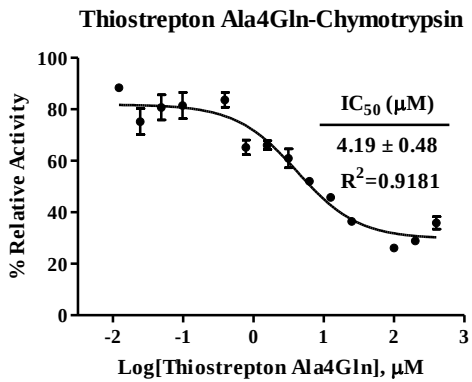

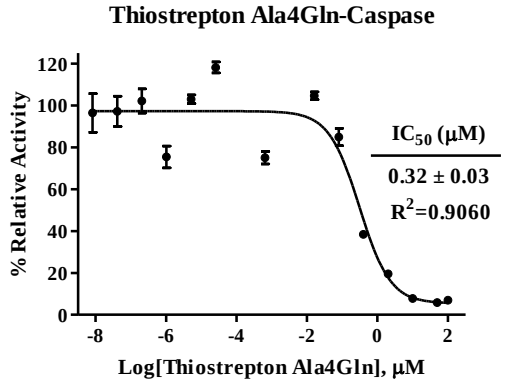

Thiostrepton Ala4Gly

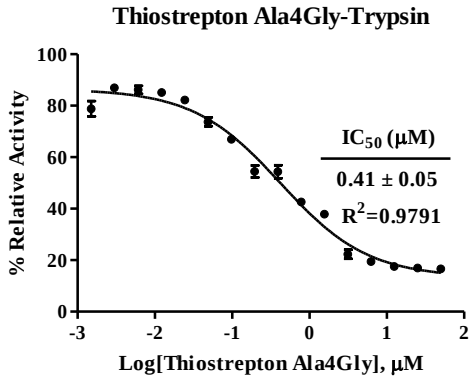

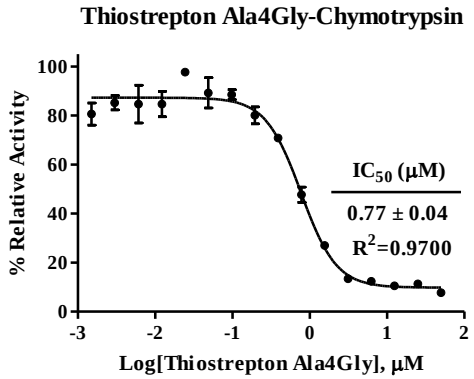

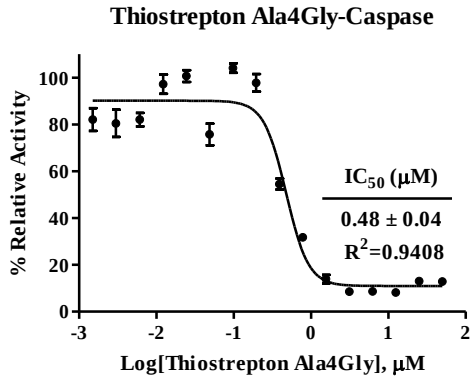

Thiostrepton Ala4His

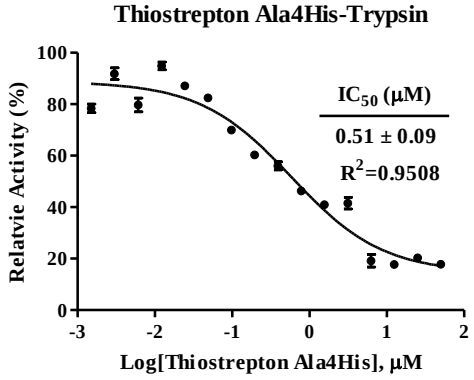

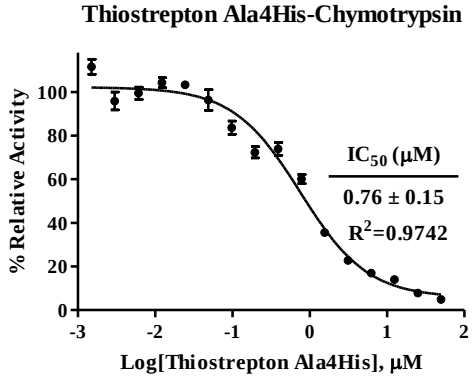

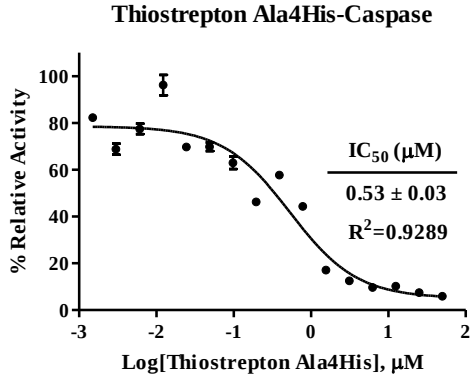

Thiostrepton Ala4Ile

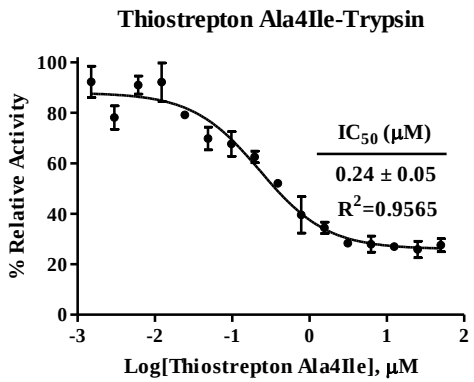

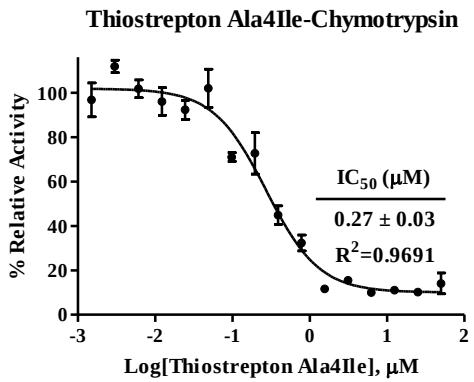

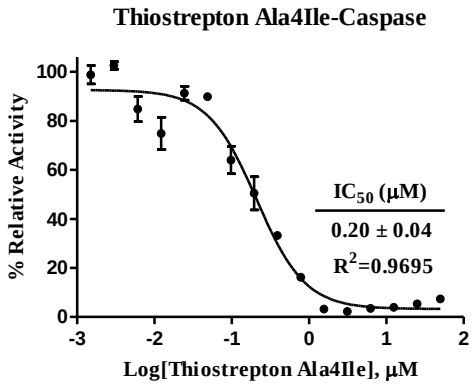

Thiostrepton Ala4Leu

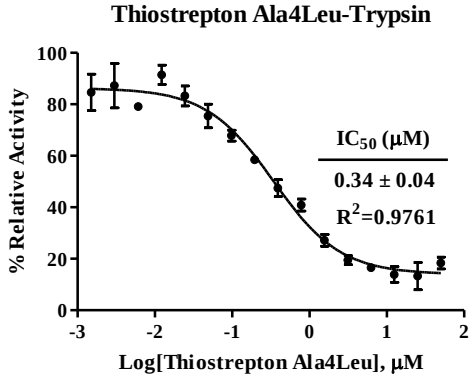

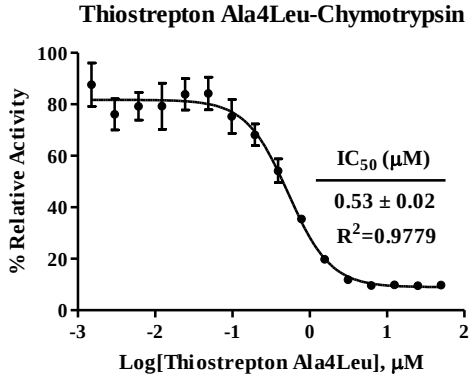

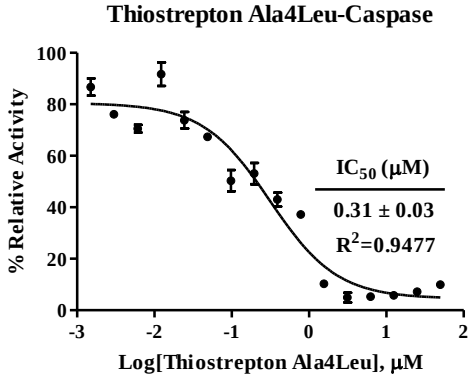

Thiostrepton Ala4Met

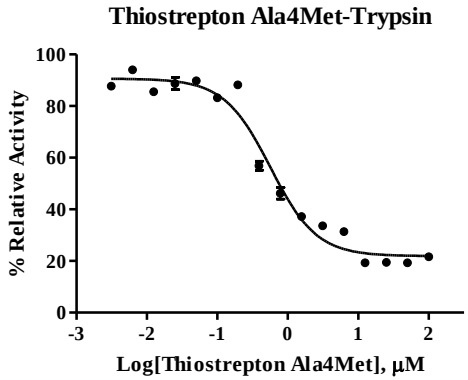

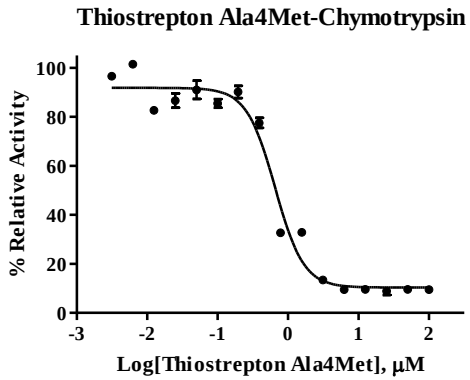

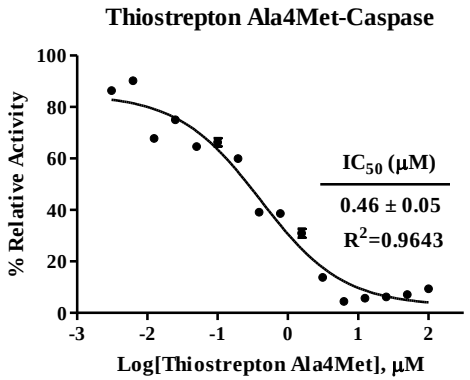

Thiostrepton Ala4Phe

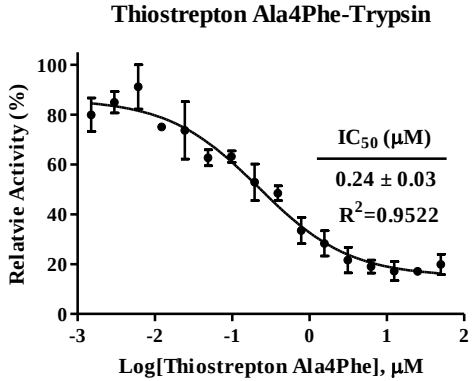

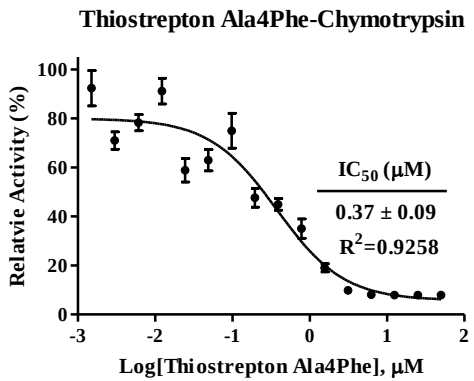

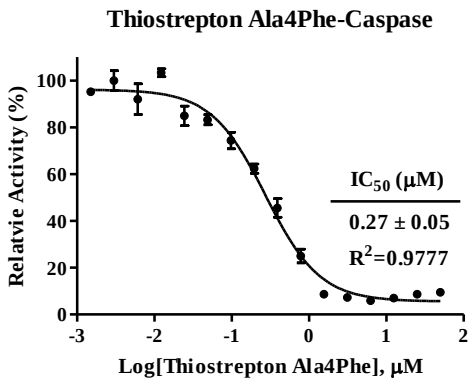

Thiostrepton Ala4Ser

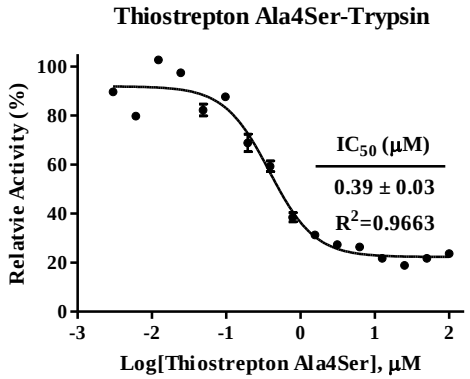

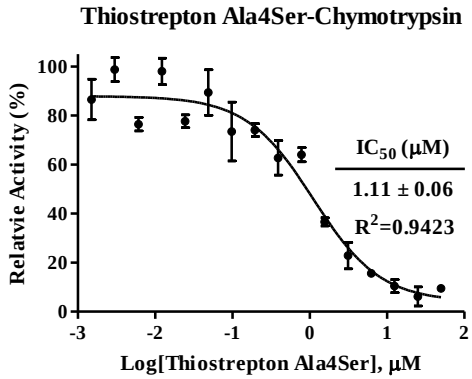

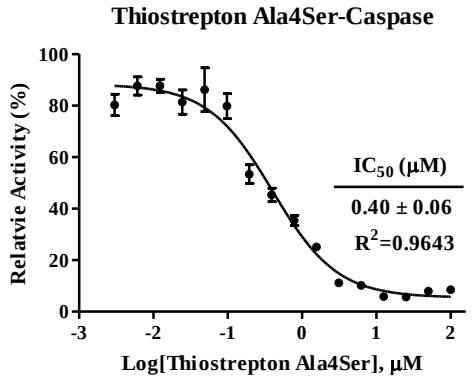

Thiostrepton Ala4Trp

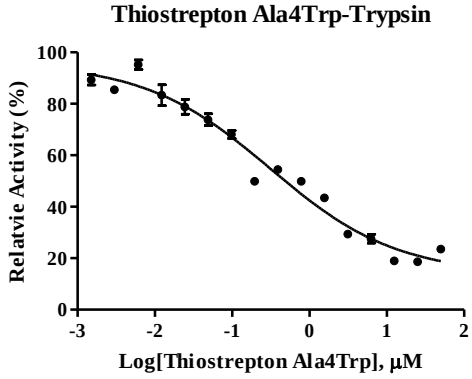

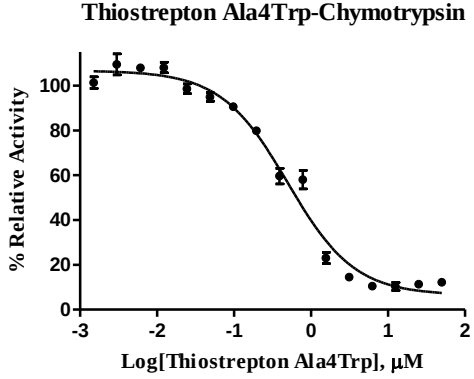

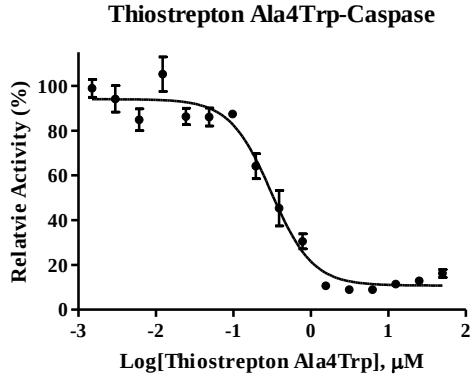

Thiostrepton Ala4Tyr

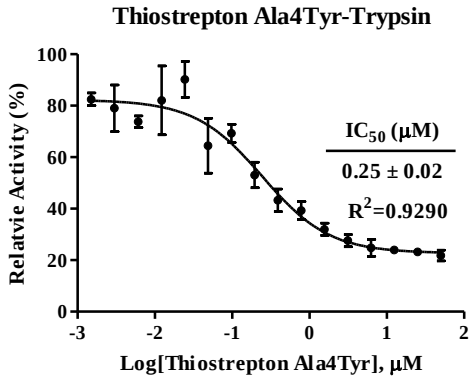

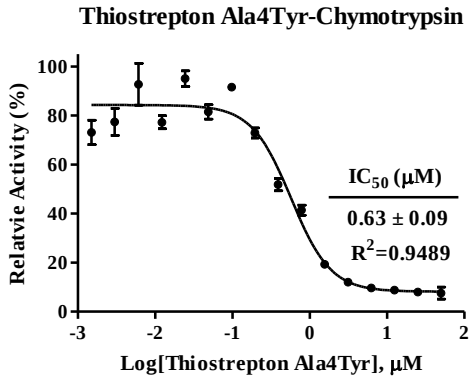

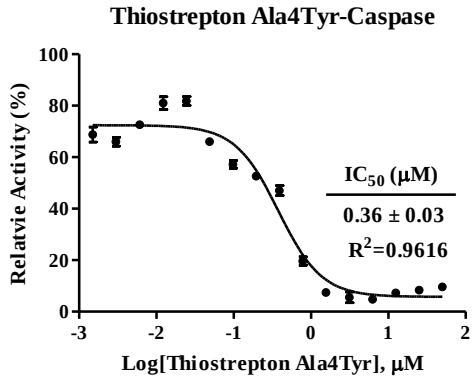

Thiostrepton Ala4Val

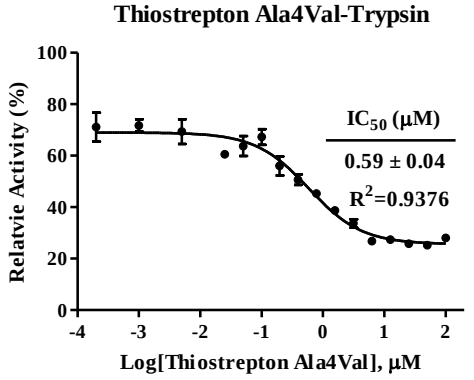

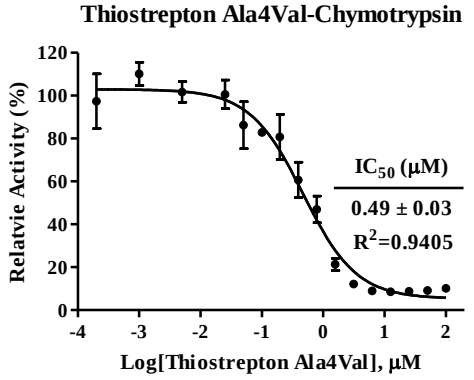

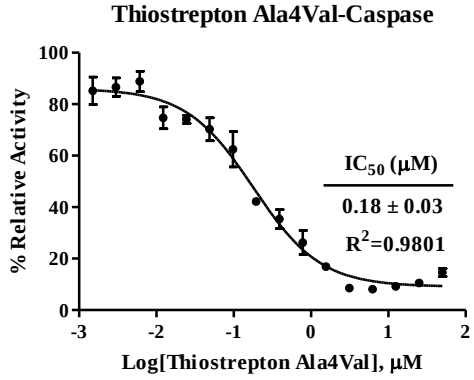

Thiostrepton Thr7Ala

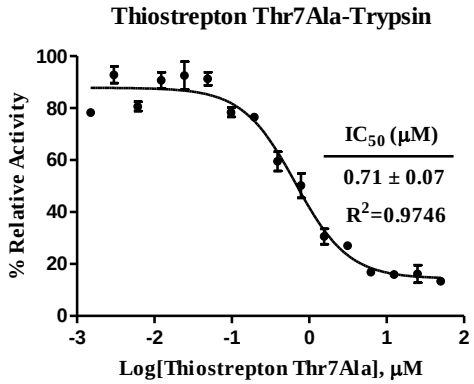

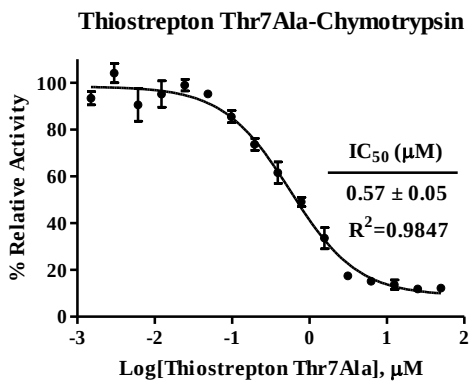

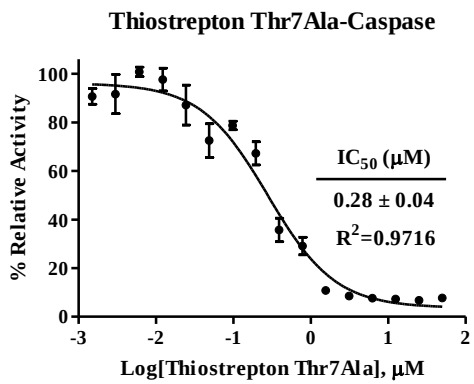

SL105-1

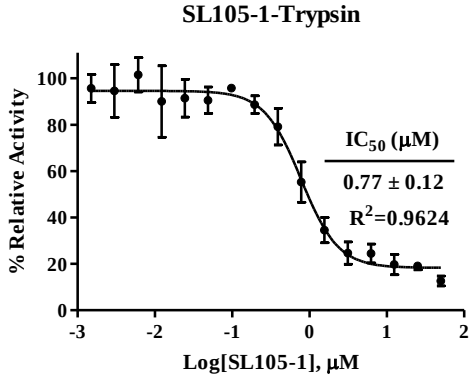

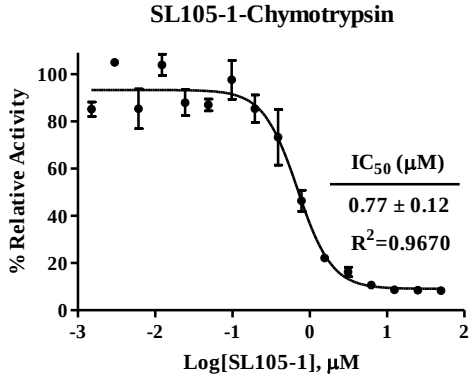

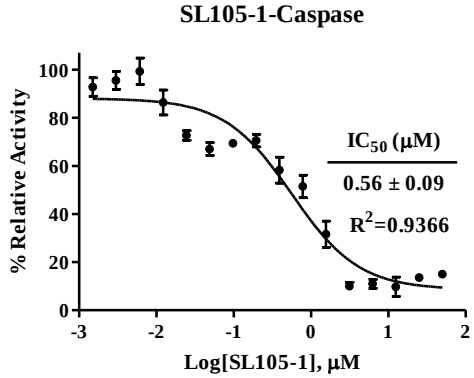

Thiostrepton Thr7Ala

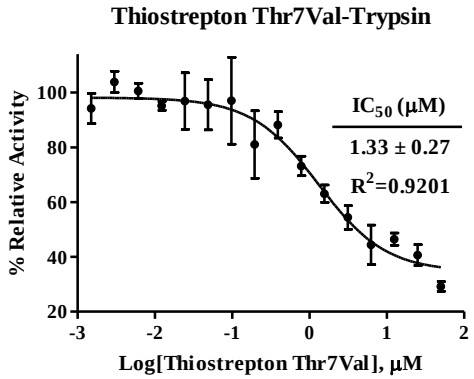

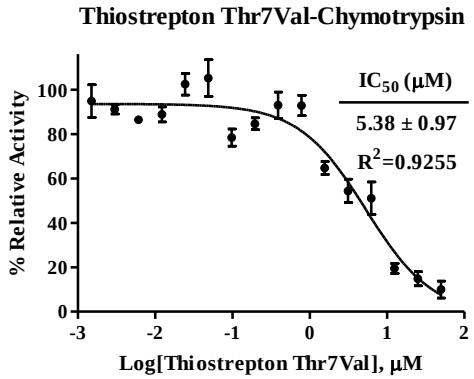

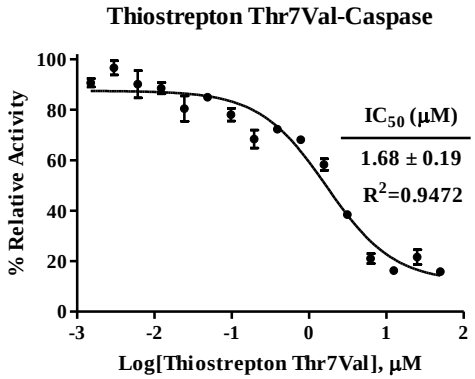

SL106-1

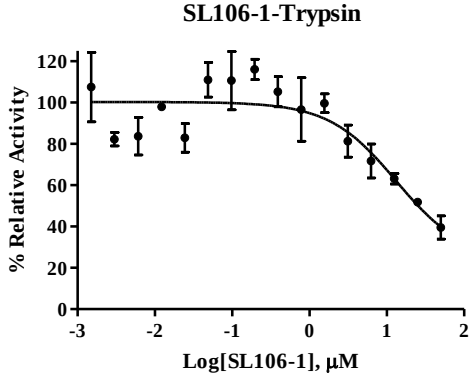

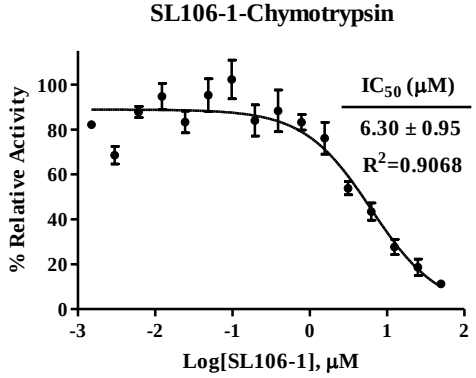

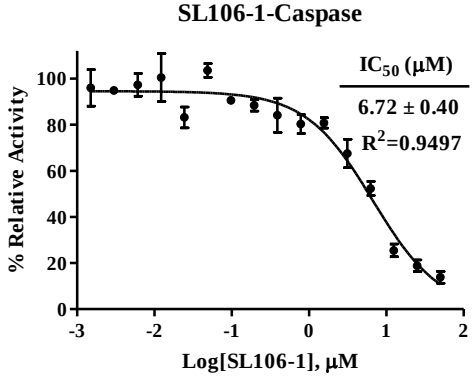

Figure G.4. *In vitro* translation inhibition curves for compounds from chapter 5.

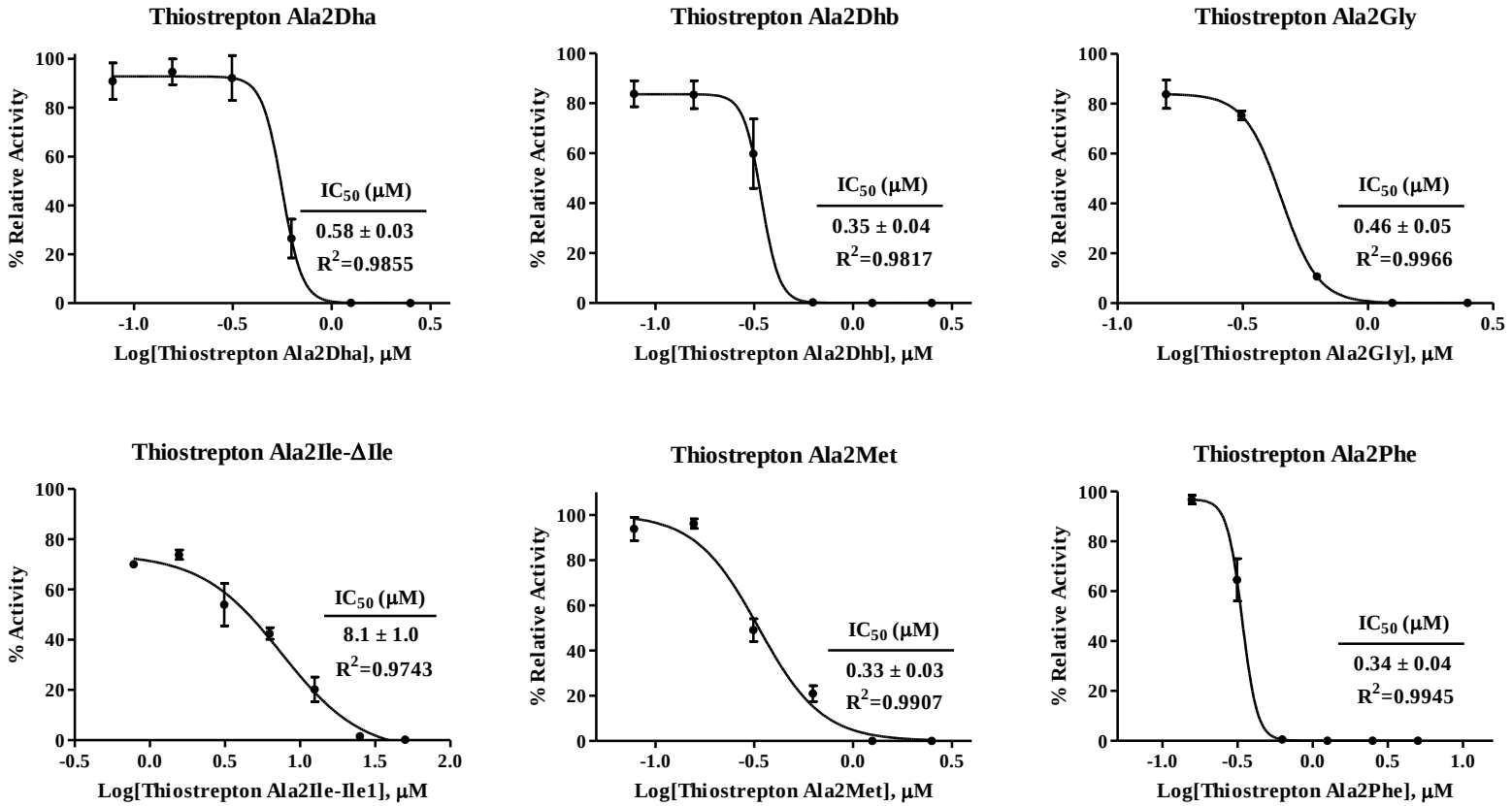

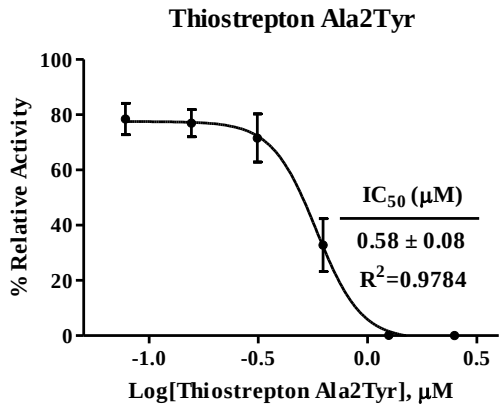
Thiostrepton Ala2Tyr
% Relative Activity
100
80
60
40
20
0
-1.0
-0.5
0.0
0.5
Log[Thiostrepton Ala2Tyr], µM
IC50 (µM)
0.58 ± 0.08
R2=0.9784

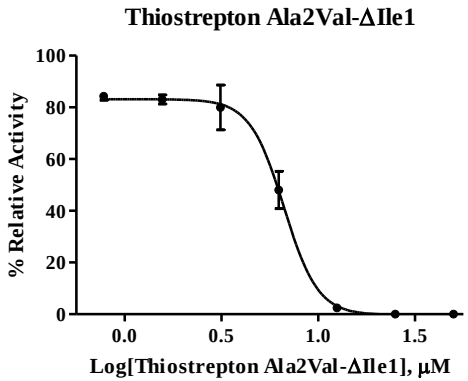
Thiostrepton Ala2Val-ΔIle1
% Relative Activity
100
80
60
40
20
0
0.0
0.5
1.0
1.5
Log[Thiostrepton Ala2Val-ΔIle1], µM

Figure G.5. 20S proteasome inhibition curves for compounds from chapter 5.

Thiostrepton Ala2Dha

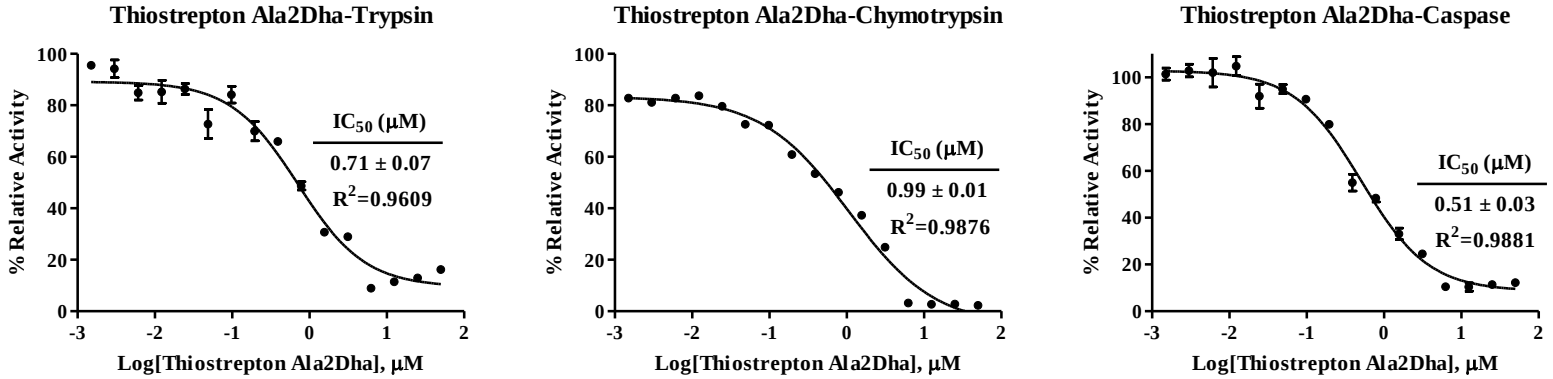

Thiostrepton Ala2Dhb

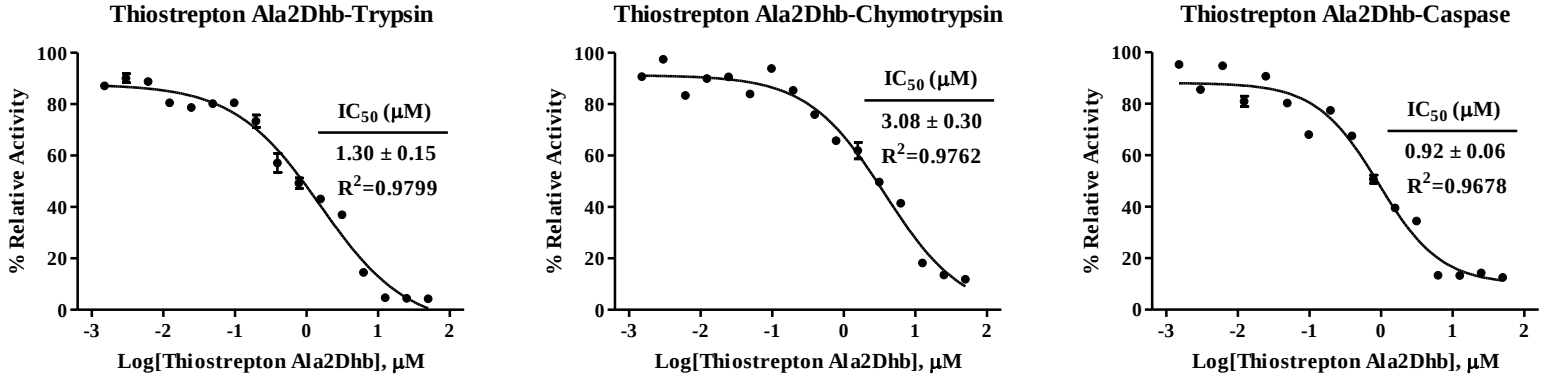

Thiostrepton Ala2Gly

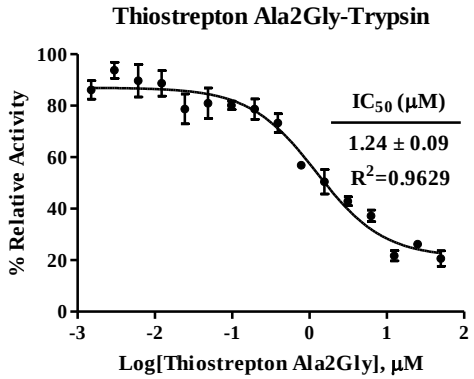

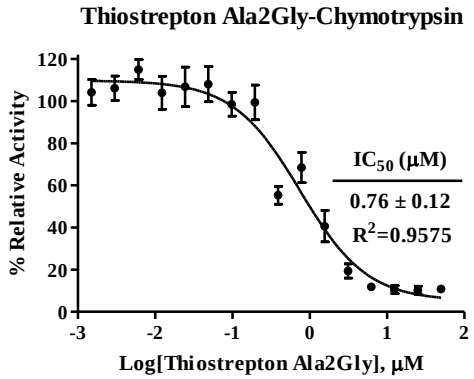

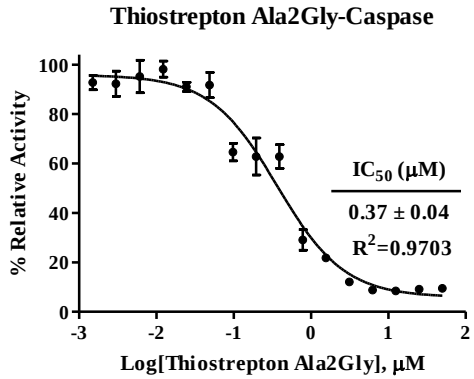

Thiostrepton Ala2Ile-ΔIle

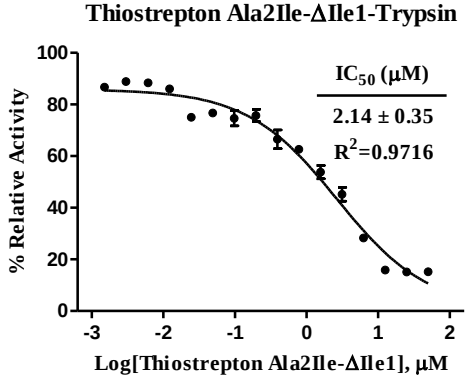

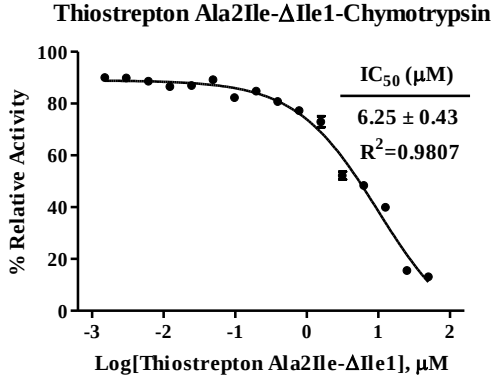

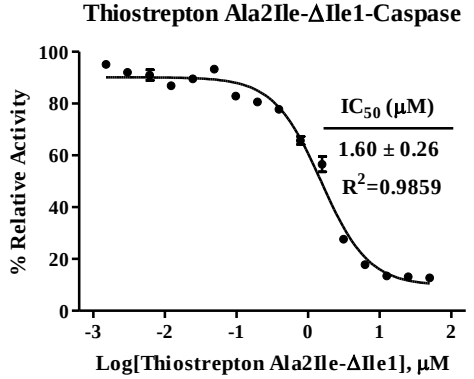

Thiostrepton Ala2Met

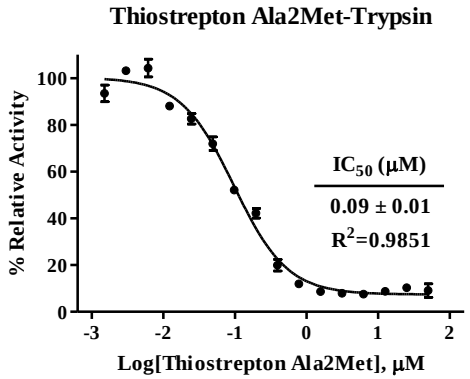

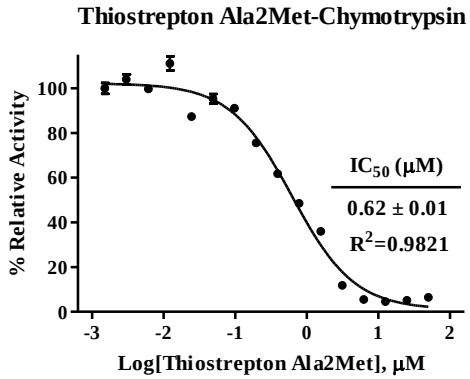

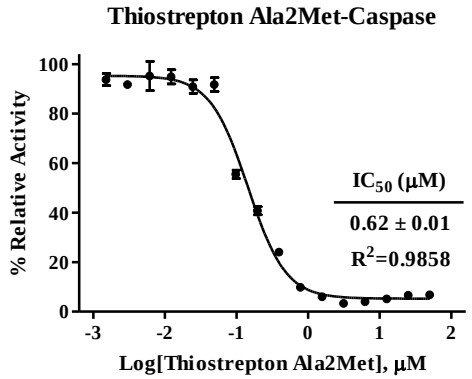

Thiostrepton Ala2Phe

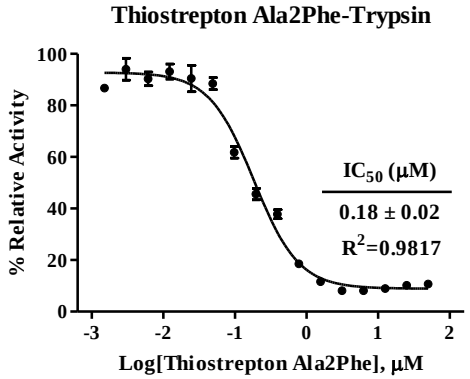

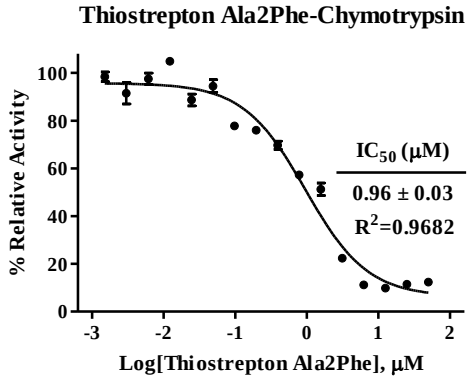

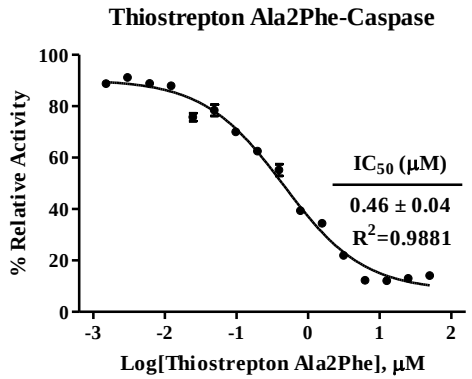

Thiostrepton Ala2Tyr

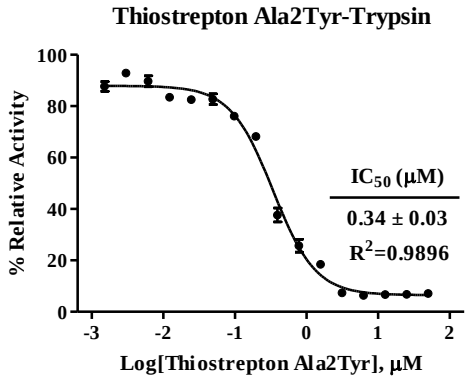

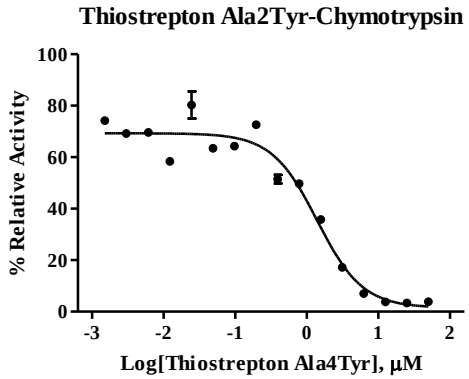

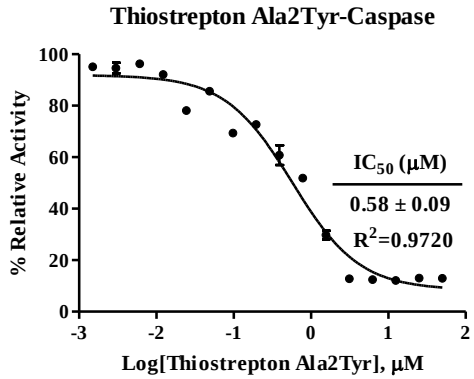

Thiostrepton Ala2Val-ΔIle